A book intended to bring unity and depth to basic concepts and principles of mechanics in the analysis of structures

Tung Au

Elementary Structural Mechanics

Civil Engineering and Engineering Mechanics Series

ELEMENTARY STRUCTURAL MECHANICS

by Tung Au

This book provides an introduction to the application of principles of mechanics in structural analysis. It deals primarily with statically determinate structures subjected to static or equivalent static loads and thoroughly treats the internal forces and deformations of these structures.

In addition to a logical consideration of statics and geometry of structures, applications of energy principles to structural analysis are systematically presented. Throughout the book, emphasis is placed on the application of principles of mechanics to the formulation and solution of structural problems in a general manner, rather than the routine techniques of solution for special types of structures.

By stressing the difference between real structures and their mathematical models, the book brings home to the reader the significance of intuitive perception so that he may gain a broad insight beyond that obtained through formal mathematical solutions.

SPECIAL FEATURES

- A fresh approach is presented by constantly pointing out the inter-

(Continued on back flap)

495 [illegible]ASANT ST.
[illegible]ELD, WISC. 53005

Civil Engineering and

Engineering Mechanics Series

N. M. Newmark and W. J. Hall, Editors

ELEMENTARY STRUCTURAL MECHANICS, by Tung Au
FOUNDATION DESIGN, by Wayne C. Teng
THEORY OF PRESTRESSED CONCRETE, by Michael Chi and Frank A. Biberstein

PRENTICE-HALL INTERNATIONAL, INC.
London Tokyo Sydney Paris
PRENTICE-HALL OF CANADA, LTD.
PRENTICE-HALL DE MÉXICO, S.A.

ELEMENTARY STRUCTURAL MECHANICS

Civil Engineering and
Engineering Mechanics Series

N. M. Newmark and W. J. Hall, Editors

ELEMENTARY STRUCTURAL MECHANICS

Tung Au

Associate Professor of Civil Engineering
Carnegie Institute of Technology

Prentice-Hall, Inc.
Englewood Cliffs, New Jersey

© 1963 by
PRENTICE-HALL, INC.
Englewood Cliffs, New Jersey

All rights reserved.
No part of this book may be reproduced
in any form, by mimeograph
or any other means,
without permission
in writing from the publisher.

Current printing (last digit):
11 10 9 8 7 6

Library of Congress Catalog Card Number 63–7562

Printed in the United States of America
26045C

PREFACE

This book is intended to bring unity and depth to basic concepts and principles of mechanics in the analysis of structures. It is written as a text for an introductory course in structural mechanics at the undergraduate level. It deals primarily with statically determinate structures subjected to static or equivalent static loads and thoroughly treats the deformations as well as the internal forces of these structures. In addition to a logical consideration of the fundamental principles of statics and the geometry of structures, the application of energy principles to the analysis of structures has been systematically presented. The student is expected to have, as prerequisite, adequate knowledge of the mechanics of rigid and deformable solids and properties of materials.

Throughout the entire text, emphasis is placed on the application of the principles of mechanics to the analysis of structures rather than the routine solution of certain types and classes of existing structures. By stressing the difference between real structures and their mathematical models at the very beginning, the text brings home to the student the significance of intuitive perception and gives a broad insight beyond that obtained through a formal mathematical solution. However, troublesome details of application are by no means neglected. Ample examples are completely worked out to illustrate the methods of approach for a great variety of problems. Numerous homework problems with varying degrees of difficulty are given to challenge the student's facility and improve his proficiency in problem solving. The book contains more than sufficient material for a one-semester course. However, a substantial part of it is devoted to the review of mechanics of rigid and deformable solids, which may be omitted if such a review is deemed unnecessary. On the other hand, some of the more ad-

vanced topics may be left out of the course if much time must be spent in the review of basic principles. For example, much of Chapters 4 and 5 and the latter part of Chapter 6 may be omitted so that more time can be devoted to Chapters 7 and 8; or full coverage may be accorded to the first six chapters, leaving the last two chapters to a more advanced course. The thorough treatment of the subject matter permits unusual flexibility in selection of the course content, at the discretion of the instructor.

The development of this book has been influenced by many previous publications by others in this field to whom the author is greatly indebted. The sources of reference are far too numerous to be cited here, but many of them are listed at the end of each chapter. However, a fresh approach has been presented by constantly pointing out the interaction of forces and displacements in structural systems. The chapter on energy principles contains material which has long been neglected in elementary books on structures but is invaluable in structural analysis, and it may be of interest to practicing engineers. The unity of purpose of many different theorems and methods has been stressed throughout the book.

The author is indebted to many of his colleagues and students at Carnegie Institute of Technology in the preparation of the manuscript; especially to Dr. James P. Romualdi for numerous constructive criticisms, to Messrs. Robert B. Anderson and Robert J. Brungraber for their assistance in proofreading, to Mrs. Sara Ennis for typing the manuscript, and to Dr. Thomas E. Stelson for his support in many ways. The author also wishes to acknowledge his appreciation to Dr. William J. Hall and Dr. Nathan M. Newmark, both of the University of Illinois, who reviewed the manuscript and offered invaluable suggestions.

TUNG AU

CONTENTS

1 INTRODUCTION 1

1–1 Structural engineering, 1. 1–2 Structural mechanics, 6. 1–3 Structural forms, 9. 1–4 Idealization of structural systems, 13. 1–5 Loads on structures, 21. 1–6 Serviceability and safety of structures, 33. 1–7 Design specifications, 38. 1–8 Formulation and solution of elementary problems, 44.

2 STRUCTURAL SYSTEMS 52

2–1 Definitions, 52. 2–2 Conditions of equilibrium, 54. 2–3 Degrees of freedom, 57. 2–4 Simple systems, 60. 2–5 Compound systems, 68. 2–6 Redundant systems, 75. 2–7 Compatibility of displacements, 80. 2–8 Force-deformation relations, 84. 2–9 Prestressing and self-straining, 95. 2–10 Linear structural systems, 99. 2–11 Nonlinear structural systems, 103. 2–12 Conservative systems—energy approach, 105. 2–13 Potential energy, 106. 2–14 Principle of virtual work, 110. 2–15 Strain energy and complementary energy, 112. 2–16 Summary, 114.

3 FORCES AND MOMENTS 122

3–1 Simple plane structures, 122. 3–2 Axial forces, shears, and moments, 123. 3–3 Differential relationships

3 *FORCES AND MOMENTS—Continued*

in beams, 130. 3–4 Integration of singularity functions, 135. 3–5 Shear and moment diagrams for beams and frames, 139. 3–6 Girders supporting floor beams, 149. 3–7 Beams subjected to irregular loading, 152. 3–8 Numerical procedure for computing shears and moments, 157. 3–9 Three-hinged arches, 163. 3–10 Cables, 173. 3–11 Suspended girders, 179. 3–12 Simple structures in space, 183. 3–13 Circular bow girders, 186. 3–14 Summary, 189.

4 *BAR FORCES IN TRUSSES* 200

4–1 Definitions, 200. 4–2 Common patterns of plane trusses, 203. 4–3 Bar forces in simple trusses, 206. 4–4 Application of method of joints, 208. 4–5 Application of method of sections, 212. 4–6 Special application to parallel chord trusses, 217. 4–7 Compound trusses, 219. 4–8 Trusses with secondary systems, 224. 4–9 Complex trusses, 228. 4–10 Method of virtual displacements, 233. 4–11 Simple trusses in space, 236. 4–12 Summary, 241.

5 *GRAPHIC STATICS* 249

5–1 Basic concepts, 249. 5–2 General graphical procedure, 252. 5–3 Applications of graphical method, 254. 5–4 Reactions, 255. 5–5 Moments in beams, 262. 5–6 Three-hinged arches, 267. 5–7 Pressure lines, 271. 5–8 Application to statically indeterminate frames, 275. 5–9 Bar forces in simple trusses, 278. 5–10 Compound trusses, 282. 5–11 Virtual displacement diagrams, 284. 5–12 Application of virtual displacement diagrams to trusses, 289. 5–13 Summary, 292.

6 *INFLUENCE LINES* 295

6–1 Definitions, 295. 6–2 Influence lines as virtual displacement diagrams, 298. 6–3 Application of influence lines, 302. 6–4 Compound beams, 307. 6–5 Girders supporting floor beams, 310. 6–6 Three-hinged arches, 314. 6–7 Simple trusses, 319. 6–8 Compound trusses, 326. 6–9 Moment tables for concentrated loads, 330. 6–10 Criteria for maximum effects on beams, 335. 6–11

6 *INFLUENCE LINES—Continued*

Absolute maximum shear and moment in beams, 345. 6–12 Criteria for maximum effects on trusses, 349. 6–13 Summary, 358.

7 *DISPLACEMENTS* 368

7–1 Elastic deflections of simple structures, 368. 7–2 Moment-curvature relation, 369. 7–3 Deflection of beams, 373. 7–4 Successive integrations of singularity functions, 379. 7–5 Moment-area method, 383. 7–6 Concept of conjugate beams, 389. 7–7 Numerical method for computing beam deflections, 393. 7–8 Geometry of deflected rigid frames, 397. 7–9 General procedure for computing deflections in rigid frames, 401. 7–10 Deflection of arches, 406. 7–11 Geometry of deflected trusses, 408. 7–12 Williot-Mohr diagram for truss deflection, 410. 7–13 Angle changes in deflected trusses, 417. 7–14 Conjugate beam method for computing truss deflections, 420. 7–15 Deflection of cables, 425. 7–16 Summary, 429.

8 *ENERGY PRINCIPLES* 436

8–1 Energy relations in structural systems, 436. 8–2 Real work and complementary work, 438. 8–3 Strain energy in linear elastic systems, 441. 8–4 Method of real work, 446. 8–5 Strain energy and complementary energy methods, 448. 8–6. Principle of virtual work, 450. 8–7 Method of virtual work for linear elastic systems, 457. 8–8 Castigliano's theorems, 460. 8–9 Deflections of nonlinear elastic systems, 465. 8–10 Maxwell-Betti theorem of reciprocal displacements, 469. 8–11 Influence lines for deflections, 474. 8–12 Analysis of redundant structures, 476. 8–13 Influence coefficients for linear systems, 482. 8–14 Müller-Breslau's Principle, 484. 8–15 Application of Castigliano's theorems, 490. 8–16 Principle of stationary potential energy, 496. 8–17 Principle of stationary complementary energy, 502. 8–18 Summary, 506.

ANSWERS TO PROBLEMS 513

INDEX 517

ELEMENTARY STRUCTURAL MECHANICS

1 INTRODUCTION

1-1 Structural Engineering

Structural engineering involves the utilization of art and science in the planning, analysis, design, and construction of structures. *Planning* consists of the development of a general layout of the structure that satisfies functional, economical, and esthetic requirements. *Analysis* is the process of constructing a mathematical model for the real structure and seeking the numerical solution of the idealized problem. *Design* involves the selection of proper materials for the structure and the determination of the shapes and sizes of its components. *Construction* pertains to fabrication, erection, and inspection of the structure. The final completion of a safe but efficient and economical structure depends on the satisfactory execution of the project through all stages.

It should be noted, however, that these basic steps are by no means distinct but rather are interdependent. Some of them involve mathematical analysis; others require judgment based on experience. Quite frequently it is necessary to have a balanced combination of both, depending on the degree of complexity of the structure. We shall examine each step in detail in order to gain a better understanding of the over-all approach to a structural problem.

Planning. This is the initial phase of a project, which requires above all creative imagination and sound judgment. If the structure is a highway bridge, for instance, the topography, soil conditions, and traffic patterns near the bridge site must be studied. Next the type of structure most suitable for the crossing must be considered. A girder, truss, arch, or suspension bridge are common alternatives. Experience with similar problems is often a guide for selecting the type of structure. However, the existing standard

structural forms may fail to satisfy all the requirements and new ones must be developed. Here the engineer needs both creative imagination and traditional conservatism. Otherwise, he may be too absorbed in the existing types of structure to recognize that a new approach is possible. On the other hand, he may see all the virtues and none of the weaknesses of the new form so that only later experience may reveal its undesirable or even disastrous aspects. It is important, therefore, that he has a broad understanding of the principles of mechanics and some practical experience so that he can exercise his judgment wisely.

For purposes of comparison it is often necessary to make preliminary designs and cost estimates for several structural schemes. As a matter of practical necessity, crude approximations may be introduced in the analysis. Once a particular structure is chosen, however, more precise data and methods are used to obtain better and more reliable solutions. Such operations are usually carried out by trial and error until a satisfactory solution is obtained.

Analysis. The analysis of structural systems is founded on the principles of mechanics. Before the formulation and solution of a problem, however, the system is usually idealized and simplified so that the conceptual model will be simple enough to analyze and yet not too different from the real structure. A great deal of judgment is involved in making simplifying assumptions, which can only be verified by experiment or justified by experience. At this stage three distinct phases should be recognized. First, the real structure may be divided into appropriate component systems that can be analyzed separately—one part at a time if necessary and possible. In a steel-framed building, for example, the beams and columns at each level can be considered as separate elements. Second, we must determine the loads that are transmitted and resisted by each system, considering not only the magnitude, location, and distribution of these loads, but also the frequency of their occurrence and the nature of their action. Third, it is necessary to examine the characteristics of the system against the consequences of failure or unserviceability of the structure. Thus, the concept of structural safety will not be lost in the idealization. These three phases are closely related to each other, and all three of them affect the method of analysis. Although the analysis itself is a rather mechanical procedure, the consideration of these factors involves a great deal of judgment.

As an example, consider the effect of a locomotive on a plate-girder bridge. It is customary to replace the rolling effect by an equivalent stationary load. Under such circumstances, the mathematical model will be the same as that for a static load and the problem can be solved by statics. On the other hand, if the rolling loads and the unbalanced weights of the driving wheels are treated as dynamic loads, the mass of the bridge must

be included in the idealized system, and the vibration of the bridge becomes important in the analysis. Moreover, the system is considered to be elastic if the criterion of unserviceability of the structure is defined by the initial yielding of the material in any part of the girder. However, it will be treated as an elastic-plastic system when the ultimate strength of the beam at collapse is the criterion of failure.

Courtesy of Richardson, Gordon & Associates, Consulting Engineers

Fort Pitt Bridge, Pennsylvania Department of Highways. This double-deck tied-arch bridge is statically indeterminate to the fifteenth degree. The arches are box girders and the trusses serve as ties.

Design. This phase involves the proportioning of the components or members of the structural system. The choice of materials for the structure depends not only on the suitability of the materials but also on their availability; for this reason the materials should be determined in the early planning stage. This is especially true if the choice of materials may influence the form of the structure, or vice versa. For example, in the design of a mill building, a steel skeleton frame may be selected because a similar frame in reinforced concrete will limit the span of the structure owing to the unfavorable ratio of resistance to weight of the material. However, if a thin-shelled roof is adopted, reinforced concrete may prove to be more suitable

than steel. Again, the interplay of these factors definitely affects the structural system, and a thorough knowledge of the properties of materials is indispensable in selecting the proper materials for specific structures.

The proportions of the component members of a structure must be so chosen that the structure as a whole can safely and economically perform the intended services under the prescribed loading conditions. Failure in certain parts of a structure may have only local effects, but in other cases it may cause the complete collapse of the structure. For this reason no member or connection in a structure should be overlooked. Because of the elements of uncertainty and perhaps ignorance of the expected loads, the material properties, and the criteria for failure, a *factor of safety* is introduced in proportioning the structural members. This may be accomplished either by providing a comfortable margin below the yield strengths of materials in specifying the allowable stresses, as is often done in the *elastic design* of structures, or by adopting ultimate design loads several times higher than the loads expected in the lifetime of the structure, as is generally practiced in the *plastic design* of structures.

It should be observed that design is almost inseparable from analysis. The exact sizes of structural members can be determined only after a complete analysis of the structure. On the other hand, there are certain items

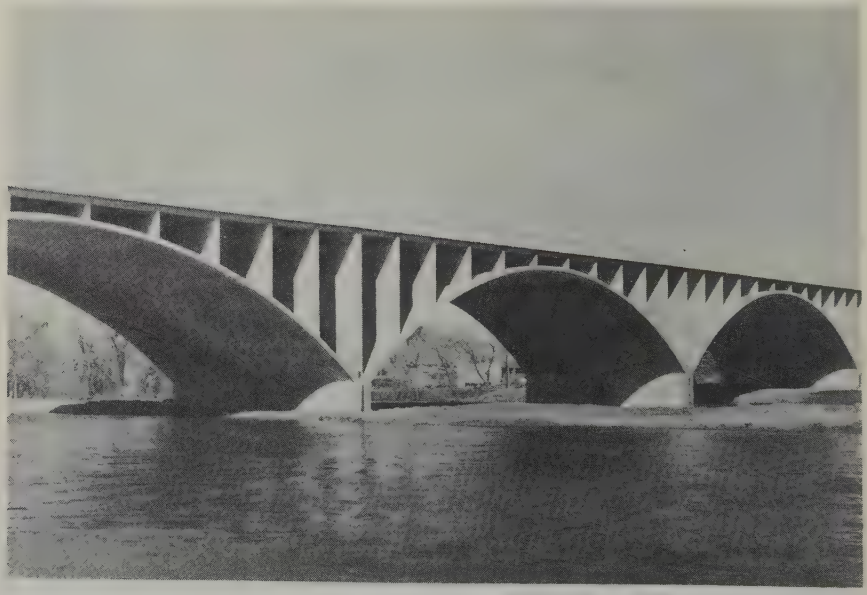

Courtesy of Vogt, Ivers and Associates, Consulting Engineers

Fox River Valley Bridge, Northern Illinois Toll Highway. The bridge consists of five thin concrete arches, each with a span of 178 ft. The arch barrels are 14 in. thick and are on a circular arc of 133 ft radius.

in analysis that depend on the results of design. One example is the weight of the structure, which cannot be determined exactly until all members of the structure are proportioned. Hence, the procedure of analysis and design may involve cycles of successive corrections.

Construction. As the project reaches its final stage, the work shifts from design office to plant and field, where the structure is fabricated and erected. The structural engineer may no longer have direct control over the job, but he should provide adequate supervision to ensure that the structure is satisfactorily completed. It is also important that an engineer be familiar with the various techniques of construction and their limitations because this will certainly influence his thinking in planning as well as in analysis and design.

The cost of construction, for instance, is affected by the availability of materials and skilled labor trained for the work at the location of the structure. Hence, an ideal structure for one locality may not be the best solution in another situation. The techniques of construction also have direct effects in analysis and design. One of the most striking examples is the computation of erection stresses for a long-span bridge. During construction, a part of the structure first erected may sometimes be used to support derricks and other construction equipment for the erection of an adjacent unit. The stresses in the members of the partially completed structure may exceed those in the completed structure under the most severe loading condition. It is imperative, therefore, to design the structure properly to withstand the expected loads at various stages of construction. This also applies to falsework and formwork used in construction.

The foregoing discussion clearly indicates the importance of an integrated knowledge of structural engineering in order to obtain the best possible solution of a structural problem. Inasmuch as engineering is an art, it cannot be completely replaced by an exact science. Engineers have learned to rely more and more on the methodology of science but they cannot entirely dispense with judgment. Paradoxically, a good understanding of the basic principles in structural mechanics can often lead to a better appreciation of the actual behavior of structures if the mathematical analysis is kept in proper perspective and proportion. Intuitive perception and insight are invaluable but not infallible. Hence, judgment based on experience must be tempered by rational analysis. A proper balance of theoretical preparation and practicality based on a sense of judgment is essential to a successful structural engineer.

During the short time available for undergraduate study, however, emphasis can be placed only on basic principles that cannot be readily acquired in practice. On the other hand, the details of design and construction can best be learned in the design office and field, where experience

is the teacher. Because of the general emphasis on theory rather than practice in most courses of study, students are urged to broaden their outlook by outside reading, field trips, and subsequent practice. Related references are given at the end of each chapter of this book.

1-2 *Structural Mechanics*

Structural mechanics is the branch of mechanics that deals with forces and motions of structural systems. It is a continuation and extension in application of the mechanics of rigid and deformable solids. The basic principles of mechanics will be briefly reviewed and developed as needed, but the main emphasis will be placed on the rational application of these principles to the analysis of structures.

In the remainder of this chapter we shall further discuss the factors influencing the idealization and simplification of the structural system. At present, however, let us consider how the principles of mechanics are applied to the formulation of a structural problem. Since structural mechanics deals with forces and motions of structural systems, it is necessary to study the forces, the motions, and the relation between them.

Force is an interaction between systems or between different parts of an isolated system. The former is referred to as the *external force* and the

Courtesy of Ammann & Whitney, Consulting Engineers

Civic Auditorium, Pittsburgh, Pennsylvania. The retractable dome has a maximum diameter of 417 ft and a rise of 109 ft. It is supported by a cantilever curved space frame outside of the structure.

latter as the *internal force* for the specific system under consideration. Each individual force is characterized by (a) its magnitude, (b) its vector direction, i.e., the sense as well as the direction, and (c) its point of application, which, combined with the direction, gives the line of action of the force. *Motion* indicates a displacement that, in general, is a function of time. Two types of motion are important in structural mechanics: one is the over-all change in position or *rigid-body movement* of the system, and the other is the displacement due to change in shape or *deformation* of the system. The first type of motion with respect to time involves velocity and acceleration, which can be related to the force causing the motion by Newton's laws of motion. The second type of motion, i.e., deformation or time rate of deformation, is related to the applied force and is a function of the material characteristics of the system.

The general principles involved in the formulation of a structural problem are so broad that they may be applied to any continuous medium or *continuum*. However, we shall confine ourselves here to a more limited scope of study, with only occasional reference to the unified principles. First, let us consider a perfectly rigid system completely constrained and subjected to stationary loads. Since no motion of any kind is involved, we are only concerned with the forces in the system. According to Newton's first law of motion, there must be no unbalanced external force when the system is at rest. In other words, the external forces acting on the isolated system are in a state of *static equilibrium*. These external forces include the expected loads and the resisting forces at the constraints or supporting points known as *reactions*. By the application of Newton's third law of motion, the resultant of the reactions is equal and opposite to the resultant of the loads.

Next let us consider a deformable system that is also properly constrained and subjected to stationary loads. In this case, the only possible motion that may occur is the deformation of the system under loads. We must consider the condition of equilibrium of forces as before but, in addition, we must consider deformations and the relation between forces and deformations. In studying the geometry of the system, we note that the deformations of the individual parts must be consistent with the over-all deformation. This is known as the *condition of continuity* or the *compatibility condition*. In relating the forces to the deformations, we take into account the special properties of the specific materials involved in the system, such as *elasticity*, *plasticity*, and so forth.

If a perfectly rigid system is supported on springs and subjected to dynamic loads, the problem becomes one involving force and motion. For motions at small velocities compared with the velocity of light, the force acting on a particle is proportional to the acceleration of the particle, according to Newton's second law of motion. The resultant of all forces that

act on a particle having a mass and an acceleration is called the *effective force*, which has a magnitude equal to the product of the mass and the acceleration and a direction that is the same as that of the acceleration. A force equal to this resultant but of opposite sense is called the *reversed effective force* or the *inertia force*. Using d'Alembert's principle, which states that the resultant of the effective forces for all the particles of a body, if reversed and assumed to act on the body with external forces, will hold the body in equilibrium, we can apply to the system its inertia forces and put the system in *dynamic equilibrium*. This allows us to write *equations of motion* as *equilibrium equations*.

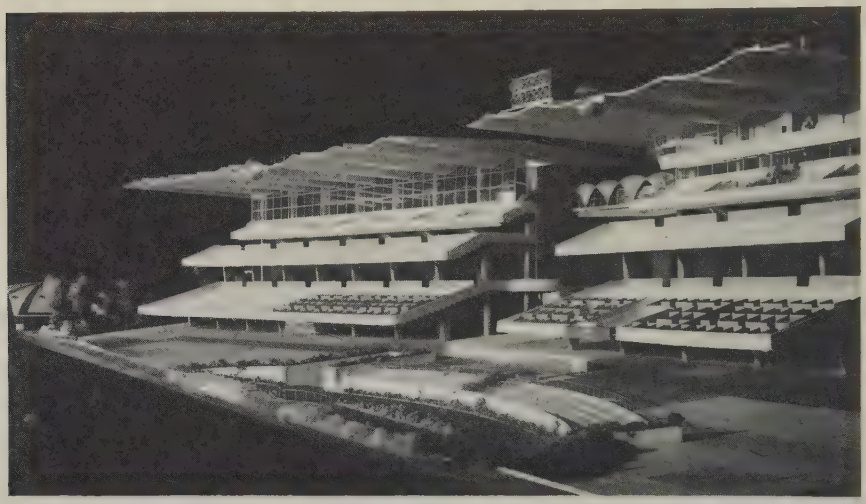

Courtesy of Arthur Froelich, Architect, Henry Layne, Structural Engineer, and T. Y. Lin, consultant on prestressed roof

Model of Hipodromo Nacional, Caracas, Venezuela. The thin-shell cantilever roofs over the grandstands are constructed of prestressed concrete. They are 100 ft above the ground floor and extend 90 ft from the supporting columns.

For a deformable system under dynamic loads, the situation is much more complicated, but the same principles may be applied. We consider the conditions of dynamic equilibrium or the equations of motion, we take into account the geometry of the system, and finally we relate the forces to the deformations according to the properties of materials.

Students who have had an introductory course in fluid mechanics should have no trouble in recognizing these steps. Although its medium of transmission is different, fluid mechanics also deals with forces, motions, and fluid properties relating forces and motions. In fluid mechanics the equations of motion are often formulated by the principle of *conservation of momentum*. The continuity condition can be obtained from the principle of *conservation*

of matter. The relation between forces and deformations is expressed by properties such as *viscosity* and *compressibility* of fluids. Since all solids and fluids are usually treated as a continuum in engineering mechanics, this parallel in approach is not surprising. The student should observe and compare such similarities at every possible opportunity.

In addition to the basic principles already cited, there is another important principle that deals with the *conservation of energy*. This principle is widely used in both solid and fluid mechanics and is the foundation of many special energy theorems that we shall encounter in structural mechanics. By using the energy theorems we can also derive the requirements of equilibrium and compatibility of a structural system. This alternative approach is very valuable, especially for more complex problems.

1-3 Structural Forms

The selection of a suitable structural form for a given situation is one of the most important steps in structural analysis. New structural forms are developed constantly to satisfy ever-increasing needs. Buildings, bridges, towers, hangars, and the like represent but a few of the manifestations of diversified structural forms. The development of structural forms is also influenced by the properties of new materials. Thin shell structures, for example, have become popular in recent years because reinforced concrete can be utilized more efficiently in this type of structure than in framed structures. High-strength steels with large ductility have made possible many new applications in bridge design. Included in this chapter are photographs of several modern structures that illustrate the use of different structural forms for different purposes.

From the point of view of efficiency, the structural forms may be classified into two broad categories: the *uniform stress* form and the *varying stress* form. In the former every element is subjected to a uniform stress. Thus, if the stress at a point of the structure becomes critical, the stresses in all parts of the structure will be critical. In the latter nonuniform stress distribution prevails. As a result, even if the stresses at certain points of the structure approach the critical value, the stresses in other parts of the same structure may still be much below the critical value. It is obvious that the uniform stress form makes more efficient use of the material.

Strictly speaking, no real structural form or member has uniform stress throughout because in reality the edges or ends of the member are so fastened that stress concentrations are introduced at such locations. However, this does not alter the fact that the state of uniform stress exists in the member at distances removed from the regions near fastened edges or ends. Such a conclusion is based on *Saint-Venant's principle*, which states that if the forces acting on a small portion of the surface of an elastic body are replaced

by another statically equivalent system of forces at the same portion of the surface, this redistribution of loading produces substantial changes in stresses locally but has a negligible effect on the stresses at distances that are large in comparison with the linear dimensions of the surface on which the forces are changed.* Thus, the practical utility of the concept of uniform stress is unimpaired.

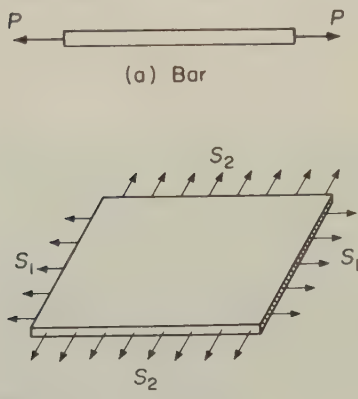

Figure 1–1

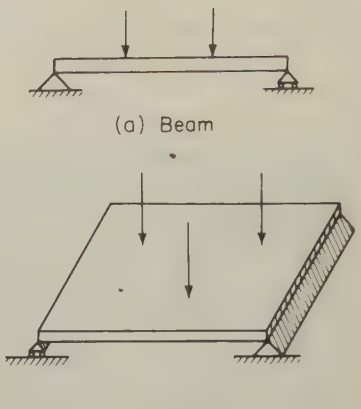

Figure 1–2

The simplest example of the uniform stress form is a member subjected to an axial force. Fig. 1-1(a) shows a bar of uniform cross section that is acted on by a tensile force distributed uniformly over the cross section. The state of stress at every point of the bar, therefore, is uniaxial tension. Fig. 1-1(b) shows a plate of uniform thickness that is acted on by tensile forces S_1 and S_2 distributed uniformly over the respective parallel edges of the plate. Then, the state of stress at every point of the plate is biaxial tension.

When a slender member is supported and loaded laterally, as shown in Fig. 1-2(a), it is subjected to shear and bending and is called a *beam*. Under such circumstances, the shearing and bending stresses vary from point to point at a cross section as well as along the length of the member. If a plate is supported and loaded laterally, in general it will be subjected to shear, bending, and twisting, and is called a *slab*. Again, the stresses due to shear, bending, and twisting vary from point to point along the width as well as along the length of the slab.

For flexible structural forms which can resist neither compression, shear, nor bending, only tensile forces will result in the system even if lateral forces

*See, for instance, p. 33 of Reference 1-4.

are applied. In this case, the magnitude and location of the applied forces dictate the shape of the flexible structure. For example, consider a cable subjected to vertical loads uniformly distributed along the horizontal span of the cable. It can be demonstrated that the cable takes the shape of a parabola, as shown in Fig. 1-3(a). Since the slope of the cable varies and the *horizontal component* of the tension in the cable remains constant along its

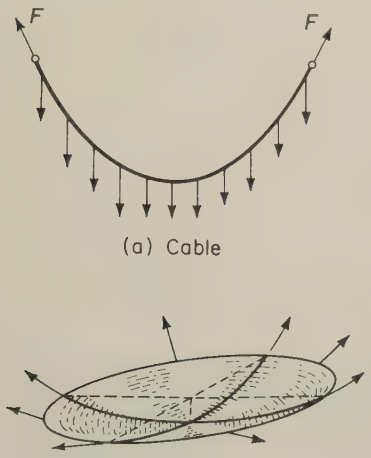

Figure 1–3

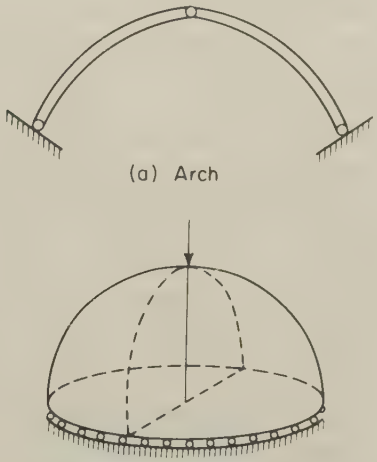

Figure 1–4

length, the tensile force along the cable varies from point to point along its length. However, the distribution of this tensile force at a particular cross section is uniform owing to the absence of shear and bending, and, theoretically at least, the state of stress can be made uniform throughout the entire length if the cross-sectional area of the cable varies in the same proportion as the tensile force acting on it. The cable may, therefore, be considered as a *pseudo-uniform* stress form. Similarly, a circular membrane subjected to a uniform pressure, as shown in Fig. 1-3(b), will be stretched like a balloon. In general, however, the tensile stresses in the membrane are not uniform because the inflated shape may be any surface of revolution. The membrane therefore represents a pseudo-uniform stress form and the tensile stresses are called *membrane stresses*. In the special case of a spherical surface, the membrane stresses are uniform in all directions.

On the other hand, inflexible curved structural forms that are properly constrained may also be subjected to direct stresses only under certain loading conditions. Fig. 1-4(a) shows a parabolic arch with three hinges. If the vertical loads are uniformly distributed along the horizontal span of the arch, the arch will be subjected only to an axial compressive force, usually

called *thrust*, along its curved length. For any other loading, shear and bending as well as thrust exist at a section normal to the axis of the arch. Thus, the parabolic arch acts as a pseudo-uniform stress form under one loading condition and becomes a varying stress form under other loading conditions. Similarly, only membrane stresses exist in a shell of revolution whose bottom edge is completely unrestrained and on which the loading is axisymmetrical, as shown in Fig. 1-4(b). If the bottom edge of the shell is fixed or otherwise restrained, however, the structure will be subjected to shear and bending as well as membrane stresses. Again, this structure acts as a pseudo-uniform stress form for one edge condition and becomes a varying stress form for another edge condition.

Uniform stress forms of structures can be built up from a number of uniform stress elements. Pin-connected trusses are typical examples. Fig. 1-5(a) shows a plane truss subjected to external loads. However, each of the

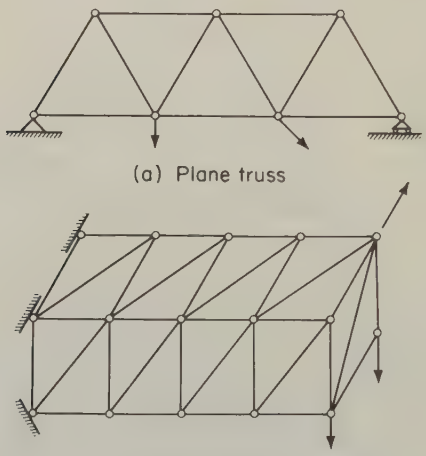

(a) Plane truss

(b) Space truss

Figure 1–5

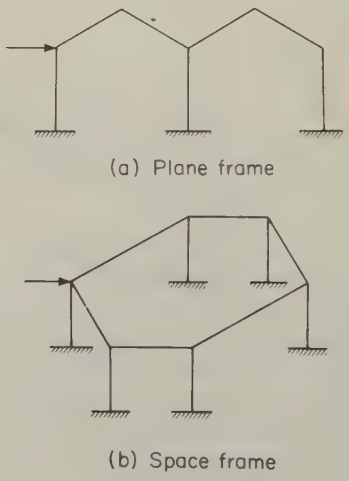

(a) Plane frame

(b) Space frame

Figure 1–6

members in the truss is subjected to a uniform stress even though the truss as a whole tends to bend under the action of the loads. Fig. 1-5(b) shows a space truss which is subjected to twisting as well as bending. Nevertheless, the stress in each member is uniform.

Quite frequently, the efficiency of varying stress members may be improved by reducing the bending at the critical section while increasing the bending in other parts of the same member. This concept leads to the development of rigid frames in which the bending effects in the center part of its members are reduced owing to the presence of the rigid joints that resist bending. Fig. 1-6(a) indicates a rigid frame with all elements lying in the same plane, and Fig. 1-6(b) shows a rigid frame in space. In the

former the members of the frame are subjected to axial force, shear, and bending only, but in the latter the members of the frame are also subjected to twisting.

1-4 Idealization of Structural Systems

Actual structures exist in three dimensions and generally consist of an assembly of intricate elements and connections. In order to effectively analyze such structures, it is convenient to break up the structure into component parts of manageable order and to convert these parts into conceptual models. Because of such simplifying assumptions, the results of analysis should be subjected to judicious interpretations.

In order to compare results of theoretical analysis with the behavior of the actual structure, we rely on experience or experiment. For conventional structures we can exercise our judgment based on experience. On the other hand, unusual structures for which no previous experience is available will require experiment. The latter approach underlines the importance of research in an ever-expanding industrial world in which we are confronted with many problems and situations that are completely new and unexplored.

A general principle for idealizing a structure is that, whenever possible, the actual three-dimensional structure should be reduced to component two-dimensional systems because the techniques of analyzing three-dimensional structures are rather complicated. Of course, there are structures for which the variation of stresses and strains in three dimensions is

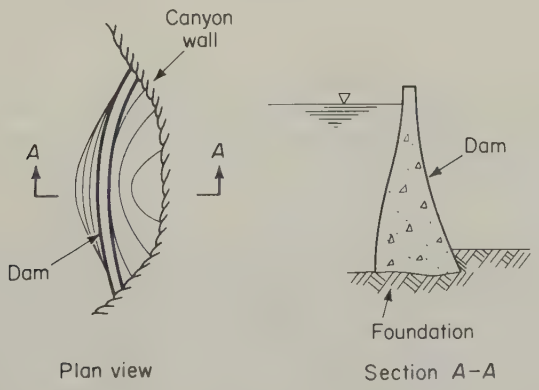

Figure 1–7

important and that cannot be reduced to simpler systems. Consider, for example, the arch dam shown in Fig. 1-7. This structure transmits the upstream hydrostatic pressure to the canyon wall by arch action as well as to the foundation by cantilever action. Thus, the state of stress at

any point in the dam must be treated as a three-dimensional problem in elasticity.*

However, a reasonable simplification may be accomplished for thin structural systems of uniform thickness, such as the plate shown in Fig. 1-8(a),

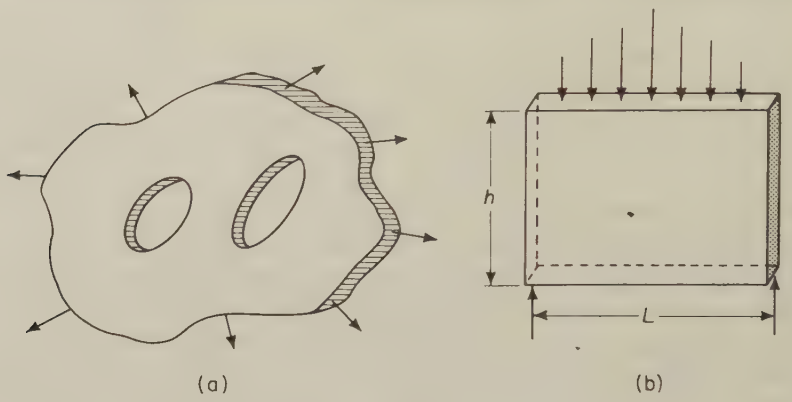

Figure 1–8

for which the external forces applied at the edges are distributed uniformly over the thickness. Since no force is acting in the direction transverse to the plate, it may be assumed that the stress components in that direction are zero and the stress components in directions parallel to the faces of the plate do not vary through the thickness. Problems such as this are called *plane stress* problems. An example of a plane stress problem is a deep beam as shown in Fig. 1-8(b). On the other hand, a similar simplification is possible for long structures, such as retaining walls, culverts, tunnels, and so forth, for which the applied forces as well as the shape of the cross section do not vary along the length. In such cases, it may be assumed that the end sections are confined between two fixed rigid planes such that the displace-

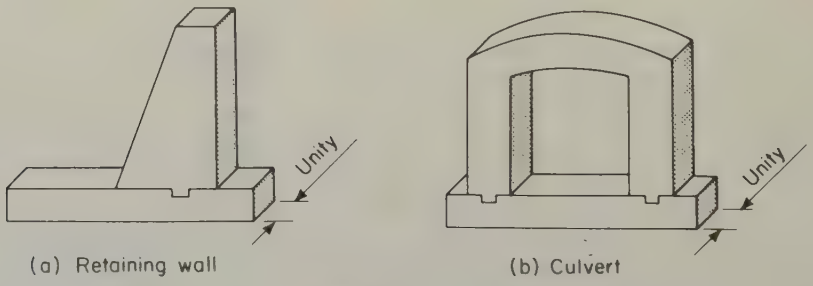

Figure 1–9

*See, for example, pp. 245–257 of Reference 1-4.

ment and hence the strain in the long direction is prevented. Since all cross sections are in the same condition in regard to loading and geometry of the cross section, it is necessary to consider only a slice between two sections at a unit distance apart, as shown in Fig. 1-9. Problems of this type are called *plane strain* problems. It can be demonstrated that the plane strain problem, like the plane stress problem, reduces to the determination of stress components in two dimensions only.*

There are other structures in the form of surfaces whose thickness, although not necessarily uniform, is small in comparison with the other two dimensions, but the applied forces in general do not lie in the middle surface. The middle surface is that surface that everywhere bisects the thickness of the element. This group of structures can be further classified into two categories: slabs and shells.† In the case of slabs, i.e., flat plates subjected to lateral loads, a satisfactory approximate theory may be developed by neglecting the normal stresses in the direction transverse to the middle surface of the plate. For thin shells, i.e., curved surfaces whose thicknesses are small in comparison with their radii of curvature as well as with the other dimensions, the bending stresses are usually small and the stresses due to strains in the middle surface are more important except in the vicinity of restrained edges. If the edge conditions of a shell are such that bending can be neglected, the problem is greatly simplified. The theory of shells based on the omission of bending stresses is called the *membrane theory*.

Structures may also consist of slender members, not necessarily of uniform cross section, whose length is large in comparison with the other two dimensions, but the applied forces may vary along the length of the member. Cables, arches, beams, frames, and trusses belong to this category. Although cables, arches, and beams are generally classified as two-dimensional systems, frames and trusses may be either two-dimensional or three-dimensional.

Two-dimensional structures are by far the most common systems encountered in structural analysis. In this introductory text we shall deal primarily with two-dimensional systems consisting of slender members, with occasional reference to three-dimensional frames and trusses. We shall therefore consider a few conventional structures and examine how they are idealized in the light of experience. Fig. 1-10(a) illustrates a through-truss railroad bridge. The structure may be separated into several structural units: the main trusses, the lateral bracing systems, and the floor framing. The main trusses are designed primarily to carry vertical loads that are transmitted to the trusses through the floor framing (stringers and floor beams). The portal frame, the top chord bracings, and the bottom chord bracings are designed to resist the horizontal or lateral forces and are known

*See, for instance, pp. 11–130 of Reference 1-4.

†See, for instance, Reference 1-5 for detailed discussions.

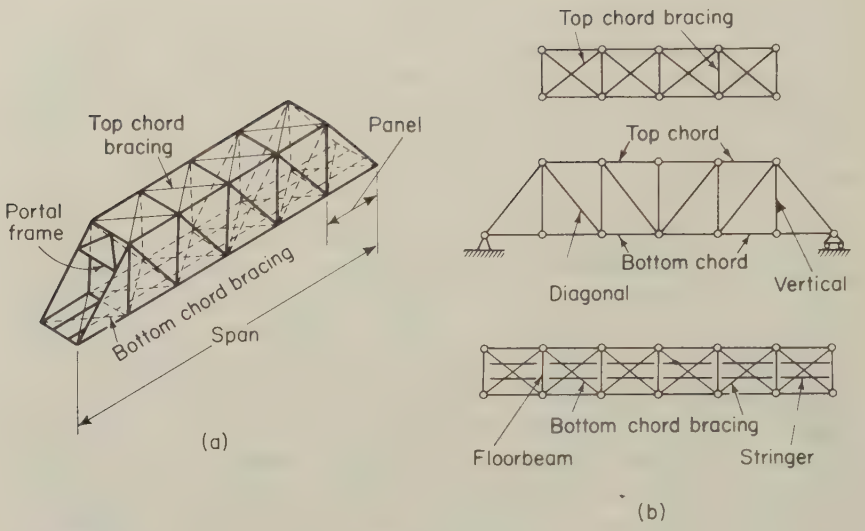

Figure 1–10

as *lateral bracing systems*. In addition to transmitting floor loads to the joints of the trusses, the floor beams also act as part of the bottom chord bracing. Fig. 1-10(b) shows the idealized plane truss, the analysis of which is usually based on the following assumptions:

1. The members of the truss are connected together by smooth pins at their ends.

2. The weight of the truss as well as the imposed loads and reactions will act only at the joints.

3. The members are straight.

The first assumption can be well justified if the members consist of eyebars with pin-connected joints. Even then, the pins are not perfectly smooth, and rough pins lead to friction between the pin and the eyebar. In modern practice, the connections are usually riveted, bolted or welded to gusset plates. Furthermore, the top and bottom chords of the truss usually are made up of members continuous over several panels instead of shorter members connected at the joints. However, errors due to neglect of these end restraints are usually not serious, and the secondary effects due to restraint at the joints can be evaluated later if greater refinement is necessary. The second assumption is usually valid for imposed loads since the floor beams are connected to the bottom chords of the trusses at the joints. For all practical purposes, the weight of the truss can be apportioned as loads at the joints of the truss; the error due to such practice is small. The third assumption implies that no bending exists in any member of the truss.

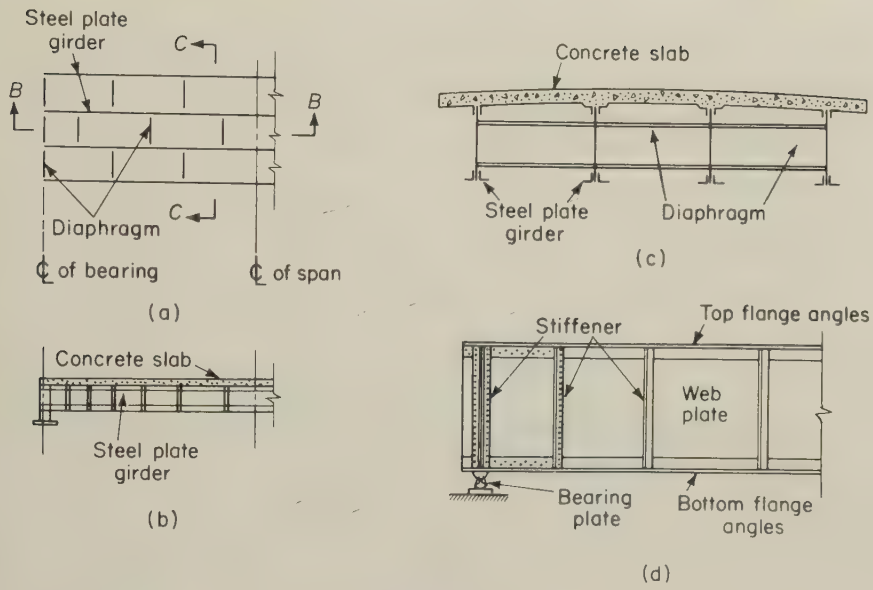

Figure 1–11

Fig. 1-11(a) shows the framing plan of a highway bridge deck, the longitudinal and transverse sections of which are shown in Fig. 1-11(b) and 1-11(c), respectively. (Note that Fig. 1-11(c) is drawn in a different scale.) The concrete deck is considered as a separate unit if no adequate bond is provided between the concrete slab and the steel plate girders. On the other hand, if suitable devices are used to ensure the bonding of the concrete to the steel, the floor system can be designed as a composite unit. The idealized model in this case is a group of simply supported beams subjected to vertical loads, whereas the diaphragm bracings are counted on to resist horizontal or lateral forces. The analysis of the system based on the elementary theory of flexure involves the following approximations:

1. The girder is straight and prismatic, and its cross section has at least one axis of symmetry.

2. The loads are applied along the axis of symmetry of the girder section.

3. The girder is adequately braced and stiffened to avoid buckling in the flange or the web of the girder.

The first two assumptions can be easily justified. In order to justify the third assumption, we count on the concrete slab to guard against lateral buckling of the top flange as indicated in Fig. 1-11(c) and add vertical stiffeners as shown in Fig. 1-11(d) to prevent buckling of the web of the girder. The diaphragms shown in Fig. 1-11(a) and (c) are provided to

maintain alignment of the girders and lateral transmission of loads, thus permitting even distribution of deformation. If the girder is continuous over two or more spans, however, the diaphragms will also serve the purpose of providing lateral supports against buckling of the bottom flange of the girder.

A suspended bridge can also be divided into component parts by separating the main span from the side spans as shown in Fig. 1-12. Since the cable

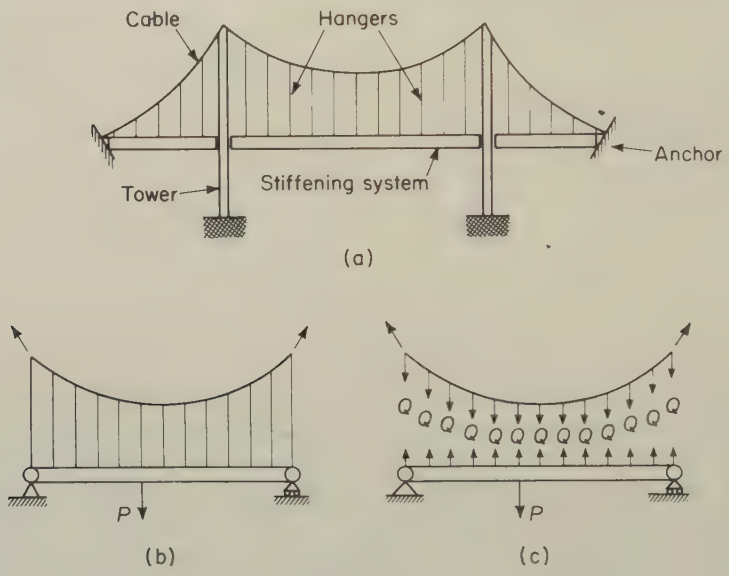

Figure 1–12

is flexible, a stiffening system is tied to the traffic deck so that the cable will not change shape while a load is moving on the bridge. The stiffening system may be a girder or a truss known as a *stiffening girder* or *stiffening truss*, as the case may be. The cable and the stiffening system for the main span can be isolated as shown in Fig. 1-12(c). In idealizing the structure, the following assumptions are usually made:

1. If the load is uniformly distributed along the horizontal span, such as the weight of the floor system, it will be carried entirely by the cable.

2. If the load on the bridge is not uniform, as in the case of moving vehicles, it will be distributed among the hangers through the stiffening system, which may be a girder or a truss.

3. Since the hangers are closely and uniformly spaced and the hanger loads are approximately equal, the shape of the cable may be assumed to be parabolic.

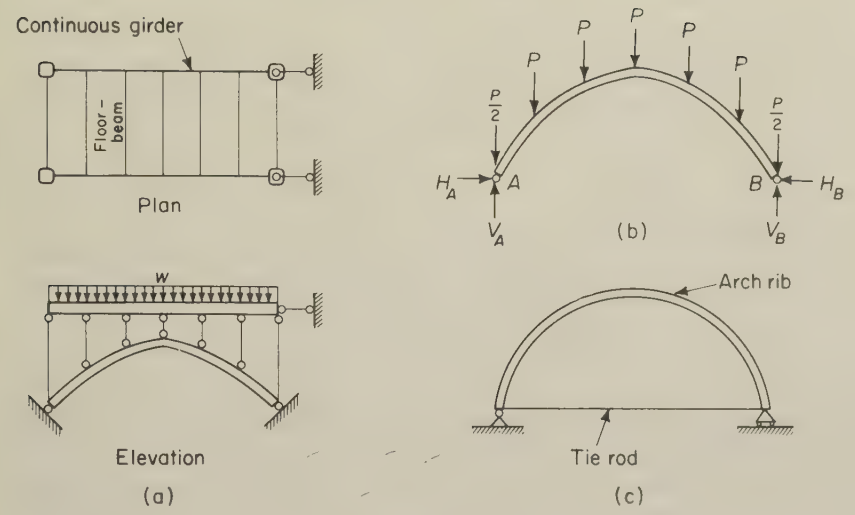

Figure 1–13

Fig. 1-13 shows an arch bridge in which the main girders are continuous over the vertical supports and are prevented from horizontal movement by the links at the right end of the girders. If the joints at the ends of the vertical posts are assumed to be pin-connected, the girders can be analyzed as continuous beams with multiple supports. Thus, the uniform load shown in Fig. 1-13(a) will eventually be transmitted to the arch rib through the vertical posts, and the resulting concentrated loads acting on the arch rib may be represented by Fig. 1-13(b).

Another important characteristic of an arch is that there will be horizontal components of reactions at supports as a result of the arch action—even if all applied loads are vertical. Hence, we can take full advantage of an arch structure only if the foundation is such that it offers resistance to horizontal thrust. Occasionally, however, especially in the design of arch roofs, the horizontal thrust at the supports of the arch are provided by a tie-rod as shown in Fig. 1-13(c). In actual construction the tie-rod is either hidden below the floor or above the ceiling in a building, but the necessity for its existence should not escape the attention of the student.

Consider next a typical framing plan for a steel-framed office building, as shown in Fig. 1-14(a). The idealized model of the girder at the center of the framing plan is given in Fig. 1-14(b). Since the girder is assumed to be simply supported, the connection from girder to column shown in Fig. 1-14(c) is designed to transmit only the vertical reaction of the girder. The end restraint of the connection for rotation is negligibly small. In cases where such a simplification is not assumed, the end of the girder may be subjected to a moment and the connection must be designed accord-

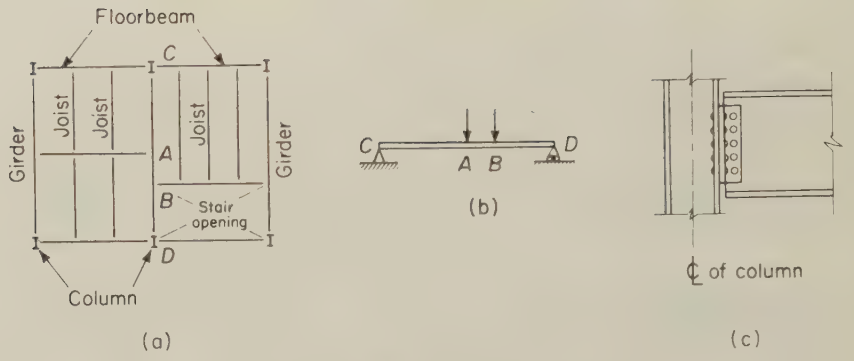

Figure 1–14

ingly. A similar situation exists for the gable frames supporting the roof of the mill building shown in Fig. 1-15(a). The conceptual model of the gable frame shown in Fig. 1-15(b) is assumed to have fixed supports because the ends of the columns are embedded in heavy concrete footings. Since large deformation of the frame is undesirable, the joints connecting the members of the frame are made to be as rigid as possible, permitting practically no *relative* rotation between connecting members at the joints. Fig. 1-15(c) illustrates a welded connection of this type. Frames consisting only of rigid connections between members are called *rigid frames.*

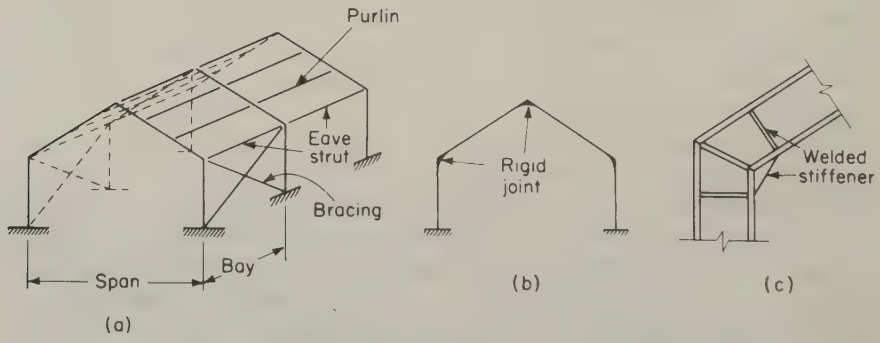

Figure 1–15

In actual practice, a perfectly rigid joint is difficult to attain. Therefore, it is desirable in some instances to use semirigid connections. The percentage of rigidity assumed in such connections is a matter the designer must decide according to his judgment.

In determining the span length of an idealized beam or frame, there is always the question of whether the distance from centerline to centerline of columns or the clear dimension should be used. Similarly, the same problem arises in determining the column height between floors. In general,

the distance from centerline to centerline is considered sufficiently accurate for analysis. If further refinement is necessary, modifications may be made later, as is often done in the analysis of continuous frames.

1-5 Loads on Structures

Because of the wide variation in the nature of loads on structures, a detailed discussion of such loads is beyond the scope of this book. However, the sources of such loads can be classified broadly into two major categories: the *body forces* and the *surface forces*. Forces distributed over the body of a structure, such as gravitational forces, magnetic forces, or inertia forces, are called body forces. Forces distributed over the surface of a structure, such as traffic loads, hydrostatic pressure, or wind pressure, are called surface forces. From another point of view, these forces may be classified as *static loads* and *dynamic loads*. The former includes forces that are either stationary, such as the weight of the structure, or movable, such as furniture or people in a building. The latter refers to forces which either produce dynamic effects on a structure, such as traffic and wind pressure, or are associated with the motion of the structure, such as earthquake forces on a building or the inertia forces on an airplane during flight. In order to simplify the analysis, we often attempt to approximate the effects of dynamic loads by the use of *equivalent* static loads. In this introductory text we shall confine our discussion to static loads and equivalent static loads only.

Even within this scope, however, the determination of loads on structures is not a simple matter. We must consider first of all the magnitude, location, and distribution of loads that may act on a structure. However, from the standpoint of design, we must be ready to answer several other questions. For instance, what are the combinations of loads that will have the most severe effect? What is the likelihood or probability of the occurrence of such combinations? Should a structure be designed to resist the worst possible loads that may occur only a few times during its life of service, or to support loads under normal conditions? These questions belong to the realm of structural safety and will be discussed in Section 1-6.

The intensities of static loads and equivalent static loads that must be imposed on a structure for design purposes may be found in the design specifications recommended by various national organizations and local authorities.* The nature and occurrence of these loads are briefly described here.

Dead loads. The weight of the basic frame of a structure and other immovable parts attached to it is called *dead load*. Although the actual weight of a structure can be accurately computed only after the sizes of all

*See, for instance, the specifications listed in Section 1-7.

structural members are determined, the dead loads must be estimated for the purpose of analysis at a very early stage. It may be observed that the ratio of dead load to total load on a structure is an important factor in influencing the dead load calculation. In short-span structures, for example, such a ratio is small and the dead load is relatively unimportant. Then, a reasonably good estimate of the dead weight is usually sufficient. For long-span structures, however, such a ratio is relatively large and the dead load becomes predominant. Hence, an accurate appraisal of the actual weight of the structure becomes necessary. In order to facilitate the work of estimating dead load for long-span structures, numerous empirical formulas have been proposed for roof trusses and bridges made of various materials. However, the formulas should be used only as a guide for preliminary analysis. After the completion of the design, it is good practice to check the actual weight of the structure against the estimated dead load and make proper adjustments or revisions if the discrepancy is substantial.

Example 1-1. A roof is supported by steel trusses that are spaced at 20-ft intervals. The dimensions of each truss are shown in Fig. 1-16. An empirical relation for the dead load representative of average conditions, say 50-ft to 100-ft span, is given by*

$$w = 0.75(1 + 0.1L)$$

in which w is the weight of the truss in pounds per square foot of horizontal projection of the roof and L is the span in feet.

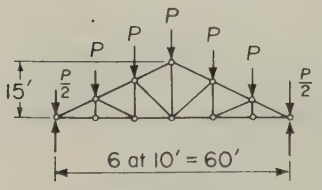

Figure 1-16

Since the roof load is transmitted through the purlins to the joints of roof trusses, the roof area contributing to a typical interior panel point has a horizontal projection equal to the product of the bay length and the span length divided by the number of panels. The panel load may then be obtained by multiplying the intensity of the weight of the truss by this projection. Thus,

$$w = 0.75\,[1 + (0.1)(60)] = 5.25 \text{ psf}$$

$$P = (5.25)\,(20)\,(60/6) = 1{,}050 \text{ lb.}$$

Live loads. Broadly speaking, all loads that are movable or moving are called *live loads.* In a narrower sense, however, the term is usually reserved for gravity loads of that nature excluding the dynamic effects due to vibratory motion or other causes. The dynamic effects are usually taken into

*See, for instance, p. 402 of Reference 1-17 for formulas for estimating weights of roof trusses.

consideration by an *impact factor*, which is the percentage increase in weight over the same load at rest. Thus, the equivalent static load in this case is equal to the stationary vertical load times the sum of one plus the impact factor. The external *horizontal loads* are usually referred to as *lateral* or *longitudinal* forces, depending on the direction of the force with respect to the structure. Horizontal loads may be caused by wind or hydrostatic pressure, or by the acceleration or swaying motion of the moving vehicles. Some of these forces are dynamic in nature but are often replaced by equivalent static loads. We shall now discuss more fully some different types of live loads that are frequently encountered.

Movable loads for buildings. Floor loads such as people, furniture, and merchandise are usually considered to be uniformly distributed except for floor areas with special arrangements of equipment consisting of large concentrated loads. The intensity of the floor loads varies according to the type of occupancy for which the floor area is designed. Because of the random distribution of the actual loads on building floors, the maximum uniform floor load tends to decrease with increase in the floor area under consideration. Thus, the uniform design load on a small floor area supported by a joist may be greater than the uniform load on a neighboring girder supporting a large floor area. Similarly, in multistoried buildings, maximum floor loads are not expected to be placed on all floors simultaneously. A column at a lower level of the building is not likely to carry the full loads from all floors above it. Most building codes permit the reduction of uniform floor load on a member as the number of floors supported by the column increases.

Moving loads for bridges. Motor vehicles on highway bridges and locomotives and rolling stock on railroad bridges are included in this category. Because of the wide variations in the distribution of highway traffic, it is expedient to adopt a rational loading pattern for highway bridges. The American Association of State Highway Officials (AASHO) specifies that either standard truck loads or lane loads should be used. The *standard truck load* shall be either a two-axle truck or a tractor truck with semitrailer. The corresponding *lane loading* shall consist of a uniform load per linear foot of traffic lane combined with a single concentrated load (or two concentrated loads in the case of continuous spans), so placed on the span as to produce maximum effect. The wheel spacing, weight distribution, and clearance of the standard trucks and the corresponding lane loads are given by the AASHO in the *Standard Specifications for Highway Bridges*. Shown in Fig. 1-17 is an example of weight distribution of a standard truck in which v may vary from

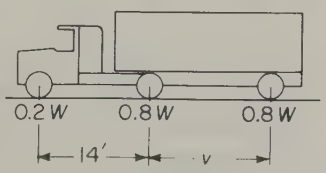

Figure 1–17

14 to 30 ft. The loading is designated as H20, H15, or H10, corresponding to W = 20 tons, 15 tons, or 10 tons. The *train loading* on railroad bridges recommended by the American Railway Engineering Association (AREA) is a series of wheel loads representing two locomotives followed by a uniform load corresponding to the weight of the cars. The loading, usually known as *Cooper's loading*, was developed by Theodore Cooper for steam locomotives. As an example, a train load represented by Cooper's E-60 loading is shown in Fig. 1-18. Other Cooper's loadings, such as E-50 and E-72, have the same spacings for the axle loads but are respectively 50/60 and

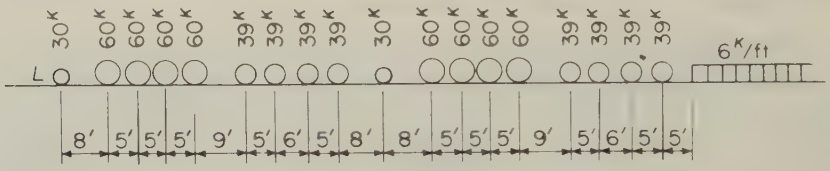

Figure 1–18

72/60 times the weights of the axles and the uniform load. In recent years, many other loadings (such as Steinman loadings) have been proposed to simulate diesel-engine locomotives more accurately. However, loadings based on steam locomotives remain in use because they are heavier and may accommodate possible future increase in design loads.

Impact. The impact factors for highway and railroad bridges in current specifications are empirical. The impact factor I, in fraction or per cent of live load, is usually expressed solely as a function of span length L in feet. For highway bridges, the impact factor is specified as a fraction of the live load by AASHO as follows:

$$I = \frac{50}{L + 125} \qquad \text{(maximum 30 per cent)}$$

For railroad bridges, different impact factors are suggested by AREA for different types of locomotives as well as different types of structures. The impact factors representing the direct vertical effect of steam locomotives are given in per cent as follows:

1. For beams, stringers, girders, floor beams:

   For L less than 100 ft: $I = 60 - \dfrac{L^2}{500}$

   For L = 100 ft or more: $I = \dfrac{1{,}800}{L - 40} + 10$

2. For truss spans: $I = \dfrac{4{,}000}{L + 25} + 15$

Extensive research investigations are currently being conducted to correlate various factors that influence the impact on highway and railroad bridges. It is expected that such investigations will lead to more realistic approaches for impact computations in the near future.

Example 1-2. For a plate-girder bridge of 120-ft span, determine the impact factor according to (1) AASHO specifications and (2) AREA specifications.

1. $I = \dfrac{50}{120 + 125} = 0.204$ or 20.4 per cent

2. $I = \dfrac{1{,}800}{120 - 40} + 10 = 22.5 + 10 = 32.5$ per cent

Horizontal forces. Inertia forces resulting from the acceleration or deceleration of vehicles in the direction of motion are called *longitudinal forces*. These forces act through the centers of gravity of the vehicles and are transmitted to the bridge deck. Forces transverse to the direction of motion of vehicles caused by wind on moving vehicles or on the bridge are called *transverse forces*. For bridges supporting curved roadways or tracks, the *centrifugal forces* should also be considered. All these horizontal forces lead to unbalanced tipping forces on the substructure supporting the bridge deck and are usually specified in bridge design specifications. Horizontal forces are also produced by moving cranes on crane runways and should be included in the design of crane runway girders.

Snow loads. The weight of snow on building roofs may be treated as vertical live load whose magnitude, of course, depends on the climate of the locality. For flat roofs, the full weight of the snow should be used in design; for pitched roofs the intensity may be reduced. Snow is seldom considered in the design of bridges since a heavy snowfall would either slow the speed of the traffic and reduce the impact on the bridge or make the bridge impassable.

Wind loads. The actions of wind on structures represent rather complicated aerodynamic phenomena that involve the velocity of wind and the orientation, area, and shape of structures and structural elements. In this connection, let us consider briefly the theory of two-dimensional flow,* i.e., flow around a body of infinite length that has a uniform cross section, as shown in Fig. 1-19. When the air stream is obstructed, it exerts a force on the body that may be resolved into two components, one along the direction of the velocity, called *drag*, and the other at right angles to it,

*See, for instance, pp. 163–182 of Reference 1-6.

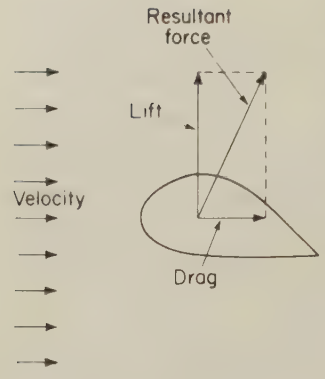

Figure 1–19

called *lift*. Thus, the force exerted by air on the body depends on the *relative* velocity between the body and the air. The theory can also be applied to flow around bodies of finite length. Hence, the analysis is equally applicable to airplanes as well as to buildings and bridges.

The drag may be caused by the skin friction or by the pressure difference over the surface of the body. It is customary to express the total drag P as follows:

$$P = AC_d \frac{\rho V^2}{2}$$

in which A is the projected area normal to the direction of the wind, C_d is known as the *drag coefficient*, and $\rho V^2/2$ is called the *dynamic pressure*, which is a function of the mass density ρ of air and the velocity V of wind. At sea level, air weighs approximately 0.0765 lb per cu ft at 60°F. If V denotes the velocity of wind in *mph*, the average wind pressure p in *psf* is equal to

$$p = \frac{P}{A} = C_d(0.00256V^2)$$

The drag coefficient is a function of Reynolds number, which is the dimensionless ratio of inertia force to viscous force of the air and is equal to

$$N_R = \frac{\rho VL}{\mu}$$

in which L is the characteristic length of the body, V is the characteristic velocity, μ is the viscosity, and ρ is the mass density of the air. In some ranges of Reynolds number, the drag coefficient is practically constant, but in other ranges it varies with the velocity. The drag coefficients for various surfaces and structural shapes may be found in the final report of a task committee of the American Society of Civil Engineers.*

The wind pressure on an inclined surface may be related to that acting on a vertical surface. The average wind pressure p_n normal to an inclined surface that has an angle of inclination θ with a horizontal plane may be expressed in terms of the horizontal wind pressure p by a formula suggested by Duchemin:†

$$p_n = p \frac{2 \sin \theta}{1 + \sin^2 \theta}$$

*See Reference 1-7.

†See, for example, p. 403 of Reference 1-17.

For enclosed structures such as conventional buildings, the wind pressure on a plane surface normal to the direction of the wind may be treated as equivalent static load because the relationship between the time variation of the wind and the natural frequency of the structure is such as to cause essentially static response. However, the wind may not only exert positive pressure on the windward side but may also create negative pressure or suction on the leeward side of a building, as shown in Fig. 1-20. It is recommended by the task committee of the American Society of Civil Engineers that, for tall buildings with plane vertical surfaces normal to wind, the following approximate relation may be used:

$$p = 0.0033V^2$$

This pressure represents the total combined force on the outside of the windward and leeward vertical surfaces. According to this formula, a pressure of 20 psf corresponds to a wind velocity of 77.8 mph.

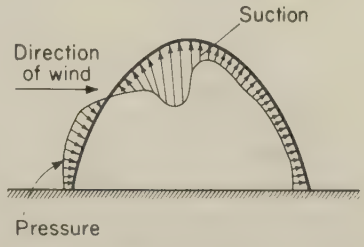

Figure 1-20

For buildings with pitched roofs spanning over large areas, such as hangars, auditoriums, or mill buildings, the pressure on the windward side and that on the leeward side of the roof should be treated separately. In the case of roofs with round surfaces, the suction may appear even on the windward side. For roofs with sharp corners, the pattern of eddy formation at the corners greatly influences the pressure at various points of the surface. The situation is further complicated by the fact that most of the buildings are not airtight, and the leakage through small openings in the building walls may give rise to internal pressure or internal suction on the roof, depending on the side of the building at which the leakage occurs. Recommendations concerning wind pressure on buildings may be found in the final report of the task committee of the American Society of Civil Engineers.*

Example 1-3. A billboard 30 ft by 30 ft is placed at an angle of inclination of 45 degrees and is supported by two trusses at the inclined edges. The wind pressure on the billboard is transmitted through horizontal members to the joints of the trusses as shown in Fig. 1-21. Determine the panel loads normal to the inclined surface due to a horizontal wind pressure of 25 psf.

$$p_n = \frac{(25)\,(2)\,(0.707)}{1 + (0.707)^2} = 23.6 \text{ psf}$$

$$P = p_n A = (23.6)(30/2)(5) = 1{,}766 \text{ lb}$$

*See Reference 1-7 for further discussion.

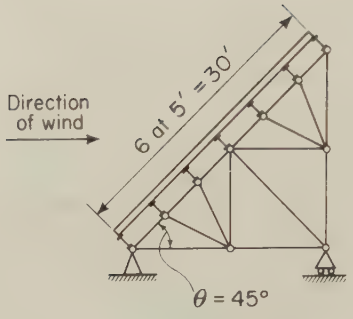

Figure 1–21

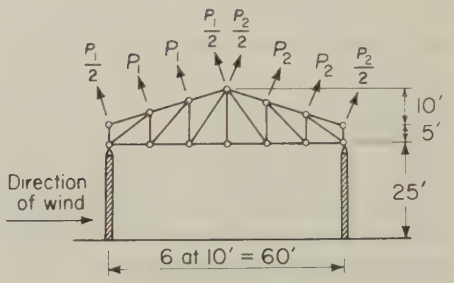

Figure 1–22

Example 1-4. A normally airtight mill building with pitched roof as shown in Fig. 1-22 has a bay length of 20 ft. The external wind force causes negative pressure (suction) almost everywhere except on the vertical wall on the windward side. Positive internal pressure may be caused by leakage in the vertical wall on the windward side, and negative internal pressure may result from leakage in the vertical wall on the leeward side. For the given truss, a suction of 12 psf for the windward slope and a suction of 9 psf for the leeward slope are recommended. Furthermore, a positive or negative internal wind pressure of 4.5 psf normal to the roof is assumed. Compute loads P_1 and P_2 in Fig. 1-22 based on a combination of:

1. external suction and positive internal pressure.
2. external suction and negative internal pressure.

The inclined length of one side of the pitched roof is

$$\sqrt{(30)^2 + (10)^2} = 31.6 \text{ ft}$$

Then, the area contributing to each panel load is

$$(20)\,(31.6/3) = 211 \text{ ft}^2$$

1. $P_1 = (12 + 4.5)\,(211) = 3{,}467$ lb
   $P_2 = (\ 9 + 4.5)\,(211) = 2{,}843$ lb
2. $P_1 = (12 - 4.5)\,(211) = 1{,}577$ lb
   $P_2 = (\ 9 - 4.5)\,(211) = \ \ 947$ lb

For long slender structures, such as suspension bridges, smokestacks, and electric power transmission wires, the possibility of oscillation under the action of wind is always present for the reason that, when the air flows around a slender body, there is an eddying wake behind the body which produces a periodic alternating force acting on the body normal to the direction of the undisturbed flow. The vibration of structures under such an

influence may be classified into two categories: the "aeolian" vibration with a relatively small amplitude and high frequency, and the "galloping" vibration with a relatively large amplitude and low frequency.

The aeolian vibration is caused by the formation of eddies breaking alternately on each side of an obstacle in a periodic manner, as shown in

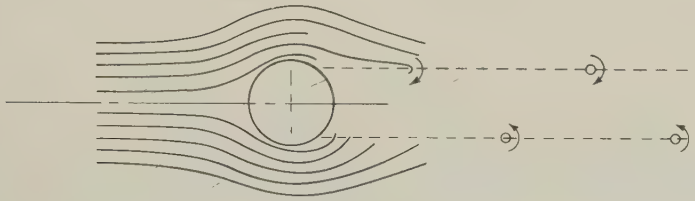

Figure 1–23

Fig. 1-23. Such a pattern of eddy formation is known as the *Karman vortex trail.* It is difficult to correlate the Karman vortex trail formation with Reynolds number, but there is evidence to indicate that the vortex trail is formed only in a certain velocity range for a particular type of body. For example, the vortex trail may be formed in the range of wind velocity from 15 mph to 40 mph for a circular cylinder, and in the range of 2 mph to 6 mph for some unsymmetrical sections. Thus, the danger of oscillation is not associated with extremely high wind velocity. Steel smokestacks have been observed to sway violently in a direction perpendicular to that of the wind at a wind velocity of 40 mph or less, and the situation may be remedied by the introduction of guy wires. Electrical transmission lines and telephone wires are known to vibrate under the action of a lateral wind of considerable strength, but such vibrations can be relieved by friction dampers. Musical tones are produced in the vibration of wires having a high frequency, and from such phenomena the name "aeolian" vibration is derived.

The galloping vibration is the result of the *aerodynamic instability* of the cross section of certain slender members. In such cases, the lift as well as the drag on the member may cause rotational vibration. This type of vibration is said to be *self-excited* because the alternating force that sustains the motion is created by the motion itself. Since the dramatic failure of the Tacoma Narrows bridge in 1940, there has been considerable study of the aerodynamic stability of structures. Although the theory is too complex to be introduced in this text, the student must be aware of the pitfalls in the design of this type of structure.*

Earthquake motions. The behavior of structures in earthquakes has generally been recognized as a dynamic vibration phenomenon of à transient

*See, for example, pp. 366–377 of Reference 1-8 for further discussion.

nature. Although an earthquake causes vertical as well as horizontal movements, the vertical component of acceleration is usually neglected. The response of a structure to an earthquake depends on a great number of factors, such as the acceleration patterns of the ground motion and the natural period of vibration of the structure. The effects of these and other factors on the behavior of structures in earthquakes are still under intensive study at the present time.

The ground accelerations may be recorded on accelerographs, which indicate the applied accelerations as functions of time. According to a joint committee report of the San Francisco Section of American Society of Civil Engineers and the Structural Engineers Association of Northern California,* the existing ground motion records seem to indicate that the peak acceleration periods of minor and moderate earthquakes in the United States are in the range of 0.1 to 0.3 seconds. The accelerations produced by explosive shocks also exhibit the predominance of such short periods of vibration. If the fundamental period of natural vibration of a structural system lies in the range of dominant earthquake acceleration periods, the structure will produce a great response or resonance. When the natural period of the system is remote from the range, its response will be small. A rational method for establishing the design forces on a structure has been suggested by the above-mentioned joint committee. This method involves the determination of the total lateral force or the base shear transmitted to the structure from the ground, and the distribution of that shear as equivalent forces applied to the structure.

The base shear for a structure subjected to ground motion varies with time in an irregular manner, depending on the irregular nature of the acceleration pattern. The absolute maximum base shear that will develop in an idealized structural system of period T during a certain earthquake is called the *spectral value* of the base shear. Let $\bar{a}$ be defined as the spectral acceleration, or the intensity of the earthquake corresponding to the absolute maximum base shear for the period T. Then, from Newton's second law of motion, the maximum base shear or total lateral force F is given by

$$F = \frac{W}{g}\bar{a} = \frac{\bar{a}}{g}W = CW$$

in which W is the weight of the structure, g is the gravitational acceleration, and $C = \bar{a}/g$ is a dimensionless coefficient depending on T. If a number of values of a is determined for varying periods T, and if $\bar{a}$ is plotted against T, the resulting curve represents the characteristic of the specific earthquake and is called the *acceleration spectrum* of the earthquake. For a real structure, the lateral force coefficient C is also influenced by the effects of damping,

*See Reference 1-9 for details.

tilting, slipping, and other factors that tend to reduce the shear transmitted from the ground. It is recommended by the joint committee that this coefficient be selected between the limits of maximum $C = 0.06$ and minimum $C = 0.02$ for the periods T as follows:

$$C = 0.06 \quad \text{for} \quad T \leqslant 0.25 \text{ sec}$$

$$C = \frac{0.015}{T} \quad \text{for} \quad 0.25 < T < 0.75 \text{ sec}$$

$$C = 0.02 \quad \text{for} \quad T \geqslant 0.75 \text{ sec}$$

The weight W of the structure should be the probable load existent at the time of the earthquake. For the design of buildings, it may be defined as the total weight of the structure above the base including all dead load plus 50 per cent of the design live load for storage and warehouse floors, 25 per cent of the design live load for all other floors, and no live load for roofs. For structures other than buildings, W is defined as dead load plus normal operating live loads.

The distribution of the base shear as equivalent lateral forces on the structure depends on the lateral deflections of the structure. For structures having uniform weight per unit height, the distribution may be approximated by a triangular loading, zero at the base and twice the average lateral load at the top. A general form of distribution of the total lateral force that permits variable distribution of masses of the structure is suggested by the joint committee as follows:

$$F_x = F \left[\frac{w_x h_x}{\sum (wh)} \right]$$

in which F_x is the lateral force at any level of a structure, w_x is the weight of the structure at that level, h_x is the height of that level above the base, and the summation term represents the sum of products of w and h at all levels. For uniform weight per unit height, this formula reduces to a triangular lateral loading.

Example 1-5. A two-story building as shown in Fig. 1-24 is designed to withstand a total lateral earthquake force $F = 0.05W$, where W is the weight of the building including all dead load plus 25 per cent of live load for all floors and no live load for the roof. If w_1 ,w_2, and w_3 denote the prescribed weights on the first floor, second floor, and roof of the building respectively, then $W = w_1 + w_2 + w_3$. Let h_1, h_2, and h_3 be the heights of the mass centers at first floor, second floor, and roof level from the base of the structure, and F_1, F_2, and F_3 be the lateral forces applied at the mass center of these floors respectively. Then, the total force $F = F_1 + F_2 + F_3$,

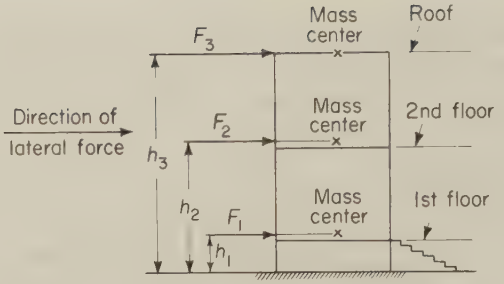

Figure 1–24

and the distribution of the lateral force F at various levels may be computed in accordance with the following formula:

$$F_x = \frac{Fw_xh_x}{(w_1h_1 + w_2h_2 + w_3h_3)}$$

in which the subscript x may denote 1, 2, and 3, referring to first floor, second floor, and roof level, respectively. If $w_1 = 300$ kips, $w_2 = 250$ kips, and $w_3 = 150$ kips, and $h_1 = 4$ ft, $h_2 = 16$ ft, and $h_3 = 28$ ft, compute F_1, F_2, and F_3.

$$W = w_1 + w_2 + w_3 = 300 + 250 + 150 = 700 \text{ kips}$$
$$F = 0.05W = (0.05)(700) = 35 \text{ kips}$$

$$w_1h_1 = (300)(4) = 1{,}200$$
$$w_2h_2 = (250)(16) = 4{,}000$$
$$w_3h_3 = (150)(28) = 4{,}200$$
$$\text{Total} = 9{,}400 \text{ ft-kips}$$

$$F_1 = \frac{(35)(1{,}200)}{9{,}400} = 4.5 \text{ kips}$$

$$F_2 = \frac{(35)(4{,}000)}{9{,}400} = 14.9 \text{ kips}$$

$$F_3 = \frac{(35)(4{,}200)}{9{,}400} = 15.6 \text{ kips}$$

Note the distribution of lateral forces at various levels of the building, as indicated by F_1, F_2, and F_3.

Blast loads. A structure may be subjected to a strong pressure that radiates from the center of a violent explosion, such as occurs during a nuclear blast.* Very shortly after the detonation, the pressure wave advances

*See, for instance, Reference 1-10.

to a neighboring point and almost instantaneously increases its pressure from atmospheric to that of the wave front, which is many times in excess of the atmospheric pressure, depending on the distance from the center of explosion. The pressure at the wave front is called the frontal or peak *overpressure*. The advancing wave is called the *shock wave*, which drops to atmospheric pressure very rapidly after the wave front passes and leaves a trailing strong wind. When the shock wave is obstructed by a structure in its path, the pressure in the wave is increased owing to reflection but the reflected overpressure drops off rapidly as the shock wave moves on. This is followed by the trailing wind that creates a drag as it passes the structure. Although the phenomenon is dynamic in nature, a design procedure essentially based on equivalent static loading has been proposed.* A more detailed analysis of structural response to blast loads can be made by considering the system as a dynamic problem.

Since the dynamic effects on structures involve mass, displacement, velocity, acceleration, and energy in the system, we must base our preliminary analysis on an assumed structure with characteristics sufficiently similar to the final structure. By using equivalent static loads and other simplified concepts, a reasonable structure may be selected without too many complications. If this is done intelligently, further dynamic analysis will be only a process of confirming the preliminary choice of the structure. Thus, analysis based on equivalent static loads has its place in structural design but it also has its limitations. If we are not aware of all the important factors in a situation, we cannot properly provide for variation and generalization in those factors. For this reason, the use of equivalent static load concepts for dynamic problems must be rather judicious.

1-6 Serviceability and Safety of Structures

The final test of a well-designed engineering structure lies in its serviceability and safety. Serviceability requires that the structure be free from excessive deformation or vibration under loads, and safety is characterized by the structural resistance against failure or the ultimate load-carrying capacity of the structure. A satisfactory design for serviceability will usually result in adequate safety if the relation between load and deformation is linear. When the load-deformation relation is nonlinear, an adequate design for one does not assure a satisfactory answer for the other.

Let us illustrate this point by means of two simple examples. Fig. 1-25(a) shows a structural steel member subjected to an axial tensile load P. The load-deformation relation of the member is represented by the curve in Fig. 1-25(b), which shows the elastic range OA, the plastic region AB, the

*See References 1-11 and 1-18.

work-hardening zone BC, and the point of rupture D. The member will be in serviceable condition if the actual load in the member does not exceed the yield load P_y, and it will fail in rupture only if the actual load in the member reaches the ultimate load P_u. For a load P_1 corresponding to point E in the elastic portion of the curve, the member is safe and in serviceable condition. On the other hand, for a load P_2 corresponding to point F in the work-hardening region of the curve, the member may no longer be in serviceable condition because of large deformations but may still be safe

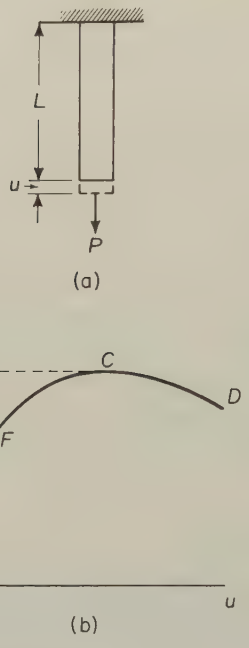

Figure 1–25

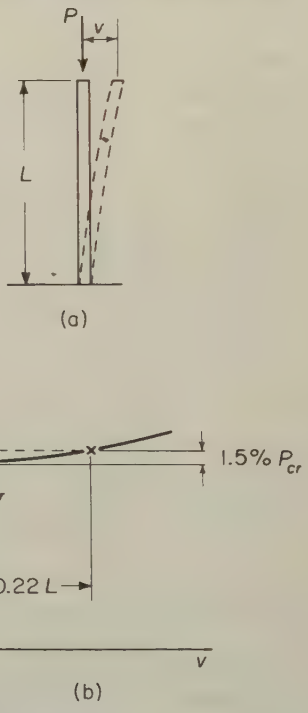

Figure 1–26

in the sense that rupture is not impending. Fig. 1-26(a) shows an ideal long compression member subjected to an axial compressive load P. If the force P is very small, the member will be slightly compressed but will remain straight. In addition to the axial force P, if a very small lateral force is applied at the free end and then removed, the member will return to its original straight position. As the load P is increased, a magnitude will be reached such that the member will not return to its initial position if a small lateral force is applied and then released. This load is called the critical load P_{cr}. It is possible to determine the relation between load and lateral deflection beyond the critical load by using an exact differential relationship

for curvature.* It has been found that, if the axial load is increased by 1.5 per cent, the lateral deflection will equal 22 per cent of the length of the member, as shown by the load-deflection relation in Fig. 1-26(b). If the actual load in such a member is P_3, which is slightly below P_{cr}, the member is in serviceable condition but not safe since a slight increase in load may cause uncontrollable lateral deflection. Although the example cited here is an ideal or perfect member, similar arguments may be applied to real members.

From the standpoint of analysis, to which the greater part of this book is devoted, we are concerned only with choosing a mode of behavior of the structure that will cause either unserviceability or failure so that we can analyze it. From the standpoint of design, however, the problem is interwoven with many intricate factors that are not immediately obvious. Many of these are skillfully hidden in the design codes and specifications or completely by-passed by these codes so that we are not fully aware of their significance. We shall bring these factors to light by further examining the criteria for serviceability and safety of structures.

In order to satisfy both criteria, a structure must be so designed that it has sufficient strength and suffers no excessive deformation. Although the elastic strength of a structure is limited by the yielding of the material, its ultimate load-carrying capacity may be characterized by one of the following modes of behavior:

1. *Plastic deformation of ductile materials.* For structural members of ductile materials such as mild steel, large plastic deformation with increasing load-carrying capacity precedes rupture, as can be visualized from the stress-strain relation in Fig. 1-25(b). In such a case, usually the appearance of excessive deformation will give sufficient warning of the impending danger. Furthermore, the ultimate collapse loads on a structure may be predicted by the method of plastic analysis. Thus, this type of failure may be prevented by the removal of the overload or by temporary shoring.

2. *Buckling of compression members.* Large lateral deflection may result from the buckling of a compression member, as indicated by the load-deflection relationship of Fig. 1-26(b). Since the deflection appears suddenly at the critical load, this mode of failure usually occurs rather abruptly. Buckling may also occur locally, such as in the outstanding flange or web of an I-section or in the lattice lacings of built-up compression members such as those shown in Fig. 1-27. For long slender members subjected to compression, buckling may occur even if the stresses in the entire member are below the proportional limit of the material. Such a phenomenon is called *elastic buckling*. If part of the compression member

*See p. 72 of Reference 1-12.

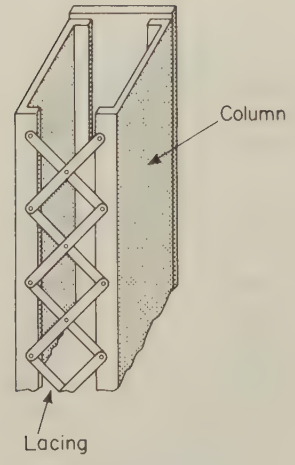

Figure 1–27

is stressed beyond the proportional limit in the process of developing a large lateral deflection, it is called *plastic buckling*. Thus, a compression member must be designed against elastic and plastic buckling.

3. *Brittle fracture under static loads.* For brittle materials such as concrete, rupture may occur without apparent deformation. Hence, it is a good practice to proportion reinforced concrete beams so that the ultimate strength of the beam is governed by the yielding of the reinforcing steel rather than by crushing or diagonal tension in concrete. Even for normally ductile materials, brittle fracture may occur as a result of a combination of adverse factors such as low temperature, combined tensile stresses, or cracks of critical size in the material. Many metals exhibit a range of transition temperature under which the material becomes susceptible to brittle fracture. This is especially true if a flaw is present in the area where the state of stress is biaxial or triaxial. Once a crack is formed near the flaw, it propagates rapidly and a brittle fracture occurs in the member. Extensive research is presently in progress to study the exact cause of crack formations and methods to arrest them. There has been some success in arresting these cracks for specific types of structural members but, generally speaking, no sure method has been discovered for preventing their formation.

4. *Fatigue fracture under dynamic repeated loads.* When a structural member is subjected to a large number of cycles of loading and unloading, rupture may occur at a stress level considerably lower than the ultimate strength of the material under static load. Since repeated loads are usually applied to the structure by dynamic means, such as locomotives or machinery that produces unbalanced driving forces, the dynamic effect should be separated from the effect arising from repeated loads. The former is classified as *impact*, whereas the latter is known as *fatigue*. For reinforced concrete structures, there is some evidence that the bond and shear strengths of concrete may be considerably reduced after a relatively small number of cycles of reversal of stress. On the other hand, steel structures are found to be unaffected, except at welded joints, geometry changes, and flaws, by relatively large number of cycles of loading and unloading for the type of moving loads that normally travel on bridges. However, steel members may suffer fatigue failure if severe vibration is present. Even plastic fatigue is possible in the case of aeolian vibration of transmission lines.

From the study of these modes of failure, it is obvious that elastic strength alone does not always give a complete picture of either the safety or serviceability of a structure. Whenever the situation indicates that this is the case, we must safeguard against other possibilities of failure or unserviceability.

The factor of safety plays a very important role in this regard. In order to ensure elasticity in a structure, the maximum stress permitted in any part of the structure under expected loads must be below the yield stress of the material by a certain margin. If the term *factor of serviceability* is defined as the ratio of yield stress to allowable stress, then the *margin of serviceability* equals this ratio minus one. Even if the actual load on the structure is slightly greater than the expected load, the structure will still behave elastically as long as the maximum stress in the structure does not exceed the yield stress. If the overload is so large that the structure begins to deform plastically, there is still no imminent danger of failure since ductility and work-hardening properties of the material provide reserve strength that cannot be predicted by the elastic analysis. On the other hand, structures designed for a criterion of ultimate load-carrying capacity usually carry only a fraction of the ultimate load under operating or service conditions. The ratio of ultimate load to operating load is called the *load factor* or *factor of safety*. However, the term "factor of safety" is commonly used in a broader sense to mean either load factor or factor of serviceability. By adopting a generous load factor, the structure will behave elastically under operating conditions although the maximum stress in the structure under such conditions cannot readily be obtained. Thus, one approach can be used to obtain the elastic behavior of the structure under operating conditions but not to predict its ultimate load-carrying capacity. The other approach will lead to the ultimate load-carrying capacity of the structure without considering its elastic behavior.

These two concepts of design are by no means contradictory. As a matter of fact, such dichotomy leads to a more sophisticated philosophy of design. In the light of different design criteria, it is possible to consider the loading conditions on structures more intelligently. For instance, the analysis of a structure under ordinary operating loads may be based on the elastic criterion, but the same structure under some possible but highly improbable loads or combinations of loads may be analyzed on the basis of the plastic criterion. In other words, a structure is expected to be serviceable under normal loading conditions, but under unusual circumstances of disastrous nature, such as earthquakes or blasts of a highly improbable magnitude, it may be sufficient to design the structure to survive imminent danger of collapse without concern for large deformation. Hence, the serviceability and load factors can be adjusted for the situation.

This leads to the important question of how to determine the factor of safety. In practice, the factor of safety usually represents a rather elusive

compromise between safety and economy based on past experience and judgment. It does not provide maximum efficiency or economy consistent with adequate safety. The structural significance of a specified condition can only be evaluated by the application of the theory of probability. In 1935, Hardy Cross remarked on the subject of structural failures in these words:

> Particularly we may wish to investigate the probability of such things happening, for engineers must always ask what rate of insurance they are willing to pay against failure. The whole field of probability of occurrence is inadequately treated in any formal way in present literature. It is, however, a question which must have some investigation in all cases where analysis is to be used as a basis for design. It is at the root of all factor-of-safety determinations.*

Since then, some progress has been made in this direction,† but a great deal of work remains to be done in order to develop more rationally based design specifications in which operating conditions and structural actions are integrated with the probability of their occurrence. This is a task of considerable urgency that requires more and better research in virtually every phase of structural analysis and design.

1-7 Design Specifications

Many national organizations as well as local authorities assume the responsibility for public safety by recommending specifications and requirements for design. These recommendations are based on the best evidence and judgment currently available and are revised periodically to keep up with the latest research and development. Some of the specifications most frequently encountered by civil engineers are listed below:

1. *American Standard Building Code*, National Bureau of Standards, Department of Commerce.
2. *Uniform Building Code*, International Conference of Building Officials (Subsidiary of Pacific Coast Conference of Building Officials).
3. *Specifications for the Design Fabrication and Erection of Structural Steel for Buildings*, American Institute of Steel Construction (AISC).
4. *Building Code Requirements for Reinforced Concrete*, American Concrete Institute (ACI).
5. *Aluminum Construction Manual*, The Aluminum Association.
6. *National Design Specification for Stress-Grade Lumber and Its Fastenings*, National Lumber Manufacturers Association.
7. *Standard Specifications for Highway Bridges*, The American Association of State Highway Officials (AASHO).
8. *Specifications for Steel Railway Bridges*, American Railway Association (AREA).
9. *Standards*, American Society for Testing Materials (ASTM).

*See Reference 1-13.
†See Reference 1-14, through 1-16.

It is difficult for the student to realize the importance of the role of design specifications. Actually, many major decisions, including the nature and magnitude of applied loads, the properties of materials, the factors of safety, the design criteria, and sometimes even the methods of analysis, are dictated by the specifications. The student should acquire some of these specifications and investigate the reasoning behind these requirements. He should learn to reach his own decisions as his experience grows and should never be content to follow blindly the provisions of the specifications. In actual practice, an engineer is often called upon to solve new problems that lie beyond the scope of existing specifications, and he must decide for himself what the design requirements are under those circumstances—and often he must convince his client.

Since the requirements of design specification affect the serviceability and safety of a structure, we shall illustrate the significance of these requirements by examining a few excerpts from the sections of sample specifications that are directly related to the factors of safety. Usually, such pertinent information may be found in the provisions for allowable stresses or load factors. The excerpts from these provisions are presented here in the order most suitable for the purpose of illustration and are not necessarily quoted verbatim.

Allowable stresses. In the elastic analysis of structures, the total effects of loads on structures are usually expressed in terms of components of stresses (such as normal stresses and shearing stresses) at critical sections of the structure. These stress components must not exceed the limits which are deemed necessary to maintain the safety and serviceability of the structure. Such limits are called *allowable stresses* or *working stresses*. The allowable stresses for elastic design are usually determined by multiplying the respective yield strengths or other appropriate limiting stresses by a suitable coefficient. Then, the factor of serviceability may be defined as the reciprocal of this coefficient and is equal to

$$n = \frac{\text{yield strength or other limiting stress}}{\text{allowable stress in design}}$$

More often than not, however, the factor of serviceability is not explicitly given in the specifications because other considerations are also involved in the determination of the allowable stresses.

As examples, let us consider the allowable stresses for structural steel recommended by the AISC specifications, 1961 edition. Since several grades of steel are permitted for bridge and building construction, the allowable stresses in general are expressed in terms of the respective yield strengths. For the sake of illustration, however, the round-off values in pounds per square inch for structural steel with a yield strength of $F_y = 33{,}000$ psi

(designated as ASTM A-7 steel) as well as the general formulas are given below:

A. Dead load and live load stresses:
   1. Tension—on the net section:
      Except at pin holes: $F_t = 0.60F_y = 20{,}000$
      At pin holes in eyebars: $F_t = 0.45F_y = 15{,}000$
   2. Shear—on the gross section:
      Beam and plate girder webs: $F_v = 0.40F_y = 13{,}000$.
   3. Compression on the gross section of axially loaded compression members having an *effective* unbraced length L and a least radius of gyration r. The ratio L/r is called the *slenderness ratio.*
      (a) When L/r is less than $C_c = \sqrt{2\pi^2 E/F_y} = 131.7$

$$F_a = \left[1 - \frac{(L/r)^2}{2C_c^2}\right]\frac{F_y}{n} \tag{1}$$

where n is the factor of safety and is equal to

$$n = \frac{5}{3} + \frac{3(L/r)}{8C_c} - \frac{(L/r)^3}{8C_c^3}$$

(b) When L/r exceeds C_c,

$$F_a = \frac{149{,}000{,}000}{(L/r)^2} \tag{2}$$

(c) When bracing and secondary members have L/r greater than 120,

$$F_{as} = \frac{F_a}{1.6 - L/200r} \tag{3}$$

where F_a is obtained by formula (1) or (2).

   4. Bending:
      (a) Tension on extreme fibers of ordinary rolled shapes, built-up members, and plate girders except compact sections having an axis of symmetry in the plane of loading for which the allowable stress may be increased: $F_b = 0.60F_y = 20{,}000$
      (b) Compression on extreme fibers of rolled shapes, plate girders, and built-up members having an axis of symmetry in the plane of their web, the larger value computed by formulas (4) and (5), but not more than $F_b = 0.60F_y = 20{,}000$:

$$F_b = \left[1 - \frac{(L/r)^2}{2C_c^2 C_b}\right] 0.60F_y \tag{4}$$

$$F_b = \frac{12{,}000{,}000}{Ld/A_f} \tag{5}$$

where L is the unbraced length of the compression flange, r is the radius of gyration of a tee section comprising the flange and 1/6 of

the web area, about an axis in the plane of the web, A_f is the area of the compression flange, C_c is defined in formula (1), and C_b can conservatively be taken as unity or otherwise computed in accordance with the specifications.

(c) Tension and compression on extreme fibers of large pins:

$$F_b = 0.90F_y = 30{,}000$$

B. Wind and seismic stresses:

Allowable stresses may be increased one-third above the values provided for dead and live loads when they are produced by wind or seismic loading, acting alone or in combination with the design dead and live loads, provided the required section computed on this basis is not less than that required for the design dead and live load and impact (if any), computed without the one-third stress increase, nor less than that required by repeated variation of stress (if it is applicable).

The net section for tension members refers to the net area of the most critical transverse section passing through the rivet holes. The gross area for compression members, on the other hand, refers to the entire transverse section without reductions for rivet holes because well-driven rivets are assumed to be tightly fitted to the holes so that compressive stresses can be transferred through the rivets. The allowable tension on net section except at pin holes is given as $0.60F_y$, thus providing a factor of serviceability of $1/0.60 = 1.67$. On the other hand, the allowable tension on a net section at pin holes in eyebars is $0.45F_y$. This does not mean that a greater margin of serviceability is provided because this reduction of allowable stress takes into consideration the higher stress concentration near the holes in the elastic range of the material as shown by the stress distribution in Fig. 1-28.*

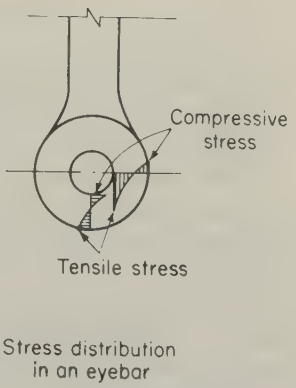

Figure 1–28

Although the yield strength in shear of structural steel has been variously estimated as between one-half and five-eighths of the tensile yield strength, the allowable shearing stress is given as two-thirds the recommended basic tensile stress. This apparent reduction in the factor of serviceability is justified by the minor consequences of shear yielding as compared with those associated with tension and compression yielding, and by the effect of strain hardening.

Although the yield point in compression for steel is substantially the same as yield point in tension, the allowable stresses for compression members

*See p. 122 of Reference 1-4 for details.

are much lower in the specifications for the reason that the buckling of long compression members depends primarily on the slenderness ratio L/r rather than on the compressive stresses. Thus, the allowable stresses are expressed as functions of the ratio L/r. For compression members whose mode of failure is by inelastic buckling, the slenderness ratio corresponding to the upper limit of inelastic buckling may be assumed to be $C_c = \sqrt{2\pi^2 E/F_y}$. Thus, C_c is used as the lower limit of long columns. A varied factor of safety has been applied to the column strength to obtain allowable working stresses. For very short columns, this factor has been taken as equal to or slightly greater than that required for axially loaded tension members. For longer columns, the serviceability factor is increased. Also note the smaller factor of safety assigned to axially loaded secondary members with values of L/r greater than 120 in comparison with the allowable stress for main members with the same L/r values. For example, if $L/r = 200$, the reduction in factor of safety is

$$1.6 - \frac{L}{200r} = 1.6 - 1 = 0.6 ,$$

or 60 per cent of the value accorded to main members.

For rolled beams and built-up girders subjected to bending, the allowable stress for compression flange is also reduced if local buckling is involved. Note also the higher allowable stress accorded to pins in bending because the ultimate flexural strength of members with circular cross sections can be shown to be almost 50 per cent higher than that of I-beams or girders.

Finally, we may note the selection of the combination of loads on a structure. It is required that the structure be designed for the full effects of dead load, live load, and impact, if any. However, if wind and seismic loads are included, the allowable stresses may be increased by one-third. The stresses caused by wind and seismic loads are of temporary duration, and it is unlikely that full live load and full wind and seismic loads would occur at the same time. Hence, a reduction in the factor of serviceability is justified.

Load factors. In plastic design, a structure is so proportioned that it can barely sustain the ultimate loads, which are obtained by multiplying the actual service loads by a load factor. Thus, the load factor K may be defined as follows:

$$K = \frac{\text{ultimate load}}{\text{corresponding service load}}$$

In general, when there is more than one load on the structure, all loads are multiplied by the same factor, as indicated by the example in Fig. 1-29. Because the relationship between loads and deformations in the plastic

range is not linear, the principle of superposition cannot be applied. Hence, all loads on the structure must be in place simultaneously for the analysis.

Consider, for example, the load factors recommended for rigid frame buildings by the AISC Specifications. We have

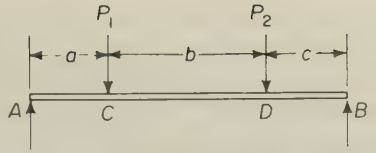

(a) Service load

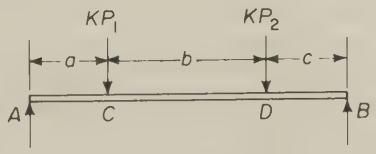

(b) Ultimate load

Figure 1–29

1. For dead and live loads only, $K = 1.85$:

$$U = 1.85(D + L)$$

in which U is the ultimate load and D and L are the expected dead and live loads respectively on the structure.

2. For wind, earthquake, and other forces, $K = 1.40$:

$$U = 1.40(D + L + W + E)$$

in which W represents the wind force and E is the earthquake force, if any, in addition to dead and live loads. Usually, either wind or earthquake force is specified—whichever has more serious effects on the structure.

We may note the relation between the load factors and the combination of loads. The load factor is reduced for the same reasons as in the case of elastic analysis when wind or earthquake forces or both are acting on the structure.

Although a single load factor is often specified as the minimum requirement for each combination of loads, it is possible to assign a different load factor for each type of load in any combination. In the case of dead and live loads only, for example, the ultimate load may be expressed as

$$U = K_1D + K_2L$$

in which K_1 and K_2 are different. As a matter of fact, there are strong reasons for suggesting different load factors for dead load and live load because the degrees of uncertainty of the two types of load are different. In general, the dead load of a structure can be estimated accurately but the live load is much less certain, especially in regard to future overloads. For instance, a warehouse that has been designed for the storage of a certain type of merchandise may be used later for some other purpose. If such a situation is anticipated, a higher load factor may be chosen for the live load.

1-8 Formulation and Solution of Elementary Problems

After discussing various aspects of structural engineering, we shall now summarize our conclusions and define the scope of this book. In general, we shall confine our discussions primarily to the analysis of structural systems made up of slender members such as cables, beams, frames, and trusses that are subjected to static loads or equivalent static loads. We shall emphasize two-dimensional systems although the same principles will occasionally be applied to three-dimensional systems for the sake of illustration.

In a broad sense, the procedure of structural analysis includes the following steps:

1. Recognize the problem.
2. Formulate the problem.
3. Solve the problem.
4. Interpret the solution of the problem judiciously.

Although the first and the last steps depend to a very large extent on judgment based on experience, an effort has been made in this chapter to point out the important factors involved. In the remaining chapters, we shall consider mainly the second and third steps, i.e., the formulation and solution of the problems.

The basic considerations in the formulation of such problems may be outlined as follows:

1. Analyze the forces and the conditions of equilibrium.
2. Study the deformations and the requirements of geometrical compatibility.
3. Establish the force-deformation relations from the properties of materials.

These principles may be applied to formulate a structural problem of any degree of complexity although it is sometimes preferable to tackle more complicated problems by means of the principles of work and energy.

For certain simple systems, however, the reactions and internal forces in the system can be completely analyzed from the conditions of equilibrium. Then, the deformations can be derived from the known internal forces and the given load-deformation characteristics of the material. Such systems are classified as *statically determinate structures*. For other systems, in which the reactions and internal forces cannot be determined from the conditions of equilibrium alone, the requirements of geometrical compatibility and the load-deformation relations will be needed to furnish additional conditions for the complete solution of a problem. These latter systems are

called *statically indeterminate structures*. Although we shall discuss the principles of analysis applicable to all structural systems in general terms, only the detailed applications of these principles to statically determinate structures will be treated here.

In connection with the computation of deformations, we shall primarily be concerned with load-deformation relations that are linear although, in some instances, the same principles are extended to the solution of deformations of members with nonlinear characteristics. Hence, the emphasis will be placed on the elastic method of analysis, with only occasional reference to the plastic method of design.

After the structural problems are formulated, a variety of methods can be used to obtain a solution. In general, a problem presents itself in the form of either a set of algebraic equations or differential equations that can be solved analytically, numerically, or sometimes graphically. Ample numerical examples are given throughout the text to illustrate the applications of basic principles to specific problems.

Although computational techniques are of great importance to structural engineers because of their influence on the choice of methods of structural analysis as well as on the accuracy of numerical solutions and the speed of obtaining them, it is not our purpose here to consider these techniques in great detail. Since high-speed electronic computers have made possible the solution of problems of great complexity, the subject of numerical analysis has become a broad field in itself, and cannot be treated thoroughly in this book.

References

1-1 H. Cross, *Engineers and Ivory Towers*, McGraw-Hill Book Co., Inc., New York, 1952.

1-2 P. L. Nervi, *Structures*, trans. G. and M. Salvadori, F. W. Dodge Corp. New York, 1956

1-3 E. Torroja, *Philosophy of Structures*, English version by J. J. Polivka and M. Polivka, University of California Press, Berkeley and Los Angeles, 1958.

1-4 S. Timoshenko and J. N. Goodier, *Theory of Elasticity*, 2nd ed., McGraw-Hill Book Co., Inc., New York, 1951.

1-5 S. Timoshenko and S. Woinowsky-Krieger, *Theory of Plates and Shells*, 2nd ed., McGraw-Hill Book Co., Inc., New York, 1959.

1-6 R. C. Binder, *Fluid Mechanics*, 4th ed., Prentice-Hall, Inc., Englewood Cliffs, N.J., 1962.

1-7 Final Report of Task Committee on Wind Forces, Structural Division, "Wind Forces on Structures," *Trans. ASCE*, Vol. 126, Part 2, 1961, p. 1124.

1-8 J. P. Den Hartog, *Mechanical Vibrations*, 3rd ed., McGraw-Hill Book Co., Inc., New York, 1947.

1-9 Joint Committee, "Lateral Forces of Earthquake and Wind," *Trans. ASCE*, Vol. 117, 1952, p. 716.

1-10 S. Glasstone, ed., *The Effects of Nuclear Weapons*, Department of Defense, U.S. Government Printing Office, Washington, D.C., 1957.

1-11 N. M. Newmark, "An Engineering Approach to Blast Resistant Design," *Trans. ASCE*, Vol. 121, 1956, p. 45.

1-12 S. Timoshenko and J. M. Gere, *Theory of Elastic Stability*, 2nd ed., McGraw-Hill Book Co., Inc., New York, 1961.

1-13 H. Cross, "Limitations and Applications of Structural Analysis," *Engineering News-Record*, Vol. 115, 1935, p. 535.

1-14 A. M. Freudenthal, "The Safety of Structures," *Trans. ASCE*, Vol. 112, 1947, p. 125.

1-15 A. M. Freudenthal, "Reflections on Standard Specifications for Structural Design," *Trans. ASCE*, Vol. 113, 1948, p. 269.

1-16 A. M. Freudenthal, "Safety and the Probability of Structural Failure," *Trans. ASCE*, Vol. 121, 1956, p. 1337.

1-17 L. C. Urquhart, ed., *Civil Engineering Handbook*, 3rd ed., McGraw-Hill Book Co., Inc., New York, 1950.

1-18 Committee on Structural Dynamics, *Design of Structures to Resist Nuclear Weapons Effects*, ASCE Manual No. 42, 1962.

Problems

1-1 The roof truss shown in Fig. P1-1 is designed to support a uniform snow

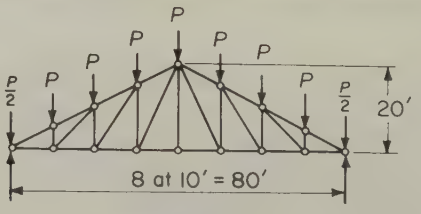

Figure P1–1

load of 40 psf on the horizontal projection of the roof, and the bay length between trusses is 20 ft. In estimating its dead weight, the following empirical formula is suggested:

$$w = \frac{pL}{150 + 5L + ps/3}$$

in which w is the truss weight in pounds per square foot of horizontal projection of the roof, L is the span length of the truss in feet, s is the distance center to center of trusses in feet, and p is the load in pounds per square foot of horizontal projection supported by the roof. If the dead weight of the truss is assumed to act at the joints in the upper chords as shown in Fig. P1-1, determine the magnitude of P caused by the dead weight only.

1-2 For a two-lane highway bridge of 180-ft span as shown in Fig. P1-2,

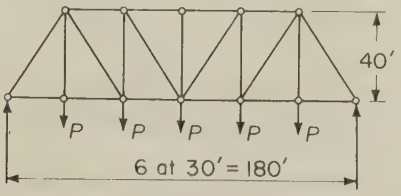

Figure P1–2

it has been suggested that the dead weight of each truss may be estimated by the following formula:

$$w = \frac{L\sqrt{p}}{20} + \frac{L(b - 16)}{10} + 50$$

in which w is the weight of each truss in pounds per linear foot, L is the span length in feet, b is the width of the roadway in feet, and p is the live load on each truss in pounds per linear foot. If the width of the roadway is 22 ft, and the live load may be considered as 1,200 plf on each truss, compute the panel load P due to dead load only.

1-3 For a deck plate-girder railroad bridge with a cross section as shown in

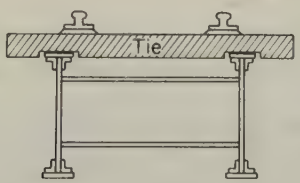

Figure P1–3

Fig. P1-3, it has been suggested that the dead weight of the bridge including girders, stringers, and floor beams may be estimated by the following formula:

$$w = k(12.5L + 100)$$

in which w is the weight of the entire bridge in pounds per linear foot, L is the length of span in feet, and k is a constant depending on the live load. If the span length of the bridge is 200 ft, determine the uniform dead load on each girder for

(a) $k = 1.1$ for Cooper's E-60 loading,
(b) $k = 1.0$ for Cooper's E-50 loading.

1-4 For the six-story building shown in Fig. P1-4, a typical interior column

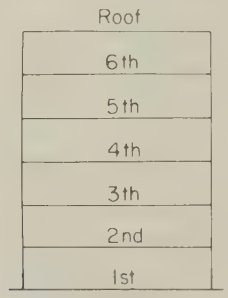

Figure P1–4

supports a floor area of 20 ft by 24 ft on each floor. Assume that the dead weight of the roof is 20 psf and that of all other floors is 40 psf per floor. The snow load on the roof is 30 psf and the movable load on each floor is 60 psf. Determine the load transmitted to the column at a level above the first floor considering only

(a) dead load,
(b) live load with the following reduction:

Floor level	*Per cent of live load used for design*
Roof	100
6th floor	95
5th floor	90
4th floor	85
All other floors	80

1-5 For a truss bridge of 240-ft span, determine the impact factor according to (a) AASHO specifications and (b) AREA specifications.

1-6 A chimney 250 ft high and 15 ft in diameter is subjected to a lateral pressure due to a 60-mph wind. If the drag coefficient $C_d = 0.75$ for chimneys of rough surface, determine the overturning moment at the base of the chimney due to wind.

1-7 For mill buildings with wall openings varying from 0 to 30 per cent of the wall surface, it is recommended that roofs with an angle of inclination of between 20 to 30 degrees be designed for the following wind loads normal to the roof surface:

(a) on the windward slope, an external suction of $p = (36 - 1.2\alpha)$, where α is the angle of inclination in degrees and p is in pounds per square foot;
(b) on the leeward slope, an external suction of 9 psf;
(c) on both slopes, an internal pressure of $p = 4.5 + 0.25n$ or an internal

suction of $p = 4.5 + 0.15n$, where n is the percentage of opening of the wall surface.

Compute the panel loads due to wind on the truss shown in Fig. P1-7, with a

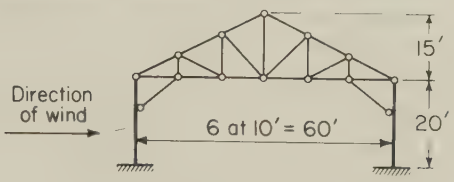

Figure P1–7

bay length between trusses equal to 20 ft, if a 10 per cent opening is assumed for the building.

1-8 For a tall building subjected to earthquake, the lateral force applied at the mass center of each floor may be computed by the formula

$$F_x = CW\left[\frac{w_x h_x}{\sum w_i h_i}\right]$$

in which C is a lateral force coefficient, W is the total weight of the building, w_x is the weight of the floor under consideration, and h_x is the height of the mass center of that floor from the ground level. The summation of $w_i h_i$ is taken from $i = 1$ to $i = n$, which is the total number of floors. If $C = 0.05$, compute the lateral forces at the mass centers of various levels for which w_i and h_i are given as follows:

i (floor level)	w_i, *kips*	h_i, *ft*
1	2,000	2
2	1,500	18
3	1,500	32
4	1,500	46
5	1,500	60
6	1,500	74
7 (roof)	500	88

1-9 The system shown in Fig. P1-9 consists of two bars of 5 sq in. each in

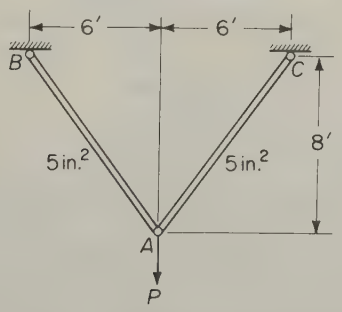

Figure P1–9

cross-sectional area that are pin-connected to support a service load $P = 160$ kips at joint A. If the load P is increased gradually, yielding of the material in both members AB and BC is noticed when P reaches $P_y = 264$ kips, and the maximum ultimate load prior to rupture is found to be 480 kips. What are the serviceability and load factors of the system?

1-10 A steel beam is to be selected to span 20 ft and to support a uniformly distributed load of $w = 3.3$ kips/ft under operating conditions. Three different beam sections that have almost the same section modulus in bending are being considered:

(a) standard wide flange section 18 WF 55,
(b) rectangular bar of 5.9-in width by 10-in depth,
(c) circular bar of 10-in diameter.

It has been found that, if the uniform load w is gradually increased, the extreme fibers at the center of all three beams begin to yield when w reaches $w_y = 5.45$ kips/ft. On the other hand, the three beams begin to exhibit excessive deformation at different loads w_u. For case (a), $w_u = 6.2$ kips/ft, for case (b), $w_u = 8.2$ kips/ft, and for case (c), $w_u = 9.2$ kips/ft. Determine the serviceability and load factors for each of these beams.

1-11 A steel bar 10 ft long with 2-in by 2-in cross section may be subjected to an axial tensile or compressive force at each end. When the bar is in tension, it is designed for an operating load of $P = 80$ kips whereas the bar is capable of resisting a maximum ultimate load of 240 kips before rupture. When the bar is subjected to compression, it begins to buckle at a load $P_c = \pi^2 EI/L^2$, in which E is the modulus of elasticity ($E = 30{,}000$ ksi for steel), I is the least moment of inertia of the section, and L is the length of the bar. If the same load factor is maintained in compression and tension, what should be the maximum load P under operating conditions when the member is subjected to compression?

1-12 The maximum stress σ_{max} in an eccentrically loaded column corresponding to the critical buckling load P_c is given by the so-called secant formula

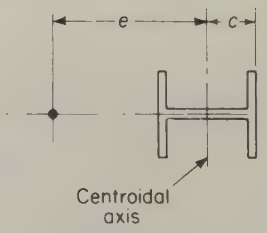

Figure P1-12

$$\sigma_{max} = \frac{P_c}{A}\left(1 + \frac{ec}{r^2}\sec\frac{L}{2r}\sqrt{\frac{P_c}{EA}}\right)$$

in which A is the cross-sectional area of the column, e is the eccentricity along

one of the principal axes of the section, c is the distance from the centroidal axis of the column section to the extreme outer fiber of the column in the direction of the column, r is the radius of gyration in the same direction, and L is the length of the column. If a load factor n is used, express the secant formula in terms of the allowable stress σ, the allowable load P, and the load factor n in place of σ_{max} and P_c while other terms in the formula remain unchanged.

2 STRUCTURAL SYSTEMS

2-1 *Definitions*

A *structural system* may be defined as an assembly of members such as bars, cables, arches, etc. with the purpose of transmitting external loads to the surrounding environment or foundation. A structural system cut away from a larger structural system—or from its foundation—is called a *free body*. To replace the influence of the members or supports that have been cut away, constraining forces are introduced at the supporting points of the isolated system; such forces are known as *reactions*. In order to determine the internal resistance of a structural system, imaginary sections may be passed through typical elements or members of the system. The portion of the system thus isolated from the rest of the system is also a free body in which the surrounding influences are replaced by *internal forces*. If a structural system is in static equilibrium, the free body isolated from any portion of the system must also be in equilibrium.

An internal force is sometimes called a *stress resultant*, which represents the total effect of stress components acting on the cross-sectional area of a member intersected by an imaginary plane. An internal couple is also known as a *stress couple* and refers to the couple resulting from these stress components. *Stress* is defined as the intensity of *force per unit area*, and in general varies over the cross-sectional area of a member. The components of stress may include *normal stress*, which is perpendicular to the section, and *shearing stress*, which is tangential to the section. Accordingly, a stress resultant may be either a *normal force* or a *shearing force*, depending on whether it is acting normal or tangential to the plane of the section. Similarly, a stress couple may be a *bending moment* resulting from the normal

stress components, or a *twisting moment* resulting from the shearing stress components. A twisting moment is also called a *torque*. Broadly speaking, the term "force" is sometimes used to imply either force or couple. Hence, the term "applied load" may refer to either external force or external couple, and the term "stress resultant" may be used to designate either internal force or internal couple.

A structural member subjected to the action of external forces or couples experiences certain deformations that usually include translational and rotational displacements. In a narrower sense, however, the term *displacement* refers only to translational movement, and the term *rotation* is used to denote rotational movement. Displacements and rotations are the outward indications of the strain in a member. *Strain* is defined as the *deformation per unit length*, and has a dimensionless unit. The components of strain may include axial strain normal to the section, called *normal strain*, and angular distortion in the plane of the section, called *shearing strain*. Thus, the geometry of a deformed structure is specified by the displacements and rotations resulting from the normal and shearing strains in its members.

The deformations tolerated in engineering structures are in general very small. Hence, the analysis of internal forces may be based on the dimensions of the undeformed shape without appreciable error, and the computation of the displacements may in turn be based on the internal forces thus obtained. This approach to the solution of structural systems is called the *small deflection theory*. Within the limitation of small deflection, structural systems are usually stressed below the elastic limit of the material. Hence, the small deflection theory is also known as the *elastic theory*. For unusually flexible structures in which displacements are large in comparison with the cross-sectional dimensions of the member although small in comparison with the length of the member, such as the cable of a long-span suspension bridge, the dimensions of the deformed structure must be used for more accurate analysis. Such an approach is known as the *large deflection theory* or *deflection theory*. Although only small deflection theory will be considered in this book, the deformations are usually exaggerated in illustrations solely for the sake of clarity.

The simultaneous positions of all particles of a system are called the *configuration* of the system. For structural systems consisting of slender members, the configuration is specified by centerlines passing through the centroids of the cross sections of the members. The centerline of a member is sometimes referred to as the *axis* of the member. When a structure is treated as a rigid system, the configuration is assumed to remain unchanged upon application of loads. On the other hand, when a structure is considered as a deformable system, the structure changes from one configuration

to another as loads are applied. The set of all configurations that a deformable system assumes during the course of deformation is called the *path* described by the system.

2-2 *Conditions of Equilibrium*

A structural system is in a state of equilibrium if the constraints permit no rigid-body movement upon application of loads. The system is assumed to be rigid in the sense that displacements due to deformation are negligible in comparison with the dimensions of the structure. The necessary and sufficient conditions to ensure equilibrium of an isolated system are that the resultant force in any direction and the resultant moment about any point be zero. Expressing these conditions for a space structure in a rectangular Cartesian coordinate shown in Fig. 2-1(a), we obtain the following set of equations of equilibrium:

$$\begin{aligned} \sum F_x &= 0, \quad \sum F_y = 0, \quad \sum F_z = 0 \\ \sum M_x &= 0, \quad \sum M_y = 0, \quad \sum M_z = 0 \end{aligned} \tag{2-1}$$

For a right-handed coordinate system, note that the positive direction of the moment with respect to the axis of rotation follows the right-hand rule. For example, if M_x represents the direction of rotation of a right-hand screw when tightened, the positive direction of the x-axis represents the direction of the advance of the screw.

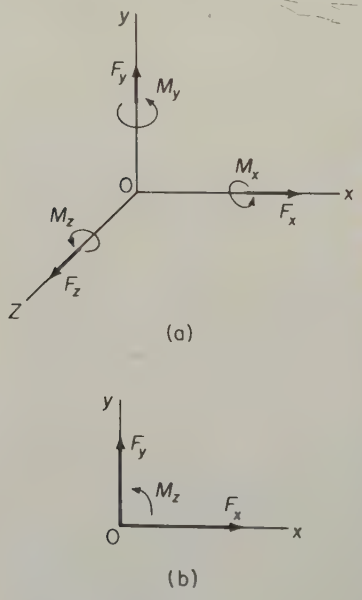

Figure 2–1

For the case of a plane structure lying in the xy-plane of the coordinate system shown in Fig. 2-1(b), the set of equations reduces to

$$\sum F_x = 0, \quad \sum F_y = 0, \quad \sum M_z = 0 \tag{2-2}$$

Note that the z-axis in space becomes a point when projected on the xy-plane. Thus, in the analysis of plane structures, the moment about a point is synonymous with the moment about an axis normal to the xy-plane passing through that point. Furthermore, in order to be consistent with the right-handed coordinate system in space, we consider counterclockwise moments as positive in coplanar systems.

The conditions of equilibrium may also be expressed in other forms.

Usually, one or more of the equations involving the summation of forces may be replaced by an equation or equations involving the summation of moments, provided that the resulting equations are independent. In general, six independent equations are available for the equilibrium of a structural system in space whereas three independent equations are available for a coplanar system. In the case of a coplanar system, for example, Eqs. (2-2) may be replaced by

$$\sum M_a = 0, \qquad \sum M_b = 0, \qquad \sum M_c = 0$$

in which a, b, and c represent points on the xy-plane not lying on the same straight line.

Several important and useful conclusions may be drawn from the simple cases of equilibrium. If a structural member is in equilibrium under the action of two forces, these two forces must be equal, opposite, and collinear, as shown in Fig. 2-2(a). If a member in equilibrium is acted on by three

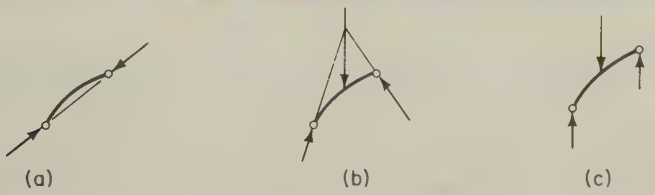

Figure 2–2

forces, these forces must be coplanar and their lines of action must be either concurrent or parallel, as shown in Figs. 2-2(b) and 2-2(c) respectively.

Since the existence of the state of equilibrium of a system is based on the tacit assumption that the system is properly constrained internally as well as externally, a structural system that satisfies this requirement is said to be in a position of *stable equilibrium*. If a system does not have a sufficient number of internal or external constraints, it will undergo a rigid-body movement upon the application of a small displacement. Such a system is said to be *statically unstable*, and is usually referred to as a *mechanism*.

Occasionally, we may encounter some unconventional structural systems that are stable under one loading condition but unstable under another. Such systems are said to be in a state of *unstable equilibrium* when the precarious balance is maintained. Although this situation is undesirable for ordinary structures such as buildings and bridges, it may be necessary for certain special-purpose structures. A precariously balanced bicycle might be cited as an example of a coplanar system in a state of unstable equilibrium. Trusses supporting the screen of a radar antenna and resting on roller bearings are typical examples of space structures that may be in a state of

unstable equilibrium. The roller bearings can be locked in a fixed position if desired. When the supports are unlocked, the structure is then in a state of unstable equilibrium.

For a stable system, we can formulate the unknown forces in terms of external loads and the conditions of equilibrium. If the unknown forces in the system can be solved by the equations of equilibrium alone, the system is said to be a *statically determinate structure*. When there are more unknown forces in a stable system than there are equations of equilibrium available for their solution, these forces cannot be solved by statics alone and the system is known as a *statically indeterminate* or *redundant structure*. The latter can further be classified into two categories. If the redundant forces appear when the structure as a whole is considered as a free body, the system is *externally* redundant. If such redundant forces occur when a part of the structure is taken as a free body, the system is *internally* redundant.

Let us consider a few simple illustrations. The beams shown in Fig. 2-3

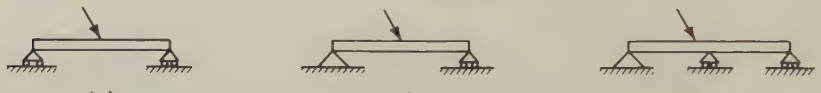

Figure 2–3

are rigid systems fixed in position by external constraints. Beam (a) is inadequately restrained and is statically unstable, beam (b) is sufficiently restrained and is statically determinate, and beam (c) is over-restrained and is externally redundant. However, if a vertical load is applied to beam (a)

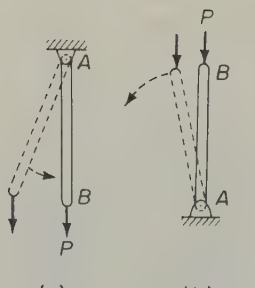

Figure 2–4

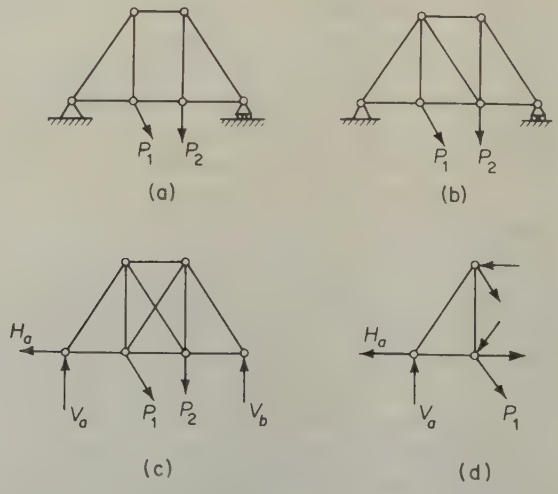

Figure 2–5

instead of an inclined load the system will be in unstable equilibrium. Similar conclusions may be drawn from the systems in Fig. 2-4. If a small lateral displacement is applied to the member in Fig. 2-4(a), it will return to its original position. On the other hand, Fig. 2-4(b) shows a system that is inherently unstable. Theoretically speaking, the member would be able to resist the external axial load if there were absolutely no disturbance in the lateral direction. In reality, however, some small lateral disturbance will exist and the member will tend to move away from the original position even if the disturbing force is later removed. Hence, the system is unstable.

We may also analyze the internal rigidity of a system by the simple examples in Fig. 2-5. Truss (a) is nonrigid and therefore statically unstable, truss (b) is just rigid and statically determinate, whereas truss (c) is overrigid and internally redundant. If we consider only part of truss (c) as a free body, as shown in Fig. 2-5(d), we find that there are four unknown internal forces although only three equations of equilibrium are available for a coplanar system. Thus, truss (c) is statically indeterminate.

2-3 *Degrees of Freedom*

If a finite number of constraints is removed from a stable system, the configuration may be specified by a finite number of variables called *generalized coordinates*. The number of generalized coordinates required to specify the configuration of a system is the number of degrees of freedom of the system. Thus, a properly constrained rigid system has no degrees of freedom whereas a deformable system may possess an infinite number of degrees of freedom.

Consider, for example, a ship on the high seas. If the ship is regarded as a floating rigid body with no external constraints, as shown in Fig. 2-6(a), its displacements may be described by the surge u, the heave v, and the sway w in the x, y, and z directions respectively, and its rotations may be defined by the roll φ_x, the yaw φ_y, and the pitch φ_z about the x, y, and z axes respectively, as shown in Fig. 2-6(b). Since the motion of the ship can be specified by six generalized coordinates u, v, w, φ_x, φ_y, and φ_z, it is said to have six degrees of freedom. On the other hand, a locomotive moving on a track can be specified by one variable. Hence, it has only one degree of freedom.

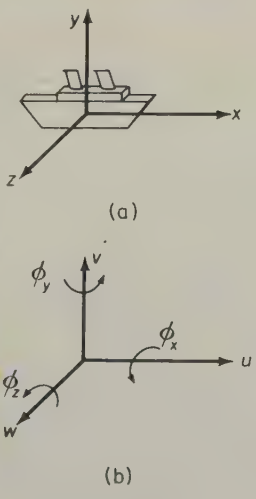

Figure 2–6

In general, a rigid system in space may have at most six degrees of freedom, whereas a coplanar rigid system may have up to three degrees of freedom. Thus, a rigid system can be restrained in a fixed position relative to the surrounding environ-

ment or foundation by a sufficient number of constraining forces at supporting points to counteract its tendency to move. However, the supports themselves may be either rigid or deformable. The former does not permit any displacement of the supporting points; the latter allows such displacements. In reality, structural supports may displace slightly owing to the settlement of the foundation or other causes but may be assumed to be rigid for most practical purposes. In cases where such an assumption cannot be made, the support itself may have various degrees of freedom. Consider, for example, the supporting springs in Fig. 2-7, which are permitted to displace in a vertical direction only. In Fig. 2-7(a), the location of the mass M can

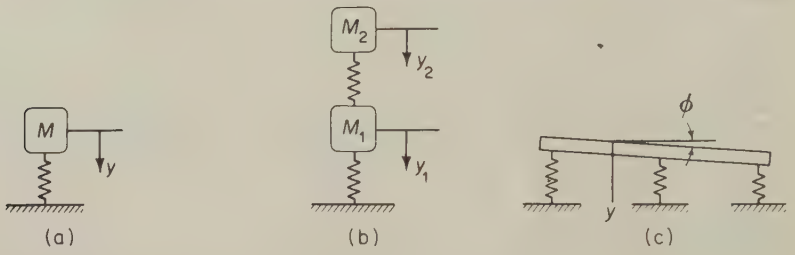

Figure 2–7

be defined by one generalized coordinate y. In Fig. 2-7(b), a spring is placed under each of the two masses. Hence, the locations of the masses M_1 and M_2 must be specified by two generalized coordinates y_1 and y_2. In Fig. 2-7(c), the rigid system is supported by three springs. However, the motion of the rigid body may be specified by a vertical displacement y referring to any point of the body and a rotation φ. Hence, the system has two degrees of freedom.

The internal constraints of a stable system may also be released to permit rigid-body movements. Consider the truss structure shown in Fig. 2-8(a). If the bottom diagonal is removed as shown in Fig. 2-8(b),

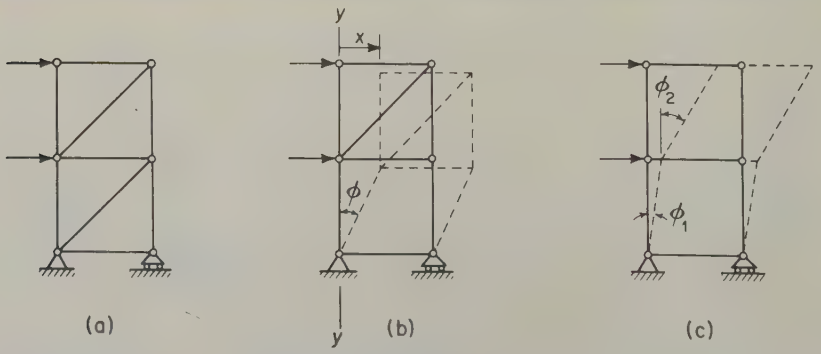

Figure 2–8

the movement of the top panel of the truss relative to a fixed line, say line y-y, can be specified by either a horizontal displacement x or a rotation φ. Hence, the system in Fig. 2-8(b) has one degree of freedom. Similarly, the system in Fig. 2-8(c), in which both diagonals have been removed, has two degrees of freedom.

When a structural system is treated as a deformable body, it no longer possesses a finite number of generalized coordinates. Consider the simple beam in Fig. 2-9(a), which is regarded as a rigid system in the analysis of

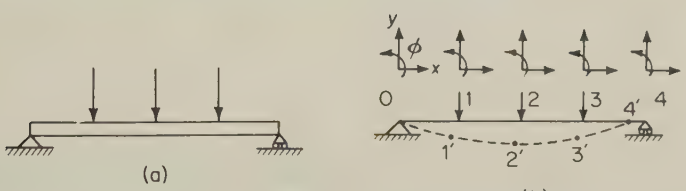

Figure 2–9

forces or moments. On the other hand, when treated as a deformable system in displacement computation, every point on the neutral axis of the beam except at the supports moves from its initial position to another position that defines the final configuration of the beam. Hence, the system has an infinite number of degrees of freedom. However, for practical purposes, the beam can be effectively approximated by a finite number of generalized coordinates as shown in Fig. 2-9(b), in which the displacements at only four points of the beam are considered. Then the system may be regarded as having a finite number of degrees of freedom.

The number of degrees of freedom chosen for an approximated system depends to a large extent on the desired accuracy of the solution. In the study of vibration of beams subjected to pulsating vertical loads, for example, it may be assumed that the mass of a beam is concentrated at the selected points. Since the horizontal displacements at these points of a beam are small compared with the corresponding vertical displacements, the horizontal displacements are negligible. Furthermore, the rotations at these points are unimportant and are usually neglected. Thus, the number of degrees of freedom in such a problem is drastically reduced. For the beam in Fig. 2-9(b), only three vertical displacements are considered, and hence the system is assumed to have three degrees of freedom in vibration analysis.

The concept of approximating a deformable system by a finite set of generalized coordinates is very useful in displacement computation. The points on a structure arbitrarily chosen for this purpose are called *nodal points*. For framed structures it is logical to select the joints as nodal points. Thus, the degrees of freedom of such systems are approximated by the

number of unknown displacement components at the nodal points. For the pin-connected truss in Fig. 2-10(a), for example, there are eight nodal points, each of which can be specified by two generalized coordinates, i.e., horizontal and vertical displacements. Since three of the displacement components are zero, there are 13 unknown displacements and the system has 13 degrees of freedom. Similarly, for the rigid frame in Fig. 2-10(b),

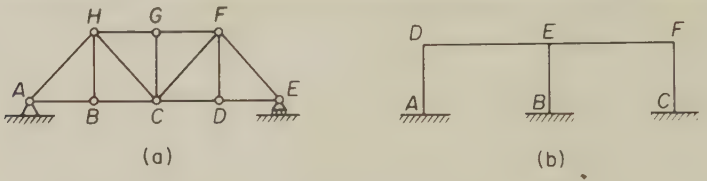

Figure 2–10

there are six nodal points, each of which can be specified by three generalized coordinates, i.e., rotation as well as horizontal and vertical displacements. Since the nodal points *A*, *B*, and *C* are completely fixed, there are nine unknown displacement components resulting from the three remaining nodal points. Hence, the system has nine degrees of freedom if all components of displacements are considered as important.

2-4 *Simple Systems*

We shall now consider some simple, statically determinate, structural systems. Such systems are internally rigid and are properly constrained externally by a sufficient number of components of reaction. These components of reaction can therefore be completely specified by the equations of equilibrium.

A plane structure may in general be completely restrained from rigid-body movement by three components of reaction defined by three equations of equilibrium. A support that can prevent rotation as well as horizontal and vertical displacements in a plane structure is called a *fixed support*. If the support can resist only horizontal and vertical displacements but not rotation, it is said to be a *hinge* or *pin*. If the support is permitted to slide in one direction as well as to rotate, it may be represented by a roller, which provides a constraining force normal to the direction of sliding. The term *roller* is used in a broad sense to allow the constraining force to act either *upward* or *downward* relative to the surface of sliding.

Similarly, a structure in space can be completely restrained by six components of reaction specified by six equations of equilibrium. A fixed support for a space structure can prevent displacements along any of the three coordinate axes as well as rotation about any of them. A ball-and-socket joint can resist only displacements along the three coordinate axes

but not rotations; hinges and rollers may also be used for supports of space structures.

The components of reaction may be described figuratively by links, each of which is used to represent one component in a specific direction. Consider, for example, the cantilever beam in Fig. 2-11(a). The components

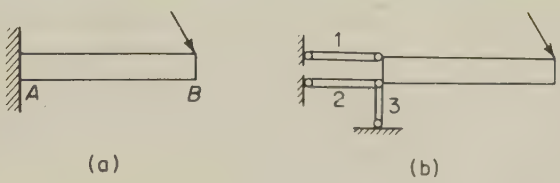

Figure 2–11

of reaction are represented by links 1, 2, and 3, as shown in Fig. 2-11(b). The rotation and the horizontal displacement at the fixed support are resisted by links 1 and 2, while the vertical displacement at the support is resisted by link 3. Similarly, for the simply supported beam in Fig. 2-12(a), the pin or hinge at support A is replaced by two links while the roller at

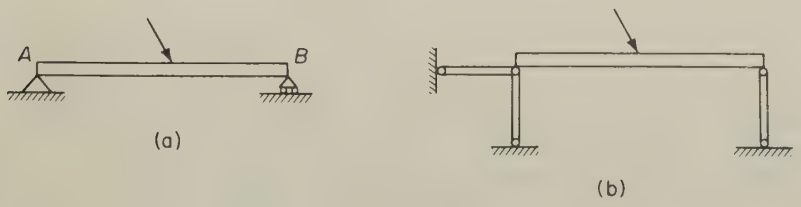

Figure 2–12

support B is equivalent to a vertical link, as shown in Fig. 2-12(b). Since the number of links equals the number of equations of equilibrium, the components of reaction can be obtained by statics. However, there are restrictions on the arrangement of the links in order to insure complete constraint of a system. If all three links supporting a system are concurrent or parallel, as shown in Figs. 2-13(a) and 2-13(b), respectively, the system

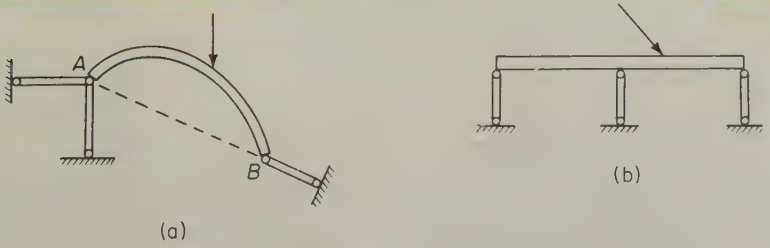

Figure 2–13

will not be completely restrained. In case (a), the components of reaction cannot resist the moment developed by the external forces about support A. In case (b), the system is unstable and will swing to the right. Systems that collapse under external loads because of the geometrical orientation of links or members are said to be *geometrically unstable*.

The idea of representing components of reaction by links may also be applied to structures in space. Consider, for instance, the rigid system in space in Fig. 2-14(a), which is subjected to external forces F_x, F_y, and F_z, and external moments M_x, M_y, and M_z. The fixed support may be replaced by six links as indicated in Fig. 2-14(b). Thus, the displacements and rotations of the support will be prevented by these links. Similarly, for the

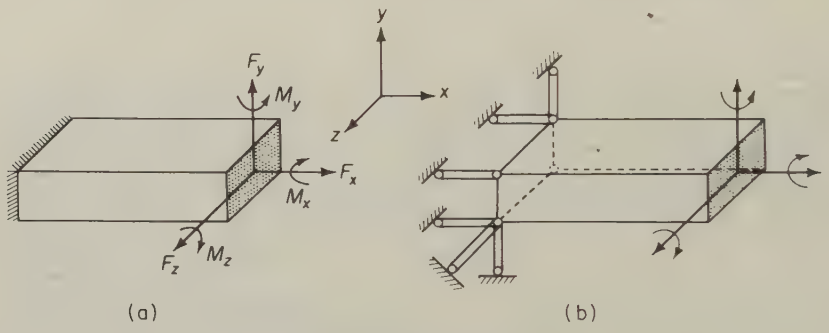

Figure 2–14

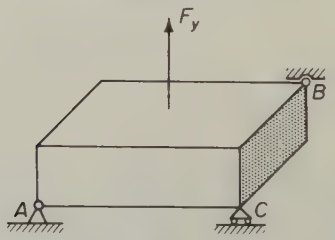

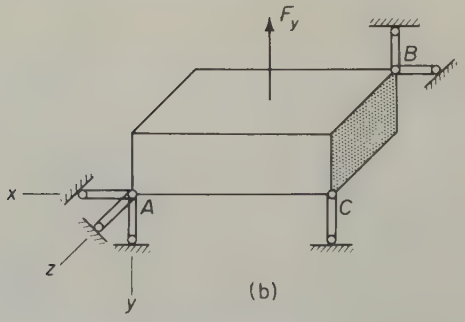

Figure 2–15

system in Fig. 2-15(a), the ball-and-socket joint at support A can be represented by three links, whereas the pin at support B and the roller at support C can respectively be replaced by two links and one link, as shown in Fig. 2-15(b). Since the number of links equals the number of equations of equilibrium, the components of reaction can be determined by statics. As in the case of plane structures, there are restrictions on the orientation or arrangement of the links supporting a system in space in order to avoid geometrical instability. If all links have lines of action which intersect a straight line, as shown in Fig. 2-16(a), there is no resistance to the moment developed by

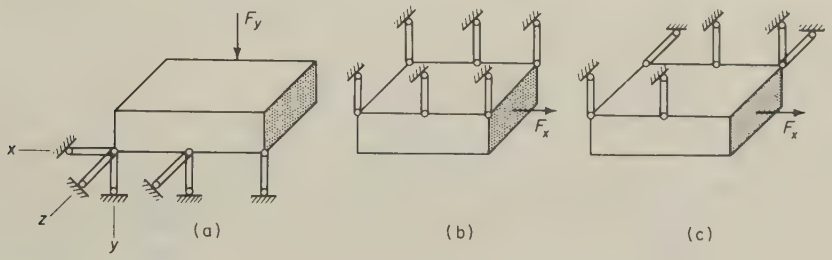

Figure 2–16

external forces about that line. Similarly, if all links are parallel, as shown in Fig. 2-16(b), the system will swing to the right upon the application of external loads. On the other hand, if all links lie on parallel planes, as shown in Fig. 2-16(c), the system is partially restrained. However, since the system must move a small distance to the right before restraining forces can be developed in the links, it is not completely restrained.

Example 2-1. Find the reactions of the simply supported beam in Fig. 2-17(a). The beam is first isolated from its supports as shown in Fig. 2-17(b), in which the components of the reactions are indicated by H_a, V_a, and V_b. If the applied load is resolved into vertical and horizontal components of 8 kips and 6 kips, respectively, the components of reaction may be obtained from the equations of equilibrium. Thus,

$$\sum M_a = 0, \qquad 8V_b - (8)(2) = 0, \quad V_b = 2 \text{ kips}$$

$$\sum F_x = 0, \qquad H_a = 6 \text{ kips}$$

$$\sum F_y = 0, \qquad V_a + V_b = 8, \quad V_a = 8 - 2 = 6 \text{ kips}$$

The same result may be obtained if we choose to use the condition that the moment of all forces be zero about any three arbitrary points not lying on the same line. Thus, from Fig. 2-17(b),

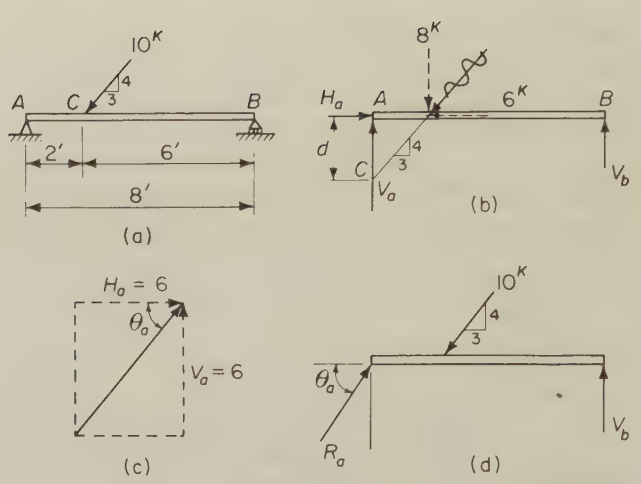

Figure 2–17

$$\sum M_a = 0, \quad 8V_b - (8)(2) = 0, \quad V_b = 2 \text{ kips}$$

$$\sum M_b = 0, \quad 8V_a - (8)(6) = 0, \quad V_a = 6 \text{ kips}$$

$$\sum M_c = 0, \quad 8V_b - H_a d = 0$$

From the relation of similar triangles, $d/2 = \frac{4}{3}$ and $d = \frac{8}{3}$. Hence,

$$H_a = \frac{(2)(8)}{\frac{8}{3}} = 6 \text{ kips}$$

If the resultant of the components of reaction at support A is desired, it may be obtained from the geometrical relation shown in Fig. 2-17(c). Then,

$$R_a = \sqrt{V_a^2 + H_a^2} = \sqrt{36 + 4} = 6.32 \text{ kips}$$

$$\theta_a = \tan^{-1} \frac{V_a}{H_a} = \tan^{-1} 3 = 70°34'$$

This result would have been obtained directly if the free-body diagram in Fig. 2-17(d) had been used. It should be noted that the number of unknowns in the system remains the same since θ_a as well as R_a must be determined in this case. From the standpoint of minimizing numerical computation, however, the solution involving vertical and horizontal components of reaction is usually preferred.

Example 2-2. Compute the reactions for the beam in Fig. 2-18(a).

Since the beam is horizontal and there are no horizontal forces acting on it, the equation of equilibrium $\Sigma F_x = 0$ immediately leads to the conclusion that the horizontal component of reaction at support A must be

zero. Thus, only vertical components of reactions at supports A and B need be considered and they can be determined from the remaining two equations of equilibrium:

$$\sum M_a = 0, \quad 20V_b - (50)(5) - (40)(10) - (30)(15) - (20)(25) - (10)(30) = 0$$
$$V_b = 95 \text{ kips}$$
$$\sum M_b = 0, \quad -20V_a + (50)(15) + (40)(10) + (30)(5) - (20)(5) - (10)(10) = 0$$
$$V_a = 55 \text{ kips}$$

It is always desirable to provide independent checks on the computations by considering another condition of equilibrium. For example,

$$\sum F_y = 0, \quad 95 + 55 - 50 - 40 - 30 - 20 - 10 = 0 \text{ (checked)}$$

There are numerous ways in which we may keep track of our computations and check them in order to avoid mistakes. As long as the solution is carried out in an orderly and systematic manner, the detail of execution is only a matter of personal preference. Fig. 2-18(b) shows computations in which the total reactions are obtained by summing up the reactions due to each external load.

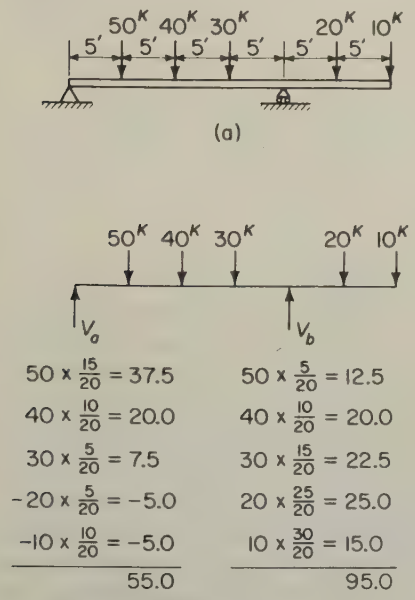

Figure 2-18

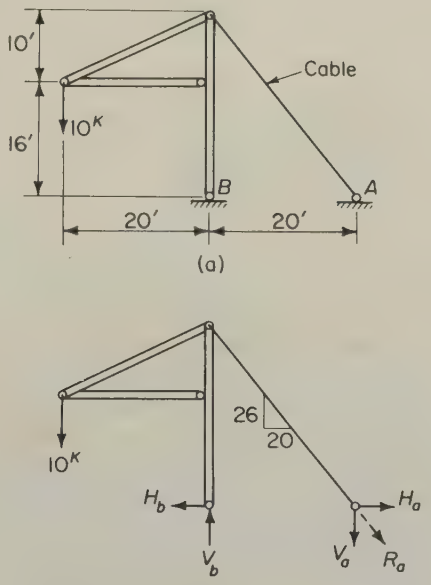

Figure 2-19

Example 2-3. Compute the reactions at supports A and B of the system in Fig. 2-19(a).

Since the cable can resist only tension, the reaction at A must have the same line of action as member AC. For the free-body diagram in Fig. 2-19(b), the vertical and horizontal components of reaction at A must bear a ratio of $V_a/H_a = 26/20$. Hence, there are only three independent unknowns that can be solved by the equations of equilibrium.

$$\sum M_b = 0, \quad -20V_a + (10)(20) = 0, \quad V_a = 10 \text{ kips}$$
$$\sum F_y = 0, \quad V_b - V_a - 10 = 0, \quad V_b = 20 \text{ kips}$$
$$\sum F_x = 0, \quad H_a - H_b = 0, \quad H_a = H_b = (^{20}\!/_{26})V_a = 7.7 \text{ kips}$$

Example 2-4. Determine the reactions at supports D, E, and F of the system in Fig. 2-20(a).

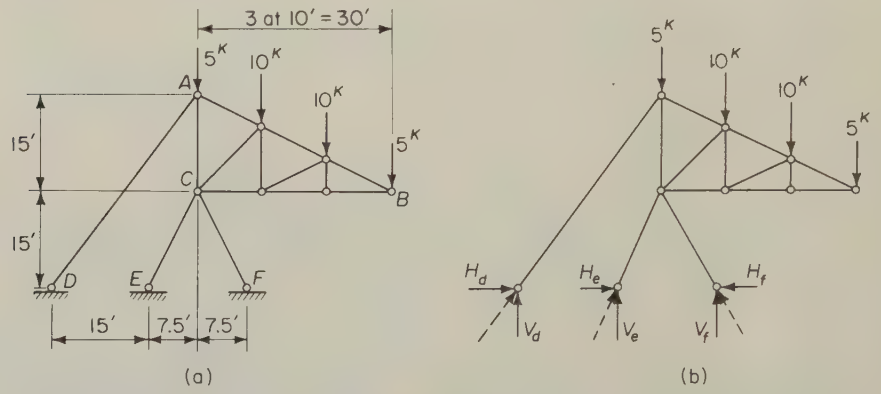

Figure 2–20

In drawing the free-body diagram for a system, it is sometimes impossible to detect the correct sense of direction of a reaction. In such a case the sense may be arbitrarily assumed. If the result obtained on such a basis is positive, the assumed sense is correct; otherwise, the actual sense of direction of the reaction is opposite the assumed sense. Considering the free-body diagram in Fig. 2-20(b), we assume the senses of direction of the reactions as indicated. Although six components of reaction are shown in the figure, there are only three independent unknowns because each of the reactions must have a line of action corresponding to the axis of the member it supports. Thus, the vertical and horizontal components of each reaction are related to each other as follows:

$$V_d/H_d = {}^4\!/_3 \text{ or } H_d = 0.75V_d$$
$$V_e/H_e = {}^2\!/_1 \text{ or } H_e = 0.5V_e$$
$$V_f/H_f = {}^2\!/_1 \text{ or } H_f = 0.5V_f$$

In order to simplify the solution, it is advisable to take moments about points that represent the intersections of some unknown components of reaction. For example,

$$\sum M_c = 0, \quad 15H_d - 22.5V_d - (10)(10) - (10)(20) - (5)(30) = 0$$
$$(15)(0.75V_d) - 22.5V_d = 450$$
$$V_d = -40 \text{ kips} \quad \text{and} \quad H_d = -30 \text{ kips}$$
$$\sum M_f = 0, \quad -(-40)(30) - 15V_e + (5)(7.5) - (10)(2.5 + 12.5) - (5)(22.5) = 0$$
$$V_e = 65 \text{ kips} \quad \text{and} \quad H_e = 32.5 \text{ kips}$$
$$\sum M_e = 0, \quad -(-40)(15) + 15V_f - (5)(7.5 + 37.5) - (10)(17.5 + 27.5) = 0$$
$$V_f = 5 \text{ kips} \quad \text{and} \quad H_f = 2.5 \text{ kips}$$

As a check, we may consider

$$\sum F_y = 0, \quad (-40) + 65 + 5 - 5 - 10 - 10 - 5 = 0$$

Note that the sense of the reaction at D has been erroneously assumed. Hence, the result is negative, and the negative sign must be consistently carried through the entire problem unless a new free-body diagram indicating the correct sense of the reaction is drawn.

Example 2-5. Find the reactions of the angle frame shown in Fig. 2-21(a). The components of the reactions H_a, V_a, and V_c are indicated in the

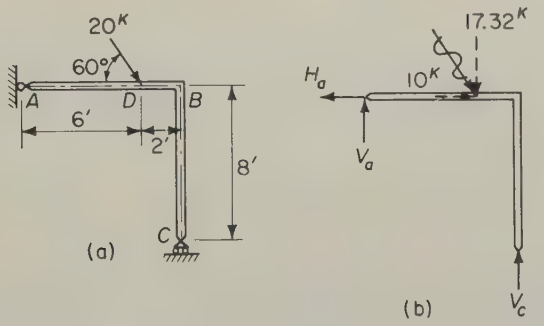

Figure 2–21

free-body diagram in Fig. 2-21(b), from which the following equations of equilibrium are obtained:

$$\sum M_a = 0, \quad 8V_c - (17.32)(6) = 0, \quad V_c = 12.99 \text{ kips}$$
$$\sum F_y = 0, \quad V_a + V_c = 17.32, \quad V_a = 4.33 \text{ kips}$$
$$\sum F_x = 0, \quad H_a = 10 \text{ kips}$$

As a check,

$$\sum M_d = 0, \quad (12.99)(2) - (4.33)(6) = 0$$

2-5 Compound Systems

A *compound system* is defined as a statically determinate system formed by interconnecting two or more simple systems. Since extra components of reaction are usually introduced in such a system, the interconnections must be so constructed that they provide additional conditions for the solution of the reactions. These additional conditions are called the *conditions of interconnection.* Consider the compound systems shown in Fig. 2-22. The compound beam in Fig. 2-22(a) is obtained by combining the simple beam

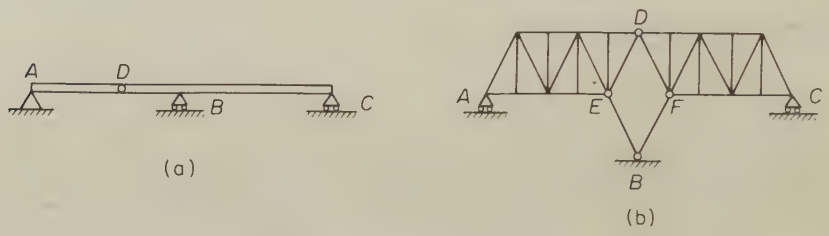

Figure 2–22

AD with the cantilever beam DC. At the interconnection point D a hinge is provided so that no moment is transmitted through that point. The components of reaction of the system may be solved by considering beam AD and beam DC as separate free bodies. Similarly, the compound truss in Fig. 2-22(b) is considered a combination of simple trusses ADE and CDF. The components of reaction can again be computed by isolating the simple trusses as free bodies.

A compound system may also be thought of as a statically determinate system formed by introducing releases to an otherwise statically indeterminate structure. A *release* is defined as a discontinuity in a structural member that is incapable of transmitting a stress resultant. If we refer again to Fig. 2-22(a), the compound beam may be regarded as a continuous beam, the continuity of which has been disrupted by the introduction of a hinge at point D. Similarly in Fig. 2-22(b), the compound truss may be considered as a continuous truss, the continuity of which has been released by the removal of member BD. The introduction of the hinge D in the former, or the removal of member BD in the latter, represents the condition of construction that produces the desired release in the structure. Hence, the conditions of interconnection may also be called the *conditions of release.*

Compound systems are especially susceptible to geometrical instability

owing to the orientation of certain members or reactions. Consider, for example, the systems shown in Fig. 2-23. Whereas systems (a) and (b) in the figure are stable, system (c) is unstable because each member tends

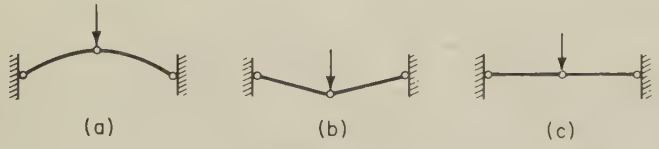

Figure 2–23

to rotate about the adjacent end hinge. The movement in system (c) can be arrested only after both members have yielded or stretched enough to cause large deformation of the center hinge. In that case, the structural system can no longer be treated as a rigid system.

In the case of the compound truss in Fig. 2-24(a), the system becomes geometrically unstable when members *BE* and *BF* are oriented in such a manner that their lines of action pass through points *G* and *H*, respectively. This can be seen from the free-body diagram representing the left half of the truss in which all forces except V_d pass through point *G*. Thus, nothing will prevent the rotation of this part of the truss under the action of V_d when we take the moment of all forces about point *G*.

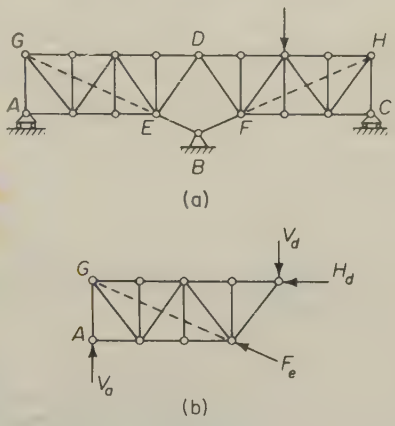

Figure 2–24

Example 2-6. Compute the reactions of the compound system shown in Fig. 2-25(a).

Since a cable can take tension only, the directions of the reactions at supports *A* and *B* must be in line with members *AE* and *BE* respectively. The reaction at support *D* can be resolved into vertical and horizontal components. When the system as a whole is taken as a free body, there are four unknown reaction components in three equations of equilibrium. However, a fourth equation may be obtained from the condition of release that no horizontal resistance be provided at point *C*. Hence, the components of reaction can be completely determined.

This problem can be readily solved by isolating the system into two parts, as shown in Figs. 2-25(b) and (c). From the former, we obtain

$$\sum F_x = 0, \quad H_d = (3/5)\,(100) = 60 \text{ kips}$$
$$\sum M_c = 0, \quad V_d = (1/50)\,(4/5)\,(100)\,(30) = 48 \text{ kips}$$
$$\sum F_y = 0, \quad V_c = (4/5)\,(100) - 48 = 32 \text{ kips}$$

From the latter it is obvious that

$$T_a = T_b = (1/2)\,(32)\,(5/3) = 26.7 \text{ kips}$$

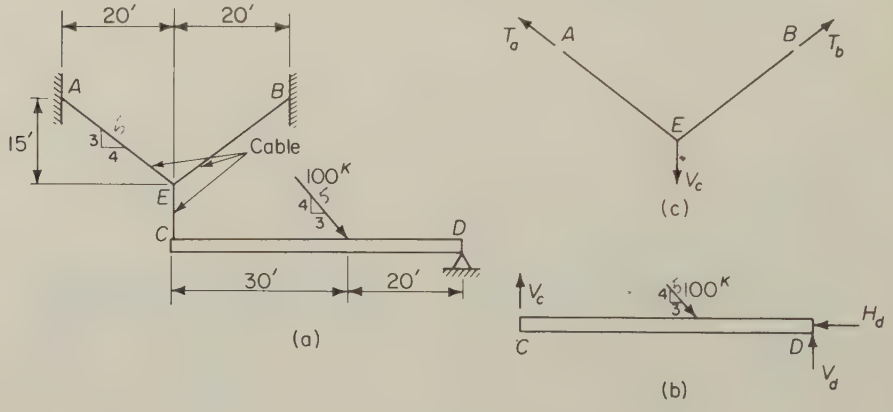

Figure 2–25

Example 2-7. Compute the reactions of the compound beam shown in Fig. 2-26(a).

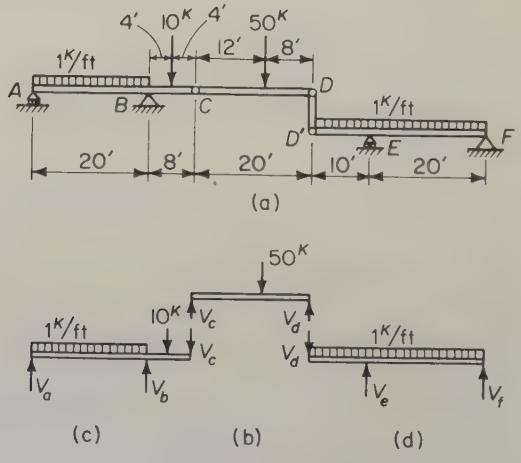

Figure 2–26

In this structure there are theoretically six components of reaction since two of the supports are on rollers and the other two are hinged. There are

also three equations resulting from the releases since $\Sigma M_c = 0$ at hinge C, and $\Sigma M_d = 0$ and $\Sigma F_x = 0$ at link DD'. Therefore, there are six equations for six unknown components of reaction. Actually, the problem can be greatly simplified since there is no horizontal load acting on the structure and thus the horizontal components of reaction become zero from the consideration of $\Sigma F_x = 0$. Four unknown vertical components of reaction V_a, V_b, V_e and V_f remain and must satisfy the equations of equilibrium $\Sigma F_y = 0$ and $\Sigma M_z = 0$, and the conditions of release $\Sigma M_c = 0$ and $\Sigma M_d = 0$. For this problem, the procedure can best be illustrated by separating the beam segments into free bodies as shown in Figs. 2-26(b), (c), and (d). Starting with Fig. 2-26(b), for which there are only two unknowns,

$$\sum M_c = 0, \quad (V_d)(20) - (50)(12) = 0, \quad V_d = 30 \text{ kips}$$

$$\sum F_y = 0, \quad V_c + V_d = 50, \quad V_c = 20 \text{ kips}$$

From Fig. 2-26(c), for $\Sigma M_a = 0$,

$$(20)(28) + (10)(24) + (1)(20)(20\tfrac{1}{2}) - (V_b)(20) = 0, \quad V_b = 50 \text{ kips}$$

For $\Sigma F_y = 0$,

$$V_a + V_b = (1)(20) + 10 + 20, \qquad V_a = 0$$

From Fig. 2-26(d), for $\Sigma M_f = 0$,

$$(30)(30) + (1)(30)(30\tfrac{1}{2}) - (V_e)(20) = 0, \quad V_e = 67.5 \text{ kips}$$

For $\Sigma F_y = 0$,

$$V_e + V_f = 30 + (1)(30), \qquad V_f = -7.5 \text{ kips}$$

It should be pointed out that the result for $V_a = 0$ is purely a coincidence. For other loads, it may be a positive or negative quantity. If it turns out to be positive, the assumed sense of direction of the reaction is correct; if it is negative, the assumed sense of the reaction should be reversed. Thus $V_f = -7.5$ kips means that the reaction should be directed downward.

Example 2-8. Compute the reactions of the three-hinged arch shown in Fig. 2-27(a).

The components of reaction of the arch, shown dotted in Fig. 2-27(a), can be related to the applied loads as follows:

$$\sum M_c = 0, \quad (V_a)(140) + (80)(3.75) - (30)(80) - (20)(40) + (H_a)(26.25) = 0$$

or

$$140V_a + 26.25H_a = 2{,}900$$

$$\sum F_x = 0, \quad H_a + H_c = 80$$

$$\sum F_y = 0, \quad V_a + V_c = 30 + 20$$

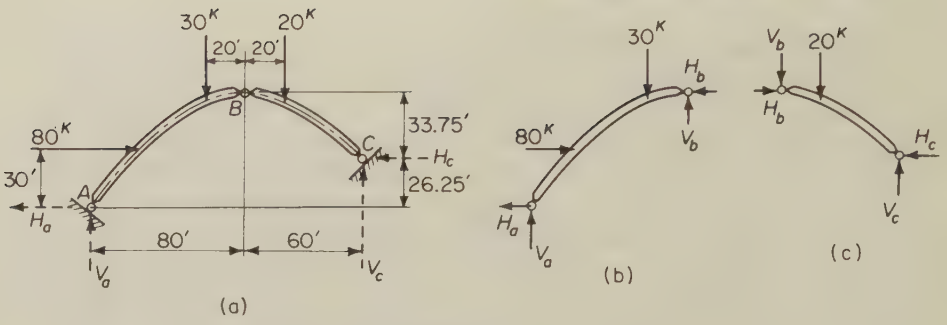

Figure 2–27

Since there are four unknowns and only three equations of equilibrium, an additional equation must be obtained from the condition of release $\Sigma M_b = 0$. Thus, by taking moments of all the forces to the left of hinge B about B, we have

$$(H_a)(60) - (80)(30) - (30)(20) + (V_a)(80) = 0$$

or

$$80V_a + 60H_a = 3{,}000$$

This last equation is equivalent to one of the equations of equilibrium, $\Sigma M_b = 0$, for the free body shown in Fig. 2-27(b). Solving these four equations simultaneously, we obtain $H_a = 29.8$ kips, $V_a = 15.1$ kips, $H_c = 50.2$ kips, and $V_c = 34.9$ kips. The reactions H_b and V_b at the hinge can also be obtained from the other two equations of equilibrium for Fig. 2-27(b).

$$\sum F_x = 0, \quad H_b = 80 - 29.8 = 50.2 \text{ kips}$$

$$\sum F_y = 0, \quad V_b = 30 - 15.1 = 14.9 \text{ kips}$$

By considering the free body shown in Fig. 2-27(c), these reactions can be checked. For $\Sigma M_b = 0$,

$$(20)(20) + (50.2)(33.75) - (34.9)(60) = 400 + 1{,}700 - 2{,}100 = 0$$

Example 2-9. Determine the components of reaction of the structure shown in Fig. 2-28(a).

If we consider the structure as a whole, the following equations of equilibrium are obtained.

$$\sum F_x = 0, \quad H_c - 40 = 0 \tag{a}$$

$$\sum F_y = 0, \quad V_a + V_b + V_c = 100 \tag{b}$$

$$\sum M_c = 0, \quad 100V_b + (40)(40) - 100V_a - (100)(40) = 0 \tag{c}$$

Since there are four unknown components of reaction V_a, V_b, V_c and H_c, an additional equation must be obtained from the condition of release. This

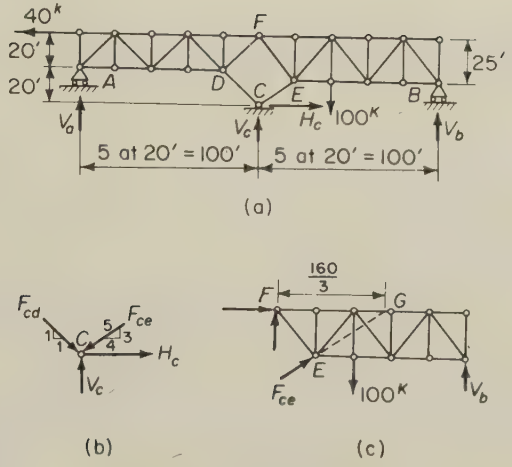

Figure 2-28

may be accomplished by considering support C as a free body as shown in Fig. 2-28(b). Thus,

$$\sum F_x = 0, \quad \frac{\sqrt{2}}{2} F_{cd} - \frac{4}{5} F_{ce} + H_c = 0 \tag{d}$$

$$\sum F_y = 0, \quad -\frac{\sqrt{2}}{2} F_{cd} - \frac{3}{5} F_{ce} + V_c = 0 \tag{e}$$

from which we may obtain

$$F_{ce} = \frac{V_c + H_c}{1.4}$$

If we now consider the right half of the truss as a free body as shown in Fig. 2-28(c), an expression relating V_b, V_c, and H_c may be obtained by taking moments about point F. Note that the force F_{ce} may be resolved into components at point G so that its horizontal component passes through point F. Then,

$$\sum M_f = 0, \quad 100V_b + \frac{3}{5} F_{ce} \left(\frac{160}{3}\right) - (100)(40) = 0$$

or

$$100V_b + (32)\left(\frac{V_c + H_c}{1.4}\right) - (100)(40) = 0 \tag{f}$$

Finally, all components of the reactions may be obtained from the simultaneous solution of Eqs. (a), (b), (c), and (f) as follows:

$H_c = 40$ kips, $V_a = 29.25$ kips, $V_b = 53.25$ kips, $V_c = 17.50$ kips

Identical results would have been obtained if F_{cd} were solved from Eqs. (d) and (e) so that an additional equation is obtained by considering the left half of the structure as a free body.

Example 2-10. Compute the reactions of the structure shown in Fig.

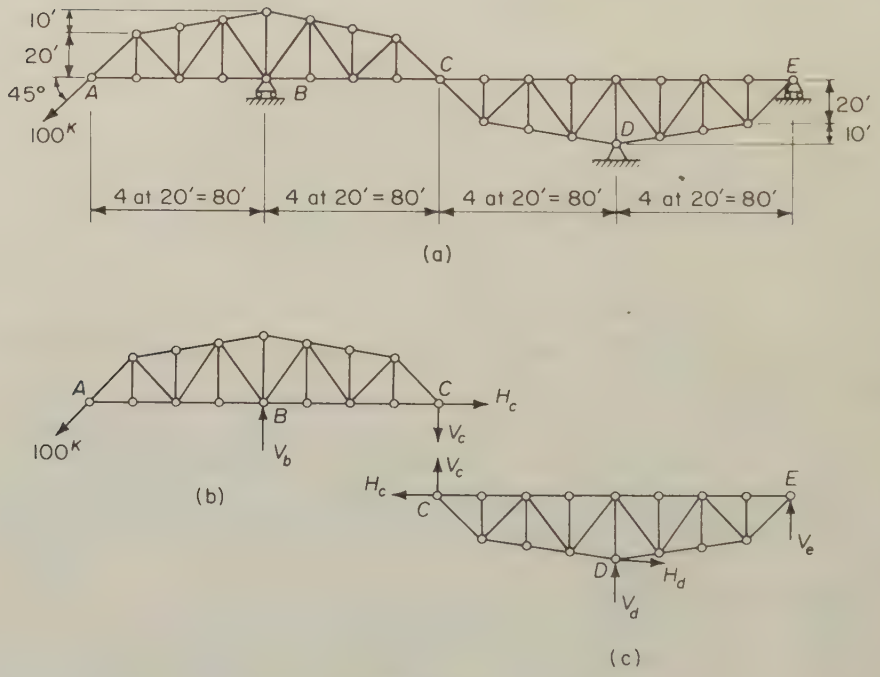

Figure 2–29

2-29(a). Since there are four unknown components of reaction and only three equations of equilibrium, an additional equation must be obtained from the condition of release $\Sigma M_c = 0$. However, we can simplify the computation by isolating the structure into two parts as shown in Figs. 2-29(b) and (c). From the former, we have

$$\sum M_c = 0, \quad 80V_b = \frac{100}{\sqrt{2}}(160), \quad V_b = 141.4 \text{ kips}$$

$$\sum F_x = 0, \quad H_c = \frac{100}{\sqrt{2}} = 70.7 \text{ kips}$$

$$\sum F_y = 0, \quad 141.4 - \frac{100}{\sqrt{2}} - V_c = 0, \quad V_c = 70.7 \text{ kips}$$

From the latter, we obtain

$$\sum M_d = 0, \quad 80V_e + (70.7)(30) - (70.7)(80) = 0, \quad V_e = 44.2 \text{ kips}$$

$$\sum F_x = 0, \quad H_d = 70.7 \text{ kips}$$

$$\sum F_y = 0, \quad V_d + 44.2 + 70.7 = 0, \quad V_d = -114.9 \text{ kips}$$

Note that the negative sign for V_d indicates that the reaction at D is downward instead of upward.

2-6 *Redundant Systems*

From the point of view of static equilibrium, structural systems may be classified as statically determinate or indeterminate. The basic approach in identifying the typical characteristics of these systems is to check first whether there are sufficient reaction components and members to maintain the equilibrium of the structure. If so, further checks should be made to insure that all reaction components and members are properly oriented so that the structure will be geometrically stable. When there are more reaction components or members than necessary, remove one redundance at a time until the structure becomes statically determinate. Then, the number of redundances removed is known as the *degree of statical indeterminacy* or *degree of redundancy*.

Consider, for example, the plane structures shown in Fig. 2-30. In

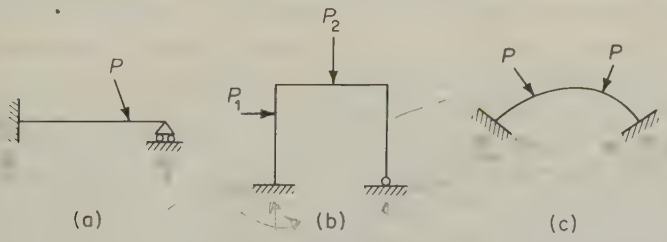

Figure 2–30

each case there are three independent equations of equilibrium when the structure as a whole is taken as a free body. The reactions at the supports are the only unknown forces acting on the structure. Since the statical indeterminacy in each case is caused by the extra components of reaction that can be removed without causing the collapse of the structure, the number of components of reaction in excess of three is the degree of indeterminacy or redundancy of the system. Since the number of independent components of reaction is four, five, and six for the structures in Figs. 2-30(a), (b), and (c) respectively, the corresponding degrees of indeterminacy are therefore equal to one, two and three.

If a section is passed through a beam, there will be at the most three stress resultants, i.e., axial force, shearing force, and bending moment, which can also be evaluated from the free-body diagram if the reactions are known. This is also true for a single-span frame or arch. Thus, the structures shown in Fig. 2-30 are only externally redundant. On the other hand, there are structures that are redundant internally as well as externally. For the structure shown in Fig. 2-31(a), the system as a whole has nine

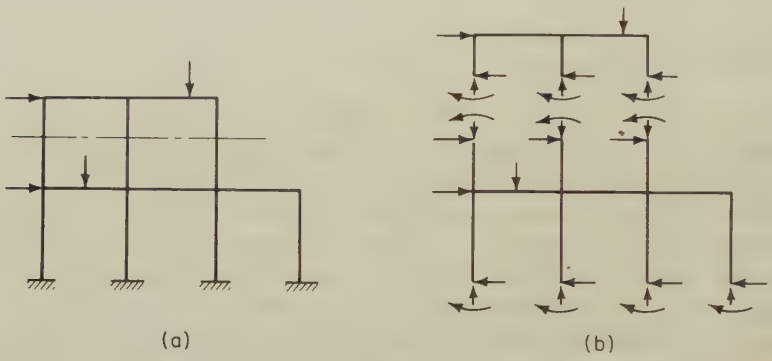

Figure 2–31

degrees of external redundancy because there are twelve components of reaction, as shown in Fig. 2-31(b). A section at the second level indicates that there are nine unknown forces and moments and only three equations of equilibrium if the top part of the structure is taken as a free body. Thus, the structure has six degrees of internal redundancy. The total number of redundances is therefore $9 + 6 = 15$.

Although this approach to identifying the degree of indeterminacy of structures is most reliable and should always be the guiding principle, simple criteria for determining the degrees of statical indeterminacy of various types of structures may be developed. These criteria are necessary but not always sufficient, and should be applied with caution. First of all, we should rule out cases that are either statically or geometrically unstable such as the systems shown in Figs. 2-32(a) and (b) respectively. Furthermore, the actual degree of indeterminacy of a system may be smaller than the nominal number given by the simple criterion. Consider, for instance, the cases shown in Figs. 2-33(a), (b), and (c), with the corresponding free-

Figure 2–32

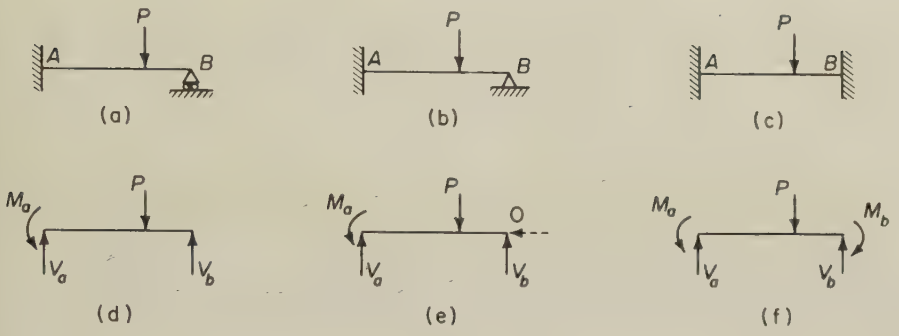

Figure 2–33

body diagrams in Figs. 2-33(d), (e), and (f). In the example of Fig. 2-33(a), the structure is statically indeterminate to the first degree as the above criterion would indicate, but the structures in Figs. 2-33(b) and (c) may be considered as only statically indeterminate to the first and second degrees respectively for practical purposes, provided that the vertical displacement of the structure will not cause significant horizontal displacement in each case. This assumption of negligible horizontal displacement is quite accurate in most cases. Thus, no horizontal reaction is included in the free-body diagrams in Figs. 2-33(e) and (f). However, these structures should be considered as statically indeterminate to the second and third degrees respectively if no such assumption can be justified.

Rigid frames. An over-all criterion for statical determinacy may be established for rigid frames. For plane frames, there are in general three stress resultants for a section passing through each member of the frame. Thus, the total number of unknowns in the frame is equal to $3m + r$, in which m is the number of members and r is the number of independent components of reaction. If j denotes the number of joints *including the points of reaction*, a total of $3j$ equations of equilibrium may be obtained by considering each of these joints as a free body. Therefore, the criterion for statical determinacy of plane rigid frames is

$$3m + r - 3j = 0 \tag{2-3}$$

If $3m + r - 3j$ is less than 0, the system is unstable; if it is greater than 0, the system is statically indeterminate to the degree indicated by $3m + r - 3j$. For the multistoried frame in Fig. 2-31(a), $m = 12$, $r = 12$, and $j = 11$. Thus,

$$3m + r - 3j = 15$$

and the structure is statically indeterminate to the 15th degree. This criterion

can be applied to the structures in Fig. 2-30, although it is hardly necessary to do this for such simple cases. For example, in Fig. 2-30(a), $m = 1$, $r = 4$, $j = 2$, and $3m + r - 3j = 1$. For Fig. 2-30(b), $m = 3, r = 5$, $j = 4$, and $3m + r - 3j = 2$. For Fig. 2-30(c), $m = 1$, $r = 6$, $j = 2$, and $3m + r - 3j = 3$.

For rigid frames in three dimensions, there are in general six stress resultants for a section passing through each member of the frame, and thus a total number of $6m$ unknowns from all members. The total number of equations of equilibrium from all joints including the points of reaction is equal to $6j$. If r is the number of independent components of reaction, the criterion for statical determinacy of a space rigid frame is

$$6m + r - 6j = 0 \tag{2-4}$$

Pin-connected trusses. In the case of trusses, the problem is simplified by the fact that the joints of the trusses are assumed to be pin-connected. This assumption leads to the simplification that there is only one stress component at a section passing through each member and that the joints can resist only direct forces but not moments. Thus, for a plane truss, the total number of unknowns in the truss is equal to $m + r$, in which m is the number of the members and r is the number of independent components of reaction. If j denotes the number of joints including the points of reaction, a total of $2j$ equations of equilibrium may be obtained by considering each of these joints as a free body. Thus, the criterion for statical determinacy of a plane truss is

$$m + r - 2j = 0 \tag{2-5}$$

This rule may be applied to the structures shown in Figs. 2-34 and 2-35. In Fig. 2-34(a), $m = 18$, $r = 3$, and $j = 10$. Since $m + r - 2j = 1$, the structure is statically indeterminate to the first degree. In Fig. 2-34(b), $m = 20$, $r = 3$, and $j = 10$. Since $m + r - 2j = 3$, the structure is statically inde-

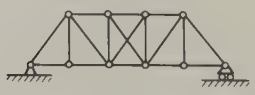

(a)

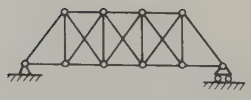

(b)

Figure 2–34

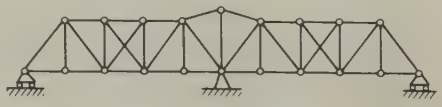

(a)

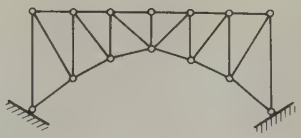

(b)

Figure 2–35

terminate to the third degree. In Fig. 2-35(a), $m = 39$, $r = 4$, and $j = 20$. Thus

$$m + r - 2j = 3$$

and the structure is statically indeterminate to the third degree. In Fig. 2-35(b), $m = 25$, $r = 4$, and $j = 14$. Since $m + r - 2j = 1$, the structure is statically indeterminate to the first degree.

For space trusses, a similar criterion may be developed. Since a total of $3j$ equations of equilibrium may be obtained by considering each of the joints as a free body, the criterion for statical determinacy of space trusses is

$$m + r - 3j = 0 \tag{2-6}$$

Structures with releases. For structures with hinges or links, the general criteria may not be applicable. Each structure must be treated as a special case.

If hinges are introduced in the members of a plane rigid frame, each hinge will provide an extra equation $\Sigma M = 0$ at the point of the hinge. Let the number of hinges in a rigid frame be denoted by n; then the criterion of statical determinacy will become

$$3m + r - 3j - n = 0$$

For the structure shown in Fig. 2-36(a), the degree of statical indeterminacy is $36 + 12 - 33 - 5 = 10$. However, if the hinges are introduced at a joint, the rotational restraints of all members meeting at the joint will be released. On the other hand, the equilibrium condition that the algebraic sum of the moments from all members meeting at the joint be zero becomes a repetitive statement in view of the existence of the hinge. Thus, the actual reduction of redundancy due to the introduction of a hinge at a joint equals the number of the members meeting at the joint minus one. For the structure shown in Fig. 2-36(b), the hinge at joint A reduces the redundancy by one, the hinge at joint B reduces the redundancy by two, and the hinge at C reduces the redundancy by three. Hence the degree of statical indeterminacy of the structure becomes $36 + 12 - 33 - 1 - 2 - 3 = 9$.

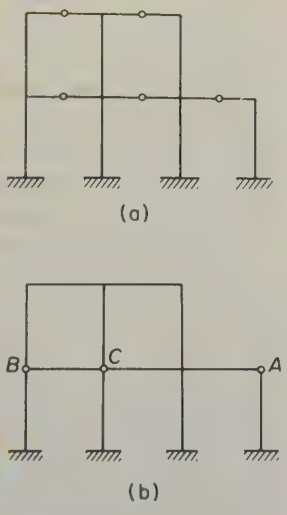

Figure 2–36

For plane trusses, the releases in structures are accomplished by omitting certain members such as those shown dotted in Fig. 2-37(a) and (b). Thus, m is reduced by one in Fig. 2-37(a) and is reduced

Figure 2–37

by two in Fig. 2-37(b). Since the reduction of each of these members is accompanied by the introduction of an additional component of reaction in the respective structures, the criterion of $m + r - 2j = 0$ may still be used. For the structure in Fig. 2-37(a), $m = 24$, $r = 4$, and $j = 14$; for the structure in Fig. 2-37(b), $m = 59$, $r = 5$, and $j = 32$. Hence, both structures are statically determinate.

For the suspension bridges shown in Fig. 2-38, there are only four known

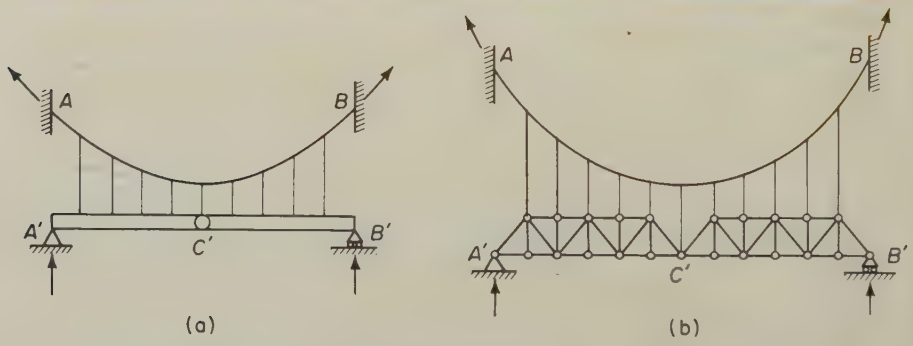

Figure 2–38

components of reaction in each system, if the stiffening girder or truss is subjected to vertical loads only. This is true because the directions of the cable reactions must be in line with the tangents of the cable at supports A and B, and the hangers are so flexible that they can transmit only vertical loads. Hence, each system is statically determinate because an additional condition of release is present in the system. In Fig. 2-38(a), the condition of release is provided by the center hinge C' in the girder, whereas in Fig. 2-38(b) no moment can be transmitted from truss $A'C'$ to truss $B'C'$. Thus, joint C' in Fig. 2-38(b) has the same effect as hinge C' in Fig. 2-38(a).

2-7 *Compatibility of Displacements*

In the analysis of redundant systems, it has been found that the equations of equilibrium alone are not sufficient for the determination of the unknowns in a system. Additional equations must be obtained from the conditions of

geometrical compatibility of displacements in the system. For this reason, the geometrical compatibility is sometimes considered as the "equilibrium" of displacements. The requirements of geometrical compatibility are based on the simple principle that the deformations of the individual elements in a system must be compatible with the over-all deformation of the entire system, and vice versa. Hence, a study of the geometry of structural systems becomes necessary in the solution of redundant systems.

Consider, for instance, the beam in Fig. 2-39(a). If the neutral axis

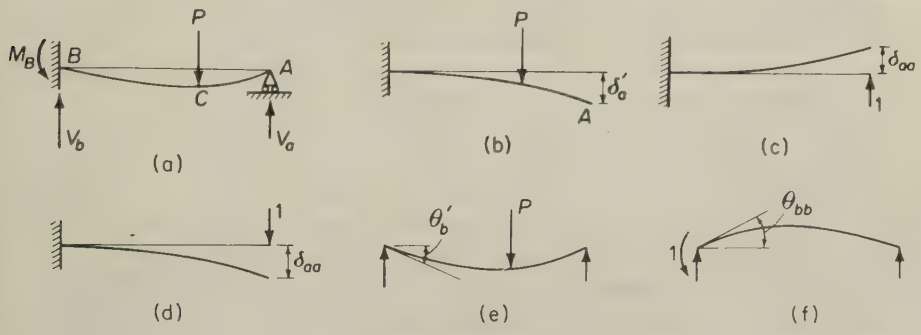

Figure 2–39

of the beam is not strained during bending, there must be a slight horizontal displacement of support A toward the left as the beam deflects downward under the action of the vertical load P. It can be demonstrated, however, that the horizontal displacement of any element in the beam is very small in comparison with its vertical displacement and is therefore negligible. Furthermore, the shape of the deflected beam is also governed by the supporting conditions. At support A, the beam is free to rotate but not to displace vertically. This implies that at support A the moment as well as the vertical displacement equals zero. At support B, the beam is neither free to rotate nor to displace vertically. Thus, at support B the slope and the vertical displacement of the beam are both zero. The conditions of forces or moments at the supporting points are called *force boundary conditions*, whereas the conditions of rotations and displacements at the supports are known as *displacement boundary conditions*. The boundary conditions of a structure are important in sketching its deflected shape qualitatively as well as for computing the displacements quantitatively.

Now that we have described the geometry of the deflected structure, we shall attempt to analyze the redundant structure in the light of the condition of geometrical compatibility. Since there are three unknown components of reaction for the structure in Fig. 2-39(a) and only two equations of equilibrium available, the third one being a trivial statement that the forces and reactions in the horizontal direction are identically zero, the structure is

statically indeterminate to the first degree. We shall therefore remove a redundance, say reaction V_a at support A, to make the structure determinate. The resulting structure, as shown in Fig. 2-39(b), is known as the *released* structure of the original system. Since point A of the released structure will deflect by an amount of δ_a' under the action of the external load P, this point must eventually be brought back by the same amount in order to satisfy the geometrical boundary conditions of the original system. This is accomplished by assuming a unit load acting upward at point A of the released structure while the external load is removed as shown in Fig. 2-39 (c). If the vertical upward displacement of point A due to a unit upward load at A is denoted by δ_{aa}, then the force necessary to restore point A to the undeformed position must be the unknown vertical reaction at A. Thus, the reaction can be obtained as follows:

$$V_a = \frac{\delta_a'}{\delta_{aa}} \qquad \text{(a)}$$

Note that the sense of direction of the unit load is arbitrarily assumed. If the assumed sense is correct, the reaction V_a will be positive. If the unit load is assumed to be acting downward and the vertical downward displacement of point A due to a unit downward load is denoted by δ_{aa} as indicated in Fig. 2-39(d), the condition of zero displacement at point A in the original system requires

$$\delta_a' + V_a\delta_{aa} = 0 \quad \text{or} \quad V_a = -\frac{\delta_a'}{\delta_{aa}}$$

It should be pointed out that in a redundant system, any component of reaction may be chosen as a redundant. For the structure in Fig. 2-39(a), the moment M_b at the fixed end may be chosen as a redundant. In that case, the released structure will deflect as shown in Fig. 2-39(e) under the external load P, and the beam undergoes a rotation θ_b' at end B as a result of the removal of the redundant M_b. Then, a unit couple may be applied at end B of the released structure, causing a rotation of θ_{bb} at end B as shown in Fig. 2-39(f). Thus,

$$M_b = \frac{\theta_b'}{\theta_{bb}} \qquad \text{(b)}$$

If we know only how to compute the displacements of the released structures due to the external loads as well as a unit load, Eq. (a) or (b) will provide the additional equation needed for the solution of the remaining unknown components of reaction.

If more than one redundance is involved in a structural system, the same principle may still be applied. Consider, for example, the continuous beam in Fig. 2-40(a), which is statically indeterminate to the second degree.

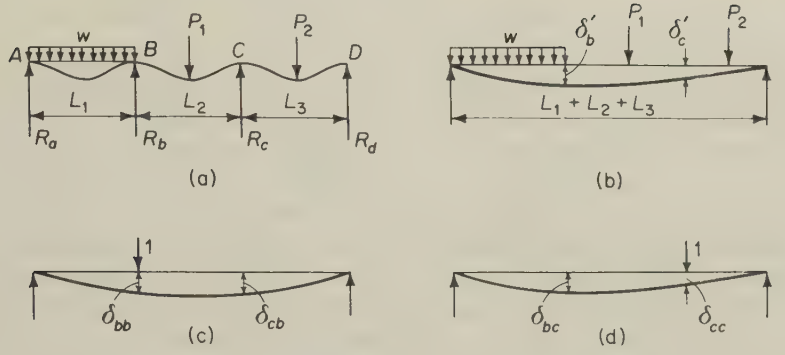

Figure 2–40

If reactions R_b and R_c are removed as redundances, the vertical displacements at points B and C of the released structure under the external loads will be δ_b' and δ_c' respectively, as shown in Fig. 2-40(b). Let δ_{bb} and δ_{cb} be the vertical displacements at B and C respectively due to a unit vertical load at B, and δ_{bc} and δ_{cc} be the vertical displacements at B and C respectively due to a unit vertical load at C, as shown in Figs. 2-40(c) and (d). Then, two equations of geometrical compatibility may be written since the vertical displacements at points B and C in the original redundant system must both be zero. Thus,

$$\delta_b' + R_b\delta_{bb} + R_c\delta_{bc} = 0 \qquad \text{(a)}$$

$$\delta_c' + R_b\delta_{cb} + R_c\delta_{cc} = 0 \qquad \text{(b)}$$

The simultaneous solution of Eqs. (a) and (b) gives the redundant reactions R_b and R_c in terms of displacements of the released structure. Hence, the remaining unknown components of reaction may be determined from the equations of equilibrium.

We may conclude, therefore, that the conditions of geometrical compatibility will in general lead to a set of simultaneous equations with as many unknowns as the number of redundances in a redundant system. This set of equations, together with the equations of equilibrium, will enable us to solve all the unknowns involved in the system. Before we can do so, however, we must know how to select a released system which is statically determinate by removing the appropriate redundances, and to compute the displacements of this statically determinate system under various loads. Although the first step involves judgment based on experience if we are to select a released system that requires a minimum of numerical computations, the second step can be handled systematically and separately. Since the computation of displacements in statically determinate structures is so vital in the analysis of redundant systems, it will be treated in greater detail later.

So far, we have approached all problems by first establishing the equations of equilibrium of forces. If the number of unknowns exceeds the number of equations, we can express the redundant forces in terms of displacements of the released system. Thus, the total number of equations will eventually be the same as the number of unknown forces. Such an approach is known as the *force method.* There is yet an entirely different approach in which the displacements at the joints of a structure are selected as unknowns whereby sufficient equations are sought to relate and solve the unknown displacements. This approach is called the *displacement method.*

Even without knowing the details of the displacement method, we can see that the degree of static indeterminacy or redundancy is no longer important in the solution of the system by this method. Instead, we want to know how many unknown displacements are involved so that the same number of equations may be formulated for their solution. Since the degree of freedom of a framed structure may be represented by the number of unknown displacements at the joints, the number of degrees of freedom in a structure is called the *degree of kinematic indeterminacy* of the system.

2-8 Force-Deformation Relations

In order to obtain the displacements of a structural system under the action of external forces, we must first establish the force-deformation relations in its members. Although a general expression for the force-deformation relations in a slender member is desirable, it is impossible to obtain without considering the member as a three-dimensional problem in the theory of elasticity. We shall therefore consider first some simple cases such as uniaxial tension, pure bending, and pure torsion of circular bars.

A few simple examples are shown in Fig. 2-41, in which the applied force is shown at the left end of each member and the state of stress on an imaginary section normal to the axis of the member is indicated at the right end of the member. The internal force or stress resultant may be obtained through proper integration of the stress over the cross-sectional area. From the condition of static equilibrium of the free bodies, the internal force is equal in magnitude but opposite in direction to the external force. In the case of uniaxial tension, the internal force F can be expressed as the sum of the normal stress σ over the cross-sectional area A as follows:

$$F = \int_A \sigma \, dA \tag{2-7a}$$

In the case of pure bending, the internal bending moment M_z may be obtained by

$$M_z = -\int_A y\sigma \, dA \tag{2-7b}$$

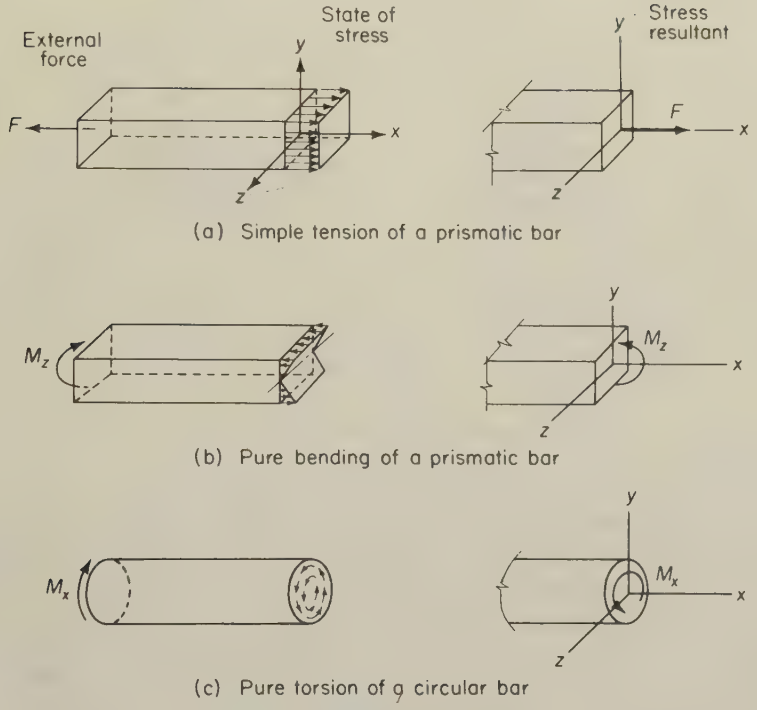

Figure 2–41

in which σ is the normal stress acting on a plane fiber at a vertical distance y from the plane of zero stress, or neutral axis, and y is the moment arm for the force $\sigma\, dA$. With the indicated direction of M_z, σ is compressive or negative when y is positive and σ is tensile or positive when y is negative. Hence, a negative sign is placed in front of the integral so that M_z is positive as indicated. In the case of pure torsion of a circular bar, the internal twisting moment or torque M_x may be obtained by

$$M_x = \int r\tau\, dA \tag{2-7c}$$

in which τ is the shearing stress acting on a circular fiber at a radius r from the center of the bar, and the radius r is the moment arm for the force $\tau\, dA$.

In general, for a slender member the state of stress at a point on a section normal to the x-axis of an orthogonal coordinate system may be represented by the normal stress σ_x and shearing stresses τ_{xy} and τ_{xz}, as shown in Fig. 2-42(a). Then, the stress resultants along the three orthogonal axes passing through the centroid of the area of the section and the stress couples about these axes, as shown in Fig. 2-42(b), may be obtained as follows:

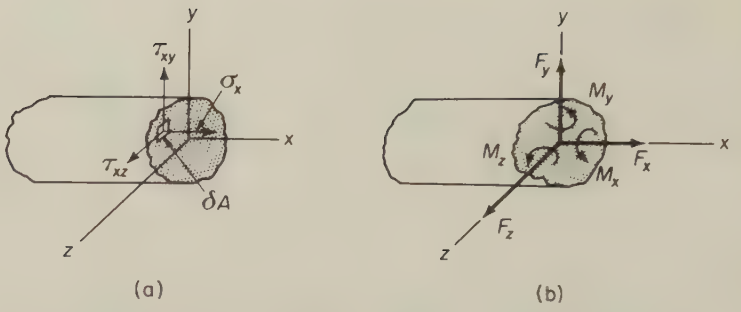

Figure 2–42

$$F_x = \int_A \sigma_x \, dA, \quad M_x = \int_A (y\tau_{xz} - z\tau_{xy}) \, dA$$

$$F_y = \int_A \tau_{xy} \, dA, \quad M_y = \int_A z\sigma_x \, dA \tag{2-8}$$

$$F_z = \int_A \tau_{xz} \, dA, \quad M_z = -\int_A y\sigma_x \, dA$$

Thus, the internal forces and couples acting on an imaginary section can be related to the state of stress at the section, and vice versa.

In order to determine the displacements at various locations of a member, we must select a frame of reference from which the displacements are measured. The relative displacement measured from the frame of reference to a section under consideration is the *deformation* between them. Thus, in the case of uniaxial tension, the tensile force F causes an elongation. If the left end of the member is fixed in position, the displacement u at the right end of the member is equal to the elongation, as shown in Fig. 2-43(a). In the case of pure bending, the bending moment M_z produces a curvature

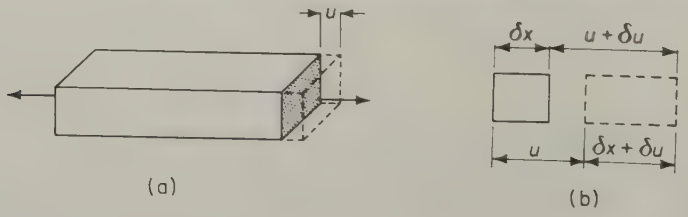

Figure 2–43

that is associated with the rotation φ_z in Fig. 2-44(a), assuming that the left end of the member is fixed in position. Similarly, in the case of pure torsion of a circular bar, the twisting moment M_x introduces an angle of twist that

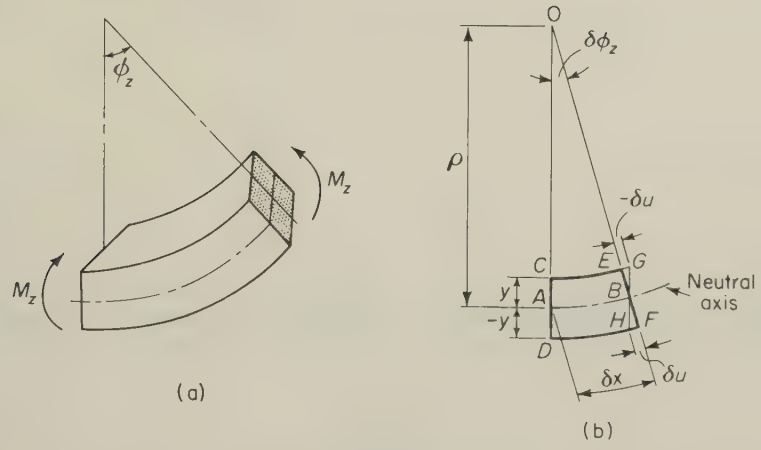

Figure 2–44

is represented by the rotation φ_x in Fig. 2-45(a), assuming again that the left end of the member is fixed in position. In the general case of a slender member shown in Fig. 2-42, the corresponding displacements and rotations may be expressed in components with respect to the orthogonal coordinate axes. Thus, there are three displacement components u, v, and w along the x, y, and z axes respectively, and three rotation components φ_x, φ_y, and φ_z about the x, y, and z axes respectively.

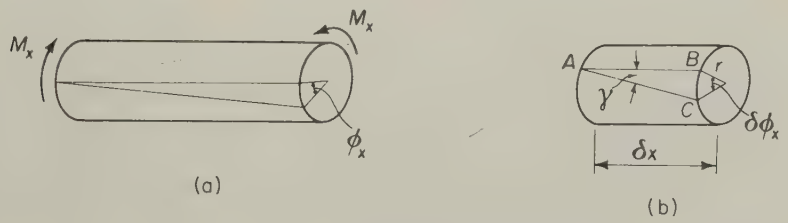

Figure 2–45

Deformations or displacements are the outward indications of the strains in a member. Wherever the displacement components depend on a fixed frame of reference, the strain components are independent of it. In the case of a bar under uniaxial tension in Fig. 2-43(a), for example, the axial strain ϵ in the bar is given by the elongation of the bar per unit length. If the bar is fixed at the left end, then the displacement u at the right end of the bar represents the accumulation of axial strains throughout the entire length. If, on the other hand, an infinitesimal element dx is taken in the axial direction of the bar, both sides of the element are displaced as indicated in Fig. 2-43(b). Let the displacement at the left side of the element be u and that at the right side be $u + \delta u$. Then, the deformed length of the element

becomes $\delta x + \delta u$. Hence, regardless of the magnitude of u, the axial strain may be obtained by the definition as follows:

$$\epsilon = \frac{(\delta x + \delta u) - \delta x}{\delta x} = \frac{\delta u}{\delta x}$$

At the limit,

$$\epsilon = \frac{du}{dx} \tag{2-9a}$$

On the other hand, the displacement u obtained from the integration of ϵ between given limits represents only the relative displacement between these limits. For example, from $x = 0$ to $x = L$,

$$u = \int_0^L \epsilon \, dx \tag{2-9b}$$

In the case of pure bending, we may also consider an infinitesimal element whose undeformed length is dx. Since the neutral axis of the member is undeformed during bending as shown in Fig. 2-44(b), the radius of curvature ρ may be related to the rotation $\delta\varphi_z$ by the arc length $\delta x = \rho \, \delta\varphi_z$. Hence, the curvature, which is defined as the reciprocal of the radius of curvature, is equal to

$$\frac{1}{\rho} = \frac{d\varphi_z}{dx} \tag{2-10a}$$

The deformation of fiber CE or DF may be measured by drawing a line GH passing through point B and parallel to side CD of the element. Obviously, the fiber CE has been shortened by the same amount as the fiber DF has been elongated if they are equidistant above and below the neutral axis respectively. Thus, if the fiber of the element at a positive distance y from the neutral axis is shortened by the amount δu, the fiber at a negative distance y from the neutral axis will be elongated by the amount δu. Since the length δx is infinitesimally small, we may consider the arc lengths as straight line segments. Then, triangles OAB, BEG, and BHF are similar to each other. From the proportionality of the corresponding sides of similar triangles, the following relation is obtained:

$$\frac{\delta x}{\rho} = -\frac{\delta u}{y}$$

If ϵ is the normal strain in the direction of the x-axis, in a fiber which is at a distance y below the neutral axis, i.e., ϵ being positive for a negative y, we have from the previous equation

$$\frac{1}{\rho} = -\frac{1}{y}\frac{du}{dx} = -\frac{\epsilon}{y} \tag{2-10b}$$

The rotation may also be expressed in terms of ϵ by noting that

$$\delta\varphi_z = \frac{\delta x}{\rho} = -\frac{\epsilon}{y}\,\delta x$$

from which

$$\varphi_z = -\int_0^L \frac{\epsilon}{y}\,dx \tag{2-10c}$$

For the torsion of a circular shaft, we may also consider an infinitesimal element dx which has an angle of twist of $\delta\varphi_x$ throughout its length as shown in Fig. 2-45(b). Then, the angle of twist per unit length is given by

$$\theta = \frac{d\varphi_x}{dx} \tag{2-11a}$$

If the shearing strain γ is defined as the angular distortion in twisting a fiber at a distance r from the center, which may be obtained by dividing the arc length BC by the length of the element δx, we have,

$$\gamma = \frac{r\,\delta\varphi_x}{\delta x} = r\,\frac{d\varphi_x}{dx} \tag{2-11b}$$

The rotation may be expressed in terms of γ by noting that

$$\delta\varphi_x = \frac{\gamma\,\delta x}{r}$$

from which we obtain

$$\varphi_x = \int_0^L \frac{\gamma}{r}\,dx \tag{2-11c}$$

In general, at a section normal to a slender member as shown in Fig. 2-42, the components of strain acting on the section are the normal strain ϵ_x in the direction of the x-axis and the shearing strain γ_{yz} in the plane defined by the y- and z-axes, as shown in Figs. 2-46(a) and (b) respectively. Note that $\partial u/\partial x$ is the rate of change of u in the direction of x, $\partial v/\partial z$ is the rate of change of v in the direction of z, and $\partial w/\partial y$ is the rate of change of w in the direction of y.

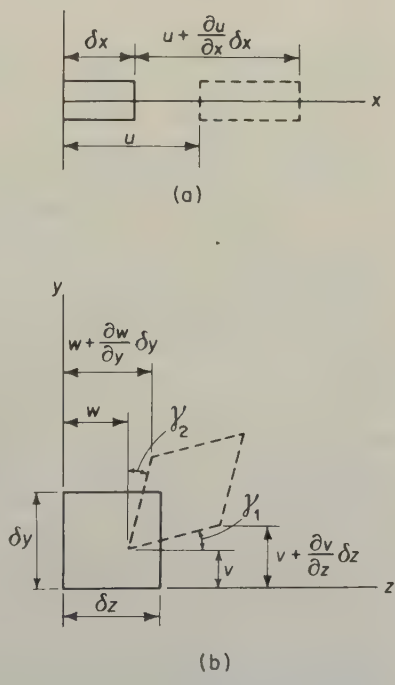

Figure 2–46

Then, the normal strain is equal to

$$\epsilon_x = \frac{(u + \dfrac{\partial u}{\partial x}\,\delta x) - u}{\delta x} = \frac{\partial u}{\partial x} \tag{2-12a}$$

The shearing strain is the total angular distortion γ_{yz} in the yz-plane. For a small angle γ, it may be assumed that $\sin\gamma = \tan\gamma = \gamma$ in radians. Thus,

$$\begin{aligned}\gamma_{yz} &= \gamma_1 + \gamma_2 \\ &= \frac{(v + \dfrac{\partial v}{\partial z}\,\delta z) - v}{\delta z} + \frac{(w + \dfrac{\partial w}{\partial y}\,\delta y) - w}{\delta y} \\ &= \frac{\partial v}{\partial z} + \frac{\partial w}{\partial y}\end{aligned} \tag{2-12b}$$

However, the state of strain for the general case of a section passing through a slender member cannot be defined by these two components of strain alone because the plane section before deformation no longer remains plane after deformation. The warping surface resulting from deformation may be a function of all components of displacement, and hence may involve strain components ϵ_y and γ_{zx} acting on a plane normal to the y-axis and strain components ϵ_z and γ_{xy} acting on a plane normal to the z-axis. A simple example of a warping surface may be seen in the twisting of a square bar. We cannot, therefore, express the components of displacement in terms of components of strain by some simple relations. Except for the simple cases of uniaxial tension, pure bending, and pure torsion of circular bars, for which the deformed sections remain plane, approximate relations will be introduced when such needs arise.

In summary, we note that internal forces can be expressed in terms of the components of stress, and for the simple cases most frequently encountered, displacements can be expressed in terms of the components of strain. If the stress-strain relation of the material is known, we can formulate the relation between internal forces and displacements in a structural system. Since the stress-strain curves of the various materials used in engineering structures are not in general expressible in simple mathematical relationships, they are usually idealized to simplify the solution of the problems. Although no real material is perfectly rigid as shown in Fig. 2-47(a), such an idealization does not introduce significant difference when applied to the analysis of forces in relatively rigid structural systems. As most materials exhibit some degree of elasticity before a limiting stress is reached, the assumption of linear elasticity as shown in Fig. 2-47(b) is most frequently used for a deformable system. Some materials, such as structural steel, have a definite yield point and undergo large plastic strain without increase in

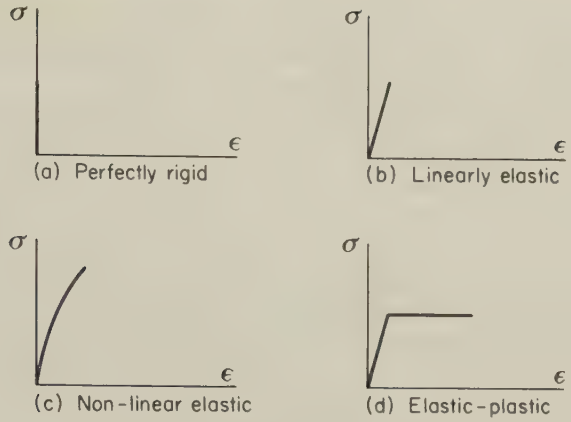

Figure 2–47

stress. The plastic region can therefore be represented by a horizontal line if the work-hardening effect is neglected. The idealization as shown in Fig. 2-47(c) represents a nonlinear elastic material. An idealized elastic-plastic material may be represented by the broken line in Fig. 2-47(d). We shall deal primarily with the linearly elastic behavior of structures in this text.

Example 2-11. Derive the force-deformation relation of a prismatic bar of length L and cross-sectional area A subjected to a uniaxial tensile force F. The material of the bar is linearly elastic, having a modulus of elasticity E.

Assuming that the stress σ is uniformly distributed over a section passing through the bar, we have from Eq. (2-7a)

$$F = \int_A \sigma dA = \sigma \int_A dA = \sigma A$$

Since the material is linearly elastic and follows Hooke's law, we obtain

$$\epsilon = \frac{\sigma}{E} = \frac{F/A}{E} = \frac{F}{AE}$$

Then, the deformation u of the bar is given by Eq. (2-9b) as follows:

$$u = \int_0^L \epsilon \, dx = \int_0^L \frac{F}{AE} dx = \frac{FL}{AE}$$

This is the relationship between the force F and the deformation u.

Example 2-12. A beam element having a length L and a depth $2c$ is subjected to a bending couple M_z, as shown in Fig. 2-44(a). Express the bending stress σ in a fiber at a distance y from the neutral axis in terms of the

bending couple M_z, the moment of inertia I about the z-axis, and the modulus of elasticity E of the linearly elastic material. Also derive an expression showing the moment-rotation relation in bending.

Assuming that plane sections before bending remain plane after bending, we have

$$\frac{y}{c} = \frac{\epsilon}{\epsilon_m}$$

in which ϵ is the strain in a fiber at a distance y from the neutral axis and ϵ_m is the maximum strain in the extreme outer fiber at a distance c from the neutral axis. From Hooke's law

$$\frac{\epsilon}{\epsilon_m} = \frac{\sigma}{\sigma_m}$$

in which σ and σ_m are stresses at fibers with strains ϵ and ϵ_m respectively. Hence,

$$\frac{y}{c} = \frac{\sigma}{\sigma_m} \quad \text{or} \quad \sigma = \frac{y}{c}\sigma_m$$

From Eq. (2-7b),

$$M_z = -\int_A y\sigma\, dA = -\frac{\sigma_m}{c}\int_A y^2 dA = -\frac{\sigma_m I}{c}$$

Thus,

$$\sigma_m = -\frac{M_z c}{I} \quad \text{or} \quad \sigma = -\frac{M_z y}{I}$$

The moment-rotation relation may be obtained directly from Eq. (2-10c) as follows:

$$\varphi_z = -\int_0^L \frac{\epsilon}{y}\, dx = -\int_0^L \frac{\sigma}{Ey}\, dx = \int_0^L \frac{M_z}{EI}\, dx$$
$$= \frac{M_z L}{EI}$$

Example 2-13. A circular bar having a length L and radius R is subjected to a twisting moment M_x as shown in Fig. 2-45(a). Express the shearing stress τ in a circular fiber at a radius r from the center of the bar in terms of the twisting moment M_x, the polar moment of inertia J of the cross section, and the modulus of elasticity in shear, G, of the linearly elastic material. Also derive an expression showing the relationship between the twisting moment and the angle of the twist.

By assuming that plane sections before twisting remain plane after twisting, we have $\tau/r = \tau_m/R$. Then, from Eq. (2-7c),

$$M_x = \int_A r\tau\, dA = \int_A \frac{\tau_m}{R} r^2\, dA = \frac{\tau_m J}{R}$$

in which τ_m is the maximum shearing stress at the outer radius R of the circular section. Hence,

$$\tau_m = \frac{M_x R}{J} \quad \text{or} \quad \tau = \frac{M_x r}{J}$$

The relationship between the twisting moment and the angle of twist may be obtained from Eq. (2-11c) as follows:

$$\varphi_x = \frac{M_x L}{GJ}$$

The intermediate steps in the derivation have been left to the student.

Example 2-14. Derive an expression for the bending stress in a curved bar subjected to pure bending as shown in Fig. 2-48(a).

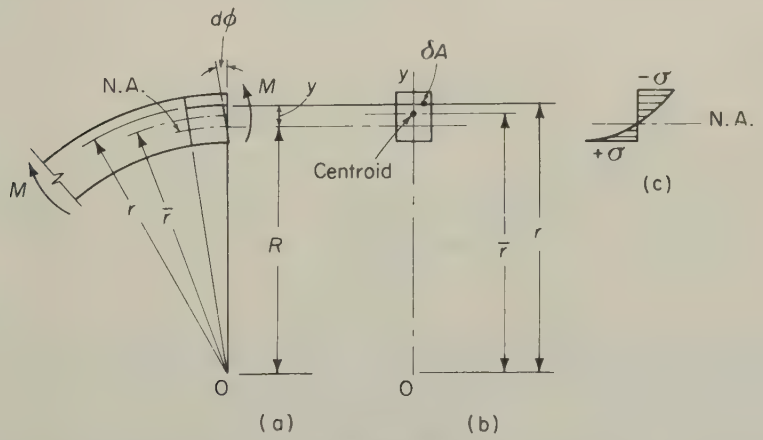

Figure 2-48

In the analysis of curved members, the neutral axis in bending does not coincide with the centroidal axis of the cross section. As a result, the distribution of normal stresses at a section is not linear as it is for straight beams. Although the basic assumptions for curved beams are the same as those for straight members, the main difference is that the initial length of a fiber in a curved beam depends on the distance from the center of curvature. Consider an element subtended by an initial central angle φ before bending as shown in Fig. 2-48(a), which is bent through a small angle of rotation $\delta\varphi$.

Although the total deformation of the fibers in the element varies linearly across the depth of the member, because of the assumption that plane sections before bending remain plane after bending, the strain or deformation per unit length of the fiber does not follow a linear distribution. Thus, the normal strain ϵ in any fiber at a distance r from the center of curvature 0 is equal to

$$\epsilon = -\frac{y\,\delta\varphi}{r\varphi} = -\frac{(r-R)\,\delta\varphi}{r\varphi} = \frac{(R-r)\,\delta\varphi}{r\varphi}$$

The negative sign indicates a compressive strain in the positive direction of y. According to Hooke's law, the normal stress σ on an element δA of the cross section, at the same distance from 0, is

$$\sigma = \epsilon E = \frac{E\,\delta\varphi}{\varphi}\left(\frac{R-r}{r}\right)$$

As in the case of straight beams, the location of the neutral axis and the distribution of normal stresses in a curved beam may be obtained from the conditions of equilibrium of the element. Since no external forces are acting on the section, the algebraic sum of the internal normal stresses over the cross-sectional area must be zero. Referring to an infinitesimal area δA in the cross section shown in Fig. 2-48(b), the sum of all stresses normal to a section leads to $\Sigma F_n = 0$, or

$$\int_A \sigma\,dA = \frac{E\,\delta\varphi}{\varphi}\int_A \frac{R-r}{r}\,dA = 0$$

By simplifying the integral, we obtain the distance R from the neutral axis to the center of curvature. The exact location of the neutral axis is given by

$$R = \frac{A}{\displaystyle\int_A \frac{dA}{r}}$$

Furthermore, the internal moment at the section resulting from the normal stresses must equal the external moment. Thus for $\Sigma M_z = 0$,

$$M = -\int_A y\sigma\,dA = \frac{E\,\delta\varphi}{\varphi}\int_A \frac{(R-r)^2}{r}\,dA$$

Performing the indicated integration, we may express the normal stress as follows:

$$\sigma = \frac{M(R-r)}{rA(\bar{r}-R)}$$

in which $\bar{r}$ is the distance from the centroid of the section to the center of curvature. It can be seen that the distribution of the normal stress across the depth of a curved member follows the pattern shown in Fig. 2-48(c).

In ordinary structures with curved members, however, the radius of curvature of a member is usually so large compared with the depth of the member that the effect of the curvature may be neglected in locating the neutral axis. Thus, for practical purposes, the centroidal axis of a curved structural member may be considered as the neutral axis for bending. As a result, the distribution of normal stress across the depth of the member is assumed to be linear in such cases.

2-9 *Prestressing and Self-straining*

In some structures the force-deformation relations may be influenced by the existence of internal stresses or internal strains without the application of external loads. Such internal stresses or internal strains usually result from prestressing, uneven temperature variations, initial lack of fit, or other similar causes. These effects must be taken into consideration in the formulation of force-deformation relations in this type of structure.

Prestressing. A prestressed structure may be defined as a system in which there have been introduced internal stresses of such magnitude and distribution that the stresses resulting from given external loadings are counteracted to a desired degree. Some common examples are prestressed concrete beams and prestressed guyed wires for tower structures.

Consider, for example, a simple rectangular beam prestressed by a tendon through its centroidal axis and subjected to external loads as shown in Fig. 2-49(a). Due to the prestress force F, a uniform compressive stress

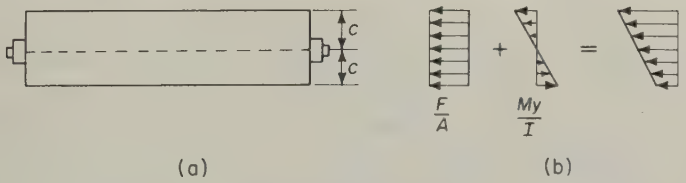

Figure 2–49

will be produced across a section of area A. The magnitude of this stress is

$$\sigma = \frac{F}{A}$$

If M is the external moment at a section due to external dead and live loads and I is the moment of inertia of the section, then the bending stress in a fiber at a distance y from the centroidal axis of the beam is

$$\sigma = \frac{My}{I}$$

Finally, the resulting stress is obtained by

$$\sigma = \frac{F}{A} \pm \frac{My}{I}$$

in which the sign for the bending stress depends on the direction of the moment M. The stress distribution based on a given moment is shown in Fig. 2-49(b).

If the tendon is placed eccentrically by a distance e with respect to the centroid of the section as shown in Fig. 2-50(a), the beam is subjected to

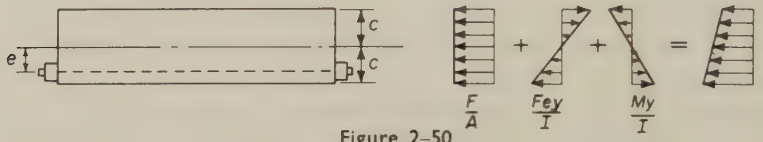

Figure 2–50

an internal moment Fe as well as the internal force F due to the eccentric prestress. Thus, the resulting stress is given by

$$\sigma = \frac{F}{A} \pm \frac{Fey}{I} \pm \frac{My}{I}$$

the distribution of which is shown in Fig. 2-50(b).

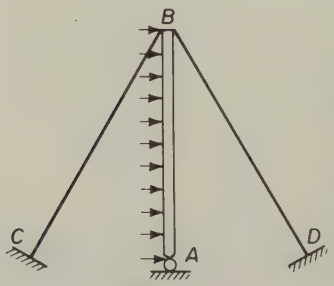

Figure 2–51

In the case of structures guyed against overturning by wires in more than one direction, the guys are usually prestressed so that they will always be in tension under loads. Consider, for example, the guyed mast in Fig. 2-51. When the uniform horizontal load is applied in the direction as shown, point B tends to move to the right as wire BC is stretched. If the wires are not prestressed, wire BD will not be able to resist the load as a slight movement of the top of the mast to the right will produce a sag in wire BD. If the wires are pretensioned to a magnitude greater than one-half of the maximum tension that may occur in the unprestressed case, the movement of the top of the mast to the right will cause only the relaxation in tension in wire BD. Thus, the prestressed wires are always in tension whether the load comes from the direction shown in the figure or from the opposite direction.

Thermal effects. Temperature changes produce effects on strains in the elastic range in two ways. First, strain may be introduced in a structure

by temperature in the absence of external forces. Secondly, the material properties such as modulus of elasticity, yield strength, and coefficient of linear expansion vary significantly with temperature in certain temperature ranges. The former occurs in all structures subjected to temperature variations wherever the latter is becoming increasingly important in the design of pressure vessels, reactors, and furnaces for industrial plants.

Thermal strains in an isotropic material must be pure expansions or contractions with no shear strains along any set of axes. For a slender structural member, only the normal strain along the axis of the member need be considered. For the ordinary range of temperature changes in structures, the thermal strains vary linearly with temperature and, for a change of temperature from T_0 to T, may be expressed by

$$\epsilon_t = \alpha (T - T_0) \tag{2-13}$$

where ϵ_t is the thermal strain and α is called the *coefficient of linear expansion* of the material. For a rise in temperature ϵ_t is positive, and for a temperature drop ϵ_t is negative. For a structural member that may expand and contract freely, the total strain due to external forces and temperature changes may be obtained by adding together the elastic strain and thermal strain. On the other hand, if the change in length of a structural member resulting from temperature encounters resistance in its axial direction, thermal expansion or contraction is retarded. This situation is identical to that of a member subjected to an elastic strain having the same magnitude but opposite sense of the retarded thermal strain ϵ_t. Thermal stresses in the member would then be given by

$$\sigma_t = - E\epsilon_t = E\alpha(T_0 - T) \tag{2-14}$$

Metals are used in a wide range of temperatures for special structures

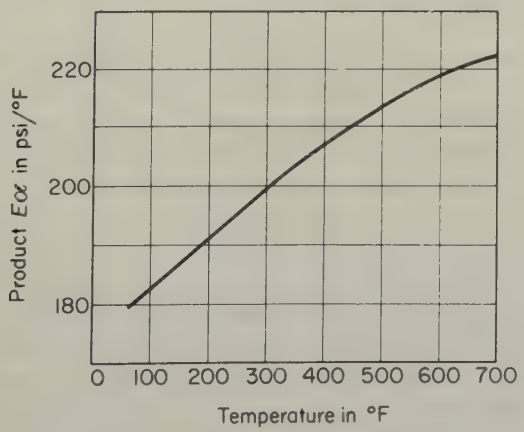

Figure 2–52

in industry. One important characteristic of ferrous metals such as mild steel is the sudden loss in toughness when a certain low temperature is reached. This temperature at which the material abruptly shows signs of brittleness is called the *transition temperature*. On the other hand, at high temperatures, some ferrous metals such as mild steel exhibit increasing ductility but decreasing yield strength. Both the modulus of elasticity and the coefficient of linear expansion vary with temperature, and the typical variation of the product $E\alpha$ with temperature for mild steel is shown in Fig. 2-52. These factors must be considered in the analysis of structures subjected to temperature variations.

Example 2-15. A concrete pavement slab 10 ft long is poured at 50°F. The material has a modulus of elasticity $E = 3 \times 10^6$ psi and a coefficient of linear expansion $\alpha = 5.5 \times 10^{-6}$ in./in./°F. Neglecting friction or other restraining forces, determine the increase in length of the slab when the temperature is 120°F. If only one-half of this thermal expansion is permitted by the expansion joint, determine the thermal stresses produced in the pavement.

When the slab is free to expand, the thermal expansion is given by

$$u_t = \epsilon_t L = \alpha(T - T_0)L$$
$$= (5.5 \times 10^{-6})(120 - 50)(10) = 3.85 \times 10^{-3} \text{ ft}$$

If only one-half of this expansion is permitted by the expansion joint, the thermal stresses in the pavement become

$$\sigma_t = -(3 \times 10^6)\left(\frac{1.925 \times 10^{-3}}{10}\right) = -578 \text{ psi}$$

The negative sign indicates that the stress is compressive.

Other causes of self-straining. Internal stresses also may result from internal strains due to initial lack of fit of a structural member. If a member of length L is made too long by an amount u, internal compressive stress will be produced when it is forced into a spacing of the intended length. Thus,

$$\sigma = -\frac{Eu}{L} \tag{2-15}$$

The same equation may be used when a structural member of length L is restrained at its ends in order to prevent the shrinkage of the member. In this case, the term u would represent the amount of shrinkage if the member were free. Thus, u is a negative quantity, and the resulting internal stress will be tensile.

Some structural members subjected to long-time sustained loads deform

progressively with time, especially at elevated temperatures. Such a phenomenon is called *creep*. If the stress in a member remains unchanged while creep deformation takes place, a study of the creep deformation-time relation of the material becomes exceedingly important if excessive deformation is to be avoided. On the other hand, in some engineering applications the stress in a member may diminish with time as a result of creep. Such a reduction of stress is called *creep relaxation*. In the analysis of this type of problem, creep stress-relaxation properties of the material must be investigated.

2-10 Linear Structural Systems

In previous sections, it has been shown that the reactions and internal forces of a statically determinate structure may be obtained from the consideration of the equilibrium of the structure as a whole or a part thereof. The reactions and internal forces can, in general, be expressed as unknowns of a set of linear simultaneous equations. For statically indeterminate structures, additional equations must be obtained from the force-deformation relations. If the stress-strain relation of the material is linearly elastic, the equations representing the force-deformation relations are also linear functions of unknown reactions or internal forces. Thus, the analysis of linear structural systems may be reduced to the solution of a large system of linear simultaneous equations.

Although this general approach is not always desirable because of the lengthy numerical computations in the solution of simultaneous equations, it does stress the simplicity of the basic theory of linear structural systems. With the aid of electronic digital computers, the numerical solution of a large system of linear simultaneous equations is no longer so objectionable. The student should be familiar with the standard procedures for solving linear simultaneous equations such as Gaussian elimination, iteration, relaxation, matrix inversion, and other methods.*

One important characteristic of linear structural systems is that the *principle of superposition* can be used for their solutions. This principle, which has wide applications in structural analysis, simply states that if several causes act simultaneously on a system and if each effect is directly proportional to its cause, then the total effect is the sum of the individual effects. For instance, the strain in a structural member resulting from several applied forces is the algebraic sum of the strains caused by the forces applied separately if each strain is linearly related to the force causing it. In view of the fact that plane sections before deformation are assumed to remain plane after deformation without significant error for a member subject to

*See, for instance, Reference 2-6.

axial force, twisting moment, or bending moment, the strain in each case is indeed directly proportional to the corresponding applied force. On the other hand, stress is proportional to strain only in the elastic range of the material. Hence the stress in a structural member resulting from several applied forces is the algebraic sum of their effects only if Hooke's law holds true. Similarly, the deflections of beams subjected to several vertical loads can also be obtained by the principle of superposition. Again, this approach is possible because the deflection caused by each load is directly proportional to the curvature thus produced in the elastic range of the material. Hence, the analysis of linear structural systems can often be simplified by using the principle of superposition.

Example 2-16. Set up a system of equations for the solution of (a) reactions and (b) reactions and internal forces in the structure in Fig. 2-53(a).

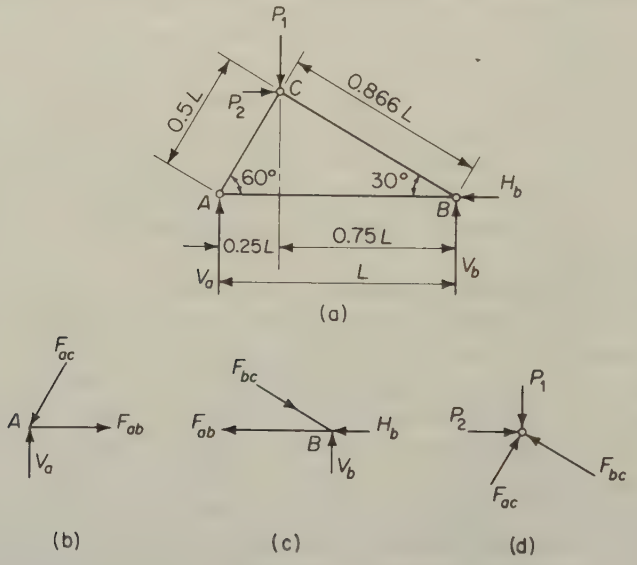

Figure 2–53

By considering the entire structure as a free body, we can establish three equations of equilibrium.

$$\sum F_x = 0, \quad P_2 - H_b = 0 \tag{a}$$

$$\sum F_y = 0, \quad V_a + V_b - P_1 = 0 \tag{b}$$

$$\sum M_a = 0, \quad V_b L - (0.25L)P_1 - (0.433L)P_2 = 0 \tag{c}$$

Thus, the components of reaction V_a, V_b, and H_b may be solved in terms of the given loads P_1 and P_2.

If the internal forces as well as the reactions are required, there are altogether six unknowns, i.e., V_a, V_b, H_b, F_{ab}, F_{ac}, and F_{bc}. Since two equations can be written for each joint of a plane truss, we shall consider joints A, B, and C as free bodies as shown in Figs. 2-53(b), (c), and (d) respectively. Then, for joint A,

$$\sum F_y = 0, \quad V_a - 0.866F_{ac} = 0 \tag{d}$$

$$\sum F_x = 0, \quad F_{ab} - 0.5F_{ac} = 0 \tag{e}$$

For joint B,

$$\sum F_x = 0, \quad 0.866F_{bc} - F_{ab} - H_b = 0 \tag{f}$$

$$\sum F_y = 0, \quad V_b - 0.5F_{bc} = 0 \tag{g}$$

For joint C,

$$\sum F_y = 0, \quad 0.866F_{ac} + 0.5F_{bc} - P_1 = 0 \tag{h}$$

$$\sum F_x = 0, \quad 0.5F_{ac} - 0.866F_{bc} + P_2 = 0 \tag{i}$$

Thus, we obtain a system of six simultaneous equations involving six unknowns.

One may question whether we have actually written nine equations for six unknowns since Eqs. (a), (b), and (c) also involve three of the unknowns. However, although there are nine equations, only six of them are independent. The remaining three can be obtained by a linear combination of the first six equations. For instance, Eqs. (a), (b), and (c) can be obtained by the following combinations respectively:

$$\text{(a)} = \text{(e)} + \text{(f)} + \text{(i)}$$

$$\text{(b)} = \text{(d)} + \text{(g)} + \text{(h)}$$

$$\text{(c)} = L \times \text{(g)} + 0.25L \times \text{(h)} - 0.433L \times \text{(i)}$$

Thus, the number of independent equations is the same as the number of unknowns.

Example 2-17. Establish a system of equations for the solution of the components of reaction of the arch in Fig. 2-54. Discuss the possibility of geometrical instability of the system.

From the condition of equilibrium, we can establish

$$\sum F_x = 0, \quad H_a - H_b = 0 \tag{a}$$

$$\sum F_y = 0, \quad V_a + V_b = P \tag{b}$$

$$\sum M_b = 0, \quad V_a L + H_a r = PL_b \tag{c}$$

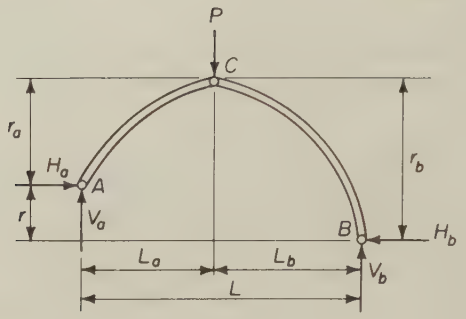

Figure 2–54

An additional equation is obtained from the condition of release at hinge C. Thus.

$$\sum M_c = 0, \quad V_a L_a - H_a r_a = 0 \tag{d}$$

This system of four equations involves four unknowns V_a, V_b, H_a, and H_b, which can be obtained from the solution of the equations.

The coefficients of the unknowns in this set of equations may be arranged in the following form:

	V_a	V_b	H_a	H_b
Eq. (a)	0	0	1	−1
Eq. (b)	1	1	0	0
Eq. (c)	L	0	r	0
Eq. (d)	L_a	0	$-r_a$	0

If we want to obtain a set of unique and finite answers from the solution of the simultaneous equations by Cramer's rule,* it is obvious that the determinant formed by the coefficients of the unknowns cannot be zero. Expanding the determinant by minors, we have

$$D = \begin{vmatrix} 0 & 0 & 1 & -1 \\ 1 & 1 & 0 & 0 \\ L & 0 & r & 0 \\ L_a & 0 & -r_a & 0 \end{vmatrix} = \begin{vmatrix} 1 & 1 & 0 \\ L & 0 & r \\ L_a & 0 & -r_a \end{vmatrix} = - \begin{vmatrix} L & r \\ L_a & -r_a \end{vmatrix}$$

$$= r_a L + r L_a = r_a(L_a + L_b) + (r_b - r_a)L_a = r_a L_b + r_b L_a$$

Since r_a, r_b, L_a, and L_b are all positive for an arch, D will always be non-zero. Hence, the structure is always stable.

*See, for instance, p. 161 of Reference 2-6.

If r_b becomes negative while r_a remains positive, it is possible for D to be zero. However, it would mean physically that while point A is located at an elevation below point C, point B is located at an elevation above point C. In that case, the structure is no longer an arch in the ordinary sense. For the special case $r_a = r_b = 0$, the determinant D is zero. This would be equivalent to a horizontal bar with a hinge at some interior point as well as at the ends. Such a system is known to be geometrically unstable, and this is confirmed by the fact that $D = 0$.

Example 2-18. Write a set of equations for the determination of the reactions of the continuous beam in Fig. 2-55.

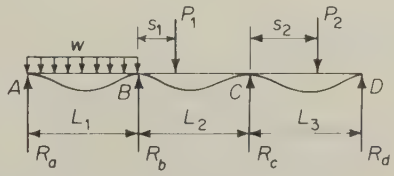

Figure 2–55

From the conditions of equilibrium, we have

$$\sum F_y = 0, \quad R_a + R_b + R_c + R_d = wL_1 + P_1 + P_2 \tag{a}$$

$$\sum M_a = 0, \quad -\frac{wL_1^2}{2} - P_1(L_1 + s_1) - P_2(L_1 + L_2 + s_2) + R_bL_1 + R_c(L_1 + L_2) + R_d(L_1 + L_2 + L_3) = 0 \tag{b}$$

Since the system is statically indeterminate to the second degree, two additional equations must be obtained from the conditions of compatibility. For this problem, we have obtained in Section 2-7

$$\delta_b' + R_b\delta_{bb} + R_c\delta_{bc} = 0 \tag{c}$$

$$\delta_c' + R_c\delta_{cb} + R_c\delta_{cc} = 0 \tag{d}$$

In Eqs. (c) and (d), the displacements can be obtained first from the released system, which is a statically determinate system and has known elastic properties. Thus, we have a set of four simultaneous equations for the four unknown reactions.

2-11 *Nonlinear Structural Systems*

The nonlinear force-deformation relation in a structural system can be caused by either the nonlinear stress-strain characteristics in the material or the state of unstable equilibrium of the system even if the material is

linearly elastic. The buckling of a column is an example of the latter. When the force-deformation relation in a structural member is nonlinear, the analysis becomes more complicated. The difficulty is further increased because the principle of superposition cannot be used in such cases. For these reasons, this type of structural system will be only briefly mentioned in this introductory text.

The determination of the force-deformation relation for a structural member due to nonlinear material characteristics will be discussed later in Section 2-15. We shall now consider an example of nonlinear force-deformation relation in a system whose members are made of a linearly elastic material.

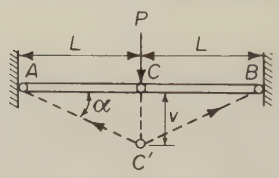

Figure 2–56

The structural system in Fig. 2-56 is in a position of unstable equilibrium because no horizontal reactions will be developed until the structure has deformed excessively. As a result, the force-deformation relation of the system is nonlinear. Let us consider the system in its deformed position as indicated by the dotted lines when the material remains in the elastic range. Because of symmetry, the internal forces in bars AC and BC are equal. Let F be the bar force when the system is in the deformed position. Then,

$$\sum F_y = 0, \quad 2F \sin \alpha = P$$

For small angles of α, we can use the approximation

$$\sin \alpha = \tan \alpha = v/L$$

Hence,

$$\frac{2Fv}{L} = P \quad \text{or} \quad F = \frac{PL}{2v}$$

The strain in each bar can be obtained from

$$\epsilon = \frac{1}{L}(\sqrt{L^2 + v^2} - L) = \left[1 + \frac{v^2}{L^2}\right]^{1/2} - 1 \approx \frac{1}{2}\frac{v^2}{L^2}$$

Then, from Hooke's law, we have $\sigma = F/A = \epsilon E$, or

$$F = A\epsilon E = \frac{AEv^2}{2L^2}$$

Hence, the relation between the load P and the displacement v is given by

$$P = \frac{2Fv}{L} = \frac{AEv^3}{L^3}$$

The internal force F in each bar may also be expressed in terms of the load P

and the geometrical and material properties of the bar. Since $v = PL/2F$, we have

$$F = \frac{AE\left(\frac{PL}{2F}\right)^2}{2L^2} = \frac{AEP^2}{8F^2}$$

Then,

$$F = \tfrac{1}{2}\sqrt[3]{AEP^2}$$

2-12 *Conservative Systems—Energy Approach*

The equilibrium of forces and the compatibility of displacements in a structural system may also be established from the consideration of the conservation of energy in the system. The *principle of conservation of energy* states that the total energy of an isolated system remains constant. In the application of this principle to any system, all major changes in a system should be included. If dissipation of energy is involved, the energy loss should be properly taken into consideration.

The work performed to displace a system slowly from one configuration to another may depend on the path of motion. Consider, for instance, a bar of constant cross section subjected to a gradually applied axial force as shown in Fig. 2-57(a). The work done by the force in deforming the bar

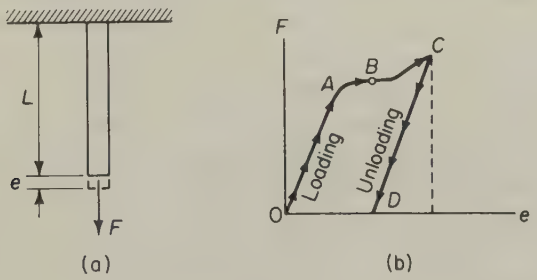

Figure 2–57

by an amount e_1 is defined as

$$W = \int_0^{e_1} F\,de$$

in which e is the displacement in the direction of the force F. Then, the work done at any instant during loading is represented by the area under the force-displacement curve corresponding to the displacement e at that instant, as shown in Fig. 2-57(b). If the force F increases linearly from zero

until it reaches point A on the curve, the bar will, upon unloading, return to its original undeformed shape. Thus, no net work is performed in a complete cycle of loading and unloading. Similarly, if the material is elastic up to point B, although the elasticity is nonlinear, all work performed up to point B is recoverable. On the other hand, if the force-displacement relation of the bar is inelastic, the unloading curve will be different from the loading curve. For example, if the bar is loaded to point C in the inelastic range and then unloaded, as shown in Fig. 2-57(b), only the portion of internal energy as represented by the area under the unloading curve CD is recoverable. The rest of the energy absorbed by the bar during loading, as represented by the area between the loading curve and the unloading curve, is dissipated in permanently deforming the body. Thus, from the principle of conservation of energy, the work done on the deformable body equals the sum of the recoverable energy and the energy dissipation or loss as a result of the permanent deformation of the material.

When the work done by the external and internal forces in a system does not depend on the path of motion, the system is called a *conservative system*. Then, the external and internal forces are both said to be *conservative forces*. All work performed on a conservative system is recoverable. If we designate a certain fixed configuration of a conservative system as the zero configuration, the work performed to displace the system slowly from the zero configuration to any other configuration is called the *potential energy* of the system at the final configuration. If a conservative system is transferred around a closed path, no net work is performed since the final configuration coincides with the initial configuration of the system.

In structural systems, external forces such as dead loads or other equivalent static loads are usually constant. In considering the potential energy of such a system, we imagine that the external forces act while the structure is deformed. If a structural system is elastic, the work done by the internal forces in the system is recoverable. Thus, such structural systems are conservative systems.*

2-13 *Potential Energy*

The potential energy of a structural system is the energy stored in the system as a result of the work performed by the external and internal forces to transfer the system from one configuration to another. The total potential energy of the system is, therefore,

$$U = U_e + U_i$$

in which U_e is the *potential energy of the external forces* and U_i is the *potential*

*See Reference 2-5 for further discussions.

energy of the internal forces. For a rigid system, the internal forces of the system perform no work since there is no relative displacement in a rigid system. If the constant gravitational force is the only external force acting on a rigid system, the potential energy of the system is equal to the weight of the system multiplied by the difference in elevation as the system is raised to a certain elevation from an initial datum. Thus, when we speak of the potential energy of a rigid system, we refer to the potential energy of the external forces only. When the rigid system is at rest, the gravitation force is the only source of the potential energy. The work done by the internal forces of a deformable system is the potential energy of deformation. Thus, the total potential energy of a deformable system consists of the potential energy of the loading U_e and the energy of deformation U_i.

Consider, for example, a spring-mass system in which the mass M is suspended by a spring of negligible mass, as shown in Fig. 2-58. The spring is stretched by an amount e_1 when the system is at rest. If h is the height of the suspended mass above an arbitrary datum and g is the gravitational acceleration, the total energy of the system with reference to the fixed datum is

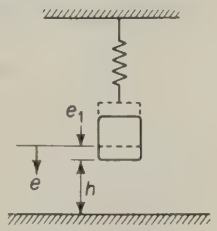

Figure 2–58

$$U = U_e + U_i = Mgh + \int_0^{e_1} F\,de \qquad \text{(a)}$$

in which F is the force in the spring. However, if the position of the mass at no stretching of the spring is used as a zero configuration, then the total potential energy of the system with reference to the latter datum is

$$U = -Mge_1 + \int_0^{e_1} F\,de \qquad \text{(b)}$$

Note that the external force Mg results from gravitation and is unaffected by the properties of the spring, whereas the internal force F is a function of the displacement e. If the spring is linearly elastic, the force is directly proportional to the displacement, i.e., $F = ke$, in which k is the spring constant. Then, Eq. (b) becomes

$$U = -Mge_1 + \tfrac{1}{2}ke_1^2 \qquad \text{(c)}$$

The application of the total potential energy to establish the conditions of equilibrium of structural systems can be illustrated by the following important principles.

Stationary potential energy. A function is said to be stationary at a point where its first derivatives all vanish. When a conservative system is in equilibrium, its potential energy is stationary. That is,

$$\delta U = \delta U_e + \delta U_i = 0 \qquad \text{(2-16)}$$

This is known as the *principle of stationary potential energy*. In general, for a conservative system with n degrees of freedom, the potential energy U of the system is a function of n generalized coordinates $(x_1, x_2, \ldots, x_n)$. If the first partial derivates of U are continuous, we have

$$\frac{\partial U}{\partial x_1} = 0, \quad \frac{\partial U}{\partial x_2} = 0, \quad \ldots, \quad \frac{\partial U}{\partial x_n} = 0 \tag{2-17}$$

Thus, the principle may also be stated as follows: A conservative system is in equilibrium if the first partial derivatives of the potential energy with respect to the generalized coordinates are all zero.

It is possible to demonstrate this principle in general terms. For the sake of simplicity, however, we consider only a specific example with one degree of freedom. If we refer again to Fig. 2-58, the increment δU of the potential energy function U can be obtained by first differentiating Eq. (c) with respect to the generalized ordinate e_1 as follows:

$$\frac{dU}{de_1} = -Mg + ke_1$$

Since $F_1 = ke_1$ when the spring is at rest, and in this instance, $F_1 = Mg$, we have

$$\frac{dU}{de_1} = -Mg + F_1 = 0$$

Then, for a small displacement δe_1 from the equilibrium position,

$$\delta U = \frac{dU}{de_1}\,\delta e_1 = 0$$

This example demonstrates the application of the principle of stationary potential energy. A more formal proof is beyond the scope of this book.

Minimum potential energy. The concept of total potential energy also provides a criterion for stability of conservative systems. As a manifestation of the efficiency of nature, the total potential energy of a system in stable equilibrium is a relative minimum whereas that of a system in unstable equilibrium is a relative maximum. However, the principle of stationary potential energy gives only the necessary but not sufficient condition for stable equilibrium. Indeed, Eq. (2-16) may point to a maximum U instead of a minimum U. Hence, a further restriction is needed by the introduction of the *principle of minimum potential energy*, which states that a conservative system is in stable equilibrium if its potential energy is a relative minimum.

Consider, for example, a solid sphere that is placed successively in three different positions A, B, and C, as shown in Fig. 2-59. The potential energy of the sphere is entirely due to the gravitational force since it is a rigid body with no internal deformation. The sphere at A is in unstable equilibrium

because it will depart completely from its summit position after a slight disturbance. Its potential energy is a relative maximum since point A is higher than its neighboring points. On the other hand, the sphere at B is in stable equilibrium because it will eventually return to its valley position after a slight disturbance. Its potential energy is a relative minimum since point B is lower than its neighboring points. The sphere at C is in neutral equilibrium because it remains in the state of equilibrium in the level region after a slight disturbance. Its potential energy is unchanged or stationary in comparison with that of its neighboring points.

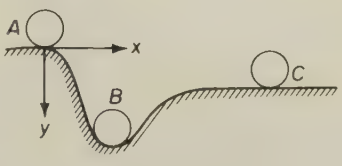

Figure 2–59

The criterion for stability can also be derived in more general terms. However, we provide here only the mathematical proof of the simple example just cited. Let $y = y(x)$ be the contour of the ground with positive directions of x and y shown in Fig. 2-59. In order that the ball be maintained in a state of equilibrium, it must be placed at a point where the tangent of the contour is horizontal because the ball will depart immediately from any position on a slope. Furthermore, in order to ensure stable equilibrium, the point on the contour must represent a valley relative to its neighboring points. We shall see that these conditions will be met if the potential energy of the sphere is a relative minimum.

The potential energy of a rigid ball of weight W placed at a point on the contour that is located at a distance y below the origin A is

$$U = -Wy$$

According to the principle of stationary potential energy, $\delta U = 0$ for a system in equilibrium. Hence

$$\delta U = -W\,\delta y = 0 \qquad \text{(d)}$$

By definition,

$$\delta y = y(x + \delta x) - y(x)$$

Expanding $y(x + \delta x)$ by Taylor's series, we get

$$\delta y = y'(x)\,\delta x + \frac{y''(x)}{2!}(\delta x)^2 + \frac{y'''(x)}{3!}(\delta x)^3 + \ldots \qquad \text{(e)}$$

Taking only the first term of Eq. (e) when δx is infinitely small and substituting into Eq. (d), we have

$$\delta U = -Wy'(x)\,\delta x = 0 \qquad \text{(f)}$$

which implies $y'(x) = 0$, or the tangent of the contour is horizontal at a point where the ball is in equilibrium.

When δx is finite but small, the change of potential energy δU can be given as

$$\delta U = -Wy'(x)\delta x + \epsilon \tag{g}$$

where

$$\epsilon = -\frac{Wy''(x)}{2!}(\delta x)^2 - \frac{Wy'''(x)}{3!}(\delta x)^3 - \cdots \tag{h}$$

If δx is sufficiently small, the sign of ϵ depends on the first term of Eq. (h). When $y''(x)$ is positive, ϵ is negative regardless of the sign of δx since it is squared. When $y''(x)$ is negative, ϵ is positive. In Fig. 2-59, a positive rate of change of slope, i.e., positive $y''(x)$, corresponds to a summit, and a negative rate of change of slope, i.e., negative $y''(x)$, corresponds to a valley. Hence, the departure from a summit causes a decrease in potential energy, since ϵ is negative in Eq. (g), whereas the displacement from a valley increases in potential energy because ϵ is positive in Eq. (g). The maximum potential energy is therefore associated with unstable equilibrium whereas the minimum potential energy is associated with stable equilibrium.

2-14 *Principle of Virtual Work*

The principle of virtual work is primarily concerned with the application of the principle of conservation of energy when a system in equilibrium is subjected to imaginary displacements, or when a system having compatible displacements and constraints is subjected to imaginary equilibrating forces. In the case of rigid systems, however, we are only dealing with the former application as developed in this section. A more general discussion of the principle of virtual work for deformable systems will be treated later in Section 8-6.

The principle of virtual work for rigid systems may be derived from the principle of minimum potential energy, which implies that a conservative system is in stable equilibrium if the potential energy is increased for every small displacement. Since work must be performed to increase the potential energy, it may be stated that a conservative system is in stable equilibrium if the total amount of work done by the forces in the system must be zero for an arbitrary displacement. The arbitrary displacement may be infinitesimal or finite. In fact, it may be imaginary as long as it is geometrically possible. Hence, such a displacement is called the *virtual displacement*, and the principle associated with it is called the *principle of virtual displacements* or the *principle of virtual work*.

However, the principle of virtual work may be proved directly by using the concept of work without referring to the principle of minimum potential energy. If a force P is given an arbitrary displacement δs in the direction of

the force, the amount of work done by the force is $\delta W = P\ \delta s$. Similarly, if a couple M acts through an arbitrary rotation $\delta\varphi$ in the direction of the couple, the amount of work done by the couple is $\delta W = M\ \delta\varphi$. Thus, the total amount of work done by a set of forces and couples in a conservative system subjected to an arbitrary displacement is the sum of the work performed by all forces and couples. If the system of forces and couples is in equilibrium, the net amount of work must be zero.

Consider a system consisting of forces P_1, $P_2, \ldots, P_n$, the resultant of which is P_r. If the system is given an arbitrary displacement δs in the direction of the resultant P_r as shown in Fig. 2-60, the work done by any force P_i is the product of the displacement δs and the projection of the force on the direction of the displacement δs. This projection of force is equal to $P_i \cos \alpha_i$, in which α_i is the angle between the positive direction of δs and the force P_i. Thus, the product representing the amount of work done by P_i is given by

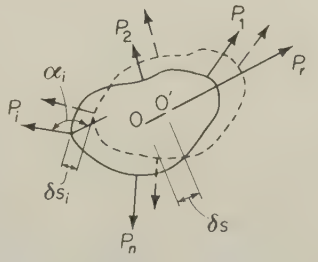

Figure 2–60

$$(P_i \cos \alpha_i)\ \delta s = P_i(\delta s \cos \alpha_i) = P_i \delta s_i$$

in which δs_i is the displacement in the direction of P_i as a result of δs in the direction P_r. Then, the total amount of work done by all forces in the system may be expressed as follows:

$$P_1\ \delta s_1 + P_2\ \delta s_2 + \ldots + P_n\ \delta s_n = P_r\ \delta s \qquad \text{(a)}$$

When the system is in equilibrium, the resultant $P_r = 0$ and the displacement δs can therefore be assumed in any arbitrary direction. For the condition of equilibrium, Eq. (a) becomes

$$P_1\ \delta s_1 + P_2\ \delta s_2 + \ldots + P_n\ \delta s_n = 0 \qquad \text{(2-18)}$$

Equation (2-18) is a statement of the principle of virtual displacements in the mathematical form. Since the displacements in the system may be finite as well as infinitesimal, the principle may also be expressed as

$$P_1 s_1 + P_2 s_2 + \ldots + P_n s_n = 0 \qquad \text{(2-19)}$$

For some problems, it is sometimes convenient to consider the instantaneous velocities along the lines of action of forces $P_1, P_2, \ldots, P_n$. In that case, we may differentiate Eq. (2-19) with respect to time. Thus,

$$P_1 \frac{ds_1}{dt} + P_2 \frac{ds_2}{dt} + \ldots + P_n \frac{ds_n}{dt} = 0 \qquad \text{(2-20)}$$

Equation (2-20) is known as the *principle of virtual velocities.*

The application of the principle of virtual work is illustrated by the cantilever beam in Fig. 2-61. The beam is in equilibrium under the action of forces P and R and moment M. The coordinate system with origin at O is arbitrarily chosen. Let the beam be given a virtual displacement δy in the direction of positive y. Then,

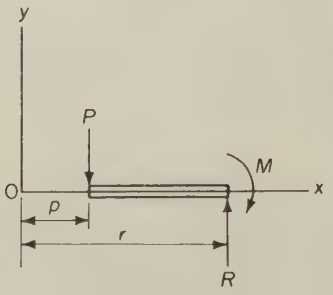

Figure 2-61

$$-P\,\delta y + R\,\delta y = 0 \qquad \text{(b)}$$

Note that the force R is preceded by a positive sign because it is in the direction of the displacement, i.e., $\cos\alpha = \cos 0^\circ = 1$, and the force P is preceded by a negative sign because it is opposite to the direction of displacement, or $\cos\alpha = \cos 180^\circ = -1$. If the beam is given a virtual displacement δx in the positive direction of x, no work is done because both R and P are perpendicular to the direction of the displacement. Thus, the equation of virtual work will be identically zero. In each case, the moment M does not enter into the picture because the moment of a couple is independent of the position. Next, the beam is given a virtual displacement in the form of a clockwise rotation $\delta\varphi$ about a fixed point, say the origin O. Then,

$$M\,\delta\varphi + Pp\,\delta\varphi - Rr\,\delta\varphi = 0 \qquad \text{(c)}$$

Simplifying Eqs. (b) and (c), we have

$$\begin{aligned} -P + R &= 0 \\ M + Pp - Rr &= 0 \end{aligned}$$

These are precisely the equations of equilibrium of the system.

2-15 *Strain Energy and Complementary Energy*

We shall now turn to the analysis of displacements by means of the energy approach. There are two energy quantities of particular interest in this regard—the strain energy and the complementary energy. The application of energy principles for the computation of displacements of deformable systems will be treated thoroughly in Chapter 8. It is sufficient to point out here that the requirement of compatibility of displacements as well as the requirement of equilibrium of forces can be derived from the energy approach.

Let us consider again a prismatic bar of length L subjected to a gradually applied axial force F. The force-deformation relation, shown in Fig. 2-62, is elastic but not necessarily linear. The area under the curve OA represents

the work done on the bar by the force. The *energy of deformation* or *strain energy* stored in the bar is given by

$$U_i = \int_0^{e_1} F\,de \qquad (2\text{-}21)$$

On the other hand, the area above the curve OA represents an integral

$$U_c = \int_0^{F_1} e\,dF \qquad (2\text{-}22)$$

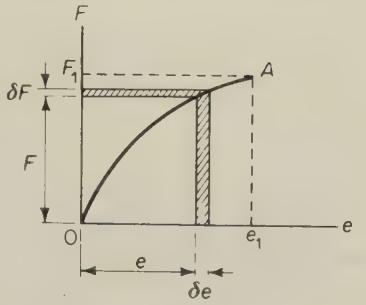

Figure 2–62

which is called the *complementary energy* or *stress energy* as opposed to strain energy. Complementary energy is a mathematical term that has in general no physical meaning, but it is very useful in the computation of displacements.

Differentiating the strain energy U_i and the complementary energy U_c, we obtain from Eqs. (2-21) and (2-22) respectively

$$F_1 = \frac{dU_i}{de} \qquad (2\text{-}23)$$

$$e_1 = \frac{dU_c}{dF} \qquad (2\text{-}24)$$

Note that, in general, the strain energy can only be used to derive the force, and the complementary energy can only be used to derive displacement. For linear systems, however, the two quantities are numerically equal and hence are interchangeable. This follows from the fact that for linear systems, the force-deformation curve is a straight line, and the areas under and above the line are both triangles of equal area. It can also be shown mathematically that, for $F = ke$, where k is a constant of proportionality, $dF = k\,de$, or $de = dF/k$. Then,

$$U_i = \int_0^{e_1} F\,de = \int_0^{F_1} ke\left(\frac{dF}{K}\right) = \int_0^{F_1} e\,dF = U_c$$

Although the derivation given in this section is confined solely to a bar subjected to axial force, the concept is equally applicable to other forms of force-displacement relations. Note, for example, the similarity of the force-displacement curves for simple tension, pure bending, and pure torsion of a circular bar, as shown in Figs. 2-63 (a), (b), and (c) respectively. Note that M_z and M_x have the unit of force-length whereas φ_z and φ_x are in radians. Thus, the unit of strain energy in bending or twisting is identical to that of uniaxial tension. Therefore, the strain energy in bending and torsion may also be obtained from the area under the corresponding

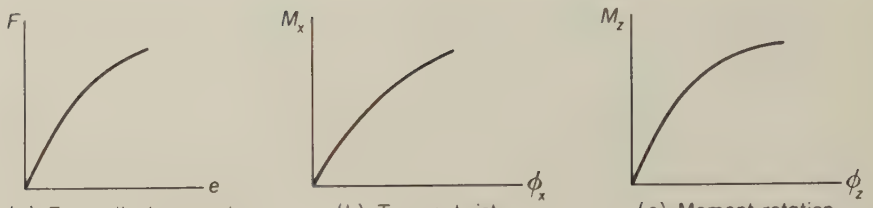

(a) Force-displacement (b) Torque-twist (c) Moment-rotation

Figure 2–63

curve, whereas the complementary energy may be found from the area above the same curve.

Example 2-19. Compute the axial deformation of a bar subjected to a gradually applied axial force P if the material characteristic of the bar is given by Fig. 2-64, in which F is the axial force and e is the axial deformation.

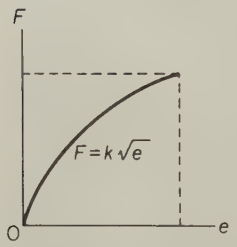

Figure 2–64

Since the material characteristic is nonlinear, the complementary energy should be used in the computation of axial deformation. Thus, the complementary energy may be obtained as

$$U_c = \int_0^{F_1} e\, dF = \int_0^{F_1} \frac{F^2}{k^2}\, dF = \frac{F_1^3}{3k^2}$$

Hence, the axial deformation is equal to

$$e_1 = \frac{dU_c}{dF} = \frac{F_1^2}{k^2}$$

The result is obvious since it can also be obtained from the equation representing the material characteristic by letting $F = F_1$ and $e = e_1$.

2-16 *Summary*

In summary, structural systems can be analyzed from either the equilibrium or the energy point of view. For both approaches, the procedure of analysis may be briefly stated as follows:

1. The reactions and internal forces in a structure can be formulated from the equations of equilibrium, or from a combination of the equations of equilibrium and the conditions of release. If the structure is statically determinate, there will be a sufficient number of equations for the solution of reactions and internal forces.
2. The deformations of a structure are related to the internal forces in the

structure according to the material characteristics of its members. For a statically determinate structure, the deformations can readily be obtained from the known internal forces, the conditions of continuity, and the stress-strain relation.

3. For statically indeterminate structures, the equations of equilibrium or a combination of equations of equilibrium and conditions of release are not sufficient to determine the unknown reactions or internal forces in the structure. Then, additional equations must be sought from the conditions of geometrical compatibility of deformations. The solution of such problems usually involves a large number of simultaneous equations with an equal number of unknowns.

This chapter has provided only a broad outline of the basic approaches. The detailed methods of analysis will be treated in subsequent chapters.

References

2-1 C. Inglis, *Applied Mechanics for Engineers*, Cambridge University Press, New York, 1951.

2-2 A. Higdon and W. B. Stiles, *Engineering Mechanics*, 2nd ed., Prentice-Hall, Inc., Englewood Cliffs, N.J., 1955.

2-3 E. Popov, *Mechanics of Materials*, Prentice-Hall, Inc., Englewood Cliffs, N.J., 1952.

2-4 I. H. Shames, *Engineering Mechanics*, Prentice-Hall, Inc., Englewood Cliffs, N.J., 1959.

2-5 T. M. Charlton, *Energy Principles in Applied Statics*, Blackie & Son Limited, London, 1959.

2-6 R. G. Stanton, *Numerical Methods for Science and Engineering*, Prentice-Hall, Inc., Englewood Cliffs, N.J., 1961.

Problems

2-1 to **2-14** In each of the systems in Figs. P2-1 to P2-14, compute the components of reaction.

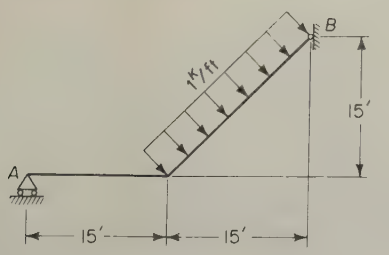

Figure P2-1

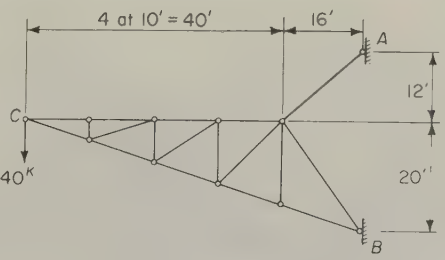

Figure P2-2

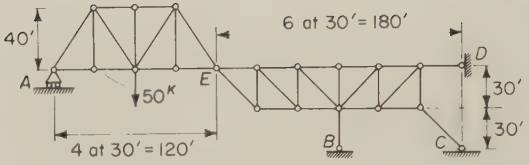

Figure P2–3

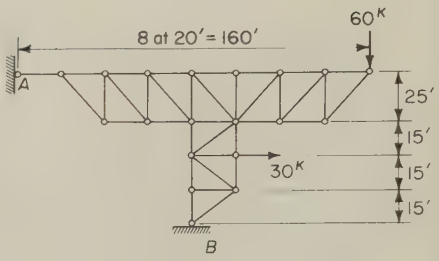

Figure P2–4

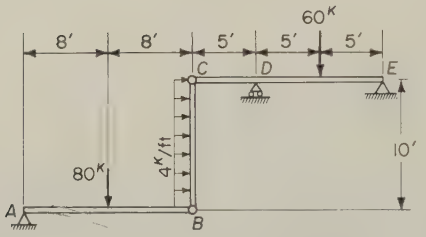

Figure P2–5

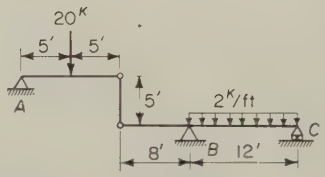

Figure P2–6

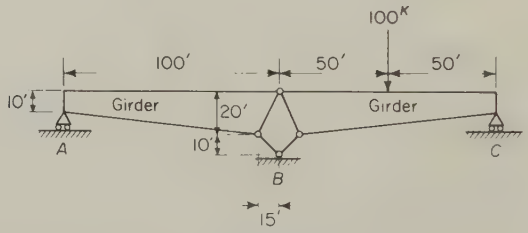

Figure P2–7

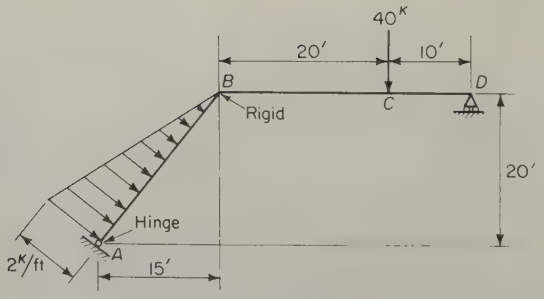

Figure P2–8

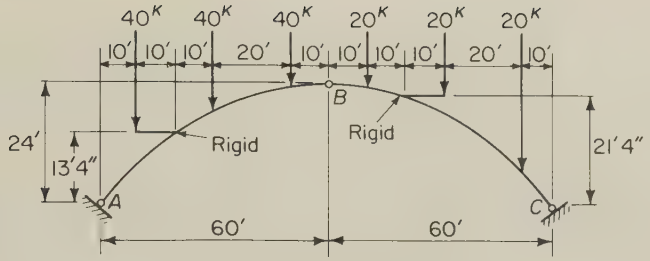

Figure P2–9

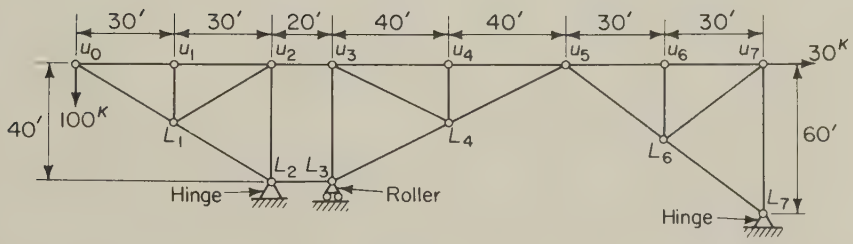

Figure P2–10

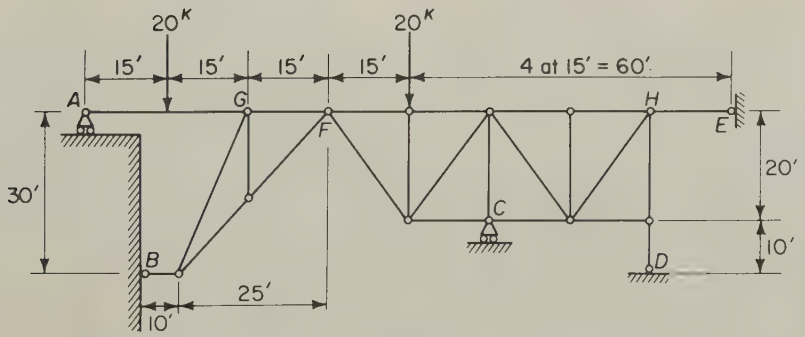

Figure P2–11

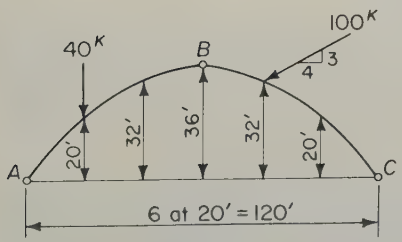

Figure P2–12

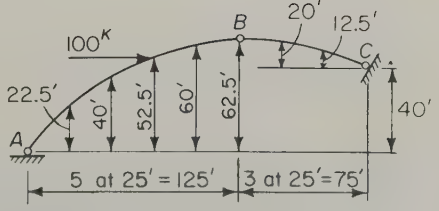

Figure P2–13

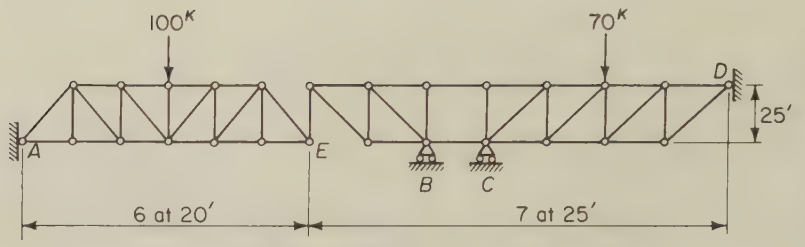

Figure P2–14

2-15 to **2-20** In each of the systems in Figs. P2-15 to P2-20, determine whether the structure is statically determinate or indeterminate. If it is statically indeterminate, state the degree of static indeterminacy.

Figure P2–15

Figure P2–16

Figure P2–17

Figure P2–18

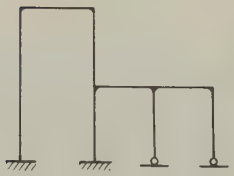

Figure P2–19

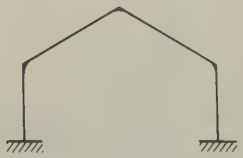

Figure P2–20

2-21 A simply supported prestressed concrete beam of 20-ft span has a uniform load of 2 kips/ft including its own weight. The cross section of the beam is rectangular, 16 in. wide by 24 in. deep. The cable is located at the lower third point of the depth and introduces an effective prestress of 200 kips. Compute the maximum stresses in the top and bottom fiber.

2-22 A 16-in. by 16-in. square concrete member is prestressed concentrically in a horizontal position. A prestress force of 320 kips is introduced by steel wires with a total area of 2 sq in. and anchored to bulkheads as shown in Fig. P2-22 before the concrete is poured. Compute the loss of prestress in

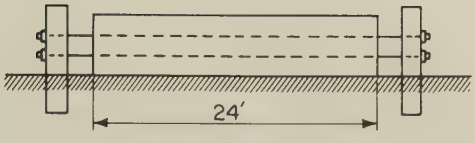

Figure P2–22

steel due to the elastic shortening of concrete when the steel wires are cut off at the ends of the beam after curing of the concrete, neglecting the shrinkage of concrete. Use $E_s = 30 \times 10^6$ psi for steel and $E_c = 3 \times 10^6$ psi for concrete.

2-23 For the beam in Problem 2-22, determine the loss of prestress in steel due to the shrinkage in concrete only, if the shrinkage strain in concrete is 0.0003 in./in.

2-24 The steel arch shown in Fig. P2-24 is erected at a temperature of 50°F.

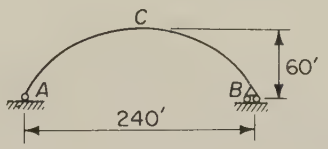

Figure P2–24

Determine the horizontal displacement at B and the vertical displacement at C when the temperature reaches 120°F, assuming that the coefficient of linear expansion for steel is $\alpha = 6.6 \times 10^{-6}$/°F.

2-25 A 6-in. by 6-in. square steel bar 10 ft long, as shown in Fig. P2-25, is fixed at the ends when the temperature in the bar is 100°F throughout. The

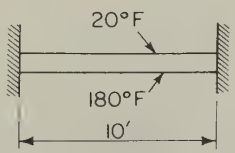

Figure P2–25

temperatures at top and bottom faces are then kept at 20°F and 180°F respectively, causing a linear temperature distribution through the depth of the bar. Compute the stresses at top and bottom fibers, using $E = 30 \times 10^6$ psi and $\alpha = 6.6 \times 10^{-6}$/°F for steel.

2-26 A rigid insulated block is suspended from two identical steel bars at a room temperature of 60°F, as shown in Fig. P2-26. The left bar is kept at room temperature while the right one is heated to a temperature of 300°F. Determine the rotation of the block if $\alpha = 6.6 \times 10^{-6}$/°F.

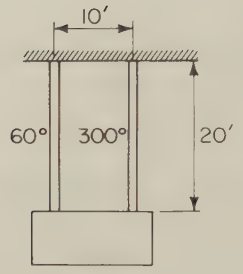

Figure P2–26

2-27 The lever shown in Fig. P2-27 is in neutral equilibrium. Determine the

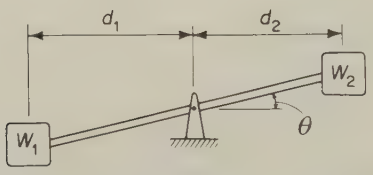

Figure P2–27

relation between d_1, d_2, W_1, and W_2 by the principle of minimum potential energy.

2-28 A rigid bar with an elastic spring at the bottom is free at the top as shown in Fig. P2-28. The spring has a constant k in resisting a rotational dis-

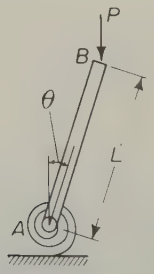

Figure P2–28

placement θ such that the resisting moment $M = k\theta$. A vertical compressive force P is applied at the top when the bar is in the vertical position. By using the principle of minimum potential energy, determine the critical value of P so that the bar will remain in the vertical position.

2-29 Derive the equations of equilibrium for the system in Fig. P2-29 by

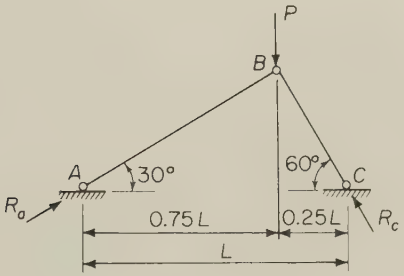

Figure P2–29

the principle of virtual displacements.

2-30 The mechanism shown in Fig. P2-30 is held in equilibrium by a hori-

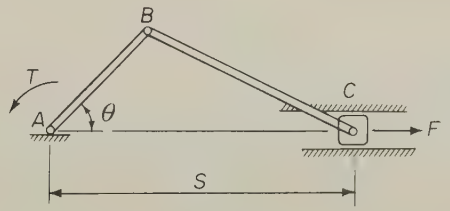

Figure P2–30

zontal force F at the slider C while a torque T is applied about the crankshaft A. Determine the force F required to resist the applied torque T in terms of the angular velocity of the crankshaft and the linear velocity of the slider.

3 FORCES AND MOMENTS

3-1 Simple Plane Structures

The analysis of all structural systems begins with the determination of reactions. After the reactions of a structure are obtained, the internal forces and moments in the desired locations of the structure may be studied by passing imaginary sections through those locations. The variations of the internal forces and moments in various members of a structure — and especially their maximum values — are of utmost importance for design purposes.

We begin with simple plane structures that are statically determinate and consist of relatively few members. In this category we include simple beams, rigid frames, cables, and arches. The stress resultants acting on a section through a member of a plane structure can in general be resolved into an axial force, a transverse shear force, and a bending moment. Plane trusses, which are widely used as structural systems, represent a special class because of the assumption of smooth pin connections for all their members, and therefore they will be treated separately in Chapter 4.

For plane structures that are statically indeterminate, the internal forces and moments as well as reactions cannot be determined by statics alone. However, these stress resultants may be obtained by the same procedure after the number of unknowns in the system has been reduced to that which may be solved by statics. Many of the simple structures used as examples in this chapter do not represent common real structures, but are the simplified versions of more complicated structures. Thus, the student should be well aware of the possibilities of other applications of the principles presented here.

3-2 Axial Forces, Shears, and Moments

Let us consider a section passing through a structural member normal to the axis of the member, as shown in Fig. 3-1(a). The stress resultants acting at the section include an axial force N, a transverse shear force S, and a

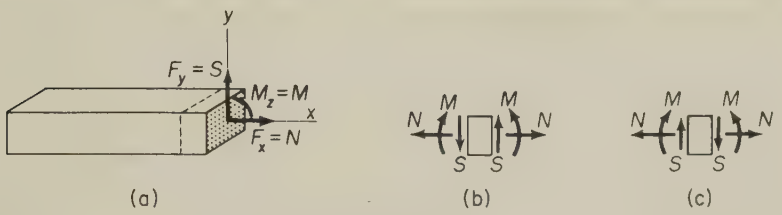

Figure 3–1

bending moment M. The transverse shear force and the bending moment will henceforth be abbreviated as "shear" and "moment," respectively, in the analysis of plane structures. If a small element such as the portion shown dotted to the left of the section in Fig. 3-1(a) is cut off from the member, equal but opposite forces should be added to the left face of the element in order to maintain the equilibrium of the free body since no external forces are acting on the element. Looking from the front of the element, these internal forces and moments can be represented as shown in Fig. 3-1(b). Looking from the back of the element, however, a mirror image as shown in Fig. 3-1(c) is obtained. Although the directions of N and M remain the same in Fig. 3-1(c) as in Fig. 3-1(b), the direction of S is reversed. It is necessary therefore to adopt a sign convention so that the situation at a section can be defined more clearly and systematically.

The selection of a particular convention is a matter of convenience. Figure 3-2 shows the sign convention that is most convenient from the viewpoint of structural design and that has been most commonly adopted in

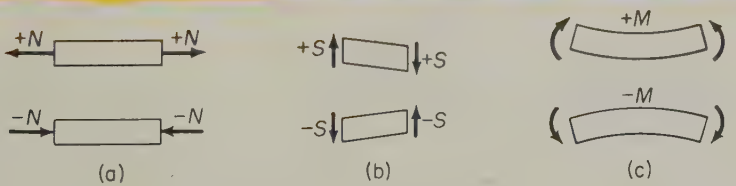

Figure 3–2

structural engineering. Unless otherwise noted for special reasons, this sign convention will be used throughout this book. As shown in Fig. 3-2(a), the pair of axial forces is considered as positive when it produces tension in a member, and is negative when it causes compression in the member. In

Fig. 3-2(b), the pair of shears is designated as positive if it tends to push the left side of a member upward, and is negative if it pushes the left side of the member downward. In Fig. 3-2(c), the pair of moments is said to be positive if it tends to bend a member concave upward causing tension in the bottom of a member, and is negative if it causes the member to bend concave downward. It should be pointed out that the position of the member is assumed to be horizontal when such a sign convention is introduced. If the member is vertical, such as member *BC* in Fig. 3-3(a), it can be looked upon from the right or the left of the member. Under such circumstances, it can be

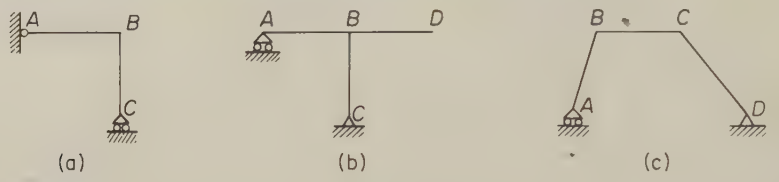

Figure 3–3

specified that either the right-hand side of member *BC* is to be considered as the bottom or that all members will be viewed from the inside of the structure. Although the former viewpoint is definitely more general, the latter also has some merits. For the structure in Fig. 3-3(b), for instance, it is impossible to differentiate which side of the vertical member is the inside of the structure. For that reason, the latter viewpoint cannot be applied to structures with more than one span or one story. The former convention will therefore be used for multispan or multistory rigid frames. On the other hand, for structures such as arches, rings, and simple frames with inclined legs such as the one shown in Fig. 3-3(c), it is much easier to view the member from the inside of the structure. The latter convention is used for such cases despite its limitations.

It may be well to mention other sign conventions and to discuss briefly their advantages or disadvantages in the analysis of structural problems. Figure 3-4(a) shows a convention for axial force that defines a positive force as one whose sense of direction points in the positive direction of the coordinate axis. Although the signs of these forces are consistent with the direction of the coordinate axis, it is not possible to determine from the

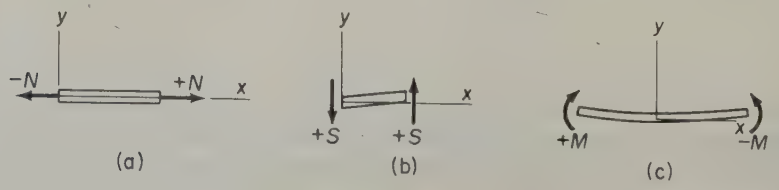

Figure 3–4

sign whether a force is tensile or compressive. However, if the section on which an axial force acts is defined as positive when its outwardly directed normal is pointing in the direction of the positive coordinate axis and as negative when the outward normal points the other way, the state of stress can be correctly obtained. Thus, the area of a section may be considered as $+A$ or $-A$ accordingly. For $+N$ and $+A$ on the right end of the member, $\sigma = N/A$ represents tensile stress in the member. For $-N$ and $-A$ on the left end of the member $\sigma = (-N)/(-A) = N/A$ also indicates tensile stress. Figure 3-4(b) shows a convention for shear that is the complete reverse of that of Fig. 3-2(b). Whereas the convention in Fig. 3-2(b) is more convenient to apply, that of Fig. 3-4(b) has the merit of being positive in the same direction as positive shearing stress defined for the general state of stress acting on an element in a right-handed coordinate system.* Figure 3-4(c) shows a convention for moment that defines positive moment as one which rotates in clockwise direction at the ends of the member. In summing up moments, this convention simplifies the operation, but it is impossible to determine from the sign of the moment whether the member is bent concave upward or downward.

The determination of axial force, shear, and moment at any section of a structure is based on the consideration of static equilibrium of the free body on either side of the section. These stress resultants acting on the free body at one side of the section are equal in magnitude but opposite in sense to the respective stress resultants acting on the free body at the other side. Thus, for a plane structure, the axial force N acting normal to any transverse section of a member may be obtained by summing up algebraically the components in that direction of all external forces and reactions acting on a free body. The shear S at any transverse section of a member is the algebraic sum of the components in the transverse direction of all external forces and reactions acting on the free body. The bending moment is the algebraic sum of the moments in the plane of the structure, taken about the intersection of the axis of the member and the transverse section, of all external loads and reactions acting on the free body. It is customary to start from the left end of the structure as the origin of the coordinate axis and to use the left-hand side of the section as a free body. However, the use of the right-hand side of the section as a free body sometimes involves less computation if there are fewer external loads and reactions on that portion of the structure.

The senses of direction of the axial force N, shear S, and moment M at any section of a structure are not always immediately obvious. If the correct senses of direction of these forces and moment cannot be detected by inspection, they can always be assumed to act in the positive direction

*See, for instance, p. 125 of Reference 3-1.

of the sign convention. In that case, a positive result will indicate that the assumed sense of direction is correct, and a negative result means that the actual sense of direction is the reverse of the assumed direction. The variations of the axial force, shear, and moment along the length of a member can be expressed algebraically or graphically as a function of the distance x along the length of the member. We shall consider here the formulation of the algebraic expressions for these quantities.

Example 3-1. For the beam shown in Fig. 3-5(a), write a general expression for the axial force, shear, and moment at typical sections of the beam.

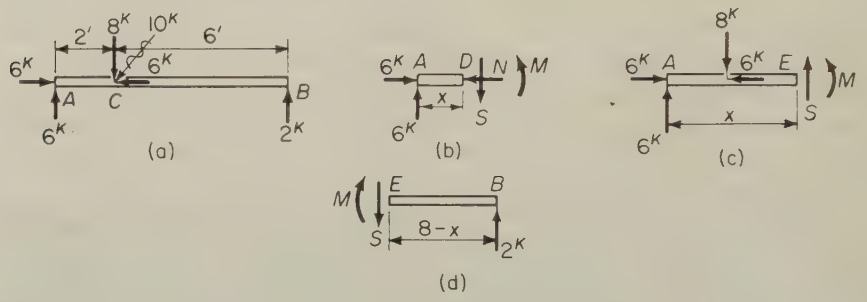

Figure 3-5

The inclined load of 10 kips is resolved into vertical and horizontal components of 8 kips and 6 kips, respectively. The components of reaction H_a, V_a, and V_b are obtained from the equations of equilibrium.

$$\sum M_a = 0, \quad 8V_b - (8)(2) = 0, \quad V_b = 2 \text{ kips}$$
$$\sum F_y = 0, \quad V_a + V_b = 8, \quad V_a = 8 - 2 = 6 \text{ kips}$$
$$\sum F_x = 0, \quad H_a = 6 \text{ kips}$$

As a check, $\Sigma M_b = 0$, $(8)(6) - 8V_a = 0$, $V_a = 6$ kips.

In obtaining the stress resultants, a section is first passed through a point D between A and C at a distance x from A. Then the free body on the left-hand side of the section will be as shown in Fig. 3-5(b). Since the correct senses of direction of forces and moment in this case are rather obvious, they have been assigned proper directions in the figure. Thus, all the results are positive.

$$\sum F_x = 0, \quad N = 6 \text{ kips}$$
$$\sum F_y = 0, \quad S = 6 \text{ kips}$$
$$\sum M_d = 0, \quad M = 6x \text{ ft-kips}$$

Note that the moment M is a function of x, the distance from the left support. The axial force N and the shear S are independent of the distance x as long as it is smaller than the distance AC.

If a section is passed through point E of the same beam as shown in Fig. 3-5(c), the same procedure may be repeated.

$$\sum F_x = 0, \quad N = 0$$

$$\sum F_y = 0, \quad S = 8 - 6 = 2 \text{ kips}$$

$$\sum M_e = 0, \quad M = 6x - 8(x - 2) = 16 - 2x \text{ ft-kips}$$

It can be seen that the same results may also be obtained from the free-body diagram in Fig. 3-5(d). Note that M and S shown in Fig. 3-5(d) are equal and opposite to those shown in Fig. 3-5(c). Thus,

$$\sum F_y = 0, \quad S = 2 \text{ kips}$$

$$\sum M_e = 0, \quad M = 2(8 - x) = 16 - 2x \text{ ft-kips}$$

Example 3-2. For the portal frame shown in Fig. 3-6(a), write a general

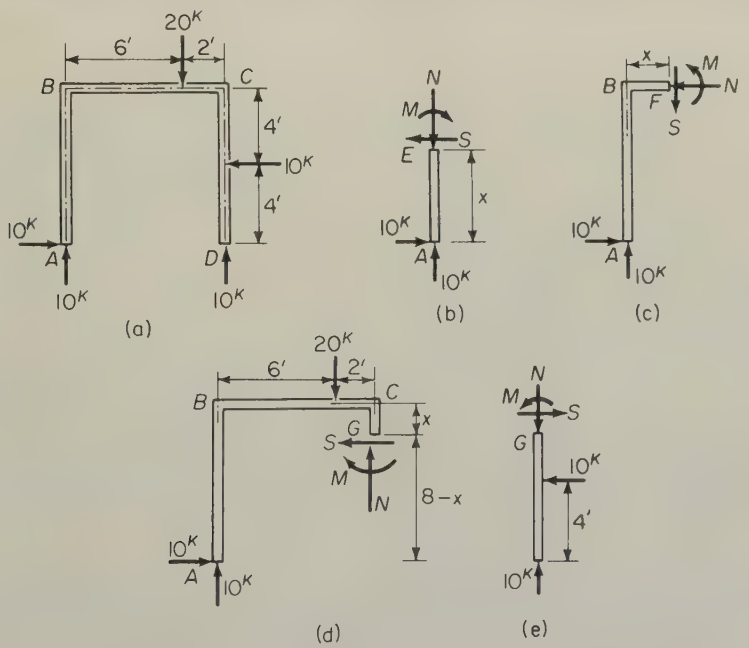

Figure 3–6

expression for the axial force, shear, and moment at typical sections of the beam.

The reaction components H_a, V_a, and V_d for the frame are obtained as follows:

$$\sum M_a = 0, \quad 8V_d + (10)(4) - (20)(6) = 0, \quad V_d = 10 \text{ kips}$$

$$\sum F_y = 0, \quad V_a + V_d = 20, \quad V_a = 10 \text{ kips}$$

$$\sum F_x = 0, \quad H_a = 10 \text{ kips}$$

As a check, $\Sigma M_d = 0$, $(10)(4) + (20)(2) - 8V_a = 0$, $V_a = 10$ kips.

When a section is passed through point E, a free-body diagram as shown in Fig. 3-6(b) is obtained. Let x be the coordinate axis along the length of the member. Then,

$$\sum F_x = 0, \quad N = 10 \text{ kips}$$

$$\sum F_y = 0, \quad S = 10 \text{ kips}$$

$$\sum M_e = 0, \quad M = 10x \text{ ft-kips}$$

For a section passed through point F, the free body representing the left-hand side is shown in Fig. 3-6(c).

$$\sum F_x = 0, \quad N = 10 \text{ kips}$$

$$\sum F_y = 0, \quad S = 10 \text{ kips}$$

$$\sum M_f = 0, \quad M = (10)(x) - (10)(8) = 10x - 80 \text{ ft-kips}$$

For a section passed through point G, the free-body diagram to the left of the section is shown in Fig. 3-6(d).

$$\sum F_x = 0, \quad N = 10 \text{ kips}$$

$$\sum F_y = 0, \quad S = 10 \text{ kips}$$

$$\sum M_g = 0, \quad M = (20)(2) + (10)(8 - x) - (10)(8) = 40 - 10x \text{ ft-kips}$$

The free-body diagram to the right of the section passed through point G may also be used. Such a diagram is shown in Fig. 3-6(e), and the results thus obtained check with those from Fig. 3-6(d).

$$\sum F_x = 0, \quad N = 10 \text{ kips}$$

$$\sum F_y = 0, \quad S = 10 \text{ kips}$$

$$\sum M_g = 0, \quad M = (10)(8 - x - 4) = 40 - 10x \text{ ft-kips}$$

Example 3-3. For the cantilever beam shown in Fig. 3-7(a), write a general expression for the axial force, shear, and moment at typical sections of the beam.

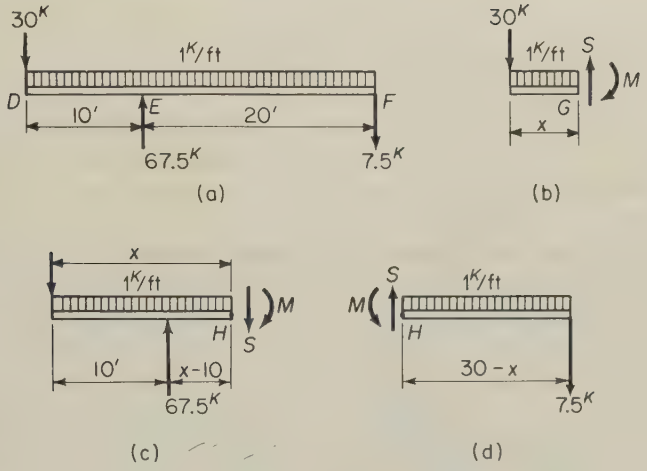

Figure 3-7

The reaction components of the beam are obtained as follows:

$$\sum M_f = 0, \quad (30)(30) + (1)(30)(30/2) - 20V_e = 0, \quad V_e = 67.5 \text{ kips}$$

$$\sum F_y = 0, \quad V_e - V_f = 30 + (1)(30), \quad V_f = 7.5 \text{ kips}$$

Since there is no horizontal force acting on the beam, there will be no axial force acting on any section normal to the length of the beam. Thus, for a section passed through point G, the free body at the left-hand side of the section will be as shown in Fig. 3-7(b).

$$\sum F_y = 0, \quad S = 30 + (1)(x) = 30 + x \text{ kips}$$

$$\sum M_g = 0, \quad M = (30)(x) + (1)(x)(x/2) = 30x + x^2/2 \text{ ft-kips}$$

For a section passed through point H, the free body at the left-hand side of the section may be represented by Fig. 3-7(c).

$$\sum F_y = 0, \quad S = 67.5 - 30 - (1)(x) = 37.5 - x \text{ kips}$$

$$\sum M_h = 0, \quad M = (30)(x) + (1)(x)(x/2) - (67.5)(x - 10)$$

$$= x^2/2 - 37.5x + 675 \text{ ft-kips}$$

As a check, the right-hand side of the section passed through H may also be used as a free body as shown in Fig. 3-7(d).

$$\sum F_y = 0, \quad S = (1)(30 - x) + 7.5 = 37.5 - x \text{ kips}$$

$$\sum M_h = 0, \quad M = (7.5)(30 - x) + (1)(30 - x)^2/2$$

$$= x^2/2 - 37.5x + 675 \text{ ft-kips}$$

3-3 Differential Relationships in Beams

Since the variation of axial forces in a beam is usually rather simple, we can dismiss it without further discussion. The variations of shears and moments can be expressed as functions of the position x along a beam, as explained in the previous section. However, they can also be obtained through successive integrations of the loading function.

Consider a beam with applied loads as shown in Fig. 3-8(a). If a differential element of length δx is isolated from the beam by two parallel

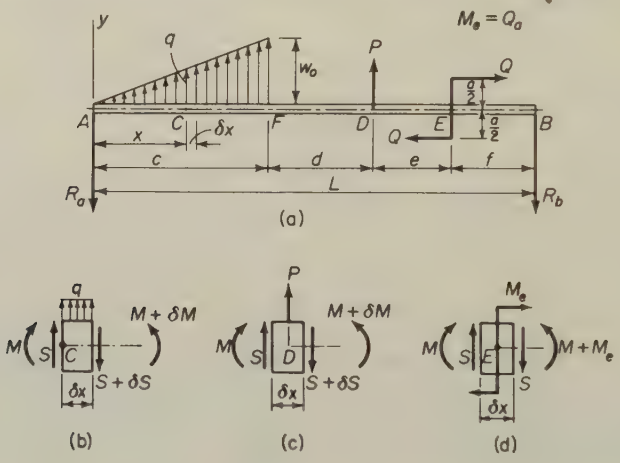

Figure 3-8

sections at x and $x + \delta x$, the forces and moments acting on the free body are as shown in Fig. 3-8(b), in which the positive directions of applied loads, shears, and moments are indicated. The intensity of load q can be considered as uniformly distributed over the length δx since the variation of q leads to higher-order terms of δx which are negligibly small compared to δx. Since the element represents a free body in equilibrium, the following conditions must be fulfilled:

$$\sum F_y = 0, \quad S + q\,\delta x - (S + \delta S) = 0$$

or

$$q = \frac{dS}{dx} \tag{3-1}$$

$$\sum M_c = 0, \quad (M + \delta M) - M - (S + \delta S)\,\delta x + q\,\delta x \frac{\delta x}{2} = 0$$

As δx approaches 0 as a limit, the higher-order terms become negligible. Thus,

$$(M + \delta M) - M - S\,\delta x = 0$$

or

$$S = \frac{dM}{dx} \tag{3-2}$$

Equation (3-1) states that the rate of change of the shear along the beam is equal to the intensity of the applied load, and Eq. (3-2) indicates that the rate of change of the moment along the beam is equal to the shear. These two equations are important because the critical values of moment and shear along the beam may be determined from them. Thus, if S is a continuous function of x for an interval $a \leqq x \leqq b$ in which the derivative dS/dx exists, the maximum or minimum shear occurs at a point where $q = dS/dx = 0$. Similarly, if M is a continuous function of x for an interval $a \leqq x \leqq b$ in which the derivative dM/dx exists, the maximum or minimum moment occurs at a point where $S = dM/dx = 0$. From a practical point of view, however, the second statement is far more useful than the first because the shear function S is seldom continuous for beams under ordinary loads. For example, if a concentrated load P is acting at point D of the beam in Fig. 3-8(a), there is a sudden change in shear between a section just to the left and another section just to the right of the load P as shown in Fig. 3-8(c). Hence, the derivative dS/dx does not exist at point D and Eq. (3-1) does not apply at this point. The moment function M may also be discontinuous as a result of applied loads such as the couple M_e at point E of the beam in Fig. 3-8(a). This couple causes a sudden change in moment from one section to another adjacent section, as shown in Fig. 3-8(d). In such a case, the derivative dM/dx does not exist, and Eq. (3-2) cannot be used for point E.

Conversely, if the loading function q is known, Eqs. (3-1) and (3-2) can be integrated and expressed in the following form:

$$S = \int q\,dx + C_1 \tag{3-3}$$

and

$$M = \int S\,dx + C_2 \tag{3-4}$$

Equation (3-3) indicates that the shear at any section of the beam is an integral of the applied loads or the *area under the loading curve*. The constant of integration C_1 can be determined from the conditions of shear at the supports of the beam. Thus, Eq. (3-3) represents the variation of shears or the *shear curve* along the length of the beam. Equation (3-4) means that

the moment at any section normal to the beam is an integral of the shear forces or the *area under the shear curve*. The constant of integration C_2 can be evaluated from the conditions of moment at the supports of the beam. Hence Eq. (3-4) represents the variation of moments or the *moment curve* along the length of the beam. The conditions of shear and moment at the supports of the beam by which the constants of integration are evaluated are called the *force boundary conditions*, or simply *boundary conditions*.

As examples, consider two beams, one cantilever and the other simply supported, subjected to downward uniformly distributed load w_0 as shown in Figs. 3-9 and 3-10. Since $q = -w_0$, where the negative sign indicates the downward direction and w_0 is a constant, then for both beams,

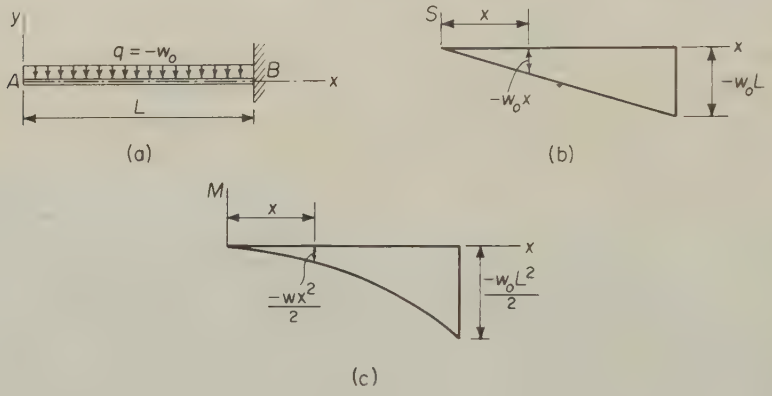

Figure 3–9

$$S = \int -w_0\,dx + C_1 = -w_0x + C_1$$

and

$$M = \int S\,dx + C_2 = -\frac{w_0x^2}{2} + C_1x + C_2$$

For the cantilever beam shown in Fig. 3-9(a), the boundary conditions are as follows: $S = 0$ at $x = 0$ and $M = 0$ at $x = 0$. Hence the constants of integration C_1 and C_2 are both zero. Then,

$$S = -w_0x$$

and

$$M = -\frac{w_0x^2}{2}$$

The shear and moment curves from these two equations are plotted in

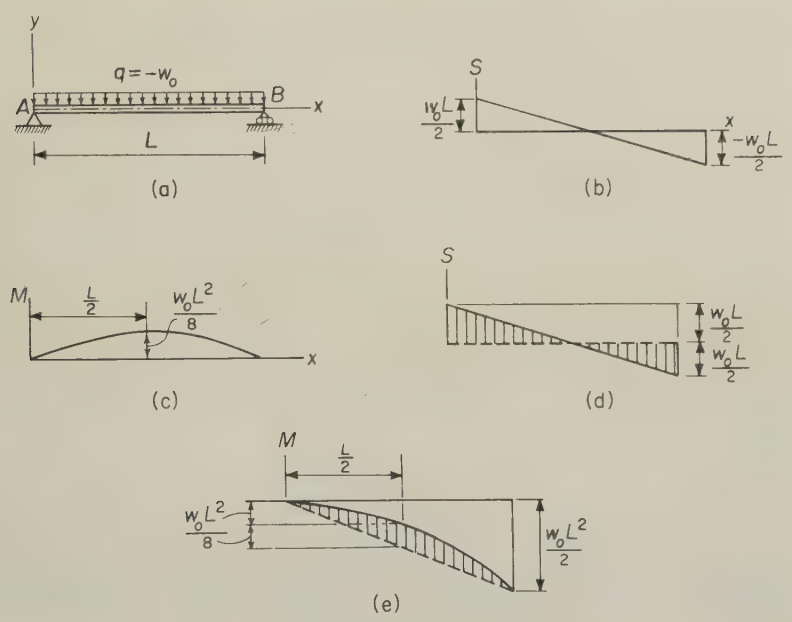

Figure 3–10

Figs. 3-9(b) and (c), respectively. For the simply supported beam shown in Fig. 3-10(a), the boundary conditions may be taken as $S = V_a$ at $x = 0$ and $M = 0$ at $x = 0$ if the reaction V_a is obtained first. However, the boundary conditions $M = 0$ at $x = 0$ and at $x = L$ may also be used without obtaining the reaction V_a. It can easily be seen in this case that $V_a = w_0L/2$. Thus, from the former set of conditions, we get $C_1 = w_0L/2$ and $C_2 = 0$, or

$$S = \frac{w_0L}{2} - w_0x$$

and

$$M = \frac{w_0Lx}{2} - \frac{w_0x^2}{2}$$

The shear and moment curves from these two equations are plotted in Figs. 3-10(b) and (c) respectively. From the latter set of conditions, the constants of integration can be obtained as follows:

$$\text{at } x = 0, M = 0: \qquad C_2 = 0$$

$$\text{at } x = L, M = 0: \qquad -\frac{w_0L^2}{2} + C_1L + C_2 = 0, \quad C_1 = \frac{w_0L}{2}$$

Thus the same results for shear and moment may be obtained.

In examining Eqs. (3-3) and (3-4) further, we observe that in general

$$S = \int q\,dx + C_1$$

and

$$M = \int S\,dx + C_2 = \int \left(\int q\,dx \right) dx + C_1 x + C_2$$

Hence, the *shape* of the shear and moment curves is defined by the corresponding integral independent of the boundary conditions. The *ordinates* of the points on the curves, of course, are influenced by the boundary conditions that are expressed in the constants of integration C_1 and C_2. The equation of the shear curve may be considered as the superposition of a diagram of

$$S = \int q\,dx \qquad \text{for } C_1 = 0$$

and a vertical translation of the x-axis equal to $S = C_1$. The equation of the moment curve may be considered as the superposition of

$$M = \int \left(\int q\,dx \right) dx \quad \text{for } C_1 = C_2 = 0$$

and a combination of vertical translation and rotation of the x-axis equivalent to $M = C_1 x + C_2$. For the special case where $C_2 = 0$, the movement of x-axis becomes pure rotation as represented by $M = C_1 x$. Since the cantilever beam in Fig. 3-9 represents the case $C_1 = C_2 = 0$, and the simply supported beam in Fig. 3-10 has $C_1 = w_0 L/2$ and $C_2 = 0$, the ordinates of the shear and moment curves of the latter may be obtained by superimposing $S = C_1$ and $M = C_1 x + C_2$ respectively to those of the former, as shown in Figs. 3-10(d) and (e) respectively. Diagrams showing proper *ordinates* as well as the *shape* of the shear curve are known as *shear diagrams*; similar diagrams showing proper *ordinates* as well as the *shape* of the moment curve are called *moment diagrams*. Thus, the shear and moment diagrams for the beam in Fig. 3-10(a) are either represented by Figs. 3-10(b) and (c) respectively, or by the *shaded portions* in Figs. 3-10(d) and (e) respectively.

In connection with the construction of shear and moment diagrams, we should first clarify several terms. The *area under a curve* is defined as the area between the curve and the coordinate axis involved. This is literally true if the curve has positive ordinates in the interval under consideration but actually means the area above the curve if the curve has negative ordinates in that interval. When a reference axis in a diagram is rotated, the *ordinates* of the curve are assumed to move *normal to the original direction*

of the reference axis. Thus, if a horizontal axis is being rotated, the ordinates of the curve will still be measured vertically. The *maximum* or *minimum* point on a curve may be considered relative only to the points on the curve in the immediate vicinity. When a function assumes its largest value algebraically in the range, the term *maximum positive* is used to denote such an absolute maximum point if it is positive. Similarly, a point representing the least value algebraically in the range is termed *maximum negative* if such an absolute minimum point is negative.

Equations (3-3) and (3-4) can also be expressed in the form of definite integrals for the interval of $a < x < b$ as follows:

$$S_b - S_a = \int_a^b q\,dx \tag{3-5}$$

and

$$M_b - M_a = \int_a^b S\,dx \tag{3-6}$$

Equation (3-5) states that the shear at any section of a beam is equal to the shear at a previous section plus the area of the loading diagram between the two sections in the positive direction of the coordinate axis. Similarly, according to Eq. (3-6), the moment at any section of a beam is equal to the moment at a previous section plus the area of the shear diagram between the two sections in the positive direction of the coordinate axis. Thus the construction of shear and moment diagrams becomes a process of summation starting from an initial point of known shear and moment.

3-4 *Integration of Singularity Functions*

In the previous section, we observed that the shear and moment in a beam can be easily obtained by integrations from Eqs. (3-3) and (3-4), or from Eqs. (3-5) and (3-6), if the loading functions are continuous. For beams with concentrated loads or distributed loads having sudden changes along its length, the loading functions may contain a number of discontinuities or singularities. It is possible to develop a general procedure for the direct integration of such loading functions if a concise notation is adopted for the treatment of the singularity functions.

The basic types of singularity functions that may appear as applied loads on a beam are shown in Fig. 3-11, and the corresponding loading functions are given in Fig. 3-12.* The actual loading function on a beam may be obtained from the superposition of these basic cases. Before considering the application of these functions, however, we shall study their properties and their integration relations.

*These figures are adapted from pp. 98-99 of Reference 3-1. See this reference for further discussions and applications.

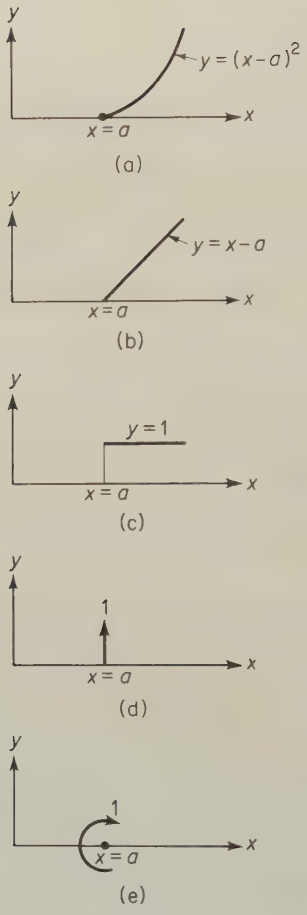

Figure 3–11

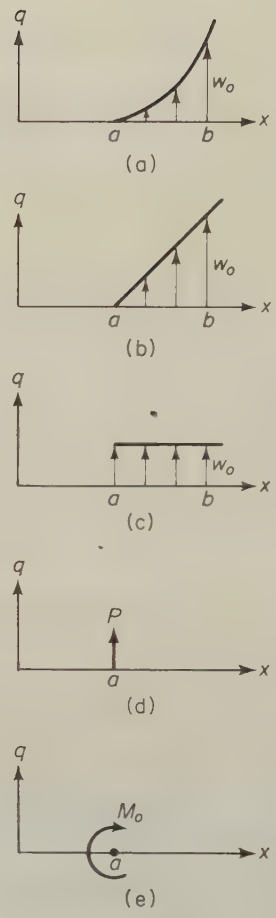

Figure 3–12

The family of singularity functions in Fig. 3-11 may be defined by a notation

$$y_n = \langle x - a \rangle^n \tag{3-7}$$

in which n is a number associated with a particular function. The bracket notation has different meanings for $n \geqq 0$ and for $n < 0$. When $n \geqq 0$, it is defined as follows:

$$y_n = 0 \qquad \text{for } x < a$$
$$y_n = (x - a)^n \quad \text{for } x \geqq a$$

Thus, the functions in Figs. 3-11(a), (b), and (c) may respectively be represented by

$$y_2 = \langle x - a \rangle^2$$
$$y_1 = \langle x - a \rangle^1$$
$$y_0 = \langle x - a \rangle^0$$

The integration of these functions is given by

$$\int_{-\infty}^{x} \langle x - a \rangle^n \, dx = \frac{\langle x - a \rangle^{n+1}}{n + 1}, \quad n \geqq 0 \tag{3-8}$$

When $n < 0$, the bracket notation is defined as

$$y_n = 0 \quad \text{for } x \neq a$$

$$y_n = 1 \quad \text{for } x = a$$

in which $y_n = 1$ is a unit concentrated force when $n = -1$ and it refers to a unit couple at $x = a$ when $n = -2$. Thus, the functions in Fig. 3-11(d) and (e) are exceptional cases that may be expressed in the bracket notation as follows:

$$y_{-1} = \langle x - a \rangle^{-1}$$

$$y_{-2} = \langle x - a \rangle^{-2}$$

These two functions are zero everywhere except at $x = a$ where they are finite. Hence, their integrations are obtained as follows:

$$\int_{-\infty}^{x} \langle x - a \rangle^{-2} \, dx = \langle x - a \rangle^{-1} \tag{3-9}$$

$$\int_{-\infty}^{x} \langle x - a \rangle^{-1} \, dx = \langle x - a \rangle^{0} \tag{3-10}$$

If the loading functions are individually represented by the curves shown in Fig. (3-12), the corresponding mathematical expressions are given by

$$q = \frac{w_0}{(b - a)^2} \langle x - a \rangle^2$$

$$q = \frac{w_0}{(b - a)} \langle x - a \rangle^1$$

$$q = w_0 \langle x - a \rangle^0$$

$$q = P_0 \langle x - a \rangle^{-1}$$

$$q = M_0 \langle x - a \rangle^{-2}$$

Note that for the first loading function, which represents a second-degree parabola starting at $x = a$, the function continues beyond $x = b$ to $x = +\infty$. The abscissa b is given only to define the shape of the parabola such that $q = w_0$ at $x = b$. The same is true for the second loading function, which is an inclined line starting at $x = a$ and continues until $x = +\infty$. The third loading function is a horizontal line representing $q = w_0$ from $x = a$ to $x = +\infty$ since $(x - a)^0 = 1$. In order to stop either of these functions at

$x = b$, we must subtract the portion of the area under the curve beyond $x = b$. No such complication is encountered in the last two loading functions, which are nonzero only at $x = a$.

As an example, let us consider the beam shown in Fig. 3-8(a). The loading function for the beam may be written according to the bracket notation as follows:

$$q(x) = \frac{w_0}{c}\langle x\rangle^1 - \frac{w_0}{c}\langle x-c\rangle^1 - w_0\langle x-c\rangle^0 + P\langle x-c-d\rangle^{-1} + M_e\langle x-c-d-e\rangle^{-2}$$

The first three terms on the right-hand side of the equation represent the triangular loading acting on the beam. The first term indicates

$$q = 0 \quad \text{for} \quad x < 0; \quad q = \frac{w_0}{c}x \quad \text{for} \quad x \geqq 0$$

The second and third terms represent respectively a triangular area and a rectangular area beyond $x = c$ that must be subtracted from the first term in order to stop the triangular loading at point $x = c$. Thus, the second term means

$$q = 0 \quad \text{for} \quad x < c; \quad q = -\frac{w_0}{c}(x-c) \quad \text{for} \quad x \geqq c$$

and the third term indicates that

$$q = 0 \quad \text{for} \quad x < c; \quad q = -w_0(x-c)^0 = -w_0 \quad \text{for} \quad x \geqq c$$

The fourth and fifth terms on the right-hand side of the equation represent the concentrated load P and the couple M_e respectively as follows:

$$q = 0 \quad \text{for } x \neq c+d; \qquad q = P \quad \text{for } x = c+d$$

$$q = 0 \quad \text{for } x \neq c+d+e; \qquad q = M_e \quad \text{for } x = c+d+e$$

For the purpose of obtaining the shear and moment equations in a beam, it is convenient to include the reactions as concentrated forces in the loading function. These reactions can be computed first from the external loads. Thus, the loading function including the reactions R_a and R_b for the beam in Fig. 3-8(a) is given by

$$q(x) = -R_a\langle x\rangle^{-1} + \frac{w_0}{c}\langle x\rangle^1 - \frac{w_0}{c}\langle x-c\rangle^1 - w_0\langle x-c\rangle^0 + P\langle x-c-d\rangle^{-1} + M_e\langle x-c-d-e\rangle^{-2} - R_b\langle x-L\rangle^{-1}$$

in which the reaction terms are negative since the reactions are acting downward. For a beam of finite length, we have the conditions $S = 0$ and $M = 0$

at $x = -\infty$. Then, according to Eqs. (3-7) and (3-8), the shear and moment functions may be obtained by successive integrations as follows:

$$S(x) = \int_{-\infty}^{x} q\,dx = -R_a\langle x\rangle^0 + \frac{w_0}{2c}\langle x\rangle^2 - \frac{w_0}{2c}\langle x-c\rangle^2 - w_0\langle x-c\rangle^1 + P\langle x-c-d\rangle^0 + M_e\langle x-c-d-e\rangle^{-1} - R_b\langle x-L\rangle^0$$

$$M(x) = \int_{-\infty}^{x} S\,dx = -R_a\langle x\rangle^1 + \frac{w_0}{6c}\langle x\rangle^3 - \frac{w_0}{6c}\langle x-c\rangle^3 - \frac{w_0}{2}\langle x-c\rangle^2 + P\langle x-c-d\rangle^1 + M_e\langle x-c-d-e\rangle^0 - R_b\langle x-L\rangle^1$$

This method of treating singularity functions makes possible the generalization of the concept of obtaining shears and moments in beams by successive integrations. Thus, the integration formulas represented by Eqs. (3-3) to (3-6) are, theoretically at least, no longer limited to continuous functions only. On the other hand, solutions of problems involving discontinuous functions are rather lengthy in spite of the simplified technique introduced in this section so we shall not elaborate further on its application. For the actual solutions of problems involving irregular loadings, a numerical procedure is suggested in Sections 3-7 and 3-8.

3-5 *Shear and Moment Diagrams for Beams and Frames*

For beams and rigid frames consisting of straight members, the variations of shears and moments along the length of a member may be represented graphically by the shear and moment diagrams, respectively, for the member. It is convenient to make these diagrams directly below the loading diagram of the member, using the same horizontal scale in the direction of the member. Shears and moments at the critical points may be computed directly from the equilibrium of the free body, or by the summation process as represented by Eqs. (3-5) and (3-6).

The summation process is rather straightforward and can be used to great advantage. However, each integration means raising the degree of the equation representing the curve by one. For instance, if the loading intensity is uniform, the equation representing such intensity is a horizontal line that can be conceived as involving the zero power of x. The integral for the shear diagram will be an inclined line that is a linear function of x. Similarly, the equation for a uniformly varying load is linear, but the resulting curve in the shear diagram is a second-degree parabola. So long as the elements of areas composing the loading and shear diagrams involve only rectangles, triangles, and second-degree parabolas, the summation process is very effective. For irregular loadings, however, approximations must be made in order to obtain a reasonable answer by the summation process.

Example 3-4. Construct shear and moment diagrams for the beam shown in Fig. 3-13(a).

The reactions of the beam are obtained from the conditions of equilibrium as follows:

$$\sum M_b = 0, \quad 30V_g - (27)(2) - (30)(18) - (20)(12) - (\tfrac{1}{2})(6)(6)(8) - (6)(6)(3) + (\tfrac{1}{2})(6)(6)(2) = 0$$

or

$$V_g = 35.0 \text{ kips}$$

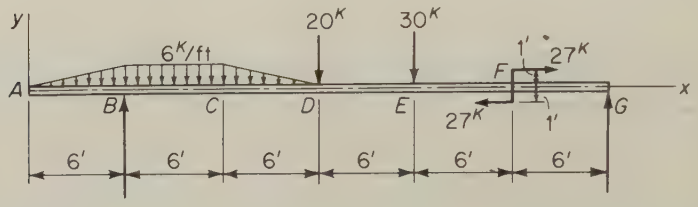

(a)

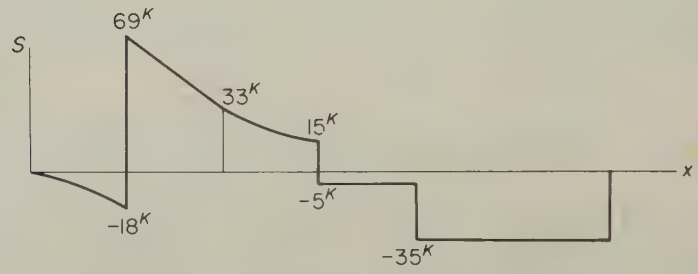

(b)

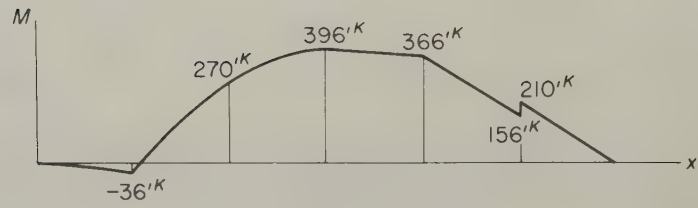

(c)

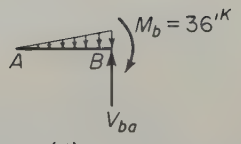

(d)

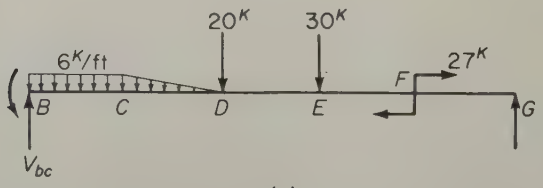

(e)

Figure 3-13

$$\sum F_y = 0, \quad V_b + 35 = (\tfrac{1}{2})(6)(6) + (6)(6) + (\tfrac{1}{2})(6)(6) + 20 + 30$$

or

$$V_b = 87.0 \text{ kips}$$

The reactions should always be checked in order to avoid carrying the errors to subsequent steps. From $\Sigma M_g = 0$,

$$30V_b - (\tfrac{1}{2})(6)(6)(32) - (6)(6)(27) - (\tfrac{1}{2})(6)(6)(22) - (20)(18) - (30)(12) + (27)(2) = 0$$

or

$$V_b = 87.0 \text{ kips}$$

Shears at various sections of the beam are obtained by the summation of the area of the loading diagram, starting from point A. Where there are vertical forces acting, such as points B, D, and E, sections should be cut just to the left and just to the right of the force since each of these sections may represent critical values of shear. The horizontal forces forming an external couple at point F do not contribute to vertical shears. We shall use a single subscript to denote the function at a point if the function is continuous at that point, and use double subscripts if the function is discontinuous at the point. In the latter case, the second subscript indicates whether we refer to the left or the right of the point in question.

$$\begin{aligned}
S_a &= 0 \text{ from the given boundary condition} \\
S_{ba} &= -(\tfrac{1}{2})(6)(6) = -18 \text{ kips} \\
S_{bc} &= -18 + 87 = 69 \text{ kips} \\
S_c &= 69 - (6)(6) = 33 \text{ kips} \\
S_{dc} &= 33 - (\tfrac{1}{2})(6)(6) = 15 \text{ kips} \\
S_{de} &= 15 - 20 = -5 \text{ kips} \\
S_{ed} &= -5 + 0 = -5 \text{ kips} \\
S_{eg} &= -5 - 30 = -35 \text{ kips}
\end{aligned}$$

The curves joining the critical points in Fig. 3-13(b) are drawn in accordance with the differential relationship given by Eq. (3-1). Since the loading diagram between A and B indicates a negative distributed load of varying intensity that increases in magnitude with the positive x-axis, the slope of the shear diagram from A to B is negative and increases in magnitude in the positive direction of the x-axis. Thus the resulting curve is concave downward. From B to C, the loading intensity is uniform and negative, and so is the slope in the shear diagram. From C to D, the loading intensity is negative and decreases in magnitude in the positive x-axis. Thus, the shear diagram between C and D is represented by a curve concave upward. Since there is no vertical load between D and E, or between E and G, each of these intervals is represented by a horizontal line in the shear diagram.

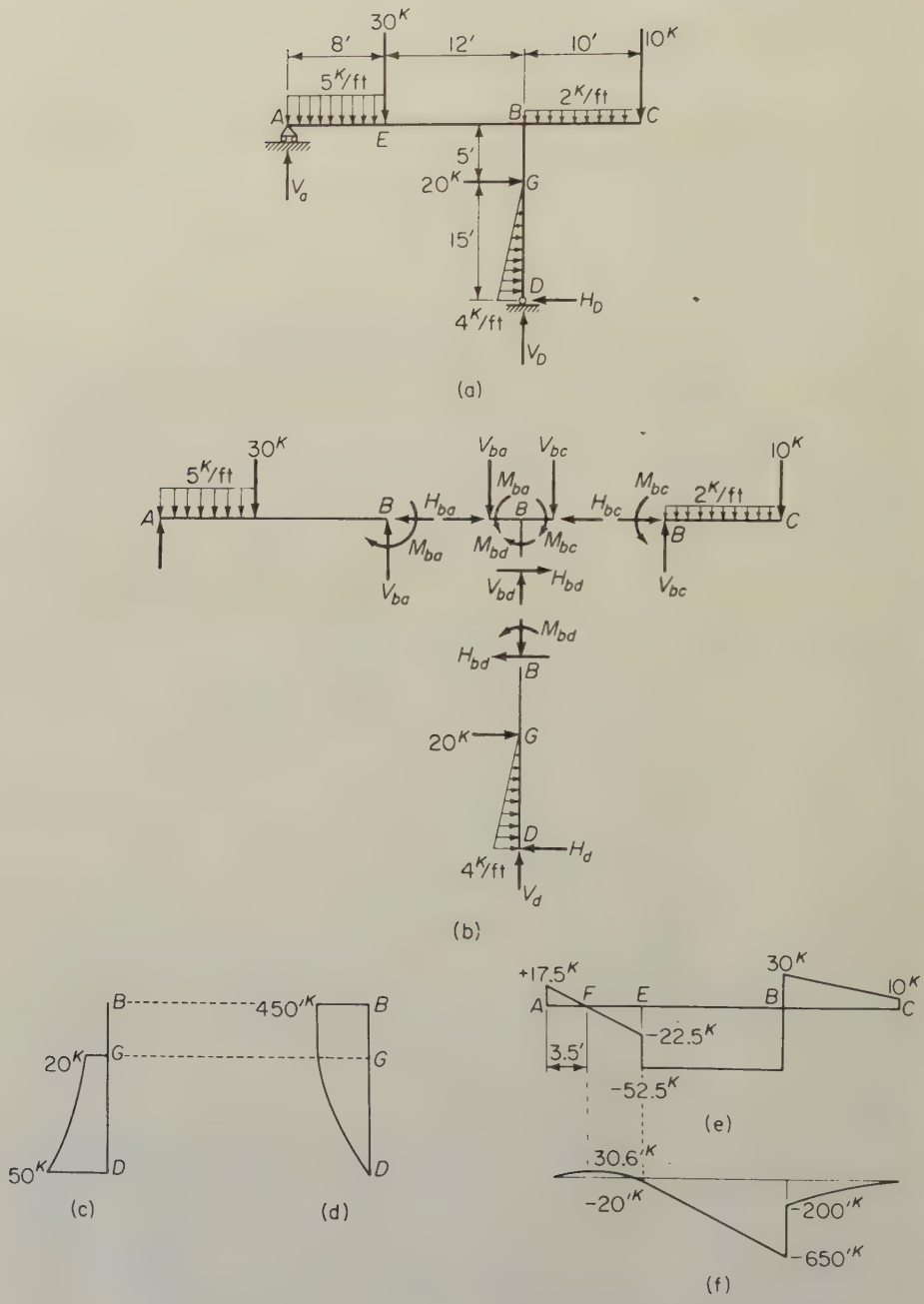
30K
8′
12′
10′
10K
5K/ft
2K/ft
A
E
B
C
5′
20K
G
15′
D
HD
4K/ft
VD
Va
(a)
Vba
Vbc
Mba
Hba
Hbc
Mbc
Mbd
Hbd
Vbd
Vba
Vbc
Hd
Vd
(b)
50K
20K
450′K
(c)
(d)
+17.5K
-22.5K
-52.5K
3.5′
30.6′K
-20′K
-200′K
-650′K
(e)
(f)

Figure 3–14

Moments at various sections of the beam are obtained by the summation of the area of the shear diagram, starting again from point A. For the external couple at point F, there is a sudden change in moment from the left to the right of the section. Hence,

$$\begin{aligned}
M_a &= 0 \text{ from the given boundary condition} \\
M_b &= -(\tfrac{1}{3})(6)(18) = -36 \text{ ft-kips} \\
M_c &= -36 + (6)(33) + (\tfrac{1}{2})(6)(69 - 33) = 270 \text{ ft-kips} \\
M_d &= 270 + (6)(15) + (\tfrac{1}{3})(6)(33 - 15) = 396 \text{ ft-kips} \\
M_e &= 396 + (6)(-5) = 366 \text{ ft-kips} \\
M_{fe} &= 366 + (6)(-35) = 156 \text{ ft-kips} \\
M_{fg} &= 156 + (27)(2) = 210 \text{ ft-kips}
\end{aligned}$$

The curves joining the critical points in Fig. 3-13(c) are drawn in accordance with the differential relationship given by Eq. (3-2). It should be pointed out that the curve segments from A to B and from C to D are cubical parabolas, but the curve segment from B to C is a second-degree parabola. Note also that the maximum positive and negative moments occur at points D and B, respectively, where the vertical lines at D and B intersect the x-axis in the shear diagram.

We may digress to point out that the beam in Fig. 3-13(a) can be isolated into free bodies as shown in Figs. 3-13(d) and (e). The moment at B can easily be determined from the free body in Fig. 3-13(d) and can be applied to the free body in Fig. 3-13(e) as a known moment. This does not alter the shear and moment diagrams of the original beam. However, the reaction R_b of the original beam is equal to the sum of V_{ba} and V_{bc} in Figs. 3-13(d) and (e) respectively. The reaction V_{ba} in Fig. 3-13(d) corresponds to the shear S_{ba} just to the left of point B of the original beam and the reaction V_{bc} in Fig. 3-13(e) corresponds to the shear S_{bc} just to the right of point B of the beam. Neither of them is equal to its reaction R_b. This point is important because very often we may wish to simplify a problem as given in Fig. 3-13(a) to equivalent systems as shown in Figs. 3-13(d) and (e). In that case, we should realize that the reaction at point B of the original beam must be obtained from the shears at *both* sides of point B.

Example 3-5. Construct shear and moment diagrams for the rigid frame shown in Fig. 3-14(a).

The reactions of the frame are first obtained as follows:

$$\sum M_d = 0 \quad 20V_a - (5)(8)(16) - (30)(12) + (2)(10)(5) + (10)(10) + (20)(15) + (\tfrac{1}{2})(4)(15)(\tfrac{15}{3}) = 0$$

$$V_a = 17.5 \text{ kips}$$

$$\sum F_y = 0, \quad V_d = (5)(8) + 30 + (2)(10) + 10 - 17.5 = 82.5 \text{ kips}$$

$$\sum F_x = 0, \quad H_d = (\tfrac{1}{2})(4)(15) + 20 = 50 \text{ kips}$$

$$\sum M_a = 0, \quad (5)(8)(4) + (30)(8) + (2)(10)(25) + (10)(30) - (20)(5) - (\tfrac{1}{2})(4)(15)(15) - (82.5)(20) + (50)(20) = 0 \quad \text{(checked)}$$

In constructing the shear and moment diagrams, we can first isolate all the members meeting at joint B as free bodies as shown in Fig. 3-14(b). The members may be thought of being cut just outside of the joint, and joint B is held in equilibrium by forces and moments equal but opposite to those at the ends of the members. The senses of forces and moments at point B are arbitrarily assumed. If the sense of a force or moment is correct, the result will have the same sign as assumed; otherwise, the result will be of opposite sign. In general, the unknowns at end B of each member may be obtained from the conditions of equilibrium of that member. Their results can be checked by the consideration of equilibrium of joint B. With the assumed senses of forces and moment as shown, we have

$$\sum F_x = 0, \quad H_{bc} - H_{ba} - H_{bd} = 0$$

$$\sum F_y = 0, \quad V_{bc} + V_{ba} - V_{bd} = 0$$

$$\sum M_b = 0, \quad M_{ba} - M_{bd} - M_{bc} = 0$$

Since no external horizontal forces act on members AB and BC, H_{ba} and H_{bc} are obviously zero. In such a case, we can easily consider members AB and BC together.

The shear and moment diagrams for the vertical member DB are shown in Figs. 3-14(c) and (d), respectively. Shears at the critical sections of the vertical member are obtained by the summation of the area in the loading diagram.

$$S_d = 50 \text{ kips from the boundary condition}$$

$$S_{gd} = 50 - (\tfrac{1}{2})(4)(15) = 20 \text{ kips}$$

$$S_{gh} = 20 - 20 = 0$$

Moments at the critical sections of the member are obtained from the summation of the area in the shear diagram.

$$M_d = 0 \text{ from the boundary condition}$$

$$M_g = (15)(20) + (\tfrac{1}{3})(15)(50 - 20) = 450 \text{ ft-kips}$$

$$M_b = 450 + 0 = 450 \text{ ft-kips}$$

The curves joining the critical points in the shear and moment diagrams are plotted according to the differential relationships given by Eqs. (3-1) and (3-2).

The shear and moment diagrams of the horizontal member AC are shown

in Figs. 3-14(e) and (f), respectively. Shears at various sections of the girder are determined as follows:

$$S_a = 17.5 \text{ kips from the boundary condition}$$
$$S_{ea} = 17.5 - (5)(8) = -22.5 \text{ kips}$$
$$S_{eb} = -22.5 - 30 = -52.5 \text{ kips}$$
$$S_{bc} = -52.5 + 82.5 = 30 \text{ kips}$$
$$S_{cb} = 30 - (2)(10) = 10 \text{ kips}$$

Point F of zero shear in the shear diagram corresponds to the point of maximum moment in the moment diagram. The distance AF can be obtained from the relation of similar triangles, or $AF = (17.5)(8)/(40) = 3.5$ ft. Then, moments at various sections of the girders can also be obtained from the summation of the area in the shear diagram.

$$M_a = 0 \text{ from the boundary condition}$$
$$M_f = (\tfrac{1}{2})(3.5)(17.5) = 30.6 \text{ ft-kips}$$
$$M_e = 30.6 + (\tfrac{1}{2})(4.5)(-22.5) = -20 \text{ ft-kips}$$
$$M_{be} = -20 + (12)(-52.5) = -650 \text{ ft-kips}$$
$$M_{bc} = -650 + 450 = -200 \text{ ft-kips}$$

It should be pointed out that there is a sudden change in moment along the girder at point B owing to the moment of 450 ft-kips introduced at joint B by the vertical member DB. As shown in Fig. 3-14(b), the algebraic sum of moments from all members meeting at joint B must be zero, i.e.,

$$M_{ba} - M_{bd} - M_{bc} = 650 - 450 - 200 = 0$$

The moment M_{bc} can also be obtained from the consideration of the portion BC of the girder as a free body. Thus,

$$M_{bc} = -(10)(10) - (2)(10)^2/2 = -200 \text{ ft-kips}$$

Example 3-6. Draw shear and moment diagrams for the gable frame with pitched roof as shown in Fig. 3-15(a).

To simplify the solution of the problem, the loads are resolved into vertical and horizontal components. The reactions are obtained as follows:

$$\sum M_a = 0, \quad (2)(20)^2/2 + (\tfrac{5}{13})(26)(25 + 30) + (\tfrac{12}{13})(26)(12 + 24) + (20)(46) - 56V_e = 0$$

$$V_e = 48.8 \text{ kips}$$

$$\sum F_x = 0, \quad H_a = (\tfrac{5}{13})(26)(2) + (2)(20) = 60 \text{ kips}$$

$$\sum F_y = 0, \quad V_a = (\tfrac{12}{13})(26)(2) + 20 - 48.8 = 19.2 \text{ kips}$$

$$\sum M_e = 0, \quad (19.2)(56) + (2)(20)^2/2 - (\tfrac{12}{13})(26)(44 + 32) + (\tfrac{5}{13})(26)(25 + 30) - (20)(10) = 0 \quad \text{(checked)}$$

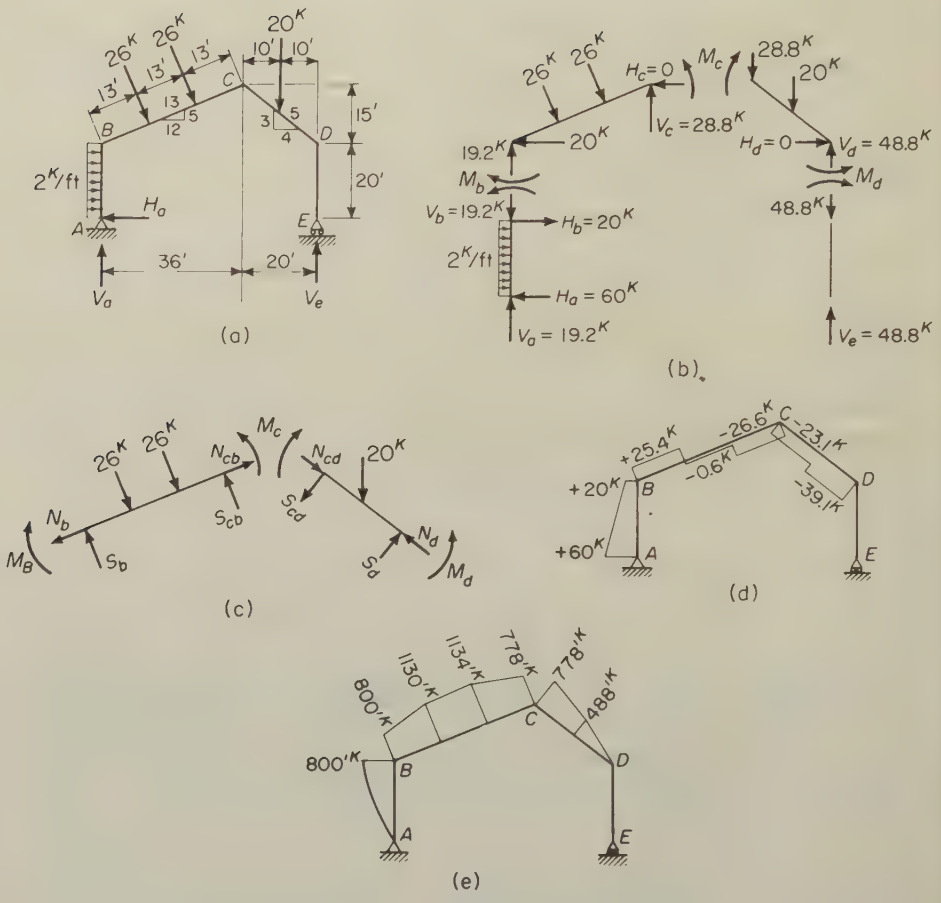

Figure 3–15

From the free-body diagrams of the individual members in Fig. 3-15(b), it can easily be seen that $H_b = 20$ kips, $H_c = 0$, and $H_d = 0$; $V_b = 19.2$ kips, $V_c = 28.8$ kips, and $V_d = 48.8$ kips. Furthermore,

$$M_b = (60)(20) - (40)(10) = 800 \text{ ft-kips}$$

$$M_c = 800 + (19.2)(36) + (20)(15) - (26)(26 + 13) = 778 \text{ ft-kips}$$

$$M_d = 778 - (28.8)(20) - (20)(10) = 0$$

For the vertical members, the steps of computing axial force, shear, and moment in the member are obvious. For the inclined members, however, only the horizontal and vertical components of the axial force and shear are given with the moment at the rigid joints. Thus, the axial force and shear for the free-body diagrams shown in Fig. 3-15(c) must be obtained from the

horizontal and vertical components. For the free body on the left-hand side of the figure,

$$N_b = (20)(12/13) - (19.2)(5/13) = 11.1 \text{ kips}$$
$$S_b = (20)(5/13) + (19.2)(12/13) = 25.4 \text{ kips}$$
$$N_{cb} = 11.1 \text{ kips}$$
$$S_{cb} = (2)(26) - 25.4 = 26.6 \text{ kips}$$

For the free body on the right-hand side of the figure,

$$N_d = (48.8)(3/5) = 29.3 \text{ kips}$$
$$S_d = (48.8)(4/5) = 39.1 \text{ kips}$$
$$N_{cd} = 29.3 - (3/5)(20) = 17.3 \text{ kips}$$
$$S_{cd} = 39.1 - (4/5)(20) = 23.1 \text{ kips}$$

Finally, the shear and moment diagrams are plotted in Figs. 3-15(d) and (e), respectively.

Example 3-7. Draw the shear and moment diagrams for the beam shown in Fig. 3-16(a).

The reactions of the beam are first obtained as follows:

$$\sum M_b = 0, \quad 200 - 100 + 30V_a - (2)(16)(8 + 7 + 7) - (80)(7) = 0$$
$$V_a = 38.8 \text{ kips}$$
$$\sum F_y = 0, \quad V_b = (2)(16) + 80 - 38.8 = 73.2 \text{ kips}$$

Thus, the shear and moment diagrams may be plotted as shown in Figs. 3-16(b) and (c), respectively.

However, we may also obtain the shear and moment diagrams by the principle of superposition if the external loads are applied to the beam separately. For example, we can consider first the vertical loads on the beam without the end moments. Then, the reactions become

$$\sum M_b = 0, \quad 30V_a - (2)(16)(8 + 7 + 7) - (80)(7) = 0$$
$$V_a = 42.1 \text{ kips}$$
$$\sum F_y = 0, \quad V_b = (2)(16) + 80 - 42.1 = 69.9 \text{ kips}$$

The shear and moment diagrams for the beam due to the vertical loads alone are indicated by the solid lines in Figs. 3-16(d) and (e), respectively. Next, we consider only the end moments acting on the beam without the vertical loads. Thus, the reactions are obtained as follows:

$$\sum M_b = 0, \quad 30V_a + 200 - 100 = 0, \quad V_a = -3.3 \text{ kips}$$
$$\sum F_y = 0, \quad V_a + V_b = 0, \quad V_b = 3.3 \text{ kips}$$

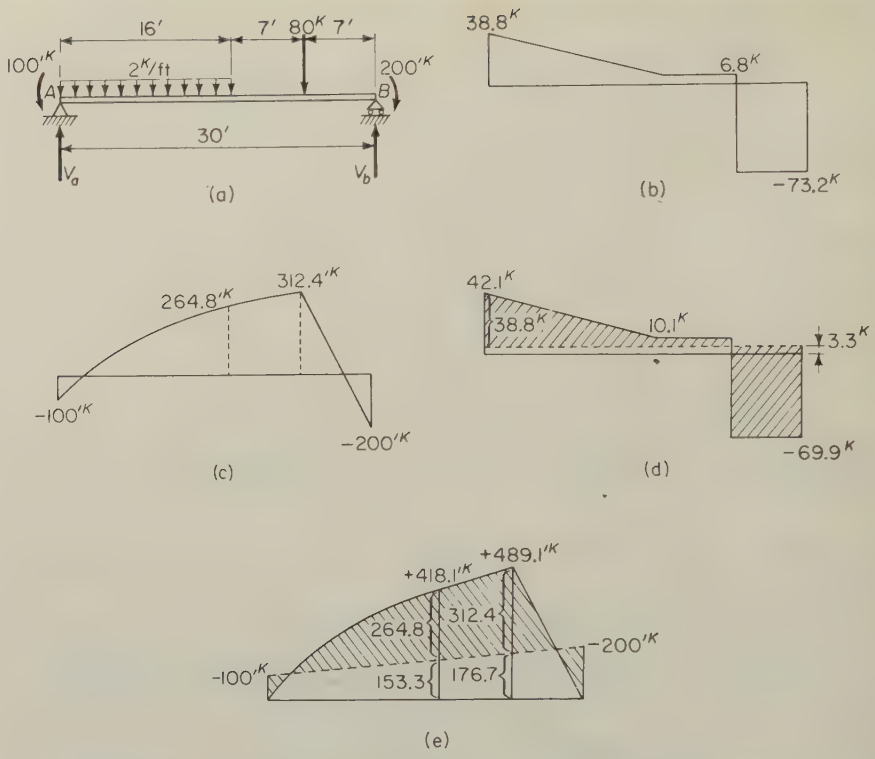

Figure 3–16

This indicates that a pair of forces, equal and opposite, is acting at the supports to balance the external end moments. The shear and moment diagrams for the beam due to the end moments alone are indicated by the dotted lines in Figs. 3-16(d) and (e), respectively. Note that the shear and moment diagrams resulting from vertical loads are plotted with *positive* ordinates above the horizontal base line whereas those due to end moments are plotted with *negative* ordinates above the horizontal base line. When the diagrams resulting from vertical loads are superimposed on those due to end moments, the overlapping areas will be cancelled and the remaining shaded areas represent the final diagrams due to vertical loads and end moments.

In comparing Figs. 3-16(b) and (c) with Figs. 3-16(d) and (e), it can be seen that the results are identical although the diagrams may appear slightly different because of different base lines for measuring the ordinates. We may also view the case with vertical loads only as a beam with boundary conditions $M_a = 0$ and $M_b = 0$. With the given boundary conditions $M_a = -100$ ft-kips and $M_b = -200$ ft-kips, the shapes of shear and moment

curves remain the same but the ordinates of the shear and moment diagrams are different from those of the beam with no end moments. The reason is that the base line of the shear diagram for the beam without end moments is translated upward, and the base line of the moment diagram is both translated upward and rotated in a counterclockwise direction as a result of the end moments. Thus, in the analysis of a beam acted on by end moments as well as vertical loading, the effect of end moments may be superimposed upon that of an identical beam having the same vertical loading but no end moments.

3-6 *Girders Supporting Floor Beams*

In many structures, the external loads are applied to a floor system that in turn transmits these loads to the main member or main system of the structure. As an example, a girder supporting floor beams is shown in Fig. 3-17(a). In general, the span lengths of the stringers need not be equal and

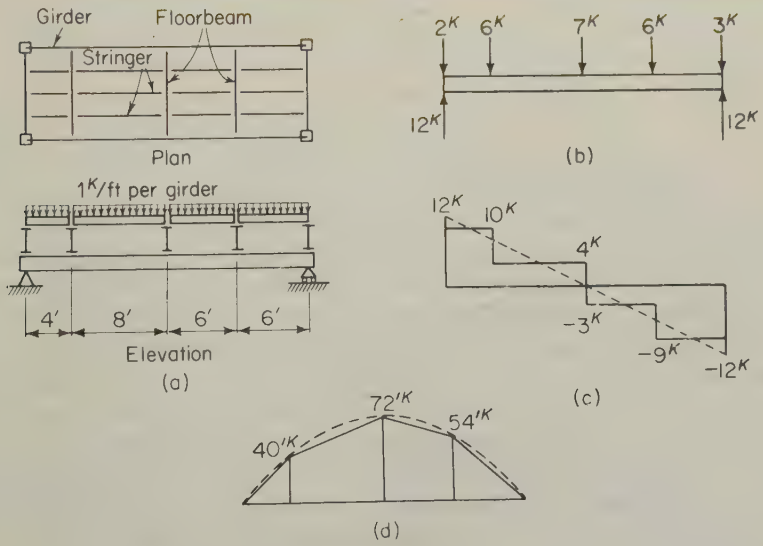

Figure 3–17

thus the floor beams are irregularly spaced. The locations of the floor beams are called *panel points* whereas the distances between them are considered as the panels of the girder. The load transmission from stringers to floor beams and then to the girder is straightforward since the reactions of the stringers are the applied loads on the girder. Thus, the concentrated loads at the panel points may be computed as shown in Fig. 3-17(b). Obviously, the reactions of the girder remain unchanged whether or not a floor

system is used to transmit the applied loads. However, the shears and moments at some locations are affected by the presence of the floor system.

The shear and moment diagrams for the girder in Fig. 3-17(a) are indicated by the solid lines in Figs. 3-17(c) and (d), respectively. If the uniformly distributed loads were applied directly to an identical girder without a floor system, the resulting shear and moment diagrams would be as shown by the dotted lines in the corresponding figures. Note that the shear at each panel point of the girder between floor beams is constant and is called the *panel shear*. Thus, the shear at a point just to the left of a panel point is different from that just to the right of the same panel point. Note also that the moments at the panel points of the girder are not influenced by the use of a floor system.

Example 3-8. Draw the shear and moment diagrams for the girder shown in Fig. 3-18(a).

This same girder, without floor beams but under the same loading, has been treated in Example 3-4, and the reactions of the girder in this case are identical to those given in that example. The shear and moment diagrams in Example 3-4 are indicated by dotted lines on the corresponding diagrams of this problem for the purpose of comparison.

Since only stringers AB, BC, and CD are subjected to applied loads, the loading, shear, and moment diagrams for these individual stringers are shown in Figs. 3-18(b), (c), and (d), respectively. Thus, the final loads acting on the girder may be represented by Fig. 3-17(e). The pairs of vertical loads at points B, C, and D could have been combined, but they are shown separately so that their effects can be more readily seen in the shear diagram of the girder. The distance between the two forces in each pair is considered to be infinitesimal or zero. The shear and moment diagrams of the girder are represented by the solid lines in Figs. 3-18(f) and (g), respectively. It can be seen that the dotted lines in Fig. 3-18(f) may be obtained by superimposing the individual shear diagrams in Fig. 3-18(c) onto the solid lines representing the shear diagram of the girder, and the dotted lines in Fig. 3-18 (g) may be obtained by superimposing the individual moment diagrams in Fig. 3-18(d) onto the solid lines representing the moment diagram of the girder. Hence, the shears and moments along a girder subjected to applied loads directly may be obtained by superposition of the corresponding shears and moments in a similar girder supporting floor beams and the shears and moments in the individual stringers between floor beams. Such conclusions lead to some very useful applications in determining shears and moments in beams subjected to irregular loading.

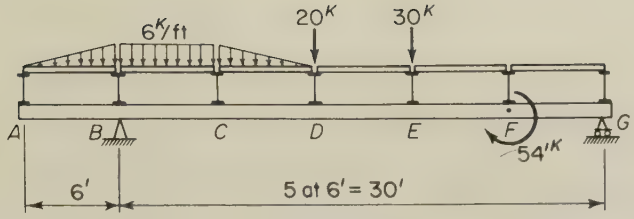

(a)

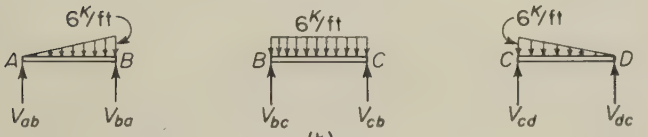

(b)

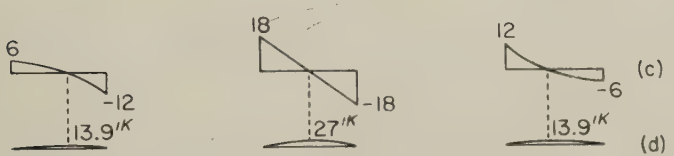

(c)

(d)

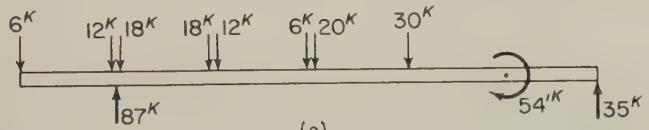

(e)

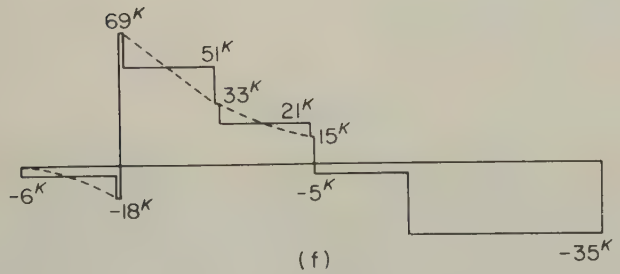

(f)

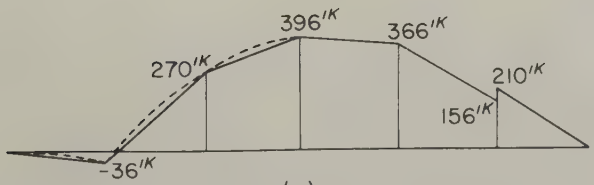

(g)

Figure 3–18

3-7 Beams Subjected to Irregular Loading

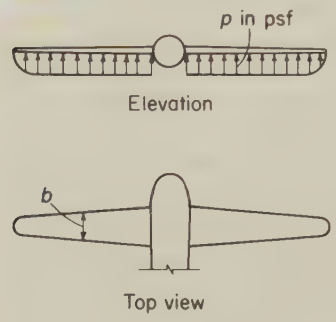

Figure 3–19

In engineering applications, beams may be subjected to rather irregular loading patterns. Usually such irregular loading patterns can be approximated by some simple mathematical curves without introducing significant errors. For instance, an airplane subjected to lift pressure is shown in Fig. 3-19. Each wing can be considered as a cantilever beam subjected to a loading intensity along its length as shown in Fig. 3-20(a). Since the width of the wing varies, the loading intensity q per unit length of the beam is obtained from the product of the wing width b and the lift pressure p, which is expressed in force per unit area.

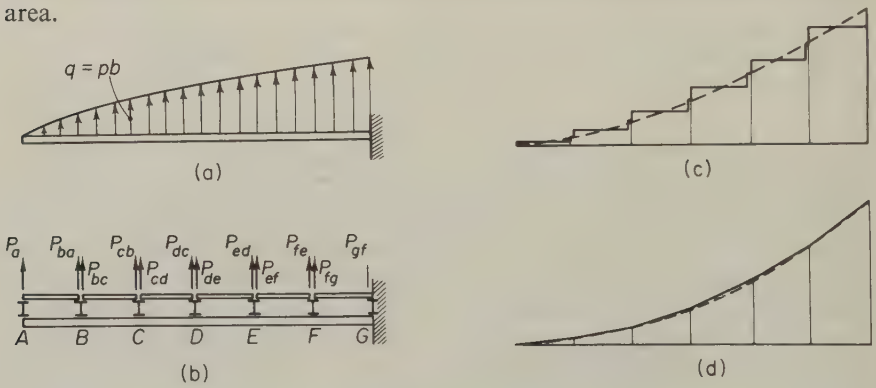

Figure 3–20

Imagine that stringers and floor beams are introduced for transmitting the distributed load to the cantilever beam. Then, the distributed load along the length of the beam can be replaced by equivalent concentrated loads at the locations of the imaginary floor beams. For the sake of simplicity, the floor beams may be equally spaced, and the fictitious panel length depends only on the accuracy desired for the resulting shears and moment in the beam. For instance, the cantilever beam in Fig. 3-20(b) is divided into six equal panels, which may be considered as six imaginary stringers. The concentrated loads shown in the figure are equal in magnitude to the corresponding reactions of the imaginary stringers. The shear and moment diagrams for the given irregular loading intensity are shown dotted in Figs. 3-20(c) and (d) respectively; those for the equivalent concentrated loads are indicated by the solid lines in the corresponding diagrams.

If the shears and moments for the individual imaginary stringers can be computed, they can be superimposed on the corresponding quantities obtained from the equivalent concentrated loads to obtain the true shears and moments in the cantilever beam due to the original loading. For design purposes, however, only the shears and moments at a finite number of points on the beams are usually desired. Thus, those points on the beam may be designated as the fictitious panel points. As the number of panels increases, greater accuracy may be obtained for the approximation of the loading curve.

The loading curve may be approximated by segments of straight lines, second-degree curves, or higher-degree curves. Two points are required to define a straight line, three points for a second-degree curve, and one more point for each increase in the degree of a curve. It has been found that straight line segments or second-degree curves are sufficiently accurate for practical purposes, and further refinements by higher-degree curves are not necessary.

Consider first the case of approximation by straight line segments. Let h be the length of the equal panels selected for the purpose of computing equivalent concentrated loads. If the loading intensity q is distributed along the length of the x-axis as shown in Fig. 3-21(a), the panel at each panel

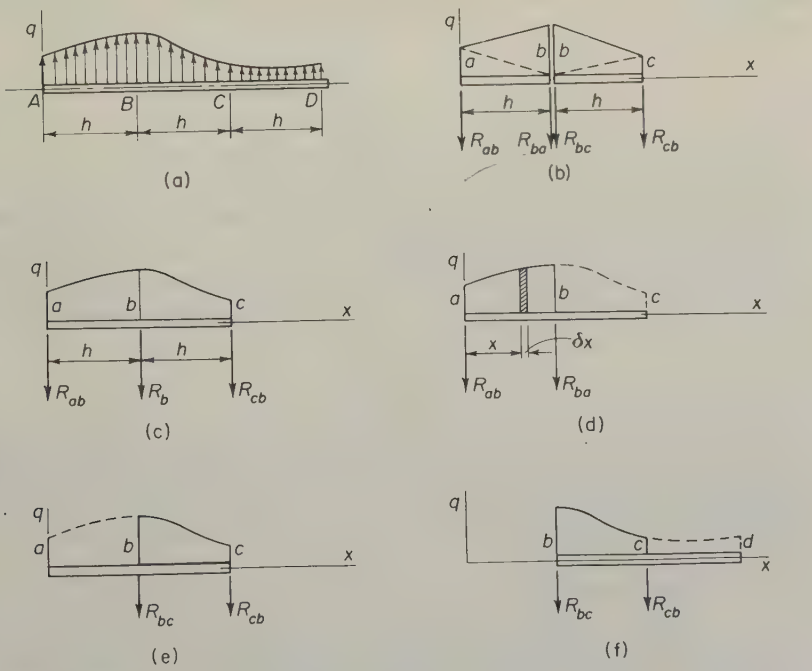

Figure 3–21

point is influenced by the loading on the panels immediately adjacent to the panel point only if straight line approximation is used. Thus, for the end point A, we need to consider only panel AB, whereas for the interior panel B, we will consider both panels AB and BC as shown in Fig. 3-21(b). If the ordinates of the loading at points A, B, and C are denoted by a, b, and c respectively, the reactions of the imaginary stringers may be obtained from the trapezoidal areas in the loading diagram. Thus, from Fig. 3-21(b),

$$R_{ab} = \frac{1}{3}ah + \frac{1}{6}bh = \frac{h}{6}(2a + b) \tag{3-11a}$$

$$R_{ba} = \frac{1}{6}ah + \frac{1}{3}bh = \frac{h}{6}(a + 2b) \tag{3-11b}$$

Similarly,

$$R_{bc} = \frac{h}{6}(c + 2b)$$

$$R_{cb} = \frac{h}{6}(b + 2c)$$

The equivalent concentrated load at a typical interior point is equal in magnitude to the sum of the reactions from both sides of that point. Thus, for point B,

$$R_b = R_{ba} + R_{bc} = \frac{h}{6}(a + 4b + c) \tag{3-11c}$$

If the loading curve in Fig. 3-21(a) is approximated by a second-degree curve, three ordinates are necessary to define such a curve. For the interior point B, it is logical to select the ordinates a, b, and c. Thus, the loading curve between A and C will be considered. For the end point A, however, the best we can do is to choose ordinates a, b, and c. If a, b, and c are known, we can obtain a second-degree curve to pass through these points as follows:

$$q = \frac{a}{2h^2}(x - h)(x - 2h) - \frac{b}{h^2}x(x - 2h) + \frac{c}{2h^2}x(x - h)$$

It can be readily verified that this second-degree function satisfies the requirement that $q = a$, b, and c at $x = 0$, h, and $2h$ respectively. From the conditions of equilibrium of panel AB shown in Fig. 3-21(d), the following equations are obtained:

$$\sum F_y = 0, \quad R_{ab} + R_{ba} = \int_0^h q\,dx$$

$$\sum M_a = 0, \quad R_{ba}h = \int_0^h qx\,dx$$

Solving these two equations simultaneously, one obtains

$$R_{ab} = \frac{h}{24}(7a + 6b - c) \tag{3-12a}$$

$$R_{ba} = \frac{h}{24}(3a + 10b - c) \tag{3-12b}$$

Similarly, for panel BC in Fig. 3-21(e), the following relations may be derived:

$$R_{bc} = \frac{h}{24}(3c + 10b - a)$$

$$R_{cb} = \frac{h}{24}(7c + 6b - a)$$

Thus, the equivalent concentrated load at a typical interior point is equal in magnitude to the sum of the reactions from both sides of that point. For point B,

$$R_b = R_{ba} + R_{bc} = \frac{h}{12}(a + 10b + c) \tag{3-12c}$$

It should be pointed out that the reactions for panel BC may also be obtained from the ordinates b, c, and d shown in Fig. 3-21(d) as follows:

$$R_{bc} = \frac{h}{24}(7b + 10c - d)$$

$$R_{cd} = \frac{h}{24}(3b + 10c - d)$$

However, these values are not used in computing R_b because we have selected ordinates a, b, and c for approximating the panel load at point B. On the other hand, these values are needed in the computation of the panel load at point C. If D is the terminal point, the panel load at D is equal to

$$R_{dc} = \frac{h}{24}(7d + 10c - b) \tag{3-12d}$$

Note that in Eqs. (3-12), the ordinate at a panel point has the greatest influence on the panel load at that point. For the panel load at A, for instance, the ordinate a has the largest coefficient and the ordinate c has only a minor influence in Eq. (3-12a). For the panel load at B, the influence of ordinate b in Eq. (3-12c) is obvious.

Example 3-9. Figure 3-22 shows a cantilever beam subject to a distributed loading that can be approximated by straight line segments. Determine the equivalent concentrated loads at the panel points.

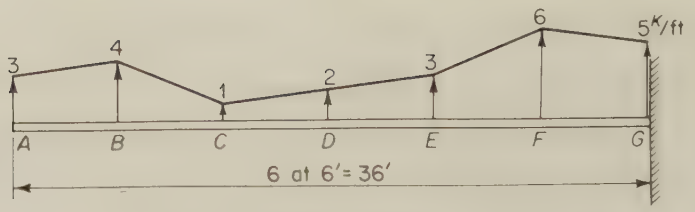

Figure 3–22

Since the beam is divided into six equal panels, the equivalent concentrated loads may be computed by either Eqs. (3-11a) and (3-11b) for separate reactions from stringers to the left and to the right of a panel point or Eq. (3-11c) for the combined reactions from the stringers on both sides of the panel point. Thus,

$$R_{ab} = \tfrac{6}{6}\,[(2)\,(3) + 4] = 10; \quad R_{ba} = \tfrac{6}{6}\,[(2)\,(4) + 3] = 11$$

$$R_{bc} = \tfrac{6}{6}\,[(2)\,(4) + 1] = 9; \quad R_{cb} = \tfrac{6}{6}\,[(2)\,(1) + 4] = 6$$

$$R_{cd} = \tfrac{6}{6}\,[(2)\,(1) + 2] = 4; \quad R_{dc} = \tfrac{6}{6}\,[(2)\,(2) + 1] = 5$$

$$R_{de} = \tfrac{6}{6}\,[(2)\,(2) + 3] = 7; \quad R_{ed} = \tfrac{6}{6}\,[(2)\,(3) + 2] = 8$$

$$R_{ef} = \tfrac{6}{6}\,[(2)\,(3) + 6] = 12; \quad R_{fe} = \tfrac{6}{6}\,[(2)\,(6) + 3] = 15$$

$$R_{fg} = \tfrac{6}{6}\,[(2)\,(6) + 5] = 17; \quad R_{gf} = \tfrac{6}{6}\,[(2)\,(5) + 6] = 16$$

or

$$R_a = R_{ab} = 10$$

$$R_b = R_{ba} + R_{bc} = 20$$

$$R_c = R_{cb} + R_{cd} = 10$$

$$R_d = R_{dc} + R_{de} = 12$$

$$R_e = R_{ed} + R_{ef} = 20$$

$$R_f = R_{fe} + R_{fg} = 32$$

$$R_g = R_{gf} = 16$$

Example 3-10. Figure 3-23 shows a simply supported beam subjected to a

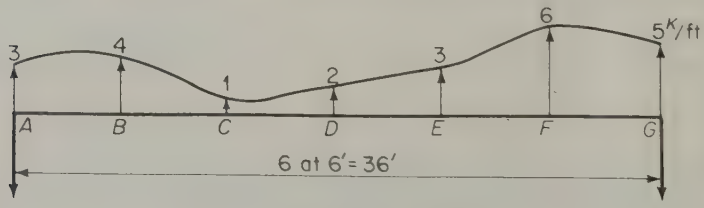

Figure 3–23

distributed loading that can be approximated by a second-degree curve. Compute the equivalent concentrated loads at the panel points.

The beam is divided into six equal panels and the equivalent concentrated loads at the panel points may be computed by Eq. (3-12) as follows:

$$R_a = \tfrac{6}{24}[(7)(3) + (6)(4) - 1] = 11$$

$$R_b = \tfrac{6}{12}[3 + (10)(4) + 1] = 22$$

$$R_c = \tfrac{6}{12}[4 + (10)(1) + 2] = 8$$

$$R_d = \tfrac{6}{12}[1 + (10)(2) + 3] = 12$$

$$R_e = \tfrac{6}{12}[2 + (10)(3) + 6] = 19$$

$$R_f = \tfrac{6}{12}[3 + (10)(6) + 5] = 34$$

$$R_g = \tfrac{6}{24}[(7)(5) + (6)(6) - 3] = 17$$

3-8 Numerical Procedure for Computing Shears and Moments

After the equivalent concentrated loads are computed, a numerical procedure may be used for rapid and systematic calculation of shears and moments in a beam. Essentially, the procedure is based on the summation process explained in Section 3-3 and represented by Eqs. (3-5) and (3-6). In applying the process to a beam subjected to concentrated loads only, the procedure is greatly simplified since the area in the loading diagram is zero and the area in the shear diagram consists of rectangular elements that may be considered as products of the shear in a panel and the panel length. Thus, the procedure is reduced to computing the shears from one end of the beam to the other by adding or subtracting the successive loads, and then to computing the moments by adding or subtracting the successive shears multiplied by the panel length over which the shear acts. By considering upward loads as positive, the successive calculation of shears and moments can be carried out by adding, respectively, loads and shears from left to right, starting from a point of known shear and moment.

For example, the free end of the cantilever beam in Fig. 3-20(b) is a point of zero shear and zero moment. If the equivalent concentrated loads in the figure are known, the ordinates of the shear diagram can be obtained by adding the series of concentrated loads from left to right as indicated by the solid lines in Fig. 3-20(c). It may be noted that the *actual shear* due to the original loading varies within a panel, whereas the *panel shear* due to the equivalent concentrated loads remains constant within a panel. The true shears at the panel points may be obtained easily if the equivalent concentrated loads to the right and to the left of a panel point are computed separately. In most cases, however, the average shears are accurate enough for design purposes, particularly if the number of panels is large.

The ordinates of the moment diagram in Fig. 3-20(d) are obtained by the summation from left to right of the area in the shear diagram. The moments at the panel points are identical to the actual moments at the corresponding points due to the original loading.

When only the moments at two points are known, such as zero moment at the two supports of a simply supported beam, the summation process must be modified. Either the shear at one of the two points of known moments is first computed by statics, or the shear at that point may be assumed to have an arbitrary value that will be subsequently corrected. The latter approach is based on Eqs. (3-3) and (3-4) as well as Eqs. (3-5) and (3-6), and involves a translational correction for shears and a rotational correction for moments.

The numerical procedure for computing shears and moments may be summarized as follows.*

1. Compute the equivalent concentrated loads by making a proper approximation of the loading curve, using either straight line segments or a second-degree curve. If the actual shears at the panel points are required, separate reactions from stringers to the left and to the right of a panel point should be computed. If only the panel shears are needed, equivalent concentrated loads representing combined reactions from stringers at the panel points are sufficient.

2. Starting from a point of known shear and moment, add the equivalent concentrated loads from left to right, or subtract the loads from right to left, to obtain shears. Similarly, add the products of shear and the panel length from left to right, or subtract the same products from right to left, to obtain moments.

3. The procedure can be simplified by postponing the multiplication of the shears by the panel length until the end of the computations. As a matter of fact, common factors of multiplication involved in all steps may be left out until the end of the computations.

4. When only the moments at two points are known, the shear at one of these two points can be arbitrarily assumed, and the same procedure may still be used. If the resulting moment at the second point is different from the known moment at that point, the correction for moment may be made by a linear moment diagram which corresponds to a constant shear correction. Thus, the final moments may be obtained from the sum of the linear moment correction and the corresponding trial moments based on arbitrarily assumed shear at a point, and the final shears may be obtained from the constant shear correction and the corresponding trial shears.

The above procedure can be conveniently carried out in a tabulated form using the following notations: q for the intensity of distributed load at

*See Reference 3-2 for further discussions.

a panel point, Q for the equivalent concentrated load at a panel point, S for the panel shear, and M for the moment at a panel point. If the actual shear at a panel point is needed, it will be denoted by $\bar{S}$. For solutions involving trial shears and moments, S' is used for the trial shear in a panel, M' for the trial moment at a panel point, S'' for the shear correction, and M'' for the moment correction.

Example 3-11. For the cantilever beam subjected to a distributed loading shown in Fig. 3-24(a), compute the shears and moments at the panel points.

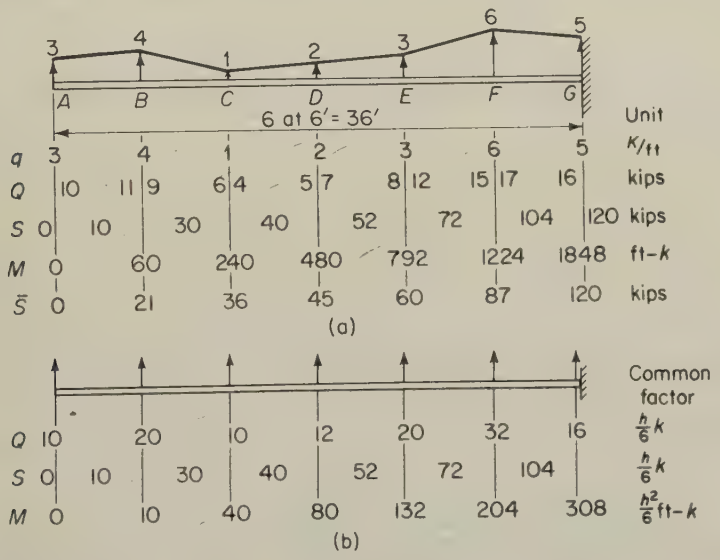

Figure 3-24

The equivalent concentrated loads for this beam have already been computed in Example 3-9. The computation of shears and moments can be carried out in the figure. The first line in the table is the given distributed loading. The second line represents the equivalent concentrated loads to the left and to the right of the panel points. The third line shows the average shears in the panels, which are obtained by starting with zero shear to the left of point A and by adding the equivalent concentrated loads successively from left to right. Thus,

$$S_{ab} = 0 + 10 = 10$$

$$S_{bc} = 10 + 11 + 9 = 30, \text{ etc.}$$

The fourth line indicates the moments at the panel points by starting with zero moment at point A and by adding the product of the shears and the

panel length successively from left to right. Or,

$$M_b = 0 + (10)(6) = 60$$
$$M_c = 60 + (30)(6) = 240, \text{ etc.}$$

The last line in the figure gives the actual shears at the panel points, which are obtained in the same manner as the panel shears except that only the equivalent concentrated load to the left of a panel point under consideration is included in the summation. For instance,

$$\bar{S}_b = 10 + 11 = 21$$
$$\bar{S}_c = 21 + 9 + 6 = 36, \text{ etc.}$$

The units of the computed quantities are shown at the right-hand column of the figure.

The procedure can be simplified as shown in Fig. 3-24(b). In general, the computation of equivalent concentrated loads may involve fractions if h is not divisible by 6. It is therefore advisable to leave out the factor $h/6$ in the computation of the equivalent concentrated loads and to consider it as a common factor in the right-hand column of the figure. For this particular problem, this factor is reduced to $h/6 = 6/6 = 1$. In the computation of moments, another common factor h may be taken out as indicated by the term $h^2/6$ in the right-hand column.

Example 3-12. For the simply supported beam subjected to a distributed

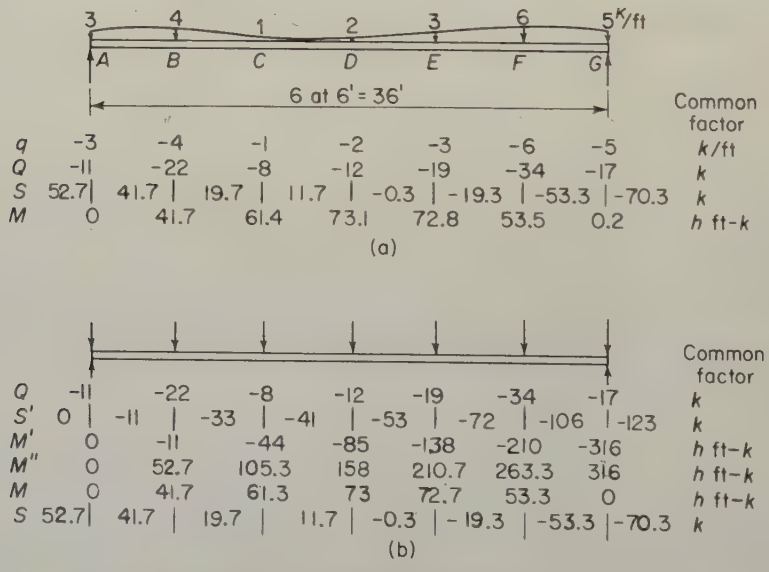

Figure 3–25

loading shown in Fig. 3-25(a), compute the panel shears and the moments at panel points.

The equivalent concentrated loads for this beam have been computed in Example 3-10. The computation of shears and moments can be carried out in the figure after the reaction at A is obtained. Thus, for $R_a = 52.7$ kips, a shear of 52.7 is shown to the left of point A. If we carry through the computation as shown, the resulting moment at point G should be zero. The computed value of 0.2 for the moment at point G is due to the rounding off of the decimal points, and it serves the purpose of showing how errors can be accumulated in such a procedure. Figure 3-25(b) shows the solution of the same problem by assuming arbitrarily a zero shear at the left of point A. Since the resulting moment at point G is $-316h$, a linear moment correction corresponding to the rotation of the base line in the moment diagram is applied so that the moment at point G will be zero. Then the correction for other panel points may be obtained by a simple ratio as follows:

$$M'' \text{ for point } G = +316h$$

$$M'' \text{ for point } F = (\tfrac{5}{6})\ (316h) = 263.3h$$

$$M'' \text{ for point } E = (\tfrac{4}{6})\ (316h) = 210.7h, \text{ etc.}$$

The shear correction is constant throughout corresponding to the translation of the base line in the shear diagram and is equal to the moment correction at point G divided by the span length of the beam, or

$$S'' = \frac{316h}{6h} = 52.7$$

The final panel shears and the final moments at panel points may be obtained by superposition as follows:

$$S = S' + S''$$

$$M = M' + M''$$

If M'' at G is a negative quantity instead of a positive quantity, the negative sign should be included in the summations for final shears and moments.

It should be pointed out that the arbitrarily assumed shear at point A can be any value, including zero. As a matter of fact, if a value of + 50 is used, the resulting moment at point G will be much smaller and the moment correction will be smaller. From a practical point of view, the latter assumed value leads to less numerical work. Hence, it is advisable to assume an arbitrary value for shear approximately equal to the magnitude of the reaction at that point if it can be estimated intelligently.

Example 3-13. For the beam with a distributed loading shown in Fig.

3-26(a), compute the shears in the panels and the moments at the panel points.

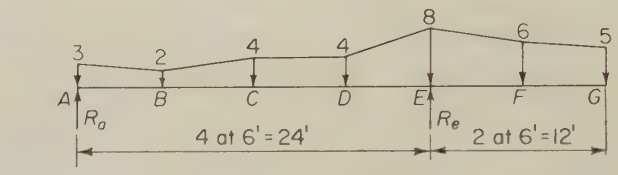

									Common factor
q	-3	-2	-4	-4	-8	-6	-5		k/ft
Q	-8	-15	-22	-28	-42	-37	-16		k
S	20	12	-3	-25	-53	+53	16	0	k
M	0	12	9	-16	-69	-16	0		6 ft-k

(a)

Q	-8	-15	-22	-28	-42	-37	-16		k
S'	0	-8	-23	-45	-73	-115	-152		k
M'	0	-8	-31	-76	-149	-264	-416		6 ft-k
M''	0	+20	+40	+60	+80	+248	+416		6 ft-k
M	0	12	9	-16	-69	-16	0		6 ft-k
S	20	+12	-3	-25	-53	53	16	0	k

(b)

Figure 3-26

The equivalent concentrated loads at the panel points may be obtained from Eqs. (3-11), and are indicated in the second line in the figure. The reactions are found to be $R_a = 20$ kips and $R_e = 148$ kips. Then, the shears and moments may be computed as shown in the figure. It is only necessary to point out that at point E there is an upward force of 148 as well as a downward force of 42. Thus, the shear in panel EF is obtained from the shear in panel DE as follows:

$$S_{ef} = -53 - 42 + 148 = 53$$

The rest of the computation is rather routine and needs no further explanation.

However, if the reactions are not found, and the shears and moments are obtained by assuming arbitrarily a shear at the boundary, we must be very careful in making the corrections. This approach is shown in Fig. 3-26(b). Note that the shear to the left of point A is first assumed to be zero and that the reaction at point E is assumed to be zero in the computation of the shear in panel EF in the second line of the figure. These assumptions lead to the moments in the third line, which must be corrected according to the requirements that the moment at point G be zero and the moment

at point E be equal to that caused by the loads in the cantilever end of the beam. Before going into the fourth line in the figure, we try to compute this moment at E. Starting from the right end of the sixth line, we make use of the known condition that the shear to the right of point G is zero and subtract the equivalent concentrated loads successively to obtain the shear in panels FG and EF. Thus,

$$S_{fg} = 0 - (-16) = 16$$
$$S_{ef} = 16 - (-37) = 53$$

Similarly, starting from the right end of the fifth line, we know that the moment at point G is zero and can therefore compute the moments at panel points F and E as follows:

$$M_f = (0 - 16)h = -16h$$
$$M_e = (-16 - 53)h = -69h$$

Note that $h = 6$ is the common factor taken out of the computation in the figure. In order to make $M_e = -69$ and $M_g = 0$, we must apply corrections $M_e'' = 80$ and $M_g'' = 416$ as shown in the fourth line in the figure. The moment corrections at other points of the beam are obtained by observing the linear relationships from point A to point E and from point E to point G. Thus, by neglecting the common factor h, we have

$$M_b'' = {}^{80}\!/_{4} = 20$$
$$M_c'' = {}^{80}\!/_{2} = 40$$
$$M_d'' = (80)\,({}^{3}\!/_{4}) = 60$$
$$M_f'' = 80 + (416 - 80)/2 = 248$$

3-9 Three-hinged Arches

In ordinary structures with curved members such as arches, the radius of curvature of a member is usually so large in comparison with the depth of the member that the effect of the curvature may be neglected in locating the neutral axis of the member. Thus, the centroidal axis of the member may be considered as the neutral axis for bending. The axial force, shear, and moment at a section of a curved member can be as readily obtained as those for straight members. However, the location of a point on a curved member is specified by two coordinates instead of one. Thus, it is desirable to obtain an equation representing the curve by which the two coordinates are related. Furthermore, the slopes of the tangents at various points of the curve can also be determined from the derivative of the equation. Then, the axial force and the shear at any section can be specified in the axial and transverse directions of that particular section, respectively.

Consider, for example, an arch rib that is a second-degree parabola as shown in Fig. 3-27. We can choose a convenient set of coordinate axes

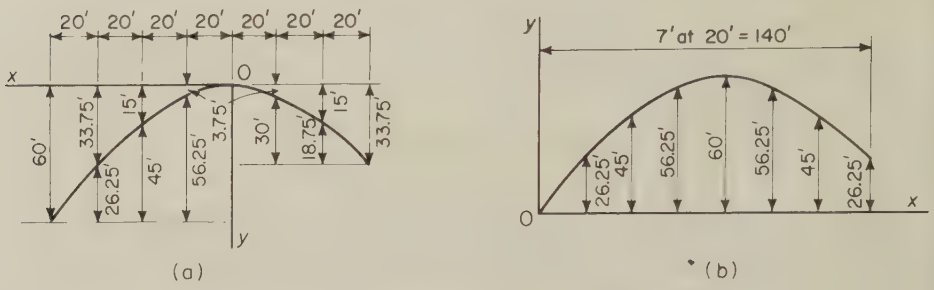

Figure 3–27

for which the equation of a second-degree parabola is given by

$$y = Ax^2 + Bx + C$$

in which A, B, and C are constant. For the coordinate system in Fig. 3-27(a), we have $y = 0$ at $x = 0$, and $y = 33.75$ for $x = \pm 60$. Thus, $A = 3/320$, $B = 0$, and $C = 0$. The resulting equation is

$$y = \frac{3}{320}x^2 \quad \text{and} \quad \frac{dy}{dx} = \frac{3}{160}x$$

Thus, the slope at any point of the arch can be obtained by substituting the value of x into the first derivative of the curve.

If another coordinate system is chosen as shown in Fig. 3-27(b), we can proceed in the same manner in evaluating the constants in the equation for a second-degree parabola. In this case, $y = 0$ at $x = 0$, $y = 60$ at $x = 80$, and $dy/dx = 0$ at $x = 80$. Thus, $A = -3/320$, $B = 3/2$, and $C = 0$. The equation of the arch axis then becomes

$$y = -3/320x^2 + 3/2x.$$

Again, the slope at a point of the arch can be obtained from the first derivative of this equation.

In order to draw the shear and moment diagrams for a curved member, however, we encounter difficulties that are not present in the case of straight members. First, the direction of the axis of the member changes along its length. Thus, the axial force and shear at any section depend on the angle between a horizontal line and the tangent to the curve at that point. Secondly, the base line for the shear and moment diagrams is a curve instead of a straight line. As a matter of convenience, shear and moment diagrams on the *horizontal projection* of the axis of the curved member are sometimes

used if the external loads are all vertical. These diagrams are useful for design purposes, but their limitations should be recognized.

Example 3-14. Figure 3-28(a) shows a three-hinged arch whose axis is represented by the parabolic curve in Fig. 3-27(a). Determine the axial force, shear, and moment at points D and E of the arch, if $x_1 = 40$ ft, $y_1 = 45$ ft, $x_2 = 40$ ft, and $y_2 = 30$ ft.

If a section is passed through point D of the arch axis, the free body on

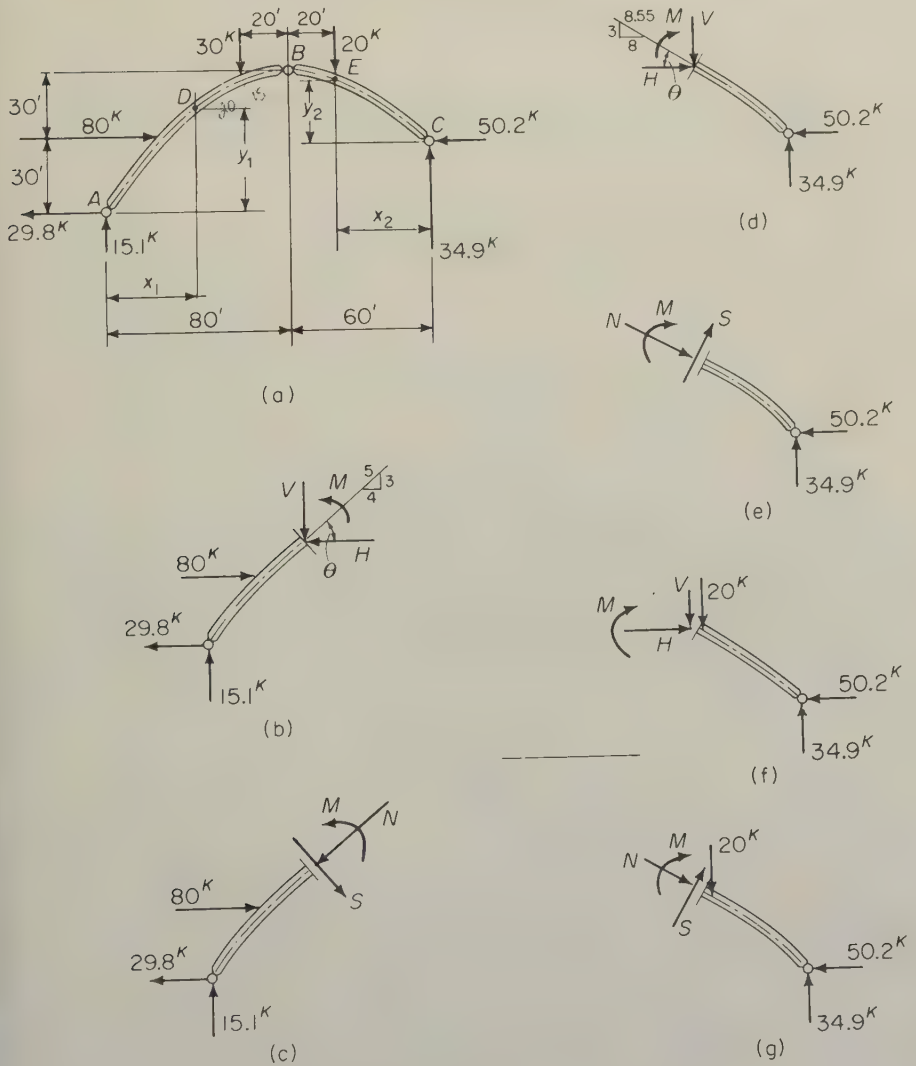

Figure 3–28

the left-hand side of the section can be represented by either Fig. 3-28(b) or 3-28(c). In the former case, the components of forces at the section are resolved into horizontal and vertical directions whereas in the latter, the components of forces at the section are shown in axial and transverse directions. Since the direction of the arch axis changes from point to point, it is easier to sum up all the external forces and reactions acting on the free body in horizontal and vertical directions. Thus, from Fig. 3-28(b),

$$\sum F_x = 0, \quad H = 50.2 \text{ kips}$$
$$\sum F_y = 0, \quad V = 15.1 \text{ kips}$$
$$\sum M_d = 0, \quad M = 15.1x_1 + 29.8y_1 - 80(y_1 - 30) \text{ ft-kips}$$

The axial force N and the shear S in Fig. 3-28(c) can easily be obtained from the consideration of the equilibrium of the free body, or they may be expressed in the following form:

$$N = H \cos \theta + V \sin \theta$$
$$S = -H \sin \theta + V \cos \theta$$

For example, if $x_1 = 40$ ft and $y_1 = 45$ ft, $\tan \theta = \frac{3}{4}$. Then, $\sin \theta = \frac{3}{5}$ and $\cos \theta = \frac{4}{5}$. Hence,

$$N = (50.2)(\tfrac{4}{5}) + (15.1)(\tfrac{3}{5}) = 40.2 + 9.1 = 49.3 \text{ kips}$$
$$S = (15.1)(\tfrac{4}{5}) - (50.2)(\tfrac{3}{5}) = 12.1 - 30.1 = -18.0 \text{ kips}$$
$$M = (15.1)(40) + (29.8)(45) - (80)(15) = 744 \text{ ft-kips}$$

When a section is passed through point E, the right-hand side of the section may be considered as a free body. For $x_2 = 40$ and $y_2 = 30$, the section coincides with the vertical load of 20 kips. Therefore, we can only take a section either just to the right or just to the left of the vertical load. The former is shown by the free body in Fig. 3-28(d) or 3-28(e), and the latter is illustrated by the free body in Fig. 3-28(f) or 3-28(g). For either case, we obtain the following relations:

$$N = H \cos \theta + V \sin \theta$$
$$S = H \sin \theta - V \cos \theta$$

Since $\tan \theta = \frac{3}{8}$ for $x_2 = 40$ and $y_2 = 30$,

$$\sin \theta = 3/8.55 = 0.351 \quad \text{and} \quad \cos \theta = 8/8.55 = 0.936$$

From Fig. 3-28(d) for a section just to the right of point E,

$$\sum F_x = 0, \quad H = 50.2 \text{ kips}$$
$$\sum F_y = 0, \quad V = 34.9 \text{ kips}$$
$$\sum M_e = 0, \quad M = 34.9x_2 - 50.2y_2 \text{ ft-kips}$$

Then from Fig. 3-28(e),

$$N = (50.2)(0.936) + (34.9)(0.351) = 47.1 + 12.2 = 59.3 \text{ kips}$$
$$S = (50.2)(0.351) - (34.9)(0.936) = 17.6 - 32.6 = -15.0 \text{ kips}$$
$$M = (34.9)(40) - (50.2)(30) = -110 \text{ ft-kips}$$

Similarly, from Fig. 3-28(f) for a section just to the left of point E,

$$\sum F_x = 0, \quad H = 50.2 \text{ kips}$$
$$\sum F_y = 0, \quad V = 34.9 - 20 = 14.9 \text{ kips}$$
$$\sum M_e = 0, \quad M = 34.9x_2 - 50.2y_2 \text{ ft-kips}$$

Then from Fig. 3-28(h),

$$N = (50.2)(0.936) + (14.9)(0.351) = 47.1 + 5.2 = 52.3 \text{ kips}$$
$$S = (50.2)(0.351) - (14.9)(0.936) = 17.6 - 14.0 = 3.6 \text{ kips}$$
$$M = -110 \text{ ft-kips}$$

Note that N and S are influenced by the location of the section because of different values of V just to the left or to the right of point E, but M is unaffected since the moment arm for the vertical load at point E is zero for all practical purposes.

Example 3-15. Figure 3-29(a) shows a three-hinged arch, the right half

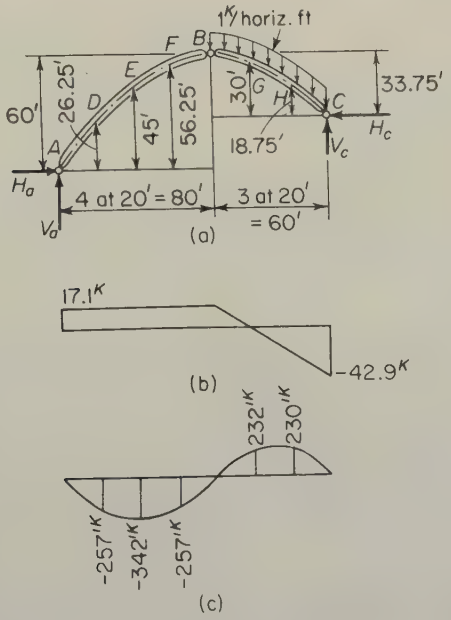

Figure 3–29

of which has a uniform load of 1 kip per horizontal foot. Draw the shear and moment diagrams on the horizontal projection of the arch axis.

The reactions at A and C are first obtained as follows:

$$\sum M_c = 0, \quad 140V_a - 26.25H_a - (1)(60)^2/2 = 0$$
$$\sum F_x = 0, \quad H_a = H_c$$
$$\sum F_y = 0, \quad V_a + V_c = (1)(60)$$
$$\sum M_b = 0, \quad 80V_a = 60H_a$$

Hence, $H_a = 22.8$ kips, $V_a = 17.1$ kips, $H_c = 22.8$ kips, and $V_c = 42.9$ kips.

Since there is no external load on the segment AB, the resultant of H_a and V_a must pass through hinge B in order to maintain the equilibrium of the two-force member AB when it is separated as a free body. This requirement is indicated by the condition of release $\Sigma M_b = 0$, which implies that $V_a/H_a = {}^{60}\!/_{80} = {}^{3}\!/_{4}$. As a check, this same relation is obtained from the ratio of the actual components of reaction at A, or $V_a/H_a = 17.1/22.8 = {}^{3}\!/_{4}$.

Since there is no external horizontal load, the horizontal component of forces acting at any section of the arch is constant. The vertical component of these forces at the same section varies along the horizontal projection of the arch axis, and such variation is indicated by the shear diagram in Fig. 3-29(b). Hence, the axial force and transverse shear at any section normal to the arch axis may be obtained by resolving the horizontal and vertical components of forces at that section into axial and transverse components. Moments are computed for points on the arch axis at 20-ft intervals of the horizontal projection, and are plotted on the moment diagram with the horizontal projection of the arch axis as the base line as shown in Fig. 3-29(c). For instance,

$$M_d = (17.1)(20) - (22.8)(26.25) = -257 \text{ ft-kips}$$
$$M_e = (17.1)(40) - (22.8)(45.0) = -342 \text{ ft-kips}$$
$$M_f = (17.1)(60) - (22.8)(56.25) = -257 \text{ ft-kips}$$
$$M_b = 0$$
$$M_g = (42.9)(40) - (22.8)(30) - (1)(40)^2/2 = 232 \text{ ft-kips}$$
$$M_h = (42.9)(20) - (22.8)(18.75) - (1)(20)^2/2 = 230 \text{ ft-kips}$$

It should be pointed out that such a moment diagram does not give the true variation of moments along the arch axis; it serves only as a convenient framework for tabulating the computed moments at the desired locations.

Example 3-16. Figure 3-30 shows a three-hinged arch with a uniform load of 1 kip per horizontal foot throughout the entire span. Draw the shear and moment diagrams on the horizontal projection of the arch axis.

In this case, the reactions are found to be as follows: $H_a = 53.3$ kips, $V_a = 80$ kips, $H_c = 53.3$ kips, and $V_c = 60$ kips. Again, the horizontal component of forces acting at any section of the arch is constant, and the variation of the vertical component can be represented by the shear diagram based on the horizontal projection of the arch axis as shown in Fig. 3-30(b). Moments at various points of the arch are found to be zero. For example,

$$M_e = (80)(40) - (53.3)(45) - (1)(40)^2/2 = 0$$

Thus, the moment diagram plotted on the horizontal projection of the arch axis has zero area as shown in Fig. 3-30(c).

This example points out a very important feature of arches. While the vertical reaction from the vertical loads on an arch tends to produce a positive moment at a section, the horizontal reaction tends to reduce such a moment. Hence, the moment at any section of an arch is much smaller than the moment at the same section of a beam with equal span and subjected to the same vertical loads. For an arch span fully loaded with a uniform vertical load, the moment curve resulting from vertical forces alone has the shape of a second-degree parabola. If the arch axis is also a second-degree parabola, the negative moment at a section caused by the horizontal reaction eliminates exactly the positive moment at that section caused by the vertical forces. That is the reason for the zero moment at any point along the arch axis.

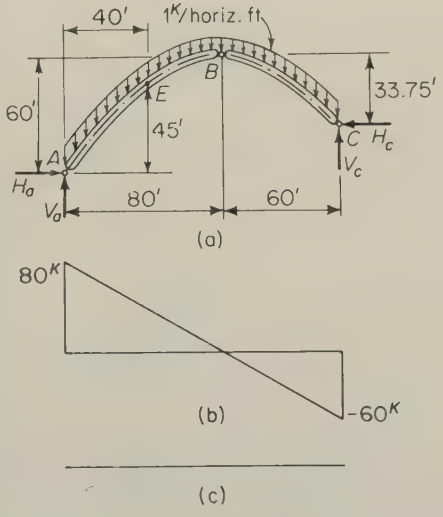

Figure 3–30

The reduction of moment along the arch axis is a very desirable characteristic. On the other hand, large horizontal reactions and axial forces are introduced even if the structure is subjected to vertical loads only. Broadly speaking, the term *arch action* refers to the tendency to develop horizontal resistance at the supports of a structure that is subjected only to vertical loads. Hence an arch may be defined as a curved member that results in inward horizontal reactions under vertical loads. This emphasizes the importance of adequate supports for arches.

Example 3-17. The arch in Fig. 3-31(a) is supporting a floor system. The distributed load on the girder is transmitted to the arch through the

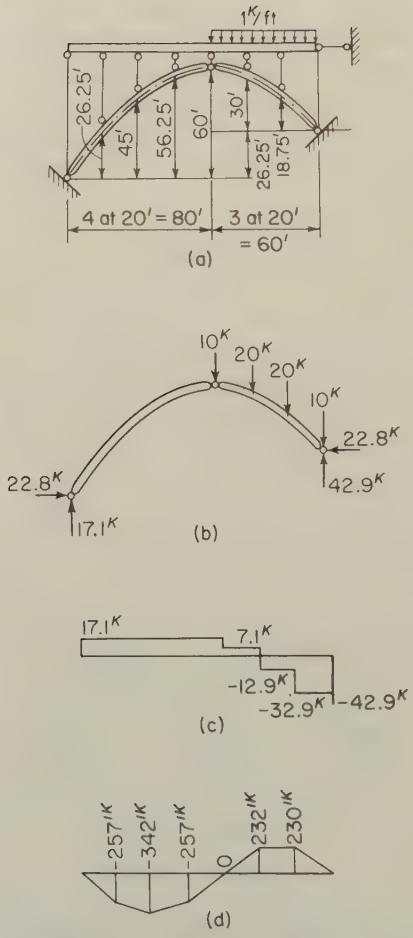

Figure 3-31

vertical posts. Draw the shear and moment diagrams on the horizontal projection of the arch axis.

The vertical loads transmitted to the arch rib through the vertical posts are shown in Fig. 3-31(b). Thus, the reactions at the supports are computed accordingly. The vertical shears are shown on a horizontal base in Fig. 3-31(c); the moments are plotted on the horizontal projection of the arch axis as shown in Fig. 3-31(d). These diagrams may be compared with those of Fig. 3-29 for the same arch without vertical posts for transmitting floor loads. Note that the vertical shears are affected by the introduction of the vertical posts to the system, but the moments at the panel points remain unchanged. We should point out again that the variation of moments along the arch axis cannot be correctly represented by a moment diagram based on the horizontal projection. Ordinates of the moments other than those at the panel points are not true values. The straight line segments joining the moments at panel points in Fig. 3-27(d) are introduced for the sake of simplicity. Fortunately, shears and moments at the panel points are usually the only points of interest for design purposes. Hence, from a practical point of view, the ordinates of the moment diagram between panel points are not important.

Example 3-18. Prove that the bending moment at any point of the three-hinged arch shown in Fig. 3-32(a) is equal to the corresponding vertical ordinate of the shaded area multiplied by a constant factor. If the arch axis is a semicircle that is represented by the equation

$$(x - r)^2 + y^2 = r^2$$

in which r is the radius of the circle, evaluate this constant factor.

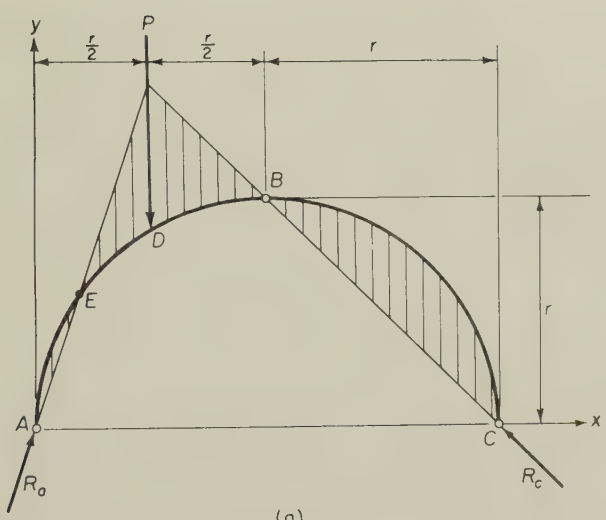

(a)

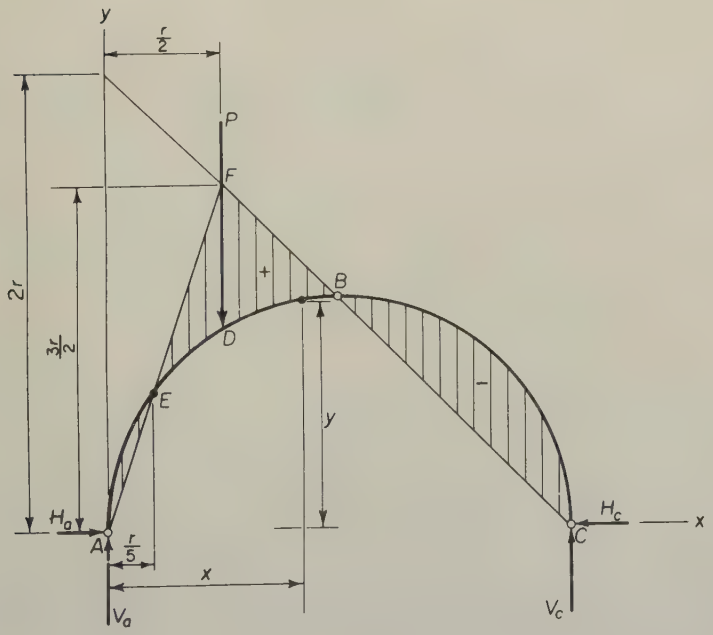

(b)

Figure 3–32

Since no external load is applied on segment BC of the arch, the reaction R_c must pass through hinge B in order to maintain the equilibrium of the segment when it is isolated as a free body. When the entire arch is considered as a free body, there are three forces acting on the structure, i.e., the external load P and the reactions R_a and R_c. Thus, R_a must pass through the intersection of P and R_c. Line AF and CF in Fig. 3-32(b) represent the lines of action of reactions R_a and R_c respectively.

From the equation of the circle, the ordinate y of a point on the circle may be expressed as

$$y = \sqrt{r^2 - (x - r)^2} = \sqrt{2rx - x^2} \tag{a}$$

The equation for line AF is given by

$$y = 3x \tag{b}$$

whereas the equation for line CF is

$$y = 2r - x \tag{c}$$

The intersection E of line AF and the circle may be obtained from the simultaneous solution of Eqs. (a) and (b). Thus, $x = r/5$.

Let t be the ordinate of the shaded area that is the vertical intercept between two curves, i.e., the difference of the ordinates of two curves. Thus,

$$t = \sqrt{2rx - x^2} - 3x \qquad \text{for } 0 \leqq x \leqq r/5$$

$$t = 3x - \sqrt{2rx - x^2} \qquad \text{for } r/5 \leqq x \leqq r/2$$

$$t = 2r - x - \sqrt{2rx - x^2} \qquad \text{for } r/2 \leqq x \leqq r$$

$$t = \sqrt{2rx - x^2} - 2r + x \qquad \text{for } r \leqq x \leqq 2r$$

From the conditions of equilibrium of the entire structure, we obtain the components of reactions as follows:

$$\sum F_x = 0, \quad H_a = H_c = H$$

$$\sum F_y = 0, \quad V_a + V_c = P$$

$$\sum M_a = 0, \quad 2rV_c - Pr/2 = 0$$

From the condition of release at B, we obtain an additional equation by considering only segment BC of the arch.

$$\sum M_b = 0, \quad rV_c - rH = 0$$

Thus,

$$V_a = 3P/4, \; V_c = P/4, \text{ and } H = P/4$$

The bending moment at any point on the arch whose ordinate is (x, y) may be obtained as follows:

$$\text{for } 0 \leqq x \leqq r/5, \quad M = V_a x - Hy = -\frac{P}{4}(\sqrt{2rx - x^2} - 3x)$$

$$\text{for } r/5 \leqq x \leqq r/2, \quad M = V_a x - Hy = \frac{P}{4}(3x - \sqrt{2rx - x^2})$$

$$\text{for } r/2 \leqq x \leqq r, \quad M = V_a x - Hy - P\left(x - \frac{r}{2}\right)$$

$$= \frac{P}{4}(2r - x - \sqrt{2rx - x^2})$$

$$\text{for } r \leqq x \leqq 2r, \quad M = V_c(2r - x) - Hy$$

$$= -\frac{P}{4}(\sqrt{2rx - x^2} - 2r + x)$$

It may be noted that for all values of x, the bending moment at a point on the arch is equal to $P/4$ times the corresponding ordinate of the shaded area. Hence, $P/4$ is the constant factor.

It is interesting to note that the moments at various points of the arch can be measured directly from the shaded area in the figure if a proper scale is used. More important is the fact that such a conclusion is also applicable to arches of any shape with any loading as long as the lines of action between reactions and loads can be drawn. Thus, the determination of moments at various sections of an arch will be greatly simplified by this consideration, which will be discussed furthur in Section 5-7.

3-10 *Cables*

In many engineering structures, such as suspension bridges and transmission lines, cables are suspended between supports and subjected to vertical loads. Since a cable is flexible and cannot resist bending or compression, the internal force acting on any section of a cable can only be axial tension. When a cable of a given length is suspended between two supports, the shape of the cable is defined by the applied loads. For example, a cable uniformly loaded along the horizontal span takes the shape of a parabola, whereas a cable uniformly loaded along its length assumes the shape of a catenary. Cables loaded uniformly along the horizontal span are by far the type most commonly used in structures—for example, cables supporting the roadway of a suspension bridge.

If a set of vertical loads $P_1, P_2, \ldots, P_i, \ldots, P_n$ is applied on a cable suspended between two supports as shown in Fig. 3-33(a), the cable will

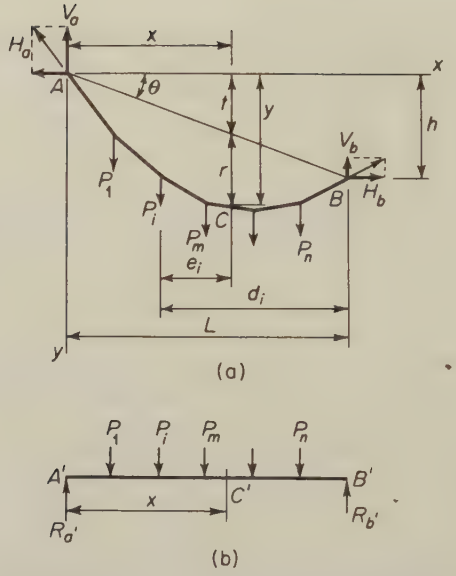

Figure 3–33

assume the shape of a polygonal curve that depends on the magnitude and location of the loads. Since the cable cannot transmit moment or shear, only axial tension T is present at any section. The reactions T_a and T_b at supports A and B may be resolved into vertical and horizontal components. Then, from the conditions of equilibrium, we obtain

$$\sum F_x = 0, \quad H_a = H_b = H, \text{ a constant}$$

$$\sum F_y = 0, \quad V_a + V_b = \sum_{i=1}^{n} P_i$$

$$\sum M_b = 0, \quad V_a L - \sum_{i=1}^{n} P_i d_i - Hh = 0$$

where d_i is the horizontal distance from the load P_i to support B. Since there are four unknown components of reaction and only three equations of equilibrium, the fourth equation is supplied by the requirement that the moment at any section of the cable be zero. Thus, in a free body either to the right or to the left of a section, the sum of the moments of all forces about the section point on the cable must be zero. For the free body to the left of a section through point C, which is at a horizontal distance x from the left support A as shown in Fig. 3-33(a), the following equation may be obtained:

$$\sum M_c = 0, \quad V_a x - \sum_{i=1}^{m} P_i e_i - Hy = 0$$

Hence, from $\Sigma M_b = 0$ and $\Sigma M_c = 0$, it may be derived that

$$\sum_{i=1}^{n} \frac{P_i d_i}{L} + \frac{Hh}{L} = \sum_{i=1}^{m} \frac{P_i e_i}{x} + \frac{Hy}{x}$$

or

$$H\left(y - \frac{hx}{L}\right) = \frac{x}{L} \sum_{i=1}^{n} P_i d_i - \sum_{i=1}^{m} P_i e_i$$

Noting that $t = hx/L$ and $r = y - t$ in Fig. 3-33(a) and denoting

$$M' = \frac{x}{L} \sum_{i=1}^{n} P_i d_i - \sum_{i=1}^{m} P_i e_i \tag{3-13a}$$

we obtain

$$Hr = M' \quad \text{or} \quad H = \frac{M'}{r} \tag{3-13b}$$

in which the distance r is called the *sag* of the cable. If the sag r at any point of the cable is known, the horizontal component of reaction H may be computed by Eq. (3-13b). The H component is sometimes referred to as the *horizontal tension*. The vertical components of reaction V_a and V_b can be obtained from the remaining equations of equilibrium as follows:

$$V_a = \frac{1}{L} \sum_{i=1}^{n} P_i d_i + \frac{Hh}{L} \tag{3-13c}$$

and

$$V_b = \sum_{i=1}^{n} P_i - \frac{1}{L} \sum_{i=1}^{n} P_i d_i - \frac{Hh}{L} \tag{3-13d}$$

Let us digress at this point to imagine a simple beam that has the same horizontal span as the cable and is acted on by the same vertical loads as shown in Fig. 3-33(b). It can be seen that the reactions at supports A' and B' of this beam are equal to

$$R_{a'} = \frac{1}{L} \sum_{i=1}^{n} P_i d_i \tag{3-14a}$$

$$R_{b'} = \sum_{i=1}^{n} P_i - \frac{1}{L} \sum_{i=1}^{n} P_i d_i \tag{3-14b}$$

and the moment at a point C' of the beam is equal to M' as indicated in Eq. (3-13a). Thus, we may conclude that the vertical reactions at the supports of a cable are related to the reactions of the imaginary beam as follows:

$$V_a = R_{a'} + \frac{Hh}{L} \tag{3-14c}$$

$$V_b = R_{b'} - \frac{Hh}{L} \tag{3-14d}$$

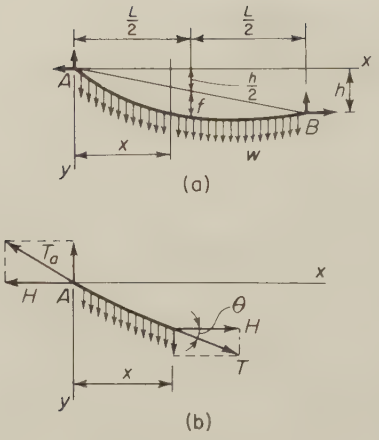

Figure 3–34

When the supports A and B of the cable are at the same elevation, i.e., $h = 0$, then $V_a = R_{a'}$ and $V_b = R_{b'}$. The horizontal tension in a cable may be expressed in terms of the moment M' at a point C' of the imaginary beam by Eq. (3-13b). Thus, the calculation of reactions in a cable can readily be related to the familiar procedure of computing beam reactions and moments.

When a cable is loaded uniformly along the horizontal span, it assumes the shape of a parabola. This can easily be demonstrated by referring to Fig. 3-34(a). For any section at a horizontal distance x from the left support, the horizontal tension H due to the uniform load w may be obtained from Eq. (3-13a) as follows:

$$Hr = \tfrac{1}{2}wLx - \tfrac{1}{2}wx^2$$

At $x = L/2$, for which the sag r is equal to f, then

$$H = \frac{wL^2}{8f} \tag{3-15}$$

Substituting this value of H into the previous equation, we obtain

$$r = \frac{4fx}{L^2}(L - x)$$

Since $y = r + t = r + hx/L$,

$$y = \frac{4fx}{L^2}(L - x) + \frac{hx}{L} \tag{3-16}$$

This is the equation of a parabola having point A as the origin and the positive coordinate axes directed as shown in Fig. 3-34(a).

The tension at any point of the cable may be obtained from the free body cut by a section through that point, as shown in Fig. 3-34(b). If the horizontal tension H is known, the tension T at any point in the cable at a horizontal distance x from the left support is given by

$$T = H \sec\theta = H\frac{ds}{dx}$$

where ds is measured along the length of the cable.

By taking the derivative of Eq. (3-16), we obtain

$$\frac{dy}{dx} = \frac{4f}{L^2}(L - 2x) + \frac{h}{L}$$

Thus,

$$\frac{ds}{dx} = \sqrt{1 + \left(\frac{dy}{dx}\right)^2} = \left[1 + \left(\frac{4f}{L} - \frac{8fx}{L^2} + \frac{h}{L}\right)^2\right]^{1/2}$$

If $n = f/L$ is defined as the sag ratio of a cable, the tension in the cable is equal to

$$T = H\left[1 + 16n^2 + \frac{64n^2x^2}{L^2} + \frac{h^2}{L^2} - \frac{64n^2x}{L} - \frac{16nxh}{L^2} + \frac{8nh}{L}\right]^{1/2} \tag{3-17a}$$

The maximum tension occurs at one of the supports where the slope of the curve has maximum numerical value. Thus, for $x = 0$,

$$T_a = H\left[1 + 16n^2 + \frac{h^2}{L^2} + \frac{8nh}{L}\right]^{1/2} \tag{3-17b}$$

and for $x = L$,

$$T_b = H\left[1 + 16n^2 + \frac{h^2}{L^2} - \frac{8nh}{L}\right]^{1/2} \tag{3-17c}$$

Hence, T_a represents the maximum tension in the cable.

If the supports of a cable are at the same elevation, Eqs. (3-16) and (3-17) may be simplified by letting $h = 0$, i.e.,

$$y = \frac{4fx}{L^2}(L - x) \tag{3-18}$$

and

$$T = H\left[1 + 16n^2 + \frac{64n^2x}{L}\left(\frac{x}{L} - 1\right)\right]^{1/2} \tag{3-19a}$$

For $x = 0$ or $x = L$,

$$T_{\max} = H\left[1 + 16n^2\right]^{1/2} \tag{3-19b}$$

Example 3-19. Determine the component of reactions for the cable shown in Fig. 3-35, for which $r = 30$ ft and $t = 30$ ft at point C.

For an imaginary beam corresponding to the horizontal projection of the cable, we have from Eqs. (3-13a) and (3-14a)

$$R_{a'} = \tfrac{1}{120}\left[(10)(20)(1 + 2 + 3 + 4 + 5)\right] = 25 \text{ kips}$$

$$M' = (25)(80) - (10)(20)(1 + 2 + 3) = 800 \text{ ft-kips}$$

Then, from Eqs. (3-13b), (3-14c), and (3-14d),

$$H = {}^{800}\!/_{30} = 26.7 \text{ kips}$$

$$V_a = 25 + (26.7)(45)/(120) = 35 \text{ kips}$$

$$V_b = 50 - 25 - (26.7)(45)/(120) = 15 \text{ kips}$$

It should be noted that once the vertical loads are given, the polygonal curve is uniquely determined. In other words, the ordinates at various points of the polygonal curve are interrelated in accordance with the applied loads and cannot be arbitrarily assumed. If the sag r at one point in the cable is known, the sag at any other point may be obtained after the horizontal tension H is computed. Thus, for the cable in Fig. 3-35, $r_c = 30$ ft and $H = 26.7$ kips. Therefore,

$$r_d = \frac{M'}{H} = \frac{1}{26.7}(25)(20) = 18.75 \text{ ft}$$

$$r_e = \frac{1}{26.7}[(25)(40) - (10)(20)] = 30.0 \text{ ft}$$

$$r_f = \frac{1}{26.7}[(25)(60) - (10)(40 + 20)] = 33.75 \text{ ft}$$

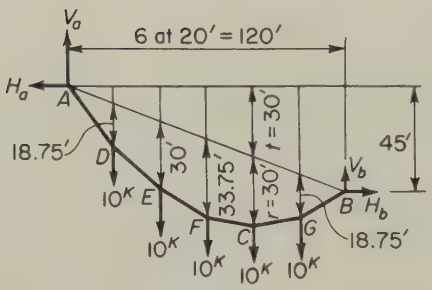

Figure 3–35

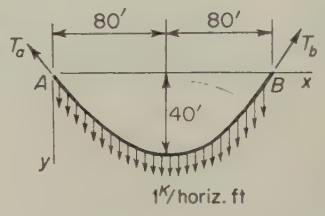

Figure 3–36

Example 3-20. The cable shown in Fig. 3-36 is subjected to a uniform load of 1 kip/ft. The supports of the cable are at the same elevation. $L = 160$ ft, $f = 40$ ft, and $n = f/L = 0.25$. Determine the maximum tension in the cable.

From Eq. (3-15), we have

$$H = \frac{(1)(160)^2}{(8)(40)} = 80 \text{ kips}$$

and from Eq. (3-18),

$$y = \frac{(4)(0.25)x}{160}(160 - x) = x - \frac{x^2}{160}$$

The tension in the cable can be obtained from Eq. (3-19a):

$$T = (80)\left[1 + (16)(0.25)^2 + \frac{(64)(0.25)^2 x}{160}\left(\frac{x}{160} - 1\right)\right]^{1/2}$$

$$= (80)\left[2 + \frac{x}{40}\left(\frac{x}{160} - 1\right)\right]^{1/2}$$

At supports A and B, where $x = 0$ and $x = L$, respectively,

$$T_a = T_b = 80\sqrt{2} = 106.5 \text{ kips}$$

3-11 *Suspended Girders*

If a girder is suspended from a cable at uniformly spaced intervals, and hinged at the center as well as at the ends, as shown in Fig. 3-37, a simple statically determinate suspension bridge is formed. The cable tends to take the form of an equilibrium polygon for any set of applied loads. Thus, the cable takes a parabolic shape under the dead load, which is uniformly distributed along the horizontal span. The main function of the girder is to distribute the moving loads so that the cable remains essentially parabolic under the action of such loads. The girder transmits very little load to its supports and all loads are primarily carried by the hangers. It may be assumed that, with the stiffening system, the hanger loads are equal throughout the entire span.

Consider, for example, the system in Fig. 3-37(a) for which the load is concentrated at point D'. A free-body diagram of the entire system may be drawn as in Fig. 3-37(b), in which there are six unknown components of reaction. Since there are only three equations of equilibrium, we must seek additional equations from other considerations. If a vertical section is cut through the cable and the girder arbitrarily as shown in Fig. 3-37(c), there will be a vertical component as well as the horizontal component of tension H in the cable, and there are in general shear and moment in the girder. However, if the section is passed through CC', the vertical component of the tension in the cable is zero since C is the lowest point of the cable, and the moment in the girder is zero because of the hinge at C'. Thus, the problem is greatly simplified, and one more independent equation is gained from the condition of the release. When the cable is separated from the girder as shown in Fig. 3-37(d), the vertical loads Q from the hangers can be related to the components of reaction of the cable. With the given condition of release $\Sigma M_{c'} = 0$, all components of reaction acting on the cable, i.e., V_a, V_b, and H, may be obtained by Eqs. (3-13) and (3-14). The remaining components of reaction $V_{a'}$ and $V_{b'}$ acting on the girder may then be obtained from the equations of equilibrium when the

entire system is taken as a free body, or from the free-body diagrams shown in Fig. 3-37(e).

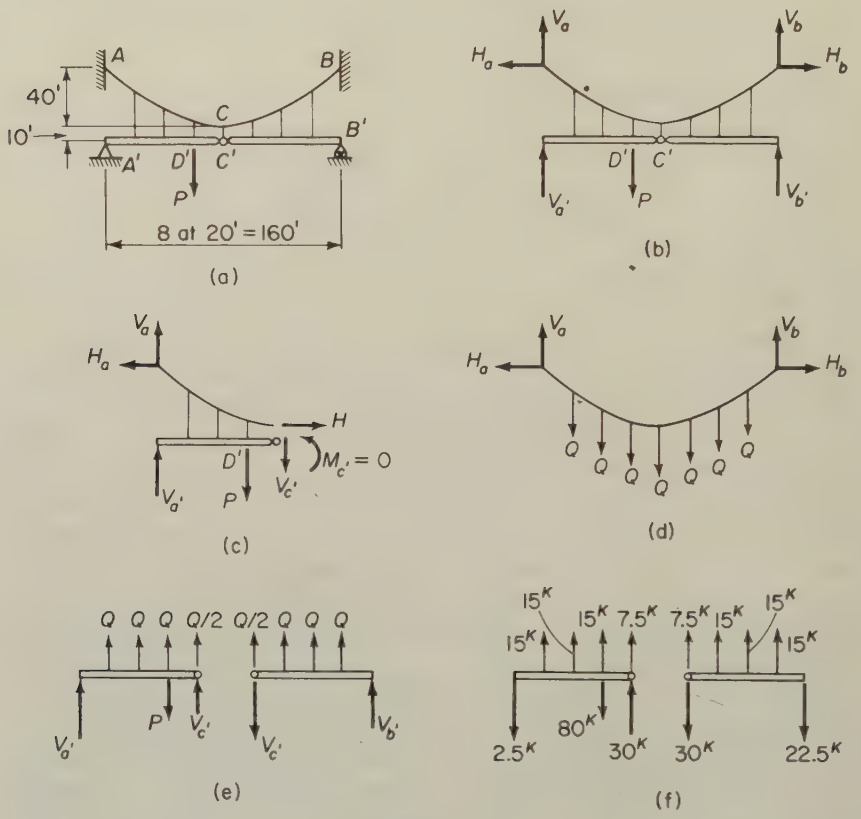

Figure 3–37

The tension at any section of the cable may be obtained from Eq. (3-19a), with maximum tension at the supports as given by Eq. (3-19b). The shear and moment at any section of the girder may be obtained from the free-body diagrams in Fig. 3-37(e) after the magnitude of the vertical loads Q has been found.

Example 3-21. The dimensions of the statically determinate suspended bridge shown in Fig. 3-37(a) are given as follows: $L = 8 @ 20$ ft $= 160$ ft, $f = 40$ ft, and $CC' = 10$ ft. A concentrated load of $P = 80$ kips is acting at point D'. Compute the reactions at all supports.

From the consideration of the entire system as a free body, as it is shown in Fig. 3-37(b),

$$\sum M_b = 0, \quad (V_a + V_{a'})(160) - (80)(100) = 0, \quad V_a + V_{a'} = 50 \text{ kips}$$

$$\sum F_x = 0, \quad H_a = H_b = H$$

$$\sum F_y = 0, \quad (V_a + V_{a'}) + (V_b + V_{b'}) = 80, \quad V_b + V_{b'} = 30 \text{ kips}$$

From the consideration of the left half of the system as a free body, as shown in Fig. 3-37(c), $\Sigma M_{c'} = 0$,

$$(V_a + V_{a'})(80) - 40H - (80)(20) = 0,$$

$$40H = (50)(80) - (80)(20) = 2{,}400, \quad H = 60 \text{ kips}$$

From the consideration of equilibrium of the cable isolated from the girder, as shown in Fig. 3-37(d), Eqs. (3-13) and (3-14) lead to the following:

$$M' = (7Q/2)(80) - (Q)(3 + 2 + 1)(20) = 160Q$$

$$Hr = (60)(40) = 160Q, \quad Q = 15 \text{ kips}$$

$$V_a = 3.5Q = 52.5 \text{ kips}, \quad V_b = 52.5 \text{ kips}$$

Hence,

$$V_{a'} = 50 - V_a = 50 - 52.5 = -2.5 \text{ kips}$$

$$V_{b'} = 30 - V_b = 30 - 52.5 = -22.5 \text{ kips}$$

Finally, consider the left half of the girder as a free body as shown in Fig. 3-37(e), $\Sigma M_{c'} = 0$,

$$(V_{a'})(80) + (15)(3 + 2 + 1)(20) - (80)(20) = 0$$

$$V_{a'} = -2.5 \text{ kips (checked)}$$

The minus sign indicates that the sense of direction of $V_{a'}$ shown in Fig. 3-37(e) should be reversed. Similarly, $V_{b'}$ may be obtained by considering the right half of the girder as a free body. Thus, the components of reaction of the girder can be completely determined from Fig. 3-37(e). Such results with correct senses of direction are shown in Fig. 3-37(f).

Example 3-22. For the suspension bridge shown in Fig. 3-38(a), draw the shear and moment diagrams for the girder.

This structure is identical to that of the previous example except that hangers are present at points A and B also. When the entire system is considered as a free body, the equations of equilibrium obtained in the previous example still hold. Thus, $H = 60$ kips. When the cable is isolated as a free body, the hanger loads at A and B are each $Q/2$ as shown in Fig. 3-38(b).

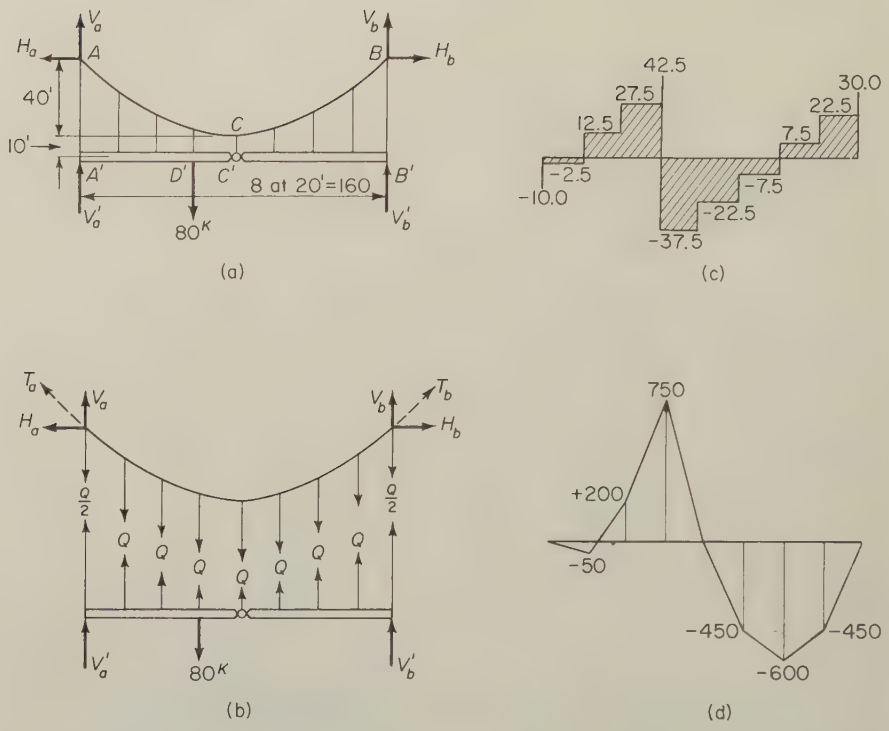

Figure 3–38

Hence, the cable may be considered as uniformly loaded with $w = 8Q/160 = Q/20$. Then, from Eq. (3-15), we get

$$H = \frac{(Q/20)\,(160)^2}{(8)\,(40)} = 4Q$$

or

$$Q = \frac{H}{4} = 15 \text{ kips}$$

Thus, the vertical reactions may be obtained in a manner similar to the previous example as follows:

$$V_a = 60 \text{ kips}, \qquad V_b = 60 \text{ kips}$$

$$V_{a'} = -10 \text{ kips}, \quad V_{b'} = -30 \text{ kips}$$

Obviously, each cable reaction has been increased by an amount of $Q/2 = 7.5$ kips over that in the previous example while each girder reaction has been decreased by the same amount.

Since this problem can be treated as one with uniformly distributed load, the vertical reactions in the cable can also be obtained directly from the slope of the cable at each support. Note that in this case,

$$\frac{dy}{dx} = \frac{4f}{L^2}(L - 2x) = \frac{(4)(40)}{(160)^2}(160 - 2x) = 1 - \frac{2x}{160}$$

For $x = 0$, $dy/dx = 1$, and for $x = 160$ ft, $dy/dx = -1$. Hence

$$V_a = V_b = H = 60 \text{ kips}$$

The shear and moment diagrams for the girder are shown in Figs. 3-38(c) and (d) respectively. It may be observed from the shear diagram that the load $Q/2$ in each end hanger does not affect the shears in the girder. The ordinates in the shear diagram are obtained by the summation of loads from left to right of the girder whereas the ordinates in the moment diagram are obtained by the summation of the areas in the shear diagram.

3-12 *Simple Structures in Space*

When a plane rigid frame or curved member is subjected to loads that do not lie in the plane of the structure, there are in general six stress resultants at a section normal to the axis of a member. Such a structure constitutes a system in space even if the structure itself lies in a plane. Although most structures in space are statically indeterminate, we shall discuss a few simple cases that can be solved by statics alone.

Consider, for example, the cantilever beam in Fig. 3-39(a), which is

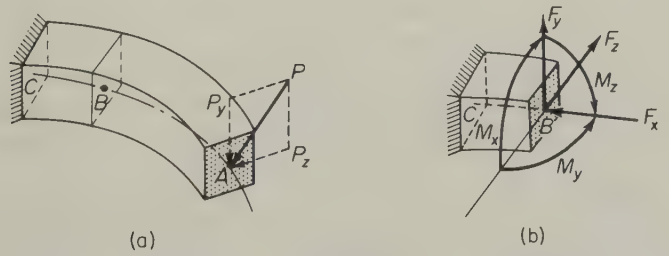

Figure 3–39

curved in the horizontal plane and is subjected to an inclined load P lying in a plane normal to the curved axis at point A. If a section is passed through any point B along the axis of the curve, the six stress resultants acting on the section are represented by internal forces F_x, F_y, and F_z, and internal moments M_x, M_y, and M_z, as shown in Fig. 3-39(b). Let the positive direc-

tions of the stress resultants be indicated by the positive directions of a right-handed coordinate system as shown when the section at B is viewed from A. These stress resultants are identified as follows:

F_x = axial force normal to the plane of the section

F_y = shear force in the vertical direction

F_z = shear force in the horizontal direction

M_x = torque about x-axis

M_y = bending moment in the horizontal plane about y-axis

M_z = bending moment in the vertical plane about z-axis

Since six equations of equilibrium can be established for a free body in space, the six stress resultants at a section can be determined from the conditions of equilibrium.

If the inclined load P is resolved into vertical and horizontal components P_y and P_z at point A, the component P_z lies in the plane of the structure and causes F_x, F_z, and M_y at a section while the component P_y is acting normal to the plane of the structure and produces F_y, M_x and M_z. Since the former case has been fully dealt with in the discussion of arches, we shall consider only the latter case here. The total effect of the inclined load P on the girder may be obtained from the superposition of the separate effects of each component.

A curved member subjected to loads normal to the plane of the curved axis is commonly known as a *bow girder*. In general, the axis of the girder may be a smooth curve or a broken line with straight or curved segments. In order to obtain the stress resultants at any section along the member, however, the axis of the member must be described by a consistent coordinate system. Figure 3-40(a) shows the plan view of a bow girder with loads acting normal to the plane. Let s be defined as the distance along the axis of the member, starting from the free end. Such a coordinate system is convenient and useful only if the member consists of straight segments.

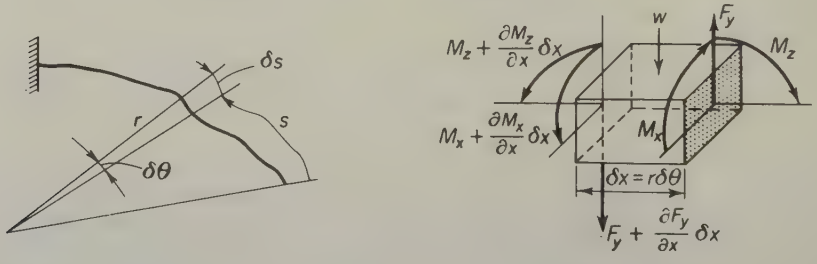

(a) (b)

Figure 3–40

On the other hand, polar coordinates (r, θ) may be used to describe a curve. Even in the latter case, the complexity of the solution depends on the shape of the curve and the loading. When an infinitesimal element $\delta s = r\ \delta\theta$ is isolated from the member in Fig. 3-40(a), the equilibrium of the element is maintained by the stress resultants shown in Fig. 3-40(b), in which w is the intensity of the external load acting on the element. The positive directions for the stress resultants on each face of the element are given in the figure. Thus, the differential relationship of the stress resultants may also be established.

Example 3-23. Write a set of general expressions for the vertical shear F_y, torque M_x, and bending moment M_z at a section of a cantilever bow girder whose axis is shown by the plan view in Fig. 3-41(a). A downward load P is applied at point A of the girder.

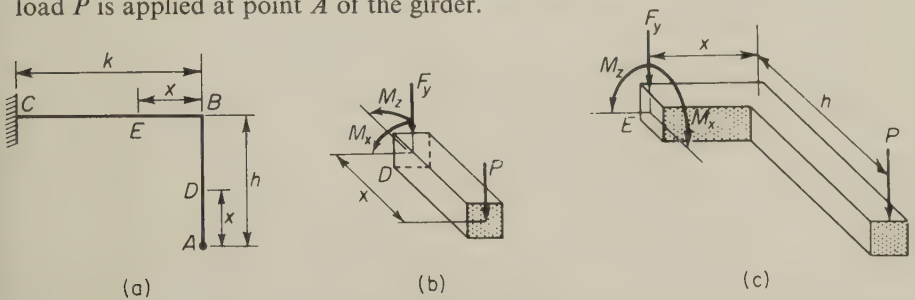

Figure 3–41

Since the axis of the girder consists of two straight segments AB and BC, we can consider the two segments separately. For a general point D in segment AB, part AD is isolated as a free body as shown in Fig. 3-41(b). Thus,

$$\sum F_y = 0, \quad F_y = -P$$
$$\sum (M_x)_d = 0, \quad M_x = 0$$
$$\sum (M_z)_d = 0, \quad M_z = Px$$

Similarly, for a general point E in segment BC, part ABE is isolated as shown in Fig. 3-41(c). Then,

$$\sum F_y = 0, \quad F_y = -P$$
$$\sum (M_x)_e = 0, \quad M_x = -Ph$$
$$\sum (M_z)_e = 0, \quad M_z = Px$$

Example 3-24. For the bow girder in Example 3-23, write a set of general expressions for the vertical shear F_y, torque M_x, and bending moment M_z if a downward uniformly distributed load w is applied on the full length of segment AB instead of a concentrated load P applied at point A.

For a general point D in segment AB, we have

$$\sum F_y = 0, \quad F_y = wx$$
$$\sum (M_x)_d = 0, \quad M_x = 0$$
$$\sum (M_z)_d = 0, \quad M_z = wx^2/2$$

For a general point E in segment BC, we get

$$\sum F_y = 0, \quad F_y = wh$$
$$\sum (M_x)_e = 0, \quad M_x = -wh^2/2$$
$$\sum (M_z)_e = 0, \quad M_z = whx$$

3-13 Circular Bow Girders

When the axis of a bow girder is described by a circular arc, the problem can easily be solved by using the polar coordinates. Consider, for instance, the cantilever bow girder whose axis is shown in the plan view in Fig. 3-42(a). The axis of the girder is a circular arc of radius r, and the angle subtended

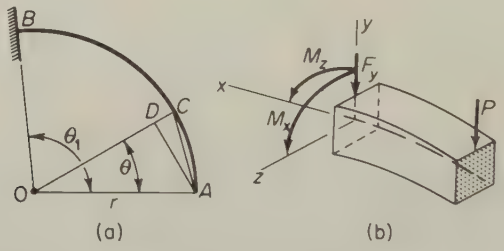

Figure 3–42

between the free and fixed ends of the girder is θ_1. A point C on the curve may be located by the angle θ measured from the free end A to point C. If a downward concentrated load P is applied at point A, the stress resultants at a section passing through point C are as shown in Fig. 3-42(b). Since the distances AD and CD in Fig. 3-42(a) are given by the geometrical relations

$$AD = r \sin \theta$$
$$CD = r(1 - \cos \theta)$$

the stress resultants at section C are obtained from the conditions of equilibrium as follows:

$$\sum F_y = 0, \quad F_y = -P$$
$$\sum (M_x)_c = 0, \quad M_x = -Pr(1 - \cos \theta)$$
$$\sum (M_z)_c = 0, \quad M_z = Pr \sin \theta$$

Thus, the components of reaction at the fixed support B may be computed by letting $\theta = \theta_1$ in the above equations.

If the cantilever bow girder is loaded with a downward uniformly distributed load w along the entire arc length, the same approach may be used. Consider, for example, an infinitesimal element subtended by the central angle $\delta\alpha$ as shown in Fig. 3-43. Since the length of the arc $\delta s = r\,\delta\alpha$, the load acting on the element is $wr\,\delta\alpha$. Thus, the stress resultants at point C due to the downward load acting on the infinitesimal element at point E are

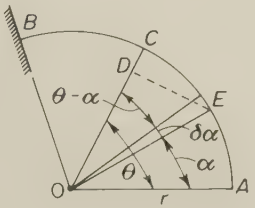

Figure 3-43

$$\delta F_y = -wr\,\delta\alpha$$

$$\delta M_x = -(wr\,\delta\alpha)r\,[1 - \cos(\theta - \alpha)] = -wr^2\,[1 - \cos(\theta - \alpha)]\,\delta\alpha$$

$$\delta M_z = (wr\,\delta\alpha)\,[r \sin(\theta - \alpha)] = wr^2 \sin(\theta - \alpha)\,\delta\alpha$$

Then, the stress resultants at point C due to the uniform load from point A to point C may be obtained by integration as follows:

$$F_y = -\int_0^\theta wr\,d\alpha = -wr\alpha\Big|_0^\theta = -wr\,\theta \tag{3-20a}$$

$$M_x = -\int_0^\theta wr^2\left[1 - \cos(\theta - \alpha)\right] d\alpha$$

$$= -wr^2\left[\alpha + \sin(\theta - \alpha)\right]_0^\theta = -wr^2\,(\theta - \sin\theta) \tag{3-20b}$$

$$M_z = \int_0^\theta wr^2 \sin(\theta - \alpha)\,d\alpha = wr^2 \cos(\theta - \alpha)\Big|_0^\theta$$

$$= wr^2\,(1 - \cos\theta) \tag{3-20c}$$

A bow girder may also be simply supported at three points, as shown in Fig. 3-44(a). The uniformly distributed load w is acting downward while the vertical reactions V_0, V_1, and V_2 are assumed to act upward. For a section at any point A between supports 0 and 1, the angle θ is measured from the

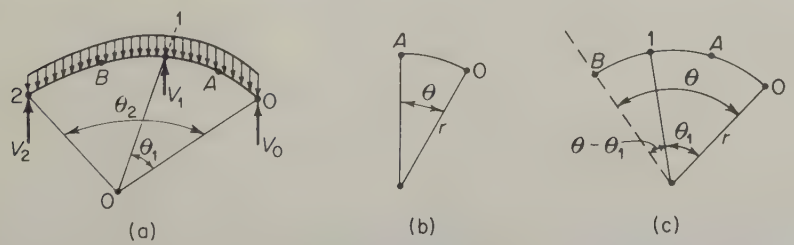

Figure 3-44

reference point 0 to point A as shown in the plan view in Fig. 3-44(b). Then, the stress resultants at A due to downward load w and upward reaction V_0 are as follows:

$$F_y = V_0 - wr\theta$$
$$M_x = V_0 r(1 - \cos\theta) - wr^2(\theta - \sin\theta)$$
$$M_z = -V_0 r \sin\theta + wr^2(1 - \cos\theta)$$

Similarly, for a section at any point B between supports 1 and 2, the angle θ is measured from the reference point 0 to point B as shown in the plan view in Fig. 3-44(c). Thus, the stress resultants at B due to downward load w and upward reactions V_0 and V_1 are

$$F_y = V_0 + V_1 - wr\theta$$
$$M_x = V_0 r(1 - \cos\theta) + V_1 r[1 - \cos(\theta - \theta_1)] - wr^2(\theta - \sin\theta)$$
$$M_z = -V_0 r \sin\theta - V_1 r \sin(\theta - \theta_1) + wr^2(1 - \cos\theta)$$

By considering the entire structure as a free body, we obtain

$$\sum F_y = 0, \quad V_0 + V_1 + V_2 - wr\theta_2 = 0 \tag{3-21a}$$

$$\sum (M_x)_2 = 0, \quad V_0 r(1 - \cos\theta_2) + V_1 r[1 - \cos(\theta_2 - \theta_1)] - wr^2(\theta_2 - \sin\theta_2) = 0 \tag{3-21b}$$

$$\sum (M_z)_2 = 0, \quad -V_0 r \sin\theta_2 - V_1 r \sin(\theta_2 - \theta_1) + wr^2(1 - \cos\theta_2) = 0 \tag{3-21c}$$

The last two equations may be simplified by dividing through each of them by a factor r. Hence, the vertical reactions can be computed from these equations of equilibrium.

Example 3-25. Compute the vertical reactions for the circular bow girder shown in Fig. 3-45(a) with a plan view shown in Fig. 3-45(b).

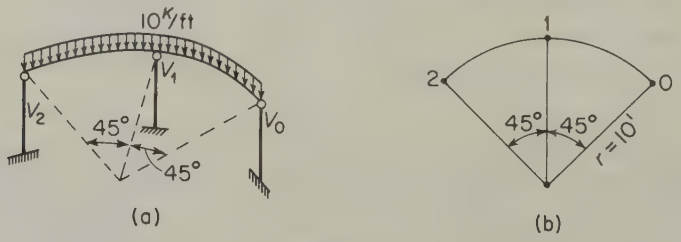

Figure 3–45

In this problem, $w = 10$ kips/ft, $r = 10$ ft, $\theta_1 = 45° = 0.7854$ radian, and $\theta_2 = 90° = 1.5708$ radians. Then, from Eqs. (3-21), we have

$$V_0 + V_1 + V_2 - (10)(10)(1.5708) = 0$$
$$V_0(1 - 0) + V_1(1 - 0.7071) - (10)(10)(1.5708 - 1) = 0$$
$$-V_0(1) - V_1(0.7071) + (10)(10)(1 - 0) = 0$$

or

$$1.0000V_0 + 1.0000V_1 + 1.0000V_2 = 157.08$$
$$1.0000V_0 + 0.2929V_1 = 57.08$$
$$1.0000V_0 = 0.7071V_1 = 100.00$$

The solution of these simultaneous equations gives

$$V_0 = V_2 = 26.73 \text{ kips}, \quad V_1 = 103.62 \text{ kips}$$

3-14 Summary

In this chapter, we have discussed the procedures for determining the internal forces and moments in simple structures in a plane and in space. For plane structures, only the axial force, shear, and moment are involved. For structures in space, the stress resultants consist of internal forces along three orthogonal axes and internal moments about these axes. Although a great variety of structures has been treated, the same principles can be applied to all of them. The variations of the stress resultants along the length of a member can also be conveniently plotted in the form of diagrams for most cases.

References

3-1 S. H. Crandall and N. C. Dahl, eds., *An Introduction to the Mechanics of Solids*, McGraw-Hill Book Co., Inc., New York, 1959.

3-2 N. M. Newmark, "Numerical Procedure for Computing Deflections, Moments, and Buckling Loads," *Trans. ASCE*, vol. 108, 1943, p. 1161.

3-3 C. H. Norris and J. B. Wilbur, *Elementary Structural Analysis*, 2nd ed., McGraw-Hill Book Co., Inc., New York, 1960.

3-4 T. C. Shedd and J. Vawter, *Theory of Simple Structures*, 2nd ed., John Wiley & Sons, Inc., New York, 1941.

3-5 F. R. Shanley, *Basic Structures*, John Wiley & Sons, Inc., New York, 1944.

3-6 D. B. Steinman, *Suspension Bridges*, John Wiley & Sons, Inc., New York, 1922.

Problems

3-1 Derive the differential relationships of load, shear, and moment in a beam using each of the sign conventions shown in Fig. P3-1.

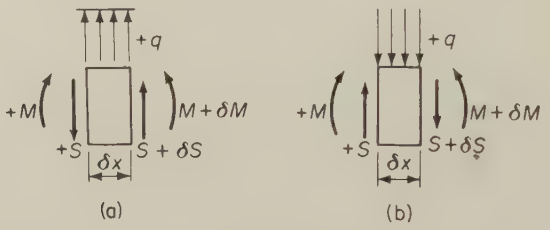

Figure P3–1

3-2 Determine the axial force, shear, and moment at a section just to the right of point *D* and those at a section just to the right of point *E* of the structure shown in Fig. P3-2.

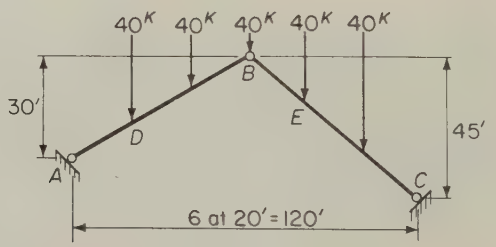

Figure P3–2

3-3 Write a set of general expressions for the axial force, shear, and moment for a section between supports *B* and *C* in Fig. P3-3. Use support *B* as the point of reference for the coordinate in locating a point between *B* and *C*.

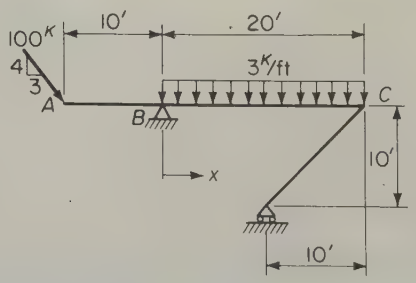

Figure P3–3

3-4 Compute the axial force, shear, and moment at points F and G in the rigid frame shown in Fig. P3-4.

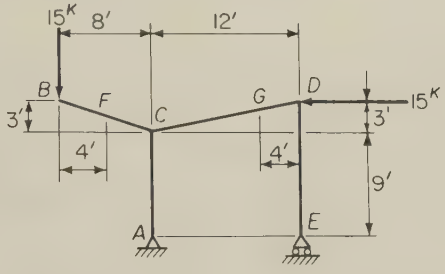

Figure P3–4

3-5 to **3-18** Draw the shear and moment diagrams for each member in each of the structures shown in Figs. P3-5 to P3-18.

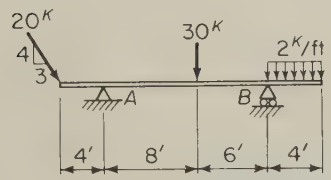

Figure P3–5

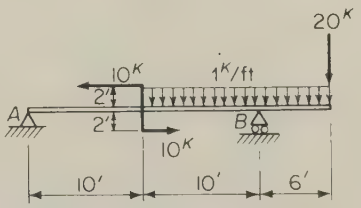

Figure P3–6

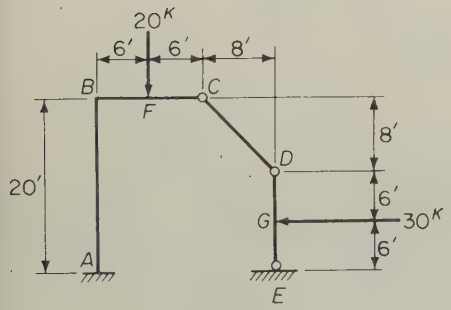

Figure P3–7

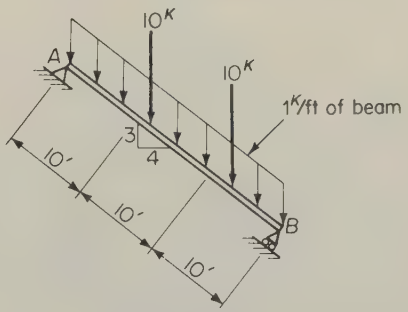

Figure P3–8

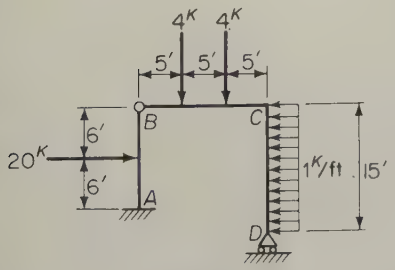

Figure P3–9

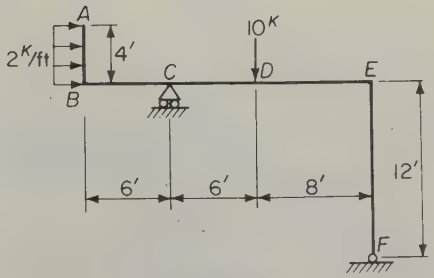

Figure P3–10

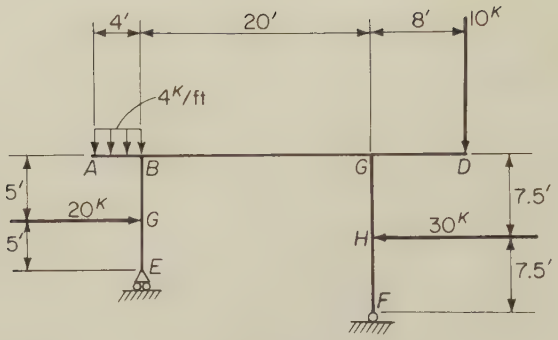

Figure P3–11

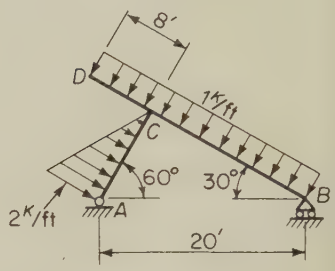

Figure P3–12

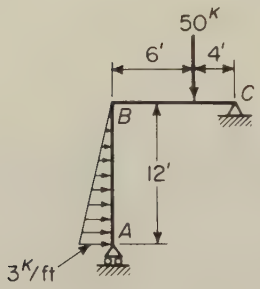

Figure P3–13

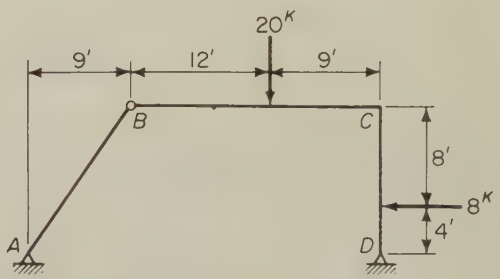

Figure P3–14

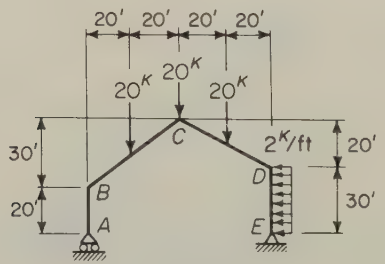

Figure P3–15

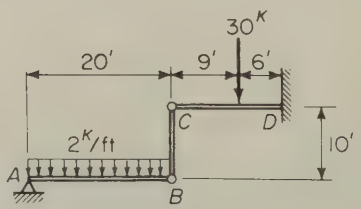

Figure P3–16

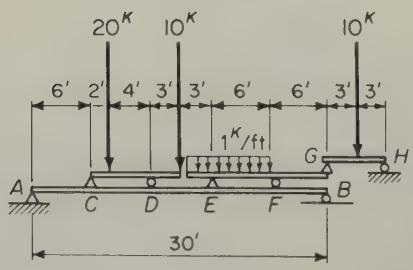

Figure P3–17

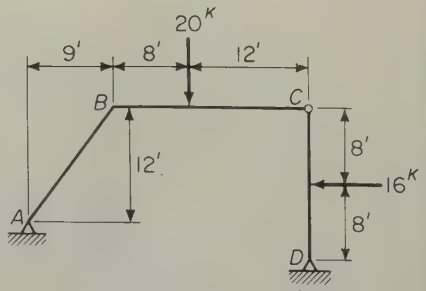

Figure P3–18

3-19 to **3-26** Compute the panel shears and the moments at the panel points for each of the beams shown in Figs. P3-19 to P3-26.

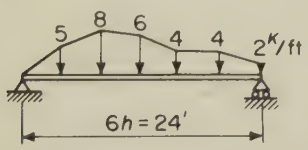

Figure P3–19

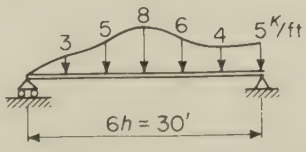

Figure P3–20

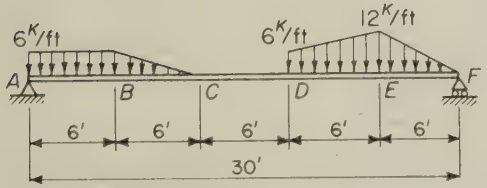

Figure P3–21

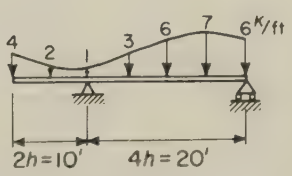

Figure P3–22

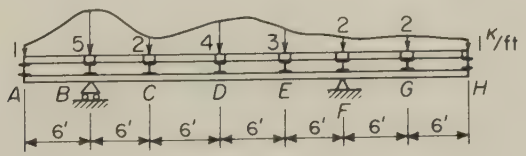

Figure P3–23

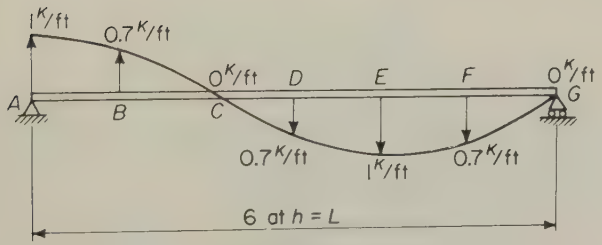

Figure P3–24

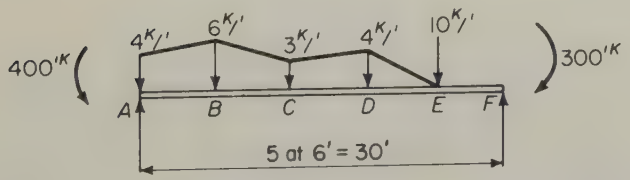

Figure P3–25

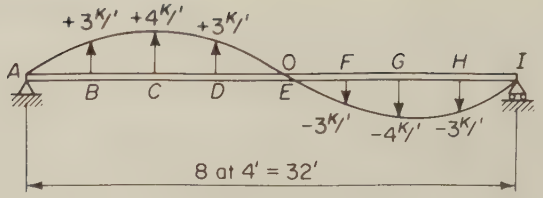

Figure P3–26

3-27 The three-hinged arch shown in Fig. P3-27(a) consists of two segments whose equations are shown in Fig. P3-27(b). Determine the axial force, shear, and moment at a section just to the right of point D and those at a section just to the right of point E of the structure.

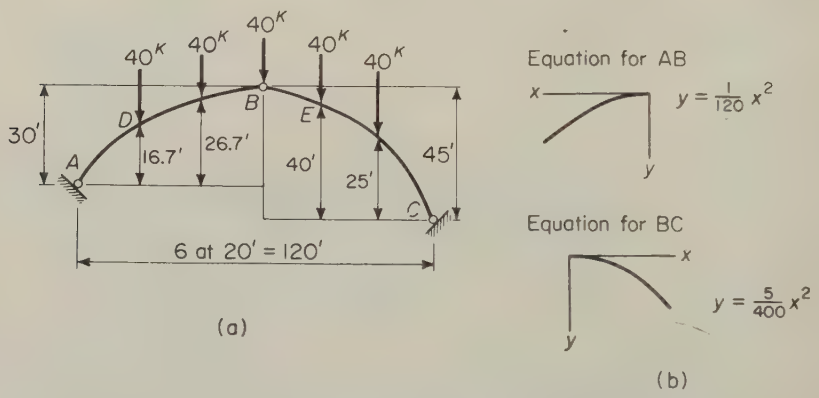

Figure P3–27

3-28 The axis of the three-hinged arch shown in Fig. P3-28 is a semicircle. The brackets inside the arch are rigidly attached. Compute the axial force, shear, and moment at point D of the arch.

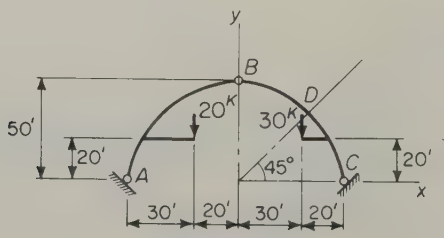

Figure P3–28

3-29 to **3-32** Draw the shear and moment diagrams on the horizontal projection of the arch axis for each of the three-hinged arches shown in Figs. P3-29 to P3-32.

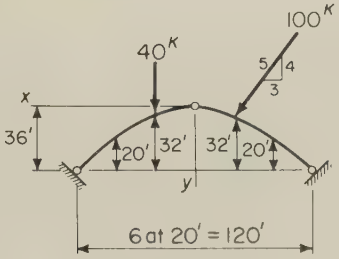

Figure P3–29

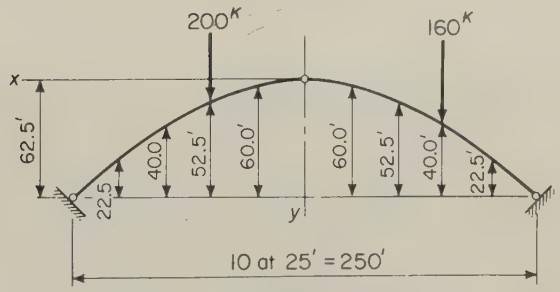

Figure P3–30

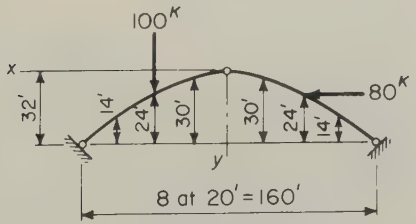

Figure P3–31

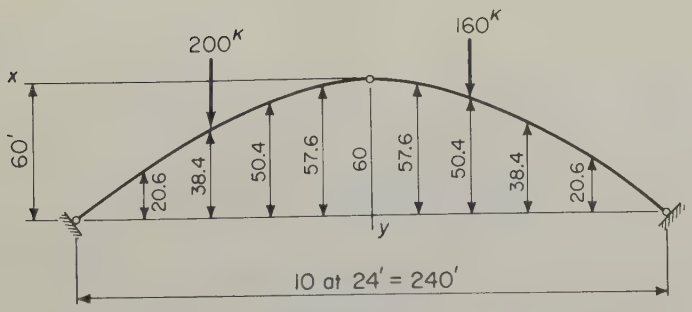

Figure P3–32

3-33 to **3-36** Compute the ordinates of the cable at the points of concentrated loads and the maximum tension in the cable for each of the cables shown in Figs. P3-33 to P3-36.

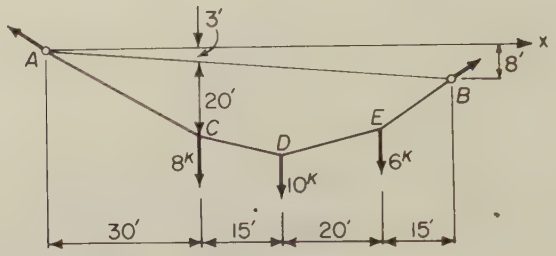

Figure P3–33

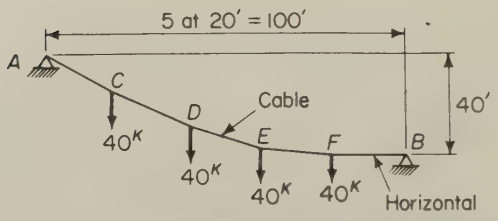

Figure P3–34

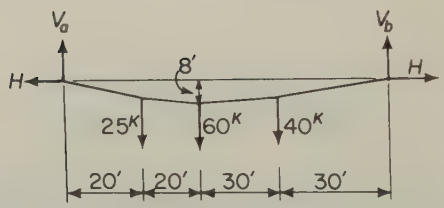

Figure P3–35

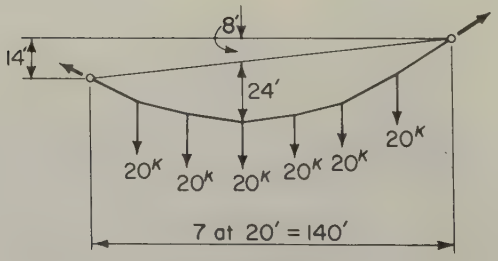

Figure P3–36

3-37 Determine the tension of the cable at points *A*, *B*, and *C* in Fig. P3-37.

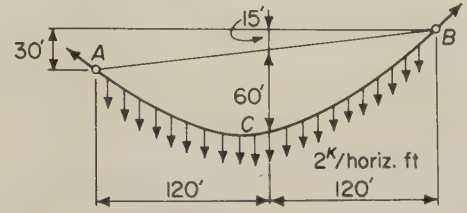

Figure P3–37

3-38 to **3-41** Draw the shear and moment diagrams for each of the suspended girders shown in Figs. P3-38 to P3-41.

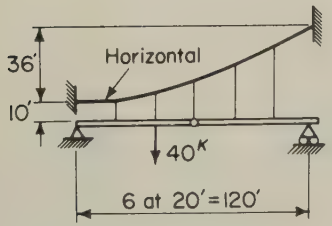

Figure P3–38

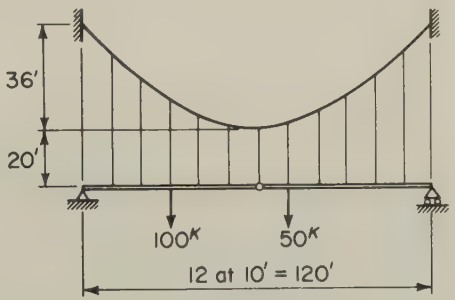

Figure P3–39

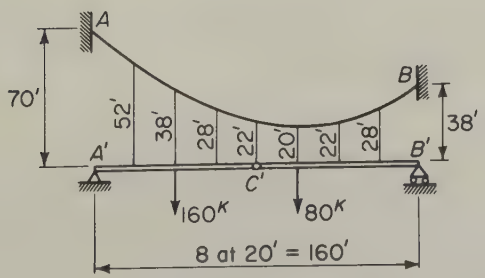

Figure P3–40

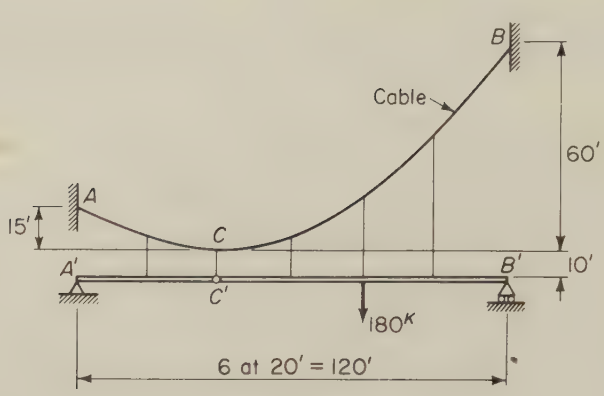

Figure P3–41

3-42 Compute the vertical shear, torque, and bending moment at the fixed support C of the cantilever bow girder whose axis in a horizontal plane is shown in Fig. P3-42. A downward vertical load of 20 kips is applied at the free end A and a downward uniformly distributed load of 1 kip/ft is applied along the length AB of the girder.

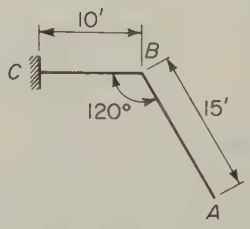

Figure P3–42

3-43 Compute the vertical shear, torque, and bending moment at the fixed support C of the cantilever circular bow girder whose axis in a horizontal plane is shown in Fig. P3-43. A downward uniformly distributed load of 2 kips/ft is applied along arc AB of the girder.

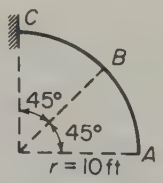

Figure P3–43

3-44 Determine the vertical reactions of the balcony girder that is loaded with a uniformly distributed load of 5 kips/ft along the entire circular girder as shown in Fig. P3-44(a). The axis of the girder in a horizontal plane is shown in Fig. P3-44(b).

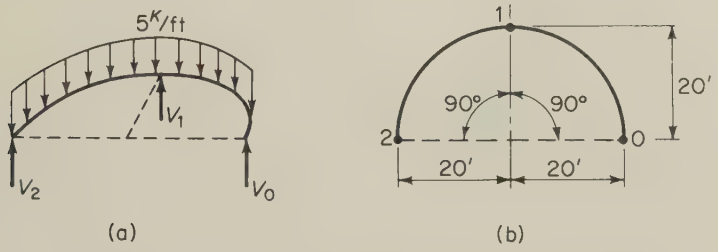

Figure P3–44

3-45 Compute the vertical shear, torque, and bending moment at the fixed support C of the cantilever bow girder in Problem 3-43 if a downward uniform load of 2 kips/ft is applied along arc BC instead of arc AB of the girder.

4 BAR FORCES IN TRUSSES

4-1 Definitions

If straight bars are joined together at their ends by frictionless pins to form a rigid system on which loads are applied only at the joints, the resulting idealized structure is known as a *truss*. The system is said to be rigid in the sense that it undergoes no movement other than small deflections under applied loads. Since the bars in such a system are arranged in the form of triangles or polygons that are not closed by solid plates as in plate girders, this type of structure is sometimes called an *open truss*. If the bars or members of a truss are confined to the same plane, the truss is termed a *plane truss*; otherwise, it is said to be a *space truss*.

An *ideal truss* is characterized by the fact that its members are subjected to axial forces only because the smooth pins at the ends of a member cannot transmit moment and the line of action of the internal force in a member must pass through the pins at its ends. The *internal axial force* in a member of the truss is called the *bar force*.* For a *real truss*, however, the joints are somewhat restrained from rotation, and the dead weight of the members is not concentrated at the joints. As a result, bending exists in the members of a real truss and causes moments and shears in the members. Since the stresses introduced by these moments and shears are relatively small compared with those caused by bar forces, especially if the centerlines of the members in a real truss meet at one point at each joint, the stresses due to

*In some textbooks, the term *stress* is used to denote the bar force, but in this book *stress* is defined strictly as the intensity of force per unit area.

bar forces are considered as *primary stresses*, whereas the stresses due to bending are termed *secondary stresses*. The latter can be superimposed on the former, and the two can be investigated as separate problems.

Trusses are used extensively in buildings, bridges, and many other important industrial constructions because they can be adapted to transmit heavy loads over relatively long spans. Since they are usually designed for specific purposes, their shapes and sizes vary greatly. In this chapter, we shall confine our discussions to the analysis of ideal plane trusses that are statically determinate and are subjected to stationary loads.

The members of a plane truss must be so arranged that the structure is statically and geometrically stable. The over-all criteria of statical determinacy for plane and space trusses have been given in Section 2-6. We should point out again that either of these conditions is necessary but not sufficient to ensure the statical determinacy of a truss. The final test is to check whether the truss constitutes a rigid system that cannot be collapsed under all loading conditions. The geometrical instability of a truss is not always obvious, but it can be detected immediately if the results of the computed reactions or bar forces in a system turn out to be infinite or inconsistent.

From the point of view of analysis, statically determinate trusses may be classified into three categories: simple, compound, and complex. A *simple truss* is defined as a system of bars assembled by first joining together three bars at their ends in the form of a triangle and then adding to this configuration two more bars for each additional joint. A *compound truss* is defined as a rigid system formed by interconnecting two or more simple trusses, the rigidity being provided by a sufficient number of independent components of constraint at the interconnection between the simple trusses. If the arrangement of bars in a truss fails to satisfy either the definition of a simple truss or that of a compound truss, even though the criterion for statical determinacy still holds true, the system is said to be a *complex truss*.

In this chapter we are primarily interested in the analysis of bar forces in plane trusses, although the same principles may be applied to the solution of space trusses. We shall, therefore, discuss the three major categories of statically determinate trusses in terms of plane trusses only. Figure 4-1 shows several simple trusses, each of which has been formed by starting with triangle ABC and then establishing the remaining joints in alphabetical

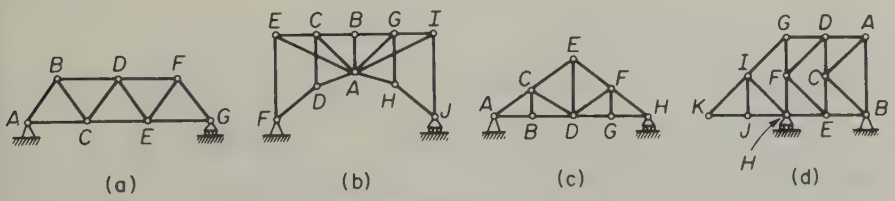

Figure 4-1

order. Intersections where bars cross each other freely without connection are not considered as joints. Figure 4-2 illustrates several compound trusses, each of which has been formed by interconnecting two simple trusses by

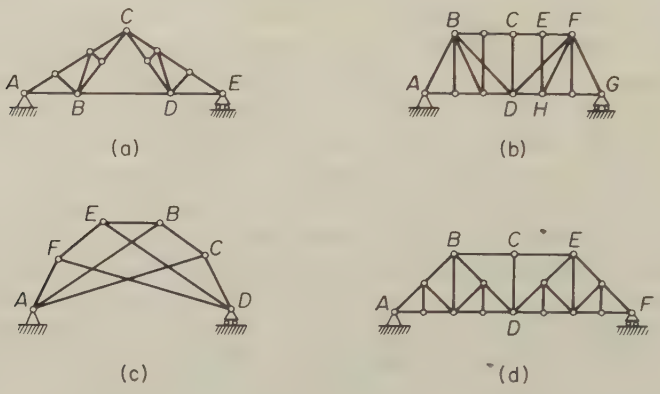

Figure 4–2

three independent components of constraint. In Fig. 4-2(a), the portion *ABC* is formed in accordance with the definition of a simple truss, but beyond points *B* and *C* this procedure cannot be applied. However, a second simple truss *CDE* may be connected to the first one by member *BD* and hinge *C*. If the portions *ABC* and *CDE* are isolated as free bodies, there will be an axial force acting along *BD* and two components of force at hinge *C*. These three components of force are necessary and sufficient to provide rigidity for the interconnected truss, and they may be determined from the condition of equilibrium of the free bodies. In Fig. 4-2(b), two simple trusses *ABCD* and *EFGH* are interconnected by members *CE*, *DH*, and *DF*, which provide three independent components of constraint; in Fig. 4-2(c), two simple trusses *ABC* and *DEF* are interconnected by members *AF*, *BE*, and *CD*, which are the components of constraint. In Fig. 4-2(d), two simple trusses *ABCD* and *DEF* are interconnected by member *CE* and hinge *D*. However, compound trusses may also be formed by two simple trusses with less than three independent components of constraint at the interconnection if extra components of reaction are added to make up the

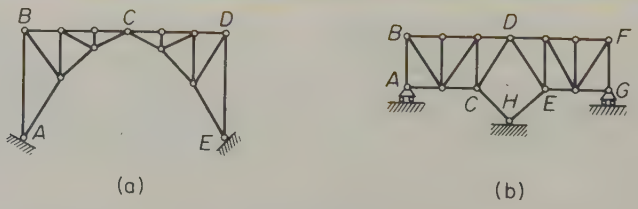

Figure 4–3

difference. Figure 4-3 shows two of these compound trusses. In Fig. 4-3(a) the structure is formed by two simple trusses ABC and CDE that are interconnected by two components of constraint plus an extra component of reaction that replaces the third component of constraint normally needed at the interconnection of simple trusses. In Fig. 4-3(b), simple trusses $ABDC$ and $EDFG$ are interconnected by two components of constraint at joint D only, but the additional support at H provides an extra component of reaction for each of the simple trusses. Figure 4-4 shows two complex trusses

(a) (b)

Figure 4-4

that do not fulfill the requirements of simple or compound trusses. Nevertheless, they satisfy the criterion of statically determinate plane trusses.

4-2 *Common Patterns of Plane Trusses*

Although plane trusses of various shapes may be adopted for specific purposes, most of those used in buildings and bridges follow a few simple patterns that have been found to be economical under ordinary conditions encountered in practice. Since the primary function of a roof or bridge truss is to transmit loads between supports, the structural action of a truss is analogous to that of a beam or girder. The members that form the perimeter of a truss are called *chord members*. The top and bottom chord members in a truss serve the same purpose as the flanges of a plate girder. The interior members between chord members are known as *web members*. They have the same function as the solid web plate of the plate girder. Whenever possible, symmetrical trusses are preferred because of the simplicity of their analysis and fabrication. We shall mention briefly here the conventional names and the general characteristics of these patterns.

Roof trusses. The top chords of roof trusses may be either pitched or flat. The ratio of rise to span length of a roof truss is called the *pitch*, which varies from 1/4 to 1/3 for ordinary pitched roof trusses. The ratio of depth to span length of flat roof trusses is usually between 1/12 and 1/8. The panel length of the trusses is determined by the spacing of the roof purlins, which are supported at the joints of top chord members. Figures 4-5(a), (b), and (c) show three common types of trusses for pitched roofs of moderate

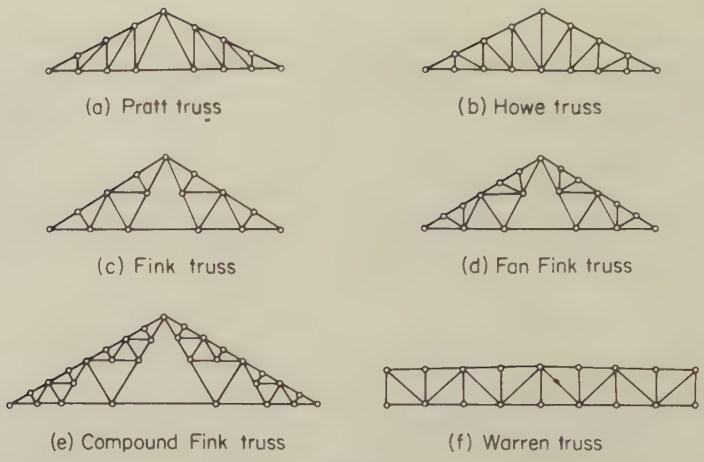

Figure 4-5

span. The Fink truss in Fig. 4-5(c) may be used for spans of greater length, but it must be modified to provide more joints at the upper chord if the roof is to be supported at relatively short intervals as shown in Fig. 4-5(d) or (e). For a relatively flat roof, the Warren truss shown in Fig. 4-5(f) may be used. However, the web system of a truss for a flat roof may also be patterned after the Pratt truss or Howe truss, shown in Figs. 4-5(a) and (b) respectively.

Bridge trusses. Bridge trusses may be classified according to the manner in which the floor loads are transmitted to the trusses. If the floor system is connected to the bottom chord of a truss, the truss is said to be a *through truss* in the sense that the traffic passes through the truss. If the floor system is connected to the top chord of a truss, the truss is called a *deck truss*. When the floor system is located between the top chord and the bottom chord, the truss is known as *half-through* or *pony truss*. Figure 4-6 shows various patterns of bridge trusses that are adaptable to either through trusses, deck trusses, or pony trusses.

For bridge trusses of moderate span, the top and bottom chord members are usually made parallel in order to simplify the fabricating process. For longer spans, polygonal top chords are used to reduce the dead weight of the truss. This is analogous to cutting off the cover plates of a plate girder in the region where the cover plates are no longer needed to resist bending. For economical designs, the ratio of maximum depth to span length of a bridge truss is usually between 1/10 and 1/5, and the slope of the diagonal web members varies from 45 deg to 60 deg with a horizontal line. Figures 4-6(a), (b), (c), and (d) represent the most common types of bridge trusses of moderate span. The type shown in Fig. 4-6(e) may be used for slightly longer spans.

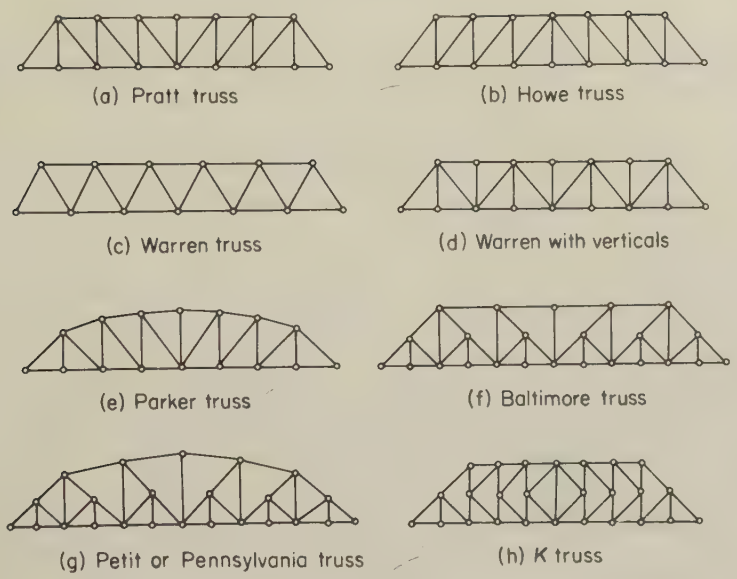

Figure 4–6

As the span length of a truss increases, the panel length also becomes longer if the slope of the diagonal web members is maintained at an angle of 45 deg to 60 deg with a horizontal line. The panel length of a truss is a factor of economy of the floor system, which in turn affects the dead weight of the truss. If a heavy floor system is to be avoided, trusses with subdivided panels such as those shown in Figs. 4-6(f) and (g) may be used. The short diagonals in trusses with subdivided panels are usually referred to as *subties* if they are tension members, or as *substruts* if they are compression members. The K-truss shown in Fig. 4-6(h) may also serve the same purpose without the introduction of subdivided panels.

Long-span trusses. For long-span structures, trusses such as those shown in Fig. 4-7 are often used. The arch truss in Fig. 4-7(a) has the advantage of gaining the rise as well as spanning over a long distance. The economy of a cantilever bridge such as the one shown in Fig. 4-7(b) over a simple truss of the same span is realized largely because the moments caused by uniform loads on a cantilever truss are in general smaller and most of the dead weight of the cantilever truss is concentrated near the supports. The cantilever truss is especially applicable where falsework is impractical or undesirable during erection. The Wichert truss shown in Fig. 4-7(c) has most of the advantages of a continuous structure while remaining statically determinate, but it may be geometrically unstable if the diagonals at the supports are not properly oriented. In Fig. 4-7(d), the stiffening truss of the suspension bridge is used to distribute the live loads uniformly to

the hangers so that the cables will not change shape when the loads move from one point to another on the bridge.

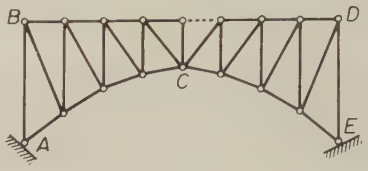

(a) Arch truss

(b) Cantilever truss

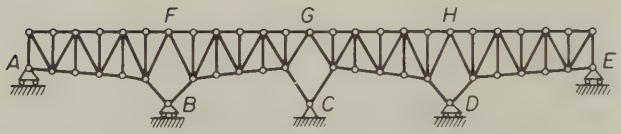

(c) Wichart truss

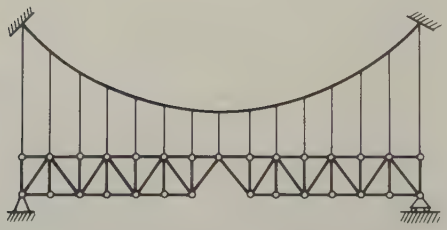

(d) Suspension bridge with stiffening truss

Figure 4–7

4-3 *Bar Forces in Simple Trusses*

The basic approach to the analysis of a truss is to study the internal forces in its members, which can be accomplished by passing imaginary sections through the members of the truss for which the bar forces are required.

Since the truss as a whole is in static equilibrium, any free body isolated from the truss must also be in equilibrium.

The bar forces in a truss may be obtained by variations of this basic approach. The two most common methods used for the solution of simple trusses are the *method of joints* and the *method of sections.* In the former, each joint of a truss is isolated as a free body. If there are not more than two unknown bar forces at a joint, these unknowns may be determined from the two equations of static equilibrium available for a coplanar concurrent force system. Thus, a joint that satisfies this requirement is first selected as the starting point, and the procedure is then carried out joint by joint so that the results of analysis from one joint may be used for the next adjacent joints. In the latter method, sections are passed through various members of the truss for which the bar forces are required. If there are not more than three unknown bar forces at a section, the unknowns may be determined from the three equations of static equilibrium available for a coplanar nonconcurrent force system. For both methods, there are exceptions to the rules stated above that will be discussed later.

Since a complete analysis of a truss involves the determination of bar forces in all of its members, they must be obtained in a well-organized sequence. A sign convention is adopted for the sense of direction of bar forces in a truss as follows: A bar force is considered as *positive* when it produces *tension* in a member and as *negative* when it causes *compression* in the member. Thus, in any free body cut by a section passing through members of a truss, a tensile or positive bar force in a member is represented by an arrowhead pulling away from a joint, and a compressive or negative bar force is represented by an arrowhead pushing toward a joint. For simple trusses, whether a member is subjected to tension or compression can easily be recognized, and correct senses of direction can be assigned to the bar forces; otherwise, the bar forces may be assumed to have a sense of direction corresponding to the positive sign convention. In that case, a positive result will indicate that the assumed sense of direction is correct, and a negative result means that actual sense of direction is the reverse of the assumed direction.

In the analysis of trusses it is often convenient to work with the horizontal and vertical components of the bar forces, since the equations of equilibrium are usually obtained by the summation of forces in two mutually perpendicular directions and by the summation of moments due to these components of forces. Because the lengths of members in a truss are known quantities while the angles between any two members are seldom computed, the horizontal and vertical components of a bar force are usually related to the corresponding projections of the member instead of being expressed in trigonometric functions.

There are numerous techniques that may be used to expedite the

determination of bar forces in plane trusses. Such techniques will be illustrated by appropriate examples.

4-4 *Application of Method of Joints*

The method of joints can always be applied to simple trusses because in any such truss there are only two bars meeting at the last joint formed in accordance with the definition. If external loads or reactions are also applied at this joint, they are either known or can be obtained first. Hence, the two unknown bar forces at the joint can be determined from the two equations of equilibrium at that joint. Then, for the next-to-the-last joint established according to the basic definition, there are also only two unknown bar forces which can be solved readily in the same manner. Hence, the bar forces in all members of a truss can be determined by considering the joints as free bodies in the reverse order from which the joints have been established. If the joints in a truss can be established in different orders, there will be more than one order according to which the bar forces in the truss may be solved by the method of joints.

In general, the two unknown bar forces at a joint can be determined from the solution of two simultaneous equations resulting from the consideration of the joint in equilibrium. However, the numerical computation may be somewhat simplified if, by the proper choice of coordinate axes, only one unknown appears in each equation. In all numerical examples in this chapter, the bar forces are in the unit of kips and the distances are in the unit of feet.

Example 4-1. Compute the bar forces in all members of the simple truss in Fig. 4-8(a).

The reactions at A and H may be computed as follows:

$$\sum M_a = 0, \qquad -80V_h + 20\,(60 + 40 + 20) + (50)\,(25) = 0, \quad V_h = 45.6$$

$$\sum F_x = 0, \qquad H_a = (\tfrac{3}{5})\,(50) = 30$$

$$\sum F_y = 0, \qquad V_a = (3)\,(20) + (\tfrac{4}{5})\,(50) - 45.6 = 54.4$$

Since there are only two unknown bar forces at either joint A or joint H, one of them can be chosen as the starting point. If we consider A as a free body as shown in Fig. 4-8(b), for instance, the internal forces in members AB and AC, as represented by F_{ab} and F_{ac} respectively, are the only unknowns. The senses of direction of F_{ab} and F_{ac} are arbitrarily assumed. However, it is not difficult to visualize in this case that, since the vertical component of reaction at A is directed upward, the vertical component of F_{ac} must be acting downward in order to maintain the equilibrium of the joint. The sense of direction of F_{ac}, therefore, is pushing toward the joint, and

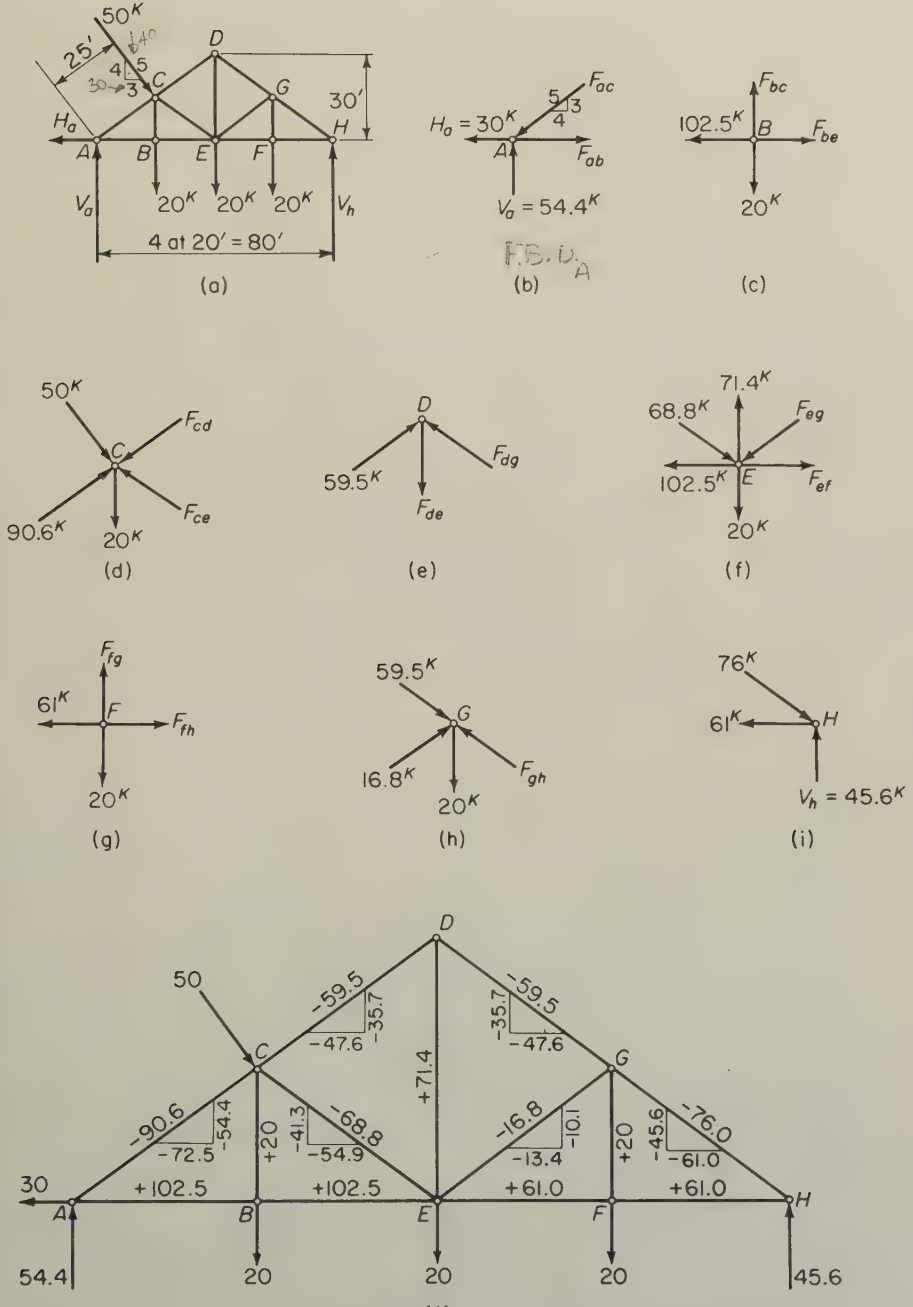
50^K
25'
4
5
3
30°
C
D
G
30'
H_a
A
B
E
F
H
V_a
20^K
20^K
20^K
V_h
4 at 20' = 80'
(a)
F_ac
5
3
4
H_a = 30^K
A
F_ab
V_a = 54.4^K
F.B.D.
A
(b)
F_bc
102.5^K
B
F_be
20^K
(c)
50^K
C
F_cd
F_ce
90.6^K
20^K
(d)
D
F_dg
59.5^K
F_de
(e)
71.4^K
68.8^K
F_eg
102.5^K
E
F_ef
20^K
(f)
F_fg
61^K
F
F_fh
20^K
(g)
59.5^K
G
16.8^K
F_gh
20^K
(h)
76^K
61^K
H
V_h = 45.6^K
(i)
D
50
-59.5
-35.7
-47.6
-59.5
-35.7
-47.6
C
G
+71.4
-90.6
-54.4
-72.5
+20
-41.3
-68.8
-54.9
-16.8
-10.1
-13.4
+20
-45.6
-76.0
-61.0
30
+102.5
+102.5
+61.0
+61.0
A
B
E
F
H
54.4
20
20
20
45.6
(j)

Figure 4–8

member AC is in compression. Again, because the horizontal component of reaction at A as well as the horizontal component of F_{ac} is directed toward the left, F_{ab} must be acting toward the right. Thus, the sense of direction of F_{ab} is pulling away from the joint, and member AB is in tension. The equations of equilibrium for the components of forces in horizontal and vertical directions at joint A can be written as follows:

$$\sum F_y = 0, \qquad 54.4 - (\tfrac{3}{5})F_{ac} = 0, \quad F_{ac} = 90.6$$

$$\sum F_x = 0, \qquad F_{ab} - (\tfrac{4}{5})F_{ac} - 30 = 0, \quad F_{ab} = 102.5$$

The positive results confirm that the assumed senses of direction for both members are correct. In order to indicate these senses of direction without referring to the free-body diagram, the magnitude of a bar force may be prefixed by a sign, such as $F_{ac} = -90.6$, indicating that the member is in compression and $F_{ab} = +102.5$, indicating that the member is in tension.

Next, proceed to joint B, at which there are only two unknown bar forces as shown in Fig. 4-8(c). Thus, from $\Sigma F_y = 0$, $F_{bc} = 20$; from $\Sigma F_x = 0$, $F_{be} = 102.5$. Similarly, for joint C shown in Fig. 4-6(d), we obtain

$$\sum F_y = 0, \quad (\tfrac{3}{5})F_{ce} - (\tfrac{3}{5})F_{cd} + 54.4 - (\tfrac{4}{5})(50) - 20 = 0$$

or

$$F_{ce} - F_{cd} = (\tfrac{5}{3})(5.6) = 9.3$$

$$\sum F_x = 0, \quad (\tfrac{3}{5})(50) + 72.5 - (\tfrac{4}{5})F_{cd} - (\tfrac{4}{5})F_{ce} = 0$$

or

$$F_{cd} + F_{ce} = (\tfrac{5}{4})(102.5) = 128.3$$

Solving these two equations simultaneously, we have $F_{cd} = 59.5$ and $F_{ce} = 68.8$. Since the results for F_{cd} and F_{ce} are positive, the assumed senses of direction are correct, i.e., both F_{cd} and F_{ce} are in compression.

The bar forces in the remaining members may be obtained in a similar manner by the consideration of joints D, E, F, and G as free bodies as shown in Figs. 4-8(e), (f), (g), and (h) respectively. It is sufficient to point out that at joint G, there is only one unknown bar force which requires only one equation of equilibrium for its solution, and the second equation of equilibrium can be used as a check. The free-body diagram for joint H shown in Fig. 4-8(i) is not needed for the solution of bar forces and is included for checking purposes only.

The results of analysis of the entire truss are summarized in Fig. 4-8(j) in which the bar forces are prefixed by either a positive or a negative sign that indicates whether the member is in tension or in compression. The vertical and horizontal components of the bar forces in inclined members are also shown in the figure. We should point out that the formal procedure of drawing separate free-body diagrams and writing equations of

equilibrium for each case is not always necessary after the student has familiarized himself with the basic idea. Referring to joint A in Fig. 4-8(j), for instance, it is obvious that the vertical component of the bar force in member AC must be equal and opposite to the vertical reaction at A since there is no other vertical force acting at joint A. The horizontal component of the bar force in member AC can be obtained by multiplying the vertical component by a ratio representing the reciprocal of the slope of the member. Then, the bar force in AC can be determined accordingly while the bar force in member AB is equal and opposite to the algebraic sum of the horizontal reaction at A and the horizontal component of the bar force in member AC. Thus, if the horizontal and vertical components of a bar force are represented by H and V respectively,

$$V_{ac} = -54.4, \quad H_{ac} = (-54.4)(\tfrac{4}{3}) = -72.5$$
$$F_{ac} = (-54.4)(\tfrac{5}{3}) = -90.6$$
$$F_{ab} = 72.5 + 30 = +102.5$$

It may also be of interest to note that if joint H were chosen as the starting point, it would involve less numerical work since there is no horizontal reaction at H. Furthermore, the bar force in member BC can be determined from the consideration of joint B alone even though there are three unknown bar forces meeting at that joint, but the bar forces in members AB and BE cannot be obtained without also considering other joints in the truss.

Example 4-2. Determine the bar forces in members AB and BC of the simple truss shown in Fig. 4-9(a).

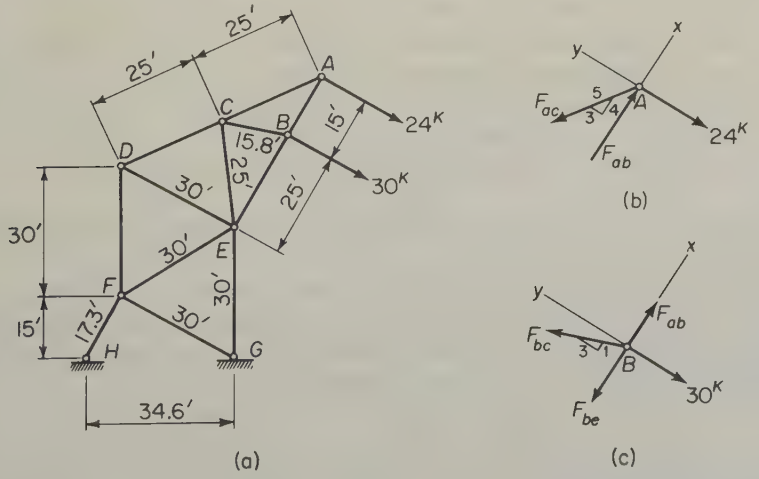

Figure 4–9

In this case the bar forces can be obtained from joints A and B without computing the reactions first since there are only two unknown bar forces at joint A. Furthermore, the numerical computation may be simplified by choosing the coordinate axes for writing the equations of equilibrium in the directions shown in Fig. 4-9(b). Thus, from $\Sigma F_y = 0$, $F_{ac} = (24)(\frac{5}{3}) = 40$, and from $\Sigma F_x = 0$, $F_{ab} = (40)(\frac{4}{5}) = 32$, with senses of direction as indicated in the figure. Similarly, the same coordinate axes may be used for the solution of the bar forces meeting at joint B, as shown in Fig. 4-9(c). It can be seen that the bar force in member BC may be determined from the consideration of joint B alone since it is the only unknown bar force acting at the joint that has a component along the y-axis. Thus, for $\Sigma F_y = 0$, $F_{bc} = (30)(\sqrt{10}/3) = 31.6$ in tension. The remaining bar forces in the truss may be obtained by going through successive considerations of equilibrium of all joints in the truss.

4-5 *Application of Method of Sections*

In the analysis of simple trusses, it is sometimes more convenient to determine the bar forces in certain members by the method of sections, which can also be used as an independent check of those bar forces obtained by the method of joints. Since the method of sections consists essentially of isolating a portion of the truss by an imaginary section passing through the members for which the bar forces are desired, the free body generally represents a coplanar nonconcurrent force system in equilibrium. For some problems it may be more expedient to cut more than one section through the members of a truss, or to use the method of sections in connection with the method of joints.

In general, the three unknown bar forces at a section can be determined from the solution of three simultaneous equations resulting from the consideration of equilibrium of the free body isolated by the section. However, the numerical computation may be greatly simplified if, by the proper choice of centers of moments, only one unknown appears in each of these equations. All bar forces in the numerical examples are in the unit of kips.

Example 4-3. Determine the bar forces in members EF, EG, and CD of the truss shown in Fig. 4-10(a).

The free body in Fig. 4-10(b) is obtained by passing a section through members DF, EF, and EG. The senses of direction of the bar forces are assumed to be positive as indicated in the figure. Then, from the summation of all forces in the vertical direction, or $\Sigma F_y = 0$,

$$V_{ef} + 40 - (2)(16) = 0, \qquad V_{ef} = -8$$

Hence,

$$F_{ef} = (-8)(\tfrac{5}{4}) = -10$$

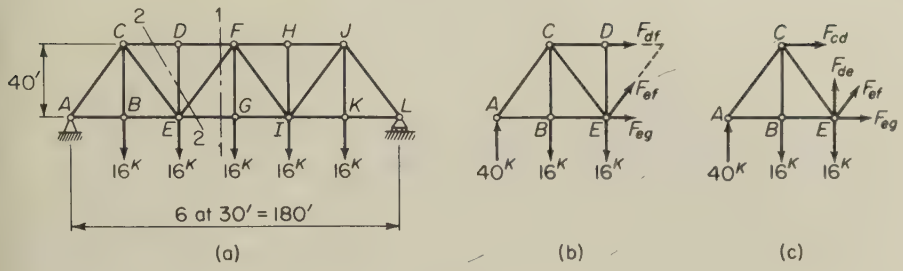

Figure 4–10

From the summation of moments of all forces about joint F, or $\Sigma M_f = 0$,

$$(40)(90) - (16)(60 + 30) - 40F_{eg} = 0, \quad F_{eg} = 54$$

The bar force in member CD can be obtained from the consideration of joint D in equilibrium if the bar force in member DF is known or determined first. Thus, by summing all forces in the horizontal direction, or $\Sigma F_x = 0$,

$$F_{df} + 54 + (-10)(\tfrac{3}{5}) = 0, \quad F_{df} = -48$$

This result may also be obtained by taking moments of all forces about joint E in Fig. 4-10(b), or $\Sigma M_e = 0$,

$$(40)(60) - (16)(30) + 40F_{df} = 0, \quad F_{df} = -48$$

Finally,

$$F_{cd} = F_{df} = -48$$

The bar force in member CD may also be obtained directly by passing section 2-2 through the truss. The free body to the left of the section is shown in Fig. 4-10(c), in which there are four unknown bar forces. However, three of these four unknown bar forces meet at one point, and it is possible to obtain the fourth by taking moments of all forces about joint E in Fig. 4-10(c). Thus, $\Sigma M_e = 0$,

$$(40)(60) - (16)(30) + 40F_{cd} = 0, \quad F_{cd} = -48$$

Example 4-4. Compute the bar forces in members BC, CD, CE, DE, and DG of the truss shown in Fig. 4-11(a).

We proceed by passing section 1-1 through members BD, CD, and CE, and passing section 2-2 through members CE, DE, and DG. The resulting free bodies to the left of sections 1-1 and 2-2 are shown in Figs. 4-11(b) and (c), respectively. Hence, three equations of static equilibrium may be written for each of the free-body diagrams, and the unknown bar forces can be obtained accordingly.

For the free-body diagram shown in Fig. 4-11(b), for instance, we can establish $\Sigma F_x = 0$, $\Sigma F_y = 0$, and $\Sigma M_c = 0$. It is obvious, however, that

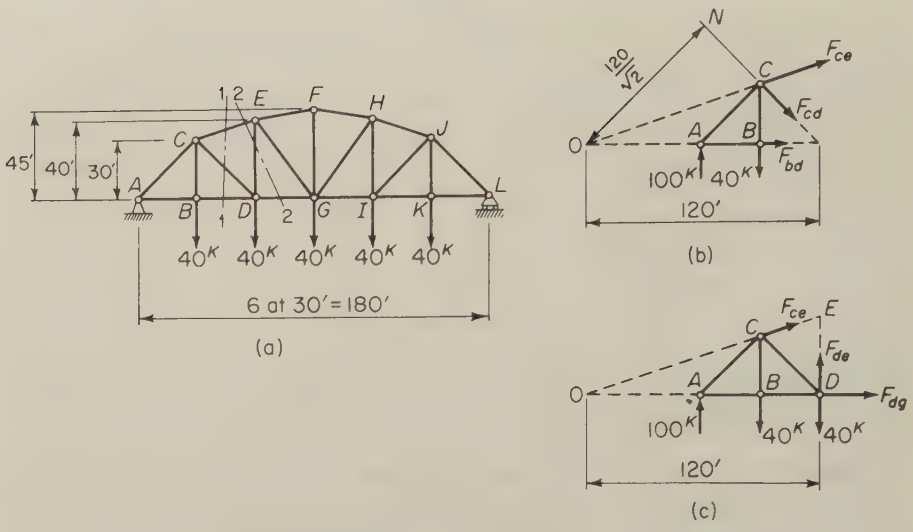

Figure 4–11

even if F_{bd} is first determined from $\Sigma M_c = 0$, both F_{cd} and F_{ce} will appear in the equations $\Sigma F_x = 0$ and $\Sigma F_y = 0$, which must be solved simultaneously. A simpler procedure may result if three independent equations of equilibrium are obtained by taking moments about three different points. Thus, $\Sigma M_c = 0$ may still be used for the solution of bar force F_{bd}, i.e.,

$$(100)(30) - 30F_{bd} = 0, \quad F_{bd} = 100$$

Similarly, from $\Sigma M_d = 0$,

$$(100)(60) - (40)(30) + \left(\frac{1}{\sqrt{10}} F_{ce}\right)(30) + \left(\frac{3}{\sqrt{10}} F_{ce}\right)(30) = 0$$

Note that the vertical and horizontal components of the bar force F_{ce} are used in the above equation since the moment arms of these components are obvious whereas the moment arm of the bar force itself must be computed from the geometry of the truss. From either consideration, $F_{ce} = -126$. The third equation may be established by taking moments about point O, which is the intersection of the lines of action of F_{bd} and F_{ce}. The moment arm for bar force F_{cd} then becomes $ON = 120/\sqrt{2}$. Hence, from $\Sigma M_o = 0$,

$$(120/\sqrt{2})F_{cd} - (100)(60) + (40)(90) = 0, \quad F_{cd} = 28.3$$

As a check, consider $\Sigma F_y = 0$,

$$100 - 40 + (1/\sqrt{10})(-126) - (1/\sqrt{2})(28.3) = 100 - 40 - 40 - 20 = 0$$

In Fig. 4-11(c), the bar forces in members DE and DG can be determined

by taking moments about points O and E respectively. Thus, for $\Sigma M_o = 0$,

$$(40)(120 + 90) - 120F_{de} - (100)(60) = 0, \quad F_{de} = 20$$

and for $\Sigma M_e = 0$,

$$(100)(60) - (40)(30) - 40F_{bd} = 0; \quad F_{bd} = 120$$

Example 4-5. For the truss shown in Fig. 4-12(a), determine the bar forces in members DF, DG, EF, and EH.

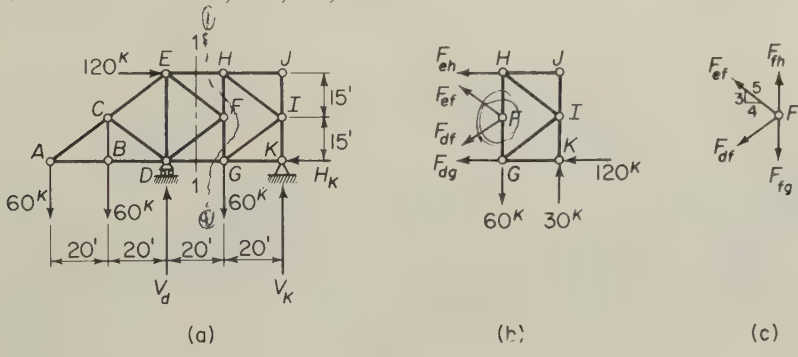

Figure 4-12

The reactions of the truss are first obtained as follows:

$$\sum F_x = 0, \quad H_k = 120$$

$$\sum M_d = 0, \quad (120)(30) + (60)(20) - (60)(40 + 20) - 40V_k = 0, \; V_k = 30$$

$$\sum F_y = 0, \quad V_d = (3)(60) - 30 = 150$$

If a part of the structure is isolated by section 1-1 as shown in Fig. 4-12(b), there are four unknown bar forces in the free body. Since only three equations of equilibrium are available, the fourth equation must be furnished by an additional requirement from the consideration of joint F in equilibrium. For the free-body diagram of joint F shown in Fig. 4-12(c), it is obvious that from $\Sigma F_x = 0$, the algebraic sum of horizontal components of F_{df} and F_{ef} must be zero. Thus,

$$\tfrac{4}{5} F_{df} + \tfrac{4}{5} F_{ef} = 0 \quad \text{or} \quad F_{df} = -F_{ef}$$

Then, from Fig. 4-12(b), we obtain

$$\sum F_y = 0, \quad \tfrac{3}{5}(F_{ef} - F_{df}) + 30 - 60 = 0, \quad F_{df} = -25 \quad \text{and} \quad F_{ef} = 25$$

$$\sum M_g = 0, \quad 30F_{eh} + (30)(20) = 0, \quad F_{eh} = -20$$

$$\sum M_h = 0, \quad 30F_{dg} + (120)(30) - (30)(20) = 0, \quad F_{dg} = -100$$

It should be noted that neither F_{df} nor F_{ef} appears in the equations for

$\Sigma M_g = 0$ and $\Sigma M_h = 0$, since the vertical components of these two forces pass through the moment center, and the horizontal components are equal and opposite to each other. As a check, $\Sigma F_x = 0$, or

$$F_{eh} + F_{dg} + 120 = -20 - 100 + 120 = 0$$

Example 4-6. Determine the bar force in member AC of the truss shown in Fig. 4-13(a).

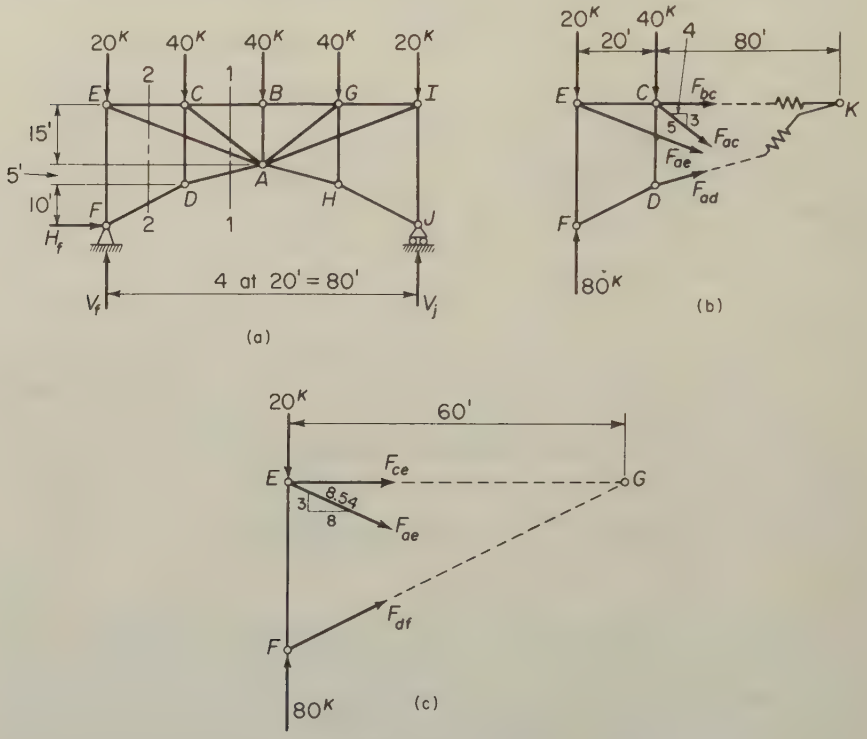

Figure 4–13

The reactions can be obtained by inspection. Since there are four unknown bar forces in the free body shown in Fig. 4-13(b), it is necessary to seek an additional equation or to eliminate one unknown from the system. This is accomplished by isolating a free body as shown in Fig. 4-13(c), from which F_{ae} may be determined. Then, F_{ac} may be obtained by taking moments of all known forces about the intersection of the lines of action of F_{ad} and F_{bc}.

Referring to Fig. 4-13(c), we take moments about point G whereby F_{ce} and F_{df} produce no moments. We can also resolve F_{ae} into vertical and horizontal components so that only the vertical component need be considered.

Thus, $\Sigma M_g = 0$ gives

$$\left(\frac{3}{8.54} F_{ae}\right)(60) + (20)(60) - (80)(60) = 0, \quad F_{ae} = 170.8$$

Similarly, in Fig. 4-13(b), we take moments about point K, with F_{ae} resolved into components at E and F_{ac} resolved into components at C. Then,

$$\left(\frac{3}{8.54} F_{ae}\right)(100) + (20)(100) - (80)(100) + \left(\frac{3}{5} F_{ac}\right)(80) + (40)(80) = 0$$

$$F_{ac} = -66.7$$

4-6 *Special Application to Parallel Chord Trusses*

For all types of parallel chord trusses with equal panels, the solution can be simplified by a slight modification of the method of sections if all panel loads are equal as in the case of dead loads. We may conceive the structural action of such a truss as a simple beam. Then the bar forces can be conveniently obtained from the shears and moments at various sections of the structure. This modified method is sometimes called the *method of shears and moments.*

Consider, for example, the parallel chord truss in Fig. 4-14(a). With height h and panel length p, all diagonal members have equal length d. In order to obtain the bar forces, sections are passed through various panels. For instance, section 1-1 is passed through panel CD in Fig. 4-14(a), resulting in the free-body diagram in Fig. 4-14(b), with the shear S and moment M at the section as indicated. The shearing resistance is provided by the vertical component of the bar force in the inclined member DI, and the resisting moment is equal to the couple produced by the bar forces in members CD and IJ. Thus, shear S is the shear in the panel CD whereas moment M may be considered as the moment about a conveniently chosen panel point such as I in this case. Thus,

$$S = 5Q - 4Q = +Q \quad \text{and} \quad M = (5Q)(2p) - (2Q)(p) = 8Qp$$

The senses of direction as well as the magnitude of the bar forces in members DI and CD can be derived from S and M as follows:

$$F_{di} = S\frac{d}{h} = \frac{Qd}{h} \quad \text{and} \quad F_{cd} = \frac{M}{h} = \frac{8Qp}{h}$$

Similarly, the bar force in a vertical member such as CI may be obtained from Fig. 3-14(c), which has been isolated by section 2-2 in Fig. 4-14(a). Hence,

$$F_{ci} = S = Q$$

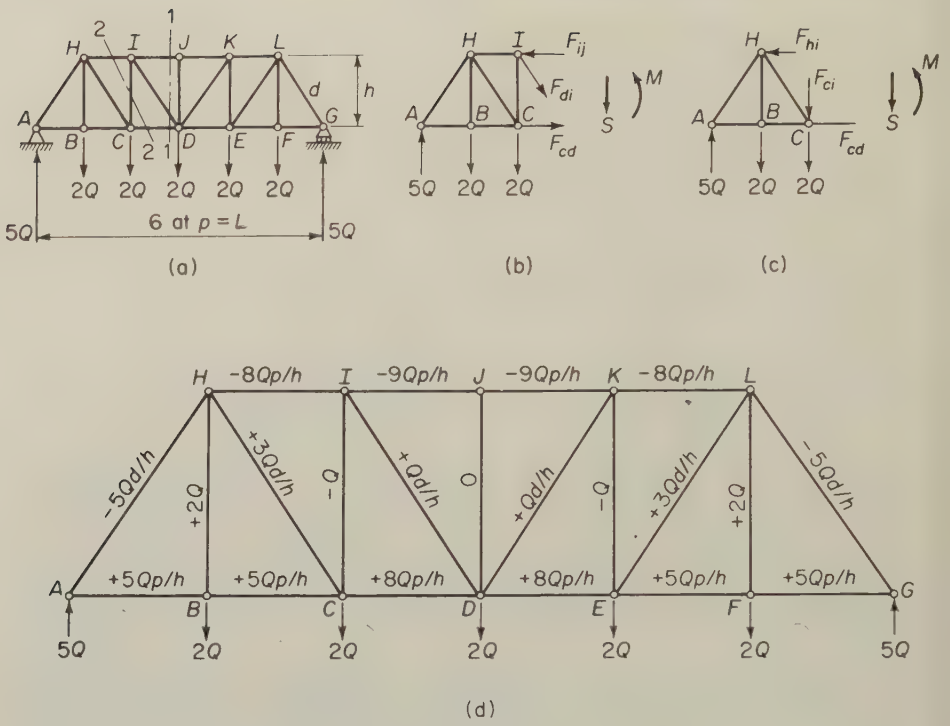

Figure 4-14

Since shears and moments at various sections of the structure can easily be obtained, the bar forces can be computed rapidly by the trigonometric relations of right triangles without drawing separate free-body diagrams. As an illustration, shears and moments for the truss are tabulated in Table 4-1.

TABLE 4-1

Panel	Shear S	Panel point	Moment M
AB	$+5Q$	B or H	$5Qp$
BC	$+3Q$	C or I	$8Qp$
CD	$+Q$	D or J	$9Qp$
DE	$-Q$	E or K	$8Qp$
EF	$-3Q$	F or L	$5Qp$
FG	$-5Q$		

Thus, the bar forces can be computed directly and are indicated in Fig. 4-14(d).

Another convenient way to obtain bar forces in a parallel chord truss with equal panel loads is through a slight modification of the method of joints. The bar forces are found by noting that the vertical components of web members are identical to the shears in the respective panels as we pass sections around successive joints. Such a method is called the *method of index forces*. Consider, for example, the truss in Fig. 4-14(d). The bar force in member AH is seen to have a magnitude of $(5Q)(d/h)$, in which $5Q$ is the shear in the panel and d/h is an index for converting the vertical component to the bar force in the inclined direction. A similar approach may be followed from joint to joint. The bar forces thus obtained are called *index forces*. Further details of the procedure will be omitted here.

4-7 Compound Trusses

The method of analysis used for the solution of simple trusses may also be applied to compound trusses. Quite frequently, however, the bar forces in a compound truss cannot be solved completely by the method of joints alone. For such cases, it is necessary to break up the compound truss into component simple trusses and to obtain the components of constraint at the interconnection between simple trusses first. This can be accomplished by the method of sections. In the compound truss shown in Fig. 4-15, for example, we may begin the solution of the truss by considering joint A as a free body after the components of reactions are determined, and proceed to joint F after obtaining the bar forces in members AB and AF. Then the next step leads to either joint B or joint G, at which there are three unknown bar forces. If we start from joint E on the other end of the truss, similar situations prevail at joints D and I. By passing section 1-1 through the truss as shown and thus isolating the simple trusses at the constraints, the bar force in member BD may be obtained by taking moments of all forces to the left or to the right of the section about joint C. As a result, the remaining two unknown bar forces at joint B can be solved by the available equations of equilibrium, and the bar forces at joint G can be obtained accordingly.

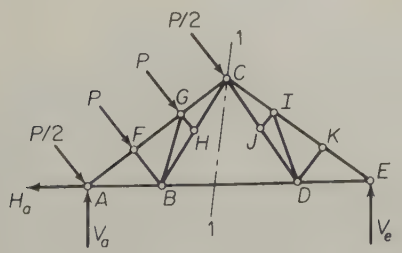

Figure 4–15

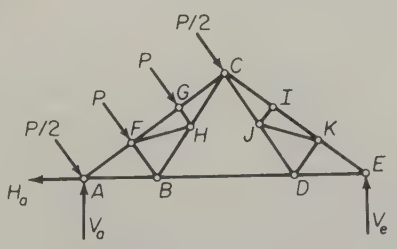

Figure 4–16

For some special cases, such as the truss shown in Fig. 4-16, the method of sections may be avoided. If we start the solution of the truss from joint A, we will immediately arrive at joint B or F, at which there are three unknown bar forces. It may be observed, however, that the bar force in member GH can be obtained from the consideration of joint G as a free body even if there are three unknown bar forces at that joint. Furthermore, the bar force in member FH can be computed by considering joint H as a free body if the bar force in member GH is known. Nevertheless, the basic approach of breaking up a compound truss at the constraints can be applied to any general case in which the method of joints or method of sections seems to fail to yield a solution.

Example 4-7. The compound truss in Fig. 4-17(a) consists of two simple trusses ABC and DEF that are linked together by three components of constraint AF, EB, and CD. Determine the bar forces in members AF, EB, and CD.

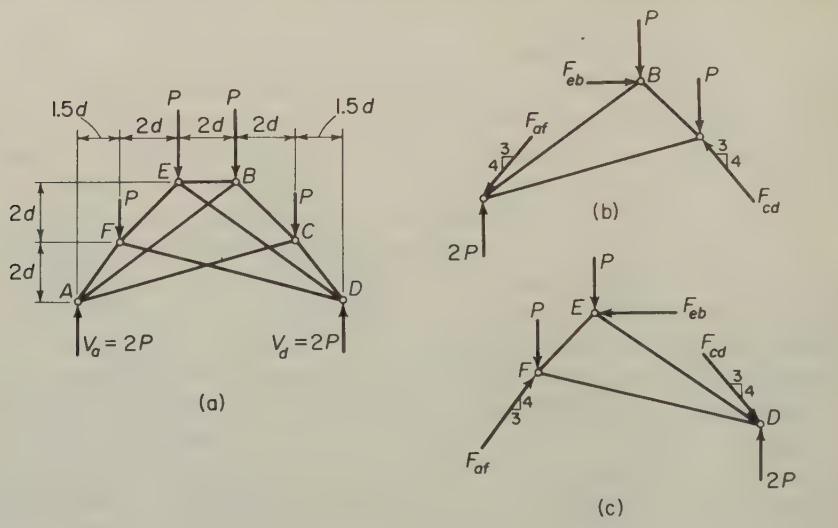

Figure 4-17

By breaking up the interconnections between two simple trusses, as shown in Figs. 4-17(b) and 4-17(c), we can obtain the bar forces in members AF, EB, and CD. From Fig. 4-17(b), we have

$$\sum F_y = 0, \quad 2P - P - P + \tfrac{4}{5}F_{cd} - \tfrac{4}{5}F_{af} = 0 \quad \text{or} \quad F_{af} = F_{cd}$$

$$\sum F_x = 0, \quad F_{eb} - \tfrac{3}{5}F_{af} - \tfrac{3}{5}F_{cd} = 0 \quad \text{or} \quad F_{eb} = \tfrac{3}{5}(F_{af} + F_{cd})$$

$$\sum M_a = 0, \quad (5.5d + 7.5d)P + (4d)F_{eb} - (7.5d)\,(\tfrac{4}{5}F_{cd}) - (2d)\,(\tfrac{3}{5}F_{cd}) = 0$$

or

$$7.2F_{cd} - 4F_{eb} = 13P$$

Solving these three equations simultaneously, we get

$$F_{af} = F_{cd} = 5.41P \quad \text{and} \quad F_{eb} = 6.5P$$

Then, the bar forces in all other members of the compound truss can be computed by the method of joints.

Example 4-8. Determine the bar forces in all members of the truss shown in Fig. 4-18(a).

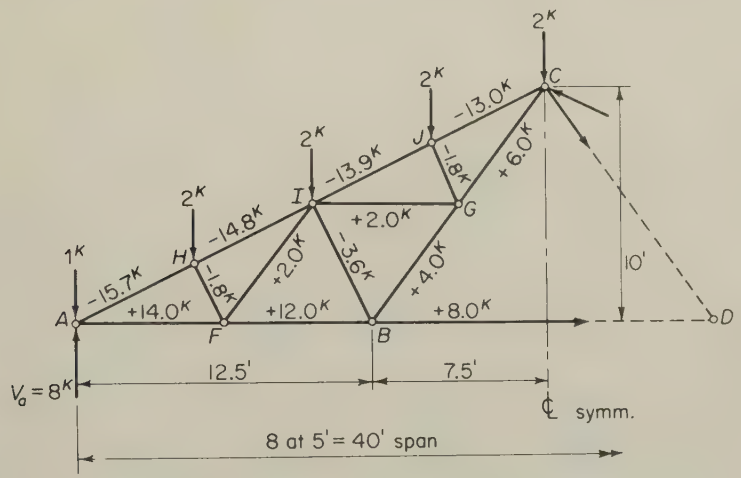

(a)

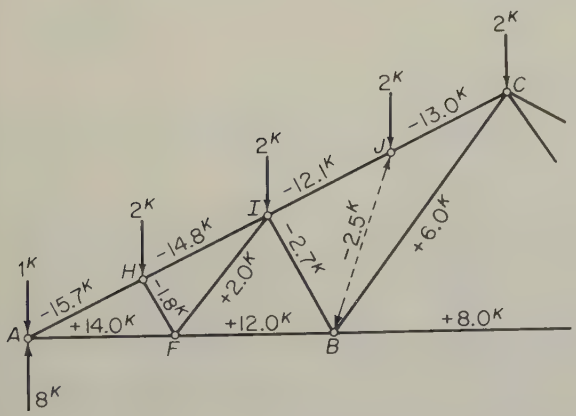

(b)

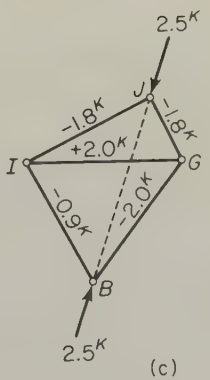

(c)

Figure 4–18

Since the truss is symmetrical with respect to its centerline, only half of it is shown in the figure. The problem can be solved by passing a section through the constraints connecting the two halves of the truss so that the bar force in member *BD* can be determined first. Then, the bar forces in all members of the truss are found by the method of joints as shown in the figure. However, the problem can also be solved without first obtaining the bar force in member *BD* by the method of sections, if the bar forces in members *GJ* and *GI* are first determined by considering successively the equilibrium of joints *J* and *G* respectively. Then the remaining bar forces can be obtained without difficulty.

A different approach involving the principle of superposition may also be used for the solution of this problem. If members *GJ* and *GI* in the truss are replaced by a substitute member *BJ* as shown in Fig. 4-18(b), the bar forces in the resulting truss can be completely solved by the method of joints. Such a substitution causes no change in the bar forces in the members of the original truss except in those members bounded by the panel *BIJG*. This can be seen from the fact that the bar forces in members *AF*, *AH*, *FH*, *HI*, *FI*, and *FB* can be solved by the method of joints starting from joint *A*, and those in members *CG* and *CJ* can also be solved after the components of reaction at *C* are obtained. All these bar forces are not related to those in panel *BIJG* and will not be affected by them. On the other hand, the bar force in the substitute member *BJ* is, in reality, nonexistent and may be construed as two equal and opposite forces temporarily placed at joints *B* and *J* that will eventually be removed. Furthermore, the panel *BIJG* shown in Fig. 4-18(c) may be considered as a separate system acted on by forces at joints *B* and *J* that are opposite to the corresponding forces representing the substitute member in Fig. 4-18(b). If Fig. 4-18(c) is superimposed on Fig. 4-18(b), the effect of the substitute member on the truss will be eliminated. The final results of superposition are identical to those shown in Fig. 4-18(a).

Example 4-9. Determine the bar forces in members *BC*, *BF*, *FK*, *IF*, *FJ*, *IJ*, *JK*, and *BI* of the symmetrical compound truss with subdivided panels in Fig. 4-19(a).

For a compound truss with subdivided panels, a section may be passed through a panel with not more than three members such as section 1-1 in Fig. 4-19(a). From the isolated free body in Fig. 4-19(b), we have

$$\sum M_k = 0, \quad \left(\frac{5}{\sqrt{26}} F_{bc}\right)(48) + (20)(60 + 40 + 20) + (10)(60 + 20) - (140)(80) = 0$$

$$F_{bc} = \frac{100}{3}\sqrt{26} = 170\ (-)$$

$$\sum M_b = 0, \quad 40F_{jk} + (20 + 10)(20) - (20 + 10)(20) - (140)(40) = 0$$

$$F_{jk} = 140\,(+)$$

$$\sum M_o = 0, \quad (140)(160) - (20)(180 + 200 + 220) - (10)(180 + 220) - \left(\frac{1}{\sqrt{2}} F_{fk}\right)(240) = 0$$

$$F_{fk} = \frac{80}{3}\sqrt{2} = 37.7\,(+)$$

Considering joint J as a free body as shown in Fig. 4-19(c), we get

$$\sum F_x = 0, \quad F_{ij} = F_{jk} = 140\,(+)$$

$$\sum F_y = 0, \quad F_{fj} = 20\,(+)$$

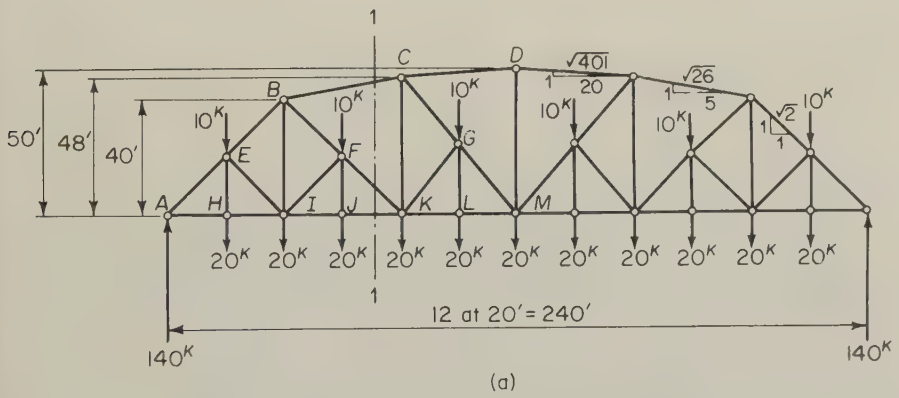

(a)

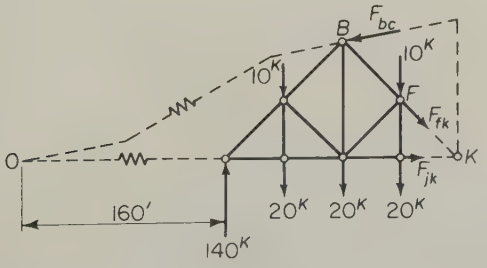

(b)

(c)

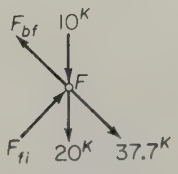

(d)

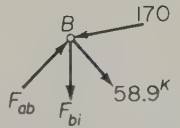

(e)

Figure 4–19

Then, from the consideration of joint F as a free body as shown in Fig. 4-19(d), we obtain

$$\sum F_x = 0, \quad \frac{1}{\sqrt{2}} F_{fi} - \frac{1}{\sqrt{2}} F_{bf} + \frac{37.7}{\sqrt{2}} = 0$$

$$\sum F_y = 0, \quad \frac{1}{\sqrt{2}} F_{fi} + \frac{1}{\sqrt{2}} F_{bf} - 20 - 10 - \frac{37.7}{\sqrt{2}} = 0$$

Hence,

$$F_{fi} = 15\sqrt{2} = 21.2\,(-), \quad F_{bf} = 41.7\sqrt{2} = 58.9\,(+)$$

Finally, by considering joint B as a free body as shown in Fig. 4-19(e), we have

$$\sum F_x = 0, \quad \frac{1}{\sqrt{2}} F_{ab} - F_{bi} - \frac{170}{\sqrt{26}} - \frac{58.9}{\sqrt{2}} = 0$$

$$\sum F_y = 0, \quad \frac{1}{\sqrt{2}} F_{ab} + \frac{58.9}{\sqrt{2}} - \left(\frac{5}{\sqrt{26}}\right)(170) = 0$$

Thus,

$$F_{ab} = 125\sqrt{2} = 176\,(-), \quad F_{bi} = 50\,(+)$$

4-8 *Trusses with Secondary Systems*

Compound trusses may be formed by superimposing several small-size simple trusses on the members of another simple truss. The basic framework

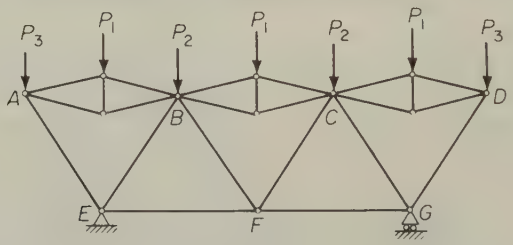

(a)

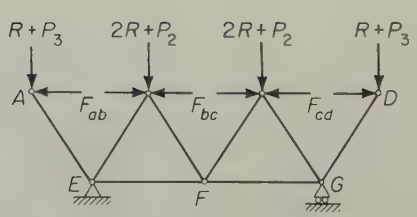

(b)

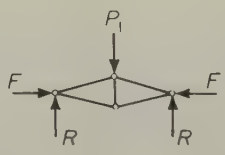

(c)

Figure 4–20

on which the smaller simple trusses are superimposed is considered as the primary system, whereas the smaller trusses themselves are regarded as secondary systems. Examples are shown in Figs. 4-20 and 4-21.

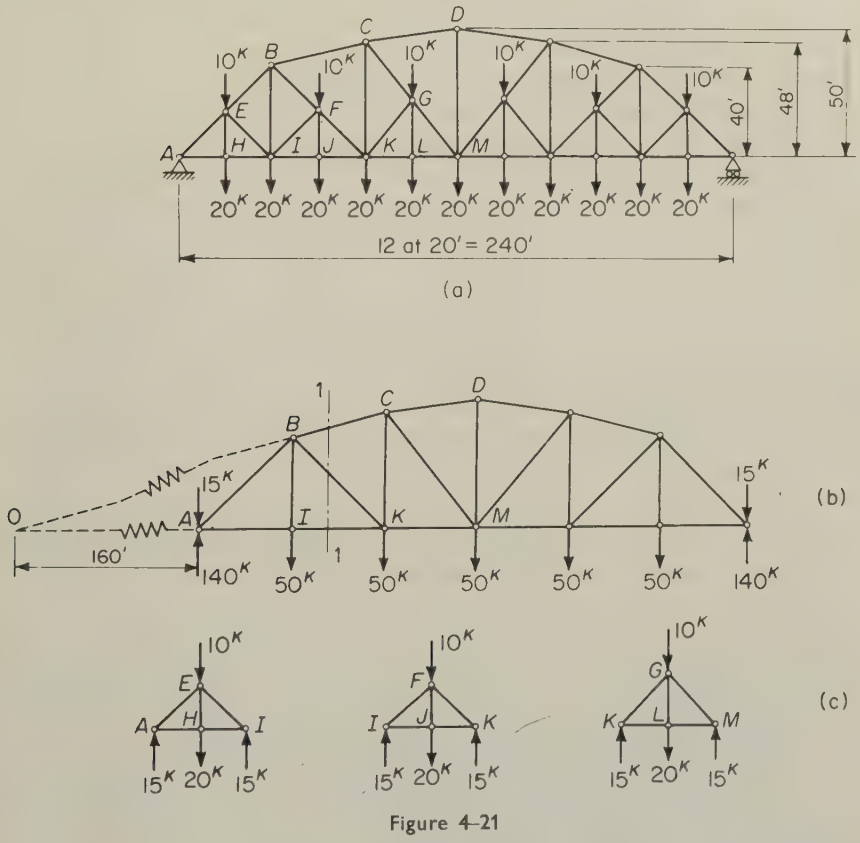

Figure 4–21

The secondary systems in a compound truss serve the dual functions of acting as individual units and of transferring their own loads to the joints of the primary system. If the external loads on the secondary systems are transferred properly to the joints of the primary system while the secondary systems are replaced by single bars, the resulting system can be solved by the method of joints or the method of sections, and the effects of the secondary systems may be superimposed later without difficulty. Consider the compound truss in Fig. 4-20(a), in which the secondary systems between joints *A* and *B*, *B* and *C*, and *C* and *D* may be replaced by bars *AB*, *BC*, and *CD* respectively, as shown in Fig. 4-20(b). Each of these secondary systems may be isolated as a free body, as shown in Fig. 4-20(c). Since all external loads in Fig. 4-20(c) are in the vertical direction, the vertical components

of reaction R at each end of the secondary system can be computed from the applied loads while the horizontal components of reaction F at each end represent the action of the primary system on the secondary system. If the bar forces in Fig. 4-20(b) are first determined, the horizontal force F for each of the secondary systems may be obtained from the corresponding substitute member in the primary system. Thus, when the results of the secondary systems are superimposed on those of the primary system, the effects of the substitute members are eliminated.

Although this general approach can be applied to any compound truss with secondary systems, it can be simplified for special cases. For instance, the compound truss with subdivided panels shown in Fig. 4-21(a) can be replaced by the primary system shown in Fig. 4-21(b) plus the secondary systems shown in Fig. 4-21(c) for each of the panels in the primary system. In this case, no substitute members are added, and therefore the bar forces in the bottom chord of the primary system can be superimposed directly upon the corresponding bar forces in the secondary systems. Thus, no horizontal forces are assumed at the ends of the secondary systems in Fig. 4-21(c) to counteract the bar forces at the bottom chord of the primary system.

Example 4-10. Determine the bar forces in members BC, BF, FK, IF, FJ, IJ, JK, and BI of the truss shown in Fig. 4-21(a) by the superposition of the primary system in Fig. 4-21(b) and the secondary systems in Fig. 4-21(c).

The panel loads in the primary system are obtained from the sum of the panel loads in the original truss and the reactions transmitted from the secondary systems to the corresponding panel points. Thus, $20+(2)(15)=50$.

By passing section 1-1 through the primary system and by considering the portion to the left of the section in Fig. 4-21(b), we have

$$\sum M_k = 0, \quad \left(\frac{5}{\sqrt{26}} F_{bc}\right)(48) + (50)(40) - (140 - 15)(80) = 0$$

$$F_{bc} = \frac{100}{3}\sqrt{26} = 170\,(-)$$

$$\sum M_b = 0, \quad 40F_{ik} - (140 - 15)(40) = 0$$

$$F_{ik} = 125\,(+)$$

$$\sum M_o = 0, \quad (140 - 15)(160) - (50)(200) - \left(\frac{1}{\sqrt{2}} F_{bk}\right)(240) = 0$$

$$F_{bk} = 41.7\sqrt{2} = 58.9\,(+)$$

Also, by considering joint I of the primary system as a free body, we get

$$\sum F_y = 0, \quad F_{bi} = 50\,(+)$$

The bar forces in the secondary system corresponding to the panel IK are obtained by the method of joints as follows:

$$F_{if} = F_{fk} = 15\sqrt{2} = 21.2\,(-), \quad F_{ij} = F_{jk} = 15\,(+), \quad F_{fj} = 20\,(+)$$

By superimposing the bar forces in the primary and secondary systems, we obtain

$$F_{bc} = 170 + 0 = 170\,(-), \qquad F_{if} = 0 + 21.2 = 21.2\,(-)$$
$$F_{bf} = 58.9 + 0 = 58.9\,(+), \qquad F_{fj} = 0 + 20 = 20\,(+)$$
$$F_{fk} = 58.9 - 21.2 = 37.7\,(+), \qquad F_{ij} = 125 + 15 = 140\,(+)$$
$$F_{bi} = 50 + 0 = 50\,(+), \qquad F_{jk} = 125 + 15 = 140\,(+)$$

These results are identical to those obtained by the methods of joints and sections in Example 4-9.

Example 4-11. Determine the bar forces in the compound truss shown in Fig. 4-22(a).

In this case, the compound truss can be considered as the superposition of the simple truss shown in Fig. 4-22(b) plus a secondary truss as shown in Fig. 4-22(c) in each panel of the primary truss. Thus, the bar forces in the primary truss can be computed by the method of sections. By considering the moments about panel points and shear across the panels, we have:

$$M_j = (360 - 40)\,(40) = 12{,}800$$
$$F_{bc} = 12{,}800/48 = 267\,(+)$$
$$M_c = M_k = (360 - 40)\,(80) - (80 + 48)\,(40) = 20{,}480$$
$$F_{jl} = 20{,}480/48 = 427\,(-), \quad F_{cd} = 427\,(+)$$
$$M_d = (360 - 40)\,(120) - (80 + 48)\,(80 + 40) = 23{,}040$$
$$F_{ln} = 23{,}040/48 = 480\,(-)$$
$$S_{ab} = 360 - 40 = 320, \qquad F_{aj} = (320)\,(7.81/6) = 416\,(-)$$
$$S_{bc} = 320 - 80 - 48 = 192, \qquad F_{cj} = (192)\,(7.81/6) = 250\,(+)$$
$$S_{cd} = 192 - 80 - 48 = 64, \qquad F_{dl} = (64)\,(7.81/6) = 83\,(+)$$

The bar forces in other members can be determined by the method of joints, and their results are given in Fig. 4-22(b). The bar forces in the secondary truss can also be found by the method of joints to be as shown in Fig. 4-22(c). The final results of the original truss are obtained by superposition and are shown in Fig. 4-22(d).

This problem can also be solved directly by the method of sections in conjunction with the method of joints without using the principle of superposition, but the solution involves more computations than the procedure given here.

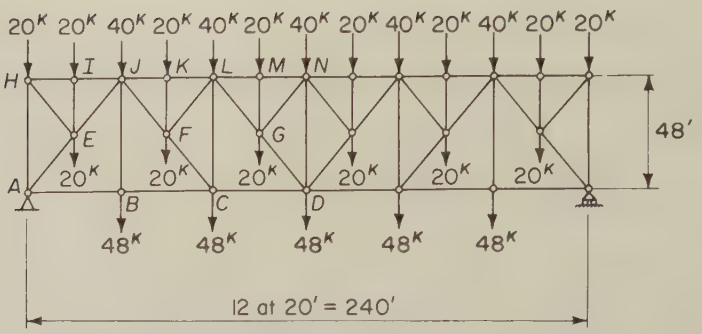

(a)

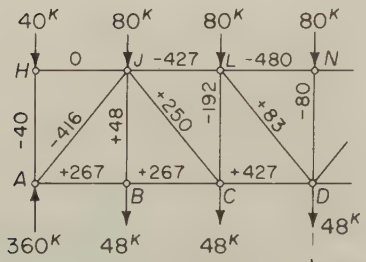

(b)

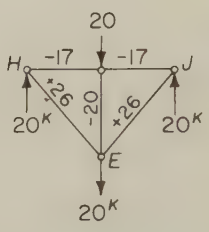

(c)

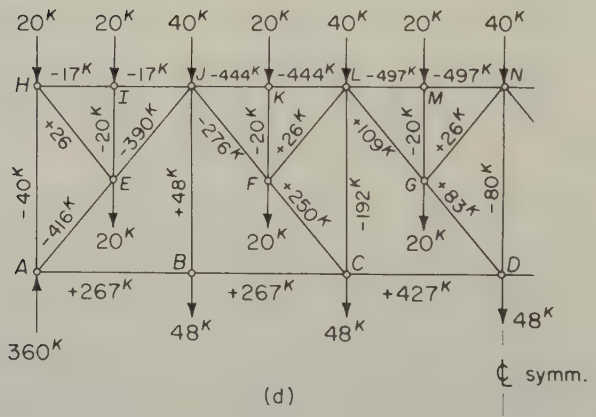

(d)

4-9 *Complex Trusses*

Since a complex truss does not satisfy either the definition of a simple truss or that of a compound truss, the method of joints or the method of sections usually fails to provide a *direct* solution of this type of truss. However,

the method of joints can always be used to establish the relations between bar forces at the joints of a truss. Then, the bar forces can be solved ultimately from a set of simultaneous equations. For a statically determinate complex truss, $m + r = 2j$, or the sum of the number of unknown bar forces and the number of unknown components of reaction must be equal to twice the number of joints in the truss. Since two equations of equilibrium can be written for the forces acting at a joint, the total number of equations available for the entire truss is $2j$. Thus, a total of $m + r$ unknowns in the system can be solved by an equal number of equations. If the unknown components of reaction can be computed first, the extra equations in the set of simultaneous equations can be used as a check.

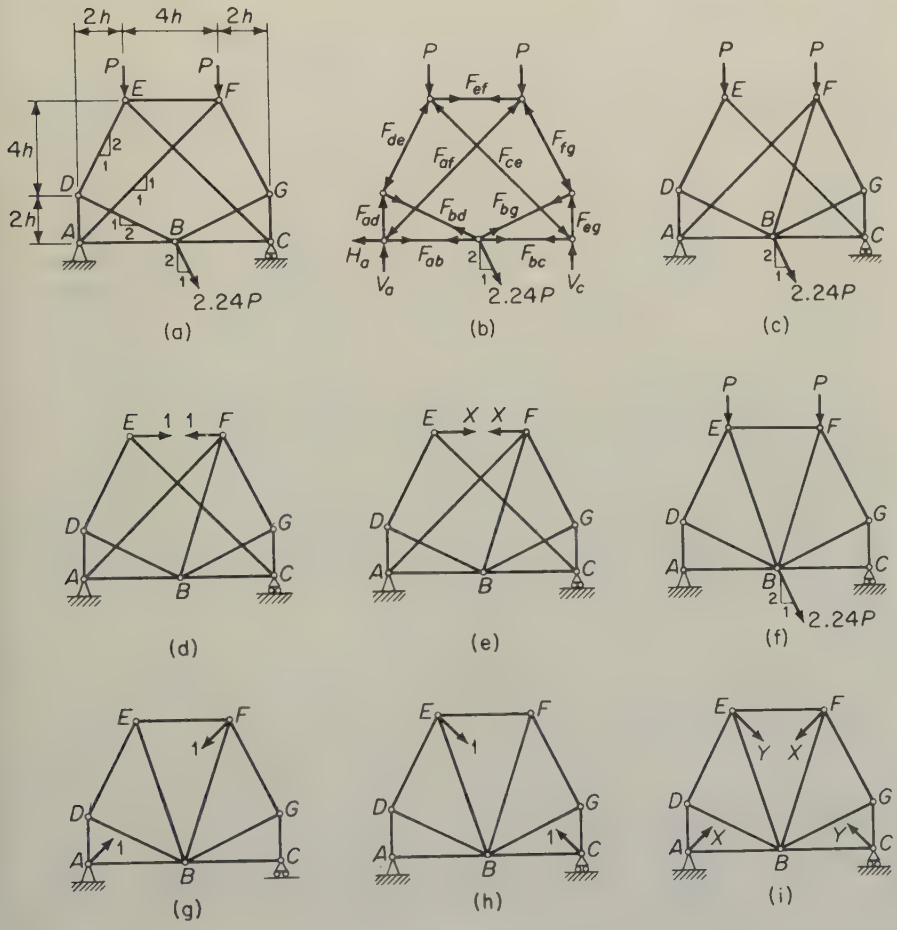

Figure 4–23

Consider, for example, the complex truss shown in Fig. 4-23(a). After the reactions are computed, it is found that there are three or more unknown bar forces at each joint of the truss. Since $m = 11$, $r = 3$, and $2j = 14$ in this case, a total number of 14 equations will be available for the solution of the problem. Referring to the designation of bar forces in Fig. 4-23(b), we can write two equations for joint A as follows:

$$\sum F_x = 0, \quad F_{ab} - 0.707F_{af} - H_a = 0$$

$$\sum F_y = 0, \quad -F_{ad} - 0.707F_{af} + V_a = 0$$

and at joint D,

$$\sum F_x = 0, \quad \frac{2}{2.24}F_{bd} - \frac{1}{2.24}F_{de} = 0$$

$$\sum F_y = 0, \quad F_{ad} - \frac{2}{2.24}F_{de} - \frac{1}{2.24}F_{bd} = 0$$

Similar equations can always be written for other joints; hence, the solution of the problem is assured. From a practical point of view, however, such an approach is undesirable since it involves the solution of a large number of simultaneous equations. We shall, therefore, seek some other alternative methods of solution.*

Before discussing further the methods of solution of complex trusses, however, we should examine the possibility of geometrical instability of such trusses. Since a complex truss in general consists of polygons as well as triangles, it is especially susceptible to geometrical instability because of the orientations of certain members. This type of instability can readily be detected if a set of simultaneous equations is set up from the consideration of equilibrium of all joints. In that case, the determinant formed by the coefficients of the unknown bar forces is the controlling factor. If this determinant is not zero, there will be a unique solution to the problem and hence the structure is statically determinate. If the determinant happens to be zero, there will be infinite sets of answers that may satisfy the simultaneous equations. The student is referred to Example 2-17 in Section 2-10 for the detailed application of such a procedure.

The concept of introducing substitute members for the solution of a truss problem may also be applied to complex trusses. Such a method of solution is known as *Henneberg's method.* By replacing one or more members in a complex truss, it is often possible to reduce such a truss to a simple truss that can be solved directly by the method of joints or the method of sections. Then, a correction may be applied later to remove the effect of the substitute member or members. For the complex truss in Fig. 4-23(a), for example, member EF may be replaced by member, BF, resulting

*See also Reference 4-1 for further discussions.

in a simple truss as shown in Fig. 4-23(c). Let the bar force in any member i of the original truss be denoted by F_i and the bar force in the same member of the resulting system be denoted by F_i'. If the external loads are now removed and two equal and opposite unit forces are applied at joints E and F on the resulting system as shown in Fig. 4-23(d), another set of bar forces f_i may be obtained. If the magnitude of the equal forces at joints E and F is X as shown in Fig. 4-23(e), the bar force in a member i of the resulting system will be $f_i X$. In order to eliminate the effect of the substitute member BF when Fig. 4-23(e) is superimposed on Fig. 4-23(c), it is necessary that

$$F_{bf} = F_{bf}' + f_{bf}X = 0$$

from which

$$X = -\frac{F_{bf}'}{f_{bf}}$$

Then the remaining bar forces may be obtained from the superposition of Figs. 4-23(c) and (e) as follows:

$$F_i = F_i' + f_i X$$

In some cases, it is necessary to introduce more than one substitute member in order to reduce the complex truss to a simple truss. Nevertheless, the same principle may still be applied. As an illustration, the complex truss in Fig. 4-23(a) may be reduced to a simple truss by replacing members CE and AF by members BE and BF. Let the bar forces in members AF and CE in the complex truss be X and Y respectively, and the bar force in a member i be F_i in the original truss. Let f_i' be a set of bar forces caused by a pair of equal and opposite unit forces applied at joints A and F of the resulting system and let f_i'' be another set of bar forces caused by a pair of equal and opposite unit forces applied at joints C and E of the resulting system. Then, in order to eliminate the effects of the substitute members CE and AF when Fig. 4-23(i) is superimposed on Fig. 4-23(f), it is necessary that

$$F_{be} = F_{be}' + f_{be}'X + f_{be}''Y = 0$$

and

$$F_{bf} = F_{bf}' + f_{bf}'X + f_{bf}''Y = 0$$

Solving these two equations simultaneously, we get

$$X = \frac{\begin{vmatrix} -F_{be}' & f_{be}'' \\ -F_{bf}' & f_{bf}'' \end{vmatrix}}{\begin{vmatrix} f_{be}' & f_{be}'' \\ f_{bf}' & f_{bf}'' \end{vmatrix}} \quad \text{and} \quad Y = \frac{\begin{vmatrix} f_{be}' & -F_{be}' \\ f_{bf}' & -F_{bf}' \end{vmatrix}}{\begin{vmatrix} f_{be}' & f_{be}'' \\ f_{bf}' & f_{bf}'' \end{vmatrix}}$$

After the values of X and Y are obtained, the remaining bar forces can be found by superposition. For any member i, the bar force is

$$F_i = F_i' + f_i' X + f_i'' Y$$

Note that the bar force F_i in the above equation has the unit of force in kips, whereas the bar force f_i resulting from a pair of unit loads at the joints of the removed member has a dimensionless unit of kips per kip of load at those joints. Hence, X and Y also have the unit of force in kips.

Example 4-12. Determine the bar forces in all members of the complex truss shown in Fig. 4-23(a), using Henneberg's method.

The procedure for the solution of this problem has been fully explained. If member EF is temporarily removed and a substitute member BF is added as shown in Fig. 4-23(c), the details of calculation can be presented in a tabulated form as shown in Table 4-2.

TABLE 4-2

Member	F_i'	f_i	$f_i X$	F_i
AB	$+2.167P$	$+0.833$	$-4.167P$	$-2.00P$
BC	$+0.333P$	$+0.667$	$-3.333P$	$-3.00P$
AD	$-0.833P$	$+0.833$	$-4.167P$	$-5.00P$
BD	$+0.373P$	-0.373	$+1.865P$	$+2.24P$
CG	$-1.667P$	$+0.667$	$-3.333P$	$-5.00P$
BG	$+0.746P$	-0.298	$+1.495P$	$+2.24P$
DE	$-0.746P$	$+0.746$	$-3.73P$	$-4.48P$
FG	$-1.495P$	$+0.596$	$-2.98P$	$-4.48P$
CE	$-0.471P$	-0.942	$+4.71P$	$+4.24P$
AF	$-1.645P$	-1.178	$+5.89P$	$+4.24P$
EF	0	$+1$	$-5.00P$	$-5.00P$
BF	$+1.580P$	$+0.316$	$-1.58P$	0

The quantity X has been obtained from the relation

$$X = -\frac{F_{fb}'}{f_{fb}} = -\frac{1.580P}{0.316} = -5P$$

Since a simple truss can be obtained by substituting one member in the complex truss for this problem, naturally it is not desirable to make a simple problem complicated by substituting two members in the original truss. For the sake of illustration, however, we shall repeat this same problem by removing members AF and CE and at the same time introducing two substitute members as shown in Fig. 4-23(f). Then, the details of calculation are carried out in Table 4-3.

TABLE 4-3

Member	F'_i	f'_i	f''_i	f'_iX	f''_iY	F_i
AB	$1.00P$	-0.707	0	$-3.0P$	0	$-2.00P$
BC	0	0	-0.707	0	$-3.0P$	$-3.00P$
AD	$-2.00P$	-0.707	0	$-3.0P$	0	$-5.00P$
BD	$+0.896P$	$+0.316$	0	$+1.34P$	0	$+2.24P$
CG	$-2.00P$	0	-0.707	0	$-3.0P$	$-5.00P$
BG	$+0.896P$	0	$+0.316$	0	$+1.34P$	$+2.24P$
DE	$-1.792P$	-0.632	0	$-2.69P$	0	$-4.48P$
FG	$-1.792P$	0	-0.632	0	$-2.69P$	$-4.48P$
EF	$-1.00P$	-0.472	-0.472	$-2.0P$	$-2.0P$	$-5.00P$
CE	0	0	1	0	$+4.24P$	$+4.24P$
AF	0	1	0	$+4.24P$	0	$+4.24P$
BE	$+0.632P$	$+0.598$	-0.742	$+2.53P$	$-3.16P$	0
BF	$+0.632P$	-0.742	$+0.598$	$-3.16P$	$+2.53P$	0

The quantities X and Y are obtained from the solution of the following simultaneous equations:

$$F_{be} = 0.632P + 0.598X - 0.742Y = 0$$

$$F_{bf} = 0.632P - 0.742X + 0.598Y = 0$$

Hence, $X = 4.24P$ and $Y = 4.24P$.

4-10 *Method of Virtual Displacements*

Another approach based on the principle of virtual displacements may be used for the analysis of plane trusses. Although the method usually offers no advantages over the other methods, the concept is generally very useful in the analysis of structures. We shall therefore briefly discuss the basic procedure and some simple applications.

The application of the principle of virtual displacements to the analysis of statically determinate trusses can be illustrated by the simple case shown in Fig. 4-24(a). Imagine that a member of the truss, say member AC for

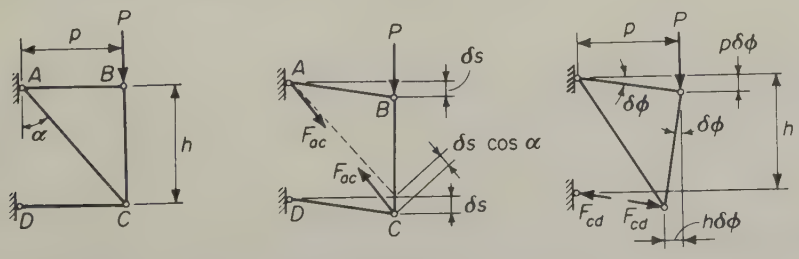

Figure 4-24

instance, is removed from the structure. The resulting system will no longer be rigid and will move as indicated in Fig. 4-24(b). However, if two equal and opposite forces F_{ac} acting in the direction of member AC are added to the resulting system when the member is removed, the forces F_{ac} tend to bring the system back to its original position. Since the displacements need not have actually taken place, they are called *virtual displacements* and are considered as infinitesimal quantities. If the virtual displacement of joint B in the direction of the external force P is denoted by δs, then the virtual displacement of joint C in the direction of the diagonal member AC is $\delta s \cos \alpha$. Since joint A has not undergone any displacement, the force F_{ac} at A produces no work. For a system in equilibrium, the total work done on the system must be zero. In this case,

$$P\,\delta s - F_{ac}\,\delta s \cos \alpha = 0$$

The first term in the equation is positive because the virtual displacement is in the same direction as the force P, whereas the second term is negative because the virtual displacement is opposite to the direction of the bar force F_{ac}. Thus, the bar force in member AC is equal to

$$F_{ac} = \frac{P}{\cos \alpha}$$

If the sense of direction of F_{ac} were assumed in the opposite direction, the term $F_{ac}\,\delta s \cos \alpha$ would be positive and F_{ac} would be negative. This indicates that the assumed direction of F_{ac} is incorrect and should be reversed.

Next imagine member CD in Fig. 4-24(a) to be removed from the structure and its action on the resulting system to be represented by two equal and opposite forces F_{cd} as shown in Fig. 4-24(c). If the infinitesimal rotation of the triangle ABC is denoted by $\delta\varphi$, then the virtual displacement of joint B in the direction of P is $p\,\delta\varphi$, and the virtual displacement of joint C in the direction of force F_{cd} is $h\,\delta\varphi$. Since the system is in equilibrium, the equation representing the total work done on the system is as follows:

$$P(p\,\delta\varphi) - F_{cd}(h\,\delta\varphi) = 0$$

The terms in this equation may also be interpreted as the work done by couples acting through an infinitesimal rotation $\delta\varphi$ about a fixed point. Since the moment of P about joint A of the truss is Pp and the moment of F_{cd} at C about joint A is $F_{cd}h$, we have

$$(Pp)\,\delta\varphi - (F_{cd}h)\,\delta\varphi = 0$$

Finally,

$$F_{cd} = \frac{Pp}{h}$$

It may be observed that the choice of δs or $\delta\varphi$ to establish virtual displacements at various points is a matter of convenience. In order to determine the bar force in any member of a truss, the virtual displacements of the points of application of all forces must be calculated. In general, a truss consists of many joints on which external loads are acting, and the procedure of computing virtual displacements may become quite tedious. Furthermore, the method of virtual displacements requires the study of the kinematics of nonrigid systems.

Example 4-13. Determine the bar forces in members BG and GH of the truss shown in Fig. 4-25(a) by the method of virtual displacements.

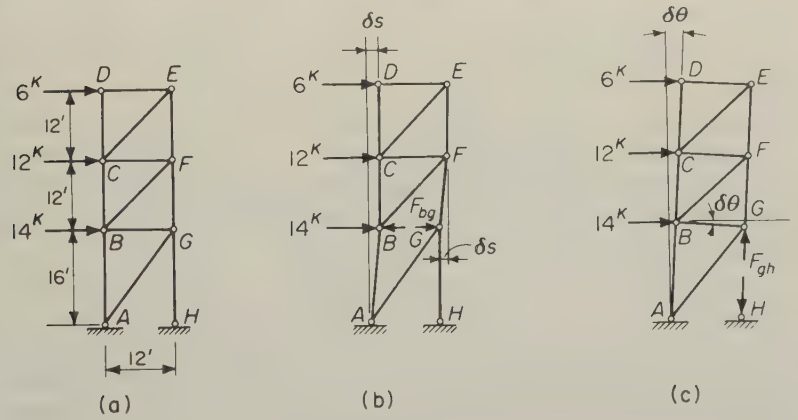

Figure 4-25

If member BG in the truss is removed and replaced by the force F_{bg} as shown in Fig. 4-25(b), the virtual displacements at the points of application of all loads are equal to δs. Thus,

$$(6 + 12 + 14)\,\delta s - F_{bg}\,\delta s = 0 \quad \text{or} \quad F_{bg} = 32$$

On the other hand, the removal of member GH causes virtual displacements of (16) $\delta\varphi$, (28) $\delta\varphi$, and (40) $\delta\varphi$ at joints B, C, and D respectively as shown in Fig. 4-25(c). For the bar force F_{gh}, the virtual displacement is (12) $\delta\varphi$. Hence,

$$(14)(16)\,\delta\varphi + (12)(28)\,\delta\varphi + (6)(40)\,\delta\varphi - F_{gh}(12)\,\delta\varphi = 0$$

or

$$F_{gh} = 66.7$$

Example 4-14. Determine the bar force in member CF of the truss shown in Fig. 4-26(a) by the method of virtual displacements.

If member CF in the truss is replaced by two equal and opposite forces

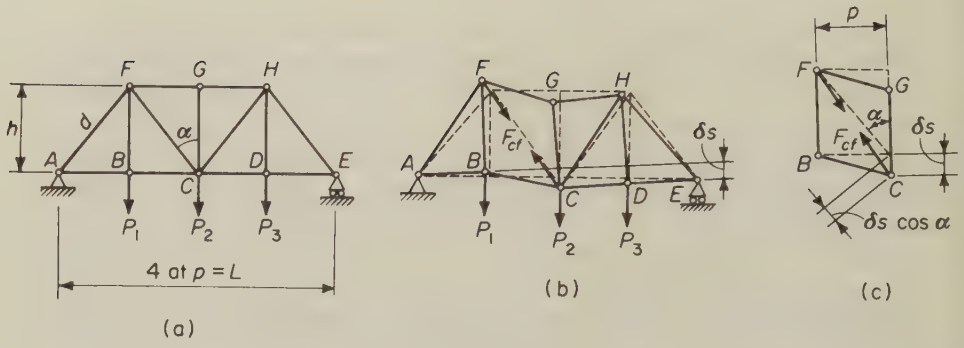

Figure 4–26

F_{cf}, the resulting system tends to take the shape shown in Fig. 4-26(b). Although the actual displacements of joint C and joint F are not readily known, the relative displacement between joints C and F can be obtained from the relative movement of the members in panel $BCGF$ as shown in Fig. 4-26(c). If ds denotes the virtual displacement of joint C in the direction of member CG when joint F is fixed in position, then the virtual displacement between joints C and F is equal to

$$ds \cos \alpha = \left(\frac{h}{d}\right) \delta s$$

The displacements of joints B, C, and D are obtained proportionally from the geometry of the system shown in Fig. 4-26(b). It should be noted, however, that while joints C and D move downward, joint B moves upward.

Thus, by the principle of virtual displacements, we have

$$-P_1\left(\frac{\delta s}{4}\right) + P_2\left(\frac{\delta s}{2}\right) + P_3\left(\frac{\delta s}{4}\right) - F_{cf}\left(\frac{h}{d}\right)(\delta s) = 0$$

As a result,

$$F_{cf} = \left(\frac{d}{4h}\right)(-P_1 + 2P_2 + P_3)$$

4-11 *Simple Trusses in Space*

Although we are primarily concerned with the analysis of plane trusses in this chapter, the same methods may also be applied to statically determinate space trusses. As a matter of fact, we have approached the problems from a general point of view with the intention of extending all applications from plane to space trusses. For example, complex trusses are more often found in space frameworks than in plane structures, but we have treated complex plane trusses in great detail. However, although the

principles for the analysis of space trusses are simple, the solution of a space truss is usually rather tedious because of the three-dimensional geometry of the structure, and the large number of members involved. We shall, therefore, confine our present discussions to simple trusses in space.

The simplest element forming a space truss consists of three bars that do not lie in one plane, as shown in Fig. 4-27, in which the bars are connected by smooth ball-and-socket joints. In general, a ball-and-socket joint

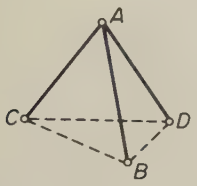

Figure 4–27

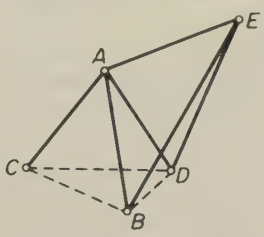

Figure 4–28

provides three components of constraint in three orthogonal directions. Thus, joint A in the figure is completely constrained in space by bars AB, AC, and AD. If joints B, C, and D are the supports in the foundation, the element is a rigid truss in space. An additional joint may be introduced by adding three more bars that do not lie in one plane and by connecting them to either previously established joints or the foundation as shown in Fig. 4-28. A simple truss in space can therefore be formed by connecting the three bars defining the first element to a rigid foundation and establishing each additional joint by three more bars that do not lie in one plane.

A simple truss formed in this manner is statically determinate regardless of the number of components of reaction because it can always be solved by the method of joints, starting from the last joint thus formed and proceeding from joint to joint in the reversed order of that in the process of formation. However, the statical determinacy of space trusses can also be checked by the criterion $m + r - 3j = 0$, as explained in Section 2-6.

Because of the large number of members often involved in a space truss, some members of the truss may be inactive or have zero bar force under a given loading condition. The analysis of a space truss can be simplified by noting these inactive members. Consider, for example, the structure shown in Fig. 4-29, which is known as a *Schwedler dome*. The directions of the horizontal components of reaction are indicated by the angle θ with respect to the corresponding sides at the base of the dome. If a vertical load P is applied at point A, the bars shown dotted in the plan view are found to be inactive. Then, the bar forces in members shown by solid lines in the plan view can be solved by the method of joints.

The method of joints is always applicable in the analysis of simple

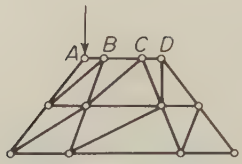

Elevation

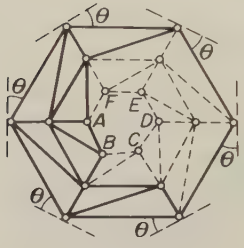

Plan

Figure 4–29

trusses in space. However, the method can be considerably simplified for systematic treatment if the ratios of the bar force to the length of the members are used instead of the bar forces themselves. Such a simplified procedure is called the *method of tension coefficients*.* Since the senses of direction of the bar forces in space trusses in general are not obvious, all bar forces can be assumed to be tension. Then, a positive answer will indicate that the assumed sense is correct and a negative result will mean that the assumed sense is opposite to that of the actual sense. Consider a simple element of a space truss consisting of three bars as shown in Fig. 4-30(a). The location of all joints can be specified by the coordinates in the x, y, and z directions. For each of the bar forces the components of force may be expressed in terms of the components of length of the member. Let $\bar{x}$, $\bar{y}$, and $\bar{z}$ be the components of length L of a member, say AB, as shown in Fig. 4-30(b), and let F_x, F_y, and F_z be the components of force F in the same member as shown in Fig. 4-30(c). Then, the components of force F may be obtained from the similar triangles as follows:

$$F_x = \frac{\bar{x}}{L} F = \frac{F}{L} \bar{x} = t\bar{x}$$

$$F_y = \frac{\bar{y}}{L} F = \frac{F}{L} \bar{y} = t\bar{y}$$

$$F_z = \frac{\bar{z}}{L} F = \frac{F}{L} \bar{z} = t\bar{z}$$

in which $L = \sqrt{\bar{x}^2 + \bar{y}^2 + \bar{z}^2}$ Then,

$$F = \sqrt{F_x^2 + F_y^2 + F_z^2} = tL$$

The ratio $t = F/L$ is called the *tension coefficient* of the member. It can be seen from Fig. 4-30(a) that, for member AB, $\bar{x} = x_b - x_a$, $\bar{y} = y_b - y_a$, and $\bar{z} = z_b - z_a$. Note that, in considering joint A, coordinates of joint A are *subtracted* from the corresponding coordinates of the joint at the far end of the member. Hence, $\bar{x}$, $\bar{y}$, and $\bar{z}$ may be positive or negative. Similar relations may be obtained for members AC and AD. Thus, the components of all bar forces meeting at joint A may be computed.

Let X, Y, and Z be external forces at joint A in the directions of x, y, and z-axes, respectively. Then, from the consideration of equilibrium of joint

*See Reference 4-2 for further discussions.

A, we have

$$\sum F_x = 0, \quad (F_{ab})_x + (F_{ac})_x + (F_{ad})_x + X = 0$$
$$\sum F_y = 0, \quad (F_{ab})_y + (F_{ac})_y + (F_{ad})_y + Y = 0$$
$$\sum F_z = 0, \quad (F_{ab})_z + (F_{ac})_z + (F_{ad})_z + Z = 0$$

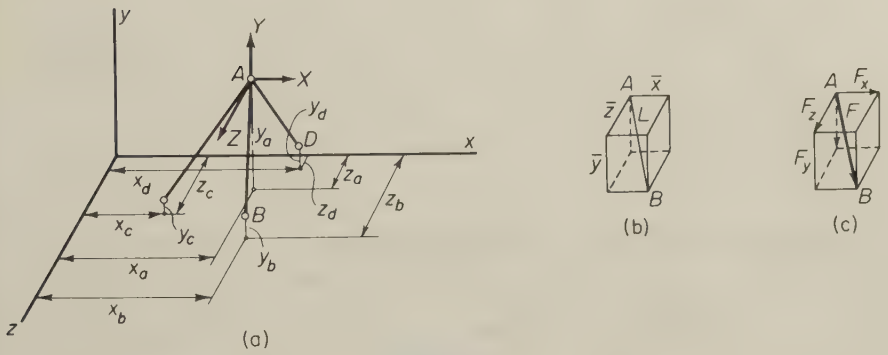

Figure 4–30

Expressed in terms of the tension coefficients, these equations become:

$$t_{ab}\bar{x}_{ab} + t_{ac}\bar{x}_{ac} + t_{ad}\bar{x}_{ad} + X = 0$$
$$t_{ab}\bar{y}_{ab} + t_{ac}\bar{y}_{ac} + t_{ad}\bar{y}_{ad} + Y = 0$$
$$t_{ab}\bar{z}_{ab} + t_{ac}\bar{z}_{ac} + t_{ad}\bar{z}_{ad} + Z = 0$$

Since $\bar{x}$, $\bar{y}$ and $\bar{z}$ for all members can be determined from the geometry of the structure, the tension coefficients can be solved from this set of simultaneous equations. Finally, the bar forces are obtained from the relations $F_{ab} = t_{ab}L_{ab}$, $F_{ac} = t_{ac}L_{ac}$, and $F_{ad} = t_{ad}L_{ad}$.

The same procedure may be used to solve the bar forces at any joint of a simple truss in space as long as the number of unknown bar forces at a joint is not greater than three. Therefore, we shall always start the solution from a joint with not more than three unknowns and proceed successively to other joints. The procedure can be efficiently carried out in a tabulated form.

Example 4-15. Compute the bar forces in all members of the space truss shown in Fig. 4-31.

For the given structure, with the x-, y-, and z-axes directed as shown, the absolute values of the components of length of each member are obtained, and the length of the member itself is computed accordingly as shown in Table 4-4. Then, from the consideration of equilibrium of each joint, we

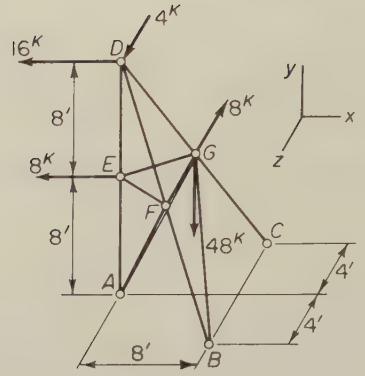

Figure 4–31

can establish three equations of equilibrium. Starting from joint D we have

$$\sum F_x = 0, \quad 4t_{df} + 4t_{dg} - 16 = 0$$
$$\sum F_z = 0, \quad 2t_{df} - 2t_{dg} + 4 = 0$$
$$\sum F_y = 0, \quad -8t_{df} - 8t_{dg} - 8t_{de} = 0$$

from which we obtain $t_{dg} = 3$, $t_{df} = 1$, and $t_{de} = -4$.

TABLE 4-4

Member	$\lvert\bar{x}\rvert$	$\lvert\bar{y}\rvert$	$\lvert\bar{z}\rvert$	L (ft)	$t\ (=F/L)$	F (kips)
DE	0	8	0	8.00	−4.0	−32.0
DF	4	8	2	9.17	1.0	+ 9.2
DG	4	8	2	9.17	3.0	+27.5
EA	0	8	0	8.00	−4.0	−32.0
EF	4	0	2	4.48	1.0	+ 4.5
EG	4	0	2	4.48	1.0	+ 4.5
FA	4	8	2	9.17	−0.5	− 4.6
FB	4	8	2	9.17	1.5	+13.7
FG	0	0	4	4.00	0	0
GA	4	8	2	9.17	−3.5	−32.1
GB	4	8	6	10.77	1.0	+10.8
GC	4	8	2	9.17	−0.5	− 4.6

With the known value of t_{de}, we may proceed to solve the unknowns in the members meeting at joint E. Thus,

$$\sum F_x = 0, \quad 4t_{ef} + 4t_{eg} - 8 = 0$$
$$\sum F_z = 0, \quad 2t_{ef} - 2t_{eg} = 0$$
$$\sum F_y = 0, \quad -8t_{ea} + 8t_{de} = 0$$

from which we obtain $t_{ef} = 1$, $t_{eg} = 1$, and $t_{ea} = -4$.

Similarly, from joint F we can establish

$$\sum F_x = 0, \quad -4t_{df} - 4t_{ef} - 4t_{fa} + 4t_{fb} = 0$$
$$\sum F_z = 0, \quad -2t_{df} - 2t_{ef} - 4t_{fg} - 2t_{fa} + 2t_{fb} = 0$$
$$\sum F_y = 0, \quad 8t_{df} - 8t_{fa} - 8t_{fb} = 0$$

Since t_{ef} and t_{df} are known, we get $t_{fa} = -0.5$, $t_{fb} = 1.5$, and $t_{fg} = 0$.

Finally, we obtain from joint G the following equations:

$$\sum F_x = 0, \quad -4t_{dg} - 4t_{eg} - 4t_{ga} + 4t_{gb} + 4t_{gc} = 0$$
$$\sum F_z = 0, \quad 2t_{dg} + 2t_{eg} + 4t_{fg} + 2t_{ga} + 6t_{gb} - 2t_{gc} - 8 = 0$$
$$\sum F_y = 0, \quad 8t_{dg} - 8t_{ga} - 8t_{gb} - 8t_{gc} - 48 = 0$$

With known values of t_{dg}, t_{eg}, and t_{fg}, the unknowns are obtained as follows: $t_{ga} = -3.5$, $t_{gb} = 1.0$, and $t_{gc} = -0.5$.

4-12 *Summary*

In this chapter we have discussed various methods of solution of plane trusses. Although each method has its own merit, we need not use only one method in a problem. It has been repeatedly demonstrated that these methods can be used to the greatest advantage when suitable combinations are made in the analysis. Although the same principles may be applied to space trusses, the solution is usually complicated by the geometry of space structures. Hence, we have confined our discussions to simple trusses in space only.

References

4-1 S. Timoshenko and D. H. Young, *Theory of Structures*, McGraw-Hill Book Co., Inc., New York, 1945.

4-2 R. V. Southwell, "Primary Stress-Determination in Space Frames," *Engineering*, vol. 109, 1920, p. 165.

4-3 M. Merriman and H. S. Jacoby, *Roofs and Bridges*, 6th ed., vol. 1, John Wiley & Sons, Inc., New York, 1928.

4-4 G. A. Hool and W. S. Kinne, eds., *Movable and Long Span Bridges*, McGraw-Hill Book Co., Inc., New York, 1923.

4-5 J. A. L. Waddell, *Economics of Bridgework*, John Wiley & Sons, Inc., New York, 1921.

4-6 D. B. Steinman, *The Wichert Truss*, D. Van Nostrand Co., Inc., Princeton, N.J., 1932.

Problems

4-1 to **4-4** Compute the bar forces in all members of the trusses shown in Figs. P4-1 to P4-4 by the method of joints.

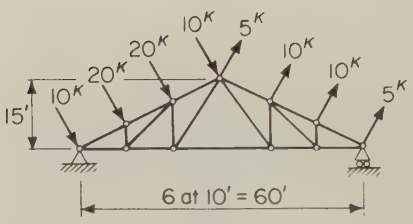

Figure P4–1

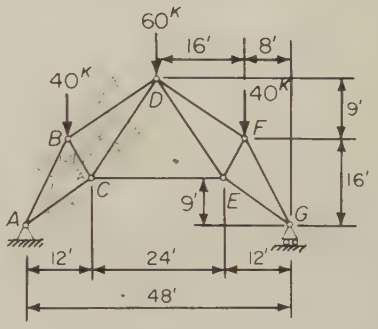

Figure P4–2

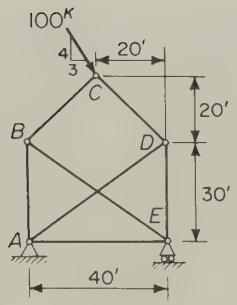

Figure P4–3

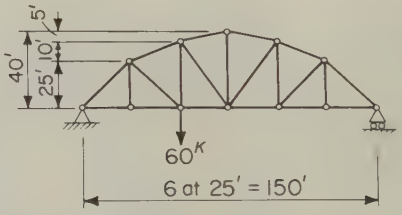

Figure P4–4

4-5 to **4-14** Calculate the bar forces in members marked by letters *a*, *b*, and *c* of the trusses shown in Figs. P4-5 to P4-14 by the method of sections.

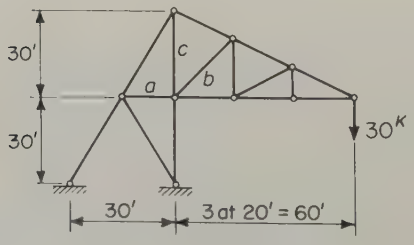

Figure P4–5

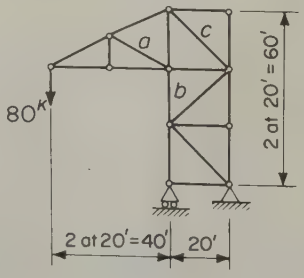

Figure P4–6

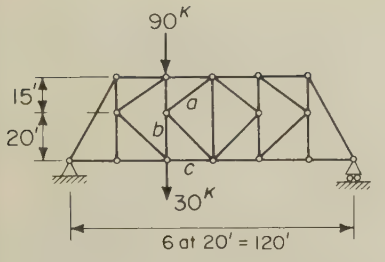

Figure P4–7

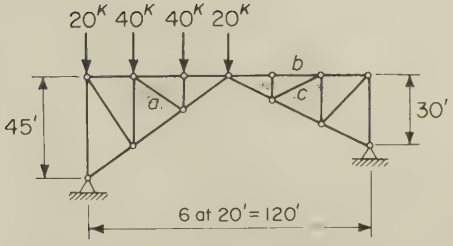

Figure P4–8

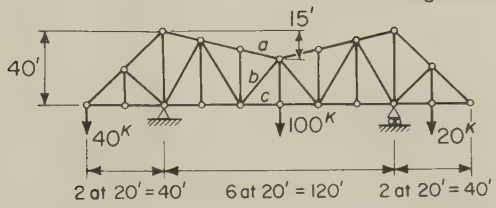

Figure P4–9

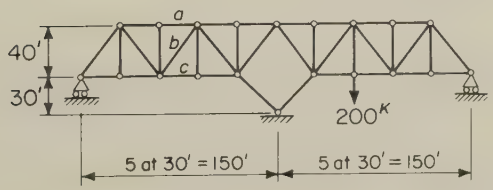

Figure P4–10

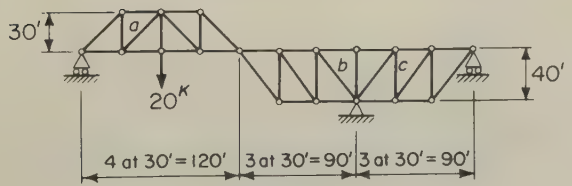

Figure P4–11

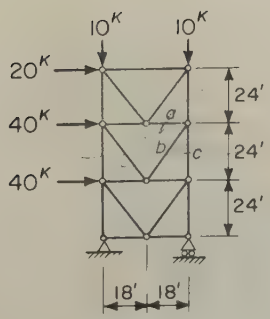

Figure P4–12

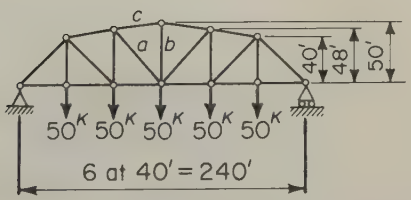

Figure P4–13

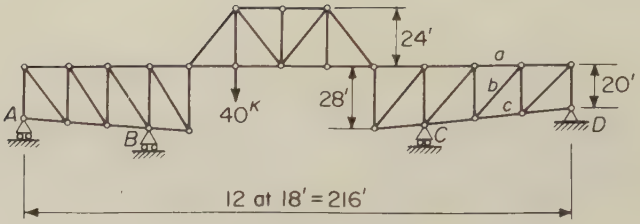

Figure P4–14

4-15 and **4-16** Solve the bar forces in all members of the trusses shown in Figs. P4-15 and P4-16 by the method of shears and moments.

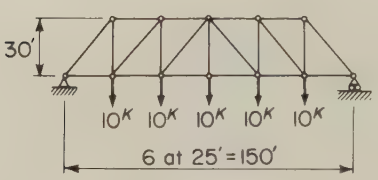

Figure P4–15

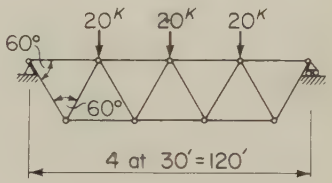

Figure P4–16

4-17 and **4-18** Compute the bar forces in members marked by letters *a*, *b*, and *c* of the stiffening trusses of the suspension bridges shown in Figs. P4-17 and P4-18.

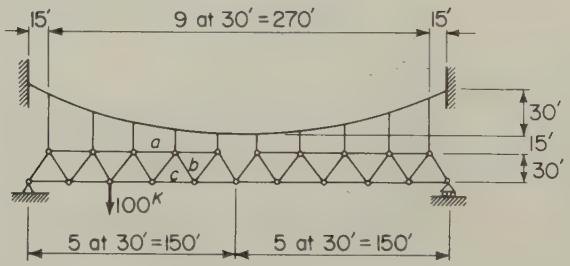

Figure P4–17

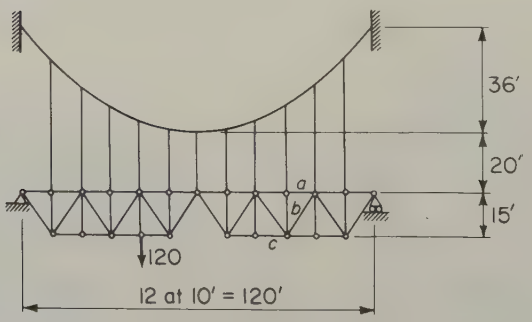

Figure P4–18

4-19 to **4-22** Calculate the bar forces in all members of the compound trusses shown in Figs. P4-19 to P4-22.

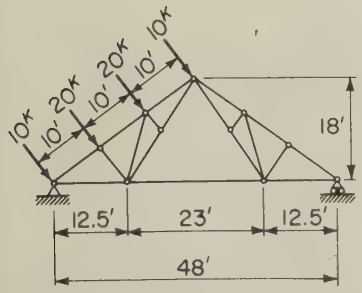

Figure P4–19

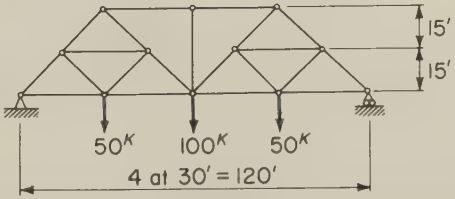

Figure P4–20

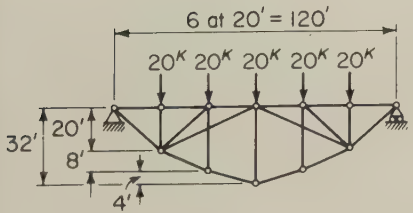

Figure P4–21

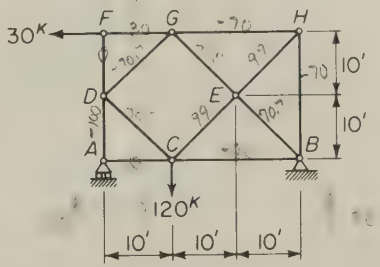

Figure P4–22

4-23 to **4-30** Calculate the bar forces in members marked by letters *a*, *b*, and *c* of the compound trusses shown in Figs. P4-23 to P4-30.

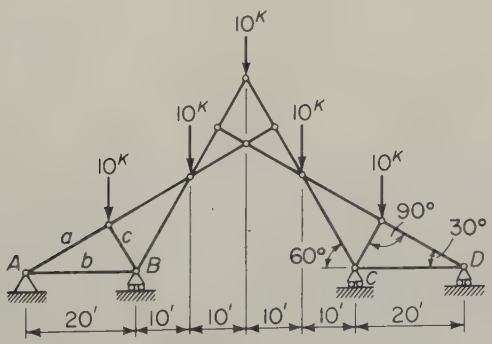

Figure P4–23

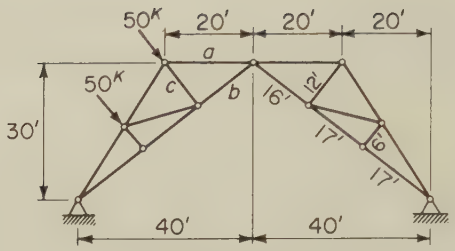

Figure P4–24

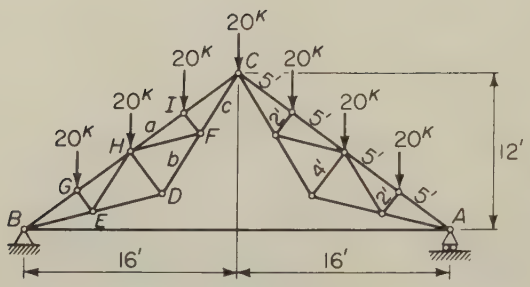

Figure P4–25

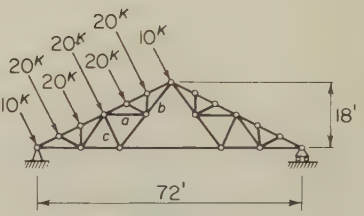

Figure P4–26

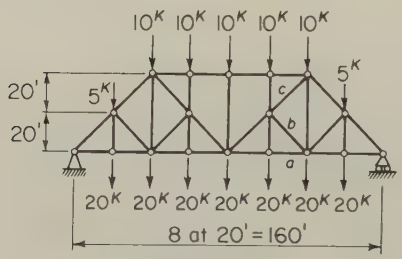

Figure P4–27

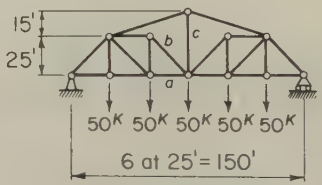

Figure P4–28

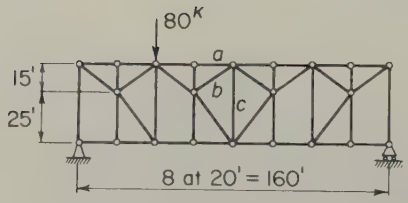

Figure P4–29

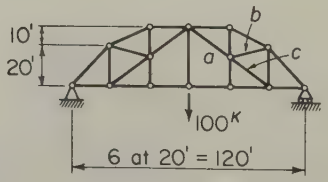

Figure P4–30

4-31 and **4-32** Calculate the bar forces in all members of the complex trusses shown in Figs. P4-31 and P4-32.

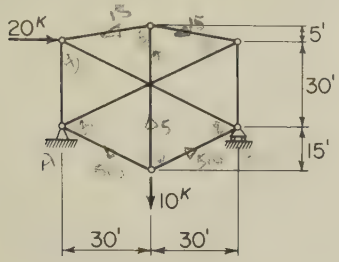

Figure P4–31

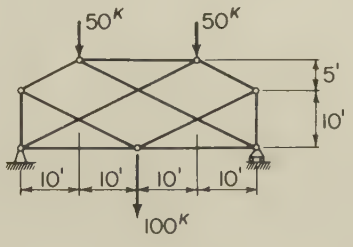

Figure P4–32

4-33 and **4-34** Using the method of virtual displacements, calculate the bar forces in members marked by the letters *a*, *b*, and *c* of the trusses shown in Figs. P4-33 and P4-34.

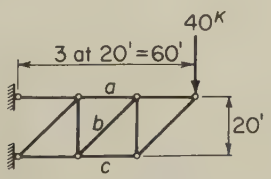

Figure P4–33

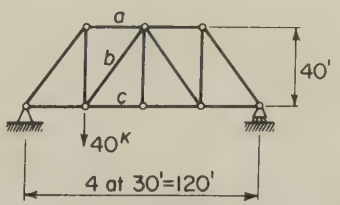

Figure P4–34

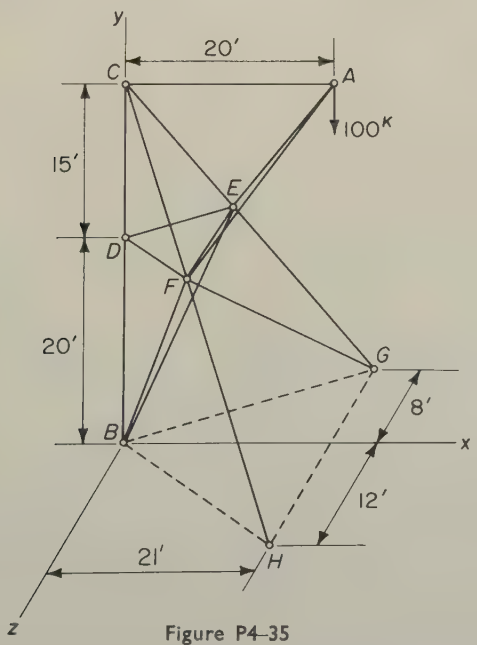

Figure P4–35

4-35 and **4-36** Calculate the bar forces in all members of the space trusses shown in Figs. P4-35 (see page 247) and P4-36.

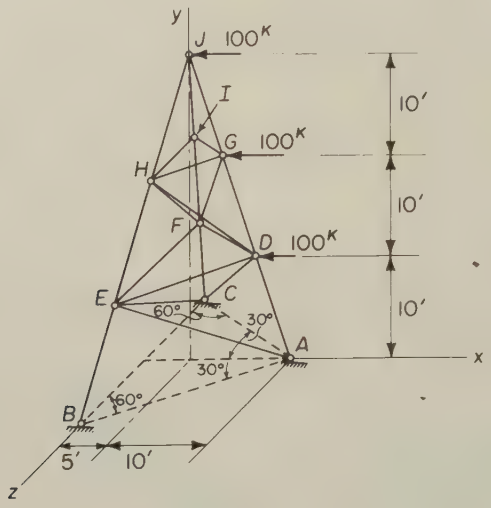

Figure P4–36

5 GRAPHIC STATICS

5-1 Basic Concept

In the analysis of simple structural systems, it is sometimes advantageous to obtain the solution of a problem by means of graphical construction. Since forces and displacements are vector quantities that are characterized by a magnitude, a vector direction, and a point of application, both the conditions of equilibrium of a structure and the geometry of its deflected shape can be represented graphically. However, a graphical solution is more than merely a convenient procedure for solving complex problems; it may lead to a basic understanding of the action of a structure under applied loads even if it is carried out in sketch form without great precision. For this reason, graphical analysis still has a place in the age of high-speed electronic computers.

The graphical representation of a vector quantity is a line segment having a given magnitude and a given direction, the sense of which in indicated by an arrowhead. A vector that has no fixed position in space is called a *free vector*; a vector that has a unique point of application is called a *fixed* or *bounded vector*. In a coplanar system, all vectors can be represented graphically in the same plane. For a noncoplanar system, the projections of the vectors can be treated graphically. In this chapter we shall confine our discussion to graphic statics of coplanar systems, which includes the graphical solution of forces and moments and the graphical procedure for obtaining the virtual displacements that are needed in the computation of forces and moments by the principle of virtual displacements.

Since the addition and subtraction of vectors are governed by the parallelogram law, a system of forces can be combined into a resultant, or each of the forces can be resolved into components in accordance with this fundamental law. The resultant of a concurrent force system is a single force, but the resultant of a nonconcurrent force system may be either a force or a couple. A force may be resolved into components along any two directions defining a plane on which the force lies. In analytical solutions, however, a force can be more conveniently resolved into components that lie in two mutually perpendicular lines such as the horizontal and vertical directions of a Cartesian coordinate system. On the other hand, the graphical composition and resolution of forces along any given directions can be carried out easily by the construction of parallelograms, triangles, or polygons whose sides represent the corresponding forces or their components.

Consider first the coplanar concurrent force systems. If two forces P_1 and P_2 which are plotted in scale and represented by the vectors OA and OB as shown in Fig. 5-1(a), are combined by the parallelogram law, the diagonal OC of the parallelogram formed by the given forces represents the

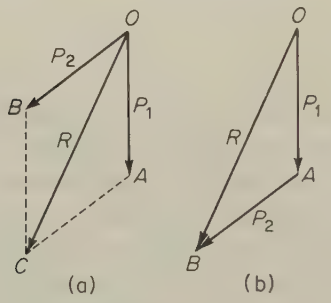

Figure 5–1

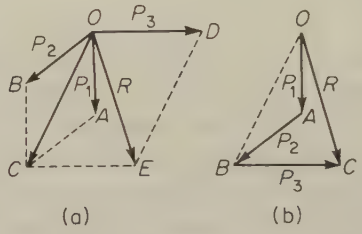

Figure 5–2

resultant R. The magnitude of the resultant is expressed in the same scale as the given forces, its vector direction is indicated by the arrowhead, and its line of action passes through the intersection O of the given forces P_1 and P_2. The same resultant may also be represented by the closing side OB of the triangle formed by the given forces, as shown in Fig. 5-1(b). Figures 5-1(a) and (b) are known as the *parallelogram* and the *triangle of forces*, respectively. If there are several forces meeting at one point such as P_1, P_2, and P_3 shown in Fig. 5-2(a), the resultant R of these forces can be obtained by successive applications of the parallelogram of forces as shown in the figure. The same resultant can also be represented by the closing side of the *polygon of forces* in Fig. 5-2(b), which has been constructed by successive applications of the triangle of forces. The line of action of this resultant must pass through the intersection of the given forces.

The construction of the polygon of forces is simpler than the graphical

representation of the parallelograms of forces and is generally preferred in determining the resultant of several forces graphically. If the force polygon constructed from the given forces forms a *closed* polygon, the resultant is then zero and the concurrent force system is said to be in equilibrium.

For nonconcurrent force systems, the same fundamental law for composition and resolution of forces may be applied. Although the forces do not meet at one point, the free vectors representing these forces can still be used in the construction of the polygon of forces. In addition, the line of application of the resultant must be located with the aid of the force polygon. Consider, for example, a system of nonconcurrent forces P_1, P_2, P_3, and P_4 as shown in Fig. 5-3(a). The force polygon is constructed in

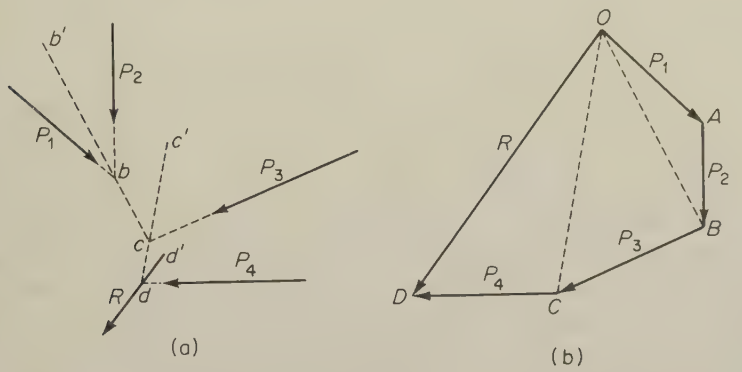

Figure 5–3

Fig. 5-3(b), in which the resultant R is represented by the vector OD. In order to locate the line of action of the resultant, we shall first connect points B and C to point O in the force polygon with dotted lines OB and OC as shown in Fig. 5-3(b). The vector OB represents the resultant of forces P_1 and P_2 while the vector OC represents the resultant of forces P_1, P_2, and P_3. If the vectors representing the forces P_1 and P_2 in Fig. 5-3(a) are extended until they meet at point b, and a line bb', is drawn to be parallel to vector OB in Fig. 5-3(b), line bb' represents the line of action of vector OB, which is the resultant of P_1 and P_2. Next, extend the vector representing force P_3 in Fig. 5-3(a) until it meets the extension of line bb' at c, and draw a line cc' parallel to vector OC in Fig. 5-3(b). Then, line cc' indicates the line of action of vector OC, which is the resultant of P_1, P_2, and P_3. In a similar manner, we can construct line dd' in Fig. 5-3(a), which is the line of action of vector OD representing the resultant R in Fig. 5-3(b).

If the force polygon constructed from the given nonconcurrent forces forms a *closed* polygon, the resultant *force* vanishes. However, it does not rule out the possibility that a resultant *couple* may exist. In order to check

this possibility, we can divide the given forces *arbitrarily* into two groups and find the resultant of each group. If the two resultants thus obtained are equal and opposite but not collinear, the resultant of the force system is a couple that has a magnitude equal to the product of one of the resultants and the perpendicular distance between them. For example, a system of four nonconcurrent forces P_1, P_2, P_3, and P_4 is shown in Fig. 5-4(a). Since the force polygon in Fig. 5-4(b) is closed, there can be no resultant force. Therefore,

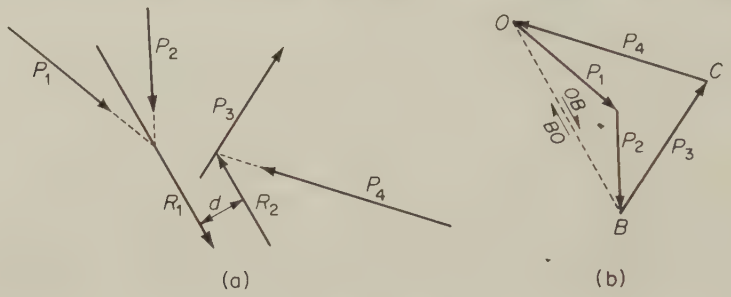

Figure 5–4

we divide the forces into two groups, one consisting of P_1 and P_2 and the other consisting of P_3 and P_4. The corresponding resultants are R_1 and R_2 which must be equal and opposite to each other since R_1 and R_2 are represented by vectors OB and BO respectively in the force polygon. It is found, however, that these two resultants are not collinear and the distance d between them can be measured. Hence the resultant couple is $M = R_1 d = R_2 d$. It should be noted that the grouping of the forces is arbitrary. If P_1, P_2, and P_3 are grouped together into one resultant and P_4 is considered as the other resultant, the same couple M will result although R_1 and d individually may differ from the corresponding values in the previous grouping. In the case of nonconcurrent force systems in which R_1 and R_2 are equal, opposite, and *collinear*, the system is in a state of equilibrium.

5-2 *General Graphical Procedure*

Although the graphical construction described in the previous section is applicable to nonconcurrent, nonparallel force systems, it is not practical to determine the line of action of the resultant by such a method if the given forces are nearly parallel and will not intersect within a reasonably large area. Furthermore, the method cannot be applied to determine the line of application of the resultant of a parallel force system. Therefore, we shall develop a general graphical procedure that has some practical advantages and is applicable to all coplanar force systems.

Consider the coplanar nonconcurrent force system as shown in Fig.

5-5(a), which is referred to as the *space diagram*. The corresponding force polygon is constructed in Fig. 5-5(b). We shall choose an arbitrary point O in Fig. 5-5(b) and join it with the apexes of the force polygon by dotted lines a, b, c, d, and e. The point O is called the *pole*, and the dotted lines are known as the *rays*. If arrowheads are placed next to the rays as shown, they may be regarded as vectors representing the components of the given forces. For example, the force P_1 may be resolved into components represented by vectors AO and OB, the force P_2 into components represented by vectors BO and OC, and so on. We shall now transfer these components

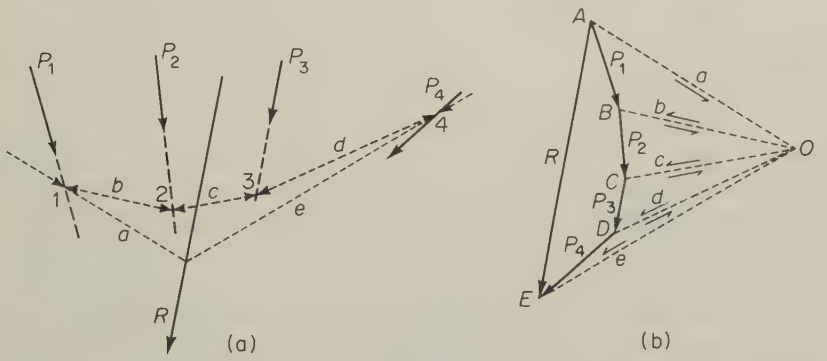

Figure 5–5

back to the space diagram in Fig. 5-5(a). By selecting a convenient point 1 on the line of action of force P_1 in the figure, we draw two lines a and b passing through point 1 and at the same time parallel, respectively, to rays a and b in Fig. 5-5(b). The lines a and b in Fig. 5-5(a) are called *strings* and represent respectively the directions of the component vectors AO and OB of the force P_1. The string b intersects the force P_2 at point 2, through which string c is drawn to be parallel to ray c in Fig. 5-5(b). The same procedure is followed so that strings d and e can be drawn in Fig. 5-5(a). The polygon formed by the strings a, b, c, d, and e is called the *string* polygon, or *funicular* polygon. It may be concluded that if P_1, P_2, P_3, and P_4 are resolved into components as shown in Fig. 5-5(b), all components except AO and OE will eliminate each other. The combination of the remaining two components AO and OE leads to the same resultant R represented by the vector AE. The line of action of this resultant must pass through the intersection of strings a and e in Fig. 5-5(a). In other words, the system of forces P_1, P_2, P_3, and P_4 may be considered as being replaced by two forces having the same magnitude and direction as vectors AO and OE in the force polygon and acting along strings a and e of the string polygon.

If the force polygon constructed from a system of given forces is closed, i.e., the ending point coincides with the starting point, the resultant force

is zero and the last ray coincides with the first ray. Consider, for example, the force system in Fig. 5-6(a), for which the force polygon is constructed in Fig. 5-6(b). Since points E and A coincide, the ray a as represented by

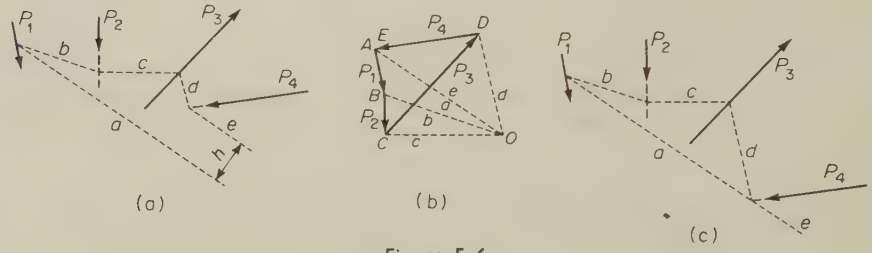

Figure 5–6

vector AO and the ray e as represented by vector OE also coincide. Hence, in the string polygon of Fig. 5-6(a), the strings a and e are parallel and at a perpendicular distance h apart. The resultant, therefore, is a couple, having a magnitude equal to the product of the vector AO and the distance h. On the other hand, the force system in Fig. 5-6(c) may also lead to the same force polygon shown in Fig. 5-6(b), but the resulting string polygon in Fig. 5-6(c) indicates that strings a and e are collinear. In this case, not only does the resultant force vanish but the resultant couple is also equal to zero. The force system is therefore in equilibrium.

The graphical procedure just discussed is perfectly general and is applicable to all coplanar force systems. The results of the graphical construction are in general represented by the force polygon together with the string polygon. If the force polygon resulting from the system of forces is not closed, the closing side represents the resultant force whose line of action must pass through the intersection of the first and the last strings of the string polygon. If the force polygon is closed but the first and the last strings of the string polygon are parallel, the resultant of the force system is a couple whose magnitude is equal to the product of the vector representing the first or last ray in the force polygon and the distance between the first and the last strings in the string polygon. If the first and last strings of the string polygon coincide, the string polygon becomes closed. In that case, both the resultant force and the resultant couple vanish and the force system is in equilibrium.

5-3 *Applications of Graphical Method*

The graphical method can be applied directly to the determination of reactions, forces, and moments in a structural system. The number of unknown quantities that can be determined graphically is identical to that

which can be solved for analytically. In general, three equations of equilibrium can be established for a coplanar nonconcurrent force system, and hence three unknowns can be determined by the graphical solution. In the case of a coplanar concurrent force system for which two equations of equilibrium can be written, only two unknowns can be determined by the graphical construction. In order to make use of the graphical method efficiently, a string polygon is sometimes drawn through certain specified points. In determining reactions of beams, frames, and trusses, for example, it is generally necessary to pass a string polygon through a point of reaction. In constructing moment diagrams for beams, it may be desirable to construct a string polygon through the two supporting points of the beam. In obtaining the reactions, forces, and moments in a three-hinged arch, it will be most convenient to pass a string polygon through all three hinges. We shall, therefore, discuss the method of construction of a string polygon passing through one, two, or three given points in connection with these problems.

5-4 *Reactions*

The procedure for the graphical determination of reactions of a structure under a single applied load can usually be simplified by observing the basic conditions of equilibrium of systems of two or three forces. If the two forces are in equilibrium, they must be equal and opposite and collinear; if three forces are in equilibrium, they must be concurrent. Thus, the reactions of a structure subjected to a single applied load can readily be determined by the triangle of forces. The same simplification may result for several given external forces if the magnitude and the line of action of the resultant of the external forces can be obtained by inspection. For distributed loads, the graphical method for finding reactions is simple and accurate only if the magnitude and the line of action of the resultant can readily be determined. Otherwise, the distributed load must be approximated by a set of concentrated loads. For a structure subjected to a large number of concentrated loads, the solution for the reactions can best be obtained by means of the general procedure involving the string polygon as well as the force polygon. In this case, it is necessary to construct a string polygon through a point of reaction. In general, for a given force system and a specified point, we can arbitrarily select a pole for the force polygon and draw the rays to the apexes of the force polygon. Then, the string polygon can be constructed by first drawing the string that is required to pass through the specified point and be parallel to the corresponding ray and then by completing the other strings accordingly. For the given forces P_1, P_2, and P_3 in Fig. 5-7(a), for example, it is required that the string polygon pass through point A. The force polygon, together with the rays drawn from

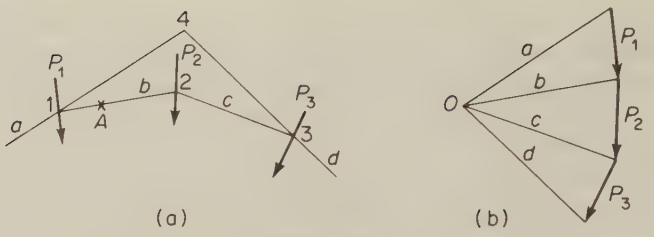

Figure 5–7

an arbitrarily chosen pole O, is shown in Fig. 5-7(b). Since the specified point A in Fig. 5-7(a) lies between the lines of action of forces P_1 and P_2, the string that passes through it must be parallel to ray b, which connects the pole to the apex between P_1 and P_2 in the force polygon. This string b intersects P_1 and P_2 at points 1 and 2, respectively, and strings a and c can be drawn to pass through points 1 and 2, respectively. Finally, string d can be constructed to pass through point 3, which is the intersection of string c and the force P_3.

Example 5-1. Determine graphically the reactions at A and B of the beam shown in Fig. 5-8(a).

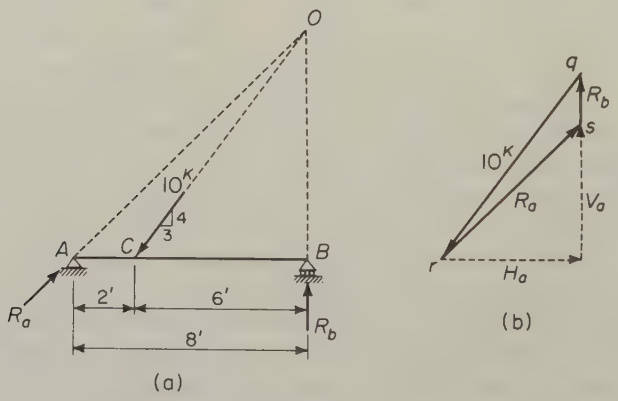

Figure 5–8

Since support B is a roller, the line of application of reaction R_b is known to be vertical. This reaction intersects the applied force of 10 kips at point O. Since there are only three forces in the system, which is in equilibrium, the reaction R_a must pass through point O also. Thus, the line of application of reaction R_a is indicated by AO in the figure. The force triangle for the system is constructed in Fig. 5-8(b) by first plotting the vector qr in a convenient scale and parallel to line OC in Fig. 5-8(a) and then by closing the triangle by drawing lines rs and sq parallel respectively to line OA and OB

in Fig. 5-8(a). Thus, reactions R_a and R_b are represented respectively by vectors *rs* and *sq*, the magnitudes of which can be measured by the same scale as that of vector *qr*. It is possible to resolve R_a into horizontal and vertical components H_a and V_a by projecting the vector *rs* on horizontal and vertical lines respectively, as indicated by the dotted lines in Fig. 5-8(b). By direct measurements with a proper scale, we obtain $R_a = 8.5$ kips, $R_b = 2$ kips, $V_a = 6$ kips, and $H_a = 6$ kips.

Example 5-2. Determine graphically the reactions at supports *A* and *C* of the frame shown in Fig. 5-9(a).

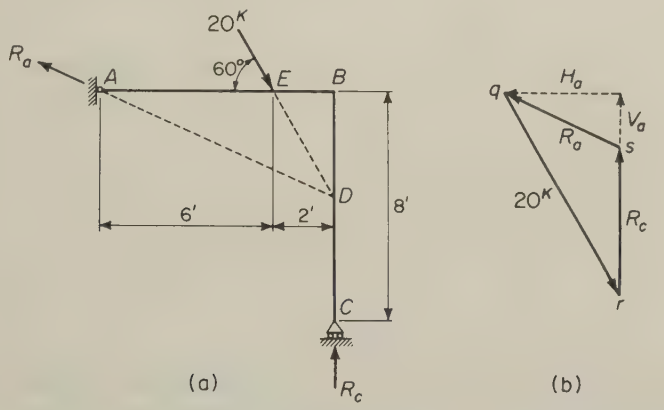

Figure 5–9

From the given conditions of the supports, the direction of the reaction R_c is known to be vertical and intersects the applied force at point *D* in Fig. 5-9(a). The line of action of the reaction R_a is then determined by the fact that it must pass through points *A* and *D*. Hence, the force triangle can be constructed as shown in Fig. 5-9(b) in a manner similar to that explained in the previous example.

Example 5-3. Determine graphically the reactions at supports *A* and *D* of the frame shown in Fig. 5-10(a).

For this problem the applied forces can first be combined as indicated by the dotted vector *qs* in the force polygon in Fig. 5-10(b). The line of action of this resultant can be located in Fig. 5-10(a) by drawing a line through the intersection of the applied forces and parallel to vector *qs* in the force polygon. Then, this resultant and the reactions R_a and R_d are the only three forces left in the system, which is in equilibrium. We can, therefore, proceed to obtain R_a and R_d graphically as in the previous example.

The problem can also be solved by means of the string or funicular polygon as shown in Figs. 5-10(c) and (d). First, construct a part of the force

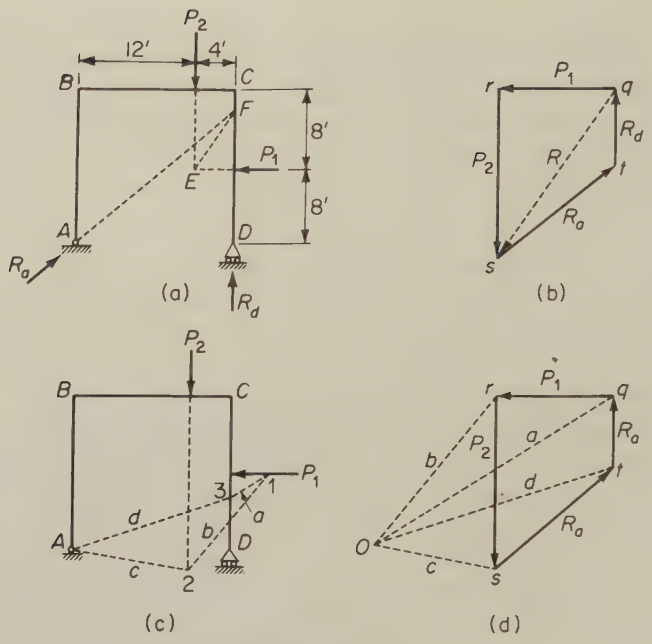

Figure 5–10

polygon with two known forces P_1 and P_2 and connect the rays between the apexes q, r, and s of the polygon and the arbitrarily chosen pole O, as shown in Fig. 5-10(d). Then, starting from point A in Fig. 5-10(c), draw string c parallel to ray c in the force polygon. From the intersection of string c and the line of action of force P_2, which is designated as point 2 in Fig. 5-10(c), construct string b parallel to ray b in the force polygon. Similarly, from the intersection of string b and the line of action of force P_1, which is designated as point 1 in Fig. 5-10(c), construct string a parallel to ray a in the force polygon. The intersection of string a and the line of action of R_d is denoted as point 3. The closing string d is represented by the line connecting points A and 3. Thus, we can construct ray d passing through the pole in the force polygon and parallel to string d of the string polygon. If a vertical line is drawn through point q intersecting ray d at point t in the force polygon, the vectors st and tq represent the reactions R_a and R_d respectively.

The physical meaning of the graphical construction can be explained in greater detail. Since the line of action of reaction R_d is known to be vertical but the line of action of reaction R_a remains to be determined, we begin the graphical construction of the string polygon from point A, which is the only known point on the line of application of the reaction R_a. As string c passes through point A, it may be considered as representing

one of the two components of reaction R_a, the other component being represented by string d which is yet to be determined. The fact that reaction R_a can be resolved into components in the directions of strings c and d is clearly shown by the relation between vector st and rays c and d in the force polygon. Similarly, force P_2 may be resolved into components in the directions of strings b and c, while force P_1 is resolved into components in the directions of strings a and b. Finally, reaction R_d may be considered as being resolved into components in the directions of strings a and d. From the force polygon, it can be seen that all components of forces will cancel each other. The net result is that the system is in equilibrium.

Example 5-4. Determine graphically the reactions at supports A and C of the three-hinged arch shown in Fig. 5-11(a).

Since no external force is applied on the part of the arch rib from C to B,

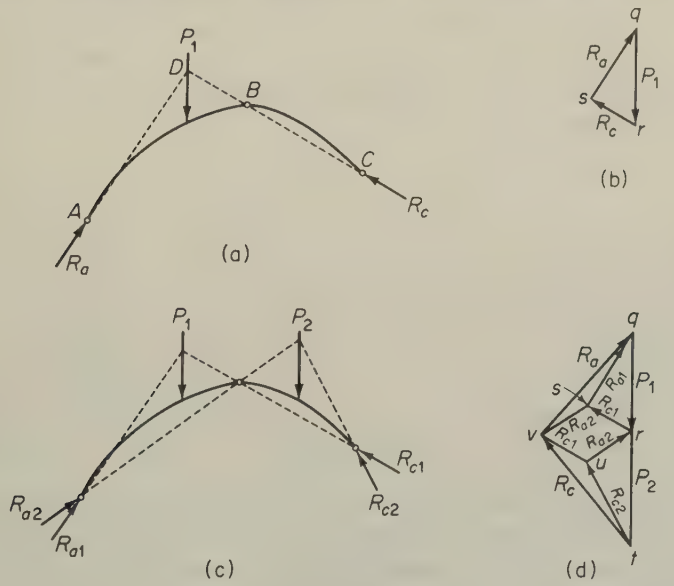

Figure 5–11

the rib CB, when isolated as a free body, is a two-force member in which the reaction acting at hinge C must be equal, opposite, and collinear to the force acting at hinge B. In other words, the line of action of the reaction R_c must pass through hinges C and B. If this line of action is extended until it intersects the applied force at point D, the line of action of the reaction R_c may be determined by the line joining points A and D. With the applied force plotted in a convenient scale, the reactions can be measured from the force polygon shown in Fig. 5-10(b).

If there is another force acting on rib BC as well as a force on rib AB of the arch, as shown in Fig. 5-11(c), we can first obtain the reactions resulting from each of the loads individually as if the other load were not acting. Hence, two force triangles qrs and rtu are obtained as indicated in Fig. 5-11(d), in which R_{a1} and R_{c1} are reactions at hinges A and C respectively due to P_1 alone and R_{a2} and R_{c2} are the corresponding reactions at A and C due to load P_2 alone. The resultant of the reactions at each support can be determined graphically by constructing lines vs parallel to ur and vu parallel to sr. Since $vsru$ is a parallelogram, the opposite sides are equal to each other. It is obvious, therefore, that vectors vq and tv represent the reactions R_a and R_c respectively.

In the case of several loads acting on each side of the center hinge of a three-hinged arch, we can first obtain graphically the resultant for the loads on each side and then proceed as before. However, a direct method of solution can be developed by introducing certain modifications to the general procedure. Such modifications will be discussed in Section 5-6.

Example 5-5. Determine graphically the reactions at supports A and B of the beam shown in Fig. 5-12(a).

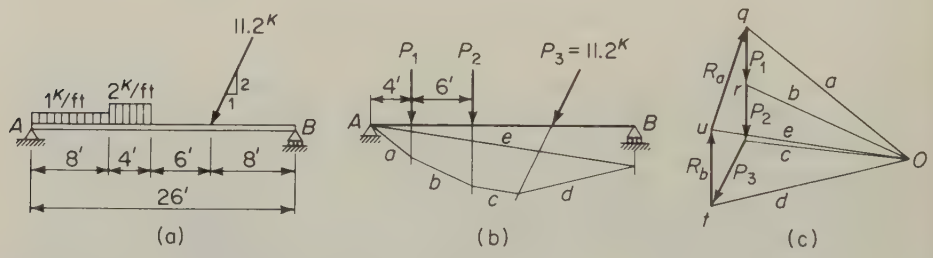

Figure 5–12

For this problem, the centers of gravity of the distributed loads can be located by inspection, and the uniformly distributed loads can therefore be replaced by equivalent concentrated loads. An equivalent force system is shown in Fig. 5-12(b), with $P_1 = (1)(8) = 8$ kips and $P_2 = (2)(4) = 8$ kips, and the lines of action of these loads are indicated in the figure. We can now construct part of the force polygon with the known forces P_1, P_2, and P_3 and connect the apexes q, r, s, and t to an arbitrarily chosen pole O with rays a, b, c, and d as shown in Fig. 5-12(b). Starting with point A in Fig. 5-12(b), we construct the string polygon with strings a, b, c, and d parallel respectively to rays a, b, c, and d in the force polygon. The closing side of the string polygon is constructed by joining point A and the point of intersection of string d and the line of action of reaction R_b. Finally, the ray e, which is parallel to string e in the string polygon, may be drawn

passing through point O in the force polygon. The intersection of this line and a vertical line passing through point t is denoted by u. Then, the vectors tu and uq represent the reactions R_b and R_a respectively.

The student should be able to follow the logic behind the method of construction since the detailed explanation of a similar solution has been given for Example 5-3.

Example 5-6. Determine graphically the reactions at supports A and B of the roof truss shown in Fig. 5-13(a).

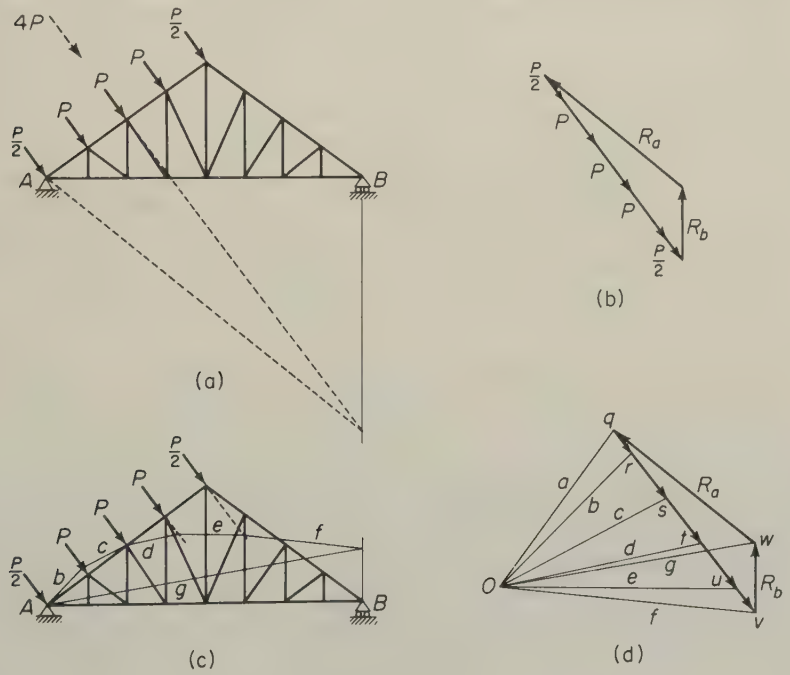

Figure 5–13

The magnitude, direction, and line of application of the resultant of the external loads on the truss can be determined by inspection. Hence, the line of action of the reaction R_a can be determined easily in Fig. 5-13(a), and the magnitudes of the reactions are obtained from the force polygon in Fig. 5-13(b).

For the sake of illustration, however, the same problem has been solved graphically by means of the general procedure. It is sufficient to point out that the string polygon and the force polygon are given in Figs. 5-13(c) and (d) respectively without further explanation.

5-5 *Moments in Beams*

The moment of a force may be obtained graphically from the product of two measured quantities, i.e., the force in force scale and the moment arm in length scale. If there are several forces in a system, the resultant of these forces may first be determined graphically and the distance from the resultant to the moment center may be measured afterwards. However, a general procedure may be developed to simplify the construction as well as the multiplication of the force and the moment arm. Consider, for instance, the system of forces shown in Fig. 5-14(a). We wish to determine graphically

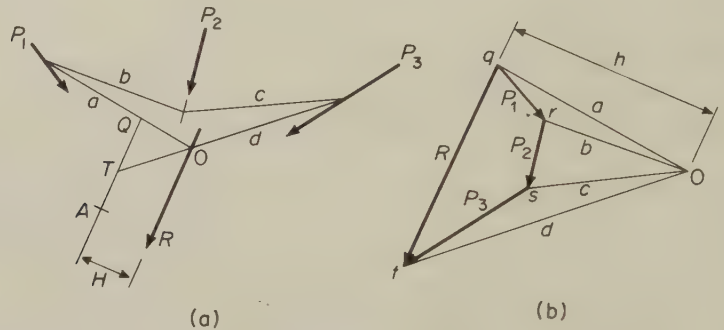

Figure 5–14

the moment of these forces about a given point A. Since the magnitude of the resultant R of the given forces can be obtained from the force polygon in Fig. 5-14(b), and the rays can be connected to the apexes of the polygon from an arbitrarily chosen pole o, the string polygon can be constructed and the point of application of the resultant R located at point O as shown in Fig. 5-14(a). If we construct a line passing through the given point A and parallel to the line of action of the resultant R, it will intersect strings a and d or their extensions at points Q and T respectively. Thus, triangles QOT and qot are similar since the sides of one are parallel to the respective sides of the other. Let H be the perpendicular distance from point O to side QT of triangle QOT, and h be the perpendicular distance from pole o to side qt of triangle qot. Then, from the relation of similar triangles, we note that

$$\frac{H}{QT} = \frac{h}{qt} \quad \text{or} \quad (qt)(H) = (QT)(h)$$

Since the moment of the resultant about point A is $(qt)(H)$, i.e., the product of the resultant R as represented by the vector qt in the force polygon and

the distance H in the diagram of the string polygon, we conclude that the moment about point A is numerically equal to

$$M_A = (QT)(h)$$

in which h is measured from the force polygon in the force scale and QT is measured from the diagram of the string polygon in the length scale. If a convenient scale is chosen for h, the moment can be readily obtained by simple calculation.

The principle of determining the moment of a force system graphically can be applied to obtain bending moments in beams. Since the shear at a section of a beam equals the vertical component of the resultant of the forces applied either to the left or to the right of the section, it can easily be found from the force polygon. The bending moment at a section is equal to the moment of the resultant of the forces applied either to the left or to the right of the section. Hence, it may be obtained by the procedure just described. If the applied loads on the beam consist of distributed loads, the length of the beam must be divided into small segments so that the distributed loads can be approximated by concentrated loads. In such a case, the simplicity of the graphical method will be lost but the concept is still useful in the construction of pressure lines, which will be discussed in Section 5-7.

In some cases, we may wish to construct a string polygon passing through both supports of a beam in order to obtain a horizontal base line for the moment diagram. We shall therefore consider the construction of a string polygon passing through two specified points that lie on the lines of action of two of the forces. As an example, a force system in equilibrium is shown in Fig. 5-15(a), for which the force polygon is constructed in Fig. 5-15(b). If a pole is chosen arbitrarily for the force polygon, we can construct a string polygon passing through one of the specified points, such as point A in Fig. 5-15(a) but not the second point B. However, if we restrict the

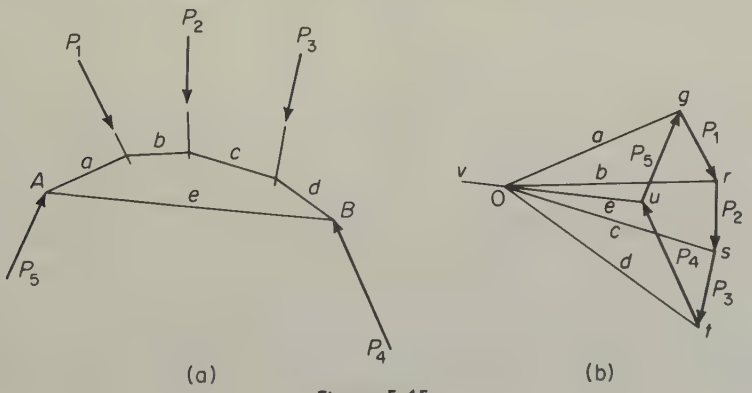

Figure 5-15

selection of the pole for the force polygon to a point on line uv in Fig. 5-15(b), which is parallel to line AB in Fig. 5-15(a), the resulting string polygon will pass through point B as well as point A. This is true because the intersection of strings d and e must lie on the line of action of P_4 regardless of how the pole for the force polygon is selected. If a point O on line uv in the force polygon is chosen, ray e is represented by the line segment Ou, which is parallel to string e in the string polygon. Hence, the intersection of strings d and e in the string polygon must fall on point B. In other words, line AB in the string polygon represents string e, which satisfies the requirements of being parallel to ray e in the force polygon and passing through the specified points A and B. It should be noted that although the selection of the pole for the force polygon has been confined to a line, it is still possible to construct an infinite number of different string polygons, each corresponding to one position of the pole on the specified line.

Example 5-7. Determine graphically the reactions for the cantilever beam shown in Fig. 5-16(a).

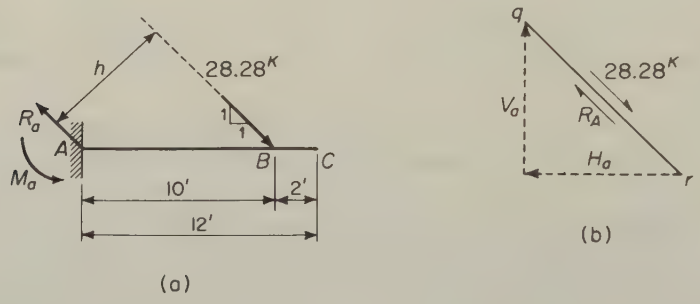

Figure 5–16

The applied force on the beam will be resisted by a force or reaction R_a and a moment M_a at the fixed support A. Since there are only two forces in the system, the force triangle is reduced to two opposite vectors coinciding with each other as shown in Fig. 5-16(b) so that the resultant force vanishes. The reaction R_a, therefore, has a magnitude equal to the applied force and its line of action can be located in Fig. 5-16(a) by drawing a line passing through point A and at the same time parallel to the applied force. The reaction R_a and the applied force form a couple that is equal in magnitude to the product of either force and the distance h between them. This couple, acting in the clockwise direction, is resisted by the moment M_a at support A. In general, the reaction R_a can be measured from the force triangle, and the distance h can be measured from Fig. 5-16(a) using the same scale by which the length of the beam has been laid out. Thus, the moment M_a can be obtained by taking the product of these two quantities.

It is again possible to obtain the horizontal and vertical components of R_a by its horizontal and vertical projections, respectively, as shown by the dotted lines in Fig. 5-16(b). From direct measurements from Fig. 5-16, we obtain $H_a = 20$ kips, $V_a = 20$ kips, $R_a = 28.28$ kips, and $h = 7.07$ ft. Hence $M_a = (28.28)(7.07) = 200$ ft-kips.

Example 5-8. Determine graphically the moments at points B, C, and D of the beam shown in Fig. 5-17(a).

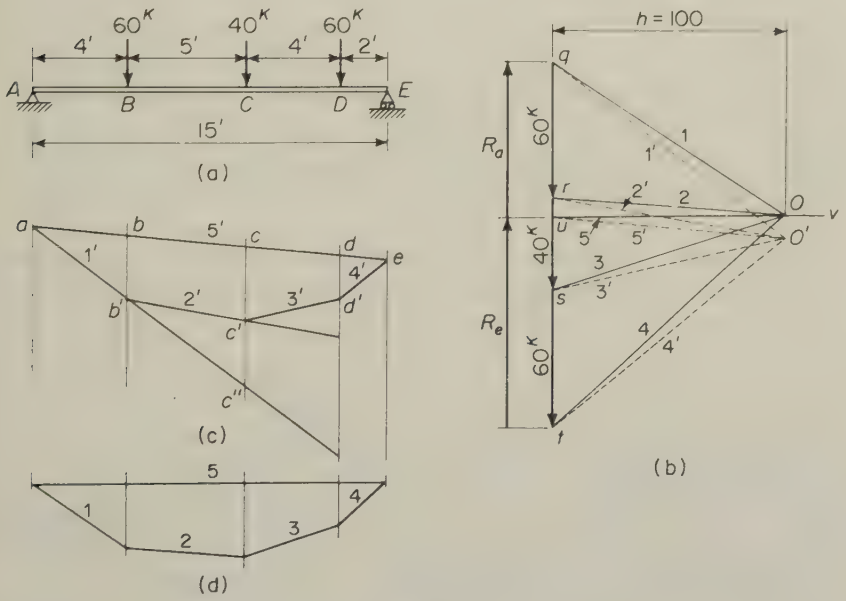

Figure 5–17

For the loading on the beam shown in Fig. 5-17(a), the force polygon is constructed in Fig. 5-17(b) by choosing a pole o' with the distance $h = 100$ kips. Then, rays 1′, 2′, 3′, 4′, and 5′ can be constructed in the force polygon in connection with the string polygon in Fig. 5-17(c). The resulting reactions are $R_a = 68$ kips and $R_e = 92$ kips, as indicated in Fig. 5-17(b). At point B of the beam, the only force to the left of the section is the reaction R_a. Thus, the moment due to R_a is equal to the product of the pole distance h and the intercept bb' since triangles abb' and $qo'u$ are similar. At point C of the beam, a downward load of 60 kips as well as the upward reaction R_a are acting to the left of the section. The moment at point C due to reaction R_a equals the product of h and the intercept cc'', whereas that due to the downward load of 60 kips is h times $c''c'$. Since the upward reaction and the downward load cause moments in opposite directions, the resulting moment at

point C is equal to the difference of the two, or the product of h and cc' in this case. The same reasoning may be used to obtain the moment at point D, which is equal to the product of h and dd' by considering either the free body to the left or to the right of the section. By direct measurements with the length scale, we get $bb' = 2.72$ ft, $cc' = 3.12$ ft, and $dd' = 1.84$ ft. Hence, the moments at points B, C, and D are respectively 272 ft-kips, 312 ft-kips, and 184 ft-kips.

If we wish to construct a string polygon passing through both points A and E of the beam, we can draw a line uv passing through point u in the force polygon and parallel to line AE of the beam after point u is located. Then, select any point on the line uv as the new pole and construct a new string polygon that will pass through points A and E. However, if the same h is maintained, i.e., if the intersection o of line uv and the vertical line representing $h = 100$ kips is chosen as the new pole, the scale remains unchanged. The resulting string polygon will be as shown in Fig. 5-17(d), which is the moment diagram of the beam plotted on a horizontal base line.

Example 5-9. Determine graphically the reactions at the supports and the moments under the applied loads of the compound beam shown in Fig. 5-18(a).

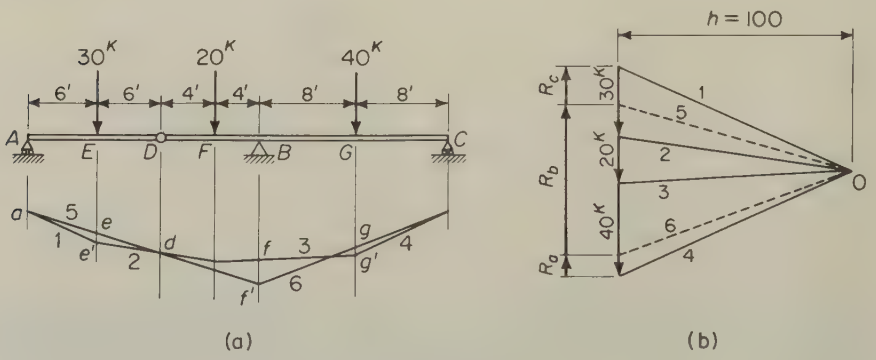

Figure 5–18

In the case of a compound beam, the fact that the string polygon is the moment diagram makes it possible to determine reactions as well as moments. Starting with the given load, a force polygon is constructed with $h = 100$ kips as shown in Fig. 5-18(b). After rays 1, 2, 3, and 4 are constructed for the force polygon and the corresponding strings for the string polygon, we cannot proceed further. However, since hinge D in the beam cannot resist moment, string 5 in the string polygon must pass through point d. Thus, point f' can be located in the string polygon by prolonging line ad, and finally string 6 can also be constructed.

The reactions can be obtained from the force polygon after completing rays 5 and 6. The moments at points E, F, and G of the beam are given by the ordinates ee', ff', and gg', respectively, in the string polygon multiplied by the factor h.

5-6 Three-hinged Arches

When a large number of applied loads appears on a three-hinged arch, it is easier to determine the reactions of the arch by the construction of a string polygon passing through the three hinges. Such a string polygon also has important applications in the graphical determination of forces and moments in the arch. Hence, we shall first develop a general procedure for constructing a string polygon passing through three given points.

Consider, for example, a force system in equilibrium as shown in Fig. 5-19(a). Let it be required to construct a string polygon through three given

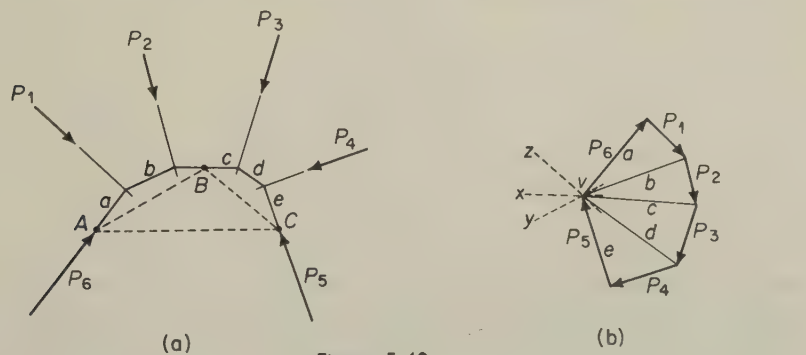

Figure 5–19

points A, B, and C. Since the system is in equilibrium, the force polygon is closed as shown in Fig. 5-19(b). By making use of the principle of construction of a string polygon through two given points, we conclude that the pole must be selected on line vx in the force polygon, which is parallel to line AC if the string polygon is to pass through points A and C. Similarly, the pole should also lie on line vy, which is parallel to line AB and on line vz, which is parallel to line BC. Hence, the point v in the force polygon is the only point that satisfies the requirement of lying on three intersecting lines and that can be located by any two of these three lines. As a result, there is only one string polygon that will pass through three specified points. Furthermore, no string polygon can be constructed to pass through more than three specified points. Once the pole of the force polygon is located, the string polygon may be constructed in a straightforward manner.

In the graphical determination of the reactions of a three-hinged arch, however, the direction and the magnitude of each reaction are not known;

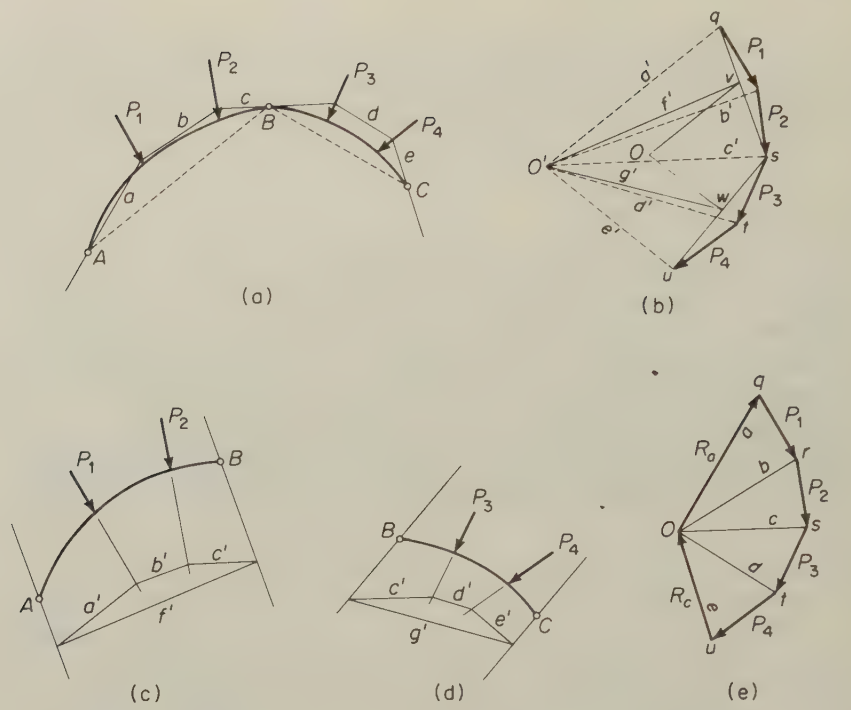

Figure 5–20

hence, the location of the pole must be determined first. Consider, for instance, the three-hinged arch shown in Fig. 5-20(a), from which a part of the force polygon may be drawn from the given forces as indicated in Fig. 5-20(b). Note that the vector qs represents the resultant of forces P_1 and P_2, and the vector su represents the resultant of forces P_3 and P_4. If we isolate the ribs AB and BC as shown in Figs. 5-20(c) and (d), and consider temporarily the two portions as completely separate units in equilibrium, the directions of the reactions at hinges A and B in Fig. 5-20(c) will be parallel to vector qs in the force polygon, and the directions of the reactions at hinges B and C in Fig. 5-20(d) will be parallel to vector su in the force polygon. We shall now select a pole O' arbitrarily, connect the rays a', b', c', d', and e' by the dotted lines shown in Fig. 5-20(b), and construct separate string polygons for the separate units as shown in Figs. 5-20(c) and (d). The closing strings f' and g' in Figs. 5-20(c) and (d) provide, respectively, the directions of rays f' and g', which can now be drawn through the arbitrarily chosen pole O'. The intersection of ray f' and vector qs is denoted by v and the intersection of ray g' and vector su is denoted by w. Thus, vectors vq and sv represent the reactions at A and B of Fig. 5-20(c), while vectors ws and uw represent the reactions at B and C in Fig. 5-20(d) respectively. If the string polygon in Fig. 5-20(c) is to pass through points

A and B, the pole for the force polygon must lie on a line passing through point v and parallel to line AB. Similarly, in order to pass the string polygon through points B and C, the pole for the force polygon must lie on a line passing through point w and parallel to line BC. Thus, the intersection O of these two lines defines the location of the pole of the force polygon from which a string polygon may be constructed through points A, B, and C. We can now draw a new set of rays in the force polygon, from which the true string polygon is constructed.

In order to avoid too many lines in one figure, the construction of the true string polygon is shown separately in Fig. 5-20(e), and the final string polygon is shown in Fig. 5-20(a). Actually, the steps of construction in Figs. 5-20(c) and (d) can also be carried out in Fig. 5-20(a), and the construction in Fig. 5-20(e) can be made in Fig. 5-20(b). It should be noted that vectors Oq and uO represent the reactions at hinges A and C respectively, while the vector Os or sO represents the reaction at hinge B, whose sense of direction depends on whether rib AB or rib BC of the arch is taken as a free body.

Let us now consider the significance of the string polygon passing through the hinges of a three-hinged arch. We have already pointed out that the reactions of such an arch can be obtained by the graphical construction of the force and string polygons. It may also be noted, however, that the forces and moments acting on various points of the arch may also be determined graphically from these polygons. Consider, for example, the string polygon drawn for the three-hinged arch in Fig. 5-20(a), which is reproduced in Fig. 5-21(a). The first and last strings in the figure represent

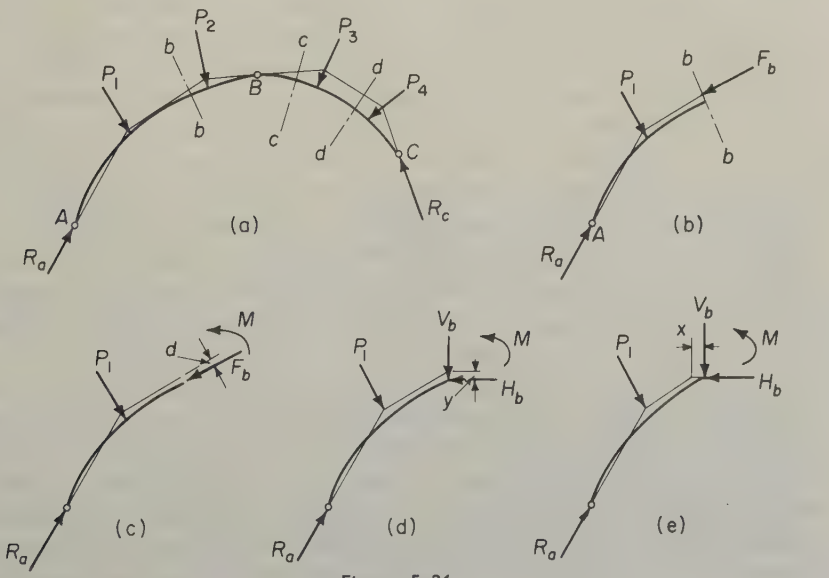

Figure 5–21

the lines of action of reactions R_a and R_c respectively. If a section b-b is passed through a point on the arch axis, the free body representing the part of the arch to the left of the section is held in equilibrium by the force F_b, as shown in Fig. 5-21(b), because the resultant R_a and P_1 is equal and opposite to F_b, as indicated by ray b in the force polygon in Fig. 5-20(e). In general, the force F_b is neither passing through the point on the arch axis nor parallel to the tangent to the arch axis at that point. However, this force may be replaced by a force of equal magnitude and same direction acting on the point of the arch axis plus a couple $M = F_b d$, as shown in Fig. 5-21(c), in which d is the perpendicular distance from the point on the arch to the line of action of F_b. Since F_b is equal to ray b in the force polygon in Fig. 5-20(e), its components in axial and tangential directions can be determined graphically once the direction of the tangent to the arch axis at that point is known. The force F_b can also be resolved into horizontal and vertical components H_b and V_b. Then, the moment M at the section can be given either by $H_b y$, where y is the *vertical* ordinate between the point of intersection of the arch axis and the string polygon as shown in Fig. 5-21(d), or by $V_b x$, where x is the *horizontal* distance between the point of intersection of the arch axis and the string polygon, as shown in Fig. 5-21(e). If a section c-c is passed through a point between P_2 and P_3, or a section d-d is passed through a point between P_3 and P_4 in Fig. 5-21(a), the same conclusion may be obtained since any string cut by a section represents the resultant of all forces acting on the free body to the left or to the right of the section, as evidenced by the rays in the force polygon in Fig. 5-20(e).

For the particular case of a three-hinged arch subjected to vertical loads only, it is obvious that the components of the horizontal reactions at the supports must be equal and opposite. At any section, therefore, the horizontal component of the force represented by a string in the string polygon is also equal to the horizontal component H of the reactions. Then, the moment at any point on the arch rib is equal to the ordinate y at that point between the arch axis and the string polygon multiplied by a constant factor H. This is true regardless of the shape of the arch axis. Thus, the string polygon passing through the three hinges of the arch is a moment curve, and the area bounded between the arch axis and the string polygon represents to some scale the moment diagram for the three-hinged arch.

Example 5-10. Determine graphically the reactions and the moment diagram for the three-hinged arch shown in Fig. 5-22(a).

We can construct the force polygon by selecting arbitrarily a pole O', as shown in Fig. 5-22(b). Then, the string polygon for each part of the arch separated by hinge B can be drawn in Figs. 5-22(c) and (d). The closing strings f' and g' in these figures provide respectively the directions of rays

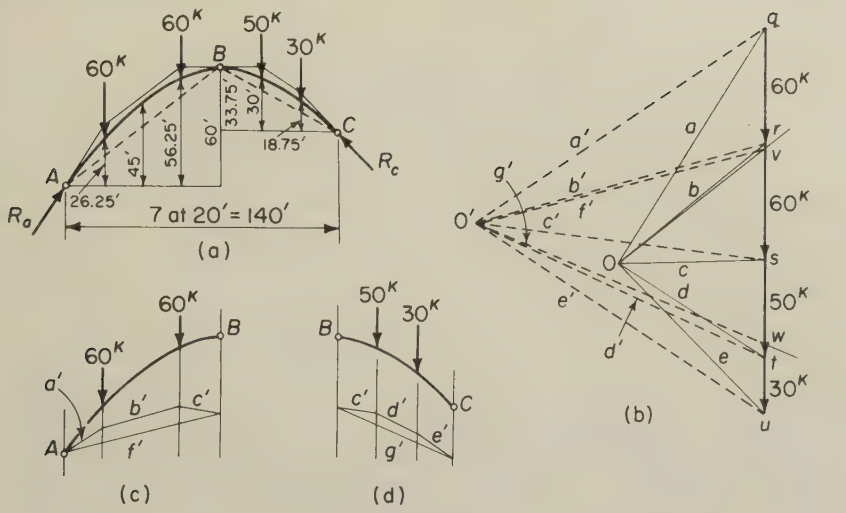

Figure 5–22

f' and g' through O' so that points v and w can be located in Fig. 5-22(b). Then, lines are drawn through points v and w in the force polygon parallel to lines AB and BC respectively in Fig. 5-22(a). The intersection of these two lines will be used as a new pole with which the reactions can be determined, and a string polygon may be constructed through the three hinges of the arch. The reactions of the arch are shown in the force polygon in Fig. 5-22(b). The string polygon, shown in Fig. 5-22(a), is the moment curve for the arch. The area between the string polygon and the arch axis represents the moment diagram. When the vertical ordinates of this area are multiplied by the pole distance h, the products give the corresponding moments at various points of the arch axis.

5-7 *Pressure Lines*

In the discussion of the construction of string polygons, we note that a system of forces such as P_1, P_2, P_3, and P_4 shown in Fig. 5-23(a) may be replaced by the two components of the resultant represented by the first and the last rays in the force polygon shown in Fig. 5-23(b). Hence, the system of forces P_1, P_2, P_3, and P_4 may be held in equilibrium by R_a and R_e, which are equal, opposite, and collinear to the respective components of the resultant. If an imaginary weightless cable or string is placed along strings a, b, c, d, and e of the string polygon, the string is in equilibrium under the action of the given forces and reactions. This concept may be generalized to include a string polygon of the shape shown in Fig. 5-23(c) as a result of the selection of the pole O' in Fig. 5-23(d). In that case, we can imagine the strings a', b', c', d', and e' of the string polygon as a bar chain capable of resisting compression that is held in equilibrium under the action of the

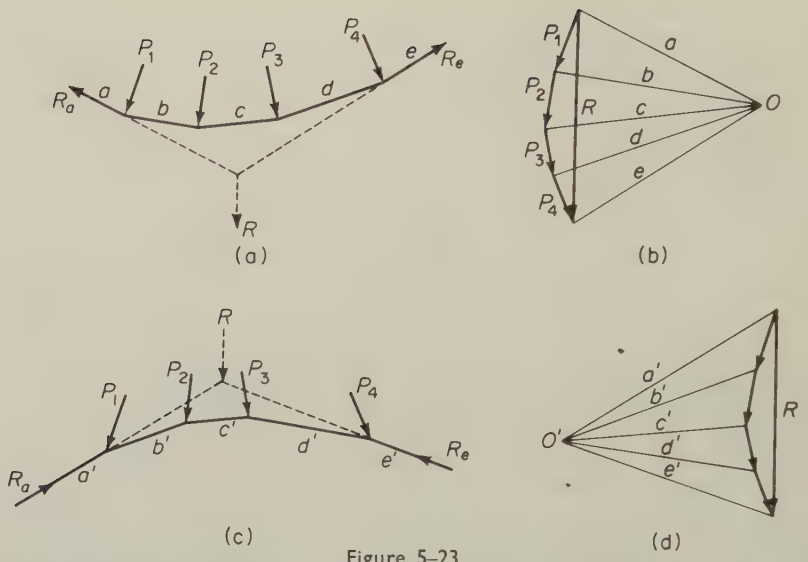

Figure 5–23

given forces and reactions. Consider, for example, a simply supported beam as shown in Fig. 5-24(a). If a string polygon is constructed to pass through supports A and B as shown in Fig. 5-24(b), the resulting configuration may be thought of as the deflected shape of a cable or string supported at A and B under the action of loads P_1 and P_2.

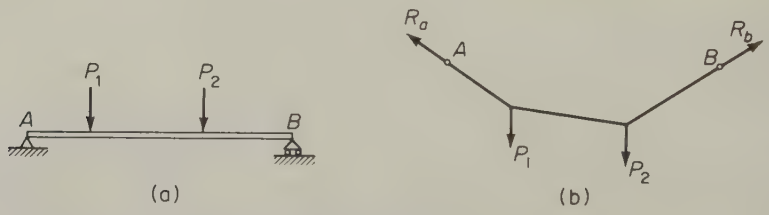

Figure 5–24

In the analysis of arches and frames, such an imaginary string or bar chain is often constructed to represent the successive resultants in their proper position along the length of the structure and is called a *pressure line*. For the three-hinged arch shown in Fig. 5-25(a), for instance, a string polygon representing the pressure line may be drawn through the three hinges as explained in the previous section. The moment at any point on the arch axis is equal to the force represented by the corresponding string of the pressure line multiplied by the perpendicular distance from this point to the string. The same concept may be applied to a rigid frame with three hinges, such as the one shown in Fig. 5-25(b). Thus, the moment at any

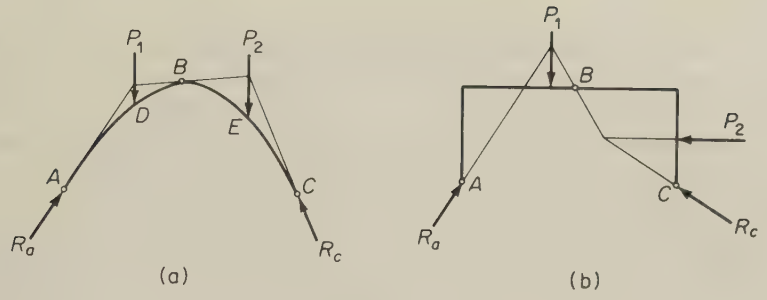

Figure 5–25

point on the horizontal member of the frame is equal to the horizontal component of the corresponding string of the pressure line multiplied by the vertical ordinate between that point and the pressure line. Similarly, the moment at any point on a vertical member of the frame is equal to the vertical component of the corresponding string of the pressure line multiplied by the horizontal distance between that point and the pressure line. Thus, the pressure line itself is a moment curve, having the axis of the structure as its base line.

We may critically examine the efficiency of structural forms by means of the pressure line concept. A structural form is most efficient if all of its parts are stressed to approximately the same level of stress. Thus, members under direct stresses are more efficient in transmitting loads than those subjected to bending stresses so far as the utilization of the material is concerned. Unless other factors are involved in the selection of structural forms, bending should be avoided or minimized whenever possible. Consider, for example, the structural systems in Fig. 5-26 in which a load is transmitted to the foundation. Since all structures shown are statically

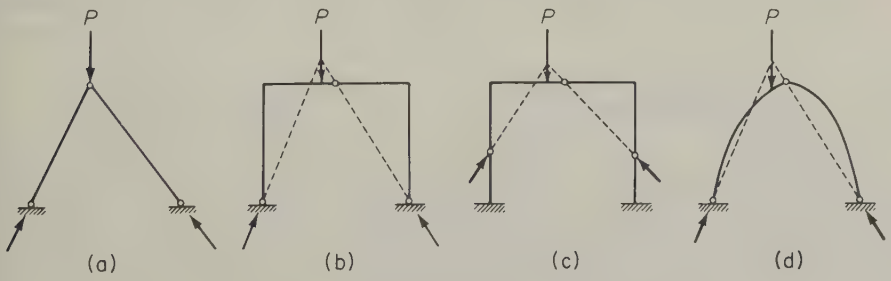

Figure 5–26

determinate and each contains three hinges, the pressure line in each case can be constructed to pass through three given points as indicated in the figures. In Fig. 5-26(a), the load is transmitted to the supports by direct

bar forces, but in Figs. 5-26(b), (c), and (d), moments exist along the length of the structure although the magnitudes of the moments vary according to the location of the pressure lines. Thus, Fig. 5-26(a) represents the most efficient system.

If there are several loads to be transmitted to the foundation, a pressure line may still be constructed through three given points. In Fig. 5-27(a),

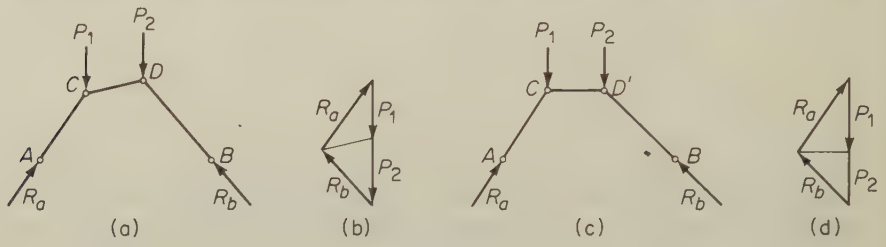

Figure 5–27

for instance, the pressure line is constructed to pass through point C on the line of action of the force P_1 as well as supports A and B, and the force polygon is shown in Fig. 5-27(b). Theoretically, a bar chain represented by the broken line $ACDB$ is the most efficient structure to transmit the forces P_1 and P_2 to the foundation. If the magnitudes of P_1 and P_2 change even slightly, however, the shape of the bar chain changes as shown in Fig. 5-27(c) corresponding to the force polygon in Fig. 5-27(d). Thus, a bar chain consisting of more than three hinges is unstable, and its shape can be uniquely determined only if the magnitudes as well as the positions of the applied loads are known.

For a uniformly distributed load transmitted to the foundation through a statically determinate structure with three hinges as shown in Fig. 5-28(a), it can easily be seen that the pressure line is parabolic. If a three-hinged parabolic arch is selected, the arch rib will be subjected to direct forces

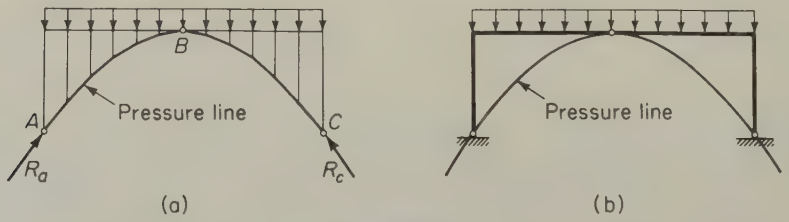

Figure 5–28

only under the action of the uniform load. On the other hand, if a rigid frame as shown in Fig. 5-28(b) is used, the moments will be large at the rigid joints.

5-8 *Application to Statically Indeterminate Frames*

The concept of pressure lines can also be applied to the analysis of statically indeterminate frames. In such cases the pressure line will be uniquely defined by three points of inflection that are analogous to three hinges in statically determinate frames. These points of inflection on a structure correspond to the points of zero moment in the moment diagrams for various members of the structure. If these points are known, the force polygon as well as the string polygon representing the pressure line can be uniquely determined.

The points of inflection of a structure are points of curvature reversal in its deflected members and can therefore be located from the deflected shape of the structure. Although the exact deflected shape of a structure can be obtained only after the forces and moments in the structure are computed, a fair approximation can be made in sketching the deflected structure. Once the approximate locations of the points of inflection are determined, we can estimate the forces and moments in the structure by using the concept of pressure lines. Hence, the pressure lines may be used for rough-checking the forces and moments in statically indeterminate frames.

The deflected shapes of structures may be sketched directly from the given constraints and applied loads. However, we can first roughly sketch the moment diagram as an intermediate step. Then, the shape of the deflected structure can be sketched in accordance with the moment diagram by noting that a positive moment produces a concave curvature and a negative moment produces a convex curvature. Consider, for instance, the statically determinate rigid frames in Examples 3-5 and 3-6 in Section 3-5 for which the moment diagrams are given. The deflected shapes can be sketched as shown in Figs. 5-29 and 5-30, respectively. The same principle

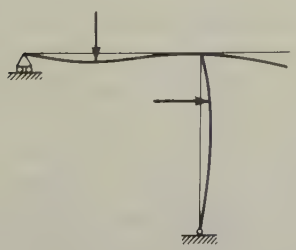

Figure 5–29

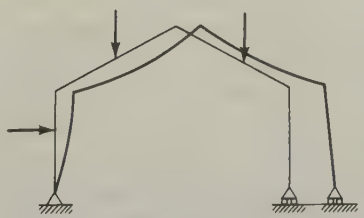

Figure 5–30

may be applied to the sketching of deflected shapes of statically indeterminate frames. The sketching of the deflected shape of a rigid frame is useful not only for the purpose of estimating forces and moments but also for the

computation of deflections by various methods based on the geometry of the structure, as explained in Sections 7-8 and 7-9.

In sketching the deflected shapes of rigid frames, it should be noted that the free-body diagram of a rigid joint must be in equilibrium. Hence, the deflected shape of the members meeting at a joint must satisfy such a requirement. If sections are passed through these members at infinitesimally small distances from the joint, certain conclusions may be drawn regarding the moment-curvature relation. Thus, in Figs. 5-31(a) and (b), the moment

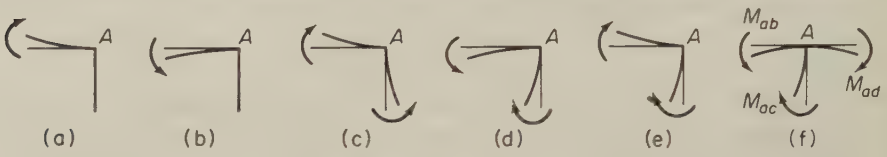

Figure 5–31

at the joint must be zero. In Figs. 5-31(c) and (d), the moments from either side of the joint must be equal and opposite to each other in order to maintain the equilibrium. Figure 5-31(e) represents an impossible case since the joint will not be in equilibrium. On the other hand, Fig. 5-31(f) is quite possible since $M_{ab} = M_{ac} + M_{ad}$ according to the direction of the moments indicated in the figure.

After the deflected shape of a statically indeterminate frame is sketched, we can apply the concept of pressure lines for estimating the forces and moments in the frame. Consider, for instance, the angle frame in Fig. 5-32(a), for which the deflected shape is shown by the dotted lines. The points of inflection are indicated by the circles on the deflected shape. However, since the deflections are greatly exaggerated in the figure, we shall use the undeflected shape of the structure in the construction of the pressure line. Thus, the points of inflection are indicated by D, E, and F, through which a pressure line is drawn as shown in Fig. 5-32(b). Since no external force is acting between points E and F, the part EBF of the frame, when isolated, is a two-force member. Hence, a string representing the reaction at point F must pass through points E and F and will intersect the vertical load. The portion $DEBF$ of the frame, when isolated from the rest of the structure, is a three-force system in which the string representing the reaction at point D must pass through the intersection of the line of action of R_f and the vertical load as shown. Hence, we have in part $DEBF$ of the frame a statically determinate system for which the reactions at points D and F can be obtained either graphically or analytically. The other portions of the frame can also be treated separately as statically determinate systems, as shown in Figs. 5-32(c) and (d). Thus, the forces and moments at any point of the entire frame can be estimated.

When there is more than one external load acting on the frame, the

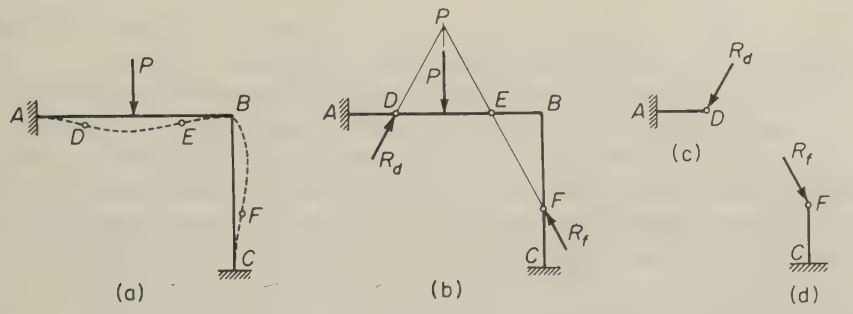

Figure 5–32

general graphical procedure for constructing the string polygon may be used. In the case of uniformly distributed loads, we may consider the resultants of these loads in the determination of reactions at the points of inflection. In obtaining the forces and moments at various points of the frame, however, a distributed load may be divided into a large number of concentrated loads spaced equally apart. The limit of the string polygon based on these concentrated loads will give the desired pressure line. Consider, for example, the portal frame shown in Fig. 5-33(a), for which the

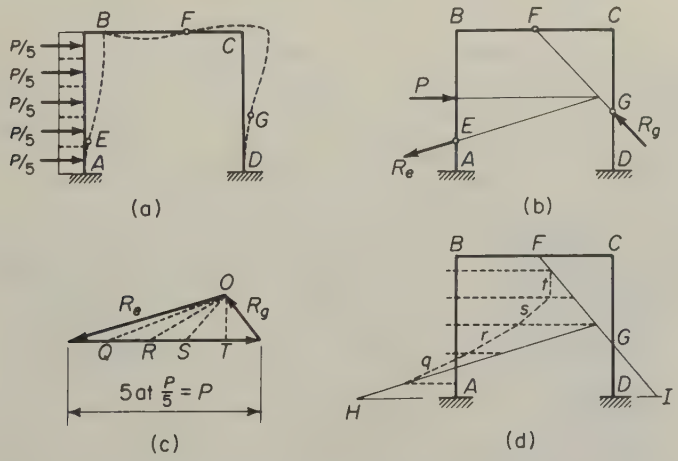

Figure 5–33

deflected shape is shown by the dotted line. If the uniform lateral pressure is replaced by its resultant as shown in Fig. 5-33(b), in which the points of inflection are also indicated, we can construct a pressure line showing the reactions at points E and G when the portion $EBFCG$ of the frame is isolated. The actual pressure line due to the uniform lateral pressure may be approximated by replacing the uniform load with five equal concentrated loads. Then, the force polygon is presented by Fig. 5-33(c), from which the string

polygon in Fig. 5-33(d) is obtained. If a large number of concentrated loads is used, the string polygon will approach a smooth curve.

From the discussion in this section, it is obvious that approximate solutions may be easily obtained for statically indeterminate frames provided that the points of inflection of the deflected structures can be fairly accurately determined. On the basis of this concept, many approximate methods have been developed for the analysis of statically indeterminate frames for which such a degree of inaccuracy can be tolerated.

5-9 *Bar Forces in Simple Trusses*

The graphical method may also be applied to determine the bar forces in trusses. In the case of simple trusses, each joint in the truss may be treated separately as a concurrent force system, beginning with a joint where there are not more than two unknown bar forces. Consider, for instance, the simple truss in Fig. 5-34(a), the reactions of which can be obtained from

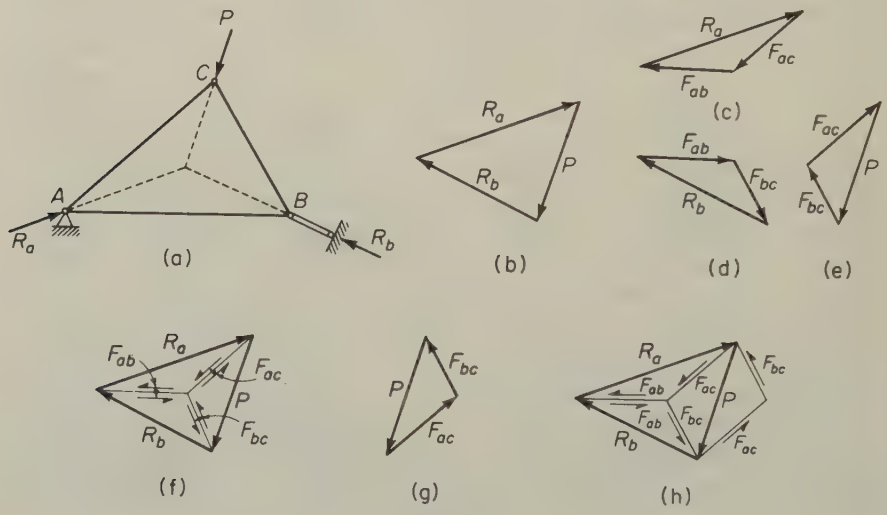

Figure 5–34

the force triangle in Fig. 5-34(b). Thus, a force triangle can be drawn for each of the three joints A, B, and C as shown in Figs. 5-34(c), (d), and (e) respectively. The bar forces in members AB, BC, and CA, which are denoted as F_{ab}, F_{bc}, and F_{ac} respectively, can be determined graphically. In order to avoid the duplication of the vectors representing the bar forces, the separate force triangles may be superimposed to form one diagram as shown in Fig. 5-34(f), which is called the *Maxwell diagram*. However, the force triangles can be compactly superimposed only if each force triangle has its

vectors arranged in the same order as their relative positions in going around the corresponding joint in Fig. 5-34(a) in *either* a clockwise or counterclockwise direction *only*. For example, if we go around joint A in a *clockwise* direction, the order of the forces acting at the joint is in the sequence of R_a, F_{ac}, and F_{ab}. Hence, the same order of arrangement of forces must be maintained in the force triangle in Fig. 5-34(c). The force triangles in Figs. 5-34(d) and (e) are drawn in a similar manner by going around joints B and C respectively in a *clockwise* direction. If a consistent order of arrangement of forces such as this is not followed, the desired purpose of avoiding the duplication of the vectors representing the bar forces will not be accomplished. For example, if the force triangle for joint C had been drawn as shown in Fig. 5-34(g), which corresponds to going around joint C in the truss in a *counterclockwise* direction while the force triangles for joints A and B remain unchanged, the resulting combined diagram would be as shown in Fig. 5-34(h) instead of Fig. 5-34(f). Therefore, in order to obtain the Maxwell diagram, it is important to follow the same direction *consistently* in going around *all* joints of the truss. Whether clockwise or counterclockwise direction is chosen is immaterial, however, the same direction must be maintained throughout the solution of the entire problem.

In the application of Maxwell diagrams to solve the bar forces in trusses, it has been found that the procedure can be simplified by the adoption of a system of notation generally known as *Bow's notation*. Let the spaces between the lines of action of the external and internal forces acting on the joints of a truss be denoted by numbers. For the truss shown in Fig. 5-35(a), for example, such spaces are labelled as 1, 2, 3, 4, and 5. Thus, each force, either external or internal, can be identified by the spaces on both sides of the line of action of that force. For instance, the reaction R_a lies between spaces 3 and 1, the external force P lies between spaces 2 and 3, and the bar force in member AD lies between spaces 1 and 4. If the reactions R_a and R_b

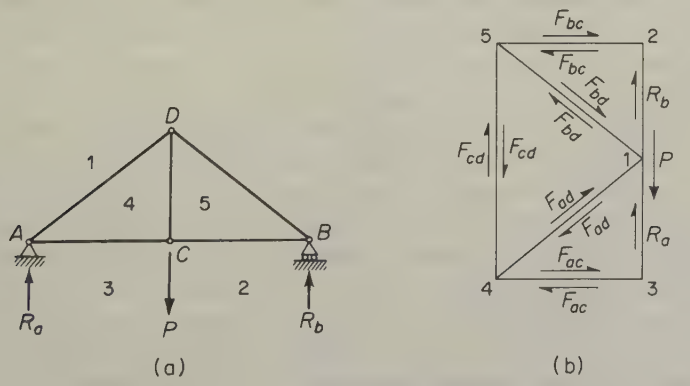

Figure 5–35

of the truss are determined first either graphically or analytically, we may construct the Maxwell diagram as shown in Fig. 5-35(b). Beginning with joint A, we go around the joint in a clockwise direction, denoting the reaction R_a as 3-1, the bar force in member AD as 1-4, and the bar force in member AC as 4-3. Then, we can construct the force triangle 3-1-4 in Fig. 5-35(b), with vectors representing these forces indicated by the arrowheads. Since the vectors 1-4 and 4-3 in triangle 3-1-4 represent the magnitude and direction of the bar forces in members AD and AC respectively when joint A is isolated as a free body, we can easily determine from the Maxwell diagram whether the member is in tension or compression. For example, the vector 1-4 is directed toward joint A, indicating that member AD is in compression, and the vector 4-3 is directed away from joint A, indicating the member is in tension. Similarly, the force triangles 1-5-4 and 1-2-5 in the same diagram may be constructed by going around joints B and C respectively in a clockwise direction.

In general, the sense of direction of the vectors representing bar forces need not be indicated by arrowheads in the Maxwell diagram since each vector is denoted by two numbers, the first number representing the starting point and the second the ending point. Thus, the vector should be pointed toward the direction of the second number. Hence, the Maxwell diagram together with Bow's notation can be conveniently used to determine the magnitude and direction of the bar forces in a truss.

Example 5-11. Determine the bar forces in all members of the truss shown in Fig. 5-36(a).

Since there is only one external load, the reactions can be determined graphically from the force polygon in Fig. 5-36(b) and their lines of action are indicated in Fig. 5-36(a). Then, we can proceed to construct the Maxwell diagram as shown in Fig. 5-36(c).

If the spaces between all forces, internal as well as external, acting on the truss are labeled by numbers, the vectors in the Maxwell diagram representing these forces can be denoted by the corresponding numbers on both sides of each force, taken in a clockwise direction around a joint. Consider, for instance, joint A of the truss, at which the three forces are denoted as 2-1, 1-9, and 9-2. Since the force denoted as 2-1 is known and can be plotted in a proper scale in Fig. 5-36(c), we can construct a line passing through point 2 parallel to member AB and a line passing through point 1 parallel to member AF. The intersection of these two lines is denoted as point 9. The vector 1-9 in the Maxwell diagram is acting in a direction away from the joint in the space diagram, and the vector 9-2 is acting toward joint A. Hence, member AF is in compression. Next, consider joint B at which the bar forces are denoted as 2-9, 9-8, and 8-2. Since the force 8-2 is known, the other two forces can be constructed in a similar manner. In this particular case, points 8 and 9 in the Maxwell diagram coincide, and the force

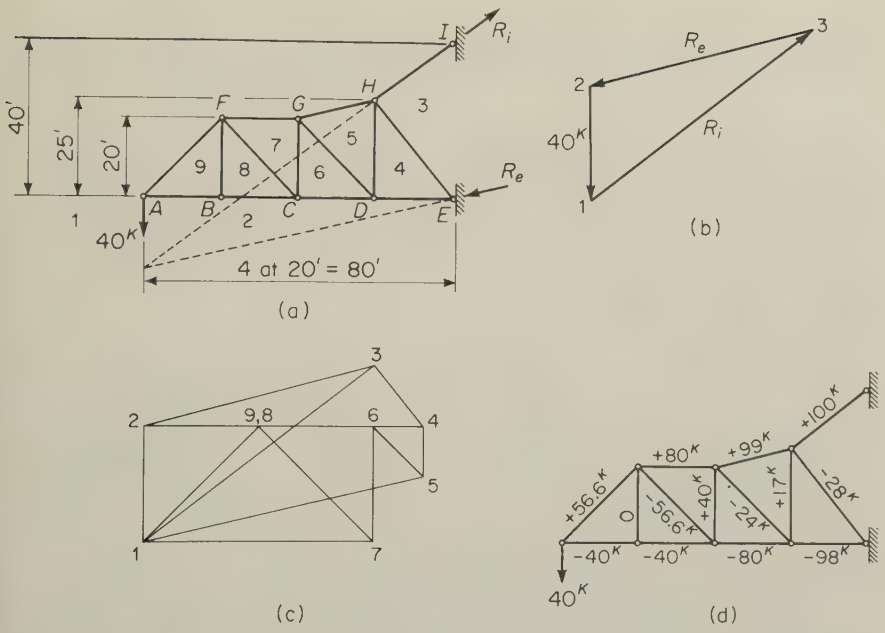

Figure 5–36

8-2 is equal in magnitude to force 2-9 but is opposite in direction, i.e., acting toward joint B of the truss. We can therefore proceed to joint F, at which the unknown bar forces 1-7 and 7-8 are obtained from the known forces 8-9 and 9-1. The same procedure will be repeated for other joints until the bar forces in all members of the truss are solved. The results are scaled off from the Maxwell diagram and recorded in Fig. 5-36(d).

Example 5-12. Determine the bar forces in all members of the truss shown in Fig. 5-37(a).

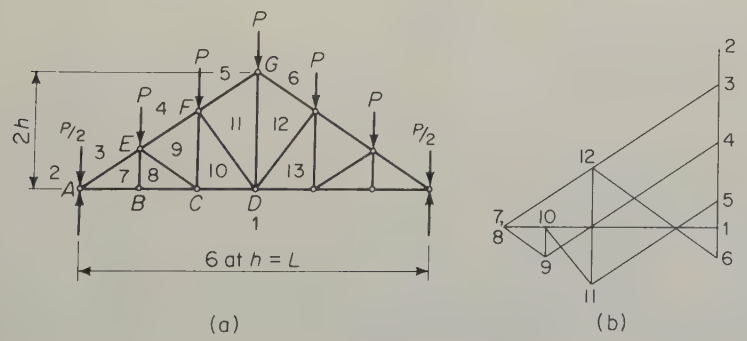

Figure 5–37

For a symmetrical truss with symmetrical loading, the reactions can readily be obtained analytically. Furthermore, because of the symmetry, only the bar forces in half of the truss are shown in the Maxwell diagram in Fig. 5-37(b).

In examining the Maxwell diagram, it can be seen that the force polygon for joint A is represented by 1-2-3-7; for joint B, it is shown to be 7-8-1; for joint E, it is indicated by 8-7-3-4-9; etc. Finally, the bar forces can be obtained by direct measurement of the vectors in the diagram.

5-10 Compound Trusses

The graphical method for the determination of the bar forces in simple trusses can also be applied to compound trusses. However, since the bar forces in a compound truss cannot be solved completely by the method of joints alone analytically, it is also necessary to modify the graphical method that has been developed for simple trusses. This is accomplished by replacing some of the members in the original truss by a substitute member or members temporarily so that the compound truss is reduced to a simple truss. In Example 4-8 of Section 4-7 we explained that such a substitution causes no change in the bar forces in the members of the original truss except in the vicinity of the substitute member. Furthermore, the bar forces in members in this vicinity can be determined later by considering the effect of the substitute member.

The bar forces in a compound truss with secondary systems may be obtained from the superposition of the corresponding bar forces in the primary and secondary systems, which may be determined graphically. Since a Maxwell diagram can be constructed for each of the constituent trusses that are simple trusses, the magnitude and direction of the bar forces in these systems can be measured directly from the Maxwell diagrams. When the results of the secondary systems are superimposed on those of the primary system, the bar forces in the original truss are obtained.

Example 5-13. Determine the bar forces in all members of the Fink truss shown in Fig. 5-38(a).

The reactions at the supports of the truss can easily be determined by inspection. Because of the symmetry of the truss and the loading, only half of the truss need be considered.

The graphical construction for the solution of this problem is similar to that for simple trusses. We can begin the construction of the Maxwell diagram by considering first the forces acting at joint A and then at joints H and F as shown in Fig. 5-38(b). However, after this point is reached, we cannot proceed any further because there are more than two unknowns at either joint I or joint B. Hence, a substitute member BJ is introduced

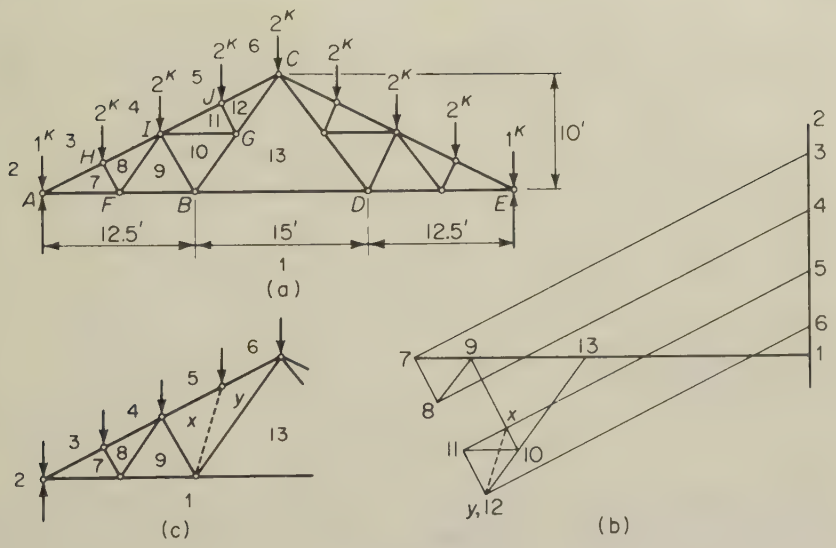

Figure 5–38

to replace members *IG* and *GJ* temporarily. It is noted that the bar forces in the members of the original truss, except those bounded within the area *IBGJ*, will not be affected. Then, the bar force in the substitute member *BJ* is sought by locating points x and y in the Maxwell diagram. Note that point y also represents the location of point 12, since the bar force 6-y in the substitute truss is the same as the bar force 6-12 in the original truss. Referring back to the original truss in Fig. 5-38(a), we can now consider joint *J* since the bar force in member *CJ* is now known. Finally, the bar forces at joints *I* and *B* can be solved accordingly.

Example 5-14. Determine the bar forces in all members of the compound truss shown in Fig. 5-39(a).

The truss can be broken up into a primary system as shown in Fig. 5-39(b) and three secondary systems each of which can be represented by Fig. 5-39(c). Because of the symmetry of the truss and the loading, a Maxwell diagram is constructed for the primary system in Fig. 5-39(d) for half of the truss. In the construction of the Maxwell diagram in Fig. 5-39(e) for the secondary system, however, the horizontal force F' acting on the secondary system in Fig. 5-39(c) is not included in order to simplify the graphical solution. Let the bar forces in members *AB*, *BC*, and *CD* in the primary system be F'_{ab}, F'_{bc} and F'_{cd} respectively. These forces would in turn act on the corresponding secondary systems they replace. Thus, the force F' in Fig. 5-39(c) represents F'_{ab}, F'_{bc} or F'_{cd}, depending on whether the secondary system *ABK*, *BCL*, or *CDM* in the original truss is being considered. If

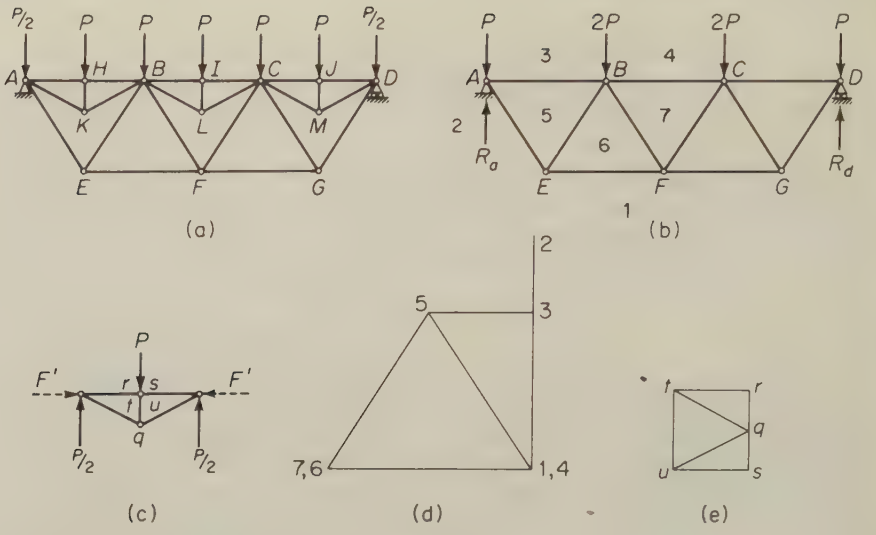

Figure 5–39

this force F' is included in the construction of the Maxwell diagram, it will be necessary to construct three separate diagrams, one for each F', from which the final results may be directly obtained. On the other hand, if F' is not included, only one diagram need be drawn, but the resulting bar forces obtained from this diagram must be superimposed on the corresponding bar forces in the primary system in order to obtain the actual bar forces in the original truss.

5-11 *Virtual Displacement Diagrams*

In the determination of bar forces by the method of virtual displacements described in Section 4-10, it is necessary to visualize the movements of nonrigid systems and to compute the virtual displacements of joints. We have pointed out that such a procedure may be quite tedious for trusses with a large number of joints and panel loads. However, a graphical method may be used to advantage in determining the virtual displacements of coplanar nonrigid systems with one degree of freedom.

Consider, for example, the simple statically determinate system in Fig. 5-40(a). In order to compute the horizontal component of reaction at C by the principle of virtual displacements, we remove this component of reaction and replace it by a horizontal force H_c. Note that the sense of direction of H_c is arbitrarily assumed. If the assumed sense is correct, the result of H_c will be positive; otherwise it will be negative. Then, the resulting system in Fig. 5-40(b) has one degree of freedom and its configuration can be completely defined by the angle φ. If the system is given a counter-

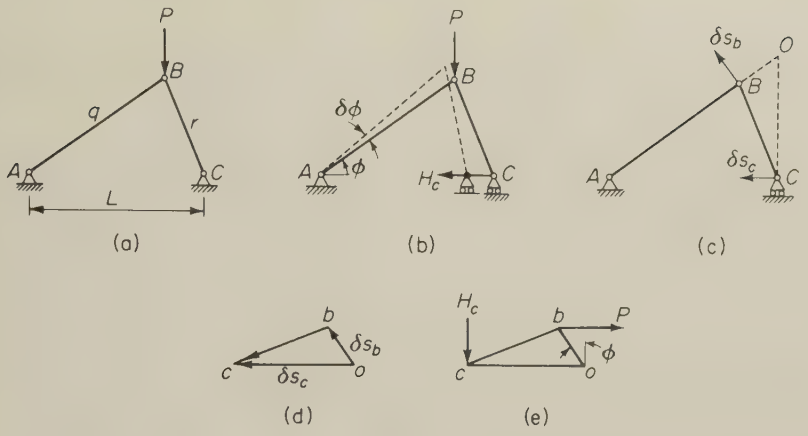

Figure 5-40

clockwise virtual rotation $\delta\varphi$, its configuration may be indicated by the dotted lines in Fig. 5-40(b). The corresponding displacements at points B and C where external forces are applied are given by δs_b and δs_c respectively. For small angle $\delta\varphi$, the displacement δs_b may be considered as being normal to member AB while the displacement δs_c is horizontal. According to the principle of virtual displacements, the virtual work done by all forces acting on the nonrigid system must be zero, i.e.,

$$\delta W = P\,\delta s_b \cos(P,\ \delta s_b) + H_c\,\delta s_c \cos(P,\ \delta s_c) = 0 \qquad \text{(a)}$$

in which the angle between the direction of a force and the direction of the displacement at the corresponding point of application of the force is identified by the force and displacement themselves. For example, $(P,\ \delta s_b)$ denotes the angle between the force P and the displacement δs_b. Note that

$$\cos(P,\ \delta s_b) = \cos(180^\circ - \varphi) = -\cos\varphi \quad \text{and} \quad \cos(P,\ \delta s_c) = \cos 0^\circ = 1$$

in this case. Hence,

$$-P\,\delta s_b \cos\varphi + H_c\,\delta s_c = 0 \qquad \text{(b)}$$

If we can determine δs_b and δs_c, the unknown component of reaction H_c can be computed in terms of the given load P and the known angle φ. Furthermore, we are only interested in the relative values of the virtual displacements rather than their absolute values. If all virtual displacements can be expressed in terms of one of them, a common factor representing this displacement can be cancelled in Eq. (b).

The relative virtual displacements of the system can be obtained from the kinematics of rigid bodies. In general, the plane motion of a rigid body can be described by its rotation about the instantaneous center, which is defined as the point of zero velocity. In the case of member AB, point

A is fixed and the member undergoes a rotation about point A only. For member BC, the instantaneous center of the plane motion may be obtained from the intersection of the lines drawn through end points B and C of the member perpendicular to displacements δs_b and δs_c respectively, as shown in Fig. 5-40(c). Thus, point O in the figure represents the instantaneous center about which member BC rotates. Since the displacement at any point on member BC is proportional to its distance from the instantaneous center O, we have

$$\frac{\delta s_b}{OB} = \frac{\delta s_c}{OC} \tag{c}$$

From the motion of member AB, we note that

$$\delta s_b = q\,\delta\varphi$$

and from Eq. (c)

$$\delta s_c = \frac{OC}{OB}\,\delta s_b = \frac{OC}{OB}\,q\,\delta\varphi$$

Hence, Eq. (b) becomes

$$Pq\,\delta\varphi\cos\varphi - \frac{OC}{OB}\,H_c q\,\delta\varphi = 0$$

or

$$H_c = \frac{OB}{OC}\,P\cos\varphi \tag{d}$$

Although distances OB and OC may be measured from the instantaneous center of member BC, the procedure becomes very complicated when a large number of members are involved. A general graphical procedure based on the geometrical relations of similar triangles may be used for determining the ratio OB/OC since only this ratio rather than the absolute values of OB and OC are needed in evaluating H_c in Eq. (d). Starting from a point o in Fig. 5-40(d), we construct lines parallel to the directions of displacements δs_b and δs_c. The magnitude of one of these displacements, say δs_b may be arbitrarily chosen and is denoted by the vector ob as shown. The closing side of the triangle in the figure may be obtained by drawing a line passing through point b and perpendicular to member BC of the system. In comparing triangle OBC in Fig. 5-40(c) and triangle obc in Fig. 5-40(d), we note that $ob \perp OB$, $oc \perp OC$, and $bc \perp BC$. Hence, the two triangles are similar, or $OB/OC = ob/oc$. Then, H_c may be obtained as follows:

$$H_c = \frac{ob}{oc}\,P\cos\varphi \tag{e}$$

The triangle thus constructed for the purpose of obtaining virtual displacements is called a *virtual displacement diagram.*

The application of the principle of virtual displacements can be further simplified if the equation of virtual displacements for an actual system is interpreted as an equation representing the moments of a set of fictitious forces acting on a fictitious system. Imagine a virtual displacement diagram to be a fictitious rigid body hinged at its initial reference point. It is possible to apply a set of fictitious forces to the appropriate points of the diagram so that the equation of equilibrium for the moments of all forces about the hinged point is *mathematically* identical to the equation obtained from the virtual displacements of the actual system, although *physically* the fictitious system and the actual system are entirely different. For the actual system in Fig. 5-40(b), for example, the relation between the forces and the virtual displacements is given by Eq. (b). By applying fictitious forces P and H_c at points b and c of the virtual displacement diagram as shown in Fig. 5-40(e) and considering counterclockwise moments as positive, the equation of equilibrium for moments about point o is given by

$$H_c\,\delta s_c - P\,\delta s_b \cos\varphi = 0$$

or

$$H_c\,oc - P\,ob\cos\varphi = 0$$

which is identical to Eq. (b). In general, the fictitious forces must have the same magnitudes as the respective forces in the actual system, and their directions correspond to those in the actual system turned 90 degrees counterclockwise. However, if clockwise moments had been defined as positive in establishing the equation of equilibrium, the directions of the fictitious forces should correspond with those in the actual system turned 90 degrees clockwise. When the virtual displacement diagram is used as a fictitious rigid body hinged at the initial point of reference, it is called a *Joukowski lever.*

In the case where external loads are applied on the members as well as the joints of the system, the same approach may still be used. The method can also be applied to systems with a large number of joints, provided that one unknown is removed at a time so that the resulting nonrigid system has only one degree of freedom.*

Example 5-15. Find the horizontal component of reaction at point C of the frame shown in Fig. 5-41(a) by the principle of virtual displacements. Determine the necessary virtual displacements graphically.

If the horizontal component of reaction at C is removed and replaced by a horizontal force H_c as shown in Fig. 5-41(b), the resulting system

*See pp. 40-43 of Reference 4-1 for further discussion.

has one degree of freedom. The portion AGB of the frame undergoes only rotation about point A while the part BFC will have a plane motion. If the angle φ of the nonrigid system in Fig. 5-41(b) is given a counterclockwise virtual rotation $\delta\varphi$, the virtual displacements at points B and D will be perpendicular to lines AB and AD respectively. The virtual displacement at point C must be horizontal, whereas that at point E is governed by the plane motion of the part BFC of the frame. Note that only the virtual displacements at the points where external forces are acting are required. Then, these displacements may be obtained from the virtual displacement diagram shown in Fig. 5-41(c). Starting from a point o, we construct the

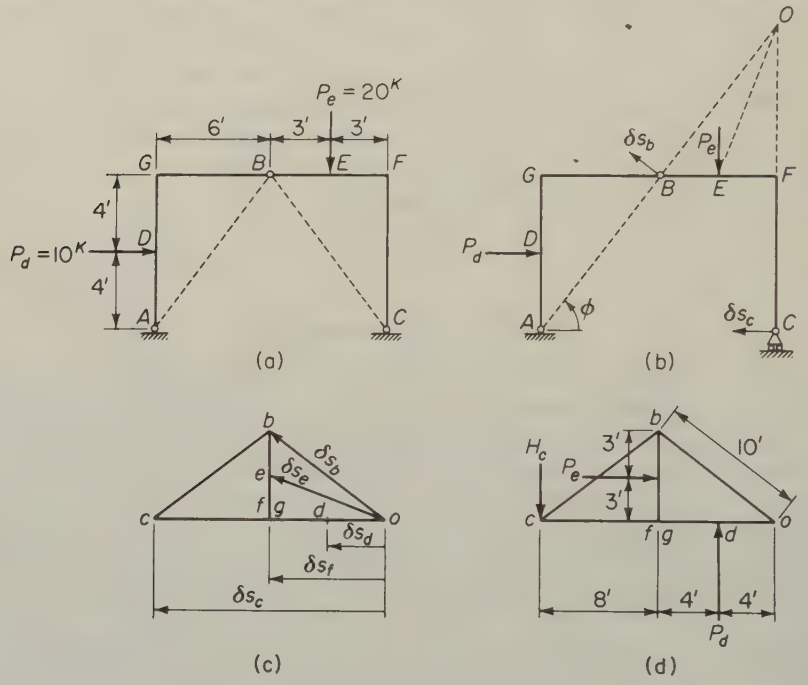

Figure 5–41

displacement vector ob of arbitrary length and parallel to δs_b in a convenient scale. Then, draw a line passing through point o and parallel to δs_c, and another line passing through point b and perpendicular to line BC in Fig. 5-41(b). The intersection of these two lines gives the point c for the displacement vector oc. The point d has the same relative position with reference to point o in the diagram as point D has to point A in the frame. Furthermore, point e in the diagram has the same relative position to point b or f as point E has to point B or F respectively in the frame. Thus, vectors od, oe, and of represent the displacements δs_d, δs_e, and δs_f respectively.

By placing the fictitious forces on the virtual displacement diagram as shown in Fig. 5-41(d), we can obtain the equation for moments about point o as follows:

$$H_c oc - P_d od - P_e ef = 0$$

By measuring the distances oc, od, and ef in the Joukowski lever by the same scale, say, on the basis of 10 for length ob, we obtain

$$16H_c - (10)(4) - (20)(3) = 0$$

Hence, $H_c = 6.25$ kips.

5-12 *Application of Virtual Displacement Diagrams to Trusses*

For structural systems with a large number of joints such as trusses, the method of constructing virtual displacement diagrams can be applied systematically joint by joint. Since the external forces on a truss are applied at the joints only, the graphical procedure is relatively simple. Upon the removal of a component of reaction or a member of a statically determinate plane truss, the resulting system will have one degree of freedom. At each step of the operation, usually one of the following three basic configurations is involved. Figure 5-42(a) shows the simplest configuration which has one

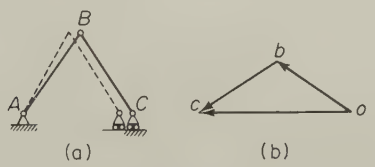

Figure 5–42

degree of freedom. We can construct the virtual displacement diagram by plotting any arbitrary length for the displacement vector ob which is perpendicular to member AB as shown in Fig. 5-42(b). Then, draw a line passing through point O and parallel to the displacement of point C, and another passing through point b and perpendicular to member BC. The intersection c of these two lines defines the displacement vector oc. The vector bc represents the relative displacement of C with respect to B in the

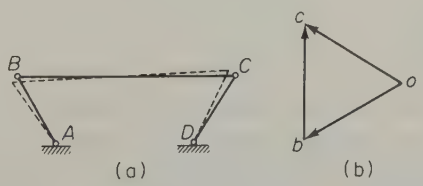

Figure 5–43

system. Hence, vector *oc* is the vector sum of *ob* and *bc*. Figure 5-43(a) shows a quadrilateral hinged at two adjacent vertices. In this case, both *A* and *D* can be used as reference points. Again, we can plot an arbitrary length for the displacement vector *ob* which is perpendicular to member *AB* as shown in Fig. 5-43(b). Then draw a line passing through point *o* and perpendicular to member *CD*, and another line passing through point *b* and perpendicular to member *BC*. The vector *oc* is the displacement of *C* while the vector *bc* is the displacement of *B* relative to *C*. The virtual displacement diagram indicates that the displacement vector *oc* is the vector sum of *ob* and *bc*. Figure 5-44(a) shows a quadrilateral hinged at one vertex and simply sup-

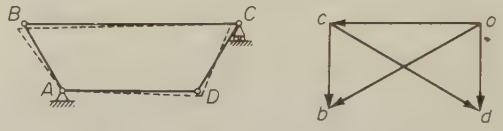

(a) (b)

Figure 5–44

ported at the opposite vertex. There is no displacement at point *A* but point *C* may move horizontally. We can therefore plot an arbitrary length for the displacement vector *ob* which is perpendicular to member *AB* as shown in Fig. 5-44(b). Then, draw a line passing through *o* and parallel to the displacement of *C*, and another line passing through *b* and perpendicular to *BC*. Thus, *oc* is the displacement of *C* and *cb* is the relative displacement of *B* with respect to *C*. Point *d* on the virtual displacement diagram is located by drawing a line through *o* perpendicular to member *AD*, and another line passing through *c* perpendicular to *CD*.

The graphical procedure is especially useful for the analysis of complex trusses. If we can determine the bar force in one member by the method of virtual displacements, the remaining bar forces may be obtained by the method of joints. The virtual displacement diagram has made possible the determination of virtual displacements of trusses with a large number of members.

Example 5-16. Determine the bar force in member *BD* of the truss shown in Fig. 5-45(a) by the virtual displacement diagram.

In order to determine the bar force in member *BD*, we remove the member and replace it with a pair of forces *Q* as shown in Fig. 5-45(b). Note that the sense of direction of *Q* is arbitrarily assumed. If the assumed sense is correct, the result will be positive; otherwise it will be negative. The resulting system then has one degree of freedom. However, part *ABC* is rigid and will displace as a unit, and so is part *CDE*. Hence, if angle φ is given a counterclockwise virtual rotation, δs_b will be perpendicular to

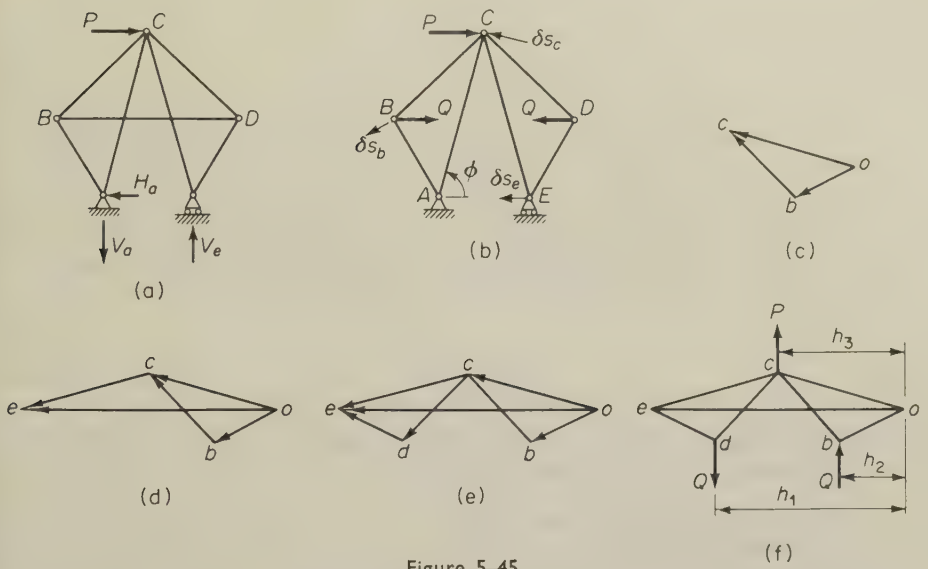

Figure 5–45

member AB and δs_c perpendicular to member AC. On the other hand, δs_e must be horizontal whereas δs_d is yet to be determined. The virtual displacement diagram may be constructed by plotting in the direction perpendicular to member AB a displacement vector ob of arbitrary length to some convenient scale, as shown in Fig. 5-45(c). Then, draw a line passing through o and perpendicular to member AC and another line passing through b and perpendicular to member BC. Then, the intersection c of these two lines defines the length of the displacement vector oc. Next, draw a horizontal line passing through o and another line passing through c and perpendicular to member CE as shown in Fig. 5-45(d). Finally, point d may be located from the intersection of lines cd and de in a similar manner. Thus, ob, oc, od, and oe in Fig. 5-45(e) represent δs_b, δs_c, δs_d, and δs_e respectively.

If fictitious forces are applied to the virtual displacement diagram in accordance with the rule of turning the actual forces on the truss counterclockwise by 90 degrees and placing them on the corresponding points of the diagram, a Joukowski lever is obtained in Fig. 5-45(f). By adopting a convenient scale for ob, the lengths of distances h_1, h_2, and h_3 can be determined graphically. Then, the bar forces can be computed by taking moments of all forces about point o as follows:

$$Qh_1 - Qh_2 - Ph_3 = 0$$

Hence,

$$Q = -\frac{Ph_3}{h_1 - h_2}$$

5-13 Summary

In this chapter we have discussed the graphical methods for determining reactions, forces, and moments in structures. However, we are not primarily concerned with the routine applications of these methods, useful though they may be. The emphasis has been placed on the visualization of the geometry of the structures under the action of forces and moments. To accomplish such purposes, the concept of pressure lines and the method of virtual displacement diagrams have been presented.

References

5-1 H. Cross and N. D. Morgan, *Continuous Frames of Reinforced Concrete*, John Wiley & Sons, Inc., New York, 1936.

5-2 J. R. Benjamin, *Statically Indeterminate Structures*, McGraw-Hill Book Co., Inc., New York, 1959.

5-3 H. Sutherland and H. L. Bowman, *An Introduction to Structural Theory and Design*, 4th ed., John Wiley & Sons, Inc., New York, 1950.

5-4 J. C. Maxwell, "On Reciprocal Figures and Diagrams of Forces," *Philosophical Magazine* (London), 4th Ser., vol. 26, 1864, p. 250.

Problems

5-1 to **5-6** Determine graphically the reactions of each of the structures corresponding to Figs. P3-5, P3-10, P3-11, P3-13, P3-14, and P3-18, respectively, at the end of Chapter 3.

5-7 to **5-10** Determine graphically the reactions at the supports and the moments at the loading points of the beams shown for these problems.

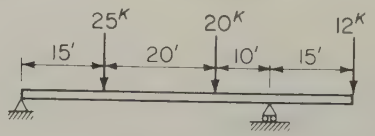

Figure P5–7

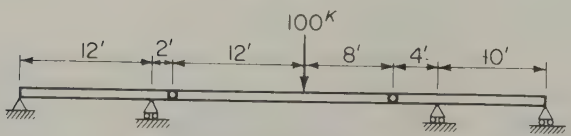

Figure P5–8

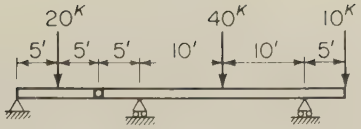

Figure P5–9

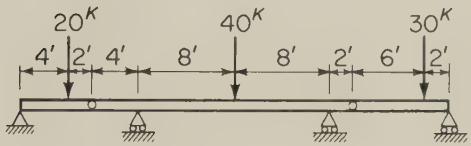

Figure P5–10

5-11 and **5-12** Determine graphically the moment diagram for each of the arches shown in Figs. P3-27 and P3-30 respectively at the end of Chapter 3.

5-13 to **5-16** Sketch the pressure lines for the frames for these problems.

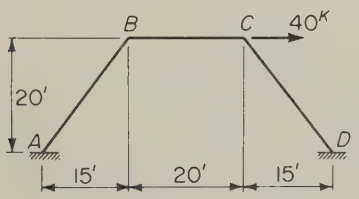

Figure P5–13

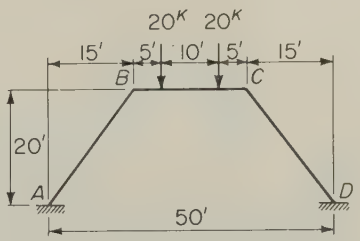

Figure P5–14

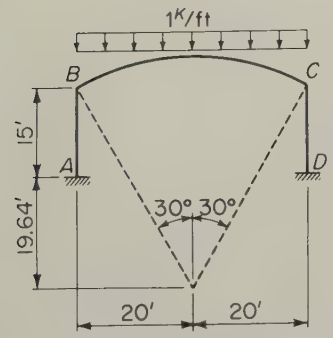

Figure P5–15

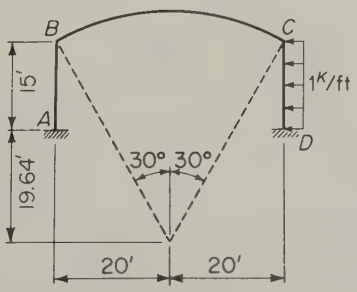

Figure P5–16

5-17 to **5-22** Determine graphically the bar forces for all members of the respective trusses shown in Figs. P4-1 to P4-6 at the end of Chapter 4.

5-23 and **5-24** Determine graphically the bar forces for all members of the trusses shown for these problems.

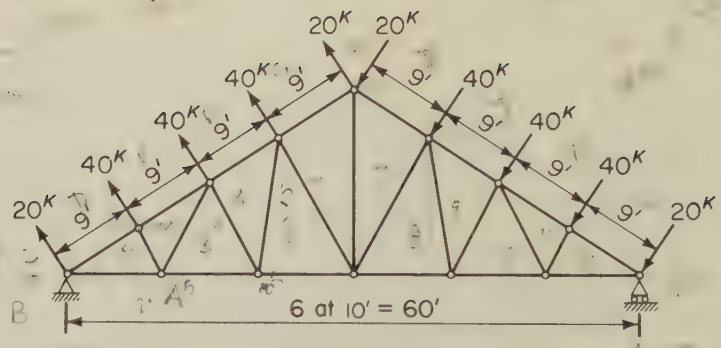

Figure P5–23

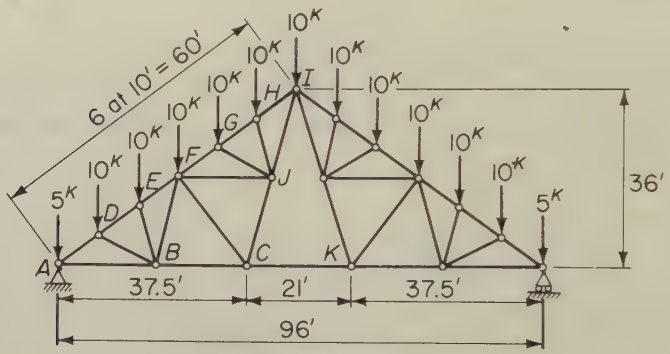

Figure P5–24

5-25 and **5-26** Determine graphically the bar forces for each of the trusses shown in Figs. P4-25 and P4-26 respectively at the end of Chapter 4.

5-27 Determine the horizontal component of reaction at point B of the structure shown for the problem by the graphical construction of virtual displacement diagram.

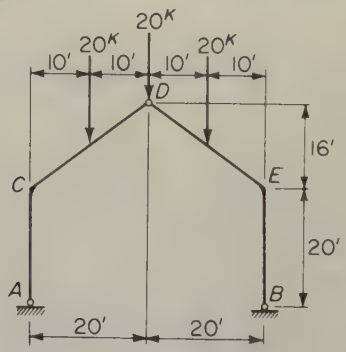

Figure P5–27

5-28 and **5-29** Determine the bar force in member AD of each of the trusses shown in Figs. P4-31 and P4-32 respectively at the end of Chapter 4.

6 INFLUENCE LINES

6-1 Definitions

When a moving load changes its position on a structure, it causes varying effects in the structure. There is always one position at which it will produce the most severe effect on a certain specified quantity of significance in the structure, such as the reaction at a support, the shear or moment at a section of a beam, or the bar force in a truss member. Sometimes it is possible to determine such a position by inspection, but in other cases it may be necessary to resort to trial-and-error procedure. In general, the variations of significant effects in a structure caused by a moving unit load can be expressed as functions of the position of the load. The graphical representations of such variations are called the *influence lines* or *influence diagrams*. Hence, the influence line for a specific effect may be defined as a curve, the ordinates of which show the variation of that effect caused by a unit load moving across the structure. The ordinate at any point represents the value of the effect when the unit load is acting at the corresponding point on the structure.

Let us consider as examples a few simple cases of influence lines for beams. Figure 6-1(a) shows a simple beam for which the influence line for the left reaction is required. If a unit load is placed at a distance x from the right support B, the left reaction $R_a = x/L$. Since a linear relation exists between R_a and x, R_a increases linearly as the unit load moves across the beam from support B to support A. Figure 6-1(b) is a plot of the variation of the left reaction where the ordinate at B is zero and the ordinate at A is unity, and the inclined line is the influence line for the left reaction.

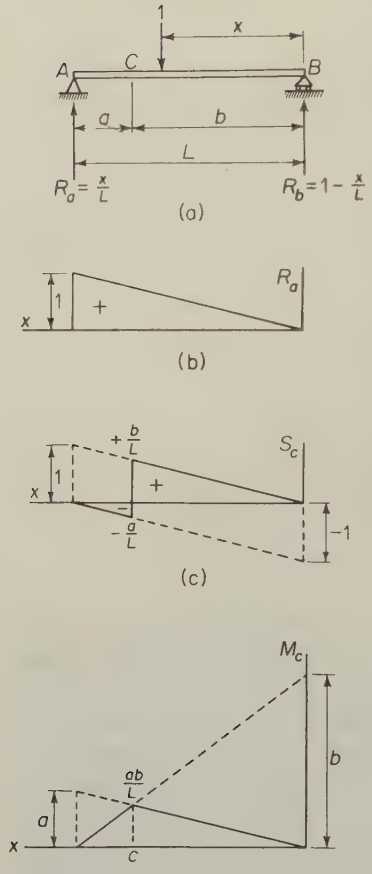

Figure 6–1

Similarly, the influence lines for shear and for bending moment at point C of a simple beam can be constructed on the same basis. In the case of the influence line for shear, the shear force at point C may be computed as follows:

for $0 < x < b$, $\quad S_c = R_a = \dfrac{x}{L}$

for $b < x < L$,

$$S_c = R_a - 1 = -R_b = -\frac{L - x}{L}$$

Note that when $x = b$, these two equations do not yield the same value for S_c. Thus, the influence line for shear at point C of the beam is represented by Fig. 6-1(c). The abrupt change of ordinate at point C indicates that the shear at point C passes suddenly from positive to negative as the load moves from a point just to the right of point C to a point just to the left of point C. In the case of the influence line for moment, the moment at point C is given by:

for $0 \leqq x \leqq b$, $\quad M_c = R_a a = \dfrac{ax}{L}$

for $b \leqq x \leqq L$, $\quad M_c = R_a a - 1(x - b)$

$$= R_b b = \frac{b(L - x)}{L}$$

Hence, the influence line for moment at point C can be plotted as shown in Fig. 6-1(d).

The unit for the ordinate of an influence line is that of the effect divided by the unit of force. For example, the unit for the ordinate of influence lines for reactions or shears is force divided by force or dimensionless. This simply means that the unit of the ordinate at any point is in pounds per pound (or kips per kip) of load applied at that point on the structure. Similarly, the unit for the ordinate of influence lines for moments is length-force divided by force or just length. This is interpreted to mean that the ordinate at any point is expressed in foot-pounds per pound of load applied at that point of the structure. The same results may be achieved if the moving load on the structure is assumed to be dimensionless. Thus, the ordinate at any point of an influence line may be considered as the *influence coefficient*

for that effect by which the load applied at that point on the structure is multiplied in order to obtain the true magnitude of the effect.

When the live load on the structure consists of a single concentrated load P, the magnitude of an effect due to this load equals the product of the load P and the ordinate of the influence line for that effect at the point of application of the load. In order to obtain the maximum value for the effect, the load P should be placed at the point for which the ordinate of the influence diagram is maximum. Thus, for the beam shown in Fig. 6-1(a), the maximum left reaction resulting from a concentrated load P is $R_a = P(1) = P$ when the load P is placed at support A. Similarly, the maximum positive shear at point C will be $S_c = Pb/L$ when the load P is placed just to the right of point C, and the maximum moment at point C will be $M_c = Pab/L$ when the load P is placed at point C of the beam. Note that reaction R_a and shear S_c have the same unit as P, which is a force, while moment M_c has the unit of force multiplied by a length. Thus, the units of these quantities obtained from the influence lines are consistent with those obtained from direct computation.

Since the influence lines shown in Fig. 6-1 are linear functions of the distance x, the construction of influence lines can be simplified by noting the geometry of these lines. In the case of reaction R_a, we can imagine that a unit load is first placed at point A and then at point B. When the load is in the former position, R_a has a magnitude of unity, when it is in the latter position, R_a is zero. After obtaining these control points in the influence diagram, we may draw a straight line between these two points as shown in Fig. 6-1(b). In the influence diagram in Fig. 6-1(c), the dotted lines indicate that the influence line for shear S_c can be obtained from the influence lines for R_a and $-R_b$ as represented by the inclined lines above and below the horizontal base line, respectively. Then, the vertical line in the influence diagram for S_c can be located easily by the relations of similar triangles. Similarly, in the influence diagram in Fig. 6-1(d), the ordinate at the control point C can be obtained from the intersection of the inclined lines if ordinates a and b are plotted at the end points in the diagram as indicated. Thus, from the relations of similar triangles, the ordinate point C is seen to be ab/L.

For statically determinate structures, the influence lines consist of straight line segments only since the effects are always related to the distance x linearly. Thus, the construction of influence lines becomes a matter of determining the ordinates of a few control points in a diagram and then connecting the proper points by straight lines.

Example 6-1. Construct the influence lines for the reaction at support B and the shear just to the right of support B of the beam shown in Fig. 6-2(a).

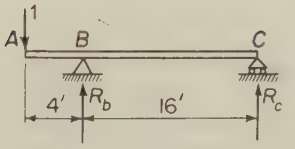

(a)

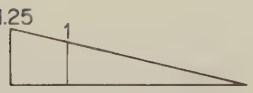

(b)

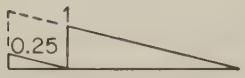

(c)

Figure 6–2

The ordinates of the control points of the influence lines can be computed by placing a unit load at points A, B, and C successively. Thus, for a unit load at A, we obtain from $\Sigma M_c = 0$,

$$16R_b = (1)(20), \quad R_b = {}^{20}\!/_{16} = 1.25$$

The shear at the point just to the right of support B is obtained from the equilibrium of the free body cut by a section just to the right of B. Thus, for a unit load at A,

$$S_{br} = -1 + R_b = -1 + 1.25 = 0.25$$

For a unit load at B, it is obvious that $R_b = 1$. However, in the determination of S_{br}, the unit load must be placed slightly to the right or left of B. In that case, R_b remains practically the same but S_{br} will have a magnitude equal to 1 or 0. When the unit load is placed at point C, we have $R_b = 0$ and $S_{br} = 0$. Thus the influence lines for R_b and S_{br} can be constructed as shown in Fig. 6-2(b) and (c) respectively. Note that the influence line in Fig. 6-2(c) can also be obtained from the influence line for R_b by subtracting the dotted portion in Fig. 6-2(c), which has an ordinate of unity for the overhang of the beam.

6-2 *Influence Lines as Virtual Displacement Diagrams*

Influence lines may also be constructed on the basis of the principle of virtual displacements. This is accomplished by removing the constraint of the structure for which the effect is desired and replacing it by a corresponding force. If the resulting nonrigid system is given a virtual displacement, it can be demonstrated that the shape of the displaced system resulting from the removal of the constraint is the influence line for that constraint.

Consider, for example, the influence line for reaction R_a of the simple beam in Fig. 6-3(a). If we remove the vertical constraint at A and replace it by reaction R_a, the resulting system has one degree of freedom. This system is then given a small virtual rotation $\delta\varphi$ about point B. For small angles of $\delta\varphi$, the movement of point A along a circular arc can be approximated by the vertical distance δs as shown in Fig. 6-3(b). If the equilibrium of the nonrigid system is to be maintained, the virtual work δW done by all forces acting on the system must be zero. Thus,

$$\delta W = R_a \delta s - Py = 0$$

Note that the sign of the virtual work is positive if the displacement is in the same direction of the force and is negative if the displacement is opposite

to the direction of the force. For a moving unit load $P = 1$ and for a unit displacement $\delta s = 1$, we have $y = R_a$. This means that the ordinate at point D of the displaced system is equal to the reaction at A due to a unit load at D. Hence, the deflected shape of the nonrigid system in Fig. 6-3(b) is the influence line for reaction R_a.

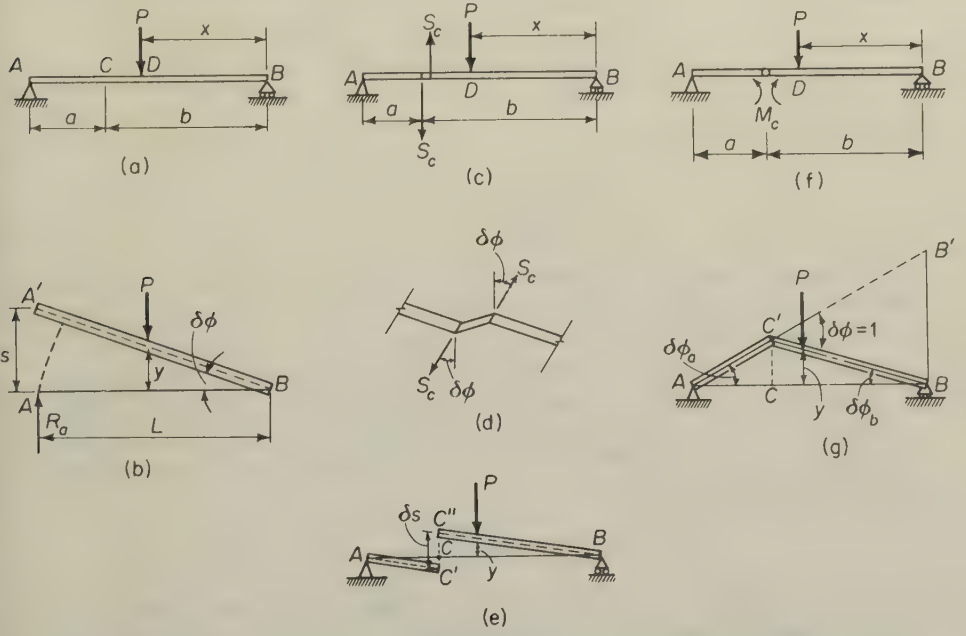

Figure 6–3

In order to obtain the influence line for shear at point C of the beam in Fig. 6-3(a), we remove the shearing constraint at point C and replace it by a pair of shear forces S_c. This may be thought of as introducing an infinitesimal element at point C so that no shear can be transmitted through the element as shown in Fig. 6-3(c). Note that the shear forces S_c on the left and right faces of the element are both positive with reference to segments AC and BC of the beam respectively. If the element is given a small displacement, causing an angular distortion $\delta\varphi$ in the element as shown in Fig. 6-3(d), it will produce rotations in beam segments AC' and BC''. Since AC' and BC'' must have the same angle of rotation $\delta\varphi$ as a result of the same angular distortion on both faces of the element, AC' and BC'' are parallel as shown in Fig. 6-3(e). For an infinitesimal element, the linear displacement $\delta s = C'C''$ may be considered as a vertical line. Thus, the virtual work done by all forces acting on the nonrigid system is

$$\delta W = S_c(CC' + CC'') - Py = S_c\delta s - Py = 0$$

For $P = 1$ and $\delta s = 1$, we obtain $y = S_c$. This implies that the ordinate at point D of the displaced system is equal to the shear at C due to a unit load at D. Hence, the deflected shape of the nonrigid system in Fig. 6-3(e) is the influence line for shear at point C of the beam. The ordinates of the influence line at C' and C'' may be obtained from the relations of similar triangles. Thus,

$$\frac{CC'}{C'C''} = \frac{a}{L} \quad \text{and} \quad \frac{CC''}{C'C''} = \frac{b}{L}$$

For $\delta s = C'C'' = 1$, we get

$$CC' = \frac{a}{L} \quad \text{and} \quad CC'' = \frac{b}{L}$$

In constructing the influence line for moment at point C of the beam, we remove the bending constraint for moment at C by introducing a hinge at that point, and replace the constraint by a moment M_c on each side of the hinge as shown in Fig. 6-3(f). Note that the moment M_c on each side of the hinge is positive with reference to the corresponding segment of the beam. If a small rotation $\delta\varphi$ is applied at hinge C, the system will displace as shown in Fig. 6-3(g). Then, the virtual work done by all forces acting on the nonrigid system is

$$\delta W = M_c(\delta\varphi_a + \delta\varphi_b) - Py = M_c\,\delta\varphi - Py = 0$$

For $P = 1$ and $\delta\varphi = 1$, we have $y = M_c$. Thus, the ordinate at point D of the displaced system is equal to the moment at C due to a unit load at D. The deflected shape of the nonrigid system in Fig. 6-3(g) is, therefore, the influence line for moment at point C of the beam. The ordinate of the influence line at C can be obtained from the relations of similar triangles. For small angles of $\delta\varphi$, the vertical distance BB' can be approximated by the arc length $b\,\delta\varphi$. Hence,

$$\frac{CC'}{BB'} = \frac{a}{L} \quad \text{or} \quad CC' = \frac{ab\,\delta\varphi}{L}$$

For $\delta\varphi = 1$, we get $CC' = ab/L$.

We have demonstrated that the principle of virtual displacements may be used to construct influence lines. It is obvious that, for statically determinate structures, the influence lines consist only of straight line segments because such structures are considered as rigid except at the point where a constraint is removed, and the deflected shape of the resulting nonrigid system obtained by the method of virtual displacements is defined by straight line segments. Once the shape of an influence line is known, the ordinates may readily be determined from the geometrical relations.

Example 6-2. Construct the influence lines by the method of virtual displacements for the following effects in the beam shown in Fig. 6-4(a): (a) reaction at support A, (b) shear at point E, and (c) moment at point F.

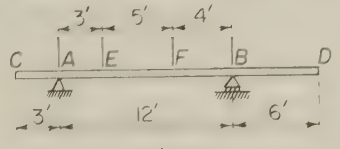

(a)

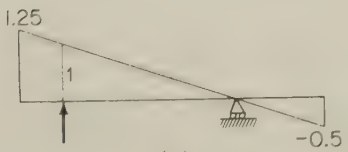

(b)

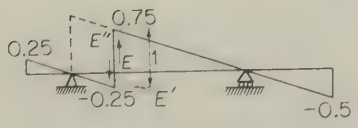

(c)

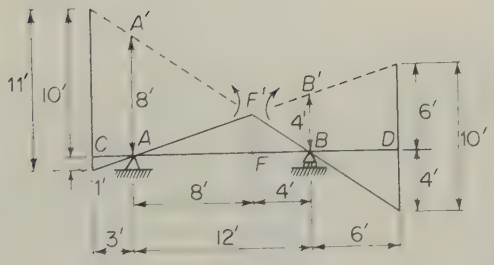

(d)

Figure 6-4

In constructing the influence line for reaction R_a, we remove the vertical constraint at A and introduce a unit vertical displacement at point A of the nonrigid system as shown in Fig. 6-4(b). The ordinates at points C and D are then obtained from the relations of similar triangles.

For the influence line for shear S_e, we remove the shearing constraint at E and introduce a unit vertical displacement at point E as shown in Fig. 6-4(c). Then, from the geometrical relations, we have

$$EE' = (1)\,(9)/12 = 0.75$$

$$EE'' = (1)\,(3)/12 = 0.25$$

The ordinates at points C and D are also obtained from the relations of similar triangles.

For the influence line for moment M_F, we remove the bending constraint at F and introduce a unit rotation at point F as shown in Fig. 6-4(d). Thus, $AA' = (1)(8) = 8$ and $BB' = (1)(4) = 4$. The ordinate FF' may be obtained from either the triangle ABB' or ABA'. Thus,

$$FF' = (8)(4)/12 = \tfrac{8}{3}$$

The ordinates at points C and D are found to be -1 and -4 respectively.

6-3 *Application of Influence Lines*

In the previous sections, two distinctly different approaches have been presented for the construction of influence lines. Each approach is based on a different concept but each is important and has wide applications. The study of the variations of effects on a structure caused by a moving unit load is a preliminary step for the determination of the position of live loads that will produce maximum effects on the structure, whereas the principle of virtual displacements leads to the visualization of the deflected shapes of systems that are released from certain constraints. Although we are dealing only with influence lines for statically determinate structures in this chapter, we shall discuss the significance of both aspects of application in broader terms.

Maximum effects of live loads. When a series of live loads moves on a structure, the maximum effects may in general be obtained from the influence lines for those effects. If the live load consists of a series of concentrated loads, the combined effect of these concentrated loads can be obtained by the principle of superposition. Consider, for instance, the beam shown in Fig. 6-5(a), on which a series of three concentrated loads P_1, P_2, and P_3, is acting. Since P_2 and P_3 are maintained at fixed distances from P_1, the locations of P_2 and P_3 are known once the location of P_1 is assigned. Let y_1, y_2, and y_3 be the ordinates of the influence line for the left reaction R_a of the beam under the loads P_1, P_2, and P_3 respectively, as shown in Fig. 6-5(b). Then, by the principle of superposition, the total left reaction R_a due to loads P_1, P_2, and P_3 is equal to

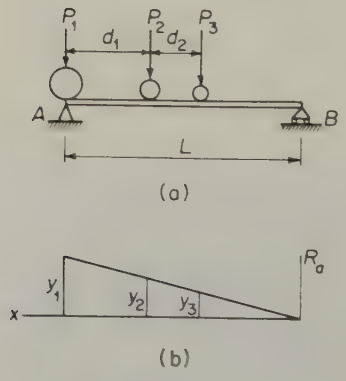

Figure 6–5

$$R_a = P_1y_1 + P_2y_2 + P_3y_3$$

In general, the effect may be the shear or moment at a point as well as the left reaction. If there are n concentrated loads $P_1, P_2, \ldots, P_n$ on the beam, and if $y_1, y_2, \ldots, y_n$ represent respectively the ordinates of the influence line for the effect involved, the effect is equal to the summation of the products of each load and influence ordinate under that load, or the total effect E is equal to

$$E = \sum_{i=1}^{i=n} P_i y_i$$

Although it is easy to compute the magnitude of a function due to a series of concentrated loads once the locations of these loads are determined, it is in general impossible to determine by inspection where these concentrated loads should be placed in order to produce a maximum value of a particular effect. In the simple case shown in Fig. 6-5, if $P_1 > P_2 > P_3$, it can be seen that the maximum value on the left reaction R_a is realized when the load P_1 is placed at point A. If the loads move toward the right, the ordinates y_1, y_2, and y_3 will be reduced and the reaction R_a will be smaller. On the other hand, if the loads move toward the left so that P_1 will be off the beam, the reaction R_a will still be smaller since P_2 and P_3 are smaller than P_1. For more complicated cases, the procedure of determining the maximum effects on the structure is essentially one of trial and error.

When the live load on the beam consists of a uniformly distributed load as shown in Fig. 6-6(a), its influence on a particular effect can also be obtained by superposition. For the left reaction R_a of the beam, for example, the load acting on an infinitesimal length δx of the beam is $w\,\delta x$. This load will cause a left reaction of $y\,w\,\delta x$, where y is the ordinate of the influence line for the left reaction as shown in Fig. 6-6(b). Thus, the total left reaction R_a due to the uniformly distributed load between D and E is

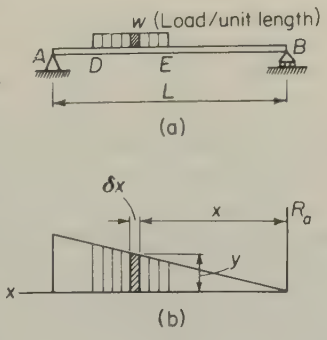

Figure 6-6

$$R_a = \int_d^e y\,w\,dx = w\int_d^e y\,dx = w\,A_{de}$$

in which A_{de} represents the area of the influence diagram bounded by the vertical lines passing through points D and E. It should be noted again that the effect on the beam under consideration may be the shear or moment at a point of the beam instead of the reaction at the left support. In general, it may be stated that the magnitude of the effect caused by a uniformly distributed load is equal to the product of the intensity of the load w and the area A_{ij} of the influence diagram bounded by the limits of the load between points i and j on the beam, or the total effect E is equal to

$$E = wA_{ij}$$

In dealing with a moving uniform load that is assumed to be longer than the span length of the beam, it is easy to determine by inspection what portion of the beam should be loaded in order to produce the particular maximum effect. In the case of the example for the left reaction shown in Fig. 6-6(a), the magnitude of the left reaction R_a is a maximum when the entire span is loaded, i.e., when the entire area of the influence diagram in Fig. 6-6(b) is included in the computation of the left reaction. On the other hand, for the maximum positive shear at point C of the beam shown in Fig. 6-7(a), only the portion CB of the beam should be loaded since the influence diagram for shear at point C in Fig. 6-7(b) indicates that the area between points C and B is positive and the area between points A and C is negative.

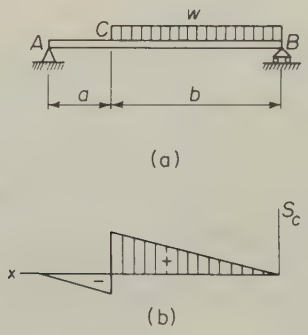

Figure 6–7

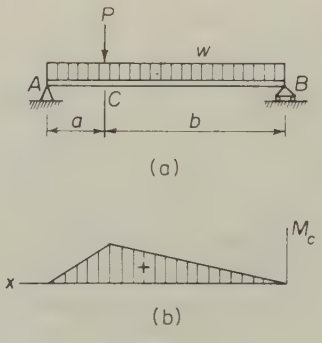

Figure 6–8

If a moving uniform load is accompanied by a single roving concentrated load which may be placed at any point so as to produce the maximum effect under consideration, the maximum effect can also be determined from the influence lines by inspection. For example, the maximum moment at point C of the beam shown in Fig. 6-8(a) is realized when the roving concentrated load is placed at C since the influence ordinate for moment at C in Fig. 6-8(b) is maximum at that point.

It may be concluded that the position of either a single concentrated load or a uniformly distributed load that will produce a certain maximum effect on a structure can be determined by inspection. When the live load consists of a series of concentrated loads, the position of the loading for producing a maximum effect can be located by trial and error. For statically determinate structures, however, criteria for maximum effects due to a series of concentrated loads can be established with the aid of influence lines.

In the design of highway bridges it is permissible to specify as live loads a uniform load plus a roving concentrated load although standard truck loads also may be used. On the other hand, locomotive wheel loads for railroad bridges or crane loads for crane runway girders are usually treated

as a series of concentrated loads. Therefore, criteria for maximum effects are primarily developed for the latter types of loading only.

Displacements of released systems. When a constraint is removed from a structure, the resulting system is said to be the released system of the original structure. For statically determinate structures, it has been demonstrated by the principle of virtual displacements that the deflected shape of the released system represents the shape of the influence line for that constraint in the original structure. Then, the ordinates of the influence line can readily be computed from the geometry of the deflected shape of the released system. For statically indeterminate structures the same concept may be applied to obtain the shape of an influence line although the computation of the ordinates of such an influence line is much more tedious because of the geometry of the deflected shape of the released system. Thus, if any constraint is removed from a statically indeterminate structure and a corresponding deforming effect is allowed to act through a unit virtual displacement, the resulting deflected shape is an influence line for the effect.* The general shape of an influence line is called a *qualitative influence line*, which is often useful in determining where to place live loads to produce a maximum effect in a statically indeterminate structure.

Consider, for example, a continuous beam with two spans as shown in Fig. 6-9(a). The structure is statically indeterminate to one degree. If a constraint is re-

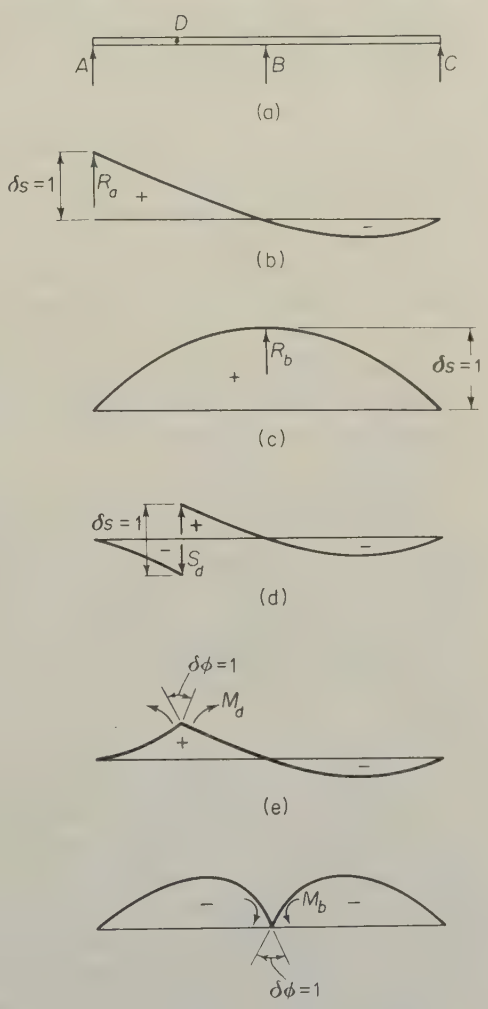

Figure 6-9

*This is known as *Müller-Breslau's principle*, the proof of which is given in Section 8-14.

moved from the structure, the resulting system will be statically determinate. In order to obtain the displacements of the released system, we must consider the load-deformation characteristics of the material of the structure. However, the general deflected shape of the released system may be sketched without actually computing the ordinates. If we remove the vertical constraint at support A and replace it by a vertical upward force at A, the deflected shape of the released system will be as shown in Fig. 6-9(b), which is also the qualitative influence for the reaction at A of the original structure. Similar influence lines have been drawn for reaction R_b, shear S_d, positive moment M_d, and negative moment M_b in Figs. 6-9(c) to (f) respectively. If a uniform live load is applied to the beam, we can determine by inspection of the influence lines what part of the beam should be loaded in order to produce certain maximum effects. If a roving concentrated load is included in the live load, its critical positions for various effects on the structure also may be located by inspection of the influence lines.

It can be seen that generally the influence lines for statically indeterminate structures consist of curves rather than straight line segments and that the ordinates of these influence lines can be obtained if the displacements of the corresponding released systems can be computed. Hence, the displacement computation of statically determinate structures is an important preliminary step in determining the ordinates of influence lines for statically indeterminate structures.

From the foregoing discussion, it is clear that the applications of influence lines will exceed by far the examples given for statically determinate structures in this chapter. On the other hand, criteria for maximum effects caused by a series of concentrated loads have only limited use for statically determinate structures. Our main emphasis, therefore, will be placed on the concept and construction of influence lines rather than their applications to determine maximum effects of live loads on statically determinate structures.

Example 6-3. A uniform live load w and a roving concentrated load P are to be placed on the continuous beam shown in Fig. 6-9(a). Determine where to place these loads in order to produce maximum effects in (a) reaction R_a, (b) reaction R_b, (c) positive shear S_d, and (d) positive moment M_d.

The positions of live loads that will produce maximum effects may be determined by inspection of the influence lines shown in Fig. 6-9. For maximum reaction R_a, the uniform load should be placed in span AB, with the roving concentrated load acting at point A. For maximum reaction R_b, both spans AB and AC should be loaded with the uniform load while the roving concentrated load should be placed at point B. For maximum positive shear S_d, only the portion DB of the beam should be loaded with the uniform load while the roving concentrated load should be placed just

to the right of point D. For maximum positive moment M_d, the uniform load should be placed in span AB, with the roving concentrated load acting at point D.

6-4 Compound Beams

The procedure for constructing influence lines for various effects on simple beams can easily be applied to compound beams. A unit load may be placed at a number of points along the beam where an abrupt change of the effect is expected. Since the effects on a statically determinate beam caused

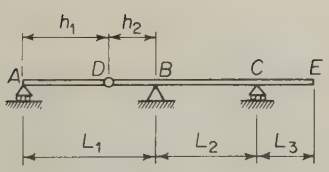

(a)

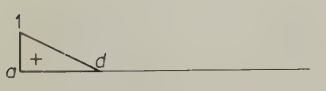

(b) R_a

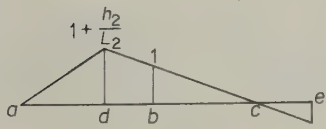

(c) R_b

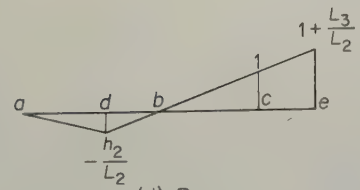

(d) R_c

Figure 6–10

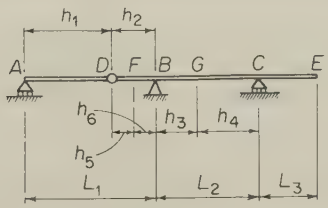

(a)

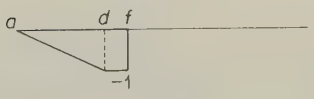

(b) S_f

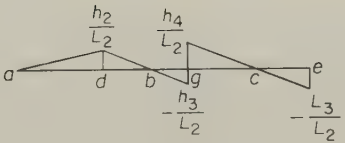

(c) S_g

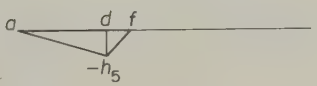

(d) M_f

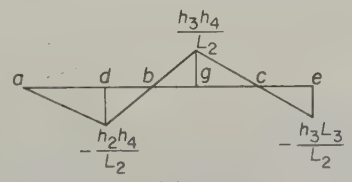

(e) M_g

Figure 6–11

by a moving unit load are found to be linear functions of the distance along the beam, the influence line between two computed ordinates can always be represented by a straight line.

Consider, for example, the construction of influence lines for reactions of the beam shown in Fig. 6-10(a). When the unit load is placed at A, the reaction $R_a = 1$ while the reactions at B and C are zero. If the unit load is placed at point D, the reaction at A is zero while the reactions at B and C are respectively

$$R_b = \frac{L_2 + h_2}{L_2} = 1 + \frac{h_2}{L_2} \quad \text{and} \quad R_c = -\frac{h_2}{L_2}$$

in which the positive result for R_b indicates an upward reaction at B and the negative sign for R_c indicates a downward reaction at C. As long as the unit load is placed outside of the beam segment AD, it will have no effect on reaction A but will continue to affect reactions B and C. Hence, the influence line for reaction at A is represented by the straight line in Fig. 6-10(b). The influence lines for reactions at B and C can be constructed by placing the unit load at points B, C, and E of the beam successively, and they are plotted in Figs. 6-10(c) and (d) respectively.

Next consider the construction of influence lines for shears at sections F and G of the same beam as shown in Fig. 6-11(a). When a unit load is placed between points A and D, the shear at F is equal to $R_a - 1$. In view of the influence line for reaction at A in Fig. 6-10(b), $S_f = 0$ at A and $S_f = -1$ at D. When the unit load is placed between D and F, the shear at F equals $S_f = -1$. As long as the unit load is placed outside of the beam segment AF, the shear at F is zero. Thus, the influence line for shear at section F is indicated in Fig. 6-11(b). The shear at section G can be obtained easily from the consideration of segment GE of the beam as a free body. When the unit load is placed anywhere between points A and G, the shear at G is equal to $-R_c$. Thus, $S_g = +h_2/L_2$ for the unit load at D and $S_g = -h_3/L_2$ for the load just to the left of G. When the unit load is placed between points G and E, the shear at G is equal to $-R_c + 1$. Thus, for the unit load just to the right of G,

$$S_g = -\frac{h_3}{L_2} + 1 = +\frac{h_4}{L_2}$$

and for the unit load at E,

$$S_g = -\left(1 + \frac{L_3}{L_2}\right) + 1 = -\frac{L_3}{L_2}$$

The influence line for shear at section G can be plotted as shown in Fig. 6-11(c). It may be noted that the influence line for shear at a section just to the left of reaction B has the same shape as that for the shear at section F when the distance h_6 approaches zero as a limit. On the other hand, the

influence line for shear just to the right of reaction B has the same shape as that for shear at section G as the distance h_3 approaches zero as a limit. Thus, the influence lines for the shears to the left and to the right of support B are entirely different.

The influence lines for moments at F and G of the same beam may be obtained in a similar manner. For a unit load at A, the moment at F is zero, and for the unit load at D, the moment at F is $-(1)(h_5) = -h_5$. The moment at F will again be zero when the unit load is placed at F or outside of the beam segment AF. Thus, the influence line for moment at F is indicated by Fig. 6-11(d). The moment at G can also be obtained easily from the consideration of segment GE of the beam as a free body. Thus, when the unit load is placed anywhere to the left of G or at G, the moment at G is equal to $R_c h_4$, or

$$M_g = 0 \qquad \text{for unit load at } A$$

$$M_g = -\frac{h_2 h_4}{L_2} \qquad \text{for unit load at } D$$

$$M_g = 0 \qquad \text{for unit load at } B$$

$$M_g = \frac{h_3 L_4}{L_2} \qquad \text{for unit load at } G$$

When the unit load is placed at a point to the right of G or at G, the moment at G is equal to $R_c h_4$ minus the product of the load and its distance from G. Hence, with the unit load at E,

$$M_g = \left(1 + \frac{L_3}{L_2}\right) h_4 - (1)(L_3 + h_4) = \frac{L_3 h_4}{L_2} - L_3$$

$$= -\left(1 - \frac{h_4}{L_2}\right) L_3 = -\frac{h_3 L_3}{L_2}$$

The influence lines shown in Figs. 6-10 and 6-11 may also be obtained by the principle of virtual displacements. Consider, for example, the influence line for reaction R_b. If the vertical constraint at B of the beam is removed and replaced by an upward force R_b, the deflected shape of the released system due to a unit virtual displacement at B will be as shown in Fig. 6-12(a). For the influence line for shear S_g, the shearing constraint at point G is removed and replaced by a pair of shear forces S_g. Then, the deflected shape of the released system resulting from a unit virtual displacement at G will be as shown in Fig. 6-12(c). For the influence line for

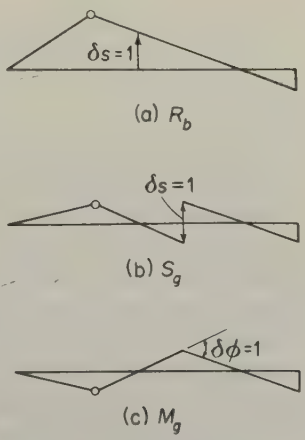

Figure 6-12

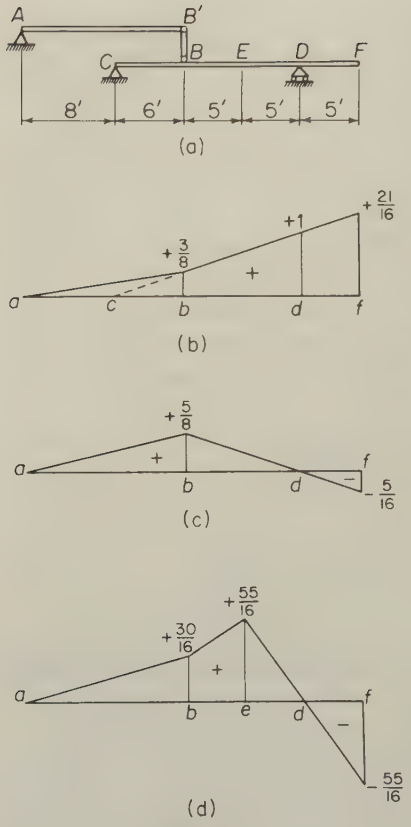

Figure 6–13

moment M_g, the bending constraint is removed and replaced by a pair of moments M_g. Thus, the deflected shape of the released system resulting from a unit virtual rotation at G will be as shown in Fig. 6-12(c). If the ordinates of the deflected shapes in Fig. 6-12 are computed from the relations of similar triangles, the results are identical to those for the corresponding influence lines obtained by the concept of a moving unit load.

Example 6-4. For the compound beam shown in Fig. 6-13(a), construct the influence line for (a) reaction at D, (b) shear at a section to the left of B, and (c) moment at E.

By placing a unit load at points A, B, E, and F successively, the specified effects on the beam can be computed as explained in this section. Hence, the required influence lines are constructed as shown in Figs. 6-13(b), (c), and (d) respectively.

6-5 *Girders Supporting Floor Beams*

In Section 3-6 we discussed the computation of reactions, shears, and moments for girders supporting floor beams under stationary loads. We pointed out that the introduction of floor beams on a girder has no effect on the reactions. Furthermore, the shear within each panel of a girder supporting floor beams is constant, and the moments at panel points of a girder supporting floor beams are identical to the moments at the corresponding points of a girder that supports applied loads directly. When a moving load is applied to a girder supporting floor beams, it can be seen that the influence line for reaction at a support remains the same as that for a girder without floor beams. The influence line for shear will be constructed for shear in a panel rather than at a section since the shear is constant within a panel. Although the influence line for moment at a panel point is not affected by the floor beams, the influence line for moment at a section

within a panel will be slightly different. We shall, therefore, discuss the modifications necessary for the construction of influence lines for shear and moment in girders supporting floor beams.

Shears. The construction of an influence line for shear in panel CD of a girder supporting floor beams is shown in Fig. 6-14(a). The ordinates

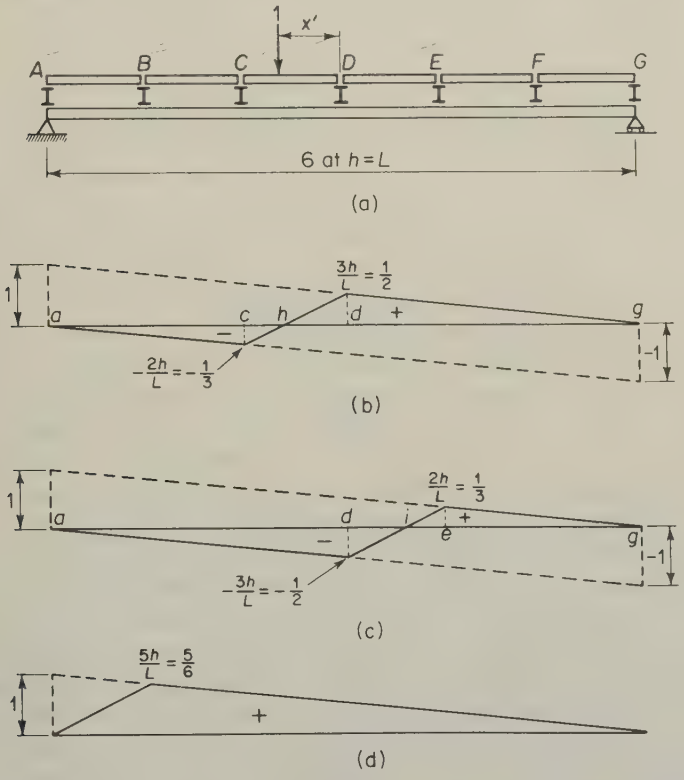

Figure 6–14

of the influence diagram can be obtained by placing the unit load at various panel points successively. As the unit load moves on a stringer from one panel point to another, the influence line between the panel points will vary linearly in the panel because the reactions of the stringer, which are in turn transmitted as loads on the girder through the floor beams, also vary linearly in the panel. As long as the unit load is in a position to the right of panel point D, the shear in panel CD equals the reaction R_a. If the unit load moves to the left of panel point C, the shear in panel CD is negative and numerically equal to reaction R_g. When the unit load is placed in panel CD, the shear in panel CD equals the reaction R_a minus the panel load at C, which is

numerically equal to the stringer reaction at C. Since the reaction $R_a = (x' + 3h)/L$ and the panel load at C is x'/h, the shear in panel CD is

$$S_{cd} = \frac{x' + 3h}{L} - \frac{x'}{h} = \frac{x' + 3h - 6x'}{6h} = \frac{1}{2} - \frac{5x'}{6h}$$

which is a linear function of x'. Thus, the influence line for shear in panel CD of the girder takes the shape as shown in Fig. 6-14(b). The influence lines for shears in other panels may be constructed in a similar manner. For example, the influence line for shear in panel DE is shown in Fig. 6-14(c), and the influence line for shear in end panel AB is shown in Fig. 6-14(d).

For a uniform load moving across the span of the girder, the maximum positive shear in a panel will occur when the uniform load extends over the portion of the span for which the influence ordinates are positive. For the shear in panel CD, this length is denoted by hg in Fig. 6-14(b); for the shear in panel DE, it is denoted by ig in Fig. 6-14(c). It may be noted that in the influence diagram for shear in panel CD, the positive area is greater than the negative area. Hence, the positive maximum shear is numerically greater than the negative maximum shear, and the absolute maximum shear in the panel CD is obtained when the uniform load is placed over the portion of span indicated by hg in Fig. 6-14(b). On the other hand, the negative maximum shear for panel DE is numerically greater than the positive shear for the panel. Then, the maximum shear in panel DE will be realized when the uniform load occupies the portion of span indicated by ai in Fig. 6-14(c). The points h and i in Figs. 6-14(b) and (c) respectively are called *neutral points*, which can be located by the geometrical relation of similar triangles. It may be further observed that for girders with floor beam spacings symmetrical with respect to a centerline at the midspan, the influence diagram for shear in a panel of the girder is antisymmetrical to that in the corresponding panel on the other side of the centerline. For example, the influence line for shear in panel CD of the girder shown in Fig. 6-14(a) is antisymmetrical to that in panel DE, as is evidenced from the influence diagrams in Figs. 6-14(b) and (c). Hence, it is only necessary to construct influence lines for shear in panels on half of the span if the maximum shear in every panel of the girder is required.

Moments. The influence line for moment at a panel point of a girder supporting floor beams has the same shape as the corresponding influence line for a girder without floor beams. For example, the influence line for moment at panel point C of the girder shown in Fig. 6-15(a) is given in Fig. 6-15(b). If the influence line for moment at some section of the girder other than the panel points is desired, it can be constructed by placing a moving unit load on the span. Consider, for example, the moment at point J of the girder shown in Fig. 6-15(a). For any position of the unit load to

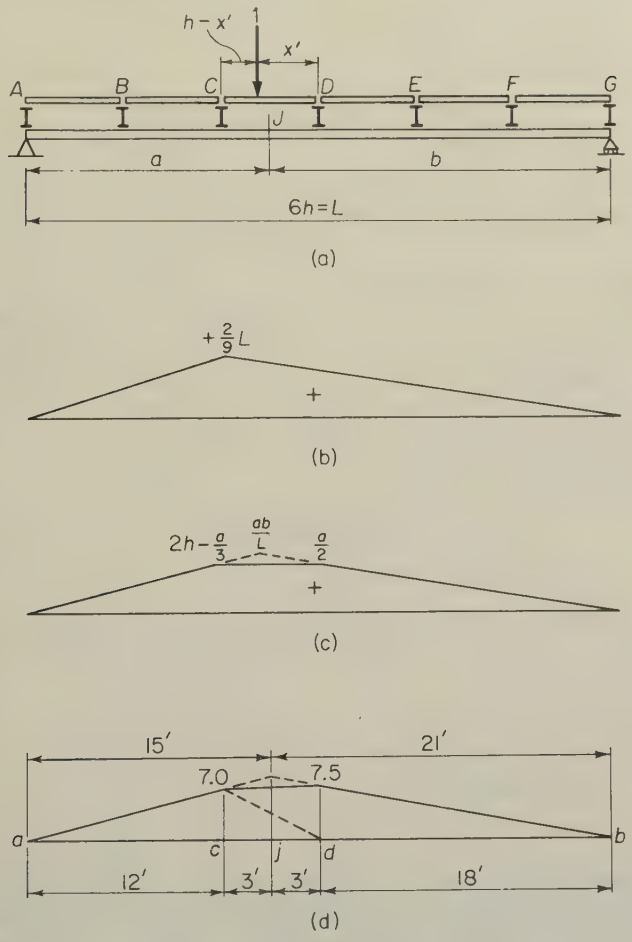

Figure 6–15

the right of panel point D, the moment at J equals $R_a a$, and for any position of the unit load to the left of panel point C, the moment at J equals $R_g b$. When the unit load is placed in panel CD, the moment at J is equal to $R_a a$ minus the moment at J due to the panel load at C caused by the reaction of the stringer CD. Thus,

$$M_j = \frac{x' + 3h}{L} a - \frac{x'}{h}(a - 2h)$$

For a given point J, the length a is constant and the moment M_j is a linear function of x'. At point D, $x' = 0$, we have

$$M_j = \frac{3h}{6h} a = \frac{a}{2}$$

At point C, $x' = h$, we get

$$M_j = \frac{4h}{6h}a - (a - 2h) = 2h - \frac{a}{3}$$

Hence, the influence line between panel points C and D is represented by a straight line joining these two ordinates as shown in Fig. 6-15(c).

Example 6-5. If the beam shown in Fig. 6-15(a) has a span length of 36 ft and point J is located 15 ft from support A, determine the maximum moment at point J due to a uniform load of 2 kips/ft and a roving concentrated load of 20 kips.

In this case, $a = 15$ ft, $b = 21$ ft, $L = 36$ ft, and $h = {}^{36}\!/_{6} = 6$ ft. For the influence line for M_j shown in Fig. 6-15(d), we have $ab/L = 8.75$. Then, the ordinates at points C and D of the beam are obtained as follows:

$$y_c = (8.75)\,({}^{12}\!/_{15}) = 7.0$$

$$y_d = (8.75)\,({}^{18}\!/_{21}) = 7.5$$

This can be checked by direct substitution into the previously given formulas for M_j. Then,

$$y_c = 2h - \frac{a}{3} = (2)\,(6) - \frac{15}{3} = 7.0$$

$$y_d = \frac{a}{2} = \frac{15}{2} = 7.5$$

The uniform load will be placed over the entire span length while the roving concentrated load should be placed at point D where the ordinate of the influence line is maximum. Thus, the maximum moment due to the given loading is equal to

$$M_j = (2)\,({}^{1}\!/_{2})\,[(12)\,(7) + (6)\,(7) + (6)\,(7.5) + (7.5)\,(18)] + (20)\,(7.5)$$

$$= 306 + 150 = 456 \text{ kips}$$

6-6 *Three-hinged Arches*

In the case of curved members, the influence lines for normal force, shear, and moment at a section are influenced by the horizontal reaction H. It is usually necessary to obtain first the influence line for the horizontal thrust H in the analysis of an arch rib.

Consider the three-hinged arch shown in Fig. 6-16(a). Let a moving concentrated load P be applied directly to the arch rib as indicated. By

considering the entire structure as a free body, we obtain

$$\sum F_x = 0, \quad H_a = H_c = H$$

$$\sum M_c = 0, \quad V_a = \frac{Px}{L} + \frac{Hh}{L}$$

$$\sum M_a = 0, \quad V_c = \frac{P(L-x)}{L} - \frac{Hh}{L}$$

By considering the left half of the structure as a free body and by taking moments about hinge B, i.e., $\Sigma M_b = 0$,

$$V_a a - H(r + t) = 0$$

Using the relation of similar triangles $t = ah/L$ in Fig. 6-16(a), we get

$$\left(\frac{Px}{L} + \frac{Hh}{L}\right) a - H\left(r + \frac{ah}{L}\right) = \frac{Pxa}{L} - Hr = 0$$

or

$$H = \frac{Pxa}{Lr}$$

Now imagine a fictitious beam having the same span length L and the same vertical loading as the three-hinged arch. Then, the vertical reactions of such a beam as shown in Fig. 6-16(b) are

$$R_a = \frac{Px}{L} \quad \text{and} \quad R_c = \frac{P(L-x)}{L}$$

The moment at point B of the beam is $M_b' = R_a a$. Then, the components of reactions of the three-hinged arch can be expressed in terms of the reactions of the fictitious simple beam as follows:

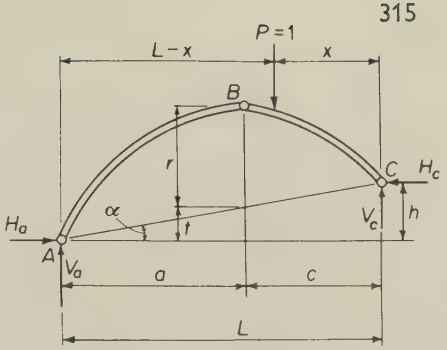

(a)

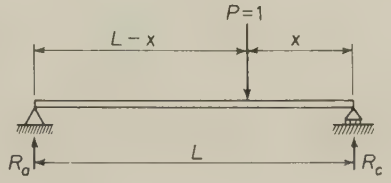

(b)

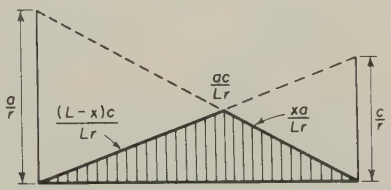

(c)

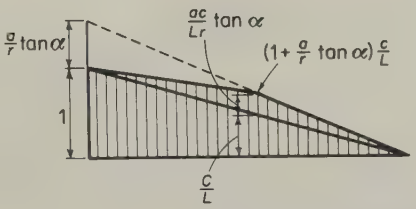

(d)

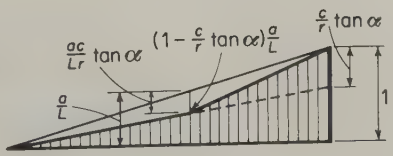

(e)

Figure 6–16

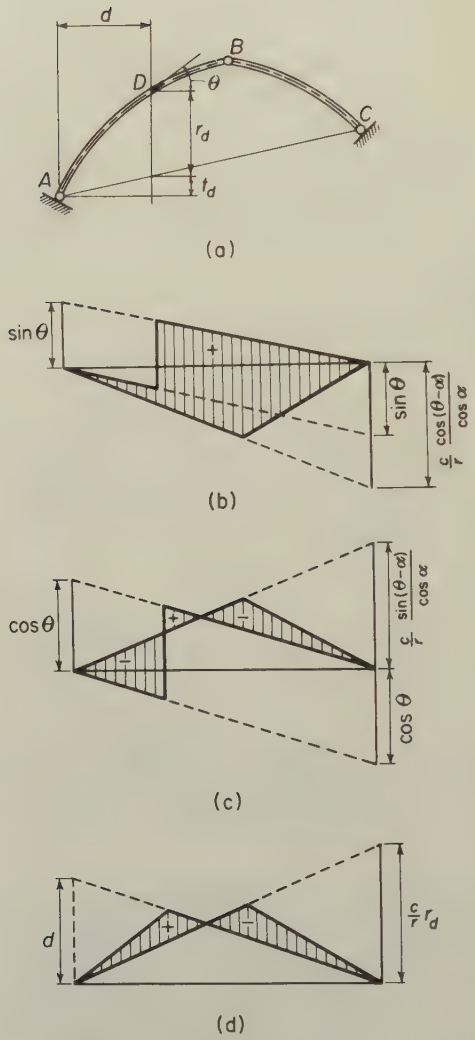

Figure 6–17

$$H = \frac{R_a a}{r} = \frac{M_b'}{r}$$

$$V_a = R_a + \frac{Hh}{L} = R_a + H\tan\alpha$$

$$V_c = R_c - \frac{Hh}{L} = R_c - H\tan\alpha$$

Thus, the influence line for the horizontal thrust H of the three-hinged arch is proportional to the moment at point B of the fictitious beam. The ordinates of the influence line for H can therefore be obtained from those for M_b' by dividing by the factor of proportionality r, and such an influence line is shown in Fig. 6-16(c). The influence lines for vertical reactions V_a and V_c can be obtained by superimposing the influence diagram representing $H\tan\alpha$ onto the corresponding influence diagrams for the vertical reactions of the fictitious beam. The results of the superposition are shown in Figs. 6-16(d) and (e) respectively.

The normal force, shear, and moment at a section passing through point D of the arch rib as shown in Fig. 6-17(a) also can be expressed in terms of the reactions of the fictitious beam. Thus, for the unit load placed at a point to the right of point D,

$$\begin{aligned} N_d &= V_a\sin\theta + H\cos\theta \\ &= (R_a + H\tan\alpha)\sin\theta + H\cos\theta \\ &= R_a\sin\theta + H\frac{(\cos\theta\cos\alpha + \sin\theta\sin\alpha)}{\cos\alpha} \\ &= R_a\sin\theta + H\frac{\cos(\theta-\alpha)}{\cos\alpha} \end{aligned}$$

$$\begin{aligned} S_d &= V_a \cos\theta - H \sin\theta \\ &= (R_a + H \tan\alpha) \cos\theta - H \sin\theta \\ &= R_a \cos\theta - H \frac{(\sin\theta \cos\alpha - \sin\alpha \cos\theta)}{\cos\alpha} \\ &= R_a \cos\theta - H \frac{\sin(\theta - \alpha)}{\cos\alpha} \end{aligned}$$

Similarly, for the unit load placed at a point to the left of point D,

$$N_d = (R_a - 1) \sin\theta + H \frac{\cos(\theta - \alpha)}{\cos\alpha}$$

$$S_d = (R_a - 1) \cos\theta - H \frac{\sin(\theta - \alpha)}{\cos\alpha}$$

When the unit load is placed to the right of point D, the moment at point D is equal to

$$M_d = V_a d - H(r_d + t_d) = \left(R_a + \frac{Hh}{L}\right) d - H\left(r_d + \frac{dh}{L}\right) = R_a d - H r_d$$

When the unit load is placed to the left of point D, M_d can be computed accordingly. For a given location of D, the angle θ can be computed from the shape of the arch rib. Hence, the influence lines for N_d, S_d, and M_d can be obtained by the principle of superposition as shown in Figs. 6-17(b), (c), and (d) respectively. It is necessary only to point out that the ordinates of the influence lines may also be plotted along a horizontal base if so desired.

Example 6-6. The parabolic rib of the three-hinged arch in Fig. 6-18(a) can be represented by the equation

$$y = (\tfrac{3}{320})\, x^2$$

with coordinate axes directed as shown. Draw the influence lines for the normal force, shear, and moment at point D of the arch.

Since $\tan\alpha = h/L = 26.25/140 = 0.1874$, we get $\sin\alpha = 0.185$ and $\cos\alpha = 0.983$. At point D, the angle θ can be obtained by

$$\tan\theta = \left.\frac{dy}{dx}\right|_{x=40} = \left.\frac{3x}{160}\right|_{x=40} = \frac{3}{4}$$

from which $\sin\theta = \frac{3}{5} = 0.6$ and $\cos\theta = \frac{4}{5} = 0.8$. Hence,

$$\frac{\cos(\theta - \alpha)}{\cos\alpha} = \frac{(0.8)(0.983) + (0.6)(0.185)}{0.983} = 0.91$$

$$\frac{\sin(\theta - \alpha)}{\cos\alpha} = \frac{(0.6)(0.983) - (0.185)(0.8)}{0.983} = 0.45$$

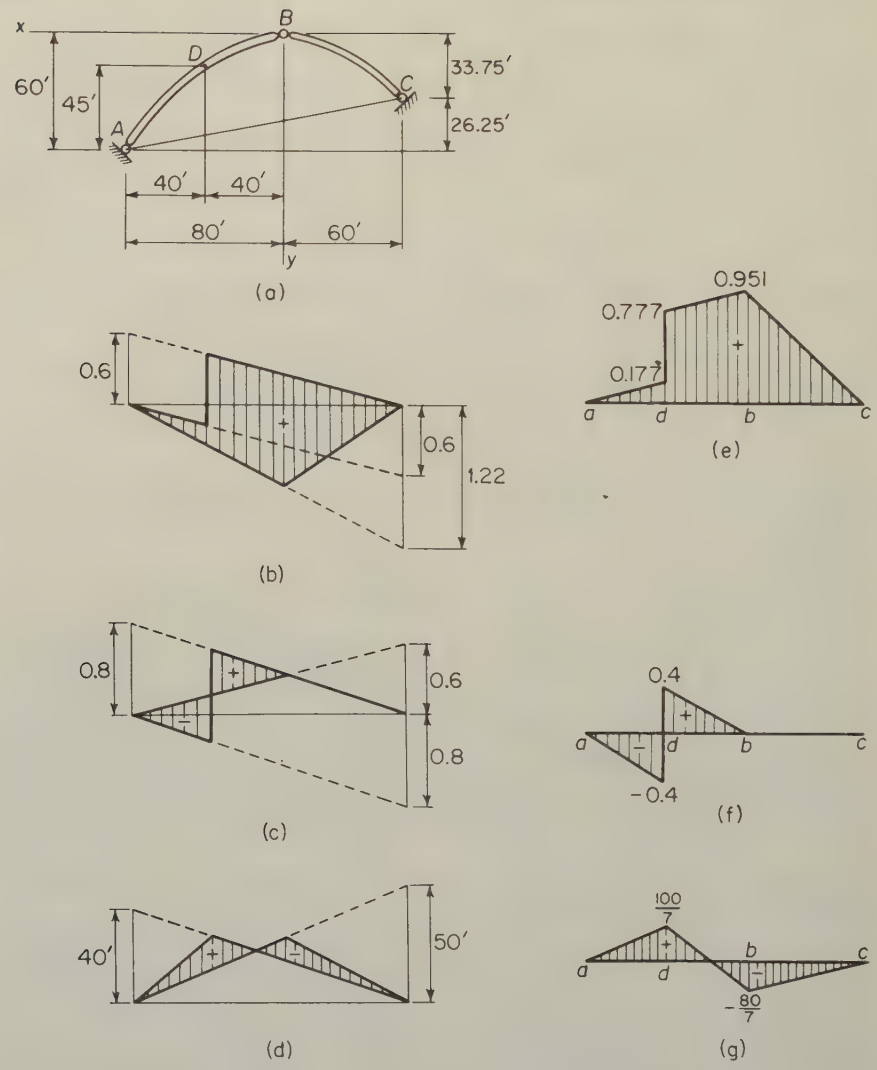

Figure 6–18

Since $c = 60$ ft, $d = 40$ ft, $r = 60 - (26.25)(8/14) = 45$ ft, and $r_d = 45 - 7.5 = 37.5$ ft,

$$\frac{c}{r}\frac{\cos(\theta - \alpha)}{\cos\alpha} = \left(\frac{60}{45}\right)(0.91) = 1.22$$

$$\frac{c}{r}\frac{\sin(\theta - \alpha)}{\cos\alpha} = \left(\frac{60}{45}\right)(0.45) = 0.6$$

$$\frac{c}{r}r_d = \left(\frac{60}{45}\right)(37.5) = 50$$

Thus, the influence lines for N_d, S_d, and M_d can be plotted as shown in Figs. 6-18(b), (c), and (d), respectively. However, these influence lines can also be plotted along a horizontal base as shown in Figs. 18(e), (f), and (g), the ordinates of which have been obtained by considering the relation of similar triangles in Figs. 6-18(b), (c), and (d), respectively.

In Fig. 6-18(e), the ordinates to the left and right of d are respectively equal to

$$y_{dl} = (40/140)(1.22 - 0.6) = 0.177$$

$$y_{dr} = (40/140)(1.22) + (100/140)(0.6) = 0.777$$

Similarly,

$$y_b = (80/140)(1.22) + (60/140)(0.6) = 0.951$$

In Fig. 6-18(f), we have

$$y_{dl} = (40/140)(-0.8) + (40/140)(-0.6) = -0.4$$

$$y_{dr} = (100/140)(0.8) + (40/140)(-0.6) = 0.4$$

In Fig. 6-18(g), we get

$$y_d = (100/140)(40) + (40/140)(-50) = 100/7$$

$$y_b = (80/140)(-50) + (60/140)(40) = -80/7$$

In the case of three-hinged arches supporting floor beams, the same procedure for the construction of influence lines may be applied with only slight modifications similar to those explained in Section 6-5 for girders supporting floor beams.

6-7 *Simple Trusses*

In constructing the influence line for the bar force in a member of a simple truss, it is necessary to determine first the most convenient approach for computing the bar force. For example, a bar force may be conveniently obtained by considering a certain part of the truss as a free body and by taking moments about a certain point, or it may be more conveniently computed from the shear force at a certain section of the truss. Thus, the effect of a moving unit load on the bar force can be directly related to that on the moment at a given point or the shear at a given section of the truss. The ordinates of the influence line for the bar force may then be obtained by proportion from that for moment or shear as the case may be.

The effects of moving loads on a truss can be determined from the influence lines for the bar forces in the truss. For a moving uniform load or a combination of moving uniform load and roving concentrated load, the procedure of computing the bar forces in a truss from the influence diagrams

for those members is straightforward and identical to that for computing the effects on beams discussed in Section 6-3. For a series of moving concentrated loads, criteria for maximum bar forces will be discussed later.

Example 6-7. Draw the influence lines for the bar forces in members U_1L_1, U_1L_2, U_1U_2, and L_2L_3 of the truss shown in Fig. 6-19(a).

For member U_1L_1, the bar force can be directly determined from the consideration of equilibrium of joint L_1. When the unit load is placed at L_1, the bar force is equal to 1 in tension. When the unit load is placed at any other joint, the bar force is zero. Thus, the influence line for the bar force in U_1L_1 is shown in Fig. 6-19(b). For member U_1L_2, the bar force can be conveniently computed by multiplying the shear in panel L_1L_2 by a factor of $\frac{5}{4}$. Thus, at joint L_1, the ordinate of the influence line is $(-\frac{1}{6})(\frac{5}{4}) = -\frac{5}{24}$, and at joint L_2, the ordinate is $(\frac{4}{6})(\frac{5}{4}) = \frac{5}{6}$. Since a positive shear at section a-a passing through panel L_1L_2 will cause tension in member U_1L_2, the sign of the influence coefficients for the bar force in U_1L_2 follows that of the shear in panel L_1L_2. The influence line for the bar force in U_1L_2 is shown in Fig. 6-19(c).

The bar force in member U_1U_2 can be obtained by considering the left of section b-b as a free body and by taking moments about joint L_2. Similarly, the bar force in member L_2L_3 is obtained by taking moments about joint U_2 of the free body. Although the unit load is placed at the bottom chord only, the unit load will cause the same moment about joint U_2 as about joint L_2. Thus, the ordinates of the influence line for the bar force in U_1U_2 are numerically equal to those for the bar force in L_2L_3. For instance, at joint L_2, the ordinates for both influence lines are numerically equal to the ordinate of the moment about joint L_2 divided by the height of the truss. Hence, at L_2, the ordinate is equal to

$$\frac{(2 \times 18)(4 \times 18)}{6 \times 18} \frac{1}{24} = 1$$

However, the signs of the ordinates of these influence lines are opposite to each other because member U_1U_2 is in compression and member L_2L_3 is in tension as a result of the consideration of equilibrium of the free body. The influence lines for the bar forces in U_1U_2 and L_2L_3 are shown in Figs. 6-19(d) and (e), respectively.

Example 6-8. Draw the influence line for the bar force in member DI of the truss shown in Fig. 6-20(a).

The bar force in member DI is obtained by first considering joint I as a free body and then the portion of the truss to the left of section a-a as a free body as shown in Figs. 6-20(b) and (c). It is possible therefore to relate

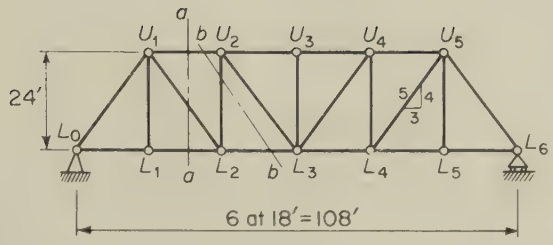

(a)

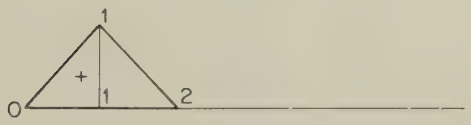

(b) U_1L_1

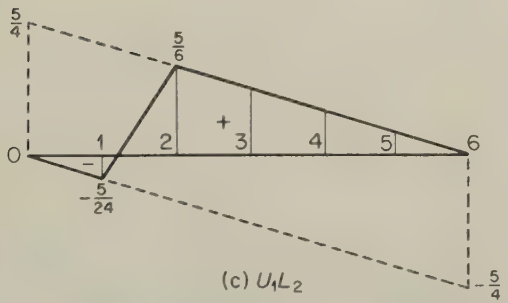

(c) U_1L_2

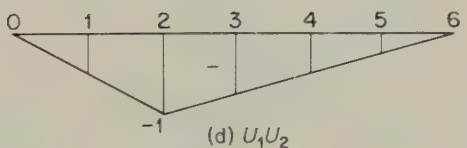

(d) U_1U_2

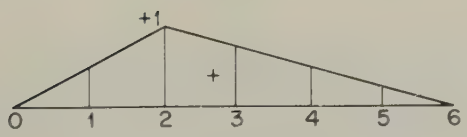

(e) L_2L_3

Figure 6–19

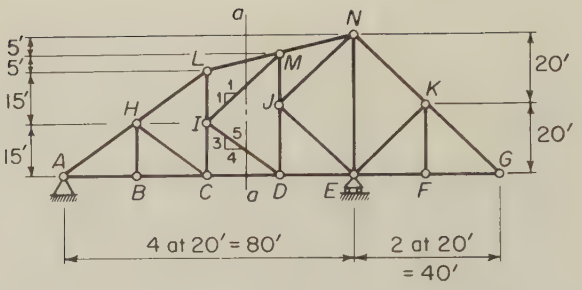

(a)

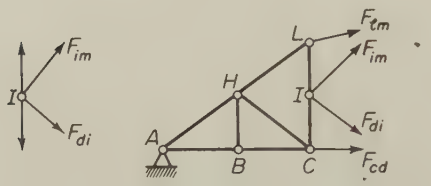

(b) (c)

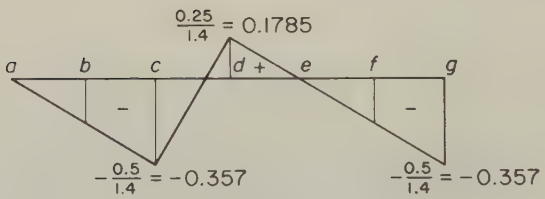

(d) $\frac{1}{1.4} S_{cd}$

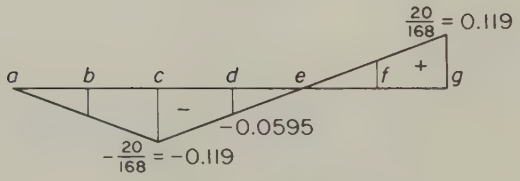

(e) $-\frac{1}{168} M_c$

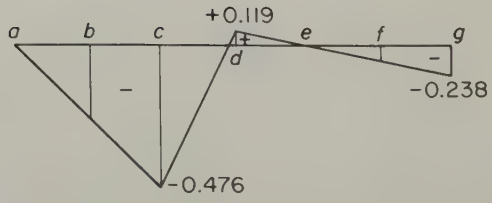

(f) F_{di}

Figure 6–20

this bar force to shear in panel CD and the moment about joint C. Let the subscripts x and y denote the components of bar forces in horizontal and vertical directions respectively, and assume that the bar forces are directed away from the joints. Then, from the sum of the horizontal forces in Fig. 6-20(b), we have

$$(F_{di})_x = -(F_{im})_x \quad \text{or} \quad \tfrac{4}{5} F_{di} = -0.707F_{im}$$

Hence, $F_{im} = -1.135F_{di}$. Furthermore, from the conditions of equilibrium of the free body in Fig. 6-20(c), we get

$$\sum M_c = 0, \quad (F_{lm})_x(30) + M_c = 0 \tag{a}$$

$$\sum F_y = 0, \quad (F_{lm})_y + (F_{im})_y - (F_{di})_y + S_{cd} = 0 \tag{b}$$

in which M_c is the moment of all *external* forces about joint C and S_{cd} is the vertical shear in panel CD due to the *external* forces, the sign convention for M_c and S_{cd} being the same as that for moment and shear in beams. Note that, in taking moments about joint C, the bar forces in members DI and IM do not enter into the equation because they can be resolved into components at joint I such that the vertical components will pass through the moment center C and the horizontal components are equal and opposite, thus cancelling each other. Hence, from Eq. (a),

$$(F_{lm})_x = -\frac{M_c}{30}$$

or

$$(F_{lm})_y = -\left(\frac{M_c}{30}\right)\left(\frac{5}{20}\right) = -\frac{M_c}{120}$$

and from Eq. (b),

$$-\frac{M_c}{120} + 0.707(F_{im}) - \frac{3}{5}(F_{di}) + S_{cd} = 0$$

Noting $F_{im} = -1.135F_{di}$, we obtain

$$1.4(F_{di}) = S_{cd} - \frac{M_c}{120} \tag{c}$$

or

$$F_{di} = \frac{1}{1.4} S_{cd} - \frac{1}{168} M_c \tag{d}$$

Thus, the influence line for F_{di} can be obtained from the influence lines for S_{cd} and M_c. The construction of the influence line for bar force in member DI is illustrated step by step in Figs. 6-20(d), (e), and (f).

Example 6-9. Determine the maximum bar forces in members U_2U_3, L_2L_3, and L_2U_3 of the truss shown in Fig. 6-21(a) due to a moving uniform load of 2 kips per foot.

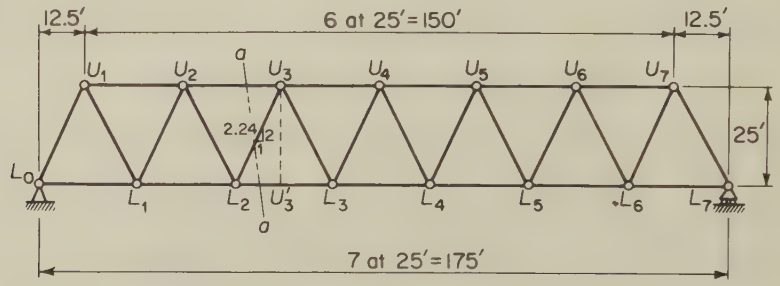

(a)

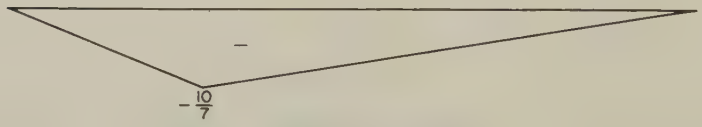

(b) Bar force in U_2U_3

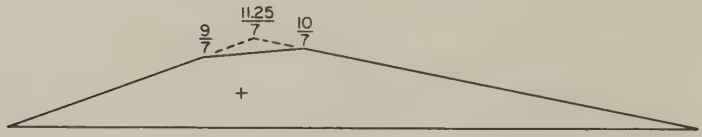

(c) Bar force in L_2L_3

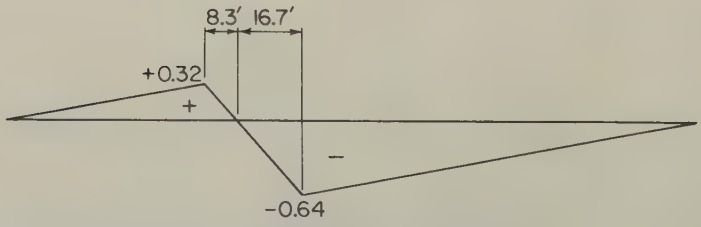

(d) Bar force in L_2U_3

Figure 6–21

Since the maximum bar force in a member of a truss subjected to a moving uniform load can be obtained from the area of the influence diagram for the bar force, the first step is to construct the influence lines for the required bar forces. By considering the portion of the truss to the left of

section *a-a* in Fig. 6-21(a) as a free body, the bar forces in members U_2U_3 and L_2L_3 can be obtained by taking moments about joints L_2 and U_3 respectively as follows:

$$F_{U_2U_3} = -\frac{M_{L_2}}{d} \quad \text{and} \quad F_{L_2L_3} = +\frac{M_{U_3}}{d}$$

in which $F_{U_2U_3}$ and $F_{L_2L_3}$ are the respective bar forces in members U_2U_3 and L_2L_3, M_{L_2} and M_{L_3} are the moments about L_2 and U_3 respectively in the free body, and d is the depth of the truss. Since the unit load is applied to the floor system and transmitted to the joints at the bottom chord of the truss, the influence line for moment about joint L_2 of the truss is identical to that for moment at the corresponding point of a beam having the same span length as the truss. The influence line for the bar force in member U_2U_3 is therefore obtained by proportion from that for moment at L_2. The result, indicated in Fig. 6-21(b), has a maximum ordinate at L_2 equal to

$$-\frac{1}{25}\frac{(50)(125)}{175} = -\frac{10}{7}$$

In order to produce maximum moment at joint U_3, the unit load should be placed in a position U_3' beneath joint U_3, as shown in Fig. 6-21(a). However, such a load is eventually transmitted through the floor system to joints L_2 and L_3 at the bottom chord of the truss. Hence, the influence line for moment at joint U_3 is identical to that for moment at point U_3' of a girder having the same span length as the truss and supporting floor beams at the same panel points as the truss. The influence line for the bar force in L_2L_3 is indicated by the solid lines in Fig. 6-21(c). The influence ordinate of the point of intersection of the dotted lines in the figure is equal to

$$+\frac{1}{25}\frac{(62.5)(112.5)}{175} = \frac{11.25}{7}$$

Then, the influence ordinates at L_2 and L_3 are respectively equal to

$$\left(\frac{11.25}{7}\right)\left(\frac{50}{62.5}\right) = \frac{9}{7} \quad \text{and} \quad \left(\frac{11.25}{7}\right)\left(\frac{100}{112.5}\right) = \frac{10}{7}$$

The bar force in member L_2U_3 can be computed from the shear at section *a-a* as follows:

$$F_{L_2U_3} = -\frac{2.24}{2} S_{23} = -1.12S_{23}$$

in which $F_{L_2U_3}$ is the bar force in the member and S_{23} is the shear in panel L_2L_3. Then, at L_2 and L_3 the ordinates of the influence line for the bar force in L_2U_3 are respectively equal to $(-1.12)(-\frac{2}{7}) = +0.32$ and (-1.12)

$(\frac{4}{7}) = -0.64$, and such an influence line is plotted in Fig. 6-21(d). The neutral point in the influence diagram is located by the relation of similar triangles.

The maximum bar forces in various members are obtained from the area of the influence diagrams for the respective members multiplied by the moving uniform load. With dimensionless coefficients for the ordinates, the product of the area of the diagram (in units of length) and the uniform load (in force per unit length) gives the bar force in the unit of force. Thus, for member U_2U_3, with the entire span loaded, the maximum bar force is

$$F_{U_2U_3} = (2)\,(\tfrac{1}{2})\,(-\tfrac{10}{7})\,(175) = -250 \text{ kips}$$

and for member L_2L_3, also with the entire span loaded, the maximum bar force is

$$F_{L_2L_3} = (2)\left(\frac{1}{2}\right)\left[\left(\frac{9}{7}\right)(50) + \left(\frac{10}{7}\right)(100) + \left(\frac{9+10}{7}\right)(25)\right] = +274 \text{ kips}$$

For member L_2U_3, however, the maximum compression is obtained when the portion of span representing the negative area of the influence diagram is loaded, and

$$F_{L_2U_3} = -(2)\,(\tfrac{1}{2})\,(0.64)\,(100 + 16.7) = -74.8 \text{ kips}$$

Similarly, the maximum tension is obtained when the positive area of the influence diagram is loaded. Then

$$F_{L_2U_3} = (2)\,(\tfrac{1}{2})\,(0.32)\,(50 + 8.3) = +18.7 \text{ kips}$$

It should be noted that when the truss is subjected to live load only, the bar force in member L_2U_3 may be in tension or in compression, depending on the location of the moving load. Under dead load, the member is subjected to compression only. Thus, the total bar force in the member due to the combination of dead load and live load may be a tension if the tension caused by the live load is greater than the compression caused by the dead load. The variation of the sense of direction of the bar force in a member as a result of the variation of the positions of the live load on a truss is known as the *reversal of bar force.*

6-8 *Compound Trusses*

The procedure for determining the maximum bar forces in a compound truss subjected to live loads is similar to that for analyzing simple trusses. As in the case of simple trusses, the effects of the moving loads on a compound truss can be studied from the influence lines for the bar forces in the truss. Here it will suffice to discuss only the modifications that are peculiar to compound trusses.

For compound trusses with secondary systems, the influence lines for bar forces in the primary systems can be obtained either by the superposition of the effects on the primary and secondary systems, or directly from the relation between the bar forces and the shears and moments at appropriate sections.

Example 6-10. Draw the influence lines for the bar forces in members L_4L_6, U_2U_4, M_3L_4, U_2M_3, U_4L_4, U_3M_3, and M_3U_4 of the Baltimore truss shown in Fig. 6-22(a) in which the upper chord is the loaded chord of the truss.

The bar force in member L_4L_6 can be obtained by taking moments about joint U_4 of the free body to the left of section *a-a* and is not affected by the presence of the secondary systems. On the other hand, the bar force in member U_2U_4 is affected by the small triangular secondary system $U_2U_4M_3$ when the unit load is placed between U_2 and U_4, although it can be computed by taking moments about joint L_4 of the free body to the left of section *b-b*. Thus, the ordinates of the influence line for the bar force in member L_4L_6 can be computed as if the secondary systems do not exist. This is shown in Fig. 6-22(b), with the ordinate at point 4 computed as follows:

$$(160/240)(80/48) = 10/9$$

Except in panel U_2U_4, the ordinates of the influence line for the bar force in member U_2U_4 will have the same magnitude as those for L_4L_6 but will be opposite in sign where the influence ordinates are affected by the secondary system. Since the effect varies linearly between U_2 and U_3, and between U_3 and U_4 due to the transmission of applied load through the floor system, it is necessary to compute only the ordinate at point 3 in order to construct the influence line for the bar force in member U_2U_4 as shown in Fig. 6-22(c). By placing the unit load at joint U_3 of the truss, the ordinate of the influence line at point 3 can be obtained as follows:

$$-(180/240)(80/48) = -5/4$$

Similarly, the bar force in member M_3L_4 can be related directly to the shear at section *c-c* in Fig. 6-22(a) without considering the effects of the secondary systems, whereas the bar force in member U_2M_3 is affected by the secondary system $U_2U_4M_3$ when the unit load is placed in panel U_2U_4. Thus, the influence line for the bar force in member M_3L_4 can be constructed as shown in Fig. 6-22(d), with ordinates at points 2 and 4 respectively equal to

$$-\left(\frac{7.88}{6}\right)\left(\frac{40}{240}\right) = -0.219$$

$$+\left(\frac{7.88}{6}\right)\left(\frac{160}{240}\right) = +0.876$$

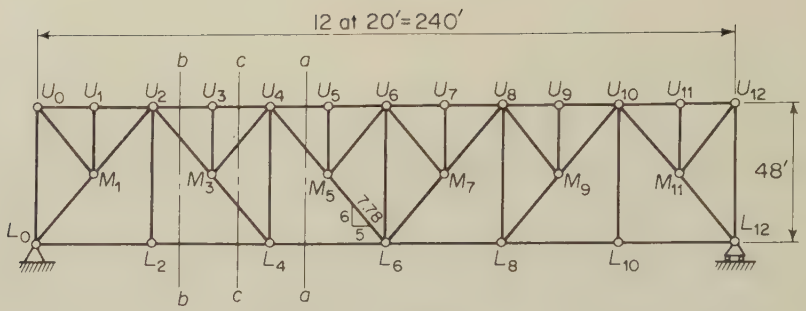

(a)

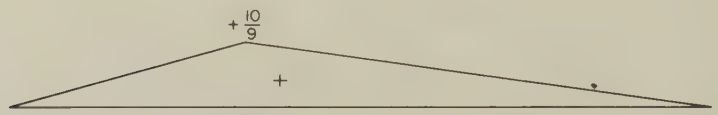

(b) Bar force in L_4L_6

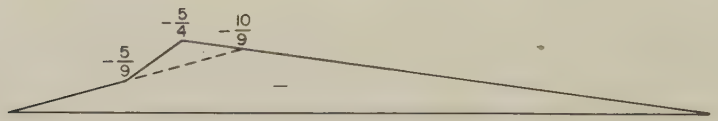

(c) Bar force in U_2U_4

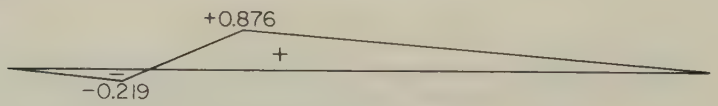

(d) Bar force in M_3L_4

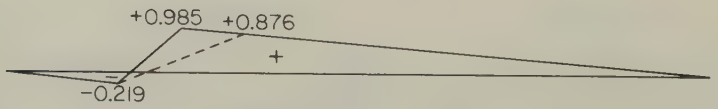

(e) Bar force in U_2M_3

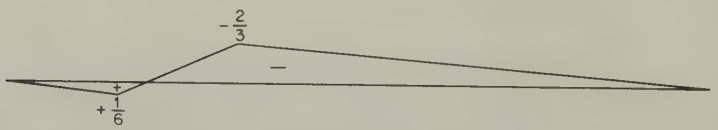

(f) Bar force in U_4L_4

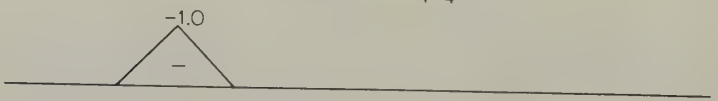

(g) Bar force in U_3M_3

(h) Bar force in M_3U_4

Figure 6–22

The influence line for the bar force in member U_2M_3 is shown in Fig. 6-22(e) in which the ordinate at point 3 can be computed by considering the shear at section *b-b* in Fig. 6-22(a) while the unit load is applied at joint U_3. Thus

$$\left(\frac{7.88}{6}\right)\left(\frac{180}{240}\right) = +0.985$$

The influence lines for the bar forces in the remaining members can be constructed in a straightforward manner as in the case of simple trusses and are shown in Figs. 6-22(f), (g), and (h) without further explanation.

Example 6-11. Draw the influence line for the bar force in member *CE* of the truss shown in Fig. 6-23(a).

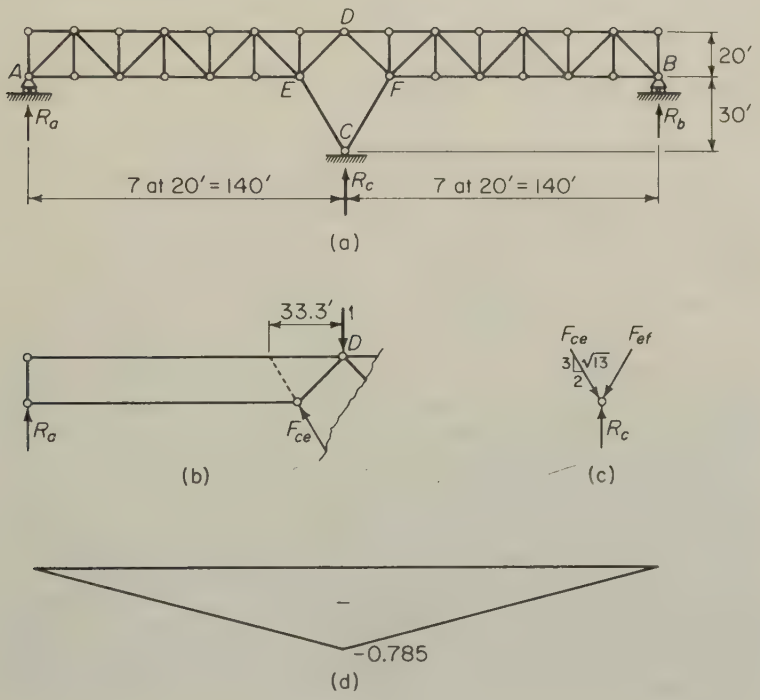

Figure 6–23

When a unit load is placed on the loaded chord over support *A* or *B*, the reaction at *C* is zero. When the unit load is placed at point *D*, we have, from $\Sigma F_y = 0$,

$$2R_a + R_c = 1$$

From the free body shown in Fig. 6-23(b), we obtain, by taking moments

about point D,

$$-140R_a - \left(\frac{3}{\sqrt{13}} F_{ce}\right)(33.3) = 0$$

From the free-body diagram in Fig. 6-23(c), we note that owing to symmetry, $\Sigma F_y = 0$ leads to

$$\frac{3}{\sqrt{13}} F_{ce} = \frac{R_c}{2}$$

Solving these three equations simultaneously, we obtain $F_{ce} = 0.785$. Since the sense of direction of the bar force has been assumed to be in compression, the positive result indicates that the assumed direction is correct. Thus, the influence line for the bar force in member CE may be plotted as shown in Fig. 6-23(d).

6-9 *Moment Tables for Concentrated Loads*

In a discussion of maximum effects of moving concentrated loads on structures, we are usually confronted with a large number of loads because, if the number of loads is small, the procedure of trial and error is quite satisfactory and there is no need for the development of criteria for maximum effects. Therefore, the direct computation of maximum reactions, shears, and moments in structures subjected to a series of concentrated loads is usually rather tedious. In order to avoid the burden of numerical calculations, the moments of a series of concentrated loads spaced at fixed distances relative to each other are taken about certain given points and are tabulated in a systematic manner. Such an arrangement is generally known as the *moment table* for the given series of concentrated loads.

Two examples of moment tables are given in Tables 6-1 and 6-2. In the numerical examples in this section and in subsequent sections, only these loadings are used so that the student will be spared unnecessary routine calculations. The application of the moment tables is based on the fact that the moment of a force system about a point may be replaced by an equivalent moment of the same magnitude and sense of direction. Consider, for example, a system of parallel forces $P_1, P_2, \ldots, P_n$ as shown in Fig. 6-24.

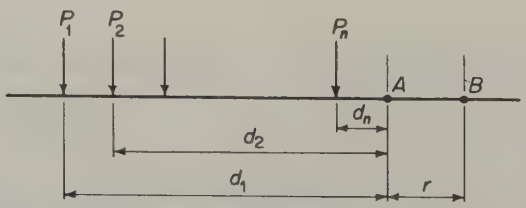

Figure 6–24

The moment of these forces about point A is equal to

$$M_a = P_1d_1 + P_2d_2 + \ldots + P_nd_n$$

Similarly, the moment of these forces about point B is

$$\begin{aligned} M_b &= P_1(d_1 + r) + P_2(d_2 + r) + \ldots + P_n(d_n + r) \\ &= P_1d_1 + P_2d_2 + \ldots + P_nd_n + (P_1 + P_2 + \ldots + P_n)r \\ &= M_a + Gr \end{aligned}$$

in which G is the sum of the forces $P_1, P_2, \ldots, P_n$. Thus, the moment of the forces about point B is equal to the moment of the same forces about point A plus a couple Gr. If the forces $P_1, P_2, \ldots, P_n$ are given and the distances $d_1, d_2, \ldots, d_n$ are fixed, we can compute the moment M_a. When the distance r is given, the computation of M_b consists of adding a couple Gr to M_a only.

TABLE 6-1

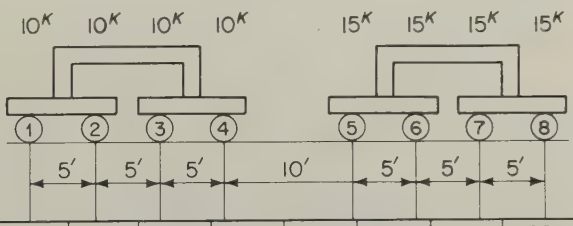

Spacings (ft)	0	5	10	15	25	30	35	40	L to R
	40	35	30	25	15	10	5	0	R to L
Loads (kips)	10	20	30	40	55	70	85	100	L to R
	100	90	80	70	60	45	30	15	R to L
Moments (ft–k) Due to loads 8 to	2	2250	50	100	150	250	300	350	400	1
	3	2200	1800	150	250	450	550	650	750	2
	4	2100	1750	1400	300	600	750	900	1050	3
	5	1950	1650	1350	1050	700	900	1100	1300	4
	6	1575	1350	1125	900	450	975	1250	1525	5
	7	1125	975	825	675	375	225	1325	1675	6
	8	600	525	450	375	225	150	75	1750	7

Moments (ft–k) Due to loads 1 to

As an example, the wheel loads for two cranes operating in tandem together with other pertinent data, are shown in Table 6-1. Under the heading for spacings in the table, the spacings between wheel loads are summed up accumulatively from left to right in the first line, and from right to left in the second line. Similarly, under the heading for loads, the wheel loads are summed up accumulatively from left to right in the first line, and from right to left in the second line. Under the heading of moments, the heavy zigzag line represents the division for the sum of moments about a point

Table 6-2

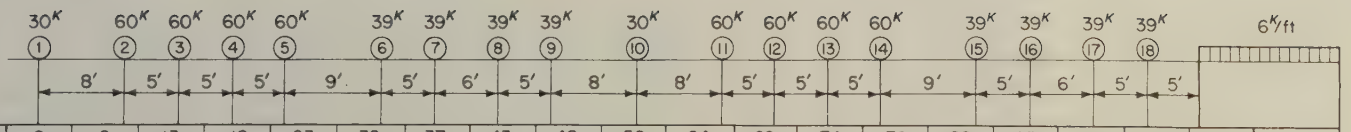

Spacings (ft)	0	8	13	18	23	32	37	43	48	56	64	69	74	79	88	93	99	104	109	L to R
	109	101	96	91	86	77	72	66	61	53	45	40	35	30	21	16	10	5	0	R to L
Loads (kips)	30	90	150	210	270	309	348	387	426	456	516	576	636	696	735	774	813	852	852	L to R
	852	822	762	702	642	582	543	504	465	426	396	336	276	216	156	117	78	39	0	R to L

Moments (ft–k) Due to loads from wheel no. 18 to wheel no.

2	43,776	240	390	540	690	960	1110	1290	1440	1680	1920	2070	2220	2370	2640	2790	2970	3120	3270	1
3	43,296	37,200	690	1140	1590	2400	2850	3390	3840	4560	5280	5730	6180	6630	7440	7890	8430	8880	9330	2
4	42,516	36,900	33,390	1440	2190	3540	4290	5190	5940	7140	8340	9090	9840	10,590	11,940	12,690	13,590	14,340	15,090	3
5	41,436	36,300	33,090	29,880	2490	4380	5430	6690	7740	9420	11,100	12,150	13,200	14,250	16,140	17,190	18,450	19,500	20,550	4
6	40,056	35,400	32,490	29,580	26,670	4920	6270	7890	9240	11,400	13,560	14,910	16,260	17,610	20,040	21,390	23,010	24,360	25,710	5
7	38,808	34,464	31,749	29,034	26,319	21,432	6456	8319	9864	12,336	14,808	16,353	17,898	19,443	22,224	23,769	25,623	27,168	28,713	6
8	37,365	33,333	30,813	28,293	25,773	21,237	18,717	8553	10,293	13,077	15,861	17,601	19,341	21,081	24,213	25,953	28,041	29,781	31,521	7
9	35,688	31,968	29,643	27,318	24,993	20,808	18,483	15,693	10,488	13,584	16,680	18,615	20,550	22,485	25,968	27,903	30,225	32,160	34,095	8
10	33,816	30,408	28,278	26,148	24,018	20,184	18,054	15,498	13,368	13,896	17,304	19,434	21,564	23,694	27,528	29,658	32,214	34,344	36,474	9
11	32,136	28,968	26,988	25,008	23,028	19,464	17,484	15,108	13,128	9960	17,544	19,824	22,104	24,384	28,488	30,768	33,504	35,784	38,064	10
12	28,296	25,608	23,928	22,248	20,568	17,544	15,864	13,848	12,168	8480	6792	20,124	22,704	25,284	29,928	32,508	35,604	38,184	40,764	11
13	24,156	21,948	20,568	19,188	17,808	15,324	13,944	12,288	10,908	7700	6492	5112	23,004	25,884	31,068	33,948	37,404	40,284	43,164	12
14	19,716	17,988	16,908	15,828	14,748	12,804	11,724	10,428	9348	6620	5892	4812	3732	26,184	31,908	35,088	38,904	42,084	45,264	13
15	14,976	13,728	12,948	12,168	11,388	9984	9204	8268	7488	5240	4992	4212	3432	2652	32,448	35,928	40,104	43,584	47,064	14
16	11,544	10,608	10,023	9438	8853	7800	7215	6513	5928	3992	4056	3471	2886	2301	1248	36,123	40,533	44,208	47,883	15
17	7917	7293	6903	6513	6123	5421	5031	4563	4173	2549	2925	2535	2145	1755	1053	663	40,767	44,637	48,507	16
18	4056	3744	3549	3354	3159	2808	2613	2379	2184	1872	1560	1365	1170	975	624	429	195	44,832	48,897	17
																			49,092	18

Moments (ft–k) Due to loads from wheel no. 1 to wheel no.

due to a group of loads to the left of the point and for those due to a group of loads to the right of the point. The numbers above the heavy zigzag line are the sums of moments about various points under consideration due to the loads to the left of the respective points as indicated by the entry on the right edge of the table. Thus, the sum of the moments at wheel 8 due to loads from wheels 1 through 5 is

$$(10)(40 + 35 + 30 + 25) + (15)(15) = 1{,}525 \text{ ft-kips}$$

This moment may be found under wheel 8 by entering the table from the right edge on the line for moment due to wheel loads 1 through 5, i.e., the fifth line under the heading for moments. On the other hand, the numbers below the heavy zigzag line are the sums of the moments about various points under consideration due to the loads to the right of the respective points as indicated by the entry on the left edge of the table. Hence, the sum of the moments at wheel 2 due to loads from wheels 8 through 3 is

$$(15)(35 + 30 + 25 + 20) + (10)(10 + 5) = 1{,}800 \text{ ft-kips}$$

This moment is found under wheel 2 by entering the table from the left edge on the line for moment due to wheel loads 8 through 3, i.e., the second line under the heading for moments.

Another example of moment tables is shown in Table 6-2 for a standard train of Cooper E-60 loading. The locomotive is represented by a series of concentrated loads that is followed by a uniform load for the cars. For a railway girder bridge supporting a single track, the live load on each girder may be taken as one-half of that of the train load shown in the table. It is obvious that the larger the number of concentrated loads, the more useful is the moment table.

Moment tables are sometimes presented in slightly modified forms. Several versions of moment tables for standard concentrated loads are available in numerous design handbooks. For other given loadings, moment tables can be constructed readily. With the aid of such tables, the reactions, shears, and moments can be conveniently computed as soon as the location of the loads for producing maximum effects are determined.

Example 6-12. The cranes in Table 6-1 are placed on a single beam of 40-ft span. With the position of the wheels located as shown in Fig. 6-25(a), determine (a) the reaction at support A, (b) the shear at a section between wheels 4 and 5, and (c) the moment under wheel 4. If some of the wheels pass out of the span as shown in Fig. 6-25(b), determine (a) the reaction at support A and (b) the reaction at support B.

Consider first the position of the wheels located as shown in Fig. 6-25(a). In computing the reaction at support A, the sum of the moments about support B due to the wheel loads on the span may be obtained with the aid

of Table 6-1. Thus,

$$M_b = 975 + (70)(4) = 1{,}255 \text{ ft-kips}$$

in which 975 is the sum of the moments of the wheel loads on the span about wheel 6, 70 is the sum of the wheel loads on the beam, and 4 is the distance between wheel 6 and support B. Hence, the reaction at support A may be computed as

$$R_a = 1{,}255/40 = 31.8 \text{ kips}$$

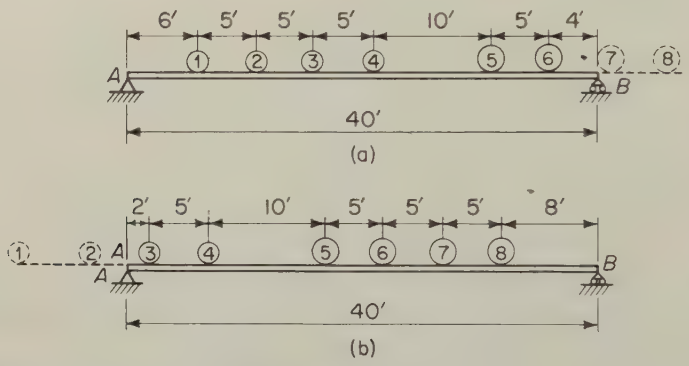

Figure 6–25

The shear at a section between wheels 4 and 5 is equal to the reaction at support A minus the sum of wheels 1 through 4, or

$$S_{4\text{-}5} = 31.8 - 40 = -8.2 \text{ kips}$$

The moment at the point of the beam under wheel 4 is

$$M_4 = (31.8)(15 + 6) - 300 = 368 \text{ ft-kips}$$

for which 15 is the sum of the spacings and 300 is the sum of the moments about wheel 4 due to wheels 1 through 3.

When some of the wheels move off the span of the beam as shown in Fig. 6-25(b), the same procedure can still be applied except that the moments caused by the loads out of the span must be subtracted from the sum of the moments due to all wheel loads. Thus, the sum of the moments of the wheel loads on the span about support B can be computed as follows:

$$M_b = (1{,}750 - 750) + (100 - 20)(8) = 1{,}640 \text{ ft-kips}$$

in which 1,750 is the sum of the moments of all wheel loads about wheel 8, 750 is the sum of the moments of wheel loads 1 and 2 about wheel 8, 100 is the sum of all wheel loads, 20 is the sum of wheel loads 1 and 2, and 8 is the distance between wheel 8 and support B. Then,

$$R_a = 1{,}640/40 = 41.0 \text{ kips}$$

After R_a is obtained, R_b can be computed directly without resorting to the moment table. However, for the sake of illustration, we shall compute R_b independent of R_a. Thus, with the aid of the moment table, the sum of the moments of the wheel loads on the span about support A is

$$M_a = 1{,}400 + (100 - 20)(2) = 1{,}560 \text{ ft-kips}$$

in which 1,400 is the sum of the moments about wheel 3 due to wheels 8 through 4, 100 is the sum of all wheel loads, 20 is the sum of wheel loads 1 and 2, and 2 is the distance from wheel 3 to support A. Finally,

$$R_b = 1{,}560/40 = 39.0 \text{ kips}$$

6-10 *Criteria for Maximum Effects on Beams*

The application of influence lines for determining the maximum effects of moving concentrated loads on beams can be illustrated by the development of criteria for maximum reactions, shears, and moments at specified locations of a simply supported beam. The criterion for the maximum of each of these effects can be established by studying the change in each effect caused by the change in position of loads.

Reactions. Consider a single load P moving across the span of a simple beam as shown in Fig. 6-26. When P is at a distance of x from support B, the reaction at support A is Px/L. If the load P moves to the left by a small distance δx, the reaction at support A will be $P(x + \delta x)/L$. In other words, the change in the reaction at support A due to the movement δx is equal to $P\,\delta x/L$. When a series of concentrated loads on the beam travels to the left by a small distance δx, each of the loads moves to the left by the same amount δx. If G denotes the sum of the loads on the beam, the change in reaction at support A will be $G\,\delta x/L$ provided that no wheel on the span has left the span and that no other wheel has entered the span.

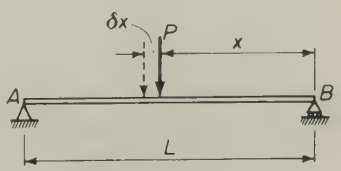

Figure 6-26

Figure 6-27(a) shows a series of concentrated loads moving onto the span. The influence line for reaction at support A is shown in Fig. 6-27(b). It can be seen from the shape of the influence line that the change in reaction at A as a result of the movement of loads to the left represents an increase until wheel 1 reaches support A. When wheel 1 leaves the span, there will be a sudden decrease in the reaction at A. However, if the movement of the loads continues, the reaction at A will again increase gradually until wheel 2 reaches support A. The same cycle will be repeated as each wheel approaches support A. In the course of each movement, it is possible that a

wheel may enter the span from the right. Although any wheel load entering the span from the right will cause an increase in the reaction at A, the influence of the new load is relatively small since the entering wheel is close to support B.

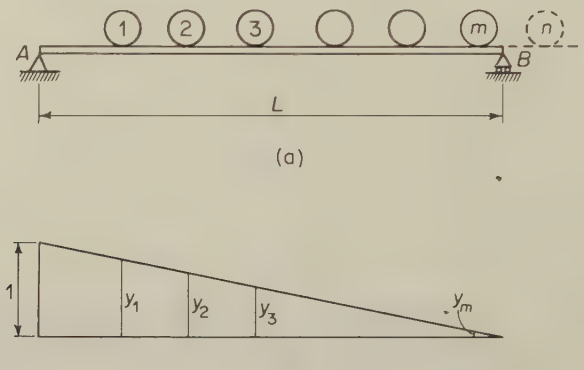

Figure 6–27

Since the reaction at A increases each time a wheel approaches support A, and decreases suddenly as that load passes support A and leaves the span, it is necessary to compare only the values of the reaction when the wheel loads successively move over support A. Thus, a general expression may be written for the change of the reaction at A by considering the loads moving off and onto the span as well as those staying on the span during the movement. Consider, for instance, the movement of the loads from the position shown in Fig. 6-28(a) to that in Fig. 6-28(b). Let G be the sum of all wheel

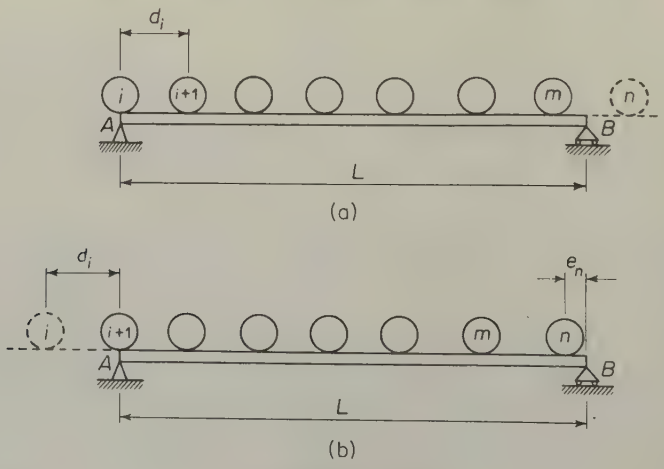

Figure 6–28

loads that are on the span and stay on during the movement, P_i be the wheel load that has just left the span, d_i be the distance between P_i and the wheel immediately following, P_n be a wheel that enters the span during the movement, and e_n be the distance that P_n travels on the span after entering. Then, the change of the reaction at support A due to the movement is

$$\delta R_a = \frac{Gd_i}{L} - P_i + \frac{P_n e_n}{L} \tag{6-1}$$

A positive value for δR_a indicates an increase in the reaction at support A and a negative value indicates a decrease. As long as the reaction at support A increases as a result of the movement, the loads should move further to the left until the next load comes directly over the support A. As soon as the reaction at support A begins to decrease, however, no further movement of loads is necessary since the maximum reaction was reached when the previous load was directly over the support. Thus, the criterion for maximum reaction at support A is given by Eq. (6-1).

Example 6-13. If a series of concentrated loads representing Cooper's E-60 loading shown in Table 6-2 moves across a simple beam of 75-ft span, compute the maximum reaction at the left support of the beam.

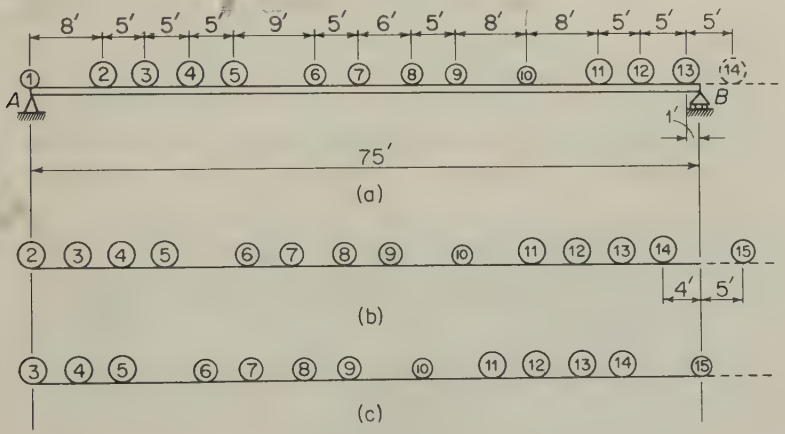

Figure 6–29

The movement of the series of concentrated loads over support A is indicated in stages by Figs. 6-29(a), (b), and (c). Then, from the position of P_1 at A to that of P_2 at A,

$$\delta R_a = (636 - 30)\,(8/75) - 30 + (14)\,(4/75) = +35.5 \text{ kips (an increase)}$$

From P_2 at A to P_3 at A,

$$\delta R_a = (696 - 90)\,(5/75) - 60 = -19.7 \text{ kips (a decrease)}$$

Note that the term $P_n e_n/L$ does not appear in the last equation since wheel 15 has not entered the span during the movement. Actually, the magnitudes of δR_a are not needed, and only the change in sign is pertinent. In this case, the maximum reaction at support A occurs when wheel 2 is directly over support A, since δR_a is negative during the movement from P_2 at A to P_3 at A.

The maximum reaction may then be computed according to Fig. 6-29(b) with the aid of Table 6-2. Thus,

$$R_a = \tfrac{1}{775}\,[26{,}184 + (696)\,(4) - 240 - (30)\,(75)] = 354 \text{ kips}$$

Shears. When a single load P moves across the span of a simple beam as shown in Fig. 6-30, the shear at a section passing through point C of the beam can be determined from the free body to the left of the section. As long as the load P is on segment BC of the beam, the shear at C equals the reaction at A. If the load moves to the left by a small distance δx within segment BC, the change in shear at C and in reaction at A will be the same. As soon as the load P moves to segment CA of the beam, the shear at C is equal to the reaction at A minus the load P. In that case, the change in shear at C due to further movement of P will be the same as the change in reaction at A minus the load P.

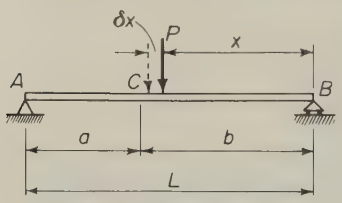

Figure 6–30

Consider next a series of concentrated loads moving onto the beam from the right as shown in Fig. 6-31(a). The influence line for shear at section C

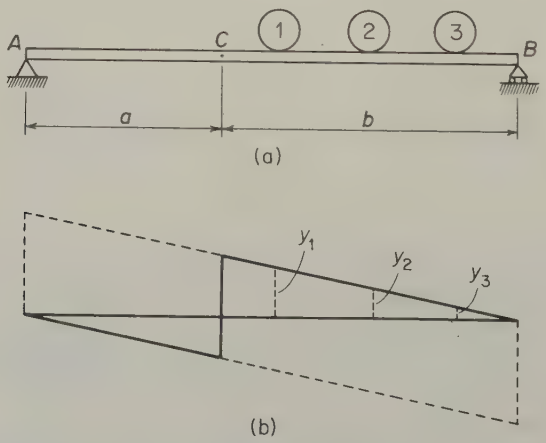

Figure 6–31

may be constructed as shown in Fig. 6-31(b). From the shape of the influence line, it is noted that the shear at C will increase when the loads move to the left until wheel 1 reaches point C. Any further movement will make wheel 1 pass to the left of point C and will cause a sudden decrease in the shear at C. However, if the movement of the loads continues, the shear at C will again increase gradually until wheel 2 reaches point C. The same cycle will be repeated as each wheel comes up to point C. In the course of each movement, it is possible that a new wheel may enter the span from the right and thus increases the shear at C. On the other hand, a wheel may leave the span from the left during the same movement, and the removal of such a load from the span will reduce the negative shear and therefore increase the positive shear.

Since the shear at C increases each time a wheel approaches point C and decreases suddenly as that load passes point C, it is necessary to compare only the values of the shear at C when the wheel loads move successively over point C. In general, the change in shear resulting from the movement as wheel succeeds wheel at the section is equal to the change in the left reaction minus the wheel that has just passed the section, provided that no wheel has left the span during the movement. If a load that was to the left of the section leaves the span during the movement, the negative shear that it caused at the section before leaving should be added to the change in shear. Thus, a general expression may be written for the change in shear at C by considering the movement of all loads that are involved. Consider, for instance, the movement of the loads from the position shown in Fig. 6-32(a) to that in Fig. 6-32(b). Let G be the sum of all wheel loads

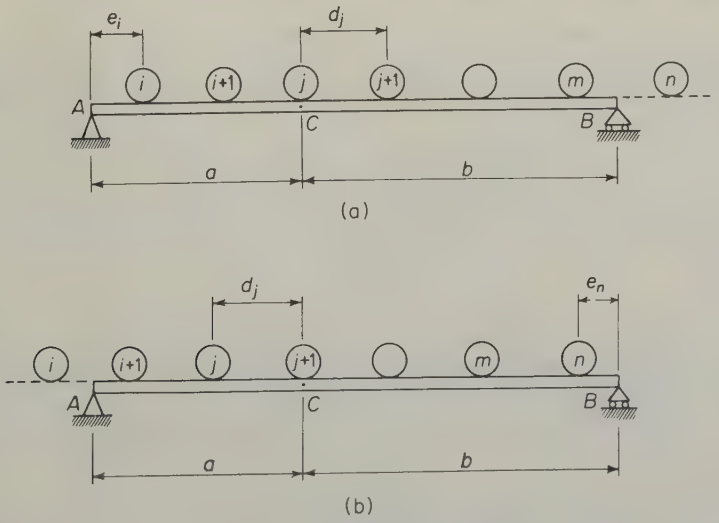

Figure 6–32

that are on the span and stay on during the movement, P_j be the wheel load that has just passed the section, d_j be the distance between P_j and the wheel immediately following, P_n be a wheel that enters the span, e_n be the distance that P_n travels on the span after entering, P_i be the wheel that has just left the span, and e_i be the distance that P_i travelled on the span before moving off. Then, the change in shear at C due to the movement is

$$\delta S_c = \frac{Gd_j}{L} - P_j + \frac{P_n e_n}{L} + \frac{P_i e_i}{L} \tag{6-2}$$

A positive value for δS_c indicates an increase in the shear and a negative value indicates a decrease. As long as the shear at C increases as a result of the movement, the load should move further to the left until the next load comes over point C. As soon as the shear at C begins to decrease, however, no further movement of loads is necessary since the maximum shear at C was reached when the previous load was directly over point C. Thus, the criterion for maximum shear at a section passing through point C is given by Eq. (6-2).

Example 6-14. For a simple beam of 75-ft span designed to support Cooper's E-60 loading shown in Table 6-2, compute the maximum shear at a section passing through point C of the beam as shown in Fig. 6-33.

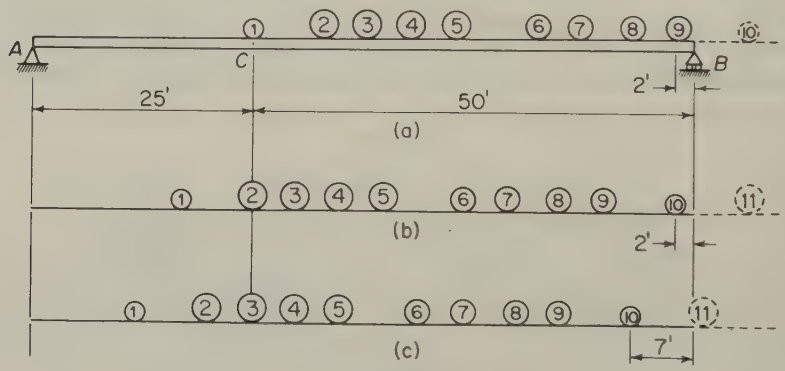

Figure 6–33

The movement of the series of concentrated loads over point C is indicated in stages by Figs. 6-33(a), (b), and (c). Then, from the position of P_1 at C to that of P_2 at C,

$$\delta S_c = (426)(\tfrac{8}{75}) - 30 + (30)(\tfrac{2}{75}) = + \text{ (an increase)}$$

From P_2 at C to P_3 at C,

$$\delta S_c = (456)(\tfrac{5}{75}) - 60 = - \text{ (a decrease)}$$

Hence, the maximum shear at C is produced when wheel 2 is placed at C. The magnitude of the maximum shear at C can be computed from Fig. 15(b) as follows:

$$\delta S_c = \tfrac{1}{75}\,[13{,}896 + (456)(2)] - 30 = 167 \text{ kips}$$

Moments. When a single load P moves across the span of a simple beam as shown in Fig. 6-34(a), the change in moment at a point C can be studied

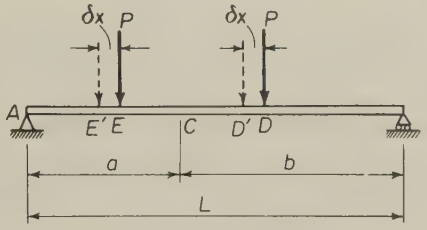

(a)

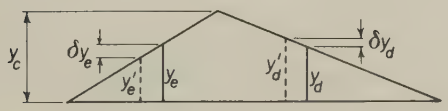

(b)

Figure 6–34

from the influence line for moment at that point as shown in Fig. 6-34(b). As long as the load P is in segment BC of the beam, any movement of load P to the left will increase the moment at C since the ordinates of the influence line increase in magnitude from B to C. As soon as the load moves to segment CA of the beam, however, any further movement of load P to the left will decrease the moment at C since the ordinates of the influence line decrease from C to A. Thus, when the load P moves a small distance δx from D to D', the change in moment at C is equal to

$$\delta M_c = P y_{d'} - P y_d = P\,\delta y_d$$

in which y_d and $y_{d'}$ are the ordinates at points D and D', respectively, of the influence diagram. From the geometrical relation of similar triangles shown in the influence diagram, it is obvious that $\delta y_d/\delta x = y_c/b$. Hence

$$\delta M_c = \frac{P y_c}{b}\,\delta x$$

Similarly, if the load P is first placed at E and then moved a small distance

δx to E', the change in moment at C is equal to

$$\delta M_c = P y_{e'} - P y_e = -P\,\delta y_e$$

in which y_e and $y_{e'}$ are the ordinates at points E and E', respectively, of the influence diagram. Again, from the relation of similar triangles, $\delta y_e/\delta x = y_c/a$. Then

$$\delta M_c = -\frac{P y_c}{a}\,\delta x$$

When a series of concentrated loads moves across the span of a simple beam as shown in Fig. 6-35(a), all loads on the span will cause moment at

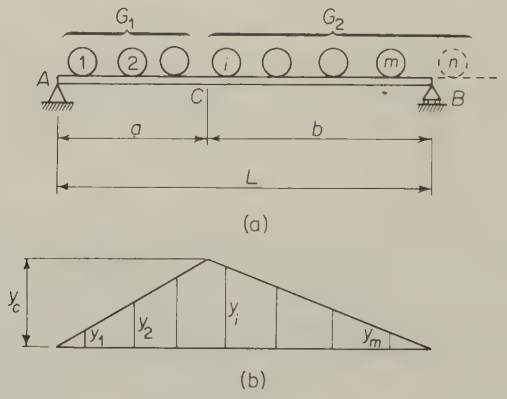

Figure 6–35

C since the ordinates of the influence line are positive throughout the entire span length. As the loads on the span move to the left, the loads that are on segment BC of the beam will cause an increase in the moment at C, whereas the loads that are on segment CA of the beam will cause a decrease in the moment at C. The change in moment at C is equal to the algebraic sum of the increase in moment caused by the loads on segment BC and the decrease in moment due to loads on segment CA of the beam. Let G_1 and G_2 be the sums of all loads on segments CA and BC of the beam respectively. Then, the change in moment at C due to a small movement δx of the loads is

$$\delta M_c = \frac{G_2 y_c}{b}\,\delta x - \frac{G_1 y_c}{a}\,\delta x$$

or

$$\frac{\delta M_c}{\delta x} = \left(\frac{G_2}{b} - \frac{G_1}{a}\right) y_c \qquad (6\text{-}3)$$

provided that no wheel enters the span from the right or leaves the span from the left during the movement.

In Eq. (6-3), a positive value for δM_c indicates an increase in moment at C and a negative value represents a decrease in moment at C. The moment at C will reach a maximum value when δM_c ceases to increase and begins to decrease. As long as no load passes through C from segment BC to segment CA, the sign of δM_c will not change during the movement of loads because the relation between G_2/b and G_1/a will remain unchanged. If a wheel passes through C during the movement, however, G_2 will decrease and G_1 will increase. Thus, the change of sign of δM_c can be detected if one wheel at a time is transferred from segment BC to segment CA of the beam. If the transfer of a wheel in this manner causes the change of sign of δM_c, the maximum moment will be produced when this wheel is placed at point C.

However, the procedure of locating the position of loads that will produce maximum moment at a section can be further simplified by proper interpretation of Eq. (6-3). As the sign of δM_c changes from positive to negative, the maximum value for moment at C is reached when $\delta M_c = 0$. In such a situation, it is necessary that

$$\frac{\delta M}{\delta x} = \left(\frac{G_2}{b} - \frac{G_1}{a}\right) y_c = 0 \quad \text{or} \quad \frac{G_1}{a} = \frac{G_2}{b}$$

However, it is usually more convenient to relate this condition to the total load and the span length as follows:

$$\frac{G_1}{a} = \frac{G_2}{b} = \frac{G_1 + G_2}{a + b} = \frac{G}{L}$$

or

$$\frac{Ga}{L} = G_1 \tag{6-4}$$

in which G is the sum of all loads on the span and L is the span length. Thus, the maximum moment at C is produced when $Ga/L = G_1$. If a load P_i in the series is first placed just to the right of C as shown in Fig. 6-35(b) and then moved to just to the left of C, the moment at C will reach a maximum value when P_i is at C if,

$$\text{for } P_i \text{ to right of } C, \quad \frac{Ga}{L} > G_1$$

$$\text{for } P_i \text{ to left of } C, \quad \frac{Ga}{L} < G_1$$

Hence, Eq. (6-4) represents the criterion for maximum moment at C.

It has been assumed so far, that no wheel enters or leaves the span during the movement of a series of loads on the span. If some wheels enter the span from the right or leave the span from the left, more than one wheel

in the series may satisfy the criterion. When successive wheels in the series satisfy the criterion, the difference in moments resulting from the corresponding wheels at point C will be very small. On the other hand, if several wheels widely scattered in the series satisfy the criterion, the maximum moment usually can be detected by inspection.

Example 6-15. For a simple beam of 75-ft span designed to support Cooper's E-60 loading shown in Table 6-2, compute the maximum moment at point C of the beam shown in Fig. 6-36(a).

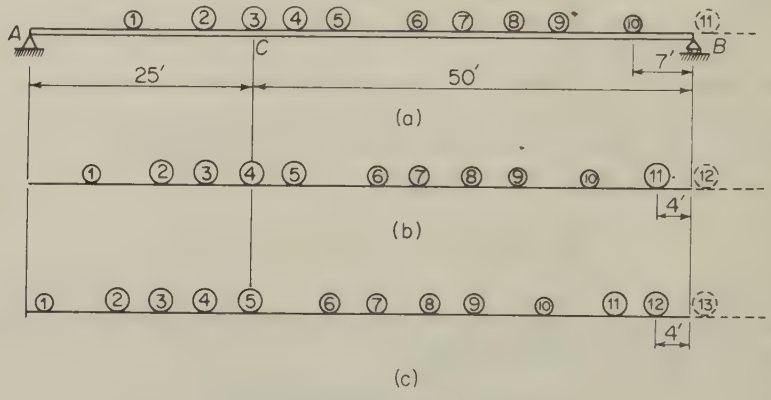

Figure 6–36

Since all loads on the span of the beam will influence the moment at C, it is unlikely that the maximum moment at C will be produced when wheel 1 or 2 is placed at C. Hence, the movement of the wheels over point C is indicated in stages by Figs. 6-36(a), (b), and (c), beginning with wheel 3 at C. The calculation is carried out in Table 6-3, in which the first column indicates the wheel load at point C. If the numbers in the second, third, and fourth columns are progressively decreasing, then the criterion of Eq. (6-4) is satisfied. Otherwise, the criterion is not satisfied.

TABLE 6-3

P_i at C	G_1 (P_i at left)	$\frac{Ga}{L}$	G_1 (P_i at right)	Criterion satisfied
P_3	150	$\frac{25}{75}(456)=152$	90	no
P_4	210	$\frac{25}{75}(516)=172$	150	yes
P_5	270	$\frac{25}{75}(576)=192$	210	no

Thus, wheel 4 satisfies the criterion and the maximum moment at C can be computed from Fig. 6-36(b) as follows:

$$M_c = \tfrac{25}{75}\,[17{,}544 + (516)\,(4)] - 1{,}440 = 5{,}096 \text{ ft-kips}$$

6-11 *Absolute Maximum Shear and Moment in Beams*

In the previous section the criteria for determining the position of loads that will produce maximum reaction, shear, and moment at a given location have been presented. In the design of beams, it is often necessary to find where this particular location should be in order to produce an absolute maximum shear or moment in the beam. For the purpose of illustration, we shall again consider a simply supported beam under the action of concentrated loads.

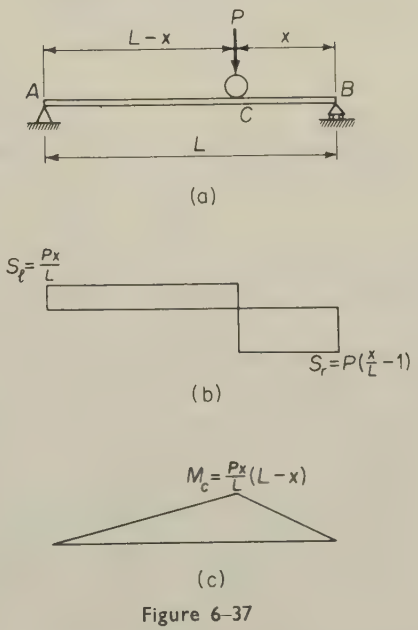

Figure 6–37

Absolute maximum shear. The absolute maximum shear in a beam resulting from moving concentrated loads will occur at a section immediately adjacent to one of the reactions. This can be seen from the shear diagram of the beam under loads. For a single moving load on a simple beam as shown in Fig. 6-37(a), the shear at a section to the left of the load is

$$S_l = \frac{Px}{L}$$

and the shear at a section to the right of the load equals

$$S_r = P\left(\frac{x}{L} - 1\right)$$

The corresponding shear diagram is shown in Fig. 6-37(b). Since x is a variable with limits from 0 to L, S_l is maximum when $x = L$ and S_r is maximum when $x = 0$. When a series of concentrated loads moves across

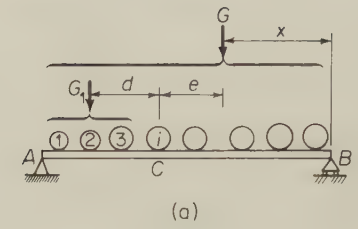

(a)

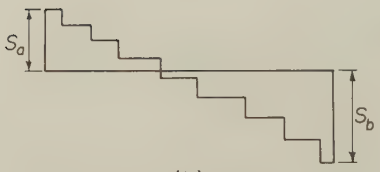

(b)

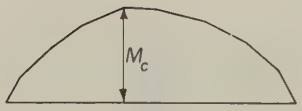

(c)

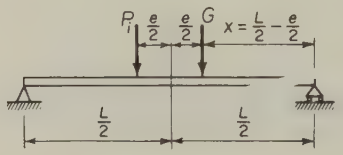

(d)

Figure 6–38

the beam as shown in Fig. 6-38(a), the shear diagram will be as shown in Fig. 6-38(b). It is obvious that the absolute maximum shear will occur at a section just to the right of support A or just to the left of support B.

Example 6-16. A series of three wheels moves across the span of a simple beam as shown in Fig. 6-39(a). Determine the absolute maximum shear in the beam.

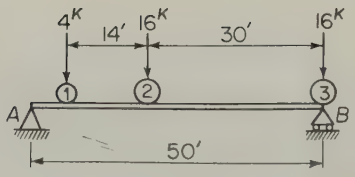

(a)

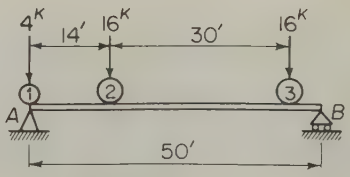

(b)

Figure 6–39

Since the absolute maximum shear occurs at either a section just to the right of support A or just to the left of support B, it is simple to compute the shear at both sections. However, by inspection of the loads, the absolute maximum shear is more likely to occur at B when wheel 3 is placed just to the left of B as shown in Fig. 6-39(a), than at A when wheel 1 is placed just to the right of A as shown in Fig. 6-39(b), because wheel 3 is much heavier than wheel 1. Thus, the absolute maximum shear in the beam is

$$S_b = -16 - \tfrac{1}{50}\,[(16)(50 - 30) + (4)(50 - 30 - 14)] = -22.8 \text{ kips}$$

As a check, the maximum shear at A can be computed according to Fig. 6-39(b).

$$S_a = 4 + \tfrac{1}{50}\,[(16)\,(50 - 14) + (16)\,(50 - 14 - 30)] = 17.4 \text{ kips}$$

Absolute maximum moment. The absolute maximum moment in a beam due to moving concentrated loads also can be studied from the moment diagram of the beam under loads. For a single moving load on a simple beam as shown in Fig. 6-37(a), the maximum moment under the load P is equal to

$$M = \frac{Px}{L}\,(L - x)$$

Since M is a function of the variable x, the absolute maximum moment may be located by setting $dM/dx = 0$. Thus,

$$\frac{P}{L}(L - 2x) = 0 \quad \text{or} \quad x = \frac{L}{2}$$

Hence, the absolute maximum moment occurs at the midspan of the beam, and the value of this moment is $PL/4$.

For a series of concentrated loads moving across the beam as shown in Fig. 6-38(a), the maximum moment will be produced under one of the concentrated loads. Let P_i be the load under which the moment is maximum as indicated by the moment diagram in Fig. 6-38(c). Also, let G be the sum of all loads on the span, x be the distance from the line of action of the resultant G to the right support B, e be the distance from the same line of action G to P_i, G_1 be the sum of all loads to the left of P_i, and d be the distance from the line of action of the resultant G_1 to P_i. Then,

$$M_i = R_a(L - e - x) - G_1 d$$

$$= \frac{Gx}{L}\,(L - e - x) - G_1 d$$

The point of absolute maximum moment may be located by setting $dM_i/dx = 0$, Thus,

$$\frac{G}{L}(L - e - 2x) = 0$$

or

$$x = \frac{L}{2} - \frac{e}{2}$$

The last equation indicates that x must be so chosen that P_i and G are equidistant from the midspan of the beam as shown in Fig. 6-38(d). If the proper P_i is located, the absolute maximum moment can be computed as follows:

$$M_i = \frac{G}{L}\left(\frac{L - e}{2}\right)^2 - G_1 d$$

Note that this equation is derived for loads placed in the order as shown

in Fig. 6-38(a), i.e., the load P_i is to the left of the line of action of G. If the load P_i is placed to the right of G, this equation still holds if the distance e is considered as negative in such a case.

In general, the load that is nearest to the line of action of the resultant G will produce the absolute moment. Otherwise, several loads adjacent to this load may be tried. In any case, the load P_i should also satisfy the criterion in Eq. (6-4) for maximum moment at a point.

Example 6-17. A series of three wheels as shown in Fig. 6-40(a) moves across a simple beam of 50-ft span. Determine the absolute maximum moment in the beam.

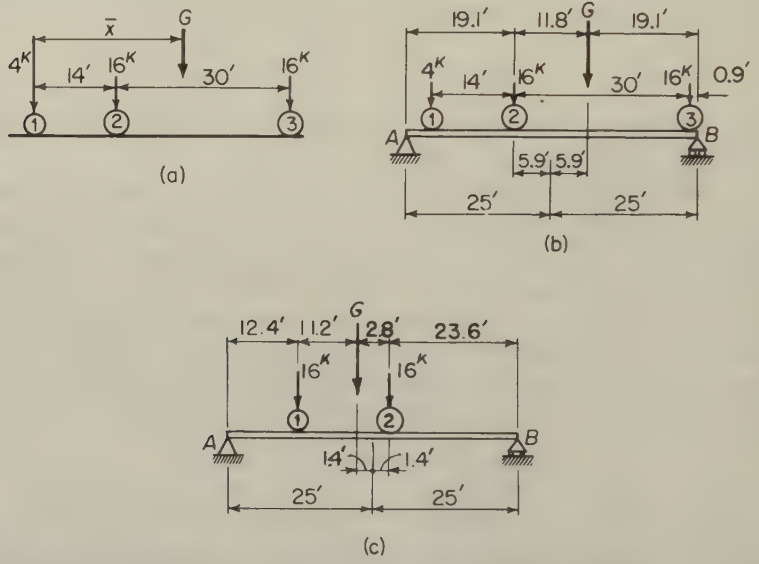

Figure 6–40

The location of the resultant of all loads with reference to wheel 1 is given by $\bar{x}$ as follows:

$$\bar{x} = \frac{16(14 + 44)}{4 + 16 + 16} = 25.8 \text{ ft}$$

If all three wheels are on the span as shown in Fig. 6-40(b), we have

$$e = 25.8 - 14 = 11.8 \text{ ft}$$

$$x = \tfrac{1}{2}(50 - 11.8) = 19.1 \text{ ft}$$

Hence, the maximum moment under wheel 2 is

$$M_i = \tfrac{36}{50}(19.1)^2 - (4)(14) = 206 \text{ ft-kips}$$

Since wheel 3 is so close to support B, its influence on the moment at wheel

2 is extremely small. It is possible, therefore, that the maximum moment may be produced when only the first two wheels are on the span. The location of the resultant of wheels 1 and 2 is given by $x = 2.8$ ft for $G = 20$ kips and $d = 14$ ft for $G_1 = 4$ kips as shown in Fig. 6-40(c). Then, $e = 2.8$ ft and $x = 23.6$ ft. The maximum moment under wheel 2 is

$$M_i = (^{2}\%_{50})(23.6)^2 = 223 \text{ ft-kips}$$

Hence, the absolute maximum moment in the beam is equal to 223 ft-kips.

6-12 *Criteria for Maximum Effects on Trusses*

Since the bar forces in a truss are usually determined either by taking moments about a certain point or by considering the shear at a certain panel of the truss, the criteria for maximum bar forces in a truss are identical to those for maximum moments or maximum shears at the appropriate locations of the truss. We may consider the loaded chord of a truss as a girder supporting floor beams. If the criteria for shears in various panels and for moments at various panel points of such a beam can be developed, the criteria for maximum bar forces in the truss itself can generally be obtained without difficulty. There are, of course, exceptions that require special treatment. However, it is not the purpose of this section to discuss all possible cases extensively, but to illustrate the principle by a few simple cases. We shall, therefore, consider first the criteria for maximum shears and moments in a girder supporting floor beams, which are equally applicable to simple trusses.

Shears. When a series of concentrated loads moves across the span from right to left, the maximum positive shear in a panel is produced when there are as many loads as possible placed on the portion of the span for which the area in the influence diagram is positive and no loads at all in the portion of the span for which the area in the influence diagram is negative, unless the movement of loads to the left beyond the neutral point causes an increase in shear in the panel. The maximum negative shear in a panel is produced either when the series of loads moves from right to left and leaves the span from the left, or when the series enters the span from the left, depending on the combination of loads. However, for girders symmetrical with respect to the centerline at midspan, we can make use of the antisymmetrical configurations of the influence lines for shear in various panels and need to consider only the case when the series of loads is moving from right to left. Hence, the criterion for maximum shear is developed only for the case when the series of loads enters the span from the right.

Consider, for instance, the maximum shear in a typical interior panel of the girder supporting floor beams in Fig. 6-41(a). The influence line for shear in such a panel, say panel CD, is shown in Fig. 6-41(b). In order to

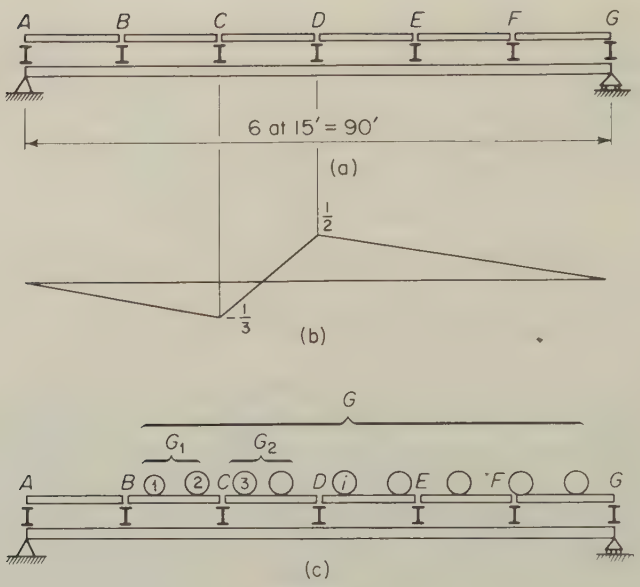

Figure 6–41

develop the criterion for maximum shear in the panel, we consider a series of concentrated loads as shown in Fig. 6-41(c), in which G_1 is the sum of all loads to the left of panel point C, G_2 is the sum of all loads in panel CD, and G is the sum of all loads on the span. If the loads move a small distance δx to the left so that no loads will move past the panel points C and D, or the supports A and G, the change in shear during the movement is equal to the change in the reaction of the girder at A minus the reaction of the stringer CD at C. From the inspection of the influence line in Fig. 6-41(b), such a change represents an increase by the amount of

$$\delta S = \frac{G\,\delta x}{L} - \frac{G_2\,\delta x}{h}$$

in which L is the span length and h is the panel length. If the span consists of n panels of equal length h, then $L = nh$. Note that the term G_1 does not appear in the above equation because the sum of the reactions at B and C of the stringer BC remains the same during the movement although the reaction at B is increased and the reaction at C is decreased at the same time. As long as the relation between G/L and G_2/h is maintained the same, the change in shear is always positive. A change in sign for δS is possible only if G_2 increases while G remains the same. This can be accomplished by moving a load just to the right of panel point D to a position just to the left of D. If there is no change in sign in δS, the next load can be moved up to a position just to the left of D until the sign of δS becomes negative. As the change in shear reverses its sign from positive to negative, the shear in the

panel reaches a maximum value when $\delta S = 0$, from which

$$\frac{G}{L} = \frac{G_2}{h}$$

or

$$\frac{G}{n} = G_2 \tag{6-5}$$

Equation (6-5) gives the criterion for maximum shear in the interior panel CD, which may be stated as follows:

$$\text{for } P_i \text{ to the right of } D, \quad \frac{G}{n} > G_2$$

$$\text{for } P_i \text{ to the left of } D, \quad \frac{G}{n} < G_2$$

If some wheel loads enter the span from the right or leave the span from the left during the movement of the series of loads to the left, it is possible to have more than one wheel load that may satisfy the criterion in Eq. (6-5). Under such circumstances, either the criterion should be modified or the maximum shear may be obtained by trial.

Since the shape of the influence diagram for shear in the end panel is a triangle, the criterion represented by Eq. (6-4) may be adapted to the determination of maximum shear in the end panel. In other words, the maximum in end panel AB for the girder shown in Fig. 6-41(a) is produced when $G_2/h = G/L$, or $G_2 = G/n$, in which G_2 is the sum of all loads in panel AB. Thus, the criterion is the same as Eq. (6-5).

Example 6-18. A series of concentrated loads representing Cooper's E-60 loading shown in Table 6-2 moves across the span of a girder supporting floor beams as shown in Fig. 6-41(a), for which $L = 90$ ft. Compute the maximum shear in panel CD.

The movement of the series of concentrated loads over panel point D is indicated in stages by Figs. 6-42(a), (b), and (c). The calculation is carried out in Table 6-4 as follows:

TABLE 6-4

P_i at D	G_2 (P_i at left)	$\frac{G}{n}$	G_2 (P_i at right)	Criterion satisfied
P_1	30	$387/6 = 64.5$	0	no
P_2	..	$430/6 = 71.7$	30	yes
	90	$456/6 = 76.0$	..	
P_3	150	$456/6 = 76.0$	90	no

Hence, only P_2 satisfies the criterion and the maximum shear in panel CD can be computed for the position of loads shown in Fig. 6-42(b). Since the reactions of the girder are not affected by the floor beams, we can compute the reaction R_a with the aid of the moment table.

$$R_a = \frac{1}{90}[10{,}488 + (465)(5)] = \frac{12{,}813}{90} = 142.4$$

Then,

$$S_{cd} = 142.4 - (30)\left(\frac{8}{15}\right) = 126.4 \text{ kips}$$

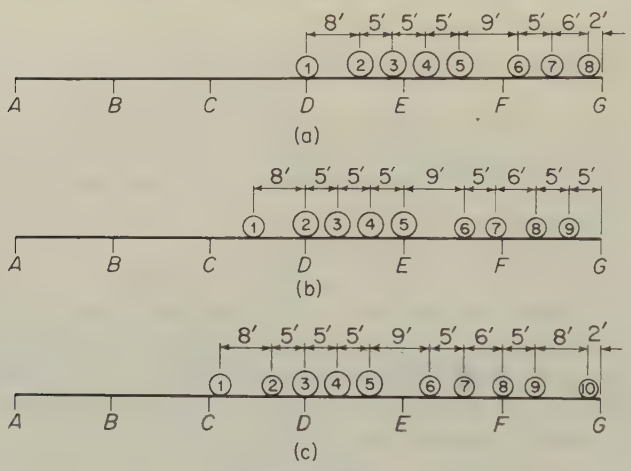

Figure 6–42

Moments. Since the influence line for the moment at a panel point of a girder supporting floor beams is identical to that of a beam of the same span without floor beams, the criterion for maximum moment in Eq. (6-4) is directly applicable to the computation of maximum moment at a panel point of a girder supporting floor beams. If the maximum moment at some point other than the panel points is desired, the criterion for maximum moment may be developed in a similar manner.

Consider, for example, the maximum moment at a point J between panel points C and D in the girder supporting floor beams shown in Fig. 6-43(a). Let h be the length of each panel, r be the number of panels to the left of point C, and s be the number of panels to the right of point D. Then, the total number of panels in the span is $n = (r + s + 1)$. The influence line for moment at point J is shown in Fig. 6-43(b). The ordinates of the influence line at c and d may be obtained by computing the moments at J due to a unit load placed at C and D of the beam, respectively. Thus, for

a unit load at C,

$$y_c = R_a a = \frac{ar}{n}$$

and for a unit load at D,

$$y_d = R_g b = \frac{bs}{n}$$

in which R_a and R_g are respectively the reactions at supports A and G due to a unit load at the given location.

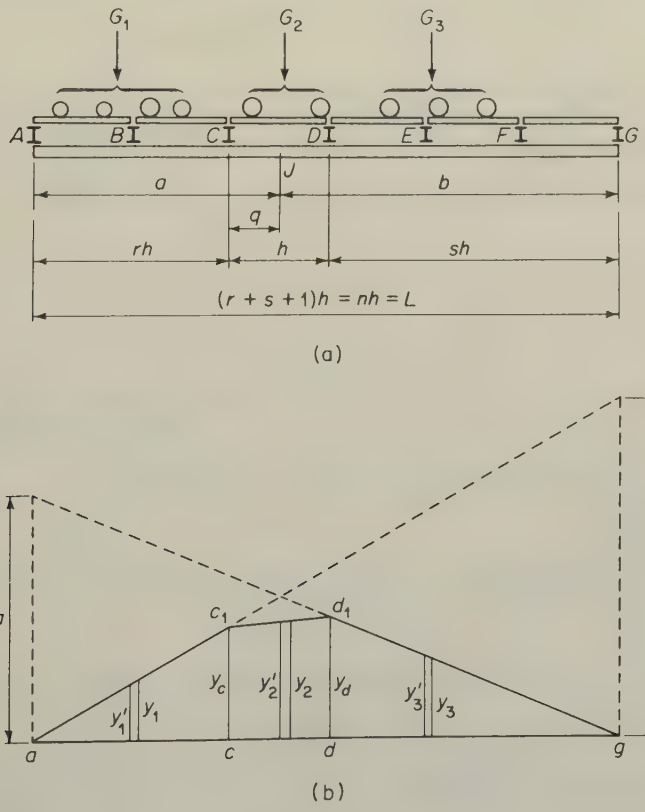

Figure 6–43

The slope of the line segment ac_1 is given by

$$\frac{y_c}{ac} = \frac{ar/n}{rh} = \frac{a}{nh} = \frac{a}{L}$$

and the slope of the line segment gd_1 is given by

$$\frac{y_d}{gd} = \frac{bs/n}{sh} = \frac{b}{nh} = \frac{b}{L}$$

The slope of the line segment c_1d_1 is equal to

$$\frac{y_d - y_c}{cd} = \frac{(as - br)/n}{h} = \frac{as - br}{L}$$

Noting that $q = a - rh$ in Fig. 6-43(a), the slope of the line segment c_1d_1 may be expressed as follows:

$$\frac{as - br}{L} = \frac{as + ar + a - ar - a - br}{L} = \frac{a(r + s + 1) - (a + b)r - a}{L}$$

$$= \frac{a}{h} - r - \frac{a}{L} = \frac{(a - rh)}{h} - \frac{a}{L} = \frac{q}{h} - \frac{a}{L}$$

If the resultants of the loads on segments AC, CD and DG of the beam are denoted by G_1, G_2, and G_3, respectively, and the ordinates of the influence line corresponding to the lines of action of these resultants are denoted y_1, y_2, and y_3, respectively, then the moment at point H is equal to

$$M_j = G_1y_1 + G_2y_2 + G_3y_3$$

If the series of loads moves a small distance δx to the left, the moment at H becomes

$$M_j' = G_1y_1' + G_2y_2' + G_3y_3'$$

in which y_1', y_2', and y_3' are the ordinates of influence lines corresponding to the new locations of the resultants of loads. Then, the change in moment M_j is equal to

$$\delta M_j = M_j' - M_j = G_1(y_1' - y_1) + G_2(y_2' - y_2) + G_3(y_3' - y_3)$$

Noting that

$$y_1' - y_1 = -\frac{b}{L}\delta x, \quad y_2' - y_2 = -\left(\frac{q}{h} - \frac{a}{L}\right)\delta x, \quad y_3' - y_3 = \frac{a}{L}\delta x$$

we have

$$\delta M_j = -G_1\frac{b}{L} - G_2\left(\frac{q}{h} - \frac{a}{L}\right) + G_3\frac{a}{L}\delta x$$

Let G be the sum of all loads on the span, or $G = G_1 + G_2 + G_3$. Then,

$$\frac{\delta M_j}{\delta x} = -G_1\frac{b}{L} - G_2\left(\frac{q}{h} - \frac{a}{L}\right) + (G - G_1 - G_2)\frac{a}{L}$$

$$= \frac{Ga}{L} - G_1\left(\frac{a + b}{L}\right) - G_2\frac{q}{h}$$

$$= \frac{Ga}{L} - \left(G_1 + G_2\frac{q}{h}\right)$$

Thus, the maximum moment at J is reached when δM_j changes from positive

to negative. This will occur when a load is placed at either panel point C or point D. When a load P_i is placed at C or D, the criterion for maximum at J is given by

$$\frac{Ga}{L} = G_1 + G_2 \frac{q}{h} \tag{6-6}$$

In other words, the criterion is satisfied if,

$$\text{for } P_i \text{ to right of } C \text{ or } D, \quad \frac{Ga}{L} > \left(G_1 + G_2 \frac{q}{h}\right)$$

$$\text{for } P_i \text{ to left of } C \text{ or } D, \quad \frac{Ga}{L} < \left(G_1 + G_2 \frac{q}{h}\right)$$

Usually the criterion is satisfied by two positions of the loading, one with a load at C and the other with a load at D. The larger of the two results is the required maximum.

It may be pointed out that, if J is a panel point, $q = 0$. Then, the criterion of Eq. (6-6) will be reduced to that of Eq. (6-4).

Example 6-19. A series of concentrated loads representing Cooper's E-60 loading shown in Table 6-2 moves across the span of a girder supporting floor beams as shown in Fig. 6-43(a), for which $n = 6$, $h = 15$ ft, and $L = 90$ ft. Compute the maximum moment at point J, which is located at 37.5 ft from support A.

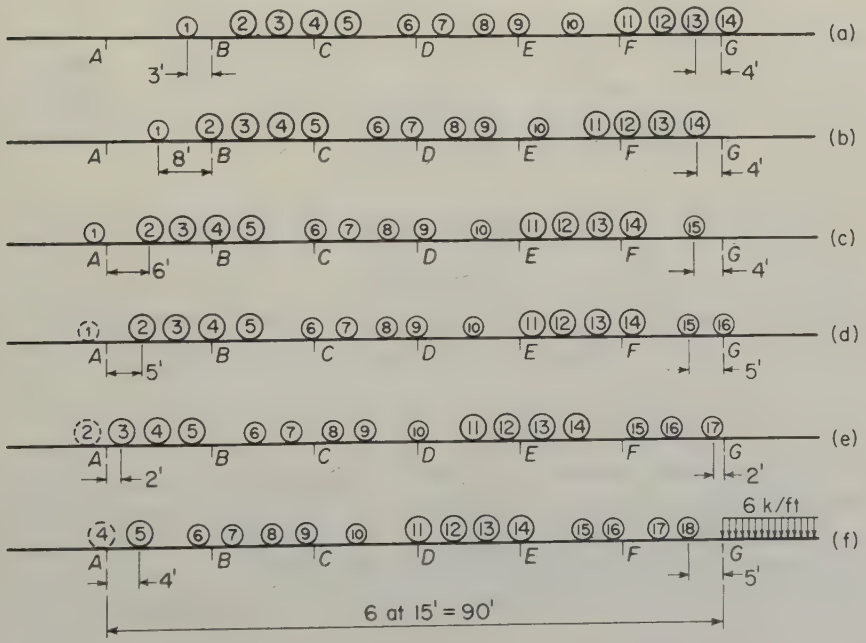

Figure 6-44

In this case, $q = 37.5 - 30 = 7.5$ ft and $q/h = 7.5/15 = \frac{1}{2}$. Hence, Eq. (6) becomes

$$\frac{Ga}{L} = G_1 + \frac{G_2}{2}$$

For a load at point C, we place the loads in positions as shown in Figs. 6-44(a), (b), and (c), and for a load at point D, we try the positions of loads shown in Figs. 6-44(d), (e), and (f). The computation for a load at C is carried out in Table 6-5 and that for a load at D is carried out in Table 6-6.

TABLE 6-5

P_i at C	$G_1 + G_2/2$ (P_i at left)	$\frac{Ga}{L}$	$G_1 + G_2/2$ (P_i at right)	Criterion satisfied
P_4	$210 + \frac{99}{2} = 259.5$	$\frac{37.5}{90}(636) = 265$	$150 + \frac{159}{2} = 229.5$	no
P_5	$270 + \frac{78}{2} = 309$	$\frac{37.5}{90}(696) = 290$	$210 + \frac{138}{2} = 279$	yes
P_6	$279 + \frac{78}{2} = 318$	$\frac{37.5}{90}(705) = 294$	$240 + \frac{117}{2} = 298.5$	no

TABLE 6-6

P_i at D	$G_1 + G_2/2$ (P_i at left)	$\frac{Ga}{L}$	$G_1 + G_2/2$ (P_i at right)	Criterion satisfied
P_9	$279 + \frac{117}{2} = 337.5$	$\frac{37.5}{90}(744) = 310$	..	no
	..	$\frac{37.5}{90}(705) = 294$	$279 + \frac{78}{2} = 318$	
P_{10}	$258 + \frac{108}{2} = 312$	$\frac{37.5}{90}(723) = 301$	$258 + \frac{78}{2} = 297$	yes
P_{11}	$216 + \frac{90}{2} = 261$	$\frac{37.5}{90}(642) = 267$	$216 + \frac{30}{2} = 231$	no

Then, the maximum moment at J for a load at C can be computed for the position of loads in Fig. 6-44(b).

$$R_a = \tfrac{1}{90}\,[26{,}184 + (696)\,(4)] = 321 \text{ kips}$$

$$M_j = (321)\,(37.5) - [2{,}490 + (270)\,(7.5)] = 7{,}480 \text{ ft-kips}$$

The maximum moment at J for a load at D can be computed for the position of loads in Fig. 6-44(e):

$$R_a = \tfrac{1}{90}\,[40{,}767 + (813)\,(2) - 240 - (90)\,(93)] = 378 \text{ kips}$$

$$M_j = (378)\,(375) - [10{,}488 + (426)\,(0.5) - 240 - (90)\,(40.5)]$$

$$= 7{,}120 \text{ ft-kips}$$

Hence, the maximum moment at J is the larger of the two, i.e., $M_j = 7{,}480$ ft-kips.

Bar forces. The maximum bar force in a member of a truss can be computed from the maximum shear in a certain panel, the maximum moment about a certain panel point, or a combination of both. Thus, the criteria developed in this section, i.e., Eqs. (6-5) and (6-6) can be used for determining maximum bar forces in trusses. We shall illustrate the applications by means of two simple examples.

Example 6-20. In member DI of the truss shown in Fig. 6-45 determine the maximum bar force due to a series of concentrated loads representing Cooper's E-60 loading.

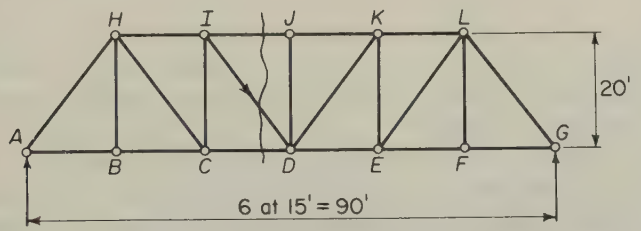

Figure 6–45

The bar force in member DI can be obtained directly from the shear in panel CD. Since the span length and the number of panels of the truss are identical respectively to those of the girder supporting floor beams in Example 6-18, the maximum shear in panel CD is equal to 126.4 kips. Hence, the maximum bar force in DI can be obtained as follows:

$$F_{di} = \tfrac{5}{4}\,S_{cd} = \tfrac{5}{4}\,(126.4) = 158 \text{ kips (tension)}$$

Example 6-21. Compute the maximum bar force in member CD of the truss shown in Fig. 6-46 resulting from a series of concentrated loads representing Cooper's E-60 loading.

The bar force in member CD can be obtained directly from the moment about panel point J. Since the span length and the number of panels of the

truss are identical respectively to those of the girder supporting floor beams in Example 6-19, the maximum moment at point J is equal to 7,480 ft-kips. Hence, the maximum bar force in CD can be obtained as follows:

$$F_{cd} = \frac{M_j}{15} = \frac{7{,}480}{15} = 499 \text{ kips (tension)}$$

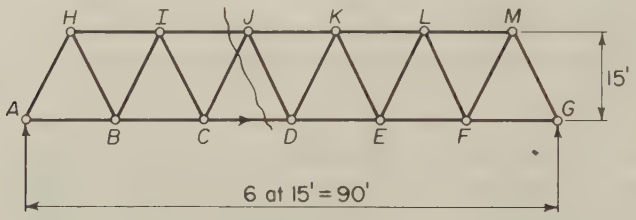

Figure 6–46

6-13 *Summary*

We have discussed the concept of influence lines and its applications and limitations. We pointed out that the scope of general applications far exceeds the examples given in this chapter, especially with regard to statically indeterminate structures. On the other hand, criteria for maximum effects due to a series of concentrated loads have only limited use for statically determinate structures. Therefore, we have emphasized the basic principles behind the development of criteria rather than extensive applications to various types of structures.

Although the method of virtual displacements does not necessarily simplify the construction of quantitative influence lines, it provides a simple means of visualizing the deflected shape of the released system which is, in itself, a qualitative influence line.

References

6-1 C. K. Wang and C. L. Eckel, *Elementary Theory of Structures*, McGraw-Hill Book Co., Inc., New York, 1957.

6-2 C. M. Spofford, *The Theory of Structures*, 3rd ed., McGraw-Hill Book Co., Inc., New York, 1928.

6-3 J. B. Johnson, C. W. Bryan, and F. E. Turneaure, *Modern Framed Structures*, 10th ed., vol. 1, John Wiley & Sons, Inc., New York, 1926.

6-4 P. Anderson and G. M. Nordby, *Introduction to Structural Mechanics*, Ronald Press Co., New York, 1960.

6-5 A. J. S. Pippard and J. F. Baker, *The Analysis of Engineering Structures*, 3rd ed., Edward Arnold Ltd., London, 1957.

Problems

6-1 For the beam shown in Fig. P6-1, draw the influence lines for the following effects: (a) reactions at supports B and C, (b) shears at a section just to the left and another section just to the right of support B, (c) moments at points B, C, E, and F.

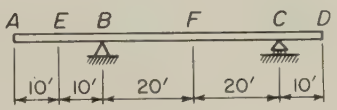

Figure P6–1

6-2 Construct influence lines for the following effects on the beam shown in Fig. P6-2: (a) reaction at A, (b) reaction at B, (c) shears at C and D, (d) moments at C and D.

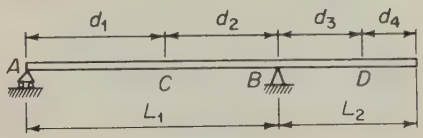

Figure P6–2

6-3 Draw the influence lines for the following effects if a unit load moves from C to A in the structure shown in Fig. P6-3: (a) shears at points E and F, (b) moments at points E and F.

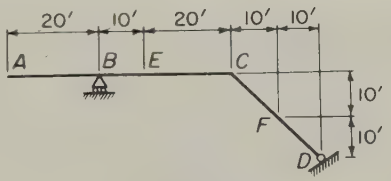

Figure P6–3

6-4 Draw the influence lines for the following effects if a unit load moves from D to A of the structure shown in Fig. P6-4: (a) vertical reaction at E, (b) shear to the right of support B, (c) moments at points C and F.

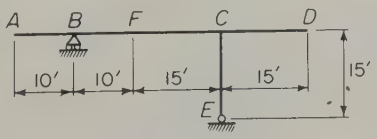

Figure P6–4

6-5 Construct the influence lines for the following effects on the beam shown in Fig. P6-5: (a) vertical reaction at F, (b) shear at a section just to the left of C, (c) shear at a section just to the right of C, (d) moment at point C, (e) moment at point E.

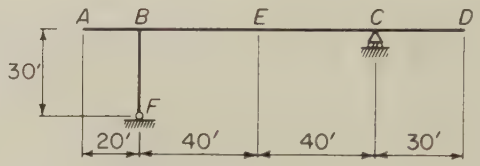

Figure P6–5

6-6 Draw the influence line for the reaction at support A of the suspended girder shown in Fig. P6-6.

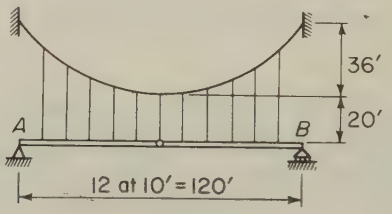

Figure P6–6

6-7 For the beam with releases shown in Fig. P6-7, draw the influence lines for the following effects, using the concept of a moving unit load: (a) reaction at support B, (b) moment at support B, (c) shear at point G.

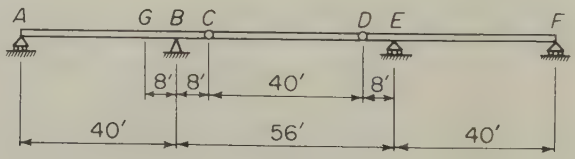

Figure P6–7

6-8 For the beam shown in Fig. P6-8, compute the maximum shear and moment at point E due to a uniform live load of 2 kips per foot plus a roving concentrated load of 20 kips.

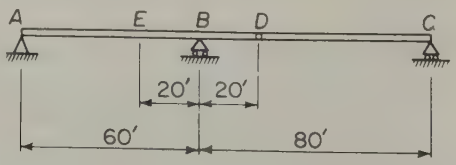

Figuer P6–8

6-9 Construct influence lines for the following effects on the beam shown in Fig. P6-9, using the concept of a moving unit load: (a) reactions at A and B, (b) shears at G and H, (c) moments at G and H.

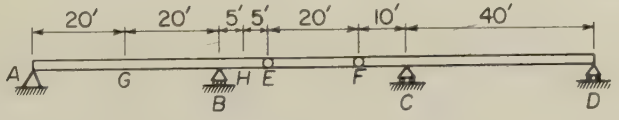

Figure P6–9

6-10 Repeat Problem 6-7 using the method of virtual displacements.

6-11 Repeat Problem 6-9 using the method of virtual displacements.

6-12 For the compound beam shown in Fig. 6-12, draw the influence lines for the following effects: (a) reaction at support B, (b) shear in panel EF, (c) moment at point F.

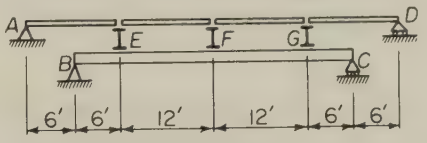

Figure P6–12

6-13 For the girder shown in Fig. P6-13, draw the influence lines for the following effects: (a) shears in panels AB and BC, (b) moments at points C and D.

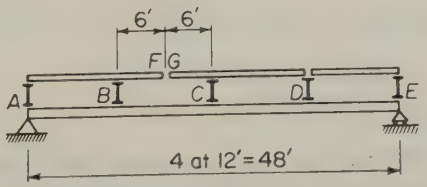

Figure P6–13

6-14 For the girder supporting floor beams shown in Fig. P6-14, draw the influence lines for the following effects: (a) reactions at supports B and F, (b) shears in panels BC and EF, (c) moments at points A and D.

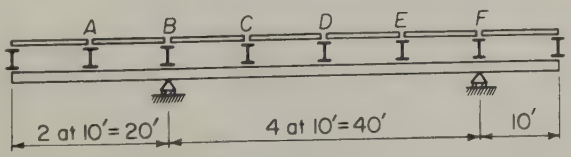

Figure P6–14

6-15 For the semicircular three-hinged arch shown in Fig. P6-15, draw the influence lines for the horizontal reaction H and for the normal force N_d, the shear S_d, and the moment M_d at point D of the arch rib if a vertical unit load moves from the right to the left of the arch.

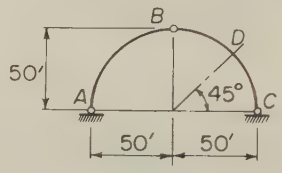

Figure P6–15

6-16 The parabolic arch shown in Fig. P6-16 supports a floor system that transmits the floor load to the arch through the vertical struts. Draw the influence line for the horizontal thrust H at the supports B and C.

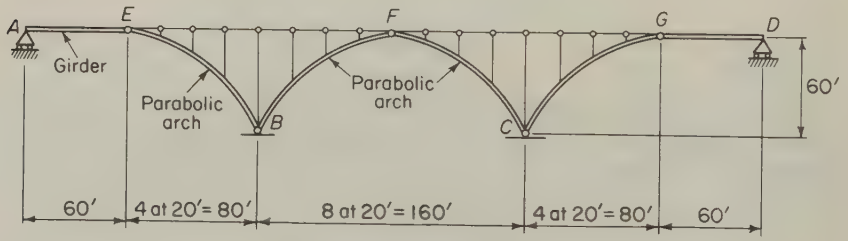

Figure P6–16

6-17 Draw the influence lines for the normal force, shear, and moment at point D of the three-hinged arch shown in Fig. P6-17. Numerical values of the key ordinates of the influence lines should be given in the diagrams. The equation of the arch rib is $y = x^2/200$.

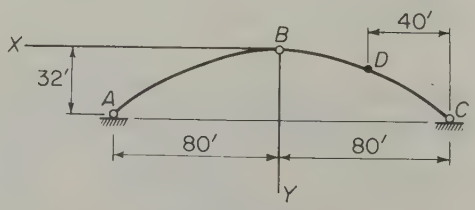

Figure P6–17

6-18 For the truss shown in Fig. P6-18, find the maximum bar forces in members U_2L_3 and L_3L_4 due to a uniform load of 1 kip/ft.

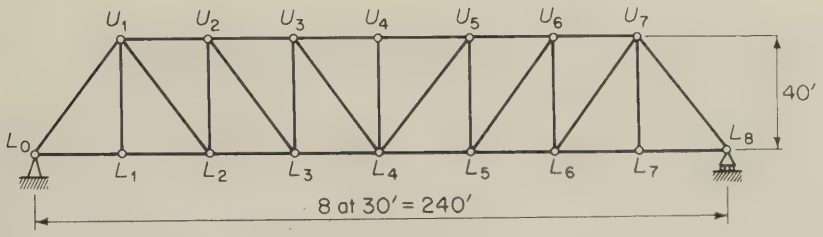

Figure P6–18

6-19 Determine the maximum bar forces in members U_2U_3, U_2L_3, L_2L_3, and U_3L_3 of the truss shown in Fig. P6-19 due to a uniform live load of 6 kips/ft.

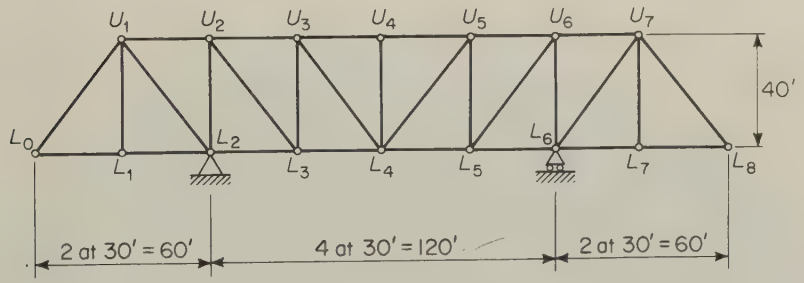

Figure P6–19

6-20 Construct the influence lines for all components of reactions as a unit load moves from A to B on the structure shown in Fig. P6-20.

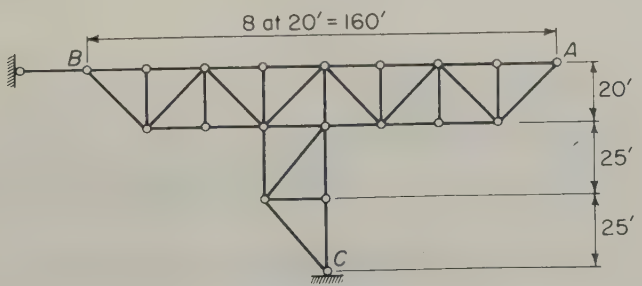

Figure P6–20

6-21 Construct the influence lines for bar forces in members U_4U_5, L_4L_5, M_4U_5, M_4L_5, U_4M_4, and M_4L_4 of the K-truss shown in Fig. P6-21.

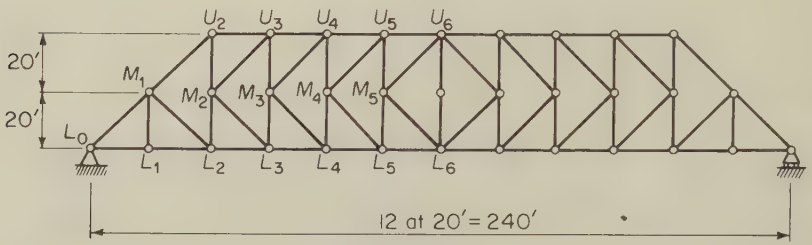

Figure P6–21

6-22 Draw the influence lines for the bar forces in members U_2U_4, L_2L_4, L_2M_3, M_3L_4, U_2M_3, and M_3L_3 of the truss shown in Fig. P6-22.

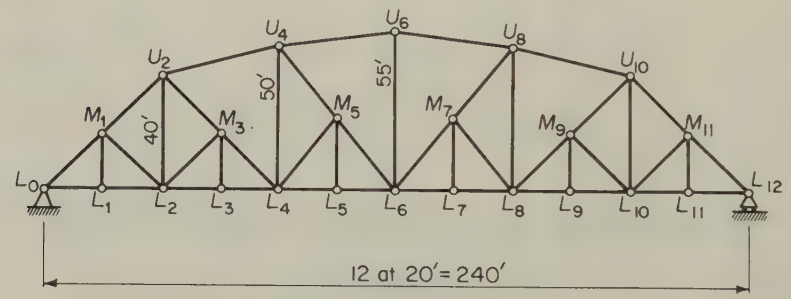

Figure P6–22

6-23 Construct the influence lines for the bar forces in members a, b, and c of the truss shown in Fig. P6-23.

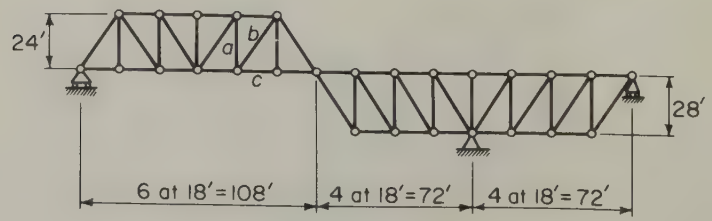

Figure P6–23

6-24 Compute the maximum tensile and/or compressive bar forces in members *a* and *b* in the structure shown in Fig. P6-24 due to a moving uniform load of 1 kip/ft.

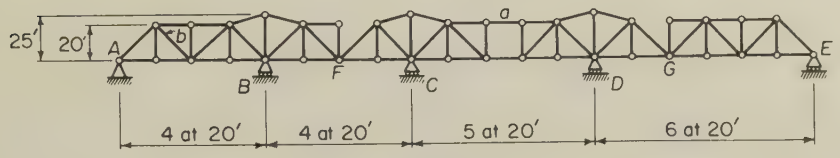

Figure P6–24

6-25 Construct the influence lines for the bar forces in members *a* and *b* and for the reaction *A* of the stiffening truss of the suspension bridge shown in Fig. P6-25.

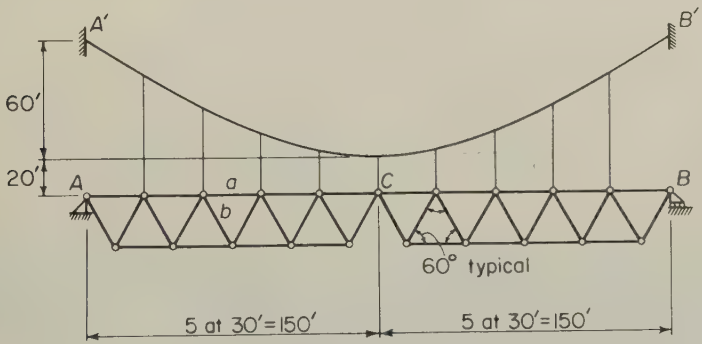

Figure P6–25

6-26 Draw the influence lines for the bar forces in members U_4U_6, U_4M_5, M_5U_6, M_5L_6, U_4L_4, and U_6L_6 for the truss shown in Fig. P6-26.

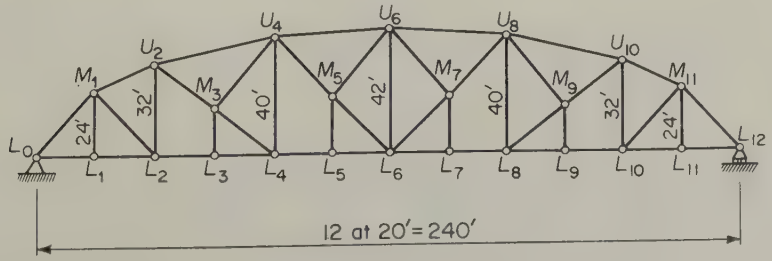

Figure P6–26

6-27 For a highway bridge girder of 45-ft single span subjected to a series of moving concentrated load as shown in Fig. P6-27, determine (a) the maximum reaction, (b) the maximum shear at the third point of the span, (c) the maximum moment at the center of the span.

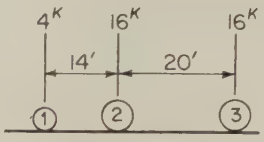

Figure P6–27

6-28 A crane runway girder of 80-ft span is designed to support two cranes in tandem. The loads applied to each girder are shown in Fig. P6-28. Compute: (a) the maximum reaction, (b) the maximum shear at the quarter point of the span, (c) the maximum moment at the center of the span.

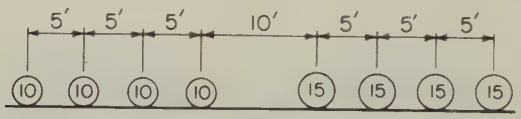

Figure P6–28

6-29 A single-track plate-girder railroad bridge of 120-ft span is designed for a Cooper's E-60 loading. Assuming that each girder carries half of the live loads, compute (a) the maximum reaction, (b) the maximum shear at the center of the span, (c) the maximum moment at the quarter point of the span.

6-30 A simple 75-ft beam is subjected to a Cooper's E-60 loading. Determine (a) the maximum shear at a point 10 ft from the left support, (b) the maximum moment at a point 15 ft from the left support.

6-31 Determine the absolute maximum moment in a simply supported beam of 60-ft span due to a series of moving loads shown in Fig. P6-31.

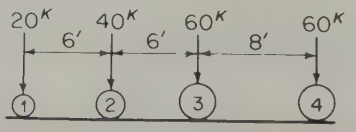

Figure P6–31

6-32 Derive a general expression for the absolute maximum moment for the beam shown in Fig. P6-32.

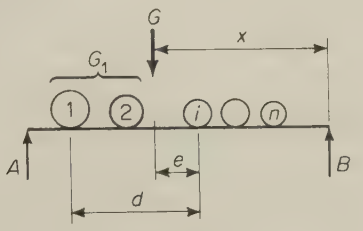

Figure P6–32

6-33 Compute the maximum bar forces in members U_1L_1, U_2L_2, U_1U_2, L_1L_2, and U_1L_2 of the truss shown in Fig. P6-33 due to Cooper's E-60 loading on the truss.

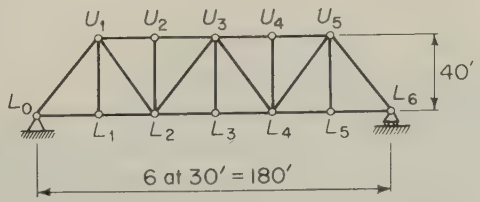

Figure P6–33

6-34 Compute the maximum bar forces in members U_2U_3, L_2U_2, L_2U_3, and L_2L_3 of the truss shown in Fig. P6-34 due to Cooper's E-60 loading on the truss.

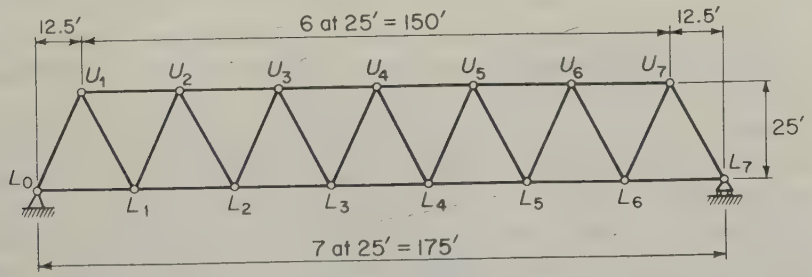

Figure P6–34

7 DISPLACEMENTS

7-1 *Elastic Deflections of Simple Structures*

The displacements of a deformable system resulting from applied loads or other causes are commonly called *deflections*. In a narrower sense, the term *deflection* is used to denote linear displacement only. The applied loads on a structure generally produce internal forces and moments in various parts of the structure. The internal forces and moments at any section of the structure may be related to the stresses acting on the section, which can in turn be expressed in terms of strains by the stress-strain relation of the material. Since deflections are the outward indications of the accumulation of strains compatible with the geometry of the structure, the deflections of a structure under loads can be computed if the stress-strain relation of the material is known.

From a broader point of view, the computation of deflections is often a preliminary step in setting up the conditions for the analysis of statically indeterminate structures. For such cases, the main point of interest will no longer be the general deflections of a structure, but rather a particular deflection for which certain conditions of geometrical compatibility must be maintained. Thus, the techniques or methods of computing deflections may be classified broadly as (1) methods for computing a number of deflections simultaneously and (2) methods for computing one particular deflection.

On the other hand, according to the basic approach used in the solution of the problem, the methods of computing deflections may be classified as the *equilibrium* approach, which is based on the conditions of equilibrium of the system, and the *energy* approach, which is derived from the principle of conservation of energy. In general, the equilibrium approach can readily be applied to the computation of deflections at a number of points on the

structure, and the energy approach is especially useful for the computation of one particular deflection at a time. Thus, each approach has certain advantages for specific purposes. In this chapter we shall confine our discussion to the equilibrium approach with emphasis on the geometry of structures; in Chapter 8 the energy approach will be developed for the calculation of deflections at specific points of structures.

In order to compute the general deflections of simple structures such as statically determinate beams, frames, and trusses by means of the equilibrium approach, we must study the geometry of the deflected structures by means of which the applied loads and the deflections are related. Since the deflections tolerated in engineering structures are usually very small, we are primarily interested in the elastic deflections. Hence, the angles of rotation as well as the displacements in a deflected structure are small quantities in comparison with the dimensions of the structure. For the sake of simplicity, in this chapter, we shall confine our discussion to linearly elastic materials in the computation of displacements and rotations.

In order to designate the senses of direction of displacements correctly and systematically, it is often convenient to adopt a sign convention. On the other hand, sign conventions have their limitations because they are not always adaptable to complicated structures. Therefore, it is sometimes easier to deal with the absolute values of these quantities if the geometry of the deflected structure is observed so that the senses of direction of displacements cannot be mistaken. Whenever a sign convention is adopted in connection with a method of solution in this chapter, it will be clearly defined. However, the physical meaning of the signs will also be explained by study of the geometry of structures.

7-2 *Moment-Curvature Relation*

If an initially straight member is subjected to bending, the shape of the deformed neutral axis is called the *elastic curve*. Consider a small element δx, as shown in Fig. 7-1 that is isolated from a member subjected to pure bending. Since no shear exists at any section of a member in pure bending, the bending moment equals M at every section of the member. Let y be the ordinate of a point from the neutral axis of the element, being positive when the point is above the neutral axis. Assuming that sections that are plane before bending remain plane after bending, the relation between bending stress and bending moment can be established

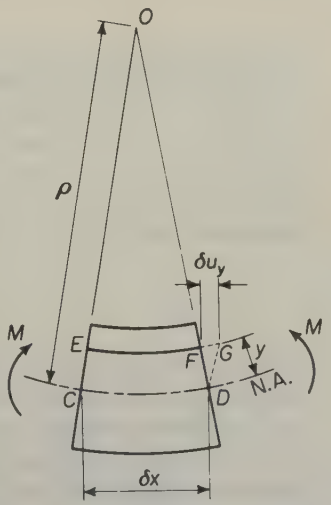

Figure 7–1

from the consideration of equilibrium of forces and moments acting on the element. In Section 2-8, the bending stress σ in a fiber at a distance y from the neutral axis is given for linearly elastic materials as follows:

$$\sigma = -\frac{My}{I} \tag{a}$$

in which M is the moment at a section and I is the moment of inertia of the cross section. The minus sign indicates compressive stress for positive y if the moment is positive. The same assumption of linear strain distribution leads to the conclusion that the initially parallel planes on the sides of an element before bending must intersect after bending as shown in Fig. 7-1. The intersection O is called the *center of curvature* and the distance ρ from the intersection O to the neutral axis is called the *radius of curvature*. For a fiber at a distance y from the neutral axis, the original length of the element δx is shortened by an amount δu_y, and the strain at that fiber is equal to $\epsilon = \delta u_y/\delta x$. As δx approaches zero as a limit,

$$\epsilon = -\frac{du_y}{dx} \tag{b}$$

Since δx is infinitely small, OCD and FGD may be considered to be similar triangles from which

$$\frac{\delta u_y}{y} = \frac{\delta x}{\rho} \quad \text{or} \quad \frac{du_y}{dx} = \frac{y}{\rho} \tag{c}$$

From Eqs. (b) and (c), we get

$$\epsilon = -\frac{y}{\rho}$$

For elastic materials for which Hooke's law applies,

$$\sigma = \epsilon E = -\frac{Ey}{\rho} \tag{d}$$

By equating Eqs. (a) and (d), the moment-curvature relation can be expressed as follows:

$$\frac{M}{EI} = \frac{1}{\rho} \tag{7-1}$$

This is essentially a force-deformation relation in which M is the applied force and the curvature $1/\rho$ is the resulting deformation. The quantity EI is called the *flexural rigidity* or *bending stiffness* of the member.

If a structural member is subjected to shear and axial force as well as bending moment, additional deformation is caused. For slender members, however, the deformation due to shear or axial force is small and negligible

in comparison with that due to bending. It is assumed, therefore, that Eq. (7-1) can generally be applied to members subjected to a combined action of axial force, shear, and bending. When shear forces exist at various sections of a member, the bending moment is no longer constant along the length of the member. When the moment changes from point to point in the member, the curvature changes accordingly. On the other hand, if the moment of inertia of the member varies along its length, the curvature also changes. In either case, $1/\rho$ will no longer be constant at different points of the beam, but the moment-curvature relation in Eq. (7-1) still holds at any particular point.

The over-all shape of the elastic curve is directly related to the curvature along the length of a member. Let u and v be the horizontal and vertical displacements respectively of a point on the elastic curve, as shown in Fig. 7-2(a). If the member is supported at point O, a point A on the neutral axis

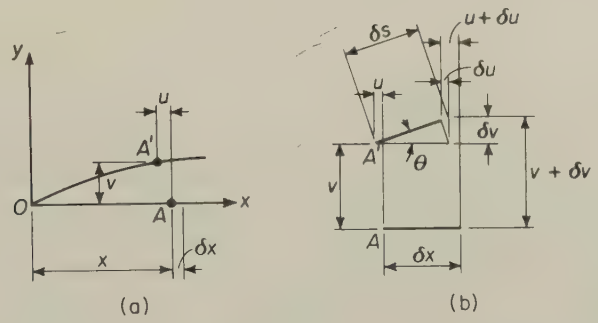

Figure 7–2

of the undeflected beam will move to point A' on the elastic curve after bending, resulting in displacement u toward the left of the original position and displacement v in the upward direction. For ordinary engineering structures, only small deflections and small slopes are involved, and the angle θ of the slope is in the order of magnitude of a thousandth of a radian. It can be assumed, therefore, that

$$\sin\theta = \tan\theta = \theta \text{ in radian}$$

and

$$\cos\theta = 1$$

For an element δx shown in Fig. 7-2(b), δu is small and negligible in comparison with δv because $\delta u = \theta\, \delta v$, in which θ is a small quantity. It is necessary, therefore, to consider only the vertical displacement v. However, the horizontal displacement u can be expressed as a function of v by observing the geometrical relation in Fig. 7-2(b). For $\delta u = \delta s - \delta x$, the

displacement u at any point on the elastic curve is equal to

$$u = \int_0^x (ds - dx) \tag{e}$$

Since δs may be expressed in terms of the slope of the elastic curve and approximated by expanding the expression into a binomial series, we have

$$\delta s = [(\delta x)^2 + (\delta v)^2]^{1/2} = \left[1 + \left(\frac{dv}{dx}\right)^2\right]^{1/2} \delta x$$

$$= \left[1 + \frac{1}{2}\left(\frac{dv}{dx}\right)^2 - \frac{1}{8}\left(\frac{dv}{dx}\right)^4 + \cdots\right] \delta x \tag{f}$$

By taking only the first two terms in the series, and by substituting Eq. (f) into Eq. (e), we obtain

$$u = \int_0^x \frac{1}{2}\left(\frac{dv}{dx}\right)^2 dx \tag{7-2}$$

Hence, the horizontal displacement u can be evaluated if the equation of the elastic curve for the vertical displacement v is first obtained.

The vertical displacement v of the elastic curve can readily be related to the curvature. In elementary calculus, it has been shown that if v denotes the ordinate and x the abscissa of a point on a curve, as shown in Fig. 7-3(a), the curvature is given by:

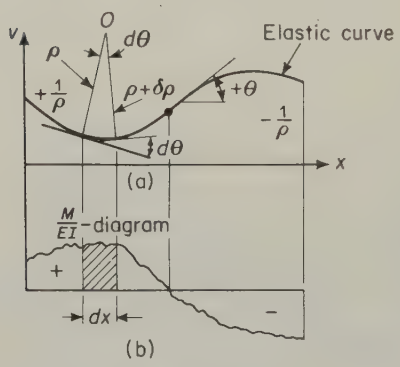

Figure 7–3

$$\frac{1}{\rho} = \frac{d^2v/dx^2}{[1 + (dv/dx)^2]^{3/2}}$$

By substituting this expression into Eq. (7-1), we obtain

$$\frac{d^2v/dx^2}{[1+(dv/dx)^2]^{3/2}} = \frac{M}{EI} \tag{7-3}$$

It may be observed that the solution of Eq. (7-3) is rather difficult to obtain. However, since the slope of the elastic curve dv/dx is small, the term $(dv/dx)^2$ is negligible in comparison with unity. Then Eq. (7-3) becomes

$$\frac{d^2v}{dx^2} = \frac{M}{EI} \tag{7-4}$$

Finally, the elastic curve of a deflected member can be obtained from the solution of the differential equation represented by Eq. (7-4).

In view of the fact that $\tan\theta = \theta$ for small angles, the slope of the elastic

curve can be represented by θ or

$$\frac{dv}{dx} = \theta \tag{7-5}$$

Then, Eq. (7-4) becomes

$$\frac{d\theta}{dx} = \frac{M}{EI} \tag{7-6}$$

Since the curvature is defined by Eq. (7-4), a positive curvature corresponds to a positive moment. Equation (7-6) further indicates that a positive change in slope between two points on the elastic curve corresponds to a positive moment as shown by the part of the deflection curve that is concave upward in Fig. 7-3(a). If the ordinates of the moment diagram along the length of a member are divided by the corresponding EI of the beam at the same section, the ordinates of the resulting M/EI diagram have the same sign as the corresponding moments. Thus, the sign of the curvature at a point on the elastic curve shown in Fig. 7-3(a) must correspond to that of the same section on the M/EI diagram in Fig. 7-3(b).

7-3 *Deflection of Beams*

The equation of the elastic curve of a beam subjected to a given loading can be obtained by integrating twice the expression M/EI in Eq. (7-4) with respect to x. Carrying out the integration in two steps, the equations for slopes and deflections of a beam can be obtained from Eqs. (7-5) and (7-6). Thus,

$$\theta = \int \frac{M}{EI} dx + C_1 \tag{7-7}$$

$$v = \int \theta \, dx + C_2 \tag{7-8}$$

In order to evaluate the integrals and the constants of integration in Eqs. (7-7) and (7-8), we proceed as follows:

1. From the conditions of equilibrium of forces and moments, the bending moment along the beam can be expressed as a function of x. The procedure for carrying out this step has been fully explained in Chapter 3.

2. The bending stiffness EI can be determined from the material characteristics and the dimensions of the cross section of the beam. If EI is constant throughout the entire length of the beam, it can be conveniently handled in Eqs. (7-7) and (7-8). If EI is variable, it must also be expressed as a function of x.

3. The constants of integration can be determined from the requirements that the continuity of the elastic curve be maintained and that the displacement boundary conditions of the elastic curve be satisfied. Continuity implies that no abrupt change in deflection or slope of the deflection

curve is permissible. The displacement boundary conditions refer to the known conditions of deflection and slope at the supports. For example, at a hinge or roller support no deflection of the elastic curve can take place, and at a fixed support no deflection or rotation of the elastic curve can occur.

The physical meaning of the displacement boundary conditions in determining the constants of integration in Eqs. (7-7) and (7-8) can easily be explained if these equations are rearranged as follows:

$$\theta = \int \frac{M}{EI}\,dx + C_1 = \int k\,dx + C_1$$

$$v = \int \theta\,dx + C_2 = \int \left(\int k\,dx \right) dx + C_1 x + C_2$$

in which the curvature M/EI is denoted by k. Thus, the integrals in the equations for slope and deflection are defined by the curvature only and are independent of the boundary conditions. The ordinates of the points on the slope and deflection curves, of course, are influenced by the boundary conditions which are represented by the constants of integration C_1 and C_2. As an example, consider two simply supported beams, one horizontal and the other inclined, as shown in Figs. 7-4(a) and (b) respectively. If the ordinate

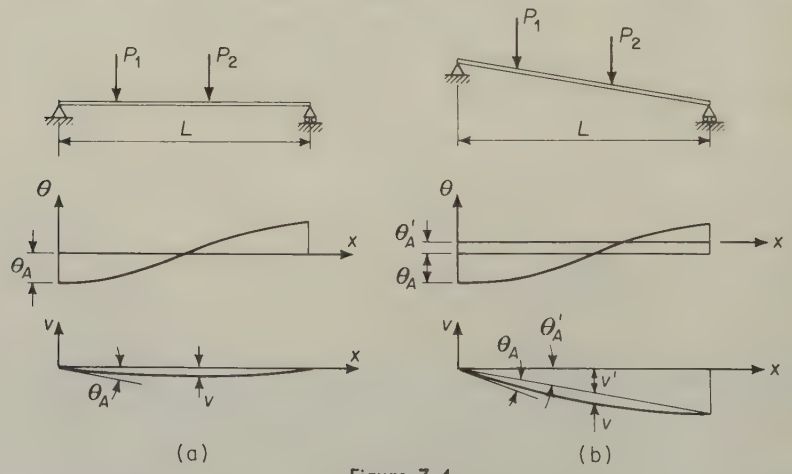

Figure 7–4

of the M/EI diagram at every *vertical* section is the same for both beams, then the slope and deflection curves for the beam in Fig. 7-4(a) have the same shapes as the respective curves for the beam in Fig. 7-4(b). Since the boundary conditions of these beams are different, the ordinates of these diagrams in Figs. 7-4(a) and (b) are not the same. However, the ordinates of the slope curve in one case may differ from those in the other case by a constant amount equivalent to the vertical translation of the x-axis, and the

ordinates of the deflection curve may differ by an amount equivalent to the rotation of the x-axis. In general, if the integrals representing the shapes of the slope and deflection curves are evaluated first by assuming $C_1 = C_2 = 0$, corrections equivalent to $\theta = C_1$ and $v = C_1x + C_2$ may be added to the corresponding integrals later.

The slope and deflection equations may also be expressed in the form of definite integrals for the interval $a < x < b$ as follows:

$$\theta_b - \theta_a = \int_a^b \frac{M}{EI}\, dx \tag{7-9}$$

$$v_b - v_a = \int_a^b \theta\, dx \tag{7-10}$$

Equation (7-9) implies that the slope at any point of a beam is equal to the slope at a previous point along the axis of the beam plus the area of the M/EI diagram between these two points. Similarly, Eq. (10) states that the deflection at any point of the beam is equal to the deflection at a previous point along the axis of the beam plus the area under the slope curve between these two points. Thus, the computation of slopes and deflections becomes a process of summation starting from an initial point of known slope and deflection.

We can make use of the relationships in Eqs. (7-5), (7-6), (7-9), and (7-10) in plotting the variations of slope and deflection along the length of the beam. For example, we observe that the point of maximum deflection is the point of zero slope, and that the point of maximum slope is the point of zero moment. The ordinates of the slope and deflection curves can be obtained from step-by-step summation as represented by Eqs. (7-9) and (7-10). However, usually only the qualitative rather than the quantitative representations of these curves are needed for the study of the geometry of deflected structures.

In view of Eqs. (7-5) and (7-6), together with Eqs. (3-1) and (3-2), it may be concluded that if the equation of the elastic curve is known, not only the slope θ of the elastic curve but also the moment M, the shear S, and the applied load q at any point of the beam may be obtained by successive differentiations as follows:

$$\begin{aligned} \theta &= \frac{dv}{dx} \\ M &= EI\frac{d\theta}{dx} = EI\frac{d^2v}{dx^2} \\ S &= \frac{dM}{dx} = EI\frac{d^3v}{dx^3} \\ q &= \frac{dS}{dx} = EI\frac{d^4v}{dx^4} \end{aligned} \tag{7-11}$$

Conversely, the equation of the elastic curve may be obtained by successive integrations from the applied load, as given by Eqs. (3-3) and (3-4), together with Eqs. (7-7) and (7-8). Denoting the curvature M/EI by k, we have

$$\begin{aligned} S &= \int q\,dx + C_1 \\ M &= \int S\,dx + C_2 \\ \theta &= \int \frac{M}{EI}\,dx + C_3 = \int k\,dx + C_3 \\ v &= \int \theta\,dx + C_4 \end{aligned} \tag{7-12}$$

in which the constants of integration C_1, C_2, C_3, and C_4 are determined from the boundary conditions. The first two equations of Eqs. (7-12) involve only the principles of statics, and the constants C_1 and C_2 depend on the force boundary conditions of shear and moment. The last two equations of Eqs. (7-12) include the material characteristics E and the geometrical properties of the section I, and the constants C_3 and C_4 depend on the displacement boundary conditions of slope and deflection.

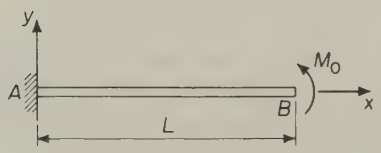

Figure 7–5

Example 7-1. A cantilever beam of span length L and of constant bending stiffness EI is subjected to a moment M_0 at the free end as shown in Fig. 7-5. Determine the equation of the elastic curve.

Since the moment along the length of the beam is constant, or $M = M_0$, we obtain from Eqs. (7-7) and (7-8).

$$\theta = \frac{M_0 x}{EI} + C_1 \tag{a}$$

$$v = \frac{M_0 x^2}{EI} + C_1 x + C_2 \tag{b}$$

The displacement boundary conditions of this beam are as follows:

$$\theta = 0 \text{ at } x = 0 \quad \text{and} \quad v = 0 \text{ at } x = 0$$

Hence, the equation of the elastic curve is

$$v = \frac{M_0 x^2}{2EI} \tag{c}$$

The last equation indicates that the elastic curve is parabolic whereas, in reality, it should be a circular arc, since the moment M_0 is constant along the length of the beam, and consequently the radius of curvature is also constant. This inconsistency is the result of the use of the expression for curvature in Eq. (7-4) instead of that in Eq. (7-3).

We can now compare the order of magnitude of the displacements u and v for this particular problem. The maximum displacements occur at the free end B of the beam where $x = L$. Thus, from Eq. (c),

$$v_b = \frac{M_0 L^2}{2EI}$$

For Eq. (7-2), we obtain first $dv/dx = M_0 x/EI$. Then,

$$u_b = \int_0^L \frac{1}{2} \left(\frac{M_0 x}{EI}\right)^2 dx = \frac{M_0^2 x^3}{6(EI)^2}\bigg|_0^L = \frac{M_0^2 L^3}{6E^2 I^2}$$

The ratio of u_b to v_b can be expressed as follows:

$$\frac{u_b}{v_b} = \frac{L}{3EI}$$

For ordinary engineering problems, $M_0 L/3EI$ is a very small quantity, and hence u_b is negligible in comparison with v_b.

Example 7-2. A simply supported beam of span length L and constant bending stiffness EI is subjected to a uniformly varying load as shown in Fig. 7-6(a). Plot the ordinates of shear, moment, slope, and deflection along the length of the beam.

If the reactions from the applied load are first obtained as shown in Fig. 7-6(a), the force boundary conditions can be expressed as $S = w_0 L/6$ at $x = 0$ and $M = 0$ at $x = 0$. Thus, by starting from $q = -w_0 x/L$,

$$S = \int q\,dx + C_1 = -\frac{w_0 x^2}{2L} + \frac{w_0 L}{6}$$

$$M = \int S\,dx + C_2 = -\frac{w_0 x^3}{6L} + \frac{w_0 L x}{6} + 0$$

$$k = \frac{M}{EI} = \frac{w_0}{6EIL}(-x^3 + L^2 x)$$

$$\theta = \int k\,dx + C_3 = \frac{w_0}{6EIL}\left(-\frac{x^4}{4} + \frac{L^2 x^2}{2}\right) + C_3$$

$$v = \int \theta\,dx + C_4 = \frac{w_0}{6EIL}\left(-\frac{x^5}{20} + \frac{L^2 x^3}{6}\right) + C_3 x + C_4$$

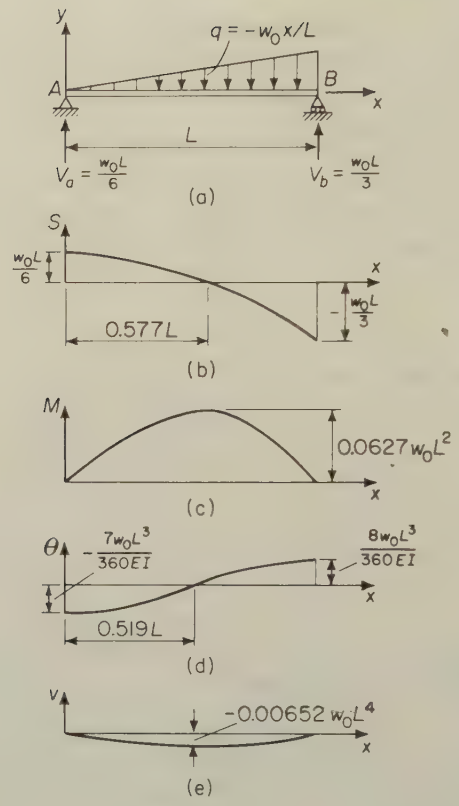

Figure 7–6

The displacement boundary conditions are $v = 0$ at $x = 0$ and $x = L$. Then,

$$C_4 = 0 \quad \text{and} \quad C_3 = -\frac{7w_0L^3}{360EI}$$

Hence,

$$\theta = \frac{w_0}{360EIL}(-15x^4 + 30L^2x^2 - 7L^4)$$

$$v = \frac{w_0}{360EIL}(-3x^5 + 10L^2x^3 - 7L^4x)$$

The maximum moment occurs at the point where $S = 0$, from which $x = 0.577L$ and $M_{\max} = 0.0627w_0L^2$. Similarly, the maximum deflection occurs at the point where $\theta = 0$, from which $x = 0.519L$ and $v_{\max} = -0.00652w_0L^4$. The equations for shear, moment, slope, and deflection are plotted in Figs. 7-6(b), (c), (d), and (e) respectively.

7-4 *Successive Integrations of Singularity Functions*

In Section 3-4, the integrations of singular functions are introduced primarily for the purpose of providing complete generality to the concept of obtaining shears and moments from the given loading functions by direct integration. We pointed out that, for practical purposes, such a method offers little advantage over other methods. In the computation of deflections, however, this general concept not only brings unity to the procedure of successive integrations but also simplifies the solution of certain types of problems.

When the applied load on a beam is not a continuous function along its length, the conditions of compatibility at each point of discontinuity must be considered in the solution of slope and deflection of the beam by direct integration if the integrations of singularity functions are not introduced. Thus, for each discontinuity, there appear two additional constants of integration in the slope and deflection of the beam which may be evaluated from the conditions of compatibility. For problems with several discontinuities, the solution leads to a large number of simultaneous equations involving constants of integration as unknowns. This situation can be avoided by the introduction of singularity functions.

In the case of beams with variable bending stiffness, such as beams with cut-off cover plates, discontinuities also exist in the curvature diagrams. Such situations can also be treated by the use of singularity functions. One of the most useful applications of the singularity functions is the computation of deflection of beams with releases. Without the benefit of singularity functions, the deflection at each part of the beam between releases or supports must be computed separately. By introducing the concept of singularity functions in the curvature diagram, it can be treated in the same way as for beams without releases.

There are other advantages in the use of singularity functions, especially in the computation of deflections of beams that are statically indeterminate. In that case, the redundant reactions can be treated as singularity functions of forces. The student is referred to Reference 3-1 for further discussion.*

Example 7-3. A simply supported beam of span length L and constant bending stiffness EI is subjected to a concentrated load P as shown in Fig. 7-7(a). Find the equation of the elastic curve.

The problem will be worked out in two ways. First, moment equations are written separately for segment AC and CB of the beam, secondly, the notations for singularity functions are used. The coordinate system shown in Fig. 7-7(b) will be adopted for both cases.

*See pp. 364-370 of Reference 3-1.

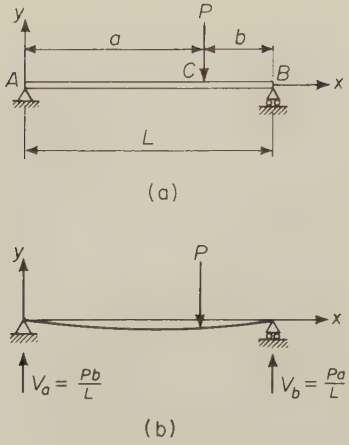

Figure 7-7

The equations for moment in segments AC and CB of the beam can be obtained by statics, and the integrations of these equations are carried out as follows:

For segment AC,

$$M = \frac{Pb}{L}x$$

$$\theta = \frac{Pbx^2}{2EIL} + C_1$$

$$v = \frac{Pbx^3}{6EIL} + C_1x + C_2$$

For segment CB,

$$M = \frac{Pb}{L}x - P(x - a)$$

$$\theta = \frac{P}{EI}\left[\frac{bx^2}{2L} - \frac{x^2}{2} + ax\right] + C_3$$

$$v = \frac{P}{EI}\left[\frac{bx^3}{6L} - \frac{x^3}{6} + \frac{ax^2}{2}\right] + C_3x + C_4$$

There are four constants of integration in the two sets of equations for slope and deflection. From the displacement boundary conditions, we have $v = 0$ at $x = 0$ and at $x = L$, from which we obtain

$$C_2 = 0$$

$$0 = \frac{PL^2}{6EI}(b - L + 3a) + C_3L + C_4 = \frac{PaL^2}{3EI} + C_3L + C_4$$

Two other conditions are sought from the continuity of the elastic curve. That is, at $x = a$ the slope and deflection are unique whether they are obtained from segment AC or segment CB. Thus, at point C

$$\theta_c = \frac{Pba^2}{2EIL} + C_1 = \frac{Pa^2}{2EI}\left(\frac{b}{L} + 1\right) + C_3$$

$$v_c = \frac{Pba^3}{6EIL} + C_1a + C_2 = \frac{Pa^3}{6EI}\left(\frac{b}{L} + 2\right) + C_3a + C_4$$

Solving these four equations simultaneously, we get

$$C_1 = -\frac{Pb}{6EIL}(L^2 - b^2), \qquad C_2 = 0$$

$$C_3 = -\frac{Pa}{6EIL}(2L^2 + a^2), \qquad C_4 = \frac{Pa^3}{6EI}$$

Finally, we obtain for $0 \leqq x \leqq a$,

$$v = \frac{Pb}{6EIL}\,[x^3 - (L^2 - b^2)x]$$

and for $a \leqq x \leqq L$,

$$v = \frac{Pb}{6EIL}\left[x^3 - \frac{L}{b}(x - a)^3 - (L^2 - b^2)x\right]$$

Using the notations for singularity functions in Section 3-4, we have in this case a loading function

$$q = -P\langle x - a\rangle^{-1}$$

Integrating twice, we get

$$S = -P\langle x - a\rangle^0 + C_1$$

$$M = -P\langle x - a\rangle^1 + C_1 x + C_2$$

From the static boundary conditions $M = 0$ at $x = 0$ and at $x = L$, we obtain $C_2 = 0$ and $C_1 = P(L - a)/L = Pb/L$. Thus,

$$S = \frac{Pb}{L} - P\langle x - a\rangle^0$$

$$M = \frac{Pbx}{L} - P\langle x - a\rangle^1$$

These are essentially identical to the equations for shear and moment obtained by statics.

In order to compute the slope and deflection, we integrate the equation for curvature. Thus,

$$k = \frac{M}{EI} = \frac{P}{EI}\left[\frac{bx}{L} - \langle x - a\rangle^1\right]$$

$$\theta = \frac{P}{2EI}\left[\frac{bx^2}{L} - \langle x - a\rangle^2\right] + C_3$$

$$v = \frac{P}{6EI}\left[\frac{bx^3}{L} - \langle x - a\rangle^3\right] + C_3 x + C_4$$

The geometrical boundary conditions are $v = 0$ at $x = 0$ and at $x = L$. Then, we get

$$C_4 = 0, \qquad C_3 = -\frac{Pb}{6EIL}(L^2 - b^2)$$

Hence,

$$v = \frac{Pb}{6EIL}\left[x^3 - \frac{L}{b}\langle x - a\rangle^3 - (L^2 - b^2)x\right]$$

Note that the second term on the right-hand side of the equation has a bracket notation because it is zero when $x < a$ and is equal to $(L/b)(x - a)^3$ when $x > a$.

Example 7-4. Derive the equation of the elastic curve for the compound beam shown in Fig. 7-8(a).

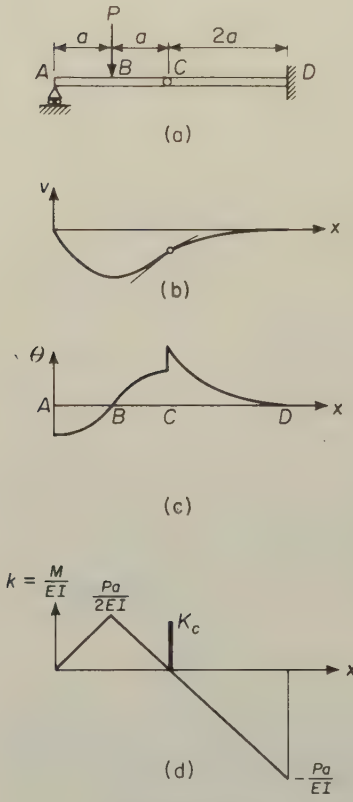

Figure 7–8

Since a hinge is present at point C, it is usually necessary to break up the compound beam into parts AC and CD because there is a kink or an abrupt change of slope in the deflection curve at point C. Exaggerating the deflection curve in Fig. 7-8(b), the tangent to the curve at the left of hinge C is seen to be different from that at the right of hinge C. Therefore, a sudden jump or step exists at point C of the curve showing the variation of slope in Fig. 7-8(c). At the corresponding point of the curvature curve or M/EI diagram in Fig. 7-8(d), an abrupt angle change or "concentrated curvature" should be introduced if the compound beam is to be treated as a single unit. Thus, by integrating the curvature curve, the abrupt angle change at point C becomes a jump or step at the corresponding point in the slope curve; and by integrating the slope curve, this step becomes a kink in the deflection curve. Hence, the compatibility conditions at the hinge will be automatically satisfied if a proper angle change is introduced at the corresponding point in the curvature curve.

Fortunately, this angle change need not be known in advance in order to solve the problem. As long as the beam is statically determinate, there will be an additional component of reaction at the support when a hinge is introduced in the beam. This additional component of reaction provides an extra boundary condition which may be used to evaluate the unknown angle change at C in the curvature curve. Since the equation of moment is given by

$$M = \frac{Px}{2} - P\langle x - a\rangle^1$$

We may introduce an arbitrary angle change K_c at point C of the curvature curve so that

$$\frac{M}{EI} = \frac{Px}{2EI} - \frac{P}{EI}\langle x - a\rangle^1 + K_c\langle x - 2a\rangle^{-1}$$

Then, by successive integrations, we have

$$\theta = \frac{Px^2}{4EI} - \frac{P}{2EI}\langle x - a\rangle^2 + K_c\langle x - 2a\rangle^0 + C_1$$

$$v = \frac{Px^3}{12EI} - \frac{P}{6EI}\langle x - a\rangle^3 + K_c\langle x - 2a\rangle^1 + C_1x + C_2$$

From the boundary condition $v = 0$ at $x = 0$, we have $C_2 = 0$. From the other two boundary conditions $v = 0$ and $\theta = 0$ at $x = 4a$, we obtain the following equations respectively:

$$0 = \frac{P(4a)^3}{12EI} - \frac{P}{6EI}(3a)^3 + K_c(2a) + C_1(4a)$$

$$0 = \frac{P(4a)^2}{4EI} - \frac{P}{2EI}(3a)^2 + K_c + C_1$$

From the solution of these two equations, we get

$$K_c = \frac{17Pa^2}{12EI} \quad \text{and} \quad C_1 = -\frac{11Pa^2}{12EI}$$

Hence, the elastic curve of the beam is given by

$$v = \frac{Px}{12EI}(x^2 - 11a^2) - \frac{P}{6EI}\langle x - a\rangle^3 + \frac{17Pa^2}{12EI}\langle x - 2a\rangle^1$$

7-5 Moment-Area Method

Another approach used in computing slopes and deflections along the length of a beam is to provide a semigraphic interpretation relating slopes and deflections *directly* to the M/EI diagram. First, we shall introduce the theorems relating the M/EI diagram and the shape of the elastic curve that are independent of the boundary conditions. Next, we shall apply the theorems to the computation of slope and deflection of beams with various boundary conditions.

According to Eq. (7-9), the change in slope between two points on the elastic curve, commonly known as the *angle change*, can be represented by the area of the M/EI diagram between these two points. However, in Eq. (7-10), the change in deflection is not expressed explicitly in terms of the area of the M/EI diagram. Therefore, we seek an indirect approach in

which the displacement of a point on the elastic curve from the tangent to the elastic curve at a second point is obtained. Since such a displacement represents the deviation of the curve from a tangent, measured vertically in this case, it is called the *tangential deviation*. Referring to Fig. 7-9(a), $\Delta\theta_{ba}$ is the angle change from point A to point B, and t_{ba} is the tangential deviation of point B from a tangent at point A. It should be noted that the

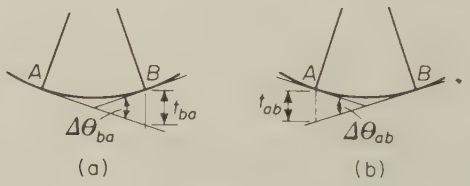

Figure 7–9

order of the subscripts in $\Delta\theta_{ba}$ and t_{ba} is important since a reverse of the order will result in $\Delta\theta_{ab}$ and t_{ab}, as shown in Fig. 7-9(b).

The procedure of computing the angle change and the tangential deviation from the area of the M/EI diagram is commonly embodied in the moment-area theorems. From Eq. (7-9), we have

$$\Delta\theta_{ba} = \theta_b - \theta_a = \int_a^b \frac{M}{EI}\,dx$$

This is known as the *first moment-area theorem*, which states that the angle change from point A to point B on the elastic curve is equal to the area of that portion of the M/EI diagram bounded by the ordinates through A and B. Similarly,

$$\Delta\theta_{ab} = \theta_a - \theta_b = -\Delta\theta_{ba}$$

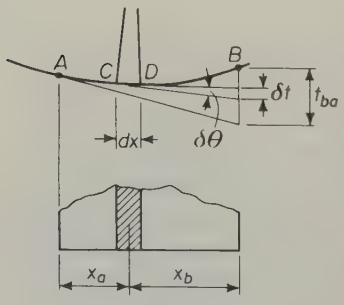

Figure 7–10

Furthermore, according to the first theorem, the infinitesimal angle $\delta\theta$ between tangents at points C and D in Fig. 7-10 is equal to the shaded portion of the M/EI diagram. Since the slopes along the elastic curve are very small, the vertical distance δt may be approximated by the arc length, which is equal to the angle change $\delta\theta$ multiplied by the horizontal distance x_b. Thus, by using point B as the origin and the positive direction of x_b as shown,

$$t_{ba} = \int_b^a x_b\,d\theta = \int_b^a x_b \frac{M}{EI}\,dx_b = \bar{x}_b \int_b^a \frac{M}{EI}\,dx_b = \bar{x}_b \int_a^b \frac{M}{EI}\,dx$$

or, by using point A as the origin and the positive direction of x_a as shown,

$$t_{ab} = \int_a^b x_a \, d\theta = \int_b^a x_a \frac{M}{EI} \, dx_a = \bar{x}_a \int_a^b \frac{M}{EI} dx_a = \bar{x}_a \int_a^b \frac{M}{EI} dx$$

in which $\bar{x}_b$ and $\bar{x}_a$ represent the distances from the centroid of the area of the M/EI diagram to points B and A respectively, and the integral represents the area of the M/EI diagram between points A and B. Thus, the *second moment-area theorem* can be stated as follows: The tangential deviation from a point B to the tangent at another point A is equal to the moment of the area of the M/EI diagram bounded by the ordinates through A and B about an axis through point B. Since $\bar{x}_a$ or $\bar{x}_b$ is always positive, the sign of the tangential deviation depends only on the sign of the M/EI diagram. For a positive moment, the tangential deviation is positive and the point on the elastic curve is *above* the tangent; for a negative moment, the tangential deviation is negative and the point on the elastic curve is *below* the tangent as shown in Fig. 7-11.

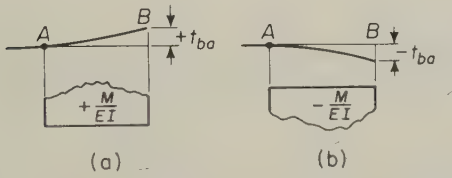

Figure 7-11

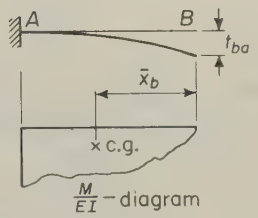

Figure 7-12

Let us now consider the significance of the boundary conditions in the application of the moment-area theorems. In general, neither the slope nor the deflection at a point on the beam is given directly by these theorems. The geometry of the deflected beam must therefore be taken into consideration in applying these theorems to the solution of a problem. In the case of a cantilever beam as shown in Fig. 7-12, the slope θ_a and the deflection v_a at the fixed end A are known to be zero. Thus, the slope θ_c and the deflection v_c at any point C of the beam under any loading may be given as follows:

$$\theta_c = \Delta\theta_{ca} = \int_a^c \frac{M}{EI} dx \tag{7-13a}$$

$$v_c = t_{ca} = \bar{x}_c \int_a^c \frac{M}{EI} dx \tag{7-13b}$$

In the case of a simply supported beam as shown in Fig. 7-13, if a tangent is drawn at point A, the slope θ_c and the deflection v_c at any point C can be

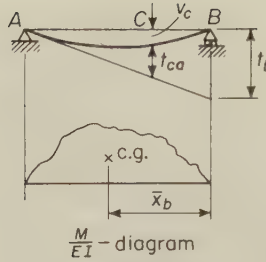

Figure 7–13

obtained from the geometry of the deflected beam as follows:

$$\theta_c = \theta_a + \Delta\theta_{ca} = -\frac{t_{ba}}{L} + \Delta\theta_{ca}$$

$$v_c = -t_{ba}\frac{x}{L} + t_{ca}$$

Note that the sign in front of t_{ba} is negative because t_{ba} is positive for a positive moment whereas θ_a and $\theta_a x$ should be negative for a positive moment. The quantities $\Delta\theta_{ca}$, t_{ca}, and t_{ba} can be computed directly from the moment-area theorems, i.e.,

$$\Delta\theta_{ca} = \int_a^c \frac{M}{EI}\,dx$$

$$t_{ca} = \bar{x}_c \int_a^c \frac{M}{EI}\,dx$$

$$t_{ba} = \bar{x}_b \int_a^b \frac{M}{EI}\,dx$$

in which $\bar{x}_c$ and $\bar{x}_b$ are the distances from points C and B to the centroids of the moment areas bounded by points A and C and by A and B respectively. Then,

$$\theta_c = -\frac{\bar{x}_b}{L}\int_a^b \frac{M}{EI}\,dx + \int_a^c \frac{M}{EI}\,dx \tag{7-14a}$$

$$v_c = -\frac{x}{L}\bar{x}_b \int_a^b \frac{M}{EI}\,dx + \bar{x}_c \int_a^c \frac{M}{EI}\,dx \tag{7-14b}$$

It can readily be seen that the computation of angle change and tangential deviation is a matter of following a set of formulas whereas the application of these theorems to compute slope and deflection depends on the ability to sketch the correct shape of the elastic curve. This is always possible if the moment diagram for a given beam is known. When the moment diagram consists of simple geometrical elements such as triangles, rectangles, and second-degree parabolas, the solution by the moment-area method is rather simple, otherwise, the computation of areas and centroids of areas becomes quite tedious. It is sometimes possible to simplify the computation of these quantities by replacing the actual moment diagram with several separate moment diagrams, each of which consists of simple geometrical elements only and all of which are superimposed to obtain the actual moment diagram. For convenient reference, the geometrical properties of triangles and second-degree parabolas are summarized in Fig. 7-14.*

*This figure is adapted from p. 497 of Reference 3-4.

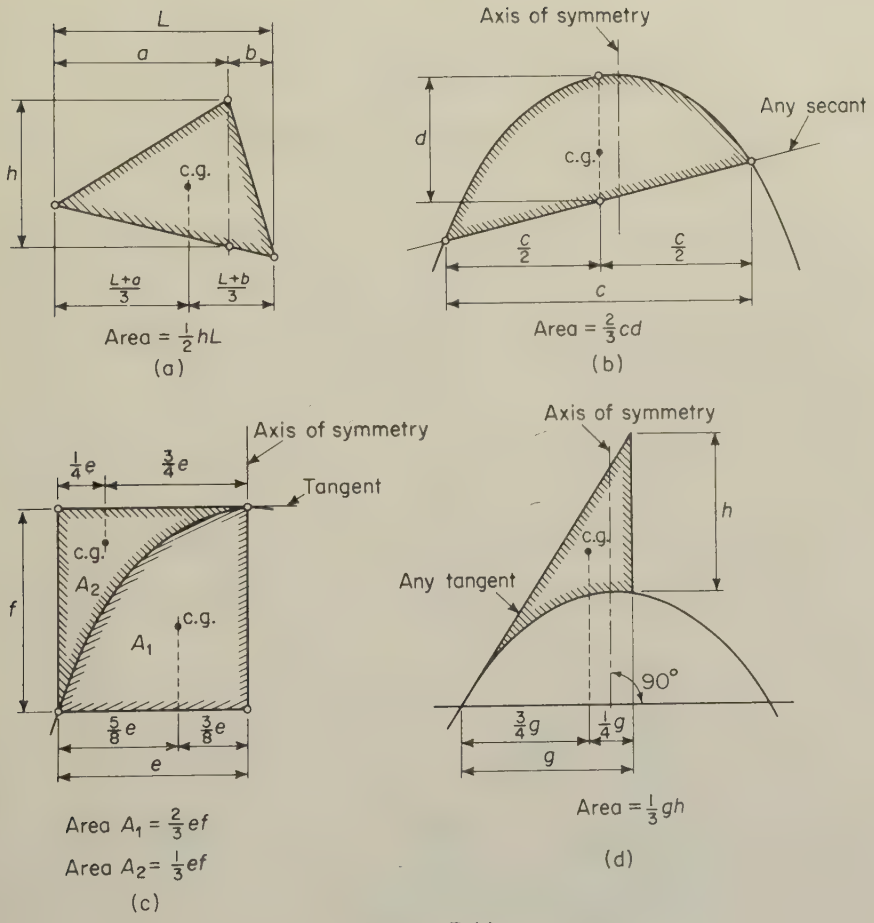

Figure 7–14

Example 7-5. Compute the deflection at point D of the beam shown in Fig. 7-15(a). $E = 30 \times 10^3$ ksi and $I = 100$ in.^{4}

First construct the moment diagram and sketch the elastic curve for the beam. Then, a tangent is drawn at point B and the following relation is established:

$$v_d = t_{db} + \theta_{ba}L_2$$

Since t_{db} is negative, corresponding to a negative moment, and θ_{ba} is positive for a positive slope, v_d will be negative indicating a downward deflection if t_{db} is numerically greater than $\theta_{ba}L_2$. The computation can be carried out

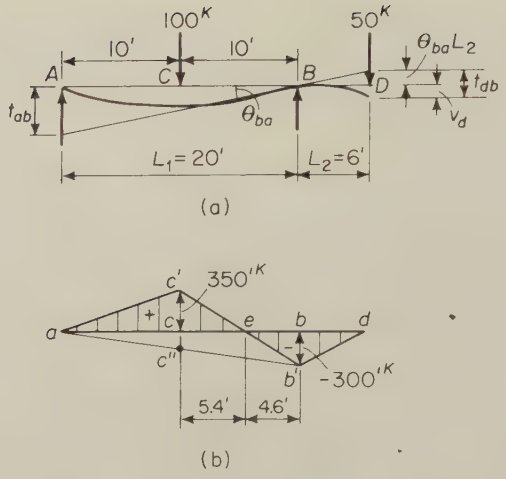

Figure 7–15

by first plotting the moment diagram as shown in Fig. 7-15(b). Then,

$$t_{ab} = \frac{1}{2}\left(\frac{350}{EI}\right)(10)(6.67) + \frac{1}{2}\left(\frac{350}{EI}\right)(5.4)(11.8) - \frac{1}{2}\left(\frac{300}{EI}\right)(4.6)(18.5)$$

$$= \frac{10{,}000}{EI}\ \text{ft}^3\text{-k}$$

$$\theta_{ba} = \frac{t_{ab}}{L} = \frac{10{,}000}{20EI} = \frac{500}{EI}\ \text{ft}^2\text{-k}$$

$$t_{db} = \frac{1}{2}\left(\frac{-300}{EI}\right)(6)(4) = -\frac{3{,}600}{EI}\ \text{ft}^3\text{-k}$$

$$v_d = -\frac{3{,}600}{EI} + \left(\frac{500}{EI}\right)(6) = -\frac{600}{EI}\ \text{ft}^3\text{-k}$$

$$= -\frac{(600)(1{,}728)}{(30{,}000)(100)} = -0.34\ \text{in.}$$

The computation of t_{ab} can be simplified if we consider the moment diagram between points a and b in Fig. 7-15(b) as the superposition of a positive triangle $ac'b'$ and a negative triangle abb', thus avoiding the necessity of locating point e. The ordinate $c'c''$ represents the moment at point C of the beam when the moment at point B of the beam is zero, i.e., when there is no load acting at point D of the beam. Thus,

$$c'c'' = (100)(20)/4 = 500$$

The areas and centroidal distances of these triangles then can be obtained

directly from Fig. 7-14. Hence,

$$t_{ab} = \frac{1}{2}\left(\frac{500}{EI}\right)(20)(10) - \frac{1}{2}\left(\frac{300}{EI}\right)(20)(13.3) = \frac{10{,}000}{EI} \text{ ft}^3\text{-k}$$

The advantage of the method of superposition is even greater when the moment diagram consists of parabolas instead of triangles.

Example 7-6. Compute the deflection at point B of the compound beam shown in Fig. 7-8(a) by the moment-area method.

The construction of the M/EI diagram for such a compound beam with a hinge has been explained in Example 7-4. From the M/EI diagram in Fig. 7-8(d), we note that K_c may be treated as a concentrated area lying on a vertical line. Hence, the centroid of the area to point A is equal to $2a$. Thus, starting from a point A with known tangential deviation of point A from a tangent at point D, we have

$$t_{ad} = \frac{1}{2}\left(-\frac{Pa}{EI}\right)(2a)\left(\frac{4a}{3} + 2a\right) + \frac{1}{2}\left(\frac{Pa}{2EI}\right)(2a)(a) + K_c(2a) = 0$$

from which $K_c = 17Pa^2/12EI$.
Then,

$$t_{bd} = \frac{1}{2}\left(-\frac{Pa}{EI}\right)(2a)\left(\frac{4a}{3} + a\right) + \frac{1}{2}\left(\frac{Pa}{2EI}\right)(a)\left(\frac{a}{3}\right) + \frac{17Pa^2}{12EI}(a)$$

$$= -\frac{5Pa^3}{6EI}$$

Hence, the deflection at point B is equal to

$$v_b = t_{bd} = -\frac{5Pa^3}{6EI}$$

7-6 *Concept of Conjugate Beams*

In the derivation of the equation of the elastic curve for a deflected beam, we observe the similarity between the procedure of obtaining deflection from curvature and that of obtaining moment from applied load, provided that comparable boundary conditions also exist in the determination of the constants of integration. A comparison of the two procedures may be made by noting Eqs. (3-3) and (3-4) for shear and moment, and Eqs. (7-7) and (7-8) for slope and deflection. The significance of the force boundary conditions in determining the constants of integration in Eqs. (3-3) and (3-4) has been discussed in Section 3-3. The physical meaning of the displacement boundary conditions in determining the constants of integration in Eqs. (7-7) and (7-8)

has been explained in Section 7-3. Thus, we can make a complete analogy of the two procedures by noting the duality of these two sets of equations.

The concept of conjugate beams is introduced for the purpose of carrying out the solution of one set of equations by referring to the solution of the other set as an analogy. Since the shear and moment at a point of a beam subject to a given loading may be computed from statics, by analogy the slope and deflection at a point of the actual beam may be thought of as the shear and moment at the corresponding point of a fictitious beam having the curvature curve or M/EI diagram as the applied load. This fictitious beam must have force boundary conditions identical to the displacement boundary conditions of the actual beam, and is therefore called a *conjugate beam.* Such a method of computing deflections is known as the *conjugate beam method* or *elastic weight method* since the M/EI diagram is used as the applied load on the conjugate beam. In many respects, the applications of this method are similar to those of the moment-area method. However, the concept of conjugate beams permits further applications in computing beam deflections by numerical methods and in computing truss deflections, which will be discussed later in this chapter.

The analogy between the roles of curvature, slope, and deflection in the actual beam and their counterparts in the conjugate beam may be given as follows:

Actual beam	*Conjugate beam*
curvature $k = M/EI$	load q
slope θ	shear S
deflection v	moment M

Imagine that the conjugate beam has the same span as that of the actual beam and has force boundary conditions identical to the displacement boundary conditions of the actual beam. Then, the equivalence of boundary conditions may be given for a few basic cases as follows:

Actual beam	*Conjugate beam*
simple support ($\theta \neq 0$, $v = 0$)	simple support ($S \neq 0$, $M = 0$)
fixed end ($\theta = 0$, $v = 0$)	free end ($S = 0$, $M = 0$)
free end ($\theta \neq 0$, $v \neq 0$)	fixed end ($S \neq 0$, $M \neq 0$)
interior hinge ($\theta \neq 0$, $v \neq 0$)	interior support ($S \neq 0$, $M \neq 0$)
interior support ($\theta \neq 0$, $v = 0$)	interior hinge ($S \neq 0$, $M = 0$)

Hence, for a simply supported beam, the supporting conditions of the conjugate beam are identical to those of the actual beam as shown in Fig. 7-16(a). For a cantilever beam, the end conditions of the conjugate beam will be the reverse of those of the actual beam as shown in Fig. 7-16(b). Other examples of statically determinate structures are given in Figs. 7-16 (c), (d), and (e).

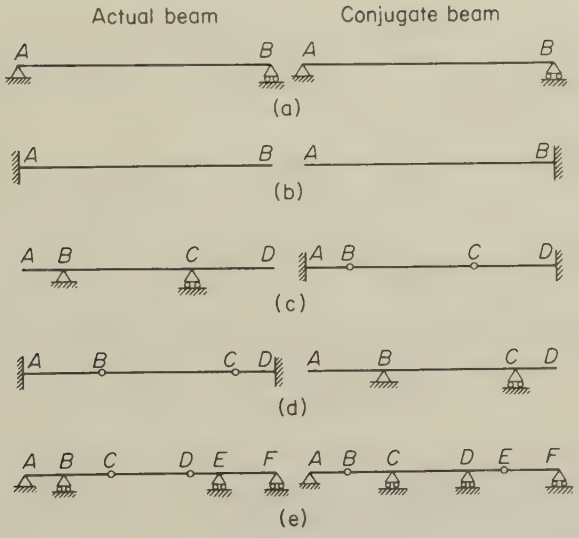

Figure 7–16

If the M/EI diagram of the actual beam is applied as a load to the conjugate beam, it can be demonstrated that the shear at any point of the conjugate beam is the slope at the corresponding point in the actual beam, and that the moment at any point of the conjugate beam is the deflection at the corresponding point in the actual beam. Consider, for instance, the special cases of cantilever beam and simply supported beam for which the slope and deflection at any point have been formulated in terms of the M/EI diagram in Section 7-5. In order to avoid confusion, the quantities

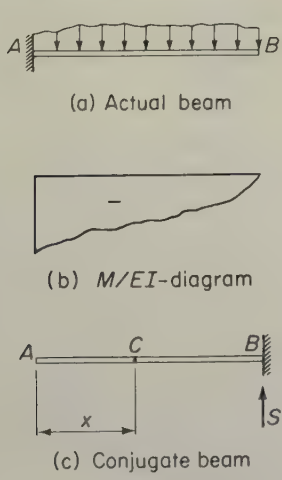

Figure 7–17

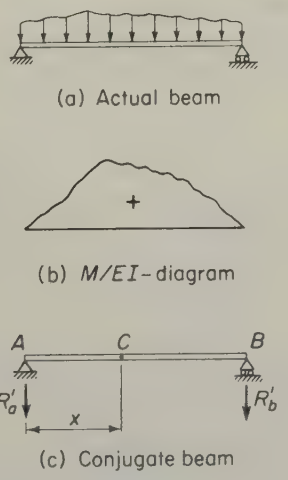

Figure 7–18

relating to the conjugate beam are given in primed notations and those for the actual beam are shown in unprimed notations. Referring to the conjugate beam in Fig. 7-17, we obtain from statics the shear and the moment at point C as follows:

$$S_c' = \int_a^c \frac{M}{EI} dx \tag{7-15a}$$

$$M_c' = \bar{x}_c \int_a^c \frac{M}{EI} dx \tag{7-15b}$$

For the conjugate beam in Fig. 7-18, we obtain by taking moments about B,

$$R_a' = \frac{\bar{x}_b}{L} \int_a^b \frac{M}{EI} dx$$

Hence,

$$S_c' = \frac{\bar{x}_b}{L} \int_a^b \frac{M}{EI} dx + \int_a^c \frac{M}{EI} dx \tag{7-16a}$$

$$M_c' = -\frac{x}{L} \bar{x}_b \int_a^b \frac{M}{EI} dx + \bar{x}_c \int_a^c \frac{M}{EI} dx \tag{7-16b}$$

in which x_c and x_d are the distances from points C and B to the centroids of the moment area bounded by points A and C and by A and B, respectively. A comparison of Eqs. (7-13) and (7-14) with Eqs. (7-15) and (7-16) will establish the fact that the conjugate beam method leads to the same results as the moment-area method for these two cases.

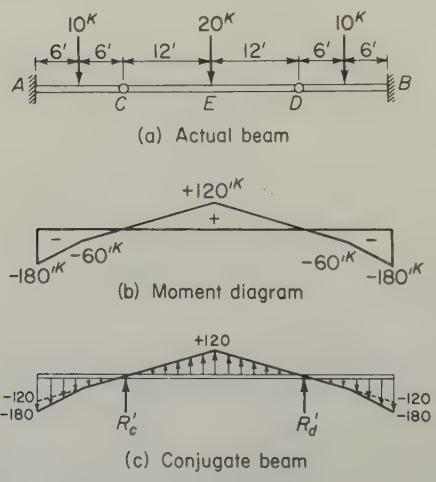

Figure 7–19

Example 7-7. For the beam shown in Fig. 7-19(a), compute the deflection at point E by the conjugate beam method. E = 30,000 ksi and I = 800 in.^{4}

The actual beam can be broken up into separate units at point C and D whereby the moment diagram can be obtained as shown in Fig. 7-19(b). The conjugate beam is shown in Fig. 7-19(c). Because of the symmetry of the structure and loading, each reaction of the conjugate beam is equal to one-half of the applied elastic loads as follows:

$$EIR_c' = -\tfrac{1}{2}(-120)(12) - \tfrac{1}{2}(-60)(6) - \tfrac{1}{2}(120)(12)$$

$$R_c' = \frac{180}{EI}\text{ ft}^2\text{-k}$$

Hence, the deflection of the actual beam at E is the same as the moment of the conjugate beam at E, or

$$EIM_e' = \tfrac{1}{2}(-120)(12)(8 + 12) + \tfrac{1}{2}(-60)(6)(4 + 6 + 12) + (180)(12) + \tfrac{1}{2}(120)(12)(4) = -12{,}940\text{ ft}^3\text{-k}$$

or

$$v_e = -\frac{12{,}940}{EI}\text{ ft}^3\text{-k} = -\frac{(12{,}940)(1{,}728)}{(30{,}000)(800)} = -0.93\text{ in.}$$

7-7 *Numerical Method for Computing Beam Deflections*

When the curvature curve or M/EI diagram of a beam consists of irregular shapes, the deflection of the beam can be obtained most conveniently by a numerical procedure commonly known as *Newmark's method.* The application of this method to compute shear and moment in a beam has been explained in Section 3-8, and by analogy, it can be used to compute slope and deflection in a beam as well. The relations between curvature, slope, and deflection of the beam are derived from the relations between load, shear, and moment of a conjugate beam. Thus, the ordinate k of the curvature curve of the actual beam can be obtained first by dividing the ordinates of the moment diagrams by the corresponding values of bending stiffness EI. Then the equivalent concentrated curvatures or angle changes at regularly spaced "panel points" can be obtained from the ordinates of the curvature curve or M/EI diagram. Let the equivalent concentrated curvatures at a panel point be denoted by K. Then, the K values at various panel points may be computed as reactions of stringers having the M/EI diagram as applied loads by Eqs. (3-11) and (3-12). These equivalent concentrated curvatures may then be applied as loads at the panel points of the conjugate beam. Finally, the slope in a panel and the deflection at a panel point of the actual beam may be obtained by the same procedure for computing shear in a panel and moment at a panel point of the actual beam.

Consider, for example, the simple beam shown in Fig. 7-20(a), the span of which is divided into four equal panels. The introduction of the panel points has the effect of replacing the elastic curve of the beam by a bar chain represented by the dotted lines insofar as computation of slopes and deflections are concerned. In the elastic curve of the beam, the change of curvature is gradual while in the bar chain the changes of curvature are concentrated at points B, C, and D as represented by the angle changes K_b, K_c, and K_d in Fig. 7-20(b). The slopes of the bar chain are constant

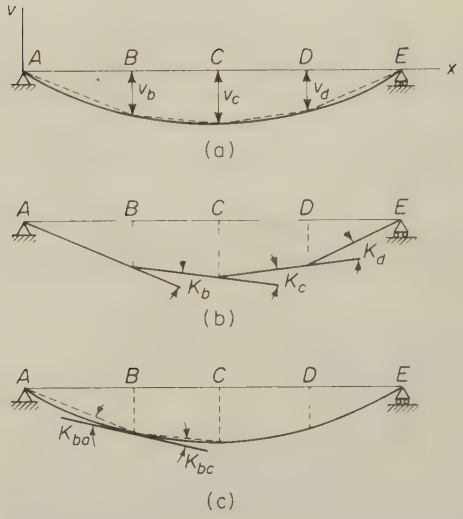

Figure 7–20

within a panel and do not represent the true slopes of the elastic curve, but the deflections at the joints of the bar chain are identical to those at the panel points of the beam. If the true slopes at the panel points of the elastic curve are desired, the equivalent concentrated curvatures to the left and right of each panel point can be computed separately. Then, the slope of the tangent to the elastic curve at a panel point may be obtained by adding the suitable part of concentrated angle change to the corresponding panel slope as shown in Fig. 7-20(*c*).

By adopting the sign convention of curvature, slope, and deflection as in Eqs. (7-5) and (7-6), the successive calculation of slopes and deflections can be carried out by adding, respectively, curvatures and slopes from left to right, or by subtracting from right to left, starting from a point of known slope and deflection. In the case of a cantilever beam, for example, the fixed end is a point of zero slope and zero deflection. The computation of slope and deflection may begin from that point. When only the deflections at two points are known, such as the conditions of no deflections at the supports of a simple beam, the slope at one of the supports may be arbitrarily assumed. After the deflections at the panel points are computed, a check is made on the deflection at the second support. If the computed deflection at that point is different from the known boundary condition, a correction equivalent to the rotation of the x-axis may be applied to the trial deflections based on the arbitrarily assumed slope at the first support. The slopes at the panel points can be corrected by an adjustment corresponding to the translation of the x-axis. For solutions given in tabulated form, the following notations are adopted: k for the curvature at a panel point, K for the equivalent concentrated curvature at a panel point, θ for the panel slope, and v for the deflection at a panel point. If the actual or true slope at a panel point is needed, it will be denoted by $\bar{\theta}$. For solutions involving trial slopes and deflections, θ' is used for the trial slope in a panel, v' for the trial deflection at a panel point, θ'' for the slope correction, and v'' for the deflection correction.

The numerical computation of slopes and deflections can also be conveniently carried out in a tabulated form. As a matter of fact, if the shears

and moments in the same beam are also computed by numerical integration, the two sets of computations can be tabulated together. The units of all quantities can be taken out to the last column of the tabulation as common factors. However, great care must be taken so that correct units will accompany the final results. It should be noted that the unit for curvature is 1/length, the unit for concentrated curvature and for slope is radian or a dimensionless quantity, and the unit for deflection is length.

Example 7-8. A cantilever beam with variable moment of inertia as shown in Fig. 7-21 is subjected to a concentrated load of 20 kips at the free end. For $I_0 = 3{,}000$ in.^{4} and $E = 30 \times 10^3$ ksi, find the deflections of the beam at intervals of 1/6 the span length by numerical integration.

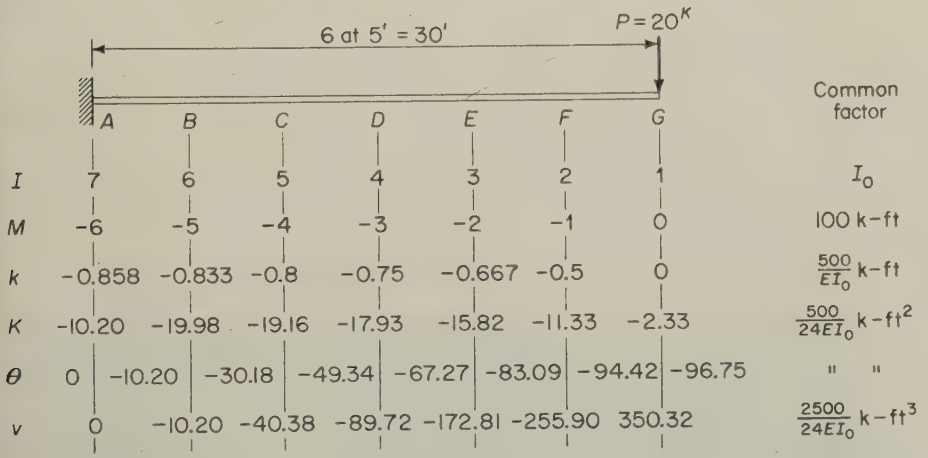

Figure 7-21

The moment of inertia of this beam varies continuously from I_0 at the free end to $7I_0$ at the fixed end, with intermediate values given at intervals of $h = L/6$. Since the ordinates of moments can readily be obtained, the ordinates of curvature k are computed by dividing the ordinates of moments by the corresponding values of EI. The equivalent concentrated curvatures K are computed by Eqs. (3-12) because the variation of curvature can best be approximated in this way. Since the slope and the deflection at the fixed end are known to be zero, the numerical integration can be carried out in a straightforward manner, starting from the left to the right both for slopes and for deflections. The common factor for deflections can be simplified at the final stage as follows:

$$\frac{(2{,}500)\ (12)^3\ \text{k-in.}^3}{(24)\ (30{,}000)\ (3{,}000)\ \text{k-in.}^2} = 0.002 \text{ in.}$$

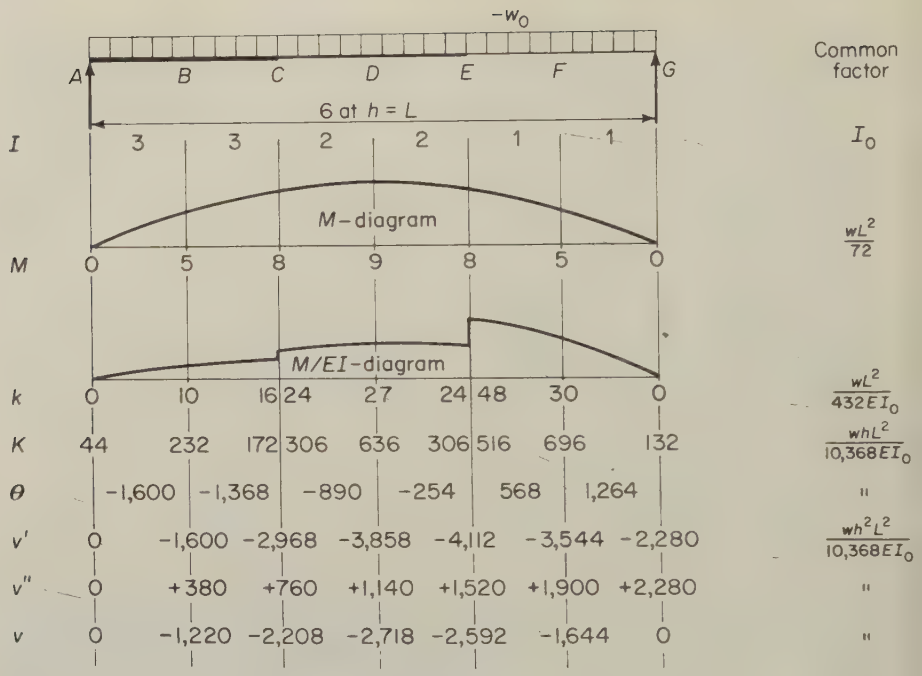

Figure 7–22

Example 7-9. A simply supported beam with variable moment of inertia as shown in Fig. 7-22 is subjected to a uniformly distributed load. Compute the deflections of the beam at intervals of 1/6 of the span length.

The ordinates of the moment diagram for a uniformly loaded simple beam are first computed and tabulated in the figure. Dividing these ordinates by the corresponding EI, we obtain the k values. At point C of the beam, for instance, the moment ordinate is $(8)(wL^2/72)$. In dividing this ordinate by EI, we have different values of k to the left and to the right of point C respectively as follows:

$$\frac{(8)\,(wL^2/72)}{3EI_0} = (16)\left(\frac{wL^2}{432EI_0}\right)$$

$$\frac{(8)\,(wL^2/72)}{2EI_0} = (24)\left(\frac{wL^2}{432EI_0}\right)$$

The equivalent concentrated curvatures K are computed from Eqs. (3-12). At point B, for instance,

$$K_b = \frac{h}{12}[0 + (10)\,(10) + 16]\frac{wL^2}{432EI_0}$$

$$= \left(\frac{116}{12}\right)\frac{wL^2h}{432EI_0} = (232)\frac{wL^2h}{10{,}368EI_0}$$

Because of the discontinuity of the M/EI diagram at point C, we should compute separately the values of K for panel BC and CD. Thus,

$$K_{cb} = \frac{h}{24}[(7)(16) + (6)(10) - 0]\frac{wL^2}{432EI_0} = (172)\frac{wL^2h}{10{,}368EI_0}$$

$$K_{cd} = \frac{h}{24}[(7)(24) + (6)(27) - 24]\frac{wL^2}{432EI_0} = (306)\frac{wL^2h}{10{,}368EI_0}$$

It should be pointed out that the expressions for R_{ab} and R_{ba} in Eqs. (3-12) are applicable even if the ordinate c in the equations is fictitious. For example, the M/EI curve for beam segment AC may be projected beyond point C in the computation of K_{cb}, and the same result will be obtained. The next step is to assume an arbitrary value for θ' at the left support A where the deflection is known to be zero. As far as the deflections are concerned, it makes no difference whether a value of θ' is assumed to the left of point A since the equivalent concentrated curvature $K = 44$ at point A does not enter into the deflection computation. Finally, a linear correction is applied to the trial deflections v' so that the deflection at the right support G becomes zero.

7-8 *Geometry of Deflected Rigid Frames*

The methods of computing beam deflections can readily be applied to the computation of deflections of rigid frames if the general shapes of the deflected structures are known. The deflected shape of the individual straight members in a rigid frame is prescribed by the M/EI diagram along the length of the member. Furthermore, the angle at a rigid joint before deformation must remain the same after deformation. Thus, if the members meeting at a rigid joint are bent into curves, the tangents to the curves at the joint must hold the same relative position to each other as the members did before deformation. With these guiding principles, the shapes of deflected rigid frames can be easily sketched as illustrated by the following examples.

Figure 7-23 shows a rigid frame with a vertical load acting on member AB. Since bending occurs only in member AB, member BC remains straight after deformation. Since the horizontal displacement of a point in member AB is small in comparison with its vertical displacement, joint B is assumed to remain in the same position. If the slope of member AB at point B is θ_b, it will also cause a rotation of θ_b in member BC because $\angle A'BC'$ must equal $\angle ABC$. Since the angle θ_b is very small, the vertical displacement of a point in member BC is small and negligible in comparison with its horizontal displacement. Thus, point B is assumed to be undeflected in horizontal and vertical directions, and the horizontal displacement at C is equal to the rotation θ_b multiplied by the length BC.

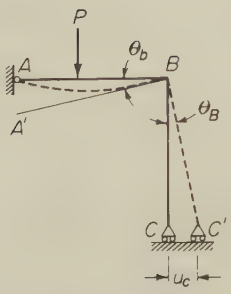

Figure 7–23

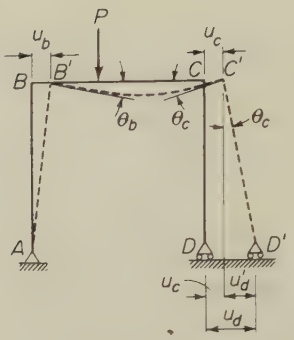

Figure 7–24

A similar case is shown in Fig. 7-24, in which member AB will also rotate as a result of the applied load on the horizontal member BC because the angle at joint B must remain 90 degrees when the horizontal member BC is subjected to bending. Since joint A is hinged, no deflection is permitted at that point, and point B will be displaced horizontally to allow rotation in member AB. Again, the vertical displacement of point B is small and negligible in comparison with its horizontal displacement so that point B' is considered to be at the same elevation as point B. For a similar reason, length $B'C'$ is taken to be equal to BC, and the horizontal displacement of point C is equal to that of point B. Finally, the horizontal displacement at any point on member CD is equal to the horizontal displacement at point C plus the horizontal displacement due to the rotation of member CD. For example, at point D, $u_d = u_c + u_d'$.

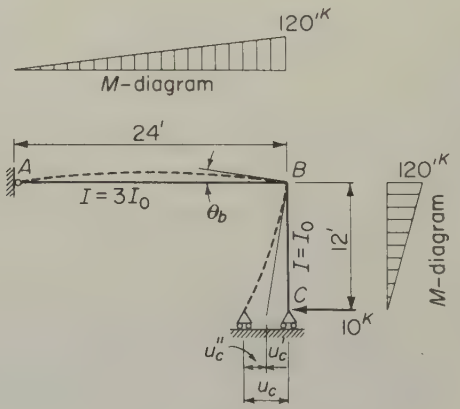

Figure 7–25

Consider another case, as shown in Fig. 7-25, in which a horizontal force is applied at point C. Since member BC as well as member AB is subjected to

bending in this case, the horizontal displacement of a point on member BC can be considered as the superposition of a displacement if end B were fixed and a displacement due to the rotation of member BC. Thus, at point C, $u_c = u_c' + u_c''$.

In some cases, the shape of the deflected structure is not obvious but it can always be sketched from the moment diagram. For the frame in Fig. 7-26, for example, the applied loads shown in Fig. 7-26(a) cause moments as shown in Fig. 7-26(b). Hence, the points of inflection can be located from the points of zero moment, and the curvatures of the individual elements follow the signs of the moment diagram as shown in Fig. 7-26(c). Without actually carrying out the computation, however, it is possible to sketch a deflected shape as shown in Fig. 7-26(d). Hence, these sketches represent only qualitatively the deflected shape of the structure.

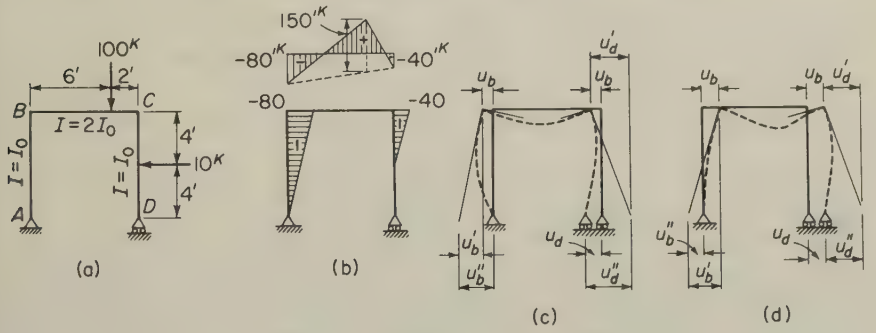

Figure 7–26

Now that we have sketched the deflected shape of a rigid frame, the influence of the deflection of individual members on that of the others with respect to a fixed reference point can be used to compute first the deflections of the individual members without the influence of the other members, and then the actual deflection is computed on the basis of superposition.

Example 7-10. Find the horizontal displacement of the point C of the frame shown in Fig. 7-25 due to a horizontal force of 10 kips acting at point C. E and I_0 are constant.

The moment diagram and the shape of the deflected frame have been plotted in the figure as previously explained. Hence, θ_b can be obtained from member AB by the method of elastic weights as follows:

$$\theta_b = \frac{1}{2}\left(\frac{-120}{3EI_0}\right)(24)\left(\frac{2}{3}\right) = -\frac{320}{EI_0}\ \text{ft}^2\text{-k}$$

The horizontal deflection of point C is caused partly by the rotation of

member BC and partly by the bending of member BC. Thus, that portion due to rotation is equal to

$$u_c' = (12)\left(-\frac{320}{EI_0}\right) = -\frac{3{,}840}{EI_0}\text{ ft}^3\text{-k}$$

The horizontal deflection due to bending also can be obtained by the method of elastic weights, or

$$u_c'' = \frac{1}{2}\left(\frac{-120}{EI_0}\right)(12)\left(\frac{2}{3}\right)(12) = -\frac{5{,}760}{EI}\text{ ft}^3\text{-k}$$

The final deflection is therefore equal to

$$u_c = u_c' + u_c'' = -\frac{9{,}600}{EI_0}\text{ ft}^3\text{-k}$$

Note that θ_b is negative because the slope of the tangent at point B of deflected member AB is negative. This in turn causes the tangent at point B of the deflected member BC to be negative if we view the member BC from the "inside" of the structure. Thus, the negative signs for all deflections mean that point C moves inward or to the left of the original position.

Example 7-11. Compute the horizontal deflection of the point D of the rigid frame in Fig. 7-26(a). E and I_0 are constant.

The shape of the deflected frame is sketched from the moment diagram as in the previous example. However, for complicated loadings it is difficult to estimate the magnitudes of the deflections as shown in the figure and to conclude whether point D moves inward or outward. However, we still can obtain the correct result if a consistent displacement diagram is used. Considering only the *absolute values* of the displacements, we obtain from the Fig. 7-26(c) the horizontal displacement at point D as follows:

$$u_d = u_d'' - u_d' + u_b = u_d'' - u_d' + u_b'' - u_b' \tag{a}$$

Or, from Fig. 7-26(d), we get

$$u_d = u_b + u_d' - u_d'' = u_b' - u_b'' + u_d' - u_d'' \tag{b}$$

Note that the sign for u_d in Eq. (a) will be opposite to that in Eq. (b) if the same *absolute values* of u_b', u_d', u_b'', and u_d'' are used in both equations. A positive result of u_d indicates that the corresponding deflected shape is correct, and a negative result means that the assumed direction of displacement should be reversed.

In carrying out the numerical computation of this problem, we may observe that the moment diagram for member BC of the frame may be considered as the superposition of a positive moment diagram on a negative moment diagram, both of which are based on the dotted line. Since we are interested in $u_b' + u_d'$ instead of each of these quantities, and since the

vertical legs AB and CD are of the same length, it can be seen that

$$u_b' + u_d' = (8)(\theta_b + \theta_c)$$

Thus, we need not even compute θ_b or θ_c but instead use the sum of θ_b and θ_c, which is nothing but the area of the M/EI diagram between B and C, or

$$\theta_b + \theta_c = \frac{1}{2}\left(\frac{150}{2EI_0}\right)(8) + \frac{1}{2}\left(\frac{-80-40}{2EI_0}\right)(8) = \frac{60}{EI_0}$$

and

$$u_b' + u_d' = (8)\left(\frac{60}{EI_0}\right) = \frac{480}{EI_0}$$

Similarly, by the method of elastic weights,

$$u_b'' = \frac{1}{2}\left(\frac{-80}{EI_0}\right)(8)\left(\frac{16}{3}\right) = -\frac{512}{3EI_0}$$

$$u_d'' = \frac{1}{2}\left(\frac{-40}{EI_0}\right)(4)\left(4+\frac{8}{3}\right) = -\frac{1{,}600}{3EI_0}$$

Finally, from Eq. (b) corresponding to Fig. 7-26(d), we get

$$u_d = \frac{480}{EI_0} - \frac{512}{3EI_0} - \frac{1{,}600}{3EI_0} = -\frac{224}{EI_0}\ \text{ft}^3\text{-k}$$

The negative sign indicates that the point D moves inward or to the left of the original position, i.e., Fig. 7-26(c) is the correct shape.

7-9 *General Procedure for Computing Deflections in Rigid Frames*

Although it is desirable to visualize the geometry of deflected structures and to exercise judgment to obtain a qualitative picture of the deflections, a systematic approach will simplify the computation, especially if the loading is complicated. We shall, therefore, develop a general procedure for computing deflections in statically determinate rigid frames.

Consider first a cantilever frame as shown in Fig. 7-27(a). Since there are only three components of constraint at support A, the frame is statically determinate. Let it be required to determine the displacement of a point on the frame with respect to its original position. We can choose any pair of mutually perpendicular axes as the reference system, and it is just as convenient to use the horizontal and vertical axes as shown in Fig. 7-27(a). Then, the displacement of a point can be determined if we can compute the components of displacement in the x and y directions. At point D, for instance, the displacement can be represented by components u_d and v_d, which are defined as positive in the positive directions of the $x =$ and $y =$ axes respectively.

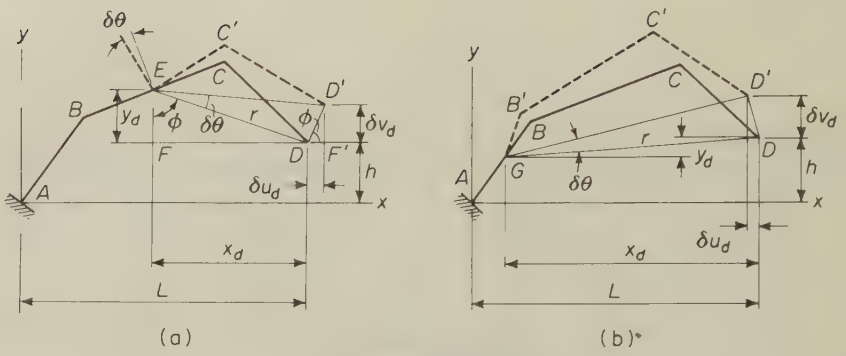

Figure 7–27

Imagine that an infinitesimally small angle change $\delta\theta$ is applied at point E of the frame while the other part of the frame is being held rigid as shown in Fig. 7-27(a). If the angle change is rotated in a counter clockwise direction, a positive curvature is introduced at that point as evidenced by the shape of BEC'. As a result of this, point D undergoes a displacement of DD' which can be resolved into components δu_d and δv_d in the x and y directions respectively. Let the distance DE be denoted by r and the angle between DE and a vertical reference line passing through point E be φ. Then, the displacement DD' may be represented by the arc length $r\ \delta\theta$. By using the ordinary assumptions of small displacement and small angle change, it can be demonstrated that $\triangle\ DEF$ and $\triangle DD'F'$ are similar triangles. If the horizontal and vertical distances between points D and E are denoted by x_d and y_d respectively, the sides of similar triangles are proportional as follows:

$$\frac{\delta u_d}{r\,\delta\theta} = \frac{y_d}{r} \quad \text{and} \quad \frac{\delta v_d}{r\,\delta\theta} = \frac{x_d}{r}$$

or

$$\delta u_d = y_d \delta\theta \quad \text{and} \quad \delta v_d = x_d \delta\theta$$

For a positive angle change $\delta\theta$ at E, both δu_d and δv_d are positive when point E is above and to the left of point D as shown in Fig. 7-27(a). Thus, the distances x_d and y_d are considered to be positive when they are directed inward and upward, respectively. If a similar $\delta\theta$ is applied at point G, which is below point D as shown in Fig. 7-27(b), δu_d then becomes negative. For a negative angle change, there is a reversal of sign for all displacement components but the positive directions of x_d and y_d remain unchanged.

When a rigid frame is subjected to external loads, the angle change at any point on the frame is caused by the bending moment M at a section passing through that point, and can be expressed as $\delta\theta = (M/EI)\ \delta s$, in

which δs denotes the length of an element along the axis of the frame. Hence, the components of deflection at point D due to external loads can be obtained as follows:

$$u_d = \int_s y_d \, d\theta = \int_s y_d \frac{M \, ds}{EI} \tag{7-17a}$$

$$v_d = \int_s x_d \, d\theta = \int_s x_d \frac{M \, ds}{EI} \tag{7-17b}$$

Note that the bending moment M due to external loads varies along the axis of the frame. An example of such variation is shown by the M/EI diagram plotted along the axis of the frame in Fig. 7-28. The integrals in Eqs. (7-17a) and (7-17b) represent the products of the area of the M/EI diagram and the corresponding distances from point D in the x and y directions. These distances are measured from point D, in horizontal and vertical directions respectively, to the projection of the centroid of the M/EI diagram on the axis of the frame, such as $\bar{x}_{d1}$ and $\bar{y}_{d1}$, $\bar{x}_{d2}$ and y_{d2}, and $\bar{x}_{d3}$ and $\bar{y}_{d3}$ for areas A_1, A_2, and A_3 respectively in Fig. 7-28. Note that the distance $\bar{y}_{d1}$ is negative in this case. Thus, the components of deflection at point D can be expressed as the summation of the moments of the M/EI diagram about point D.

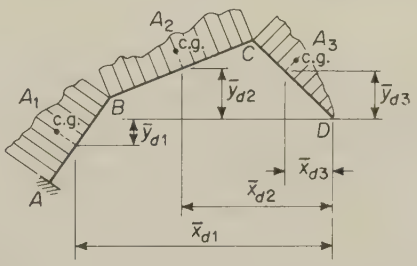

Figure 7–28

Next we shall consider another type of statically determinate frame that is hinged at one support and simply supported on the other, as shown in Fig. 7-29(a). We are primarily interested in the displacement of the roller at point D. The roller does not necessarily rest on a horizontal surface, but the x-axis can always be oriented in the direction of the displacement. Let R be the distance between point D and the fixed reference point A, and L and h be its projections on x- and y-axes respectively. Imagine that an infinitesimally small angle change $\delta\theta$ is applied at point E causing a positive curvature at that point. The frame will have a deformed shape as shown dotted in the figure, and the displacement at point D will be $\delta u_d'$. If the portion of the frame from A to E were held fixed in position while the angle change $\delta\theta$ is applied at point E, the portion of the frame from E to D would deform as shown in Fig. 7-29(b), causing a vertical displacement δv_d as well as a horizontal displacement δu_d. When the entire deformed structure is being rotated about point A so that it will be restored to the position represented by the dotted line in Fig. 7-29(b), point D'' will move to point D'. Thus, the horizontal displacement $\delta u_d'$ is the sum of δu_d and $\delta u_d''$. Again,

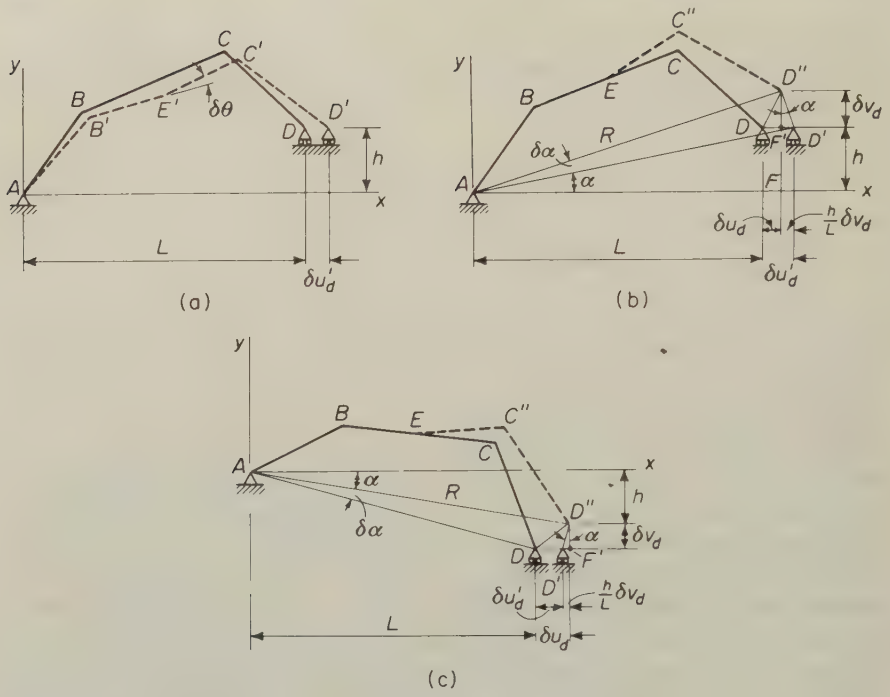

Figure 7–29

by using the ordinary assumptions of small displacement and small angle change, it can be shown that $\triangle ADF$ and $\triangle D'F'D''$ are similar triangles. Thus,

$$\frac{\delta u_d''}{\delta v_d} = \frac{h}{L} \quad \text{or} \quad \delta u_d'' = \delta v_d \frac{h}{L}$$

Hence,

$$\delta u_d' = \delta u_d + \delta v_d \frac{h}{L}$$

or, by integration,

$$u_d' = u_d + v_d \frac{h}{L} \tag{7-17c}$$

in which u_d and v_d are defined by Eqs. (7-17a) and (7-17b).

If the right support D is at a lower elevation in comparison with the left support A as shown in Fig. 7-29(c), then u_d' will be smaller than u_d since the rotation about point A tends to decrease the horizontal displacement. However, Eq. (7-17c) will still be valid if h is considered as positive when it is above the x-axis and negative when it is below the x-axis. When both supports are at the same elevation, $h = 0$ and $u_d' = u_d$.

Example 7-12. Compute the horizontal and vertical components of displacement at point D of the frame shown in Fig. 7-30(a). E and I are constant along the entire length of the frame.

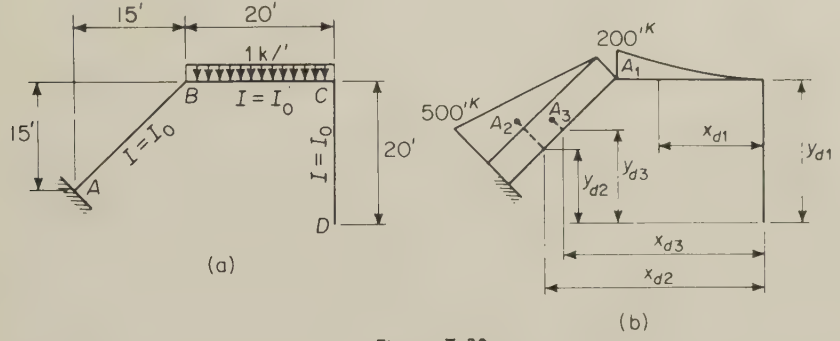

Figure 7-30

After computing the ordinates of the moment diagram as shown in Fig. 7-30(b), the calculation can be carried out in a tabulated form in Table 7-1.

TABLE 7-1

No.	$A = \int \frac{M}{EI} ds$ (ft²-k)	x_d (ft)	y_d (ft)	Ax_d (ft³-k)	Ay_d (ft³-k)
1	$\frac{1{,}333}{EI}$	15	20	$\frac{20{,}000}{EI}$	$\frac{26{,}600}{EI}$
2	$\frac{3{,}180}{EI}$	30	10	$\frac{95{,}400}{EI}$	$\frac{31{,}800}{EI}$
3	$\frac{4{,}250}{EI}$	27.5	12.5	$\frac{117{,}000}{EI}$	$\frac{53{,}100}{EI}$
				$v_d = \frac{232{,}400}{EI}$	$u_d = \frac{111{,}560}{EI}$

Example 7-13. Compute the horizontal displacement of point E in the rigid frame shown in Fig. 7-31(a). E and I_0 are constant.

The computation can also be carried out in tabulated form. As a matter of fact, the constant EI_0 can be omitted from the computation until the last step, as shown in Table 7-2, in which $EI_0 = 1$. Because of the symmetry of Fig. 7-31(b), only half of the frame need be considered.

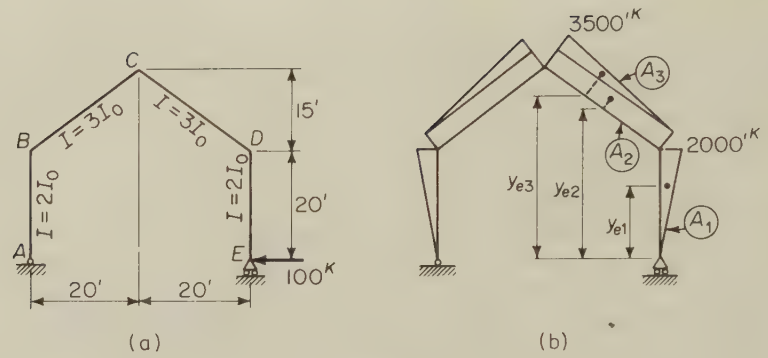

Figure 7–31

TABLE 7-2

No.	$A = \int \frac{M}{EI}\,ds$	y_e	Ay_e
1	10,000	13.33	133,300
2	16,667	27.5	458,000
3	6,250	30.0	187,500
			778,800

Hence,

$$u_e' = (2)(778{,}800)/EI_0 = 1{,}557{,}600/EI_0$$

7-10 Deflection of Arches

The general procedure for computing deflections in rigid frames can also be extended to the computation of deflections of arches. For the arch shown in Fig. 7-32, for example, Eq. (7-17c) in Section 7-9 is entirely valid since there have been no restrictions on whether the frame should consist of broken lines or a smooth curve. In evaluating the integrals in Eqs. (7-17a) and (7-17b), however, we encounter difficulties inherent in curved members. Usually, additional assumptions must be made in order to solve such problems.

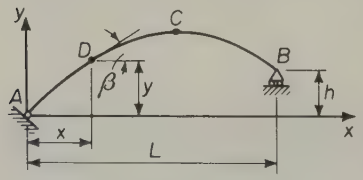

Figure 7–32

In order that the integrals in Eqs. (7-17a) and (7-17b) be integrable mathematically, we must express the terms y and ds in terms of x. Very

fortunately, many arches encountered in practice are parabolic and have a variable moment of inertia along the axis with a minimum value at the crown. Thus, the ordinate y can be expressed as a polynomial of x, and the moment of inertia I at any section can be assumed, without serious error, to be as follows:

$$I = I_c \sec \beta = I_c \frac{ds}{dx}$$

in which I_c is the moment of inertia at the crown and β is the angle between a tangent at a point on the arch axis and a horizontal line. Thus, the horizontal displacement for point B in Fig. 7-32 becomes

$$u_b' = \int_s y_b \frac{M\,dx(I/I_c)}{EI} + \frac{h}{L}\int_s x_b \frac{M\,dx(I/I_c)}{EI}$$

$$= \frac{1}{EI_c}\left[\int_0^L y_b M\,dx + \frac{h}{L}\int_0^L x_b M\,dx\right] \tag{7-18}$$

When y_b and x_b are expressed in terms of x, the integrals in Eq. (7-18) can be evaluated analytically.

Example 7-14. The parabolic arch shown in Fig. 7-33 is subjected to a concentrated load P. The equation of the arch axis, with point A as origin, is

$$y = \frac{4f}{L^2}(Lx - x^2)$$

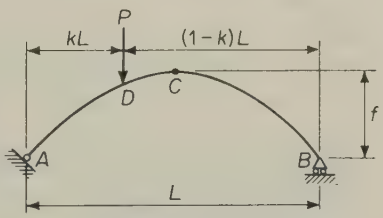

Figure 7–33

Compute the horizontal displacement at point B.

Since the moment at any section of the arch axis is

$$M = (1 - k)x \quad \text{for} \quad 0 < x < kL$$

and

$$M = k(L - x) \quad \text{for} \quad kL < x < L$$

the horizontal displacement at point B, according to Eq. (7-18), is equal to

$$u_b' = \frac{1}{EI_c}\int_0^L yM\,dx$$

$$= \frac{4f}{L^2 EI_c}\left[\int_0^{kL}(Lx - x^2)(1 - k)x\,dx + \int_{kL}^L (Lx - x^2)k(L - x)\,dx\right]$$

$$= \frac{fkL^2}{3EI_c}(1 - 2k^2 + k^3)$$

7-11 *Geometry of Deflected Trusses*

When the members of a truss change in length owing to external causes, the joints in the truss undergo displacements consistent with the deformation of individual members. Since a change in length in one or more sides of a triangle will cause changes in its interior angles, the displacements of the joints in a truss are related to the angle changes of the deflected structure. Thus, the angle changes and deflections at the joints of a truss must be compatible with the deformation of individual members.

If the change in length of the truss members is caused by external loads, the axial deformation in each member is given by $e = FL/AE$, in which F is the bar force in the member under consideration, L is the length of the member, A is the cross-sectional area of the member, and E is the modulus of elasticity of the material. If the change in length is caused by temperature changes, the axial deformation in each member can be obtained from the relation given in Section 2-9. The change in length may be deliberately made in fabrication so that the truss is cambered. Cambering is a process of changing the lengths of the members of a truss slightly so that under a specified loading condition, usually referred to as the *camber loading*, the truss will have the theoretical dimensions after the falsework is removed. The most common way of achieving such a result is to shorten the tension members by the amount they would lengthen under the specified loading and lengthen the compression members by the amount they would shorten under the same loading.

The displacements of joints of a truss can be obtained directly from the axial deformations of members. However, there are certain similarities between the deflection of a beam and that of a truss. If the chord members of the truss between supports form a straight line as shown in Fig. 7-34, the angle changes at the joints of these chord members are analogous to the concentrated angle changes at various panel points of a girder supporting floor beams. Whereas the deflected shape of a beam is represented by a smooth curve, the deflected shape of a truss consists of a series of broken lines. In Section 7-2 it was demonstrated that in the case of a beam, the horizontal displacement of a point on the neutral axis is small and

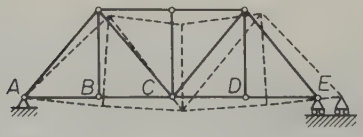

Figure 7–34

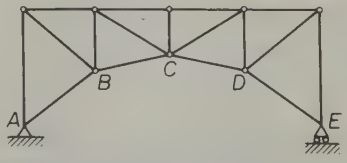

Figure 7–35

negligible in comparison with its vertical displacement. Insofar as the horizontal displacement of a joint caused by the changes in slope of the horizontal chord members in the truss is concerned, the same assumption still holds true. However, horizontal displacements of joints may also be caused by axial deformations of these chord members, which cannot be neglected in comparison with the vertical displacements of the joints. In the case of a truss in which the chord members between supports form a polygonal curve as shown in Fig. 7-35, the displacements of joints in both vertical and horizontal directions are influenced by the axial deformations of the inclined chord members as well as the angle changes at the joints. Hence, the horizontal displacements as well as vertical displacements of the joints of a truss are often required.

Among the many methods of computing truss deflections, we shall first consider a graphical method for obtaining the displacements of joints of a truss directly from the axial deformations of its members. This graphical method, generally known as the *Williot-Mohr diagram*, is preferred because of its simplicity in application although an analytical procedure based on the same principle is also available.* However, the analytical procedure is capable of providing greater accuracy if necessary. We shall also apply the conjugate beam method presented in Section 7-6 to compute the vertical displacements of joints connecting chord members between supports. If the chord members between supports form a straight and horizontal line the application is rather straightforward. The horizontal displacements of the joints may be obtained from the simple addition of the axial deformations in the horizontal chord members. In the case of a polygonal curve, however, certain modifications based on the geometry of the truss must be made in order to apply the conjugate beam method for computing vertical displacements. Furthermore, the horizontal displacements are also influenced by the geometry of the truss. Hence, there is no advantage in using the conjugate beam method when the chord members of a truss between supports form a polygonal curve, and the necessary modifications for such an application will not be discussed here.

Although these methods are applicable to all types of trusses, our discussion of their applications is confined to the computation of deflections of simple trusses. For compound trusses it may be necessary to modify the structures before these methods can be applied. The modifications include the computation of change in length of some fictitious members introduced to break up polygons into triangles. Such computations can be made by the energy methods that will be discussed in Chapter 8.

*See Reference 7-3 for details.

7-12 *Williot-Mohr Diagram for Truss Deflection*

If one side of a triangle is fixed in direction and a vertex is fixed in position, the position of the triangle is completely defined provided that the lengths of the three sides are known. For a series of triangles constituting a truss, the position of these triangles will be completely defined if the position of *one* of the triangles is fixed because the other triangles taken in the order of formation will have one side fixed in direction and a vertex fixed in position.

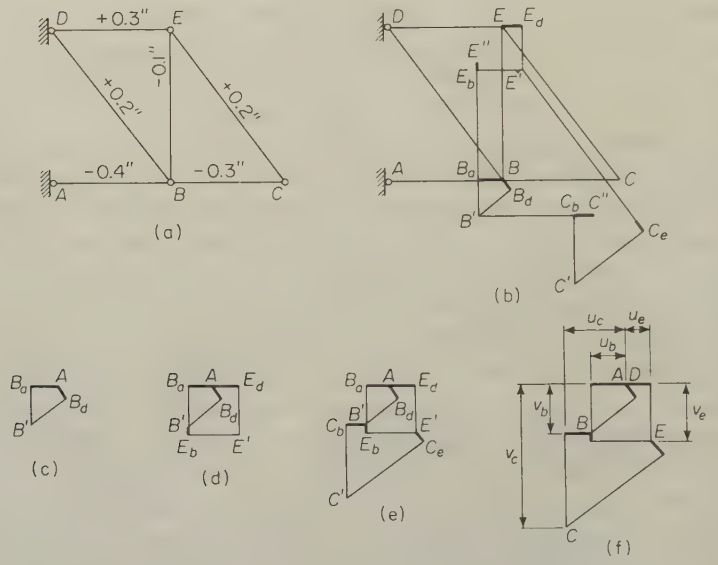

Figure 7–36

Consider the truss shown in Fig. 7-36(a), which has line AD fixed in direction and point A fixed in position. Since there is no displacement between points A and D, point D is also fixed in position in this case. The original lengths of all truss members are known, and the axial deformations of these members are as shown in Fig. 7-36(a), with positive sign indicating elongation and negative sign indicating shortening of the member. Exaggerating the deformations, we can plot the axial deformations BB_a and BB_d along members AB and BD respectively, with the sense of direction corresponding to elongation or shortening. Then, the deflected position of point B can be determined from the intersection of two arcs drawn by using points A and D as centers and distances AB_a and DB_d as radii, respectively. In

view of the assumptions of small deflections and small angle changes, these arcs can be replaced by perpendicular distances B_aB' and B_dB', which intersect at point B' or the deflected position of point B. Repeating the same procedure, we can locate point E' or the deflected position of point E from the deformed lengths of DE and BE. Finally, the point C' or the deflected position of point C can be located from the deformed lengths of BC and CE.

In Fig. 7-36(b), the axial deformations of the members are shown in heavy lines. The original lengths are represented by light lines except where parts of such lengths are overshadowed by the deformations. Thus, the length $B'E''$ is equal to length BE so that the length $B'E_b$ represents the deformed length of BE. Similarly, the length $B'C''$ is equal to length BC, and $B'C_b$ is the deformed length of BC. All other lengths are clearly indicated in the figure.

It is obvious that this is an impractical way to obtain deflections since it is impossible to make accurate measurement of the deflections no matter how large a scale is used. In examining Fig. 7-36(b), however, we note that only displacements BB', EE', and CC' are required, and we can isolate these displacements and the related deformations from the original dimensions of the truss. Imagine that the displacement BB' in Fig. 7-36(b) is translated in the horizontal direction until point B coincides with point A as shown in Fig. 7-36(c). Next, the displacement EE' in Fig. 7-36(b) is translated vertically until point E reaches point B, and then translated horizontally to point A until point E coincides with point A as shown in Fig. 7-36(d). Finally, the displacement CC' is translated in a direction parallel to EC until point C reaches point E, and then translated in stages to points B and A as before until point C coincides with point A as shown in Fig. 7-36(e). Thus, in Fig. 7-36(e), all pertinent deformations are included and the distances AB', AE', and AC' represent the displacements BB', EE', and CC', respectively. Since all lengths in Fig. 7-36(e) are small quantities, it can be reproduced in any convenient scale, such as in Fig. 7-36(f), in which the primes for B', C', and E' have been dropped.

The final graphical solution of truss deflections just described is called the *Williot diagram*. The procedure of construction can be simplified by observing some simple rules. For the truss shown in Fig. 7-36(a), we can start from the fixed point A and the fixed vertical line passing through A. Since there is no deformation in length AD, point D coincides with point A. The next step is to locate point B from points A and D. From point A, draw a line parallel to member AB of the truss and plot the deformation AB_a along this line and to the left of point A. Point B_a is plotted to the left of A because it represents the direction of the movement of joint B relative to joint A in Fig. 7-36(b). Thus, for the Williot diagram in Fig. 7-36(f), we can follow the simple procedure by laying out the deformation in the

same sense of direction as the movement of a joint relative to a previously fixed joint. By the same principle, draw a line passing through point D that coincides with point A and plot the deformation DB_d as shown in Fig. 7-36(f) because the movement of joint B relative to joint D in the truss is in that direction. Next, draw a perpendicular line to AB_a through point B_a and a perpendicular line to AB_d through point B_d. The intersection of these two perpendicular lines is denoted by B. Thus, the displacement of joint B in the truss is given by the distance AB in the Williot Diagram. Once the deflected position of point B is located, we can proceed to locate the deflected position of point E in a similar manner by considering points B and D as previously fixed points. Thus, in Fig. 7-36(f), BE_b and DE_d are located from points B and D respectively in the direction of the corresponding movement of joints in the truss. Point E is located by the intersection of perpendicular lines to BE_b and DE_d respectively. The same procedure is repeated to locate the deflected position of point C. It should be noted that the displacements of joints B, E, and C are vector quantities, the horizontal and vertical components of which are represented by the corresponding u and v in the diagram.

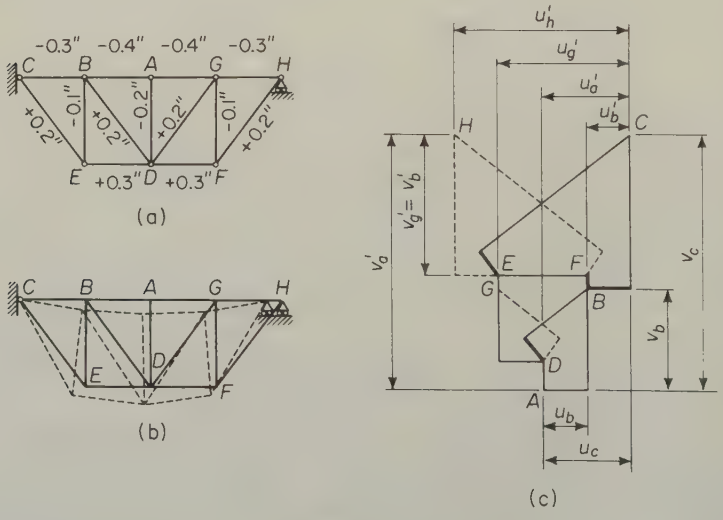

Figure 7–37

For trusses in which the point fixed in position does not lie on the fixed line, the same procedure can still be used as long as there exists a line fixed in direction as well as a line fixed in position. As an example, consider the simple truss in Fig. 7-37(a) that has perfect symmetry with respect to member AD. As the truss deflects, point C remains fixed in position because of the hinge at C and member AD remains vertical in direction because of the

symmetry. Thus, the deflected shape of the truss will be as shown in Fig. 7-37(b). In such a case, we can assume that point A is fixed in position and make use of the fact that member AD is fixed in direction. Then, we can obtain deflections of other joints on this basis by the Williot diagram. Although the results thus obtained are not the true deflections of the joints of the truss, they can easily be correlated to the true deflections from the geometry of the deflected structure. For instance, the components of deflections u and v are first obtained by the Williot diagram, shown in Fig. 7-37(c), assuming point A as fixed in position and member AD as fixed in direction. Because of symmetry, only one-half of the diagram is needed and the other half is shown by dotted lines. Also, note that the deformations need not be represented by heavy lines once we are familiar with the procedure, and the heavy lines tend to decrease the accuracy of the graphical solution. After the u and v components of deflection at various joints are obtained from the diagram, the true components of deflection u' and v' can be determined from the deflected shape in Fig. 7-37(b) by the translation of the reference axes as follows:

$$
\begin{aligned}
u_c' &= 0, & v_c' &= 0 \\
u_b' &= -u_c + u_b, & v_b' &= -v_c + v_b \\
u_a' &= -u_c, & v_a' &= -v_c \\
u_g' &= u_g - u_c, & v_g' &= -v_c + v_g \\
u_h' &= u_h - u_c = -2u_c, & v_h' &= -v_c + v_h = 0
\end{aligned}
$$

The displacement of joints at the lower chord of the truss can be obtained in a similar manner. It should be noted, however, that the components of displacement u' and v' can be measured directly from the Williot diagram by considering C as the fixed point as shown in Fig. 7-37(c).

In an unsymmetrical truss or a symmetrical truss under unsymmetrical loads, however, there is in general no member in the truss that is fixed in direction. For such cases, the Williot diagram is drawn by assuming some point fixed in position and some member fixed in direction. The deflections thus obtained are not the true deflections but can be modified and correlated to the true deflections by applying corrections generally known as *Mohr's corrections*. The resulting diagram is usually referred to as a *Williot-Mohr diagram*.

Let us consider the truss in Fig. 7-38(a), for which the deformations are unsymmetrical. We can assume *any* point as fixed in position and *any* member as fixed in direction. However, since the point C is known to be fixed in position, it will simplify the procedure to observe that fact. Furthermore, it is more convenient to assume a member passing through point C as fixed in direction, and we choose member CB for that purpose. By considering the axial deformations in all members, the deflected shape of the truss on the basis of point C as fixed in direction and member CB

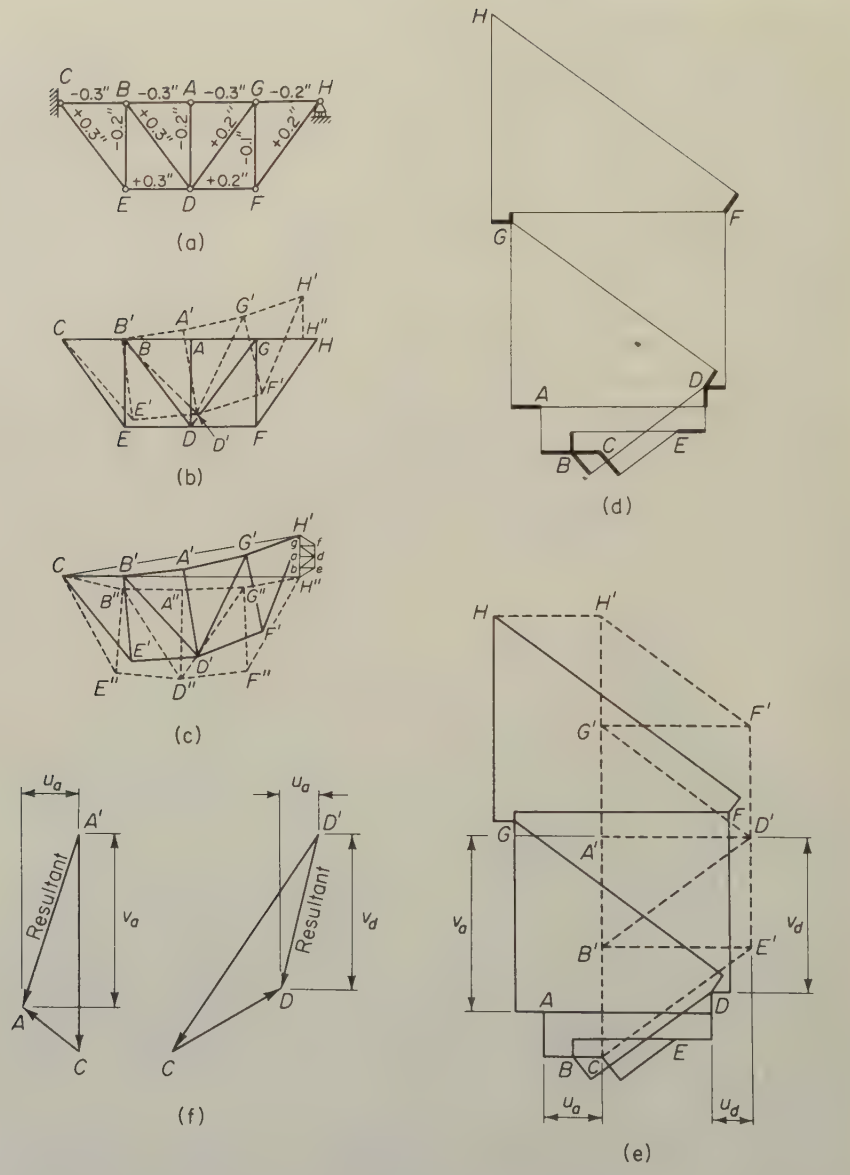

Figure 7–38

as fixed in direction may be represented by the dotted lines in Fig. 7-38(b). Note that the assumptions of small deflections and small angle changes still hold although they have been exaggerated in the figure. It is obvious that the point H' must be at the same elevation as point H since the truss is supported on rollers at that point. Therefore, the deflected truss must be

rotated about point C until point H' reaches H'', as shown in Fig. 7-38(c), in which the final positions of the joints are connected by the dotted lines. The angle of rotation of the entire body may be determined from the angle of rotation of line CH', which is equal to

$$\theta = \tan\theta = \frac{H'H''}{CH''} = \frac{H'H''}{CH}$$

Then, point A' will move to the position of A'', point D' will move to the position of D'', etc., and the distances $A'A''$, $D'D''$, etc. may be obtained from the arc length as follows:

$$A'A'' = (CA')\theta = (CA)\left(\frac{H'H''}{CH}\right)$$

$$D'D'' = (CD')\theta = (CD)\left(\frac{H'H''}{CH}\right)$$

In examining Fig. 7-38(c), we note that such distances can be represented graphically if the original truss is reduced in scale so that its span length becomes $H'H''$ and the entire truss can be fitted into the vertical position as shown at the right-hand side of the figure. Since all dimensions in the original truss and the truss of reduced size are respectively proportional, we can establish, for instance,

$$\frac{aH''}{H'H''} = \frac{CA}{CH}, \qquad \frac{dH''}{H'H''} = \frac{CD}{CH}$$

or

$$aH'' = (CA)\left(\frac{H'H''}{CH}\right), \qquad dH'' = (CD)\left(\frac{H'H''}{CH}\right)$$

Therefore, it may be concluded that $A'A'' = aH''$, $D'D'' = dH''$, etc.

In view of the displacements shown in Figs. 7-38(b) and (c), we note that each joint in the truss goes through two stages; first, the deformation with point C as fixed in position and member CB as fixed in direction, and second, the rotation through an angle θ. Thus, point A moves to A' and then A'', point D moves to D' and then D'', etc. As a result, the vector sum of AA' and $A'A''$ will result in the actual displacement of joint A, the vector sum of DD' and $D'D''$ will give the actual displacement of joint D, etc. The remaining task is to determine these displacements by the construction of the Williot-Mohr diagram.

By considering point C as fixed in position and member CB as fixed in direction, the displacements of joints can be obtained from the Williot diagram in Fig. 7-38(d). Thus, the distance CH' in the diagram represents the vertical displacement of joint H. If the original truss is now reduced in scale so that its span length becomes CH' in the Williot diagram and the

entire truss is fitted into the vertical position as shown by the dotted line in Fig. 7-38(e), the distance from a joint in the small-scale truss to point C represents the displacement of that joint due to rotation. Hence, the actual displacement of any joint in the truss can be measured from the Williot diagram with Mohr's corrections or the Williot-Mohr diagram. For example, the vector CA represents the movement of joint A in the first stage and the vector $A'C$ represents the movement of joint A in the second stage. The actual displacement of joint A is therefore represented by the vector $A'A$. Similarly, the actual displacement of joint D is represented by the vector $D'D$. The addition of such vectors is indicated in Fig. 7-38(f). Hence, the horizontal and vertical components of actual displacements can be obtained accordingly.

One may raise the question as to why the small-scale truss in Fig. 7-38(a) should be oriented 90 degrees *counterclockwise* relative to the actual truss as shown. The reason is that, through such orientation, not only the magnitude *but also the direction* of each of the dimensions such as aH'', DH'', etc. in the small truss will correspond to the respective joint displacements

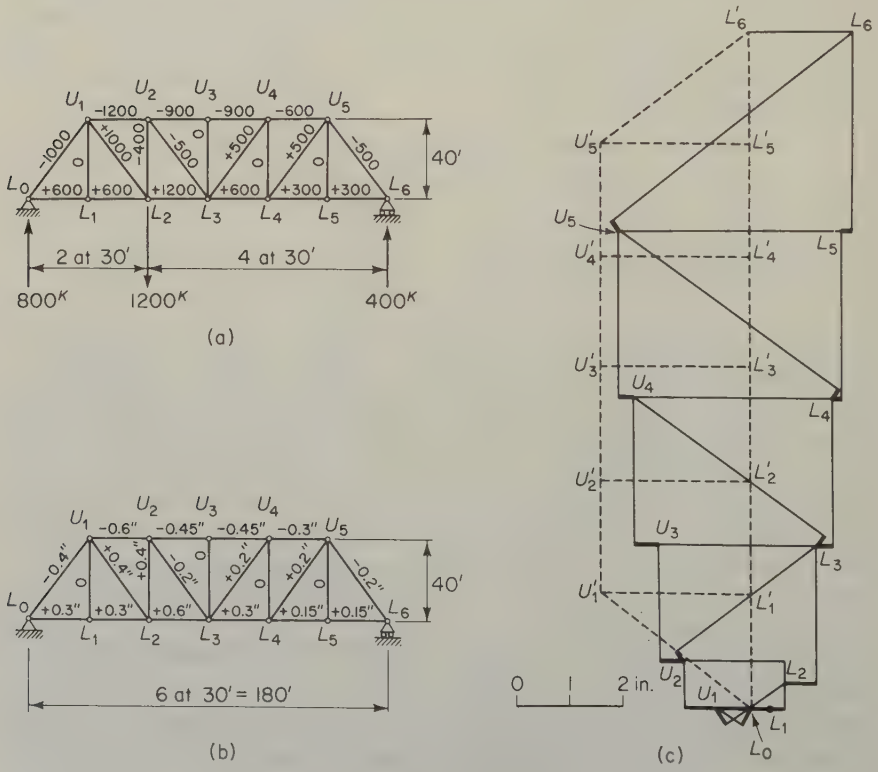

Figure 7–39

$A'A''$, $D'D''$, etc. in the actual truss. If the same orientation is followed in the Williot-Mohr diagram, it will permit the addition of the displacement vectors graphically in the diagram. Hence, the actual truss must be turned 90 degrees counterclockwise in plotting Mohr's corrections on the Williot diagram.

Example 7-15. Figure 7-39(a) shows a Pratt truss with unsymmetrical loading. The bar forces in kips are shown in the figure. Determine the deflection of all joints. The cross-sectional areas of the members are 24 in.^{2} for top and bottom chord members, 50 in.^{2} for diagonal members, and 16 in.^{2} for vertical members. The modulus of elasticity of the material $E = 30 \times 10^3$ ksi.

The axial deformation of a member due to the action of the bar force is $e = FL/AE$, in which F is the bar force, L is the length of the bar, and A is the cross-sectional area of the bar. Hence, the axial deformations are first computed and recorded along the bars in Fig. 7-39(b). The Williot-Mohr diagram is constructed by first assuming that point A is fixed in position and member AB is fixed in direction, and then by applying corrections for rotation. Note the orientation of the small-scale truss shown dotted in Fig. 7-39(c), which corresponds to the corrections for rotation in direction as well as in magnitude. The components of deflections are measured and recorded in Table 7-3.

TABLE 7-3

DEFLECTIONS IN INCHES

Joint	u	v	Joint	u	v
L_1	0.3	2.1	U_1	2.15	2.1
L_2	0.6	3.75	U_2	1.45	3.35
L_3	1.2	3.3	U_3	1.1	3.25
L_4	1.5	2.6	U_4	0.65	2.6
L_5	1.65	1.6	U_5	0.35	1.6
L_6	1.8	0			

7-13 *Angle Changes in Deflected Trusses*

Before we can apply the conjugate beam method to compute the deflections at the joints of a truss, we must first compute the angle changes at the joints as a result of the change in length of members of the truss. Since a triangle is the basic element of a truss, we shall consider first the angle changes in a triangle caused by a change in length of its sides.

Let the vertex angles of a triangle ABC be A, B, and C, and the corresponding opposite sides be a, b, and c. Let e_a, e_b, and e_c be the axial deformations of sides a, b, and c, respectively, and ΔA, ΔB, and ΔC be the changes in the vertex angles A, B, and C, respectively, with positive sign indicating an increase and negative sign indicating a decrease in each case. Since the sum of the interior angles of a triangle must be the same before and after deformation, it is necessary that the *algebraic* sum of the angle changes in all interior angles be zero, or

$$\Delta A + \Delta B + \Delta C = 0$$

Now consider the case of a triangle ABC in which only the length of side a is *increased* by an amount e_a, as shown in Fig. 7-40(a). As a result,

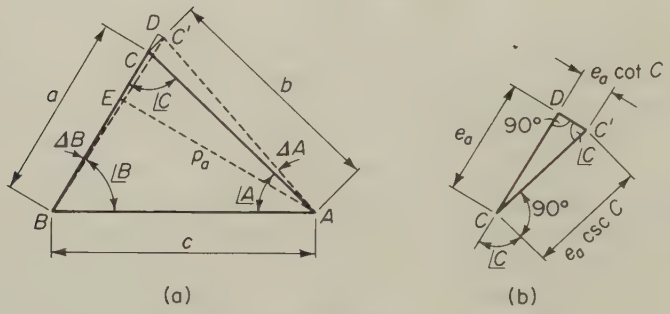

Figure 7–40

angles A and B are changed by the amount of ΔA_a and ΔB_b, respectively. Note that ΔA_a is positive and ΔB_b is negative in this case. Because of the assumption of small deflections and small angle changes, the arcs CC' and DC' with points A and B respectively as centers can be represented by straight lines perpendicular to AC and BD respectively. From the enlarged figure of triangle $CC'D$ shown in Fig. 7-40(b), it is obvious that

$$\angle CC'D = \angle ACB = \angle C$$

Hence,

$$CC' = e_a \csc C \quad \text{and} \quad DC' = e_a \cot C$$

If a perpendicular line p_a is drawn from vertex A to the opposite side a in Fig. 7-40(a), it can be seen that

$$a = BC = BE + EC = p_a(\cot B + \cot C)$$

or

$$p_a = \frac{a}{(\cot B + \cot C)}$$

Furthermore, triangles ACF and $CC'D$ are similar. Since the sides of these

triangles are proportional, $CC'/b = e_a/p_a$. The angle changes due to the change in length e_a of side a only can therefore be expressed as follows:

$$\Delta A_a = \frac{CC'}{b} = \frac{e_a}{p_a} = \frac{e_a}{a}(\cot B + \cot C)$$

$$\Delta B_a = -\frac{DC'}{a} = -\frac{e_a}{a}\cot C$$

$$\Delta C_a = -(\Delta A_a + \Delta B_a) = -\frac{e_a}{a}\cot B$$

Similarly, if the angle changes in the triangle due to the change in length e_b of side b only are denoted by ΔA_b, ΔB_b, and ΔC_b, and those due to the change in length e_c of side c only are denoted by ΔA_c, ΔB_c, and ΔC_c, the following relations can be obtained:

$$\Delta A_b = -\frac{e_b}{b}\cot C, \qquad \Delta A_c = -\frac{e_c}{c}\cot B$$

$$\Delta B_b = \frac{e_b}{b}(\cot A + \cot C), \qquad \Delta B_c = -\frac{e_c}{c}\cot A$$

$$\Delta C_b = -\frac{e_b}{b}\cot A \qquad \Delta C_c = \frac{e_c}{c}(\cot A + \cot B)$$

Thus, the total angle changes due to the change in length in all sides of a triangle equal the sums of individual changes respectively, i.e.,

$$\begin{aligned}
\Delta A &= \frac{e_a}{a}(\cot B + \cot C) - \frac{e_b}{b}\cot C - \frac{e_c}{c}\cot B \\
\Delta B &= -\frac{e_a}{a}\cot C + \frac{e_b}{b}(\cot A + \cot C) - \frac{e_c}{c}\cot A \qquad (7\text{-}19) \\
\Delta C &= -\frac{e_a}{a}\cot B - \frac{e_b}{b}\cot A + \frac{e_c}{c}(\cot A + \cot B)
\end{aligned}$$

These relations can also be expressed in another form by noting that the strain is defined as the deformation per unit length. Thus, by denoting the strains in sides a, b, and c by $\epsilon_a = e_a/a$, $\epsilon_b = e_b/b$, and $\epsilon_c = e_c/c$ respectively, we obtain:

$$\begin{aligned}
\Delta A &= (\epsilon_a - \epsilon_c)\cot B + (\epsilon_a - \epsilon_b)\cot C \\
\Delta B &= (\epsilon_b - \epsilon_a)\cot C + (\epsilon_b - \epsilon_c)\cot A \qquad (7\text{-}20) \\
\Delta C &= (\epsilon_c - \epsilon_b)\cot A + (\epsilon_c - \epsilon_a)\cot B
\end{aligned}$$

We can now proceed to compute the angle changes in a deflected truss. Consider, for instance, the deflection of the bottom chord of the truss

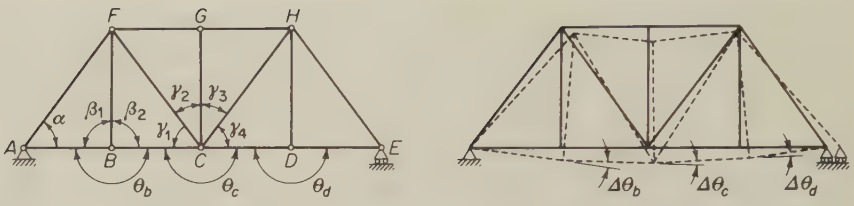

Figure 7–41

shown in Fig. 7-41(a), which is symmetrical with respect to the center line. As the truss deflects downward, θ_b and θ_c increase. Thus, $\Delta\theta_b$ and $\Delta\theta_c$ in Fig. 7-41(b) are positive. This is equivalent to the sign convention of having positive angle change corresponding to positive moment in beams. From Fig. 7-41(a), it is obvious that an increase in angle θ must be accompanied by a decrease in the sum of interior angles of triangles for a particular joint. Thus,

$$\Delta\theta_b = -(\Delta\beta_1 + \Delta\beta_2)$$
$$\Delta\theta_c = -2(\Delta\gamma_1 + \Delta\gamma_2)$$
$$\Delta\theta_d = \Delta\theta_b$$

For a cantilever truss, a similar procedure can be applied. In Fig. 7-42(a), for example, angles θ_a and θ_b will decrease if the truss deflects downward.

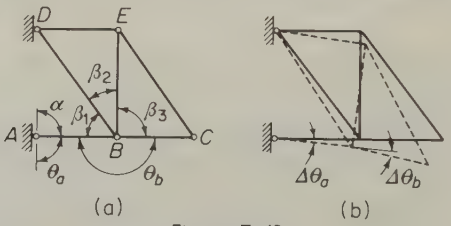

Figure 7–42

Thus, $\Delta\theta_a$ and $\Delta\theta_b$ in Fig. 7-42(b) are negative. The angle changes $\Delta\theta_a$ and $\Delta\theta_b$ can be obtained as follows:

$$\Delta\theta_a = -\Delta\alpha$$
$$\Delta\theta_b = -(\Delta\beta_1 + \Delta\beta_2 + \Delta\beta_3)$$

7-14 *Conjugate Beam Method for Computing Truss Deflections*

In sections 7-6 and 7-7, we pointed out that the relation between angle change and deflection in a beam is analogous to the relation between load and moment of a beam of the same span, provided that the displacement

boundary conditions of the former correspond with the force boundary conditions of the latter. Since the angle changes at the joints of a truss have the same characteristics as the concentrated angle changes in a girder supporting floor beams, it is obvious that the conjugate beam method may be applied to compute the vertical displacements of the joints in a truss if other requirements of the conjugate beam method are satisfied. Furthermore, the numerical computation may be tabulated in a manner similar to the numerical procedure of computing beam deflections if a large number of joints is involved in the computation. Since the chord members between supports may be considered as a bar chain, the conjugate beam method of computing truss deflections is also known as the *bar chain method.*

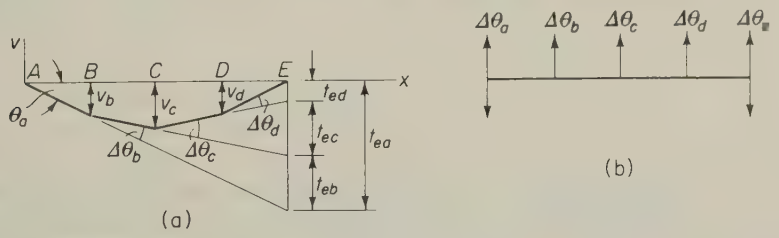

Figure 7–43

In the computation of deflections of a straight horizontal bar chain in a truss, the angle changes at the joints may be used as elastic loads on a conjugate beam. For the simply supported truss shown in Fig. 7-41(a), for example, the angle changes at the joints of the bottom chord are related to the tangential deviations at point E as shown in Fig. 7-43(a). Thus, for small angles, we have

$$\theta_a = \frac{t_{ea}}{L} = \frac{t_{eb} + t_{ec} + t_{ed}}{L}$$

Then, the vertical displacements at the joints are equal to

$$v_b = \theta_a h$$
$$v_c = \theta_a 2h - \Delta\theta_b h$$
$$v_d = \theta_a 3h - \Delta\theta_b 2h - \Delta\theta_c h$$

For a sign convention having upward displacement as positive, θ_a as well as v_b, v_c, and v_d should be preceded by a negative sign. If we take a conjugate beam of the same span length and with upward elastic loads acting as shown in Fig. 7-43(b), the reaction at A of the conjugate beam is equal to θ_a, and the moments at points B, C, and D are equal to the deflections at joints B, C, and D of the truss, respectively. Note that the upward elastic loads correspond to positive angle changes and that the angle changes at points

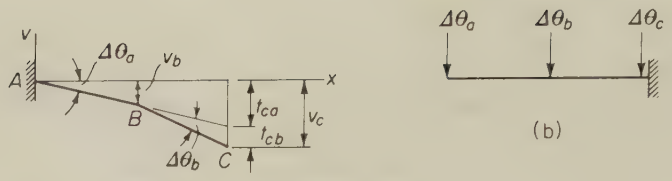

Figure 7–44

A and E need not be known since they would only influence the reactions but not the moments at points B, C, and D of the conjugate beam. For the cantilever truss shown in Fig. 7-42(a), the angle changes at the joints of the bottom chord may also be related to the tangential deviations as shown in Fig. 7-44(a). Thus, for small angles, we get

$$v_c = t_{ca} + t_{cb} = \Delta\theta_a 2h + \Delta\theta_b h$$
$$v_b = \Delta\theta_a h$$

Again, the displacements v_b and v_c should be preceded by a negative sign if upward displacement is defined as positive. The elastic loads on the conjugate beam in Fig. 7-44(b) are downward in this case because the angle changes are negative. Note that the force boundary conditions of the conjugate beam are made to correspond to the displacement boundary conditions of the truss. The angle change at C would affect the reaction at C but not the moments at points B and C of the conjugate beam and therefore need not be computed. Thus, the moments at points B and C of the conjugate beam are equal to the deflections at joints B and C of truss, respectively.

The horizontal displacement of a joint in a horizontal bar chain is equal to the accumulation of axial deformations of the chord members from the point of reference to that joint. For the truss shown in Fig. 7-43(a), for example, point A is the point of reference. Let δ_{ab}, δ_{bc}, δ_{cd}, and δ_{de} be the axial deformations of members AB, BC, CD, and DE, respectively. Then, the horizontal displacements of joints B, C, D, and E are respectively equal to

$$u_b = \delta_{ab}$$
$$u_c = \delta_{ab} + \delta_{bc}$$
$$u_d = \delta_{ab} + \delta_{bc} + \delta_{cd}$$
$$u_e = \delta_{ab} + \delta_{bc} + \delta_{cd} + \delta_{de}$$

Example 7-16. For the truss shown in Fig. 7-45(a), determine the vertical deflections at joints L_1 and L_2. The truss is symmetrical and the axial deformations in the members are noted in the figure.

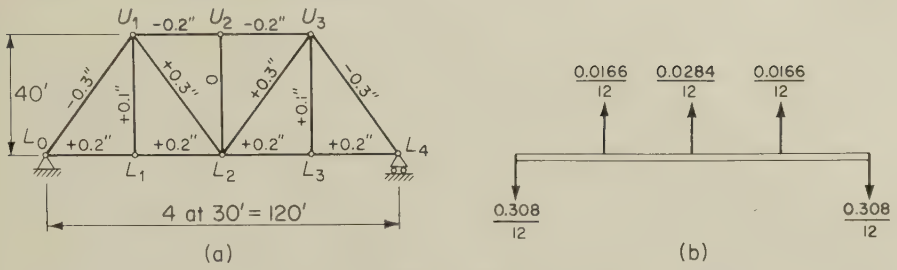

Figure 7–45

At joint L_1 the changes of angles $L_0L_1U_1$ and $L_2L_1U_1$ are needed for the computation of θ_{L_1}, and at joint L_2, only the changes of angles $L_1L_2U_1$ and $U_1L_2U_2$ are computed because of the symmetry of the truss. The calculation of these angle changes by Eq. (7-19) is carried out in Table 7-4. The last row for each joint in the table represents the algebraic sum of the changes of the interior angles at the joint. For joint L_2, the sum is multiplied by two because only half of the interior angles has been considered in the computation. The factor of 12 that is multiplied by the change of interior angles results from the conversion of the lengths of members from feet to inches. This factor need not be carried in the computation if adequate provision is made for its inclusion or cancellation later.

The conjugate beam for computing deflections is shown in Fig. 7-45(b). Note that applied loads are taken as upward because the sign of $\Delta\theta$ should be opposite to that of the sum of changes of interior angles. Since the moments at points L_1 and L_2 of the conjugate beam are negative, the deflections at joints L_1 and L_2 of the truss are negative or downward. Hence,

$$\Delta\theta_{L_1} = +\frac{0.0166}{12} \quad \text{and} \quad \Delta\theta_{L_2} = (2)\left(+\frac{0.142}{12}\right) = +\frac{0.0284}{12}$$

Then,

$$v_{L_1} = -\left(\frac{0.0308}{12}\right)(30)(12) = -0.924 \text{ in.}$$

$$v_{L_2} = -\left(\frac{0.0308}{12}\right)(60)(12) + \left(\frac{0.0166}{12}\right)(30)(12) = -1.35 \text{ in.}$$

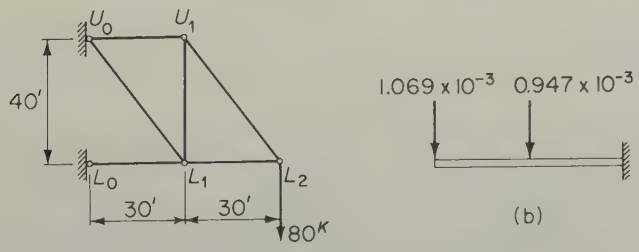

Figure 7–46

TABLE 7-4

Joint	Angle	Member	e (in.)	12 × Change of interior angles
		L_0U_1	-0.3	$-\frac{0.3}{50}\left(\frac{3}{4}+\frac{4}{3}\right) = -0.105$
	$L_0L_1U_1$	U_1L_1	$+0.1$	$-\frac{0.1}{40}\left(\frac{4}{3}\right) = -0.0033$
		L_0L_1	$+0.2$	$-\frac{0.1}{30}\left(\frac{3}{4}\right) = -0.005$
L_1		U_1L_2	$+0.3$	$\frac{0.3}{50}\left(\frac{3}{4}+\frac{4}{3}\right) = +0.105$
	$U_1L_1L_2$	U_1L_1	$+0.1$	$-\frac{0.1}{40}\left(\frac{4}{3}\right) = -0.0033$
		L_1L_2	$+0.2$	$-\frac{0.1}{30}\left(\frac{3}{4}\right) = -0.005$
	Sum			-0.0166
		U_1L_1	$+0.1$	$\frac{0.1}{40}\left(\frac{4}{3}\right) = +0.0033$
	$L_1L_2U_1$	U_1L_2	$+0.3$	$-\frac{0.3}{50}\left(\frac{4}{3}\right) = -0.008$
		L_1L_2	$+0.2$	0
		U_1U_2	-0.2	$-\frac{0.2}{50}\left(\frac{3}{4}\right) = -0.005$
L_2	$U_1L_2U_2$	U_2L_2	0	0
		U_1L_2	$+0.3$	$-\frac{0.3}{50}\left(\frac{3}{4}\right) = -0.0045$
	Sum			(2) (-0.0142)

Example 7-17. For the truss shown in Fig. 7-46(a), compute the vertical deflections at joints L_1 and L_2. $E = 30 \times 10^3$ ksi.

The bar forces in the truss members are first analyzed and the elastic strains in various members are computed as shown in Table 7-5. The computation of the angle changes has been carried out in Table 7-6. In Table

7-6 angle A represents the particular interior angle for which the change is computed, and the change ΔA is multiplied by a factor of 10^3 in the last column of the table.

TABLE 7-5

Member	Bar force F (kips)	Area A (in.^{2})	Strain $=e/L = F/AE$
L_0L_1	$-$ 120	8	$-$ 0.500 $\times$ 10^{-3}
L_1L_2	$-$ 60	8	$-$ 0.250 $\times$ 10^{-3}
U_0U_1	+ 60	8	+ 0.250 $\times$ 10^{-3}
U_0L_1	+ 100	10	+ 0.333 $\times$ 10^{-3}
U_1L_2	+ 100	10	+ 0.333 $\times$ 10^{-3}
U_1L_1	$-$ 80	6	$-$ 0.444 $\times$ 10^{-3}

TABLE 7-6

Joint	Angle A	$10^3 \times (\epsilon_a - \epsilon_c) \cot B$	$10^3 \times (\epsilon_a - \epsilon_b) \cot C$	$10^3 \times \Delta A$
L_0	$U_0L_0L_1$	$(0.333 - 0)(\frac{4}{3}) = 0.444$	$(0.333 + 0.5)(\frac{3}{4}) = 0.625$	+ 1.069
	$L_0L_1U_0$	$(0 + 0.5)(0) = 0$	$(0 - 0.333)(\frac{4}{3}) = -0.444$	$-$ 0.444
L_1	$U_0L_1U_1$	$(0.250 - 0.333)(\frac{3}{4}) = -0.063$	$(0.25 + 0.444)(0) = 0$	$-$ 0.063
	$U_1L_1L_2$	$(0.333 + 0.444)(\frac{4}{3}) = 1.016$	$(0.333 + 0.25)(\frac{3}{4}) = 0.438$	+ 1.454
	Sum			+ 0.947

The elastic load on the conjugate beam for this problem is shown in Fig. 7-46(b). Then, the vertical deflections may be computed by taking moments at points L_1 and L_2 of the conjugate beam.

$$v_{L_1} = (-1.069 \times 10^{-3})(30)(12) = -0.385 \text{ in.}$$

$$v_{L_2} = (-1.069 \times 10^{-3})(60)(12) + (-0.947 \times 10^{-3})(30)(12)$$
$$= -0.770 - 0.341 = -1.111 \text{ in.}$$

7-15 *Deflection of Cables*

When a cable is subjected to external loads, it elongates under the action of the tension; temperature variations also cause a change in length. The result is vertical deflection or change in the cable sag since the span length

between supports of the cable remains constant. We shall confine our discussion to uniformly loaded cables.

Length of cables. The total length s of a cable can be obtained by integrating the length of element ds over the entire length as follows:

$$s = \int_0^s ds = \int_0^L \left[1 + \left(\frac{dy}{dx}\right)^2\right]^{1/2} dx \tag{7-21}$$

Although it is theoretically possible to carry out the integration for the general case of a uniformly loaded cable represented by Eq. (3-16), the result is rather cumbersome. Therefore, we shall derive first an expression for a special case for which the supports are at the same elevation. Let us choose the coordinate axes as shown in Fig. 7-47. Then, the equation of a parabola can be written as

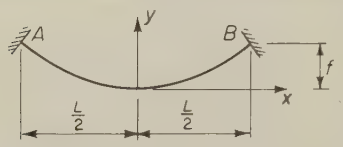

Figure 7–47

$$y = \frac{4fx^2}{L^2} \tag{a}$$

Since $dy/dx = 8fx/L^2$, we have

$$s = 2\int_0^{L/2} \left[1 + \frac{64f^2x^2}{L^4}\right]^{1/2} dx$$

Expanding the quantity under the integral sign into an infinite series by means of the binomial theorem, we obtain

$$s = 2\int_0^{L/2} \left[1 + \frac{1}{2}\left(\frac{64f^2x^2}{L^4}\right) - \frac{1}{8}\left(\frac{64f^2x^2}{L^4}\right)^2 + \cdots\right] dx$$

$$= L\left(1 + \frac{8f^2}{3L^2} - \frac{32f^4}{5L^4} + \cdots\right)$$

Taking only the first three terms and letting the sag ratio $n = f/L$,

$$s = L\left(1 + \frac{8n^2}{3} - \frac{32n^4}{5}\right) \tag{7-22}$$

When the supports of the cable are not at the same elevation, as shown in Fig. 7-48, the equation of the cable is given by

$$y = \frac{4f}{L^2}(Lx - x^2) + \frac{hx}{L} \tag{b}$$

Thus, the integral in Eq. (7-21) becomes rather complicated. However, the approximate length of the cable can be obtained from Eq. (7-22). Let L' be the length of the inclined chord between supports and f' be the sag at midspan

normal to the inclined chord. If the angle of inclination is denoted by θ, it can be seen that $L' = L \sec \theta$, and $f' = f \cos \theta$. Hence,

$$n' = \frac{f'}{L'} = \frac{f}{L} \cos^2 \theta$$

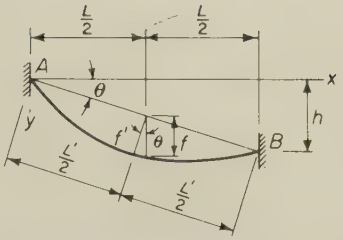

Figure 7–48

and

$$s = L' \left(1 + \frac{8n'^2}{3} - \frac{32n'^4}{5} + \dots\right)$$

$$= L \sec \theta \left(1 + \frac{8f^2}{3L^2} \cos^4 \theta - \frac{32f^4}{5L^4} \cos^8 \theta + \dots\right) \tag{7-23}$$

Elongation of cables. The elongation of a cable subjected to uniform load can be obtained by integrating the elongation of an element ds along the entire length. Thus

$$\Delta s = \int_0^s \frac{T ds}{AE} = \frac{1}{AE} \int_0^s T ds = \frac{1}{AE} \int_0^s H \frac{ds}{dx} ds$$

$$= \frac{H}{AE} \int_0^L \left(\frac{ds}{dx}\right)^2 dx = \frac{H}{AE} \int_0^L \left[1 + \left(\frac{dy}{dx}\right)^2\right] dx \tag{7-24}$$

Again, for the cable represented by Eq. (a), we have

$$\Delta s = \frac{2H}{AE} \int_0^{L/2} \left[1 + \frac{64f^2x^2}{L^4}\right] dx$$

$$= \frac{HL}{AE} \left(1 + \frac{16}{3} n^2\right) \tag{7-25}$$

If the supports of the cable are not at the same elevation, the term dy/dx in Eq. (7-24) may be obtained from Eq. (b) as follows:

$$\frac{dy}{dx} = \frac{4f}{L} - \frac{8fx}{L^2} + \frac{h}{L} \tag{c}$$

Hence,

$$\Delta s = \frac{H}{AE} \int_0^L \left[1 + \left(4n - \frac{8nx}{L} + \frac{h}{L}\right)^2\right] dx$$

$$= \frac{HL}{AE} \left(1 + \frac{h^2}{L^2} + \frac{16}{3} n^2\right) \tag{7-26}$$

Change of cable sag. From Eq. (7-22), we can write

$$s = L \left[1 + \frac{8f^2}{3L^2} - \frac{32f^4}{5L^4}\right]$$

If we differentiate s with respect to f, we obtain the following:

$$\frac{\partial s}{\partial f} = \frac{16}{3}\frac{f}{L} - \frac{128f^3}{5L^3}$$

$$= \frac{16}{3}n - \frac{128}{5}n^3$$

Physically, $\partial s/\partial f$ represents the rate of change of s with respect to f while the span length L is maintained constant. If $\partial s/\partial f$ is expressed in the form of $\Delta s/\Delta f$, in which Δs and Δf are small finite quantities, we have the following relation:

$$\Delta f = \frac{\Delta s}{16\frac{2}{3}n - 128\frac{4}{5}n^3} \tag{7-27}$$

Example 7-18. The cable shown in Fig. 7-49 is subjected to a uniform load of 1 kip/horizontal ft. The supports of the cable are at the same ele-

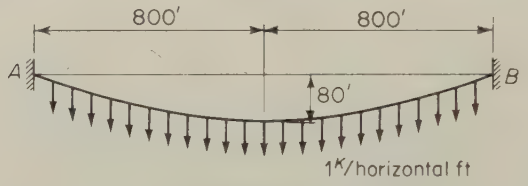

Figure 7–49

vation. $L = 1{,}600$ ft, $f = 80$ ft, and $n = f/L = 0.05$. $E = 30 \times 10^3$ ksi and $A = 80$ in.^{2} Determine the length of the cable and the elongation of the cable caused by the load.

$$s = 1{,}600\,[1 + \tfrac{8}{3}(0.05)^2 - 3\tfrac{2}{5}(0.05)^4] = 1{,}706.7 \text{ ft}$$

$$H = \frac{(1)\,(1{,}600)^2}{(8)\,(80)} = 4{,}000 \text{ kips}$$

$$\Delta s = \frac{(4{,}000)\,(1{,}600)}{(80)\,(30{,}000)}\left[1 + \frac{16}{3}(0.05)^2\right] = 2.70 \text{ ft}$$

If the shape of the cable is to remain parabolic under the load, the initial length of the cable before loading should be reduced by the amount of 2.70 ft, or the initial length is $1{,}706.7 - 2.7 = 1{,}704$ ft.

Example 7-19. For the previous example, determine the change in the cable sag under load. Also, compute the change of the sag for a temperature rise of 100 degrees F. The coefficient of linear expansion is $6.5 \times 10^{-6}/^0$F.

For the external load, $\Delta s = 2.70$ ft,

$$\Delta f = \frac{2.70}{(16\frac{2}{3})\,(0.05) - (128\frac{4}{5})\,(0.05)^3} = \frac{2.70}{0.2635} = 10.1 \text{ ft}$$

For temperature rise, $\Delta s = (100)(6.5)(10^{-6})(1{,}706.7) = 1.047$ ft,

$$\Delta f = \frac{1.047}{0.2635} = 3.98 \text{ ft}$$

7-16 Summary

In this chapter we have discussed various methods for computing deflections of simple structures such as beams, rigid frames, arches, trusses, and cables, with emphasis on the geometry of the deflected structures. It is hoped that such an approach will lead to a better understanding of the relation between the applied loads and the deflected shapes of structures.

References

7-1 H. M. Westergaard, "Deflection of Beams by Conjugate Beam Method," *Journal of the Western Society of Engineers*, vol. 26, 1921, p. 369.

7-2 M. Hetenyi, "Application of Maclaurin Series to the Analysis of Beams in Bending," *Journal of the Franklin Institute*, vol. 254, 1952, p. 369.

7-3 K. H. Chu, "Truss Deflections by the Coordinate Method," *Trans. ASCE*, vol. 117, 1952, p. 317.

7-4 J. I. Parcel and R. B. B. Moorman, *Analysis of Statically Indeterminate Structures*, John Wiley & Sons, Inc., New York, 1955.

Problems

7-1 Derive the differential relationship between moment M and deflection v for a beam using the sign convention in Fig. P7-1.

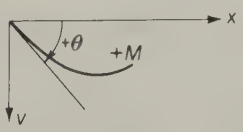

Figure P7–1

7-2 to **7-6** The beams shown in Figs. P7-2 to P7-6 have constant modulus of elasticity E and moment of inertia I. Derive the equations for slope and deflection for each beam by successive integrations. Also calculate the deflection at point C of each beam by the moment-area method.

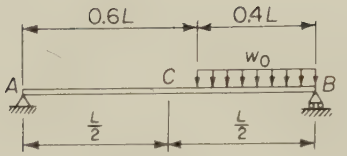

Figure P7–2

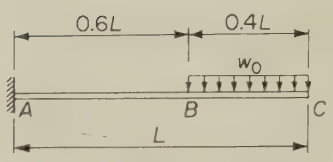

Figure P7–3

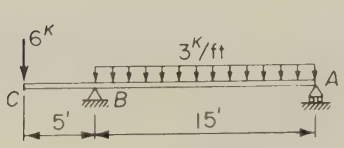

$E = 30 \times 10^3$ ksi
$I = 250$ in.^{4}

Figure P7–4

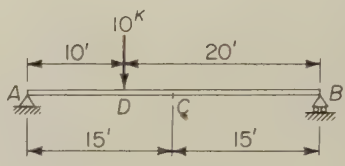

$E = 30 \times 10^3$ ksi
$I = 200$ in.^{4}

Figure P7–5

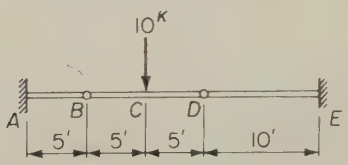

Figure P7–6

7-7 and **7-8** Calculate the slope and deflection at points A and C of the beams shown in Figs. P7-7 and P7-8 by the conjugate beam method. The modulus of elasticity E and the moment of inertia I of the beams are constant.

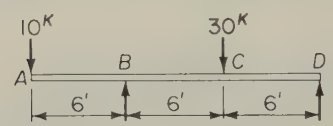

Figure P7–7

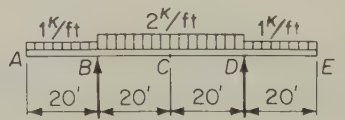

Figure P7–8

7-9 to **7-17** Calculate the deflections at the panel points of the beams shown in Figs. P7-9 through P7-17 by Newmark's method. The modulus of elasticity $E = 30 \times 10^3$ ksi.

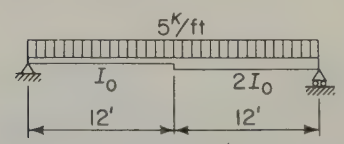

(Use $h = 6'$)

Figure P7–9

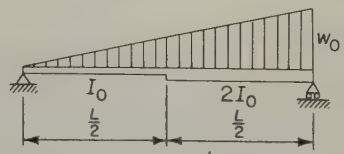

(Use $h = \frac{L}{4}$)

Figure P7–10

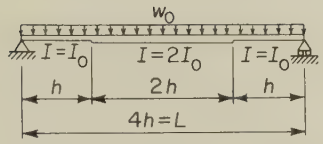

Figure P7–11

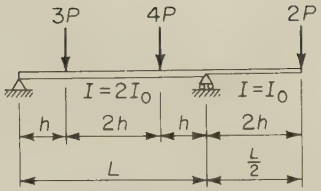

Figure P7–12

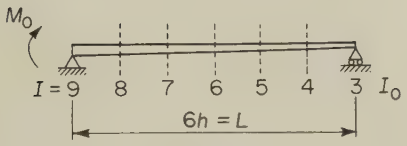

Figure P7–13

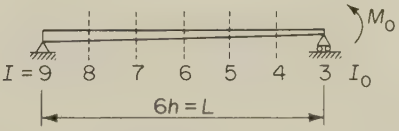

Figure P7–14

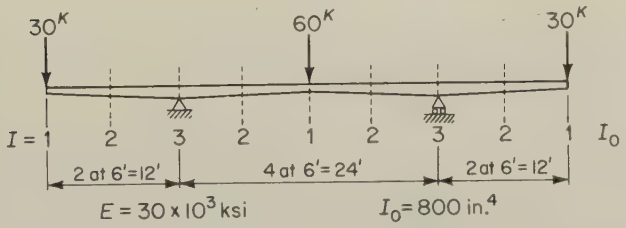

Figure P7–15

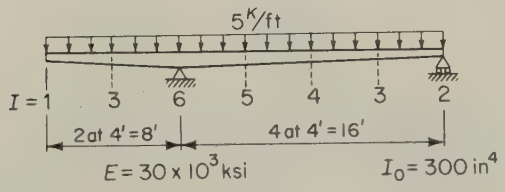

Figure P7–16

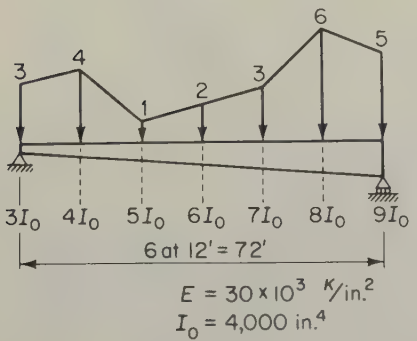

Figure P7–17

7-18 and **7-19** Calculate the horizontal and vertical displacements of joint D of the frames shown in Figs. P7-18 and P7-19.

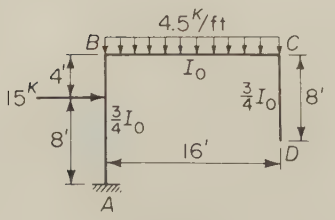

Figure P7–18

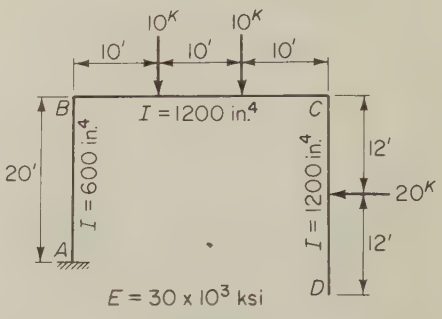

Figure P7–19

7-20 to **7-22** Calculate the horizontal displacement of joint E for the frames shown in Figs. P7-20 through P7-22.

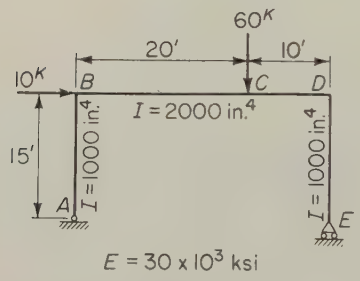

Figure P7–20

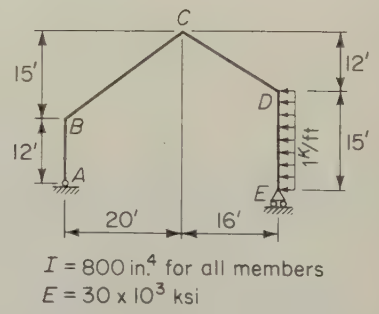

Figure P7–21

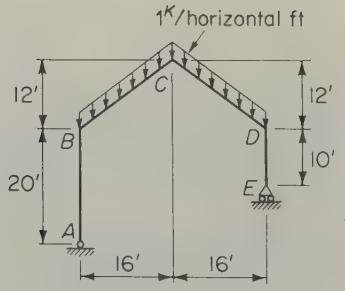

Figure P7–22

7-23 The parabolic arch shown in Fig. P7-23 has a variable moment of inertia $I = I_c \sec \beta$ in which I_c is the moment of inertia at the crown and β is the angle between a tangent at a point on the arch axis and a horizontal line. Compute the horizontal displacement of point B for $k = 0.2, 0.4, 0.6$, and 0.8.

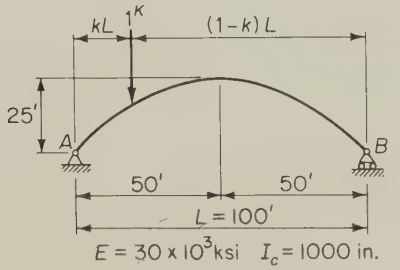

Figure P7-23

7-24 to **7-26** Find the vertical deflections of the joints at the lower chords of the trusses shown in Figs. P7-24 through P7-26 by the construction of a Williot-Mohr diagram and by the conjugate beam method.

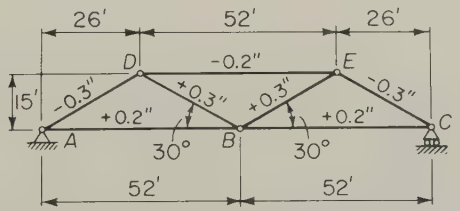

Figure P7-24

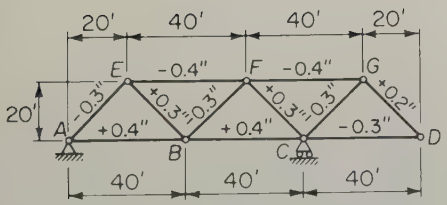

Figure P7-25

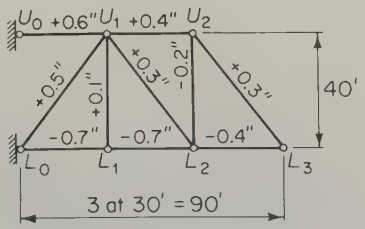

Figure P7-26

7-27 Find the vertical and horizontal deflections of all joints in the arch truss shown in Fig. P7-27 by the Williot-Mohr diagram.

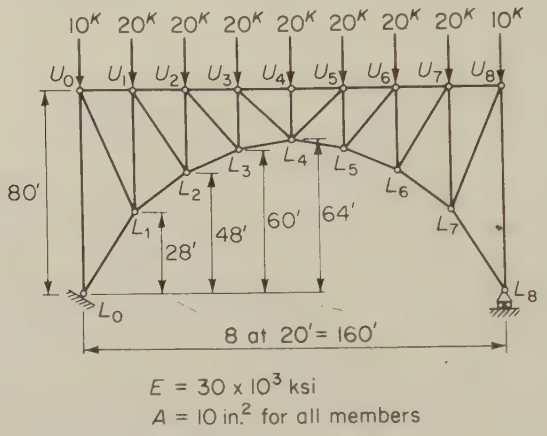

Figure P7–27

7-28 and **7-29** Compute the vertical deflections of the joints at the bottom chords of the trusses shown in Figs. P7-28 and P7-29 by the conjugate beam method.

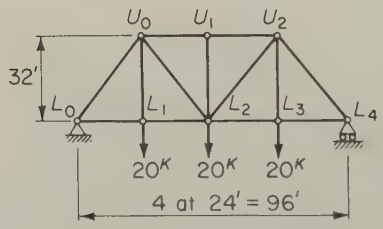

Figure P7–28

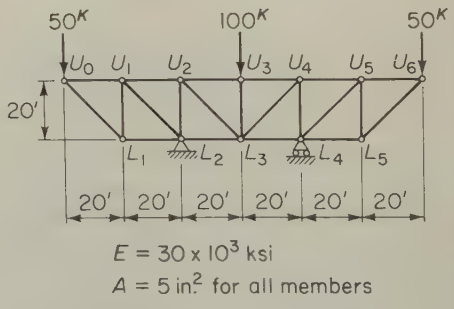

Figure P7–29

7-30 The side span of a suspension bridge cable as shown in Fig. P7-30 has a span of 600 ft and a sag of 30 ft. The load on the cable may be considered as as 1 kip/horizontal ft. The area of the cable is 60 in², and the modulus of elasticity of the material is 30,000 ksi. Compute the length of the cable under load. If the

cable is to remain parabolic under load, what should be the initial length of the cable before the load is applied?

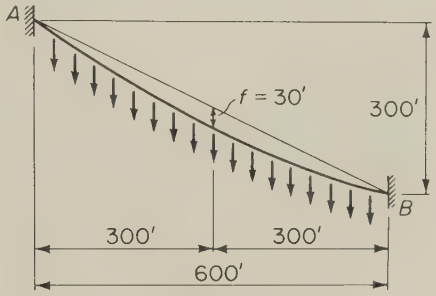

Figure P7–30

8 ENERGY PRINCIPLES

8-1 Energy Relations in Structural Systems

A structure may be considered as a conservative system if no energy is added or taken away from it when it is isolated from its environment. As a structure deforms from one configuration to another under the action of applied loads, *external work* is done on the system by the external forces. On the other hand, *internal work* is done against the deformations in the system by the internal forces during the deformation. Strictly speaking, internal work must be negative because the deformations are imposed on the system and are resisted by the internal forces. According to the principle of conservation of energy, the total energy of an isolated system remains constant. Hence, the algebraic sum of the external and internal work in a structural system must be zero. In common usage, however, we often speak of the equality of external work and internal work which implies that only the absolute values of these quantities are considered. Thus, in a structural system in which displacements are consistent with constraints, the displacements of the system can be related to the external forces by means of the energy relations.

The energy principles presented in this chapter are applicable to conservative deformable systems that are either linearly or nonlinearly elastic. Although we are primarily interested in the application of these principles to the computation of deflections of statically determinate structures, we should at least be aware of the broad scope of their application to the analysis of redundant systems. We shall, therefore, present each of the energy theorems in its entirety even if it may not be of immediate interest in the computation of deflections.

In Section 2-15 we pointed out that the forces in a deformable system are related to its strain energy whereas the displacements are associated with the complementary energy of the system. Hence, the concept of real work in general does not readily lend itself to the computation of deflections, but the concept of complementary work is useful for such a purpose.

In a broader sense, however, the strain energy and complementary energy methods may be considered as special cases of a more general principle, i.e., the principle of virtual work, which, when applied to deformable systems, may be associated with virtual displacements or virtual forces. Thus, the energy theorems encountered in structural analysis may be grouped into three categories:

A. Theorems related to strain energy:
   1. Principle of virtual displacements
   2. Castigliano's first theorem
   3. Principle of stationary potential energy
B. Theorems related to complementary energy:
   1. Principle of virtual forces
   2. Complementary energy method
   3. Principle of stationary complementary energy
C. Special applications:
   1. Dummy unit load method
   2. Castigliano's second theorem
   3. Castigliano's theorem of "least work"

The unifying factor in all these theorems is the principle of virtual work. If only one virtual force is involved, the dummy unit load method can readily be derived from the principle of virtual forces. As a special application of the principle of virtual work, Castigliano's first theorem is obtained from the strain energy of the system while the complementary energy method is derived from the complementary energy of the system. Castigliano's second theorem is merely a special case of the complementary energy method for linear elastic systems. For a more general application of the principle of virtual work, the concepts of stationary potential energy and stationary complementary energy are introduced. For linear elastic systems, the stationary values of both strain and complementary energy represent the respective minima. Castigliano's theorem of "least work" may be regarded as a special case of the principle of stationary complementary energy for linear elastic systems. The theorems in groups A and B can be developed in parallel, and the theorems in group C are special cases of those in group B.

The parallel grouping of these theorems has an important meaning in the analysis of redundant structures. The theorems in group A are used for the displacement method of analysis whereas those in group B are required for the force method of analysis. With traditional emphasis on the force method for the analysis of linear elastic structures, the theorems

in group C have historically played the most important part. With the advent of electronic digital computers, the displacement method of analysis is gradually gaining favor. Hence, both methods of analysis will be discussed briefly in order to illustrate the application of these theorems.

Linear structural systems are by far the most frequently encountered in actual application. Therefore, we shall consider in great detail the analysis of such systems. The Maxwell-Betti theorem will be derived to demonstrate the reciprocal characteristics of the stiffness and flexibility influence coefficients of linear structural systems. This theorem will be applied to obtain influence lines for deflections of statically determinate structures. Furthermore, Müller-Breslau's principle will be developed for the determination of influence lines of redundant structures.

8-2 *Real Work and Complementary Work*

When an isolated structural system deforms under the action of applied loads, there is no change in the total energy in the isolated system. Thus, according to the principle of conservation of energy, the algebraic sum of the external work W_e and the internal work W_i is equal to zero, i.e.,

$$W_e + W_i = 0 \tag{8-1}$$

For the sake of clarity, we shall always denote the internal work on a structural system as negative since the deformations are opposed by the internal forces. On the other hand, the strain energy in a structural system, which is a measure of the internal work, is defined as a positive quantity,

$$U_i = -W_i \tag{8-1a}$$

Thus, it may be stated that in an isolated structural system, the external work due to applied loads must equal the strain energy of the system as the result of deformation, i.e.,

$$W_e = U_i \tag{8-1b}$$

We shall consider the general case of a nonlinear elastic system that may be conceived schematically as consisting of n elements. Let $P_1, P_2, \ldots, P_m$ be a set of m external loads that cause displacements $s_1, s_2, \ldots, s_m$ in the directions of the respective loads as shown in Fig. 8-1. Let $F_1, F_2, \ldots, F_n$ be the internal forces in various elements of the system and $e_1, e_2, \ldots, e_n$ be the deformations in the directions of the respective internal forces. When the external loads are applied gradually to the system, increasing from

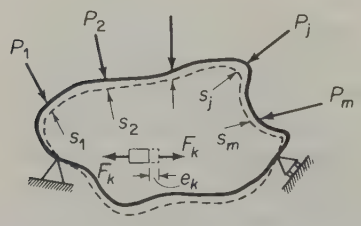

Figure 8–1

zero to their full values proportionally, the internal forces will also increase proportionally. Broadly speaking, the external work in a structural system may include the work done by the reactions as well as the applied loads if the supports are deformable. For the sake of simplicity, however, we shall confine our discussion to rigid supports. Furthermore, the effects of prestressing and self-straining as described in Section 2-9 will be excluded except for cases where they can be treated in complete generality and without introducing unnecessary complications in the discussion.

If the force-deformation characteristics of all elements of the nonlinear elastic system in Fig. 8-1 can be represented by the curve shown in Fig. 8-2(a), the strain energy of an element resulting from the deformation e in the direction of the internal force F is given by $\int F\,de$, or the area under the force-deformation curve. Hence, the total strain energy of the system is equal to

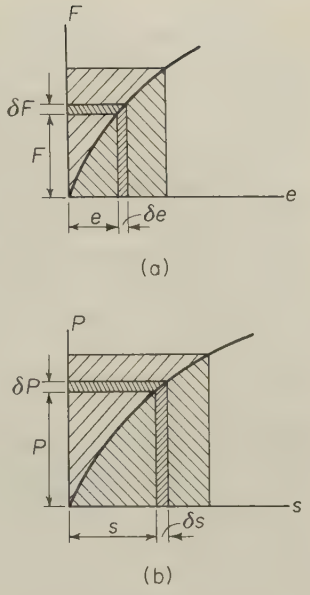

Figure 8–2

$$U_i = \sum_{k=1}^{n} \int F_k\,de_k \tag{8-2}$$

The external work done on the same system by a force P for a displacement s in the direction of P is given by $\int P\,ds$, or the area under the force-deformation curve in Fig. 8-2(b), which has the same characteristics as that in Fig. 8-2(a). Then, the total external work done on the system is equal to

$$W_e = \sum_{j=1}^{m} \int P_j\,ds_j \tag{8-3}$$

From the principle of conservation of energy, we have $W_e = U_i$, or

$$\sum_{j=1}^{m} \int P_j\,ds_j = \sum_{k=1}^{n} \int F_k\,de_k \tag{8-4}$$

Since the external loads are applied gradually to the system in proportion, the internal forces increase from zero to their full values in the same proportion. The deformations and displacements which are related to the forces also increase proportionally from zero to their respective full values. Hence, the lower limits of the integrals in Eqs. (8-2) through (8-4) are all zero, whereas the upper limits represent the respective full values of deformations and displacements when the applied loads reach their full values simultaneously. Although the limits of integration are not shown in these equations, the meaning of these integrals should be fully understood.

Parallel to the development of the concept of real work, the concept of complementary work may be introduced for the derivation of energy theorems related to the complementary energy. The complementary energy resulting from an internal force F and a deformation e in the direction of F is given by $\int e\,dF$, or the area above the force-deformation curve in 8-2(a), whereas the external complementary work resulting from an external force P for a displacement s in the direction of P is given by $\int s\,dP$, or the area above the force-deformation curve in Fig. 8-2(b). Strictly speaking, the internal complementary work must be negative. Thus, the algebraic sum of the external complementary work C_e and the internal complementary work C_i is equal to zero, i.e.,

$$C_e + C_i = 0 \tag{8-5}$$

The complementary energy is a measure of the internal complementary work and is defined as a positive quantity,

$$U_c = -C_i \tag{8-5a}$$

Hence,

$$C_e = U_c \tag{8-5b}$$

Let us again consider the nonlinear elastic system represented by Fig. 8-1. The total complementary energy of the system is given by

$$U_c = \sum_{k=1}^{n} \int e_k\,dF_k \tag{8-6}$$

The total external complementary work done on the same system is equal to

$$C_e = \sum_{j=1}^{m} \int s_j\,dP_j \tag{8-7}$$

Then, from $C_e = U_c$, we get

$$\sum_{j=1}^{m} \int s_j dP_j = \sum_{k=1}^{n} \int e_k\,dF_k \tag{8-8}$$

Without indicating the limits of integration in Eqs. (8-6) through (8-8), it is understood that the lower limits of the integrals are all zero, whereas the upper limits represent the respective full values of external and internal forces which are reached proportionately.

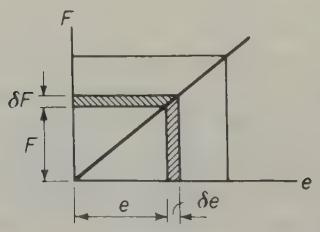

Figure 8–3

For the special case of linear elasticity as characterized by the linear load-deformation curve in Fig. 8-3, the areas below and above the curve are equal. Hence, the ex-

ternal complementary work on a linearly elastic system is identical to the real work on the system, and the complementary and strain energy of the system are interchangeable. In that case, we need be concerned only with the real work and the strain energy of the system. Then, the integrals representing the areas under load-deformation curves are reduced to areas of triangles. If the system shown in Fig. 8-1 is linearly elastic, Eqs. (8-2) and (8-3) become

$$U_i = \tfrac{1}{2} \sum_{k=1}^{n} F_k e_k \tag{8-9}$$

$$W_e = \tfrac{1}{2} \sum_{j=1}^{m} P_j s_j \tag{8-10}$$

Because of the relative simplicity in the evaluation of these expressions, linear elasticity is frequently assumed in structural analysis if the material characteristic agrees reasonably well with this assumption.

8-3 *Strain Energy in Linear Elastic Systems*

In order to evaluate the strain energy in linear elastic systems, we shall first consider different forms of strain energy that may exist in various structural systems. We are primarily concerned with systems consisting of slender elements such as bars and beams.

Strain energy due to normal stresses. Consider an infinitesimal element of volume $\delta x\, \delta y\, \delta z$ as a free body, as shown in Fig. 8-4, in which uniform stresses σ are acting on the left and right faces of the element. If the normal force $\sigma\, \delta y\, \delta z$ acting on each face increases gradually from zero to its full value, the total deformation is equal to the strain ϵ multiplied by the length δx. The strain energy δU_i stored in the infinitesimal element is

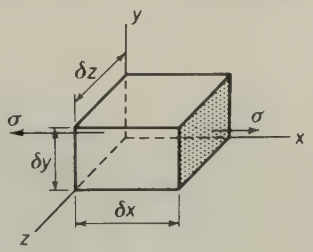

Figure 8-4

$$\delta U_i = \tfrac{1}{2} (\sigma\, \delta y\, \delta z)(\epsilon\, \delta x) = \tfrac{1}{2} \sigma\epsilon\, \delta x\, \delta y\, \delta z$$

By applying Hooke's law for linearly elastic materials, $\epsilon = \sigma/E$, where E is the modulus of elasticity, the total strain energy in a structural member of volume V due to at set of normal stresses in the direction of the x-axis becomes

$$U_i = \int\int\int_V \frac{\sigma^2}{2E}\, dx\, dy\, dz \tag{8-11}$$

For a structural member subjected to an axial force F only, $\sigma = F/A$ and

$\epsilon = e/L$, in which A is the constant cross-sectional area, e is the axial deformation, and L is the length of the member. Thus, the total strain energy in the member subject to an axial force is

$$U_i = \frac{\sigma^2 AL}{2E} = \frac{F^2 L}{2AE} \tag{8-12a}$$

However, the strain energy can also be expressed in terms of the axial deformation e instead of the axial load F, since $e = FL/AE$. Hence,

$$U_i = \frac{AEe^2}{2L} \tag{8-12b}$$

Strain energy in bending. In the case of a member subjected to bending, the bending stresses also are acting in the direction normal to a cross section of the member but are no longer uniformly distributed over the cross-sectional area. However, the total strain energy in bending can still be obtained from Eq. (8-11) if the stress σ is expressed as a function of the distance y by the formula

$$\sigma = -\frac{My}{I}$$

in which M is the moment at a section and I is the moment of inertia about the z-axis for the element shown in Fig. 8-5. Thus, the total energy in a member of volume V subjected to bending becomes

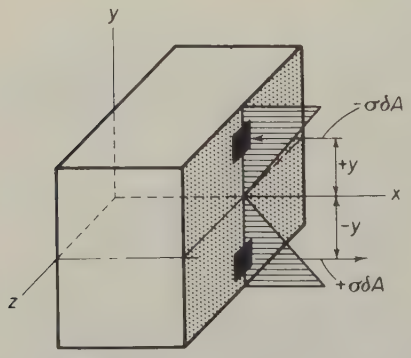

Figure 8–5

$$U_i = \int\int\int_V \frac{1}{2E}\left(-\frac{My}{I}\right)^2 dx\, dy\, dz$$

For a member of length L and cross-sectional area A, we get

$$U_i = \int_L \frac{M^2}{2EI^2}\left[\int\int_A y^2\, dy\, dz\right] dx$$

By noting $I = \int\int_A y^2\, dy\, dz$, we have

$$U_i = \int_L \frac{M^2\, dx}{2EI} \tag{8-13a}$$

Since the curvature at a section of a structural member may be approximated by d^2v/dx^2, we have $M/EI = d^2v/dx^2$, in which v is the vertical displacement of the beam. Thus, the total bending strain energy of the member can also be expressed in terms of the curvature as follows:

$$U_i = \int_L \frac{(EI\, d^2v/dx^2)^2\, dx}{2EI} = \int_L \frac{EI}{2}\left(\frac{d^2v}{dx^2}\right)^2 dx \tag{8-13b}$$

Note that Eqs. (8-13) are quite general since the moment M, the curvature d^2v/dx^2, and the bending stiffness EI in these equations may vary from section to section. In the special case of pure bending of a member with constant cross section and material properties, Eqs. (8-13) become

$$U_i = \frac{M^2L}{2EI} \quad \text{and} \quad U_i = \frac{EIL}{2}\left(\frac{d^2v}{dx^2}\right)^2$$

Strain energy for pure shear. When an infinitesimal element of volume $\delta x\ \delta y\ \delta z$ is subjected to pure shear as shown in Fig. 8-6, it is noted from the consideration of the summation of the moments of all forces about the z-axis that

$$(\tau_{xy}\, dx\, dz)\,(dy) = (\tau_{yx}\, dy\, dz)\,(dx)$$

or

$$\tau_{xy} = \tau_{yx}$$

Denoting the shearing stress by $\tau_{xy} = \tau_{yx} = \tau$ and the corresponding shearing strain by γ, the strain energy in the element resulting from pure shear is

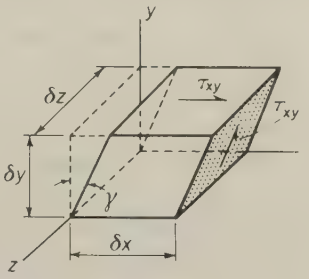

Figure 8-6

$$\delta U_i = \tfrac{1}{2}\tau\gamma\ \delta x\ \delta y\ \delta z$$

By applying Hooke's law, $\gamma = \tau/G$ in which G is the modulus of rigidity, the total strain energy in a structural member of volume V due to a set of shearing stresses in the xy-plane is equal to

$$U_i = \int\int\int_V \frac{\tau^2}{2G}\, dx\, dy\, dz \tag{8-14}$$

When a circular member of length L and constant cross-sectional area A is subjected to a constant torque T, a state of pure shear exists in the member. The shearing stress τ at a point located at a radius r from the center of the circle is given by

$$\tau = \frac{Tr}{J}$$

in which J is the polar moment of inertia. Then, the total strain energy in the circular member subjected to torsion is equal to

$$U_i = \int\int\int_V \frac{1}{2G}\left(\frac{Tr}{J}\right)^2 dx\, dy\, dz = \int_L \frac{T^2}{2GJ^2}\left[\int\int_A r^2\, dy\, dz\right] dx$$

Noting that $J = \int\int_A r^2\, dy\, dz$, we get

$$U_i = \int_L \frac{T^2\, dx}{2GJ} = \frac{T^2L}{2GJ} \tag{8-15a}$$

Since the angle of twist per unit length of a circular member is given by $\theta = T/GJ$, or $T = GJ\theta$, the total strain in the member arising from torsion may also be expressed in terms of θ. Thus,

$$U_i = \frac{(GJ\theta)^2 L}{2GJ} = \frac{GJL\theta^2}{2} \tag{8-15b}$$

Strain energy for shear in beams. In the case of a beam subjected to lateral loads, shear as well as bending occurs in the beam. However, the deformation due to shear is usually very small in comparison with that resulting from bending and is negligible except for very deep beams. In any case, the strain energy due to shear can be obtained from Eq. (8-14) since the shearing stresses on the xz- and yz-planes are assumed to be zero. However, the difficulty of its solution is caused by the fact that the variation of shearing stress in a beam depends on the shape of the cross section as well as the depth-span ratio of the beam. For a beam of rectangular cross section as shown in Fig. 8-7(a), for example, it can be shown theoretically that the distribution of shearing stress along the depth of the beam is parabolic as indicated in Fig. 8-7(b). However, if the depth h is many times greater than the width b of the cross section, the distribution of shearing stress along its depth is more complicated and has been found experimentally to have a shape as shown in Fig. 8-7(c).* For an I-beam with a cross section as shown in Fig. 8-8(a), the shearing stress is more likely to have a relatively

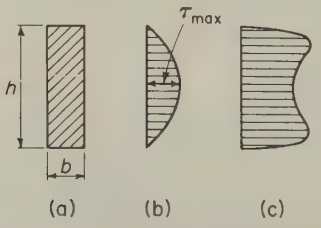

Figure 8–7

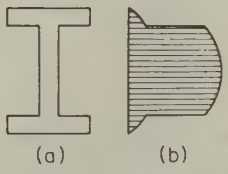

Figure 8–8

uniform distribution in the web rather than the theoretical distribution shown in Fig. 8-8(b). In the case of deep beams with large depth-span ratio, the theoretical analysis of the shearing stress is even more complicated and a detailed discussion is beyond the scope of this text. For the sake of simplicity, however, a rational approach may generally be used in the derivation of the expression for strain energy. Let S denote the total shear force acting on the section and A the area of the section that contributes to the resistance of the shear force. The shearing stress τ at any point of the cross section may be expressed in the form

$$\tau = k\frac{S}{A}$$

*See Reference 8-1 for details.

in which k is a variable factor depending on the shape of the cross section and the depth-span ratio of the beam. Then, the total strain energy due to shear in a beam of volume V is equal to

$$U_i = \int\int\int_V \frac{1}{2G}\left(k\frac{S}{A}\right)^2 dx\,dy\,dz$$

$$= \int_L \frac{S^2}{2GA^2}\left[\int\int_A k^2\,dy\,dz\right] dx$$

To simplify the solution of this expression, let us assume that

$$\int\int_A k^2\,dy\,dz = CA$$

in which C is a rational constant called the *form factor*. Then

$$U_i = \int_L \frac{CS^2\,dx}{2GA} = C\int_L \frac{S^2\,dx}{2GA} \tag{8-16}$$

Note that in Eq. (8-16), G, A, and S may vary from section to section of the beam. For beams of ordinary proportions with a rectangular cross section, the form factor may be taken as 1.2. For an ordinary I-beam, the same factor may be used for an approximate solution if A in Eq. (8-16) is taken as the area of the web of the I-beam.

Example 8-1. For a beam of ordinary proportions having a rectangular cross section and subjected to lateral loads, derive an expression for the strain energy due to shear deformation only.

For a rectangular beam with width b and depth h as shown in Fig. 8-9, the distribution of shearing stress is given by*

$$\tau = \frac{SQ}{Ib} = \frac{S}{Ib}\int_y^{h/2} by'\,dy' = \frac{S}{2I}\left(\frac{h^2}{4} - y^2\right)$$

in which Q is the statical moment of the shaded area with respect to the neutral axis. Then, from Eq. (8-14), the strain energy due to shear is equal to

$$U_i = \int\int\int_V \frac{\tau^2}{2G}\,dx\,dy\,dz = \int_L\left[\int\int_A \frac{\tau^2}{2G}\,dy\,dz\right] dx$$

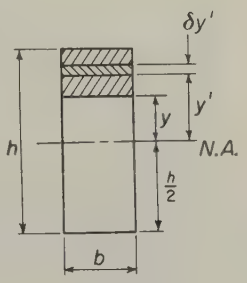

Figure 8-9

*See, for instance, pp. 138–139 of Reference 2–3.

Hence,

$$U_i = \int_L \left[\int_0^b \int_{-h/2}^{h/2} \frac{S^2}{8GI^2} \left(\frac{h^2}{4} - y^2 \right)^2 dy\, dz \right] dx$$

$$= \int_L \frac{S^2 b}{8GI^2} \left[\int_{-h/2}^{h/2} \left(\frac{h^4}{16} - \frac{h^2 y^2}{2} + y^4 \right) dy \right] dx$$

$$= \int_L \frac{S^2 b}{8GI^2} \left[\frac{h^4 y}{16} - \frac{h^2 y^3}{6} + \frac{y^5}{5} \right]_{-h/2}^{h/2} dx$$

$$= \int_L \frac{S^2 b}{8GI^2} \left[\frac{h^5}{16} - \frac{h^5}{24} + \frac{h^5}{80} \right] dx = \int_L \frac{S^2 b h^5}{240 GI^2} dx$$

Noting that $I = bh^3/12$ and $A = bh$, we obtain

$$U_i = \int_L \frac{3S^2}{5GA} dx = 1.2 \int_L \frac{S^2}{2GA} dx$$

Comparing this result with Eq. (8-16), we note that the form factor C is equal to 1.2.

8-4 Method of Real Work

By the application of the principle of conservation of energy, we can derive a relationship involving loads, displacements, and elastic and geometrical constants for an elastic structure. However, this relationship in general does not lead to the solution of the displacement in terms of other quantities. For example, if we equate the external work done on a linearly elastic system by the external loads to the strain energy stored in the system as a result of deformation, the expression thus obtained may contain many unknown quantities. The external work done on the system is expressed in terms of the products of the applied loads and the respective displacements. The strain energy of the system can be evaluated if the deformations caused by internal forces are related to the applied loads. In the case of a plane truss, for example, the members are subjected to axial forces only. Let F_k be the bar force in a member of a truss that has a length of L_k and cross-sectional area of A_k. E_k is the modulus of elasticity of the member. Then, the strain energy in the entire truss consisting of n members can be obtained from Eq. (8-12a) as follows:

$$U_i = \frac{1}{2} \sum_{k=1}^{n} \frac{F_k^2 L_k}{A_k E_k} \tag{8-17a}$$

In the case of a beam of span length L, the strain energy will be given by the sum of the strain energy due to bending and that due to shear as

represented by Eqs. (8-13a) and (8-16) respectively. Thus,

$$U_i = \frac{1}{2}\int_0^L \frac{M^2}{EI}\,dx + \frac{C}{2}\int_0^L \frac{S^2}{AG}\,dx \tag{8-17b}$$

For beams of ordinary proportions used in structures, the strain energy due to shear is very small in comparison with that due to bending and is usually neglected.

For statically determinate structures, the internal forces can be solved directly from the applied loads. Hence, the displacements s_j ($j = 1, 2, \ldots, m$) are the only unknowns when we equate Eq. (8-10) to Eq. (8-17a) or (8-17b). Even then, we cannot solve for these displacements in the equation. Only in the special case where a single external load is acting on the structure can the displacement of the point of application of this load in the direction of the load be determined. Thus, for a plane truss, the displacement s of the point of application of a load P in the direction of P may be obtained by equating Eqs. (8-10) and (8-17a) as follows:

$$s = \frac{1}{P}\sum_{j=1}^{n} \frac{F_j^2 L_j}{A_j E_j} \tag{8-17c}$$

Similarly, for a beam subjected to a single load P, the displacement of the point of application of P in the direction of P can be obtained by equating Eqs. (8-10) and (8-17b) as follows:

$$s = \frac{1}{P}\left[\int_0^L \frac{M^2\,dx}{EI}\,dx + C\int_0^L \frac{S^2\,dx}{AG}\right] \tag{8-17d}$$

This method of computing deflections, called the *method of real work*, has only very limited use.

Example 8-2. A cantilever beam of constant rectangular cross section is subjected to a single vertical load P at the free end, as shown in Fig. 8-10. Compute the vertical deflection Δ at the free end of the beam for the following cases: (a) the shearing deformation is neglected and (b) the shear deformation is not neglected.

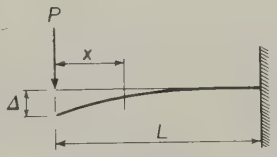

Figure 8-10

Referring to Fig. 8-10 we see that the shear at any section of the beam is $S = -P$ and the moment at any section is given by $M = -Px$. When the shear deformation is neglected, we have

$$\Delta = \frac{1}{P}\int_0^L \frac{M^2\,dx}{EI} = \frac{1}{P}\int_0^L \frac{P^2x^2\,dx}{EI} = \frac{PL^3}{3EI}$$

If the shear deformation is not neglected, the total deformation may be obtained from Eq. (8-17d) by assuming $C = 1.2$ for a rectangular beam of

ordinary proportions. Thus,

$$\Delta = \frac{PL^3}{3EI} + \frac{1.2PL}{AG}$$

It can be seen that for beams of ordinary proportions, the first term involving L^3 is much larger than the second term involving L. Hence, it is justifiable to neglect the shear deformation except for beams with large depth-span ratios where shear deformation may constitute a major portion of the deformation.

8-5 *Strain Energy and Complementary Energy Methods*

In Section 8-4, we presented a rather limited application of the method of real work in the computation of deflections. However, the concepts of real work and complementary work may have more general applications in structural analysis if the strain energy of a system is expressed as a function of the displacements and the complementary energy is expressed as a function of the external forces. Theoretically, this is always possible since the internal forces in the system are related to the external forces by the conditions of equilibrium, the deformations can be expressed in terms of the internal forces according to the stress-strain relationship of the material, and the displacements of the external forces are related to the deformations by the conditions of compatibility.

Consider, for example, the deformable system in Fig. 8-1, which in general may be nonlinear elastic. The system is subjected to a set of loads $P_1, P_2, \ldots, P_m$, producing displacements $s_1, s_2, \ldots, s_m$ at the points of application of these loads in the directions of the respective loads. The strain energy U_i stored in the system during the application of loads may be obtained from Eqs. (8-2) and (8-4) as follows:

$$U_i = \sum_{k=1}^{n} \int F_k \, de_k = \sum_{j=1}^{m} \int P_j \, ds_j$$

or

$$\delta U_i = \sum_{k=1}^{n} F_k \, \delta e_k = \sum_{j=1}^{m} P_j \, \delta s_j$$

If one of the displacements, say s_j, is increased by a small amount δs_j in the direction of the load P_j while other displacements remain unchanged, then the increment of strain energy of the system is equal to

$$\delta U_i = P_j \, \delta s_j \qquad \text{(a)}$$

If the strain energy U_i is expressed as a function of the displacements, the increment of strain energy may also be expressed as the total differential

of U_i. However, all terms except the one involving s_j will disappear since all other displacements remain unchanged. Hence,

$$\delta U_i = \frac{\partial U_i}{\partial s_1}\delta s_1 + \frac{\partial U_i}{\partial s_2}\delta s_2 + \ldots + \frac{\partial U_i}{\partial s_m}\delta s_m = \frac{\partial U_i}{\partial s_j}\delta s_j \qquad \text{(b)}$$

By equating Eqs. (a) and (b), we get

$$P_j\,\delta s_j = \frac{\partial U_i}{\partial s_j}\delta s_j$$

or

$$P_j = \frac{\partial U_i}{\partial s_j} \qquad (8\text{-}18)$$

This equation gives the external force acting at a specified point if the strain energy is expressed as a function of the displacements.

On the other hand, the complementary energy U_c of the system during the application of the loads may be obtained from Eqs. (8-6) and (8-8) as follows:

$$U_c = \sum_{k=1}^{n}\int e_k\,dF_k = \sum_{j=1}^{m}\int s_j\,dP_j$$

or

$$\delta U_c = \sum_{k=1}^{n} e_k\,\delta F_k = \sum_{j=1}^{m} s_j\,\delta P_j$$

If one of the loads, say P_j, is increased by a small amount δP_j while other forces remain unchanged, then the increment of complementary energy of the system is equal to

$$\delta U_c = s_j\,\delta P_j \qquad \text{(c)}$$

If the complementary energy U_c is expressed as a function of the external forces, the increment of complementary energy may also be expressed as the total differential of U_c. However, all terms except the one involving P_j will disappear since all other forces remain unchanged. Thus,

$$\delta U_c = \frac{\partial U_c}{\partial P_1}\delta P_1 + \frac{\partial U_c}{\partial P_2}\delta P_2 + \ldots + \frac{\partial U_c}{\partial P_m}\delta P_m = \frac{\partial U_c}{\partial P_j}\delta P_j \qquad \text{(d)}$$

By equating Eqs. (c) and (d), we obtain

$$s_j = \frac{\partial U_c}{\partial P_j} \qquad (8\text{-}19)$$

This equation gives the displacement acting at a specified point in the direction of the force if the complementary energy is expressed as a function of the external forces.

For the special case of linear elasticity, the strain energy U_i and the complementary energy U_c of the system are interchangeable. If the strain energy of a linear elastic system is expressed as a function of external forces, Eq. (8-19) may be replaced by

$$s_j = \frac{\partial U_i}{\partial P_j} \tag{8-20}$$

Equation (8-20) may be regarded as a special case of Eq. (8-19).

The methods of deriving forces, and displacements in the case of linear elasticity, from the strain energy function are called the *strain energy methods*; the method of deriving displacements from the complementary energy function is referred to as the *complementary energy method.* The application of the strain energy methods to linear elastic systems was developed by Castigliano in 1879 without the benefit of the concept of complementary energy. The application of the concept of complementary energy was introduced by Engesser in 1889 and was regarded primarily as a means for the analysis of nonlinear elastic systems. With the traditional emphasis on linear elasticity, the work of Engesser received very little attention during the half-century that followed its development. Only in recent years has the general nature of complementary energy been fully recognized. That such a concept permits the presentation of the dual roles of the energy principles has been ably expounded by Westergaard and by Argyris.*

In the application of these methods to the computation of deflections, we are confronted with the limitation that only the displacements of the points of application of the external forces can be computed. Although these methods represent an improvement over the method of real work since they are applicable to structures subjected to a large number of external forces, they are not general enough for the computation of the deflection at any specified point in any specified direction of a structure. However, the application of these methods may be extended for such a purpose if we realize that they are but special cases of a more general principle, i.e., the principle of virtual work for deformable systems. We shall, therefore, first present the principle of virtual work before discussing in detail the application of the strain energy and complementary energy methods.

8-6 *Principle of Virtual Work*

In Section 2-14 we discussed the principle of virtual work for rigid systems. When such a system in equilibrium is given an arbitrary virtual displacement, the total virtual work done by all external forces in the system must

*The student is referred to the references at the end of this chapter for further discussions. See especially References 8–2 and 8–10.

be zero. The internal forces need not be considered because the distances between any two points in a rigid system must remain constant. Hence, for a rigid system, the principle of virtual work is only used to impose the requirement of equilibrium through the introduction of a virtual displacement.

In the case of a deformable system, we can imagine that the system consists of an infinite number of mass points, the distances between which may be changed. The virtual work done on such a system may be caused by real forces acting through virtual displacements, or by virtual forces acting through real displacements. According to the principle of conservation of energy, the total virtual work done by the internal and external forces on a deformable system must be zero. Hence, the principle of virtual work may be applied to a deformable structural system in two ways. If a structure under the action of real forces is subjected to a set of virtual displacements compatible with its constraints, the principle of virtual work gives the requirement of equilibrium. On the other hand, if the system subjected to a set of real displacements is acted on by a set of equilibrating virtual forces, the principle of virtual work leads to the requirements of compatibility. To stress the dual nature of the principle, the former is referred to as the *principle of virtual displacements* whereas the latter is called the *principle of virtual forces.*

The requirements of equilibrium and compatibility of a structural system derived from the energy approach are identical to those obtained from the equilibrium approach. The conditions of equilibrium and compatibility based on the equilibrium approach have been discussed in Sections 2-2 and 2-7, respectively. Similarly, in the application of the principle of virtual work, the only requirements imposed on the system are that the forces acting on the system must be in equilibrium and that the displacements must be compatible with the constraints. The forces and displacements need not be related causes and effects, and either set of quantities can be real while the other set remains virtual.

Consider, for example, a deformable system that in general is nonlinearly elastic and may be conceived of schematically as consisting of n elements. If the system is given an infinitesimal variation of displacements compatible with the constraints, i.e., if the system is given a set of virtual dis-

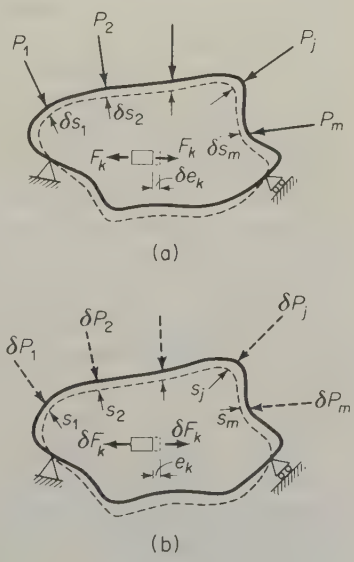

Figure 8-11

placements in the directions of the respective real forces as shown in Fig. 8-11(a), the increment of strain energy is equal to the sum of the products of the real forces and the respective virtual displacements, or

$$\delta U_i = \sum_{k=1}^{n} F_k \, \delta e_k \tag{8-21a}$$

Note that the external loads are on the structure and the real displacements under the action of these external forces have already taken place when the set of virtual displacements is introduced. Hence, the real force F_k and the virtual displacement δe_k ($k = 1, 2, \ldots, n$) need not be cause and effect. The set of virtual displacements is entirely independent of the real displacements of the structure. The corresponding increment of external work on the structure is equal to

$$\delta W_e = \sum_{j=1}^{m} P_j \, \delta s_j \tag{8-21b}$$

According to the principle of conservation of energy, the variation of the total work must be zero, i.e., $\delta W_e + \delta W_i = 0$. Hence, $\delta W_e = \delta U_i$, or

$$\sum_{j=1}^{m} P_j \, \delta s_j = \sum_{k=1}^{n} F_k \, \delta e_k \tag{8-21c}$$

Since the displacements δs_j and δe_k imposed on the system need not be real, they are called *virtual displacements*. As a matter of fact, they may be finite as well as infinitesimal as long as they do not cause a significant change in the geometry of the system. Thus, Eq. (8-21c) may be replaced by

$$\sum_{j=1}^{m} P_j s_j = \sum_{k=1}^{n} F_k e_k \tag{8-21d}$$

Equation (8-21c) or (8-21d) represents the requirement of equilibrium that must be imposed on a system when it is given a set of virtual displacements.

If a structure subjected to a set of real displacements is given an infinitesimal variation of forces, i.e., if the system is subjected to a set of equilibrating virtual forces acting in the directions of the respective real displacements as shown in Fig. 8-11(b), the increment of complementary energy is equal to the sum of the products of the real displacements and the respective virtual forces, or

$$\delta U_c = \sum_{k=1}^{n} e_k \, \delta F_k \tag{8-22a}$$

The real displacements, which may be caused by discrepancy in manufacture, temperature changes, or actual forces, are applied to the structure after the set of virtual forces is introduced. Hence, the real displacement e_k and the virtual force δF_k ($k = 1, 2, \ldots, n$) need not be cause and effect.

The set of virtual forces is completely independent of the real forces even if the real displacements in the structure are caused by real forces. The corresponding increment of complementary external work is equal to

$$\delta C_e = \sum_{j=1}^{m} s_j \, \delta P_j \tag{8-22b}$$

By equating δC_e and δU_c, we have

$$\sum_{j=1}^{m} s_j \, \delta P_j = \sum_{k=1}^{n} e_k \, \delta F_k \tag{8-22c}$$

Since the forces δP_j and δF_k imposed on the system need not be real, they are called *virtual forces*. Indeed, they may be finite as well as infinitesimal as long as they are self-equilibrating. Thus, Eq. (8-22c) may be replaced by

$$\sum_{j=1}^{m} s_j P_j = \sum_{k=1}^{n} e_k F_k \tag{8-22d}$$

Equation (8-22c) or (8-22d) represents the requirement of compatibility that must be imposed on a system when it is subjected to a set of virtual forces.

It may be observed that Eqs. (8-21d) and (8-22d) are identical although they have been derived in two different ways. In view of this, we may give a unified definition for the *principle of virtual work* as follows: if a structure is in equilibrium under the action of a set of external forces and is subjected to a set of displacements compatible with the constraints of the structure, the total work done by the external and internal forces during the displacement must be zero. We should point out again that in this statement the set of forces need not be related to the set of displacements as cause and effect and that either set can be real while the other set is virtual. Since the principle of virtual displacements imposes the requirement of equilibrium, it is usually applied to evaluate certain specified forces. On the other hand, the principle of virtual forces imposes the requirement of compatibility, and it is often used to compute certain specified displacements. For more general applications of these principles to structural analysis, the student is referred to several publications on this subject.*

One important application of the principle of virtual work is found in the computation of deflections of statically determinate structures. A convenient method of computing deflections may be developed on the basis of a special application of the principle of virtual forces. If a single external virtual force that has a magnitude of unity is placed at a point on a structure before the structure is subjected to real displacements, the displacement of this point in the direction of the unit virtual force is equal to the sum of

*See References 8–2 through 8–4.

the products of the real displacements and the respective internal virtual forces that are in equilibrium with the unit virtual force. This method of approach is called the *method of virtual work* or the *dummy unit load method.**

Consider, for example, a virtual force $P = 1$ applied to a structure as shown in Fig. 8-12(a). The displacement of the point of application of this

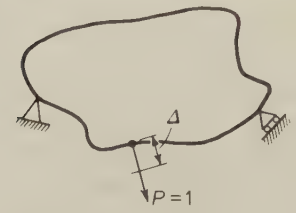

(a)

Figure 8–12

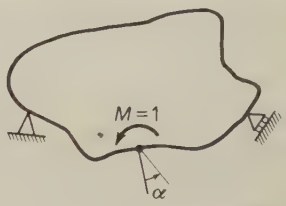

(b)

force in the direction of the force may be represented by the deflection Δ. Let f be the internal force in an element of the structure due to the virtual unit force and e be the displacement of the element in the direction of f. Then, according to the principle of virtual work, we have

$$1 \times \Delta = \sum fe \tag{8-23a}$$

in which the displacement Δ has the unit of length and the increment of strain energy on the right-hand side of the equation has the unit of force $\times$ length per unit force. Since the displacement e has the unit of length, f is expressed in terms of force per unit force and may be considered as a dimensionless coefficient.

This concept of virtual work can easily be extended to the computation of rotations. If a virtual unit moment $M = 1$ is applied to a structure as shown in Fig. 8-12(b), the rotation about a given point with respect to a given line may be defined by the angle α. Let f be the internal force in an element of the structure due to the unit moment and e be the displacement of the element in the direction of f. Then, from the principle of virtual work, we have

$$1 \times \alpha = \sum fe \tag{8-23b}$$

in which the rotation α is in radians or dimensionless, and the increment of strain energy on the right-hand side of the equation has the unit of force $\times$ length per unit moment or is dimensionless. Since the displacement e

*This method was developed independently by J. C. Maxwell in 1864 and O. Mohr in 1874, and is often called the *Maxwell-Mohr method.* Some American publications attributed the method to G. F. Swain, who first introduced the method in American literature in 1883. The versatility of this method and its relationship with other methods based on the geometry of structures have been discussed in Reference 8–5.

has the unit of length, f is expressed in terms of force per unit moment or 1/length.

This method of computing deflections is exceedingly general since the displacements e may be produced by any cause (temperature changes, misfit, or external forces). If the displacements e are caused by external forces, the material properties will be involved and the applications will be restricted to the given properties of materials.

Example 8-3. In the truss shown in Fig. 8-13(a), three members have been cut either too long or too short by a small amount as indicated by + 0.4 in., + 0.2 in., and − 0.3 in. for members L_0L_1, U_1U_2, and U_0U_1, respectively, in the figure. Compute the vertical displacement of joint L_2 due to these discrepancies in the lengths of the members.

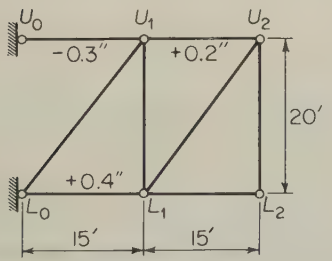

(a)

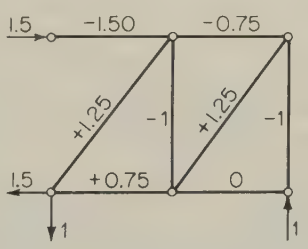

(b)

Figure 8-13

Since the vertical displacement of joint L_2 is desired, we apply a vertical unit load at that joint. The upward direction is arbitrarily assumed because an upward deflection is anticipated. A positive result will indicate that the assumed sense is correct, and a negative result will indicate a downward deflection.

The internal forces in all members of the truss due to an upward unit load at joint L_2 are solved for and indicated along the members in Fig. 8-13(b). Since the discrepancy in length occurs in members L_0L_1, U_1U_2, and U_0U_1, the change in length in other members is regarded as zero. Thus, only the internal forces in these members are required in order to compute the deflection. The vertical deflection of joint L_2 is then given by

$$\Delta = \sum fe = (-1.50)(-0.3) + (-0.75)(+0.2) + (0.75)(+0.4)$$
$$= +0.45 - 0.15 + 0.30 = 0.60 \text{ in.}$$

Since the result is positive, the deflection is directed upward as assumed.

Example 8-4. The steel bar shown in Fig. 8-14 has a 10 in. by 20 in. rectangular cross section. The top surface of the bar is maintained at a

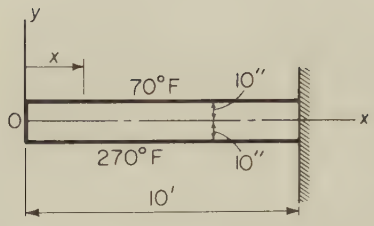

Figure 8–14

room temperature of 70°F. while the bottom surface is kept constant at a temperature of 270°F. Assuming linear distribution of temperature through the depth of the beam, determine the vertical displacement of point O at the free end of the beam. The coefficient of linear expansion of steel $\alpha = 0.6 \times 10^{-6}/°\text{F}$.

The bar is subjected to axial expansion as well as bending as a result of the temperature difference between the top and bottom surfaces. However, the contribution of axial expansion to the vertical deflection is small and negligible. Therefore, only the effect of bending need be considered.

Assuming linear distribution of temperature, the strain at any fiber at a distance y from the neutral axis is given by

$$\epsilon = -(0.6 \times 10^{-6})(270 - 70)y/20 = -0.6 \times 10^{-5}y$$

Thus, the strain is negative for a positive y. Then, the displacement in the same fiber of an element of δx in length is equal to

$$e = \epsilon\, \delta x = -0.6 \times 10^{-5} y\, \delta x$$

If a vertical upward virtual force is applied at point O in Fig. 8-14, the moment at a section at a distance x from O is $m = x$ and the internal force acting in a fiber of area δA at a distance y from the neutral axis is equal to the stress multiplied by the area, or

$$f = -\frac{my}{I}\,\delta A = -\frac{xy}{I}\,\delta A$$

Then, the vertical deflection at point O may be obtained by integrating over the entire volume V of the bar, i.e.,

$$\Delta = \sum fe = \int\int\int_V \left(-\frac{my}{I}\right)(-0.6 \times 10^{-5}y)\, dA\, dx$$

$$= \int_0^L \frac{0.6 \times 10^{-5}x}{I}\left[\int\int_A y^2\, dA\right] dx$$

$$= \int_0^{120} 0.6 \times 10^{-5}\, x\, dx = 0.3 \times 10^{-5}\, x^2\Big|_0^{120} = 0.0432 \text{ in.}$$

Note that the length of the bar $L = 10$ ft $= 120$ in. The unit of inches must be used in the evaluation of the integral because the depth of the beam has been expressed in terms of inches in the computation of strain used in formulating the integral.

8-7 *Method of Virtual Work for Linear Elastic Systems*

Although no restriction has been placed on the nature of the internal deformations of the structure in the derivation of the method of virtual work, external loads are by far the most common cause of these deformations in actual application. We shall, therefore, develop a procedure for special applications to common structural systems with linearly elastic characteristics.

Consider, for example, an elastic system acted on by a set of external forces $Q_1, Q_2, \ldots, Q_r$ as shown in Fig. 8-15. Prior to the application of these forces, however, let a virtual unit force $P = 1$ be placed at a given point and in a given direction for which the deflection is desired. As the set of external forces is gradually applied to the elastic system increasing from zero to full value and thus causing deformations in the structure, the virtual unit force simply rides along during the deformation. Let the displacements at the points of application of the external forces in the directions of the respective forces be denoted by $\Delta_1, \Delta_2, \ldots, \Delta_r$ respectively. Then, the external work done on the system from the gradual application of the external forces must equal the increment of strain energy as follows:

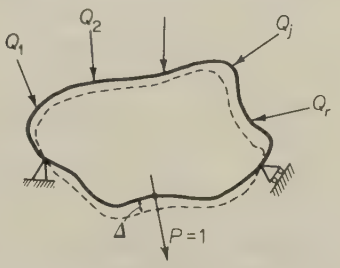

Figure 8–15

$$\tfrac{1}{2}\sum_{j=1}^{r} Q_j\Delta_j + 1 \times \Delta = \tfrac{1}{2}\sum Fe + \sum fe \qquad \text{(a)}$$

in which F is the internal force in an element of the structure and e is the corresponding deformation caused by the internal force whereas f is the internal force in the same element due to the virtual unit load. Note that the real work terms include a factor of $\frac{1}{2}$ whereas those representing virtual work do not have such a factor because the virtual unit force $P = 1$ is already on the structure when the external forces are gradually applied. Considering only the real forces, we obtain from the conservation of energy the following relation:

$$\tfrac{1}{2}\sum_{j=1}^{r} Q_j\Delta_j = \tfrac{1}{2}\sum Fe \qquad \text{(b)}$$

The virtual work done by the virtual unit force may be obtained by subtracting Eq. (b) from Eq. (a). Thus,

$$1 \times \Delta = \sum fe \qquad \text{(c)}$$

Equation (c) is identical to Eq. (8-23a) except that e is now restricted to deformations caused by external forces.

We have already established the force-deformation relations for various types of structural elements. Hence, Eq. (c) can be replaced by the direct relations developed for these structures. Wherever applicable, the notations in Section 8-3 are retained.

1. *Trusses.* In the case of a plane truss, all members are subjected to bar forces only. Hence, for a truss consisting of n members, we have

$$1 \times \Delta = \sum fe = \sum_{k=1}^{n} \frac{f_k F_k L_k}{A_k E_k} \tag{8-24a}$$

in which f_k is the bar force in a member caused by a virtual unit load and F_k is the bar force in the same member due to the external forces.

2. *Beams subject to bending.* Consider an element of a beam that has a length of δx and an area of δA. Let m be the bending moment at a section of the element caused by a virtual unit load and M be the moment at the same section due to the external forces. Then,

$$f = -\frac{my}{I}\delta A \quad \text{and} \quad e = \epsilon\,\delta x = \frac{\sigma}{E}\delta x = -\frac{My}{EI}\delta x$$

Integrating over the entire volume V of the beam, we obtain

$$1 \times \Delta = \int\int\int_V \left(-\frac{my}{I}\right)\left(-\frac{My}{EI}\right) dA\,dx$$

$$= \int_L \frac{mM dx}{EI} \tag{8-24b}$$

3. *Beams subject to shear.* In the case of a beam element subjected to shear deflection only, we may denote the shear at a section caused by a virtual unit load as s and the shear at the same section resulting from the external forces as S. By considering the average stress at a section, we obtain

$$f = k\frac{s}{A}\,\delta A \quad \text{and} \quad e = k\frac{S}{GA}\,\delta x$$

By using the same simplification in Eq. (8-16), we get

$$1 \times \Delta = \int\int\int_V k^2 \frac{sS}{GA^2}\,dA\,dx = C\int_L \frac{sS\,dx}{GA} \tag{8-24c}$$

in which C is the form factor, usually taken as 1.2 for rectangular beams and I-beams.

4. *Circular members subject to torsion.* Consider an element of a circular member subjected to torsion that has a length of δx and an area of δA. Let t be the torque at a section of the element caused by the virtual unit load and T the torque at the same section resulting from the external forces.

Then,

$$f = \frac{tr}{J}\delta A \quad \text{and} \quad e = \gamma\,\delta x = \frac{\tau}{G}\delta x = \frac{Tr}{GJ}\delta x$$

Integrating over the entire volume V of the bar, we have

$$1 \times \Delta = \int\int\int_V \left(\frac{tr}{J}\right)\left(\frac{Tr}{GJ}\right) dA\,dx$$

$$= \int_L \frac{tT\,dx}{GJ} \tag{8-24d}$$

If the rotations instead of deflections of a structure are desired, the internal force or moment in each of Eqs. (8-24) can be obtained by applying a unit couple about a point in a given direction instead of a unit load. Then, the deflection Δ may be replaced by the rotation in these equations.

Example 8-5. For the truss shown in Fig. 8-16, compute the vertical deflection at point L_2. The areas of the members in square inches are indicated along the members in parentheses in the figure. $E = 30 \times 10^3$ ksi.

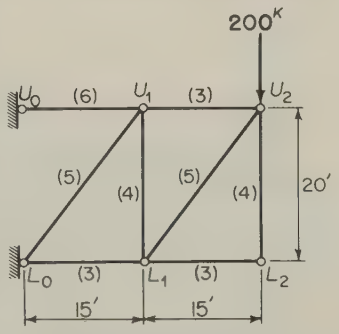

Figure 8–16

The calculation is tabulated in Table 8-1, in which the column f represents the bar forces in all members caused by a virtual unit load acting upward at joint L_2, the column F gives the bar forces in all members resulting from the external load of 200 kips at joint U_2. The other columns in the table are self-explanatory. The final result is obtained from the sum of all values in the column fe. The negative sign indicates that the assumed upward direction is incorrect and that the deflection should be downward.

TABLE 8-1

Member	f	F (kips)	L (in.)	A (in.^{2})	$e = FL/AE$ (in.)	fe (in.)
U_0U_1	− 1.50	+ 300	180	6	+ 0.30	− 0.45
U_1U_2	− 0.75	+ 150	180	3	+ 0.30	− 0.225
L_0L_1	+ 0.75	− 150	180	3	− 0.30	− 0.225
L_1L_2	0	0	180	3	0	0
L_0U_1	+ 1.25	− 250	300	5	− 0.50	− 0.625
L_1U_1	− 1.00	+ 200	240	4	+ 0.40	− 0.40
L_1U_2	+ 1.25	− 250	300	5	− 0.50	− 0.625
L_2U_2	− 1.00	0	240	4	0	0
					$\Delta =$	−2.55

Example 8-6. Compute the deflection and rotation at the free end of the cantilever beam in Fig. 8-17(a). The bending stiffness EI of the beam is constant.

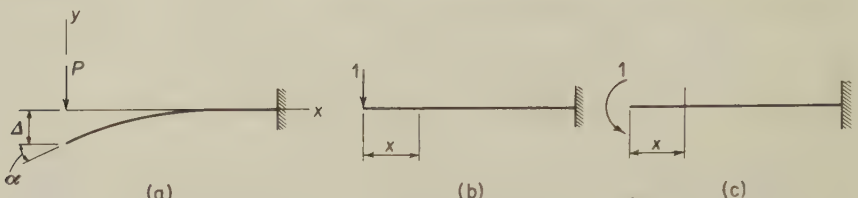

Figure 8–17

In computing the deflection Δ, we apply a downward unit load at the free end as shown in Fig. 8-17(b). At any section of the beam, we have

$$M = -Px \quad \text{and} \quad m = -x$$

Hence,

$$\Delta = \int_0^L \frac{(-Px)(-x)\,dx}{EI} = \frac{Px^3}{3EI}\bigg|_0^L = \frac{PL^3}{3EI}$$

For the computation of the rotation α, we apply a counterclockwise unit moment at the free end as shown in Fig. 8-17(c). Then, at any section, $m = -1$ while M remains the same. Hence,

$$\alpha = \int_0^L \frac{(-Px)(-1)\,dx}{EI} = \frac{Px^2}{2EI}\bigg|_0^L = \frac{PL^2}{2EI}$$

8-8 *Castigliano's Theorems*

In Section 8-3 the strain energy for various forms of linear elastic systems was expressed as a function of either the internal forces or deformations. These forces and deformations can in turn be expressed as a function of the external forces or displacements from the conditions of equilibrium and compatibility. Thus, the strain energy function may be used to derive the external forces or the displacements of their points of application. This application of the strain energy of linear elastic systems was first observed by Castigliano, who called it the *theorem of the differential coefficients of the internal work*. He stated the theorem as follows:*

Part 1. If the internal work of a framed structure is expressed as a function of the relative displacements of the external forces applied at its

*This theorem has been stated verbatim according to the translation of Castigliano's original work on p. 15 of Reference 8-6 in order to preserve the generality of his theorem.

nodes, the resulting expression is such that its differential coefficients with regard to these displacements give the values of the corresponding forces.

Part 2. If, on the contrary, the internal work of a framed structure is expressed as a function of the external forces, the resulting expression is such that its differential coefficients give the relative displacements of their points of application.

For the sake of clarity, we shall henceforth refer to part 1 of the theorem as *Castigliano's first theorem* and part 2 as *Castigliano's second theorem.* The "differential coefficients" in the statement of the theorems are the partial derivatives in Eqs. (8-18) and (8-20). We should point out again that the first theorem is applicable to all conservative systems whereas the second theorem is applicable only to linear elastic systems.

Parallel to the principle of virtual work, the first theorem imposes the requirement of equilibrium while the second theorem expresses the requirement of compatibility. With the traditional emphasis on the force method of analysis, the first theorem has been almost forgotten, but the second theorem has been used extensively for the computation of deflections of statically determinate structures and for the requirement of compatibility for statically indeterminate structures.*

Actually, Castigliano's theorems may generally be used in the analysis of statically indeterminate structures, examples of which will be given in later sections. The second theorem may also be used for computing the deflections of statically determinate structures, although any problem that can be solved by this method can also be solved by the dummy unit load method. Nevertheless, we shall illustrate the application of Castigliano's second theorem to the computation of deflections.

Let Δ_j denote the deflection at a given point along a given direction in which a force P_j acts. Then, the strain energy relations for linear elastic systems may be obtained from Sections 8-3 and 8-4 and the corresponding deflections computed as follows:

1. *Trusses*:

$$U_i = \frac{1}{2} \sum_{k=1}^{n} \frac{F_k^2 L_k}{A_k E_k}$$

Hence,

$$\Delta_j = \frac{\partial U_i}{\partial P} = \sum_{k=1}^{n} \frac{F_k L_k}{A_k E_k} \frac{\partial F_k}{\partial P} \tag{8-25a}$$

*A case in point is that in all but the most recent publications, part 1 of the original theorem does not appear at all. Part 2 appears in two forms: when applied to statically determinate structures, it is called "Castigliano's first theorem", and when applied to statically indeterminate structures, it is called "Castigliano's second theorem". This truncation of Castigliano's theorems of internal work is not followed in this text.

2. *Beams subject to bending*:

$$U_i = \int_L \frac{M^2\,dx}{2EI}$$

Hence,

$$\Delta_j = \int_L \frac{M\,dx}{EI}\frac{\partial M}{\partial P_j} \tag{8-25b}$$

3. *Beams subject to shear*:

$$U_i = C\int_L \frac{S^2\,dx}{2GA}$$

Hence,

$$\Delta_j = C\int_L \frac{S\,dx}{GA}\frac{\partial S}{\partial P_j} \tag{8-25c}$$

4. *Circular members subject to torsion*:

$$U_i = \int_L \frac{T^2\,dx}{2GJ}$$

Hence,

$$\Delta_j = \int_L \frac{T\,dx}{GJ}\frac{\partial T}{\partial P_j} \tag{8-25d}$$

The similarity between this method and the dummy unit load method is striking. It may be demonstrated later that indeed $\partial F_k/\partial P_j = f$, $\partial M/\partial P = m$, and so on. We can take advantage of this similarity and extend the usefulness of Castigliano's second theorem. If we desire to determine the deflection at a point in a given direction for which no load is acting, it is possible to assume an arbitrary load at the given point in the given direction and include its effect in the strain energy and its partial derivative. The arbitrary load may then be set equal to zero in evaluating the summation or integration in Eqs. (8-25). This is equivalent to the introduction of a dummy unit load at that point in the given direction. Furthermore, Eqs. (8-25) may be used to compute the angular rotation at a point of a structure with respect to a given line if an arbitrary moment instead of a force is applied at the desired location.

In order to demonstrate the equivalence of this method and the dummy unit load method, let us consider as an example a truss subjected to a set of loads $P_1, P_2, \ldots, P_n$. Let the bar force in a member k caused by the external loads be denoted by F_k, and the bar force in the same member due to all loads except P_j be denoted by $\bar{F}_k$. If $P_j = 1$ is applied to the truss while all other external loads are removed, the resulting bar force in member k

may be denoted by f_k. The bar force in member k due to the load P_j is therefore equal to $f_k P_j$. Thus,

$$F_k = \bar{F}_k + f_k P_j$$

Since $\bar{F}_k$ is independent of P_j, we obtain from the differentiation of F_k with respect to P_j

$$\frac{\partial F_k}{\partial P_j} = f_k \tag{8-26a}$$

Similarly, we may denote for other cases the moment, shear, and torque as follows:

$$M = \bar{M} + mP_j$$
$$S = \bar{S} + sP_j$$
$$T = \bar{T} + tP_j$$

in which $\bar{M}$, $\bar{S}$, and $\bar{T}$ are the corresponding portions of moment, shear, and torque independent of P_j and m, s, and t are the moment, shear, and torque due to $P_j = 1$. Then, by taking the partial derivative of the pertinent quantity with respect to P_j, we have

$$\frac{\partial M}{\partial P_j} = m \tag{8-26b}$$

$$\frac{\partial S}{\partial P_j} = s \tag{8-26c}$$

$$\frac{\partial T}{\partial P_j} = t \tag{8-26d}$$

If we compare Eqs. (8-25) and (8-26) with Eqs. (8-24), it is obvious that both methods lead to identical results.

Example 8-7. For the truss shown in Fig. 8-18(a), compute the relative displacement between joints B and D for a vertical load of 200 kips at joint G. The areas of the members in square inches are indicated along the members in parentheses in the Figure. $E = 30 \times 10^3$ ksi.

Since no external force is acting between B and D for which the relative displacement is required, a pair of equal, opposite, and collinear forces P is added to joints B and D as shown in Fig. 8-18(c). The senses of direction indicated for the forces P are arbitrarily assumed and will cause an increase in the distance between joints B and D. A positive answer for the displacement will indicate that the assumed increase is correct; otherwise a decrease in the distance is indicated. The bar forces in the truss caused by a vertical load of 200 kips at joint G alone are given in Fig. 8-18(b) and the bar forces

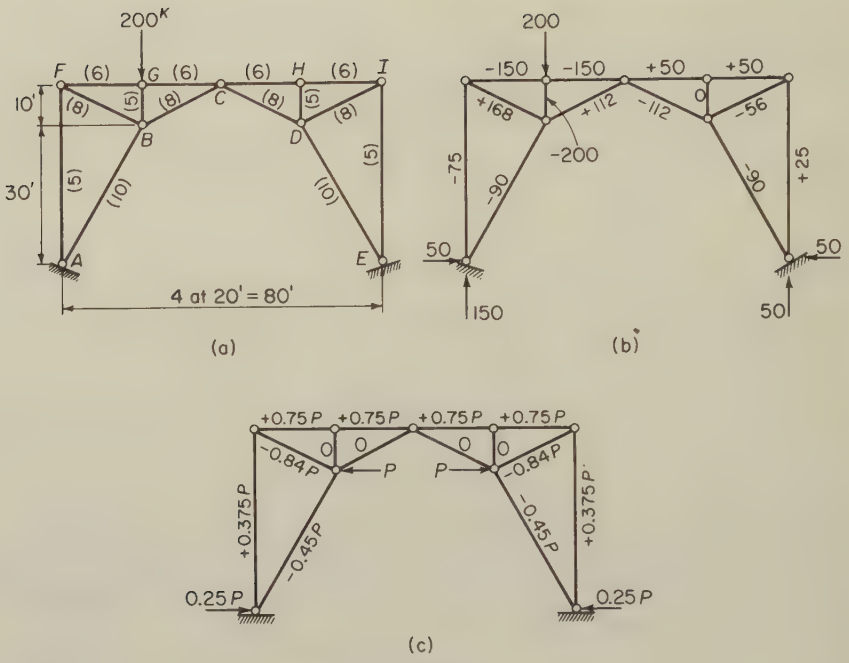

Figure 8–18

in the truss resulting from the assumed loads P are given in Fig. 8-18(c). The remaining steps of computation are shown in Table 8-2.

TABLE 8-2

Member	L (in.)	A (in.^{2})	F	$\partial F/\partial P$	FL/AE (P = 0)	$(FL/AE)(\partial F/\partial P)$ (in.)
AB	432	10	$-90 - 0.45P$	-0.45	-0.130	$+0.0585$
BC	268	8	$+112 + 0$	0	$+0.125$	0
CD	268	8	$-112 + 0$	0	-0.125	0
DE	432	10	$-90 - 0.45P$	-0.45	-0.130	$+0.0585$
FG	240	6	$-150 + 0.75P$	$+0.75$	-0.200	-0.150
GC	240	6	$-150 + 0.75P$	$+0.75$	-0.200	-0.150
CH	240	6	$+50 + 0.75P$	$+0.75$	$+0.067$	$+0.050$
HI	240	6	$+50 + 0.75P$	$+0.75$	$+0.067$	$+0.050$
AF	480	5	$-75 + 0.375P$	$+0.375$	-0.240	-0.090
BG	120	5	$-200 + 0$	0	-0.160	0
DH	120	5	$0 + 0$	0	0	0
EI	480	5	$+25 + 0.375P$	$+0.375$	$+0.080$	$+0.030$
BF	268	8	$+168 - 0.84P$	-0.84	$+0.188$	-0.158
DI	268	8	$-56 - 0.84P$	-0.84	-0.063	$+0.053$
					$\Delta =$	-0.248

Example 8-8. A cantilever girder made of a circular tube has a 90-deg. bend in the horizontal xy-plane as shown in Fig. 8-19. A vertical load P in line with the z-axis (normal to the xy-plane) is applied at the free end A of the girder. Determine the vertical deflection of point A assuming that the bending stiffness EI and torsional stiffness GJ of the tube are constant.

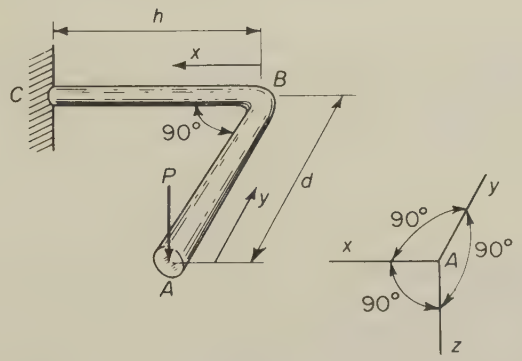

Figure 8-19

For segment AB of the girder, the moment at a section that is at a distance y from point A is given by

$$M = -Py \quad \text{and} \quad \partial M/\partial P = -y$$

The segment BC is subjected to torsion as well as bending. At a section that is at a distance x from point B, we have

$$M = -Px \quad \text{and} \quad \partial M/\partial P = -x$$

$$T = Pd \quad \text{and} \quad \partial T/\partial P = d$$

Hence,

$$\Delta = \int_0^d \frac{(-Py)(-y)\,dy}{EI} + \int_0^h \frac{(-Px)(-x)\,dx}{EI} + \int_0^h \frac{(Pd)(d)\,dx}{GJ}$$

$$= \frac{Py^3}{3EI}\bigg|_0^d + \frac{Px^3}{3EI}\bigg|_0^h + \frac{Pd^2x}{GJ}\bigg|_0^h$$

$$= \frac{P(d^3 + h^3)}{3EI} + \frac{Pd^2h}{GJ}$$

8-9 *Deflections of Nonlinear Elastic Systems*

The deflections of nonlinear elastic systems may be computed by means of the dummy unit load method or the complementary energy method. Since the latter is a special case of the former when forces and displacements in a

system are causes and effects, any problem that can be solved by the complementary energy method can also be solved by the dummy unit load method. The complementary energy of a system such as the one shown in Fig. 8-1 is given by

$$U_c = \sum_{k=1}^{n} \int e_k dF_k$$

in which e_k is the deformation of an element k and F_k is the internal force in the same element caused by the external loads. By means of the complementary energy method, the deflection at point j in the direction of the force P_j is given by Eq. (8-25) as follows:

$$\Delta_j = \frac{\partial U_c}{\partial P_j} = \sum_{k=1}^{n} e_k \frac{\partial F_k}{\partial P_j} \tag{8-27}$$

To demonstrate the equivalence of the complementary energy method and the dummy unit load method, let $\bar{F}_k$ be the internal force in an element k caused by all loads except P_j. If $P_j = 1$ is applied to the system while all other external loads are removed, the resulting internal force in the element k may be denoted by f_k. The internal force in an element k due to the load P_j is therefore equal to $f_k P_j$. Thus,

$$F_k = \bar{F}_k + f_k P_j$$

Since $\bar{F}_k$ is independent of P_j, we obtain from the differentiation of F_k with respect to P_j

$$\frac{\partial F_k}{\partial P_j} = f_k \tag{a}$$

By substituting Eq. (a) into Eq. (8-27), we obtain

$$\Delta_j = \sum_{k=1}^{n} e_k f_k$$

This is identical to Eq. (8-23a) which was obtained by the principle of virtual work.

The difficulty in the solution of a nonlinear elastic system lies in the fact that the stress-strain curve of the material may be complicated and cannot be expressed by a simple equation. In some cases, the relation between stress σ and strain ϵ may be represented by a parabolic curve

$$\sigma = C\epsilon^{1/n} \tag{b}$$

in which C and n are constants. However, even in a simple case like this, we should be aware of the additional complications that do not exist in linear elastic systems. For example, if Eq. (b) is expressed in the following

form

$$\epsilon = \frac{\sigma^n}{C^n} \tag{c}$$

and if n is even, Eq. (c) implies that ϵ is positive regardless of the sign of σ, and this is physically impossible. Therefore, the right-hand side of Eq. (c) must be preceded by a positive sign for $+\sigma$ and a negative sign for $-\sigma$.

Example 8-9. For the nonlinear elastic system shown in Fig. 8-20(a), determine the horizontal and vertical components of displacement of joint 0 if the stress-strain relation of the material for the members is given by the parabolic curve $\sigma = 1{,}000\sqrt{\epsilon}$ ksi. The cross-sectional area of each member is 5 in.^{2}, and the load $P = 100$ kips.

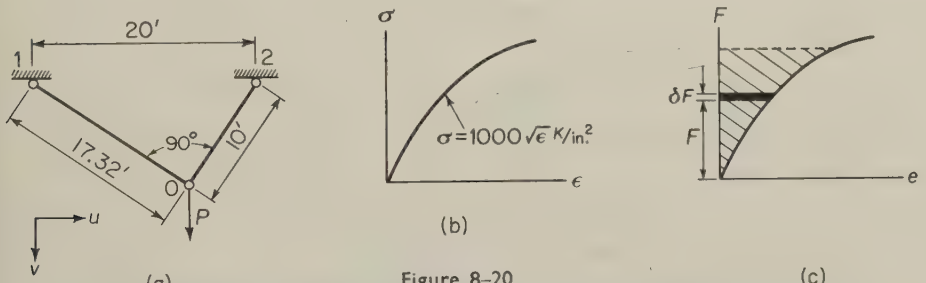

(a) (b) (c)

Figure 8–20

Let the horizontal and vertical components of displacement of joint 0 be denoted by u and v with positive directions indicated in the figure. Let F be the bar force in a member and e be the elongation in that member whose length and cross-sectional area are denoted by L and A respectively. Then, from the given stress-strain curve $\sigma = 1{,}000\sqrt{\epsilon}$ ksi, shown in Fig. 8-20(b), we have

$$\epsilon = 10^{-6}\sigma^2$$

The force-deformation relation may be represented by the curve in Fig. 8-20(c), which is given by

$$e = \epsilon L = 10^{-6}\sigma^2 L = 10^{-6}\left(\frac{F}{A}\right)^2 L = \frac{10^{-6}L}{A_2}F^2$$

Let the quantities pertaining to members 01 and 02 be denoted by subscripts 1 and 2, respectively. Assuming that the bar forces F_1 and F_2 are in tension, then from the conditions of equilibrium of joint 0 we obtain

$$\sum F_x = 0, \quad F_1 \cos 30^\circ = F_2 \cos 60^\circ$$
$$\sum F_y = 0, \quad F_1 \sin 30^\circ + F_2 \sin 60^\circ = P$$

Thus, $F_1 = 0.5P$ and $F_2 = 0.866P$. The elongations of the members can be

obtained from the force-deformation relation as follows:

$$e_1 = \frac{(10^{-6})(17.32)(12)}{5^2} F_1^2 = 8.32 \times 10^{-6} F_1^2 = 2.08 \times 10^{-6} P^2$$

$$e_2 = \frac{(10^{-6})(10)(12)}{5^2} F_2^2 = 4.8 \times 10^{-6} F_2^2 = 3.6 \times 10^{-6} P^2$$

By using Eq. (8-27), we obtain

$$v = e_1 \frac{\partial F_1}{\partial P} + e_2 \frac{\partial F_2}{\partial P} = (2.08 \times 10^{-6} P^2)(0.5) + (3.6 \times 10^{-6} P^2)(0.866)$$

$$= 1.04 \times 10^{-6} P^2 + 2.94 \times 10^{-6} P^2 = 3.98 \times 10^{-6} P^2$$

In order to determine the horizontal displacement u, we first assume a fictitious force Q in the positive direction of u. Then, from the equilibrium of joint 0, we get

$$F_1 = 0.5P + 0.866Q, \qquad F_2 = 0.866P - 0.5Q$$

Thus, by taking the partial derivatives of F_1 and F_2 with respect to Q, we have

$$\frac{\partial F_1}{\partial Q} = 0.866 \quad \text{and} \quad \frac{\partial F_2}{\partial Q} = -0.5$$

We can now evaluate e_1 and e_2 by letting $Q = 0$ in F_1 and F_2. Thus, e_1 and e_2 are identical to the respective values obtained previously when P alone is acting. Then,

$$u = e_1 \frac{\partial F_1}{\partial Q} + e_2 \frac{\partial F_2}{\partial Q} = (2.4 \times 10^{-6} P^2)(0.866) + (3.6 \times 10^{-6} P^2)(-0.5)$$

$$= 1.80 \times 10^{-6} P^2 - 1.8 \times 10^{-6} P^2 = 0$$

Note that in the calculation of v, we must retain P as a variable until the last step, whereas in the computation of u, we can let $P = 100$ kips from the beginning. In general, if there are n loads, we consider only load P_j as a variable when the displacement s_j at the point of application of P_j in the direction of P_j is required. In this problem, $P = 100$ kips and we finally obtain

$$v = 4.14 \times 10^{-6} P^2 = 0.0414 \text{ in.}$$

$$u = 0$$

For nonlinear systems with a large number of members, the calculation can be carried out systematically in tabulated form. As an example, the computations of v and u in this problem are given in Tables 8-3 and 8-4, respectively.

TABLE 8-3

Member	F	$\frac{\partial F}{\partial P} = f$	e	$e\frac{\partial F}{\partial P} = ef$
01	$0.5P$	0.5	$2.08 \times 10^{-6}P^2$	$1.04 \times 10^{-6}P^2$
02	$0.866P$	0.866	$3.60 \times 10^{-6}P^2$	$2.94 \times 10^{-6}P^2$
			$v =$	$3.98 \times 10^{-6}P^2$

TABLE 8-4

Member	F	$\frac{\partial F}{\partial Q} = f$	e $(Q = 0)$	$e\frac{\partial F}{\partial Q} = ef$
01	$0.5P + 0.866Q$	0.866	$2.08 \times 10^{-6}P^2$	$1.80 \times 10^{-6}P^2$
02	$0.866P - 0.5Q$	-0.500	$3.6 \times 10^{-6}P^2$	$-1.80 \times 10^{-6}P^2$
			$u =$	0

8-10 *Maxwell-Betti Theorem of Reciprocal Displacements*

In the study of deflections of linear elastic structures, we may observe a very useful relation indicating the reciprocity of deflections at different locations. We shall consider as an example the deflections of a simple beam. Let δ_{ab} be the deflection at point A due to a vertical load P acting at point B, and δ_{ba} be the deflection at point B due to a vertical load P acting at point A as shown in Fig. 8-21. By the method of virtual work, we obtain

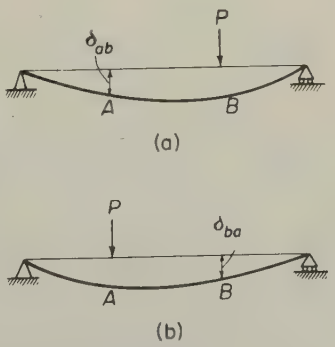

Figure 8-21

$$\delta_{ab} = \int_0^L \frac{M_b m_a \, dx}{EI}$$

$$\delta_{ba} = \int_0^L \frac{M_a m_b \, dx}{EI}$$

in which M_a and M_b are the moments at a section of the beam due to the vertical force P acting at points A and B respectively, and m_a and m_b are the moments at the same section due to a downward unit load acting at points A and B respectively. Since moments in a beam are linear functions of

external loads, we note that $M_b = Pm_b$ and $M_a = Pm_a$. Hence,

$$\delta_{ab} = \int_0^L \frac{Pm_a m_b \, dx}{EI} = \delta_{ba}$$

It should be noted that this relation is not confined to the vertical deflections of beams. Let us consider a more general case such as the linear elastic system in Fig. 8-22. If the direction of rotation of the moment M

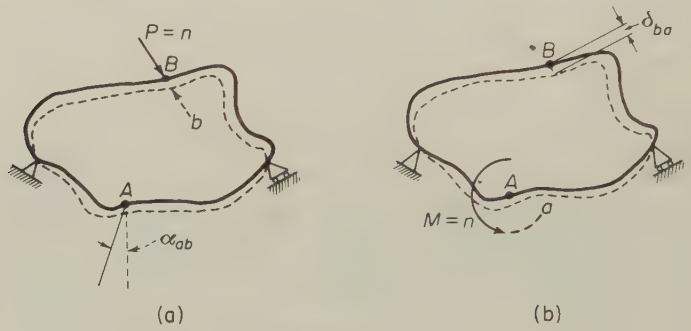

Figure 8–22

in Fig. 8-22(b) and the direction of the force P in Fig. 8-22(a) are defined as the a and b directions respectively, a force $P = n$ kips acting alone at B will cause a rotation α_{ab} at point A in the a direction, whereas a moment $M = n$ ft-kips acting alone at A will cause a deflection δ_{ba} at point B in the b direction. Then, from the method of virtual work, we have

$$1 \times \alpha_{ab} = \sum f_a e_b \quad \text{and} \quad 1 \times \delta_{ba} = \sum f_b e_a$$

where f_a = the internal force in an element due to a fictitious unit moment at point A in the a direction,

e_b = the displacement of the element in the direction of f_a due to an external force $P = n$ acting at point B in the b direction,

f_b = the internal force in an element due to a fictitious unit load at point A in the b direction,

e_a = the displacement of the element in the direction of f_b due to an external force $M = n$ acting at point A in the a direction.

Note that e_a and e_b can be expressed in terms of f_a and f_b since the internal forces and moments are linear functions of external force and moments and the displacements and rotations are linear functions of internal forces and moments. Consider, for example, a truss in which all members are subjected to axial forces only. Then,

$$1 \times \alpha_{ab} = \sum f_a e_b = \sum f_a \frac{nf_b L}{AE}$$

$$1 \times \delta_{ba} = \sum f_b e_a = \sum f_b \frac{nf_a L}{AE}$$

The units in these expressions should be carried out consistently. In the expression $1 \times \alpha_{ab}$, the unit moment has the unit of force $\times$ length and the rotation is a dimensionless quantity; whereas in the expression $1 \times \delta_{ba}$, the unit load has the unit of force and the deflection has the unit of length. If the internal forces f_a and f_b and the deformations e_a and e_b are obtained accordingly, we can equate the two expressions obtained from the principle of virtual work as follows:

$$1 \times \alpha_{ab} = 1 \times \delta_{ba}$$

Hence, we have *numerically*

$$\alpha_{ab} = \delta_{ba}$$

Another interpretation of the above equality is that for $n = 1$, α_{ab} represents the rotation at A per unit force ($P = 1$) at B, and δ_{ba} represents the deflection at B per unit moment ($M = 1$) at A. Then, the quantity on each side of the equal sign has the unit of 1/force.

In general, the reciprocal relation of displacements may be stated as follows: In a linear elastic structure, the displacement of point A in the a direction due to a load acting at a point B in the b direction is equal to the displacement of point B in the given b direction due to a load of the same magnitude acting at point A in the a direction. This is known as *Maxwell's theorem of reciprocal displacements*. The theorem is very general since the term "displacement" may refer to rotation or linear displacement and the term "load" means either moment or force.

A further generalization of the theorem has been made by Betti, and the modified form is usually called the *Maxwell-Betti theorem*.* Let two sets of forces $P_1, P_2, \ldots, P_j, \ldots, P_m$ and $P_1', P_2', \ldots, P_k', \ldots, P_n'$ act on a linear elastic system. When these two sets of forces are acting on the system separately as shown in Fig. 8-23, each set causes deformations in the system. Let

δ_{jk} = displacement of the point of application of force P_j in the direction of this force caused by the application of P_k',

δ_{kj}' = displacement of the point of application of force P_k' in the direction of this force caused by the application of P_j.

*A somewhat different proof of this theorem is given in Reference 8–7, in which the method of real work instead of the principle of virtual work is used. See p. 12 of this reference for further discussions.

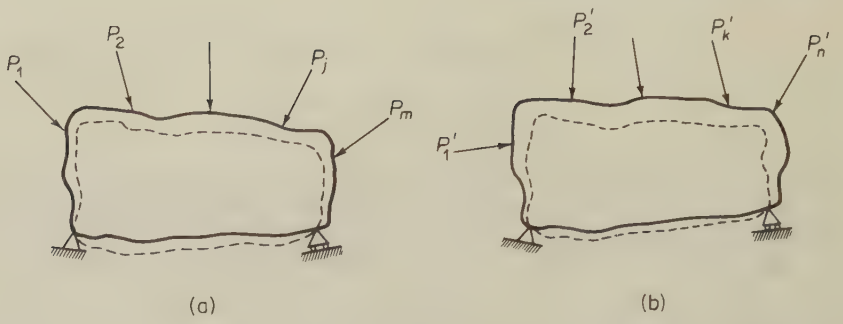

Figure 8–23

According to the principle of virtual work, δ_{jk} may be construed as being the external virtual work due to a unit load acting at the point of application of P_j in the direction of P_j as a result of the deformation caused by the application of P_k'. Then, $P_j\delta_{jk}$ = the external virtual work due to P_j as a result of the deformation caused by the application of P_k'. By summing up these terms for $k = 1, 2, \ldots, n$, we obtain the external virtual work due to P_j as a result of the deformation caused by the application of the set of loads $P_1', P_2', \ldots, P_n'$. The total external virtual work due to all loads P_1, $P_2, \ldots, P_m$ in the first set as a result of the deformation caused by the application of all loads in the second set $P_1', P_2', \ldots, P_n'$ is equal to the summation of the terms for $j = 1, 2, \ldots, m$ and $k = 1, 2, \ldots, n$. Hence,

$$W_e = \sum_{j=1}^{m} \sum_{k=1}^{n} P_j \delta_{jk}$$

Similarly, the total external virtual work due to all loads $P_1', P_2' \ldots, P_n'$ in the second set as a result of the deformation caused by the application of all loads in the first set $P_1, P_2, \ldots, P_m$ is equal to

$$W_e = \sum_{k=1}^{n} \sum_{j=1}^{m} P_k' \delta_{kj}'$$

For a linear elastic system, the order of application of the set of loads is irrelevant since the principle of superposition is valid. Hence, the total external virtual work by one set of loads due to the deformation caused by the other set is identical to the total external virtual work done by the second set of loads due to the deformation caused by the first set. That is,

$$\sum_{j=1}^{m} \sum_{k=1}^{n} P_j \delta_{jk} = \sum_{k=1}^{n} \sum_{j=1}^{m} P_k' \delta_{kj}' \tag{8-28}$$

This is the *Betti theorem* or *Maxwell-Betti theorem*, which states that in a linear elastic system, the external virtual work done by a set of forces P_m during the deformation caused by another set of forces P_n' is equal to the

external virtual work done by the set of forces P'_n during the deformation caused by the set of forces P_m.

An important special case of the theorem is obtained when each set of loads consists of the same number of loads and the lines of application of one set of loads are respectively the directions of displacements of the other set. Furthermore, if all forces of the first set except P_j and all forces of the second set except P'_k equal zero, we obtain from Eq. (8-28)

$$P_j \delta_{jk} = P'_k \delta_{kj}$$

When $P_j = P'_k = P$, the expression is reduced to *Maxwell's theorem of reciprocal displacements* as follows:

$$\delta_{jk} = \delta_{kj} \tag{8-28a}$$

Example 8-10. Determine the horizontal displacement at joint I of the truss shown in Fig. 8-24 due to a downward vertical load of 15 kips at (a) joint E and (b) joint F. The areas of the members of the truss in square inches are indicated along the members in parentheses. $E = 30 \times 10^3$ ksi.

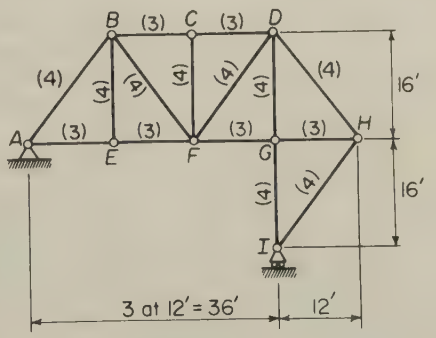

Figure 8-24

Let the horizontal displacements at joint I of the truss due to a vertical load of 15 kips at joints E and F be directed to the left and denoted by u_{ie} and u_{if} respectively. Let the downward vertical displacements at joints E and F due to a horizontal force of 15 kips acting to the left at joint I be v_{ei} and v_{fi} respectively. According to Maxwell's theorem of reciprocal displacements, we have

$$u_{ie} = v_{ei} \quad \text{and} \quad u_{if} = v_{fi}$$

We can therefore compute the deflections at two points of a truss for one position of loading instead of the deflection at one point of the truss for two different positions of loading. This usually reduces the amount of computation, especially if the deflection of one point due to a large number of positions of loading is required. In this specific example, however, the purpose is to illustrate further the application of the method of virtual work as well as Maxwell's theorem, and the possibility of saving time is not a consideration. The computation is carried out step by step in Table 8-5. Since the results for v_{ei} and v_{fi} are found to be

$$v_{ei} = -0.012 \text{ in. } (\uparrow), \quad v_{fi} = +0.0534 \text{ in. } (\downarrow)$$

we finally obtain

$$u_{ie} = -0.012 \text{ in. } (\rightarrow), \quad u_{if} = +0.534 \text{ in. } (\leftarrow)$$

Note that a positive result indicates that the assumed sense of direction is correct and a negative result indicates that it should be reversed.

TABLE 8-5

Member	15 kips horizontal at I				1 vertical at E		1 vertical at F	
	L (in.)	A (in.^{2})	F (kips)	e (in.)	f	fe (in.)	f	fe (in.)
AB	240	4	+ 8.33	+0.0167	−0.833	−0.014	−0.417	−0.0078
BC	144	3	+10.00	+0.0160	−0.250	−0.004	−0.500	+0.0080
CD	144	3	+10.00	+0.0160	−0.250	−0.004	−0.500	+0.0080
DH	240	4	+25.00	+0.0500	0	0	0	0
GH	144	3	−30.00	−0.048	0	0	0	0
FG	144	3	−30.00	−0.048	0	0	0	0
EF	144	3	−20.00	−0.032	+0.500	−0.016	+0.250	−0.0080
AE	144	3	−20.00	−0.032	+0.500	−0.016	+0.250	−0.0080
BE	192	4	0	0	+1.000	0	0	0
BF	240	4	− 8.33	−0.0167	−0.417	+0.007	+0.417	−0.0078
CF	192	4	0	0	0	0	0	0
DF	240	4	+ 8.33	+0.0167	+0.417	+0.007	+0.833	+0.0156
HI	240	4	+25.00	+0.0500	0	0	0	0
DG	192	4	−26.67	−0.0427	−0.333	+0.014	−0.667	+0.0267
GI	192	4	−26.67	−0.0427	−0.333	+0.014	−0.667	+0.0267
					$v_{ei} =$	−0.012	$v_{fi} =$	+0.0534

8-11 *Influence Lines for Deflections*

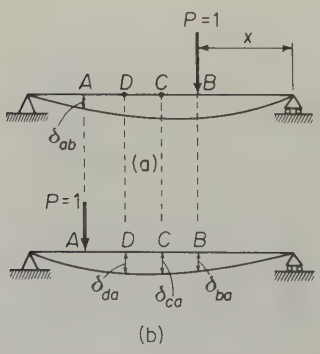

Figure 8–25

Maxwell's theorem of reciprocal displacements can readily be applied to the construction of influence lines for deflections. If, for example, we want to find the influence line for the deflection at point A of the beam shown in Fig. 8-25(a), we move a unit load $P = 1$ across the beam. For a specific location of the unit load, say point B at a distance x from the right support, the deflection δ_{ab} at point A due to a unit load at point B is equal to the deflection δ_{ba} at point B due to a unit load at point A, according to the theorem of reciprocal deflections. When

we move the unit load to the left successively to points C and D, we note $\delta_{ac} = \delta_{ca}$ and $\delta_{ad} = \delta_{da}$. Hence, the deflection curve of the beam due to a unit load at A as shown in Fig. 8-25(b) is the influence line for the deflection at point A of the beam.

The same principle of constructing influence lines for deflections may also be applied to trusses. It should be noted, however, that the influence lines for deflections of beams are smooth curves whereas those for the deflections of trusses consist of broken lines since the unit load can be applied only at the joints of the trusses. Because the influence ordinates for deflections are not linear functions of the distance x, the construction of such influence lines by the direct method of placing a unit load at various points in the structure is much more complicated than it was for influence lines for reactions, shears, or moments of statically determinate structures. Thus, Maxwell's theorem is a great help in constructing influence lines for deflections.

Example 8-11. Construct the influence line for the horizontal displacement at joint I for the truss shown in Example 8-10 due to a vertical unit load moving from point H to point A of the structure.

TABLE 8-6

Member	e (in.)	1 vertical at G		1 vertical at H	
		f	fe (in.)	f	fe (in.)
AB	+ 0.00111	0	0	+ 0.417	+ 0.000463
BC	+ 0.00107	0	0	+ 0.500	+ 0.000535
CD	+ 0.00107	0	0	+ 0.500	+ 0.000535
DH	+ 0.00333	0	0	+ 1.250	+ 0.00417
GH	− 0.00320	0	0	− 0.75	+ 0.00240
FG	− 0.00320	0	0	− 0.75	+ 0.00240
EF	− 0.00213	0	0	− 0.25	+ 0.000535
AE	− 0.00213	0	0	− 0.25	+ 0.000535
BE	0	0	0	0	0
BF	− 0.00111	0	0	− 0.417	+ 0.000463
CF	0	0	0	0	0
DF	+ 0.00111	0	0	+ 0.417	+ 0.000463
HI	− 0.00333	0	0	0	0
DG	− 0.00283	0	0	− 1.333	+ 0.00377
GI	− 0.00283	−1	+ 0.00283	− 1.333	+ 0.00377
		$u_{ig} = +0.00283$		$u_{ih} = +0.00950$	

Let the positive direction of the horizontal displacement u_i at joint I of the structure be directed to the left. We place a vertical unit load successively at the panel points H, G, F, E, and A. Since the horizontal displacement at I is zero when a unit load is at joint A, and the horizontal displacements at I due to a unit load at joints E and F may be obtained from Example 8-10 by proportion, we need to consider only the horizontal displacements at I due to a unit load at joints G and H. The computation is carried out in Table 8-6, in which the column e has also been obtained from Example 8-10 by proportion (reduced by a factor of $\frac{1}{15}$). Finally, the influence line for u_i is plotted in Fig. 8-26.

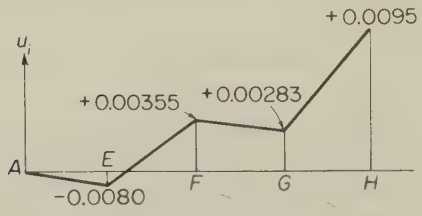

Figure 8–26

8-12 *Analysis of Redundant Structures*

In order to illustrate the broad field of application of the energy principles to redundant structures, we shall first briefly discuss the basic concept of the analysis of redundant structures. In general, we can formulate the equations of equilibrium of forces by the principles of statics and the equations of compatibility of displacements from the geometry of the structure. The equations of compatibility may be combined with material properties so that the stress-strain relation need not be given separately. Then, we can express either the displacements in terms of the forces or the forces in terms of the displacements, obtaining a set of simultaneous equations. The former is called the *force method*, the latter the *displacement method* of analysis.

In a different approach the equations of equilibrium and compatibility may be obtained from the energy principles. The principle of virtual work may be used to derive such equations for any system that in general may be nonlinearly elastic and that may involve self-straining. For the special case of linear elasticity, Castigliano's theorems may be used. The dual nature of these principles will impose both the requirements of equilibrium and the requirements of compatibility.

We should emphasize that both approaches lead to identical sets of equations. As a matter of fact, the validity of the principle of virtual work may be demonstrated from the basic requirements in the equilibrium approach. On the other hand, the equations of equilibrium and compatibility may be derived from the principle of virtual work if the concept of conservation of energy is regarded as the fundamental approach. The choice of these approaches in the solution of a problem depends primarily on which approach leads to a simpler solution for a specific problem.

In this section, we shall consider the application of the equilibrium approach in order to illustrate the basic considerations in both the force and displacement methods of analysis. For the sake of simplicity, we shall consider examples of linear elasticity. In Section 8-15 we shall discuss the solution of similar problems by the use of Castigliano's theorems. Then, we shall introduce further applications of the principle of virtual work to nonlinear elastic systems in later sections.

Example 8-12. Compute the redundant reactions R_1, R_2, and R_3 for the continuous beam in Fig. 8-27(a) by the force method. The bending stiffness EI of the beam is constant.

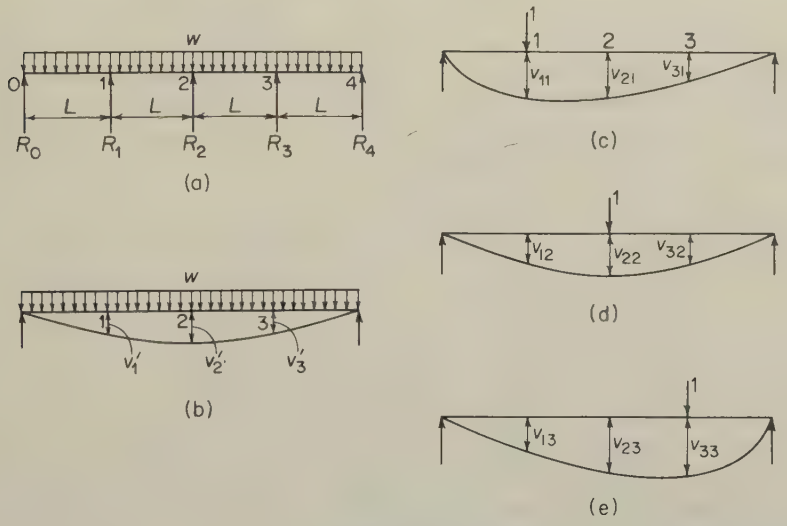

Figure 8–27

The beam is statically indeterminate to the third degree, and the reactions R_1, R_2, and R_3 are considered as redundances. We shall first remove the redundances and the released structure will deflect under the action of the external load as shown in Fig. 8-27(b). Next, place a unit load at points 1, 2, and 3 of the released structure successively as shown in Fig. 8-27(c), (d), and (e), respectively. Denoting the deflections of the auxiliary structure as shown, the conditions of compatibility require that

$$\begin{aligned} v_1' &= v_{11}R_1 + v_{12}R_2 + v_{13}R_3 \\ v_2' &= v_{21}R_1 + v_{22}R_2 + v_{23}R_3 \\ v_3' &= v_{31}R_1 + v_{32}R_2 + v_{33}R_3 \end{aligned} \tag{a}$$

Note that since the downward uniform load is considered as negative, *all*

displacements in Eqs. (a) are opposite to the senses of direction of the respective forces. Hence, no negative signs appear in the equations.

The deflection curve of a simple beam of span length $4L$ subjected to a uniform load $-w$ can readily be obtained by successive integrations as follows:

$$v = \frac{1}{24EI}\left[2w(4L)x^3 - w(4L)^3x - wx^4\right]$$

For $x = L$, $2L$, and $3L$, we obtain the displacements at points 1, 2, and 3 of the auxiliary structure as follows:

$$v_1' = -\frac{57wL^4}{24EI}, \quad v_2' = -\frac{80wL^4}{24EI}, \quad v_3' = -\frac{57wL^4}{24EI}$$

The coefficients of Eqs. (a) may be obtained from the deflections of the released structure with a unit load acting at the desired position. From Example 7-3, we note that for a simple beam of span length $4L$ subjected to a concentrated load P acting at distance a and b from the left and right supports, respectively, the deflection curve is given by

$$v = \frac{Pb}{24EIL}\left[x^3 - (16L^2 - b^2)x\right], \quad 0 \leqq x \leqq a$$

$$v = \frac{Pb}{24EIL}\left[x^3 - \frac{4L}{b}(x-a)^3 - (16L^2 - b^2)x\right], \quad a \leqq x \leqq L$$

For a unit load $P = 1$ at point 1 as shown in Fig. 8-27(c), $a = L$ and $b = 3L$. We have, for $x = L$, $2L$, and $3L$ respectively,

$$v_{11} = -\frac{3L^3}{4EI}, \quad v_{21} = -\frac{11L^3}{12EI}, \quad v_{31} = -\frac{7L^3}{12EI}$$

For a unit load $P = 1$ at point 2 as shown in Fig. 8-27(d), $a = 2L$ and $b = 2L$. We obtain, for $x = L$, $2L$, and $3L$, respectively.

$$v_{12} = -\frac{11L^3}{12EI}, \quad v_{22} = -\frac{4L^3}{3EI}, \quad v_{32} = -\frac{11L^3}{12EI}$$

For a unit load $P = 1$ at point 3 as shown in Fig. 8-27(e), $a = 3L$ and $b = L$, we get, for $x = L$, $2L$, and $3L$, respectively.

$$v_{13} = -\frac{7L^3}{12EI}, \quad v_{23} = -\frac{11L^3}{12EI}, \quad v_{33} = -\frac{3L_3}{4EI}$$

After these coefficients are computed, the redundant reactions can be obtained from the solution of Eqs. (a). The remaining reactions can be computed from the conditions of equilibrium as follows:

$$\begin{aligned} \textstyle\sum F_y &= 0, \quad R_0 + R_1 + R_2 + R_3 + R_4 = (-w)(4L) \\ \textstyle\sum M_4 &= 0, \quad 4LR_0 + 3LR_1 + 2LR_2 + LR_3 = (-w)(4L)(2L) \end{aligned} \tag{b}$$

Thus, in the force method we are primarily concerned with the solution of the compatibility equations involving redundant forces. After these redundant forces are obtained, the remaining forces can easily be computed from the equations of equilibrium.

Example 8-13. Compute the displacement components at joint 0 of the simple truss in Fig. 8-28(a). The areas of the members in square inches are indicated along the members. $E = 30 \times 10^3$ ksi.

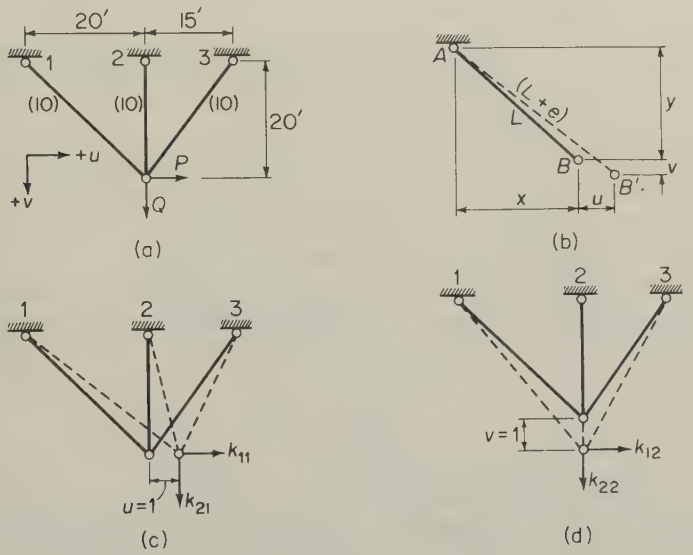

Figure 8–28

This truss is a statically indeterminate structure that will be solved by the displacement method. Hence, we are no longer interested in the degree of statical indeterminacy of the system. Instead, we should determine the degrees of kinematic indeterminacy, which are the same as the degrees of freedom. Since only one joint in the structure is free to move, and the movement can be defined by the horizontal and vertical components of displacement of this joint, the structure has two degrees of freedom or kinematic indeterminacy. Let the horizontal and vertical displacements at joint 0 be denoted by u and v respectively, with positive directions indicated in the figure. From the conditions of equilibrium of joint 0, we have

$$\begin{aligned} P &= k_{11}u + k_{12}v \\ Q &= k_{21}u + K_{22}v \end{aligned} \tag{a}$$

where k_{11} = the force at joint 0 in the direction of P due to a unit displacement in the direction of u while the displacement in the direction of v is prevented,

k_{12} = the force at joint 0 in the direction of P due to a unit displacement in the direction of v while the displacement in the direction of u is prevented,

k_{21} = the force at joint 0 in the direction of Q due to a unit displacement in the direction of u while the displacement in the direction of v is prevented,

k_{22} = the force at joint 0 in the direction of Q due to a unit displacement in the direction of v while the displacement in the direction of u is prevented.

In order to evaluate these coefficients, let us establish the relation between the displacement of joints and the deformation of members in a system. Consider first a single member of length L whose horizontal and vertical projections are x and y respectively, as shown in Fig. 8-28(b). If joint A of the member is hinged and joint B moves to point B' as the result of an elongation e in the member, the horizontal and vertical displacements of end B may be denoted by u and v respectively. From the relations of right triangles, we have

$$L^2 = x^2 + y^2 \tag{b}$$

and

$$(L + e)^2 = (x + u)^2 + (y + v)^2 \tag{c}$$

Expanding Eq. (c), we obtain

$$L^2 + 2Le + e^2 = x^2 + 2xu + u^2 + y^2 + 2yv + v^2$$

Since the deformation of a member is very small in comparison with its length, the higher-order terms of deformation and displacements are negligible. Then, Eq. (c) becomes

$$L^2 + 2Le = x^2 + 2xu + y^2 + 2vy$$

Subtracting Eq. (b) from this equation, we obtain

$$2Le = 2xu + 2yv$$

or

$$e = \frac{x}{L}u + \frac{y}{L}v \tag{d}$$

in which x/L and y/L are the direction cosines of the lines representing the member.

Let us denote the quantities pertaining to members 01, 02, and 03 of the truss shown in Fig. 8-28(a) by subscripts 1, 2, and 3 respectively. Assuming that the bar forces are in tension and that joint 0 displaces in the positive directions of u and v, we obtain from Eq. (d)

$$\begin{aligned} e_1 &= \frac{20}{20\sqrt{2}}u + \frac{20}{20\sqrt{2}}v = 0.707u + 0.707v \\ e_2 &= 0 + {}^{20}\!/_{20}\, v = v \\ e_3 &= -{}^{15}\!/_{25}\, u + {}^{20}\!/_{25}\, v = -0.6u + 0.8v \end{aligned} \tag{e}$$

These are the conditions of compatibility of the system. Using the force-deformation relation $e = FL/EA$, Eqs. (e) become

$$\begin{aligned} \frac{F_1(20\sqrt{2})\,(12)}{(30 \times 10^3)\,(10)} &= 0.707u + 0.707v \\ \frac{F_2(20)\,(12)}{(30 \times 10^3)\,(10)} &= v \\ \frac{F_3(25)\,(12)}{(30 \times 10^3)\,(10)} &= -0.6u + 0.8v \end{aligned}$$

or

$$\begin{aligned} F_1 &= 625u + 625v \\ F_2 &= 1{,}250v \\ F_3 &= -600u + 800v \end{aligned} \tag{f}$$

Hence, the bar forces in the truss can be obtained from Eqs. (f) after the displacement components u and v are obtained.

We can also make use of Eqs. (f) in determining the bar forces due to a unit displacement $u = 1$ or $v = 1$ at joint 0. For $u = 1$ and $v = 0$ as shown in Fig. 8-28(c), we have

$$F_1 = 625, \quad F_2 = 0, \quad F_3 = -600$$

Then, from the equations of equilibrium of joint 0, we get

$$k_{11} = (0.707)\,(625) - (0.6)\,(-600) = 802 \text{ kips/in.}$$

$$k_{21} = (0.707)\,(625) + (1)\,(0) + (0.8)\,(-600) = -38 \text{ kips/in.}$$

Similarly, for $u = 0$ and $v = 1$ as shown in Fig. 8-28(d), we have

$$F_1 = 625, \quad F_2 = 1{,}250, \quad F_3 = 800$$

Then, from the equilibrium of joint 0, we obtain

$$k_{12} = (0.707)\,(625) - (0.6)\,(800) = -38 \text{ kips/in.}$$

$$k_{22} = (0.707)\,(625) + (1)\,(1{,}250) + (0.8)\,(800) = 2.332 \text{ kips/in.}$$

After these coefficients are obtained, the displacement components u and v can be computed from the solution of Eqs. (a). The bar forces in the truss can in turn be computed from Eqs. (f). Thus, in the displacement method, we consider first the solution of the equations of equilibrium involving displacements. After these displacements are obtained, the internal forces can be computed from the equations of compatibility and the force-deformation relations.

8-13 *Influence Coefficients for Linear Systems*

In the analysis of linear elastic structures, we can express either the displacements in terms of forces or the forces in terms of displacements, obtaining a set of simultaneous linear equations. In the force method, the unknowns in the set of equations are forces and the coefficients are displacements per unit force; in the displacement method, the unknowns in the set of equations are displacements and the coefficients are forces per unit displacement. The coefficients of these simultaneous linear equations are called *influence coefficients*. By means of Maxwell's theorem it can be shown that these coefficients have reciprocal properties.

Let us first consider a linear spring with one degree of freedom. Let a force P be applied to the spring causing a displacement s. The force-displacement relation of the spring may be given by

$$P = ks$$

in which k is called the *spring constant* or the *stiffness coefficient* of the spring, given by $k = P/s$, which is the force required to produce a unit displacement in the spring. On the other hand, the force-displacement relation may also be expressed in the form

$$s = fP$$

in which f is called the *flexibility coefficient* of the spring and $f = s/P$ is the displacement caused by a unit force in the spring. For this simple case with one degree of freedom, it is seen that

$$k = \frac{1}{f}$$

That is, the stiffness coefficient is the inverse of the flexibility coefficient and vice versa.

For a structural system with more than one degree of freedom, the relations between the stiffness and flexibility coefficients of individual members are no longer so simple. However, the stiffness of the system as a whole is the inverse of the flexibility of the entire system. In other words, the coefficients for one set of simultaneous linear equations involving forces as

unknowns can be obtained from the solution of another set of simultaneous equations involving displacements as unknowns.

Consider, for instance, the linear system in Fig. 8-29, on which forces $P_1, P_2, \ldots, P_n$ are applied at points 1, 2, . . ., n. By the principle of superposition, the displacement at any point in a given direction is the sum of the displacements in that direction caused by each force acting separately. Let f_{ij} be a flexibility coefficient denoting the displacement at joint i in the direction of the line of action of P_i due to a unit force at joint j in the direction of s_j. Then, the displacements at various points in the lines of action of the respective forces can be expressed as follows:

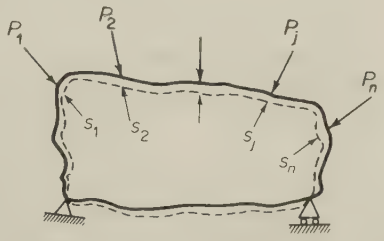

Figure 8-29

$$\begin{aligned}
s_1 &= f_{11}P_1 + f_{12}P_2 + f_{13}P_3 + \ldots + f_{1n}P_n \\
s_2 &= f_{21}P_1 + f_{22}P_2 + f_{23}P_3 + \ldots + f_{2n}P_n \\
s_3 &= f_{31}P_1 + f_{32}P_2 + f_{33}P_3 + \ldots + f_{3n}P_n \\
&\vdots \\
s_n &= f_{n1}P_1 + f_{n2}P_2 + f_{n3}P_3 + \ldots + f_{nn}P_n
\end{aligned} \tag{8-29}$$

According to Maxwell's theorem of reciprocal displacements, the displacement at joint i in the direction of the line of action of P_i due to a unit force at joint j is equal to the displacement at joint j in the direction of the line of action of P_j due to a unit force at joint i. Hence,

$$f_{ij} = f_{ji} \qquad (i = 1, 2, \ldots, n;\ j = 1, 2, \ldots, n)$$

We can also express forces in terms of displacements for the linear system in Fig. 8-29. The force at any point in a given direction is the sum of the force in that direction corresponding to each displacement applied separately. Let k_{ij} be a stiffness coefficient denoting the force at joint i in the direction of the line of action of P_i due to a unit displacement at joint j in the direction of s_j while all other displacements are prevented. Then, the forces at various points in the respective given directions can be expressed as follows:

$$\begin{aligned}
P_1 &= k_{11}s_1 + k_{12}s_2 + k_{13}s_3 + \ldots + k_{1n}s_n \\
P_2 &= k_{21}s_1 + k_{22}s_2 + k_{23}s_3 + \ldots + k_{2n}s_n \\
P_3 &= k_{31}s_1 + k_{32}s_2 + k_{33}s_3 + \ldots + k_{3n}s_n \\
&\vdots \\
P_n &= k_{n1}s_1 + k_{n2}s_2 + k_{n3}s_3 + \ldots + k_{nn}s_n
\end{aligned} \tag{8-30}$$

It can be demonstrated that the reciprocal relations of Maxwell's theorem are also applicable to this case. We have, in general,

$$k_{ij} = k_{ji}$$

It should be noted that the forces and displacements just discussed may include moments and rotations. If a linear elastic element is subjected to pure bending, for example, the rotation φ is related to M as follows:

$$M = k'\varphi \quad \text{or} \quad \varphi = f'M$$

Hence, the stiffness coefficient $k' = M/\varphi$ is the moment required to produce a unit rotation, and the flexibility coefficient $f' = \varphi/M$ is the rotation caused by a unit moment. Hence, k' is the inverse of f' and vice versa. Furthermore, the reciprocal relations of Maxwell's theorem are also applicable to flexibility and stiffness coefficients resulting from moments and rotations.

As illustrations we shall examine the coefficients of linear equations in Examples 8-12 and 8-13. In Example 8-12 the conditions of compatibility of the system yield a set of linear equations in which the unknowns are the redundant forces and the coefficients are the flexibility coefficients. The reciprocal relations $v_{12} = v_{21}$ and $v_{23} = v_{32}$ agree with Maxwell's theorem. In Example 8-13, the conditions of equilibrium of joints lead to a set of linear equations in which the unknowns are the displacements at the joints and the coefficients are the stiffness coefficients. The reciprocal relation $k_{21} = k_{12}$ also agrees with Maxwell's theorem.

The number of simultaneous equations and the amount of work in calculating the coefficients are important factors in selecting the method of solution. By observing the reciprocal relations of the coefficients, we can greatly reduce the amount of work required for a system consisting of a large number of joints and members.

8-14 *Müller-Breslau's Principle*

Another important simplification in the analysis of linear elastic structures is found in the construction of influence lines for such structures. This is accomplished by means of *Müller-Breslau's principle*, which is derived from Maxwell's theorem of reciprocal displacements. We shall discuss briefly the development of this principle and its application to statically indeterminate structures that are linearly elastic.

In the discussion of the general concept of influence lines in Section 6-3, we pointed out that an influence line for any constraint such as a reaction, shear, or moment at a point in a structure—whether it is statically determinate or indeterminate—may be obtained from the deflected shape of the released system in which the constraint has been removed. We also introduced (without proof) Müller-Breslau's principle, which states that if any

constraint is removed from a statically indeterminate structure and a corresponding deforming effect is allowed to act through a unit virtual displacement, the resulting deflected shape is an influence line for that effect. We can now demonstrate the validity of this statement by means of Maxwell's theorem of reciprocal relations.

Consider, for instance, the continuous beam in Fig. 8-30(a), for which the influence line for the reaction at support B is desired. We remove the support at B so that the released system will be as shown in Fig. 8-30(b). In the released system, the deflection at point B due to a moving unit load $P = 1$ is denoted by δ_b'. We may also remove the external load $P = 1$ and place a unit load at point B of the released structure, causing a deflection δ_{bb} at point B as shown in Fig. 8-30(c). Thus, the reaction at support B is equal to the force required to restore point B of the beam to its undeflected position. Hence,

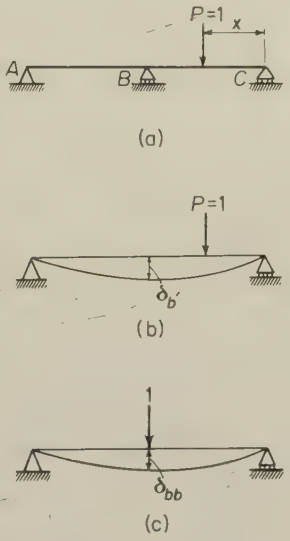

Figure 8-30

$$R_b = -\frac{\delta_b'}{\delta_{bb}}$$

Note that δ_{bb} is a constant quantity since the geometrical and material properties of the beam are known whereas δ_b' depends on the location of the moving load $P = 1$. Thus, the influence line for the reaction at support B is proportional to the influence line for deflection at point B of the released structure, the factor of proportionality being δ_{bb}. According to Maxwell's theorem of reciprocal displacements, the influence line for deflection at point B of the released structure is identical to the deflection curve of the beam with a load $P = 1$ acting at B. Hence, the ordinates of this deflection curve divided by δ_{bb} give the corresponding ordinates of the influence line for the reaction at B.

The same principle may be used for other types of constraint such as moments, shears, and bar forces in any structure provided that the material is linearly elastic. It is extremely useful in the construction of influence lines for statically indeterminate structures.

Example 8-14. The parabolic arch shown in Fig. 8-31(a) is represented by the equation

$$y = \frac{4f}{L^2}(Lx - x^2)$$

The moment of inertia at any section is $I = I_c \sec \beta$, where I_c is the moment

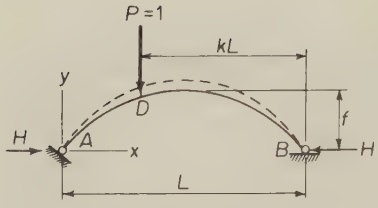

(a)

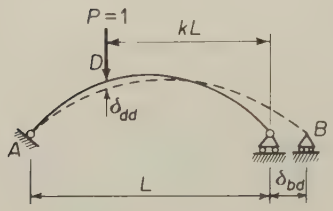

(b)

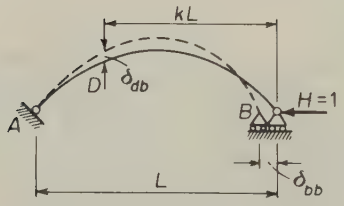

(c)

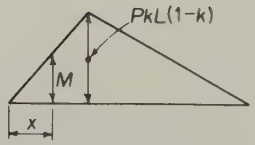

(d)

(e)

Figure 8–31

of inertia at the crown and β is the angle between a tangent at a point on the arch axis and a horizontal line. Construct the influence line for the horizontal thrust H of the arch.

In order to construct the influence line for the horizontal thrust of the arch, we shall first remove the horizontal constraint at support B and allow point B to act through a unit displacement in the direction of the horizontal force H. According to Müller-Breslau's principle, the deflected shape of the released structure as indicated by the dotted line in Fig. 8-31(a) is the influence line for the horizontal thrust of the arch.

We can also obtain the ordinates of the influence line by computing the deflections of the released system. When a moving vertical load $P = 1$ is applied at point D, which is at a distance kL from the right support of the released structure as shown in Fig. 8-31(b), the horizontal displacement of support B may be denoted by δ_{bd}. If we apply a horizontal unit load at support B of the released structure as shown in Fig. 8-31(c), the support will displace horizontally by an amount δ_{bb}. Then, the horizontal thrust H in the original structure is given by

$$H = \frac{\delta_{bd}}{\delta_{bb}}$$

Note that δ_{bb} is a constant quantity whereas δ_{bd} depends on the distance kL from the right support. Since the horizontal displacement at point B due to a vertical load $P = 1$ at point D is equal to the vertical displacement at point D due to a horizontal load $H = 1$, i.e., $\delta_{bd} = \delta_{db}$, this expression for H gives the vertical ordinates of the influence line provided that δ_{bd} and δ_{bb} can be evaluated.

For a section of the arch axis at a distance x from the left support, we have from Fig. 8-31(d),

$$M = \frac{P(1-k)Lx}{L} = P(1-k)x \quad \text{for } 0 \leqq x \leqq kL$$

$$M = \frac{PkL(L-x)}{L} = Pk(L-x) \quad \text{for } kL \leqq x \leqq L$$

and from Fig. 8-31(e), $m = y$ for all values of x. Noting that $\sec \beta = ds/dx$, in which ds is measured along the length of the arch axis, δ_{bd} and δ_{bb} may be obtained by the method of virtual work as follows:

$$\delta_{bd} = \int_0^L \frac{Mm\,ds}{EI} = \int_0^L \frac{Mm\,ds}{EI_c \sec\beta} = \int_0^L \frac{Mm\,dx}{EI_c}$$

$$= \frac{1}{EI_c}\int_0^L My\,dx$$

$$= \frac{4Pf}{L^2EI_c}\left[\int_0^{kL}(Lx - x^2)(1-k)x\,dx + \int_{kL}^{L}(Lx - x^2)k(L-x)\,dx\right]$$

$$= \frac{PfkL^2}{3EI_c}(1 - 2k^2 + k^3)$$

$$\delta_{bb} = \int_0^L \frac{y^2\,ds}{EI} = \int_0^L \frac{y^2 ds}{EI_c \sec\beta} = \frac{1}{EI_c}\int_0^L y^2\,dx$$

$$= \frac{16f^2}{EI_cL^4}\int_0^L (Lx - x^2)^2\,dx = \frac{8f^2L}{15EI_c}$$

Hence,

$$H = \frac{5PLk}{8f}(1 - 2k^2 + k^4)$$

If the span is divided into six equal divisions, for instance, the influence ordinates for H due to a unit load $P = 1$ moving along the span may be obtained as follows:

for $k = 0$ and $k = 1$, $H = 0$

for $k = \frac{1}{6}$ and $k = \frac{5}{6}$, $H = 0.099L/f$

for $k = \frac{1}{3}$ and $k = \frac{2}{3}$, $H = 0.170L/f$

for $k = \frac{1}{2}$, $H = 0.195L/f$

Since a *downward* vertical load at D will cause an *outward* horizontal displacement at B, an *inward* horizontal thrust will cause an *upward* vertical displacement in the released system. Hence, the influence ordinates are positive.

Example 8-15. Construct the influence lines for reactions R_b and R_a of a two-span continuous beam having equal spans L and constant bending stiffness EI as shown in Fig. 8-32(a).

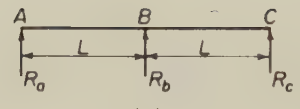

(a)

(b)

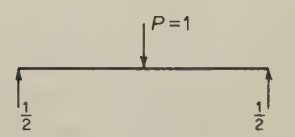

(c)

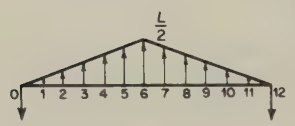

(d)

(e)

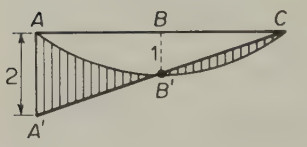

(f)

Figure 8-32

In order to obtain the influence line for reaction R_b, we remove the vertical constraint at support B and allow point B to act through a unit displacement in the direction of R_b. Then, according to Müller-Breslau's principle, the deflected shape of the released system as shown by the dotted line in Fig. 8-32(b) is the influence line for R_b.

The ordinates of the influence line can be obtained from the relation $R_b = \delta_b'/\delta_{bb}$. Since δ_b' represents the deflection at point B caused by a moving unit load at various points of the beam in Fig. 8-32(c), they are identical to the deflections at various points of the beam due to a unit load at point B. We can compute the deflections at various points of the beam due to a unit load at point B by the conjugate beam method. For the sake of convenience, let us select six points for each span, and because of symmetry, we need to consider only half of the structure. Then, from the moment diagram in Fig. 8-32(d), we obtain the vertical deflections as follows:

$$EIv_1 = \left(\frac{L^2}{4}\right)\left(\frac{L}{6}\right) - \left(\frac{1}{2}\right)\left(\frac{L}{12}\right)\left(\frac{L}{6}\right)^2\left(\frac{1}{3}\right) = \frac{107}{2{,}592}L^3$$

$$EIv_2 = \left(\frac{L^2}{4}\right)\left(\frac{L}{3}\right) - \left(\frac{1}{2}\right)\left(\frac{L}{6}\right)\left(\frac{L}{3}\right)^2\left(\frac{1}{3}\right) = \frac{13}{162}L^3$$

$$EIv_3 = \left(\frac{L^2}{4}\right)\left(\frac{L}{2}\right) - \left(\frac{1}{2}\right)\left(\frac{L}{4}\right)\left(\frac{L}{2}\right)^2\left(\frac{1}{3}\right) = \frac{11}{96}L^3$$

$$EIv_4 = \left(\frac{L^2}{4}\right)\left(\frac{2L}{3}\right) - \left(\frac{1}{2}\right)\left(\frac{L}{3}\right)\left(\frac{2L}{3}\right)^2\left(\frac{1}{3}\right) = \frac{23}{162}L^3$$

$$EIv_5 = \left(\frac{L^2}{4}\right)\left(\frac{5L}{6}\right) - \left(\frac{1}{2}\right)\left(\frac{5L}{12}\right)\left(\frac{5L}{6}\right)^2\left(\frac{1}{3}\right) = \frac{415}{2{,}592}L^3$$

$$EIv_6 = \left(\frac{L^2}{4}\right)(L) - \left(\frac{1}{2}\right)\left(\frac{L}{2}\right)(L^2)\left(\frac{1}{3}\right) = \frac{1}{6}L^3$$

Noting that $\delta_{bb} = v_6$, the influence ordinates can be obtained as follows:

$$y_0 = 0$$

$$y_1 = \frac{v_1}{v_6} = \left(\frac{107}{2{,}592}L^3\right)\left(\frac{6}{L^3}\right) = 0.248$$

$$y_2 = \frac{v_2}{v_6} = \left(\frac{13}{162}L^3\right)\left(\frac{6}{L^3}\right) = 0.481$$

$$y_3 = \frac{v_3}{v_6} = \left(\frac{11}{96}L^3\right)\left(\frac{6}{L^3}\right) = 0.688$$

$$y_4 = \frac{v_4}{v_6} = \left(\frac{23}{162}L^3\right)\left(\frac{6}{L^3}\right) = 0.851$$

$$y_5 = \frac{v_5}{v_6} = \left(\frac{415}{2{,}592}L^3\right)\left(\frac{6}{L^3}\right) = 0.961$$

$$y_6 = \frac{v_6}{v_6} = 1$$

For the influence line for reaction R_a, we remove the vertical constraint at support A and allow point A to act through a unit displacement in the direction of R_a as shown in Fig. 8-32(e). The ordinates of the influence line may be obtained in a similar manner. However, with the benefit of the influence line for R_b, the computation can be reduced by noting that the deflection curve of the beam due to a unit displacement at point A has the same shape as the one formed by a line passing through points C and B' of the deflection curve due to a unit displacement at point B. However, the absolute values of the ordinates of the former differ from those of the latter by a constant factor. We may therefore obtain AA' from BB' by the relations of similar triangles. Since $AA' = 2$ for $BB' = 1$, we can obtain the ordinates of the influence line for reaction R_a by dividing the vertical ordinates in the shaded part of Fig. 8-32(f) by a factor of 2. Thus the ordinates for the influence line for reaction R_a are obtained from the geometry of the influence line for reaction R_b as represented by the deflection curve in Fig. 8-32(f) as follows:

$y_0 = \frac{2}{2} = 1$

$y_1 = (1.833 - 0.248)/2 = 0.792$

$y_2 = (1.667 - 0.481)/2 = 0.593$

$y_3 = (1.500 - 0.688)/2 = 0.406$

$y_4 = (1.333 - 0.851)/2 = 0.241$

$y_5 = (1.167 - 0.961)/2 = 0.103$

$y_6 = (1 - 1)/2 = 0$

$y_7 = (0.833 - 0.961)/2 = -0.064$

$y_8 = (0.667 - 0.851)/2 = -0.092$

$y_9 = (0.500 - 0.688)/2 = -0.094$

$y_{10} = (0.333 - 0.481)/2 = -0.074$

$y_{11} = (0.167 - 0.248)/2 = -0.041$

$y_{12} = 0$

8-15 *Application of Castigliano's Theorems*

In the development of Castigliano's theorems, we mentioned that they are very useful in the analysis of statically indeterminate structures. We shall now discuss in detail their application to linear elastic systems.

For the displacement method of analysis, Castigliano's first theorem may be used to express the conditions of equilibrium; for the force method of analysis, Castigliano's second theorem may be used to express the conditions of compatibility. With traditional emphasis on the force method of analysis, the second theorem has been cast in a more important role than the first theorem. Castigliano himself contributed to such an unbalanced emphasis by stressing the numerous applications of the second theorem and called it the *theorem of least work*.* He stated that, among all the statically possible states of stress in a structure subjected to a variation of stress during which the conditions of equilibrium are maintained, the correct one is that which makes the strain energy of the system a minimum.

Consider, for example, a linearly elastic system with r redundant forces $X_1, X_2, \ldots, X_r$, the points of application of which remain unchanged in their positions during deformation under the action of external loads. According to Castigliano's second theorem

$$\frac{\partial U_i}{\partial X_j} = 0 \quad (j = 1, 2, \ldots, r) \tag{8-31a}$$

This set of equations is interpreted as follows: Of all possible sets of values that the redundant forces in the system may assume, the correct set of values is that which makes the strain energy U_i a minimum. Since one equation is obtained for each redundant force, a set of equations corresponding to the conditions of compatibility will result.

Castigliano further extended the theorem of least work to systems that are self-strained. In that case, the point of application of a redundant force X_j may be displaced by an amount λ_j in the direction of the force. Hence,

$$\frac{\partial U_i}{\partial X_j} = \lambda_j \quad (j = 1, 2, \ldots, r) \tag{8-31b}$$

For example, the self-straining may be caused by the settlement of the support of a redundant reaction by an amount of $-\lambda_j$ or by the initial misfit of a member by an amount λ_j too short. In the former, the negative sign of λ_j indicates that the direction of the settlement is opposite to that of the redundant reaction; in the latter, λ_j is positive for a member too short because

*See p. 18 of Reference 8-6.

the tension caused by the stretching of the member to its desired length is in the same direction as the deformation.

In examining Eq. (8-31b), it appears that the interpretation of minimum strain energy is rather artificial although the equation itself is as useful as Eq. (8-31a) for obtaining the conditions of compatibility for redundant systems. Southwell suggested that Castigliano's theorem of least work, in effect, means that the strain energy of a linearly elastic system that is initially unstrained will have less strain energy stored in it when subjected to a load system than it would have if it were self-strained.* Charlton further argued that a true principle of least work should be associated with the determination of the equations of equilibrium of self-straining systems.† Hence, if certain prescribed deflections are introduced to a linear elastic structure, the other deflections assume values such that the strain energy of the structure is a minimum. Actually, Eqs. (8-31) represent a theorem imposing the conditions of compatibility and need not be associated with a minimum of strain energy. Hence, the theorem should not be given a different name, especially not the misnomer "the theorem of least work." In this text, we shall refer to it as Castigliano's second theorem.

Example 8-16. Determine the bar forces and joint displacements in the truss shown in Example 8-13 using Castigliano's first theorem if $P = 100$ kips and $Q = 200$ kips.

For this problem, the conditions of compatibility have been previously established in Example 8-13 as follows:

$$\begin{aligned} e_1 &= 0.707u + 0.707v \\ e_2 &= v \\ e_3 &= -0.6u + 0.8v \end{aligned} \tag{a}$$

and from the force-deformation relation $e = FL/AE$, the internal forces have been obtained as follows:

$$\begin{aligned} F_1 &= 625u + 625v \\ F_2 &= 1{,}250v \\ F_3 &= -600u + 800v \end{aligned} \tag{b}$$

The strain energy of the linear elastic system is given by

$$U_i = \tfrac{1}{2}\sum Fe = \tfrac{1}{2}F_1e_1 + \tfrac{1}{2}F_2e_2 + \tfrac{1}{2}F_3e_3$$

*See Reference 8–8.
†See p. 24 of Reference 8–9.

in which

$$\tfrac{1}{2}F_1e_1 = \tfrac{1}{2}(625u + 625v)(0.707u + 0.707v) = 221u^2 + 442uv + 221v^2$$

$$\tfrac{1}{2}F_2e_2 = \tfrac{1}{2}(1{,}250v)v = 625v^2$$

$$\tfrac{1}{2}F_3e_3 = \tfrac{1}{2}(-600u + 800v)(-0.6u + 0.8v) = 180u^2 - 480uv + 320v^2$$

Hence,

$$U_i = 401u^2 - 38uv + 1{,}166v^2 \tag{c}$$

By using Castigliano's first theorem, we obtain

$$P = \frac{\partial U_i}{\partial u} = 802u - 38v$$

and (d)

$$Q = \frac{\partial U_i}{\partial v} = -38u + 2{,}332v$$

Equations (d) are the equations of equilibrium expressed in terms of displacements and stiffness coefficients. For $P = 100$ kips and $Q = 200$ kips we obtain from the solution of Eqs. (d) that $u = 0.129$ in. and $v = 0.088$ in.

The bar forces are computed from Eqs. (b) after u and v are evaluated. Thus, $F_1 = 135$ kips, $F_2 = 110$ kips and $F_3 = -7$ kips.

Example 8-17. Derive the equation of compatibility for the continuous truss shown in Fig. 8-33(a) if the center support is considered as a redundance.

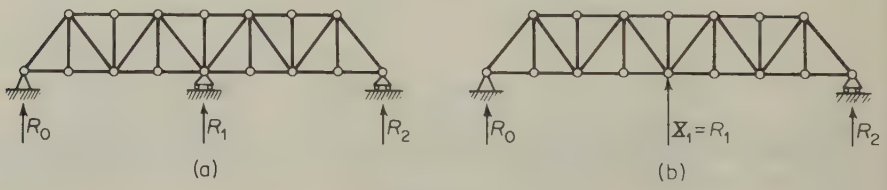

Figure 8–33

Let the center support be removed and replaced by a force $X_1 = R_1$ as shown in Fig. 8-33(b). The released structure is statically equivalent to the original structure. Then, the bar force in a member of the original truss due to the external loads may be given by

$$F = F' + X_1f_1 \tag{a}$$

in which F' is the bar force in the same member of the released structure due to the external loads when $X_1 = 0$, and f_1 is the bar force in the same member of the released structure due to $X_1 = 1$ with no other external loads.

According to Eq. (8-17a), the strain energy in the original truss is as follows:

$$U_i = \frac{1}{2}\sum \frac{F^2 L}{AE} \tag{b}$$

By using Castigliano's second theorem, we obtain

$$\frac{\partial U_i}{\partial X_1} = \sum \frac{FL}{AE}\frac{\partial F}{\partial X_1} = 0 \tag{c}$$

From Eq. (8-26a), we have

$$\frac{\partial F}{\partial X_1} = f_1 \tag{d}$$

Substituting Eqs. (a) and (d) into Eq. (c), we get

$$\sum \frac{F' L f_1}{AE} + X_1 \sum \frac{f_1^2 L}{AE} = 0 \tag{e}$$

This is the equation of compatibility for the statically indeterminate truss. We note from the principle of virtual work,

$$\delta_1' = \sum \frac{F' L f_1}{AE} \quad \text{and} \quad \delta_{11} = \frac{f_1^2 L}{AE}$$

in which δ_1' is the vertical deflection of point 1 of the released structure due to external loads when $R_1 = 0$, and δ_{11} is the vertical deflection of point 1 of the released structure due to $R_1 = 1$ without other external loads. Thus, the redundant reaction of the truss may be obtained from Eq. (e) as follows:

$$X_1 = -\frac{\sum \dfrac{F' L f_1}{AE}}{\sum \dfrac{f_1^2 L}{AE}} = -\frac{\delta_1'}{\delta_{11}} \tag{f}$$

Example 8-18. For the rigid frame in Fig. 8-34(a), determine the redundant forces by Castigliano's second theorem. The bending stiffness EI is constant for all members.

The rigid frame is statically indeterminate to three degrees and we can select any three stress resultants as redundances. The components of reaction at support D, for example, may be chosen as redundances as shown in Fig. 8-34(b). After the redundances are obtained, the stress resultants at any section of the frame can readily be determined. Using Castigliano's second theorem, the equations of compatibility will be obtained automatically without the necessity of matching the displacements at the point where the redundances are introduced. Thus, it is just as simple to choose as redundances the stress resultants at an intermediate point as those at a support of the

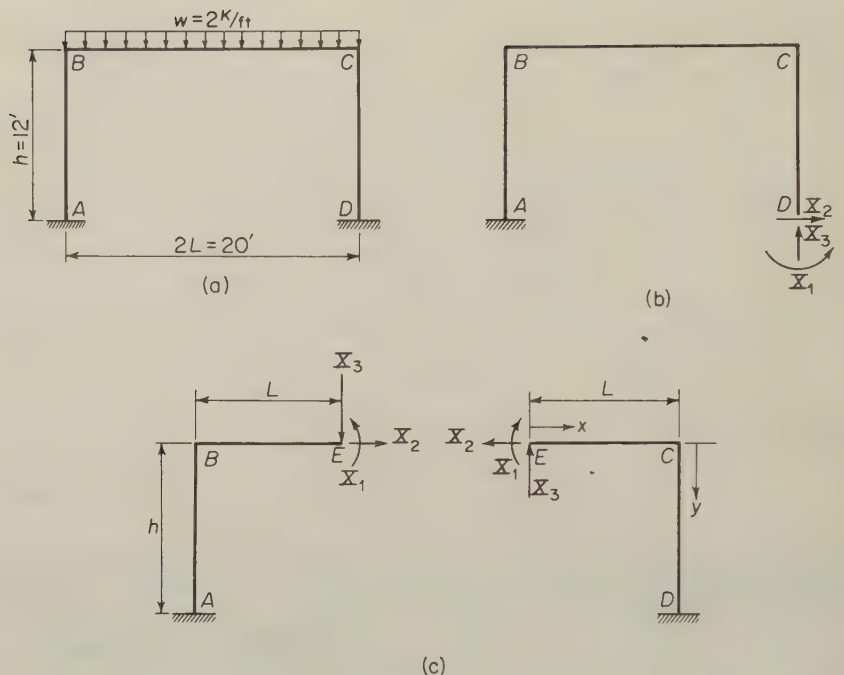

Figure 8–34

frame. Owing to the symmetry of this problem, there is much to be gained by selecting the stress resultants at the midpoint of member *BC* as redundances as shown in Fig. 8-34(c). From the condition of symmetry, it is obvious that the shear force $X_3 = 0$ because its existence would violate the symmetry of the structure and the loading. Thus, we need only two equations of compatibility instead of three for the statically equivalent structure shown in Fig. 8-34(c).

The strain energy due to axial force and shear is small in comparison with that due to bending and can therefore be neglected in establishing the strain energy expression. Thus,

$$U_i = \sum \int \frac{M^2\, ds}{EI}$$

By using Castigliano's second theorem, we have

$$\frac{\partial U_i}{\partial X_1} = 0 \quad \text{or} \quad \sum \int \frac{M\, ds}{EI} \frac{\partial M}{\partial X_1} = 0 \tag{a}$$

$$\frac{\partial U_i}{\partial X_2} = 0 \quad \text{or} \quad \sum \int \frac{M\, ds}{EI} \frac{\partial M}{\partial X_2} = 0 \tag{b}$$

At a point between E and C of the frame, we have

$$M = X_1 - \frac{wx^2}{2}$$

$$\frac{\partial M}{\partial X_1} = 1 \quad \text{and} \quad \frac{\partial M}{\partial X_2} = 0$$

At a point between C and D of the frame, we get

$$M = X_1 - X_2 y - \frac{wL^2}{2}$$

$$\frac{\partial M}{\partial X_1} = 1 \quad \text{and} \quad \frac{\partial M}{\partial X_2} = -y$$

Because of the symmetry, the moment at a point in EB is identical to that in EC, and the moment at a point in BA is the same as that in CD. Since EI is constant throughout the entire frame, it may be eliminated from Eqs. (a) and (b). Then, Eqs. (a) and (b) may be expressed as functions of X_1 and X_2 as follows:

$$\sum \int M \frac{\partial M}{\partial X_1} dx = 2 \int_0^L \left(X_1 - \frac{wx^2}{2} \right) (1)\, dx + 2 \int_0^h \left(X_1 - X_2 y - \frac{wL^2}{2} \right) (1)\, dy$$

$$= 2 \left[X_1 x - \frac{wx^3}{6} \right]_0^L + 2 \left[X_1 y - X_2 \frac{y^2}{2} - \frac{wL^2 y}{2} \right]_0^h = 0$$

or

$$2(L + h)X_1 - h^2 X_2 - wL^3 \left(\frac{1}{3} + \frac{h}{L} \right) = 0 \qquad \text{(a')}$$

$$\sum \int M \frac{\partial M}{\partial X_2} ds = 2 \int_0^L \left(X_1 - \frac{wx^2}{2} \right) (0)\, dx + 2 \int_0^h \left(X_1 - X_2 y - \frac{wL^2}{2} \right) (-y)\, dy$$

$$= -2 \left[X_1 \left(\frac{y^2}{2} \right) - X_2 \left(\frac{y^3}{3} \right) - \frac{wL^2 y^2}{4} \right]_0^h = 0$$

or

$$-h^2 X_1 + \frac{2h^3}{3} X_2 + \frac{wL^2 h^2}{2} = 0 \qquad \text{(b')}$$

By substituting the values of $w = 3$ kips/ft, $L = 10$ ft, and $h = 12$ ft into Eqs. (a') and (b'), we get

$$44X_1 - 144X_2 = 4{,}600$$

$$-144X_1 + 1{,}152X_2 = -21{,}600$$

from which we obtain $X_1 = 73.1$ ft-kips and $X_2 = -9.6$ kips.

8-16 *Principle of Stationary Potential Energy*

In the previous section, we considered the application of Castigliano's theorems to linear elastic systems. As a matter of fact, although the second theorem is restricted to linear elasticity, Castigliano's first theorem is not. We shall now consider a general application of the principle of virtual work for imposing the requirement of equilibrium, and in the next section we shall introduce a similar application for expressing the requirement of compatibility.

In the development of the principle of virtual work for rigid systems in Section 2-14, we pointed out that the principle of virtual work can be derived from the principle of minimum potential energy which is obtained first from the fundamental principle of conservation of energy. We shall now demonstrate that the principle of minimum potential energy can be derived from the principle of virtual work if the latter is obtained first from the principle of conservation of energy. For deformable systems, however, the requirement of minimum potential energy is not necessarily satisfied unless it is linearly elastic. If a potential energy function is said to be stationary when all of its partial derivatives equal zero, we can at least demonstrate that for a deformable system in equilibrium, the potential energy is stationary. If the system in equilibrium is linearly elastic, we can further show that the potential energy is a minimum.

In Section 2-13 we discussed the minimum potential energy of rigid systems. In the case of deformable systems, both external and internal forces contribute to the total potential energy. For the purpose of structural analysis, it is convenient to define a potential U_e of the external forces in such a manner that it is strictly associated with the applied external forces only. Consider, for example, two identical bars subjected to identical loads but placed in different positions, as shown in Fig. 8-35. If we consider the influence of the outside environment, say gravitation, the potential of the external forces in Fig. 8-35(a) is different from that in Fig. 8-35(b). However, if we consider as the potential of the external forces the potential capacity of performing external work by the applied forces P and Q, then the potential due to the external forces will be the same in each case. Therefore, we can simplify the formulation of the total potential energy of a structural system by introducing a concise definition of the potential of external forces.

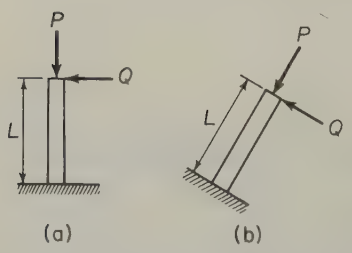

Figure 8–35

Consider a conservative deformable system in equilibrium under a set of forces $P_1, P_2, \ldots, P_m$ as shown in Fig. 8-36. If

displacements $s_1, s_2, \ldots, s_m$ are produced at the points of application of these forces in the directions of the respective forces, the work done by the external forces is given by Eq. (8-3). Let the potential of the external forces be defined as $U_e = -W_e$. The potential of the internal forces is equal to the strain energy U_i and is given by Eq. (8-2). Thus, the total potential energy of the system is

$$U = U_e + U_i$$

If the system is given a small displacement consistent with the constraints, we have

$$\delta U = \delta U_e + \delta U_i$$

or

$$\delta U = -\sum_{j=1}^{m} P_j \delta s_j + \sum_{k=1}^{n} F_k \delta e_k \qquad \text{(a)}$$

By the principle of virtual displacements, i.e., Eq. (8-21c), we get from Eq. (a)

$$\delta U = \delta U_e + \delta U_i = 0 \qquad \text{(b)}$$

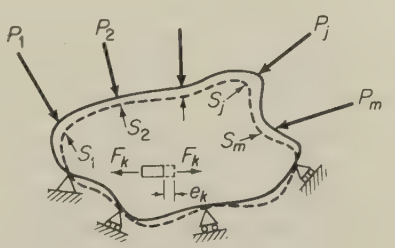

Figure 8-36

Hence, the change in total potential energy must be zero when a deformable system in equilibrium is given a virtual displacement compatible with its constraints.

If the total potential energy of a conservative system is expressed as a function of r displacements or displacement parameters $q_1, q_2, \ldots, q_r$, which represent r degrees of freedom, and if the system is given a set of virtual displacements consistent with its constraints, the conditions of equilibrium are given by

$$\delta U = \frac{\partial U}{\partial q_1}\delta q_1 + \frac{\partial U}{\partial q_2}\delta q_2 + \ldots + \frac{\partial U}{\partial q_r}\delta q_r = 0 \qquad (8\text{-}32)$$

Since $\delta q_1, \delta q_2, \ldots, \delta q_r$ are not all zero and are independent of each other, it is necessary that

$$\frac{\partial U}{\partial q_1} = \frac{\partial U}{\partial q_2} = \ldots = \frac{\partial U}{\partial q_r} = 0 \qquad (8\text{-}33)$$

It can be stated, therefore, that of all possible configurations compatible with the constraints of a deformable system, the total potential energy of the configuration that satisfies the conditions of equilibrium is stationary. This is the *principle of stationary potential energy* for deformable systems.

Let us now consider a special case in which the displacement s_j is increased by a small amount δs_j in the direction of the load P_j while the other displacements remain unchanged. Then, Eq. (b) becomes

$$\delta U = \delta U_e + \delta U_i = -P_j \delta s_j + \frac{\partial U_i}{\partial s_j}\delta s_j = 0$$

Then,

$$P_j = \frac{\partial U_i}{\partial s_j}$$

This result is identical to Eq. (8-18). Hence, Castigliano's first theorem may be considered as a special case derived from the principle of stationary potential energy. In application, the two approaches are strikingly similar. In the method based on the principle of stationary potential energy, a set of equations of equilibrium are obtained from Eqs. (8-33) whereas according to Castigliano's first theorem, one equation of equilibrium is obtained at a time from the partial derivative of the strain energy corresponding to a particular displacement. The latter approach differs from the former only in form, and they are interchangeable.

It may be interesting to note that the stationary value of the total potential energy of a linear elastic system always corresponds to a relative minimum when the equilibrium is stable. Consider, for example, a linear elastic system of volume V whose internal potential energy or strain energy is given by

$$U_i = \int\int\int_V \frac{1}{2}\sigma\epsilon\, dx\, dy\, dz = \int\int\int_V \frac{E}{2}\epsilon^2\, dx\, dy\, dz$$

If the system is given a virtual displacement, the total strain energy is

$$\begin{aligned} U_i + \delta U_i &= \int\int\int_V \frac{E}{2}(\epsilon + \delta\epsilon)^2\, dx\, dy\, dz \\ &= \int\int\int_V \frac{E}{2}\left[\epsilon^2 + 2\epsilon\,\delta\epsilon + (\delta\epsilon)^2\right] dx\, dy\, dz \end{aligned}$$

Thus, the change in strain energy is equal to

$$\begin{aligned} \delta U_i &= \int\int\int_V E\epsilon\,\delta\epsilon\, dx\, dy\, dz + \int\int\int_V \frac{E}{2}(\delta\epsilon)^2\, dx\, dy\, dz \\ &= \int\int\int_V E\epsilon\,\delta\epsilon\, dx\, dy\, dz + \zeta \end{aligned} \qquad \text{(c)}$$

in which ζ is a positive quantity of higher order since it contains the $(\delta\epsilon)^2$ term. Using the expression for external potential energy $U_e = -W_e$ and the expression for internal potential energy in Eq. (c) we obtain from Eq. (b) that

$$\delta U = -\sum P\,\delta s + \int\int\int_V E\epsilon\,\delta\epsilon\, dx\, dy\, dz + \zeta$$

If the virtual displacement is infinitesimal, the second-order term ζ approaches zero as a limit. For small finite virtual displacements, the term ζ may be

neglected. Since ζ is always greater than zero for all displacements, it means that a small virtual displacement causing a deformable system to depart from its position of equilibrium always produces an increase in potential energy. Hence, the *principle of minimum potential energy* for linear elastic systems can be stated as follows: Of all possible configurations compatible with the constraints of a linear elastic system, the configuration that satisfies the conditions of equilibrium has a minimum total potential energy.

The property of minimum potential energy of conservative systems in equilibrium can also be used to advantage in obtaining the approximate solutions of displacements of complex structural systems. If the deflected shape of the system that satisfies the boundary conditions can be approximated by an infinite series, the coefficients of the terms of the series may be determined by the condition that the total potential energy be a minimum for a configuration in stable equilibrium. Note that $q_1, q_2, \ldots, q_r$ in Eqs. (8-32) and (8-33) can be parameters of displacements, such as the coefficients in an infinite series representing displacements, instead of actual displacements. Hence, if we take a finite number of terms in the series, the coefficients of these terms can be determined from Eqs. (8-33). Although the accuracy of an approximate solution depends on the rapidity of convergence of the series and the number of terms taken, this method provides a simple means of reducing the number of displacement parameters specifying the displacements of a complex system.

Example 8-19. Determine the bar forces and joint displacements in the truss for Example 8-13 by using the principle of minimum potential energy.

The potential energy of internal forces or strain energy of the elastic system is given by

$$U_i = \tfrac{1}{2}\sum Fe = \tfrac{1}{2}F_1e_1 + \tfrac{1}{2}F_2e_2 + \tfrac{1}{2}F_3e_3$$

in which

$$\tfrac{1}{2}F_1e_1 = \tfrac{1}{2}(625u + 625v)\,(0.707u + 0.707v) = 221u^2 + 442uv + 221v^2$$

$$\tfrac{1}{2}F_2e_2 = \tfrac{1}{2}(1{,}250v)v = 625v^2$$

$$\tfrac{1}{2}F_3e_3 = \tfrac{1}{2}(-600u + 800v)\,(-0.6u + 0.8v) = 180u^2 - 480uv + 320v^2$$

Hence,

$$U_i = 401u^2 - 38uv + 1{,}166v^2$$

The potential energy of the external forces is equal to

$$U_e = -(Pu + Qv)$$

Then, the total potential energy of the system is expressed in terms of the displacements u and v as follows:

$$U = -(Pu + Qv) + 401u^2 - 38uv + 1{,}166v^2$$

By the principle of minimum potential energy, we have

$$\frac{\partial U}{\partial u} = -P + 802u - 38v = 0$$

$$\frac{\partial U}{\partial v} = -Q - 38u + 2{,}332v = 0$$

or

$$P = 802u - 38v$$

$$Q = -38u + 2{,}332v$$

These results are identical to Eqs. (d) in Example 8-16.

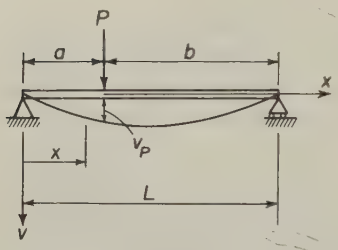

Figure 8–37

Example 8-20. Obtain an approximate deflection curve for a simple beam of constant EI subjected to a concentrated load P, as shown in Fig. 8-37, by means of the principle of minimum potential energy.

The deflection curve of the beam can be approximated by a trigonometric series that satisfies the boundary conditions. Usually, the simplest series used for such a purpose is either a sine or cosine series. Consider, for instance, a sine series of the form

$$v = c_1 \sin\frac{\pi x}{L} + c_2 \sin\frac{2\pi x}{L} + \ldots + c_n \sin\frac{n\pi x}{L} = \sum_{j=1}^{n} c_j \sin\frac{j\pi x}{L} \qquad \text{(a)}$$

in which $c_1, c_2, \ldots, c_n$ are arbitrary constants to be determined. Since $v = 0$ when $x = 0$ and $x = L$, the boundary conditions of the beam are satisfied. The integer j represents the number of half sine waves in the span length L. As examples, the first three terms in the series are plotted in Figs. 8-38(a), (b), and (c), respectively. Thus, the deflection curve of the beam is equal to the superposition of these shapes provided that $c_1, c_2, \ldots, c_n$ are first obtained by the principle of minimum potential energy.

The potential energy of the external force is equal to $U_e = -Pv_p$, in which v_p is the vertical deflection under the load at $x = a$. Hence,

$$U_e = -P \sum_{j=1}^{n} c_j \sin\frac{j\pi a}{L} \qquad \text{(b)}$$

The potential energy of the internal forces expressed as a function of displacements is given by Eq. (8-13b) as follows:

$$U_i = \frac{EI}{2} \int_0^L \left(\frac{d^2v}{dx^2}\right)^2 dx \qquad \text{(c)}$$

Noting that

$$\frac{d^2v}{dx^2} = -\sum_{j=1}^{n}\left(\frac{j\pi}{L}\right)^2 c_j \sin\frac{jn\pi}{L}$$

we get

$$\left(\frac{d^2v}{dx^2}\right)^2 = \frac{\pi^4}{L^4}\left[\sum_{j=1}^{n} j^2 c_j \sin\frac{jn\pi}{L}\right]^2 \tag{d}$$

The square of the sum of the terms inside the brackets consists of either square terms in the form of

$$j^4 c_j^2 \sin^2\frac{j\pi x}{L} \quad (j = 1, 2, \ldots, n)$$

or product terms for $k \neq j$ in the form of

$$2j^2k^2c_jc_k \sin\frac{j\pi x}{L}\sin\frac{k\pi x}{L} \quad (j = 1, 2, \ldots, n, k = 1, 2, \ldots, n)$$

It can be demonstrated by direct integration that

$$\int_0^L \sin^2\frac{j\pi x}{L}\,dx = \frac{L}{2}$$

and

$$\int_0^L \sin\frac{j\pi x}{L}\sin\frac{k\pi x}{L}\,dx = 0 \quad (j \neq k)$$

Hence, when we substitute Eq. (d) into Eq. (c), only the square terms remain. Then, we have

$$U_i = \left(\frac{EI}{2}\right)\left(\frac{\pi^4}{L^4}\right)\left(\frac{L}{2}\right)\sum_{j=1}^{n} j^4 c_j^2 \tag{e}$$

The total potential energy of the system is then equal to the sum of Eqs. (b) and (e), or

$$U = -P\sum_{j=1}^{n} c_j \sin\frac{j\pi a}{L} + \frac{\pi^4 EI}{4L^3}\sum_{j=1}^{n} j^4 c_j^2$$

By the principle of stationary potential energy, we obtain for the general case

$$\frac{\partial U}{\partial c_j} = 0, \quad P\sin\frac{j\pi a}{L} = \frac{\pi^4 EI}{2L^3} j^4 c_j$$

Hence, the general expression for the coefficient c_j is

$$c_j = \frac{2PL^3}{\pi^4 j^4 EI}\sin\frac{j\pi a}{L} \tag{f}$$

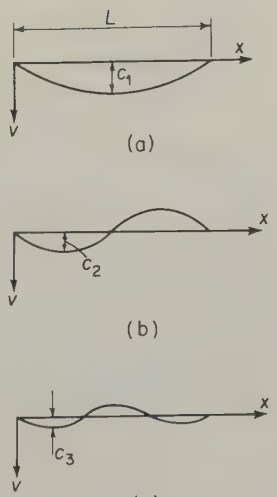

Figure 8–38

Substituting Eq. (f) into Eq. (a), we get

$$v = \frac{2PL^3}{\pi^4 EI} \sum_{j=1}^{n} \frac{1}{j^4} \sin \frac{j\pi a}{L} \sin \frac{j\pi x}{L} \tag{g}$$

To illustrate the application of Eq. (g), let us consider $a = L/2$ and take the first three terms of the series. Then,

$$v = \frac{2PL^3}{\pi^4 EI} \left[\sin^2 \frac{\pi}{2} + \frac{1}{2^4} \sin^2 \pi + \frac{1}{3^4} \sin^2 \frac{3\pi}{2} \right]$$

$$= \frac{2PL^3}{\pi^4 EI} \left[1 + 0 + \frac{1}{81} \right] = \frac{PL^3}{48.6EI}$$

It can be seen that the series converges very rapidly and, in general, a very few terms of the series will give results sufficiently accurate for practical purposes.

8-17 *Principle of Stationary Complementary Energy*

In the application of the principle of stationary potential energy, it has been shown that, if a conservative deformable system is given a variation of displacements during which the conditions of geometrical compatibility are maintained, the equations of equilibrium may be derived from the requirement of stationary potential energy. We shall now consider another application that is analogous to this principle. If a conservative deformable system is given a variation of internal forces during which the conditions of equilibrium are maintained, the equations of compatibility may be obtained from the requirement of stationary complementary energy.

Consider again a conservative deformable system in equilibrium under the action of a set of forces $P_1, P_2, \ldots, P_m$, producing displacements $s_1, s_2, \ldots, s_m$ at the points of application of these forces in the direction of the respective forces, as shown in Fig. 8-36. If the system is statically indeterminate, it is possible to produce many sets of internal forces, each of which will hold the system in equilibrium while the external forces are kept constant. Note that the deformations e are now interpreted as functions of the internal forces F, which may be varied during the equilibrium without varying the external forces. However, there is only one set of internal forces that satisfies the conditions of compatibility also. From the principle of virtual forces, i.e., Eqs. (8-22a) and (8-22c), we have

$$\delta U_c = \sum_{k=1}^{n} e_k \delta F_k = \sum_{j=1}^{m} s_j \delta P_j \tag{a}$$

The set of internal forces that satisfies the requirements of compatibility must also satisfy Eq. (a) with $\delta P_j = 0$ ($j = 1, 2, \ldots m$). Hence,

$$\delta U_c = \sum_{k=1}^{n} e_k \delta F_k = 0 \tag{b}$$

or

$$\delta U_c = 0 \tag{8-34}$$

Equation (8-34) states that of all possible states of internal forces satisfying the conditions of equilibrium of a system, the one that satisfies the conditions of compatibility causes the variation of complementary energy to vanish. This is called the *complementary energy theorem.*

In the analysis of redundant structures, the complementary energy U_c may be expressed as a function of the redundant forces. For a system with r redundances $X_1, X_2, \ldots, X_r$, we have

$$\delta U_c = \frac{\partial U_c}{\partial X_1}\delta X_1 + \frac{\partial U_c}{\partial X_2}\delta X_2 + \ldots + \frac{\partial U_c}{\partial X_r}\delta X_r = 0 \tag{8-35}$$

Since $\delta X_1, \delta X_2, \ldots, \delta X_r$ are not all zero and are independent of each other, it is necessary that

$$\frac{\partial U_c}{\partial X_1} = \frac{\partial U_c}{\partial X_2} = \ldots = \frac{\partial U_c}{\partial X_r} = 0 \tag{8-36}$$

In other words, of all possible states of internal forces satisfying the conditions of equilibrium, the one that also satisfies the conditions of compatibility makes the complementary energy function stationary. This is known as the *principle of stationary complementary energy.* Except for the special case of linear elastic systems, the stationary value of complementary energy is not always a minimum. However, in the application of this principle, it is immaterial whether the stationary value is a relative maximum or minimum.

For a given redundant structure, we can always establish the equations of equilibrium first. If the structure has r redundant forces $X_1, X_2, \ldots, X_r$, the complementary energy U_c can be expressed as a function of the redundant forces only since the other forces may be eliminated by using the relation of forces in the equations of equilibrium. Then, the compatibility conditions, which are as numerous as the redundant forces, can be obtained by Eqs. (8-36), with one equation corresponding to a redundant force.

If a redundant system is self-strained, the point of application of a redundant force X_j may be displaced by an amount λ_j in the direction of the force. If all redundant forces are affected, we have

$$\delta U_c = \sum_{k=1}^{n} e_k \delta F_k + \sum_{j=1}^{r} \lambda_j \delta X_j$$

Hence,

$$\frac{\partial U_c}{\partial X_j} = \lambda_j \qquad (j = 1, 2, \ldots, r) \tag{8-37}$$

Thus, the complementary energy is stationary only for systems without self-straining. For linear elastic systems, $U_c = U_i$. Then, Eq. (8-37) becomes Eq. (8-31b).

The complementary energy theorem may also be applied to obtain approximate solutions for deflections of complex systems in a manner similar to that using the principle of minimum potential energy. The detailed discussion of the method, however, is beyond the scope of this book.*

Example 8-21. Determine the bar forces in the redundant nonlinear elastic system shown in Fig. 8-39(a) if the stress-strain relation of the material for all members is given by the parabolic curve $\sigma = 1{,}000\sqrt{\epsilon}$ ksi. The cross-sectional areas of the members in square inches are indicated along the members.

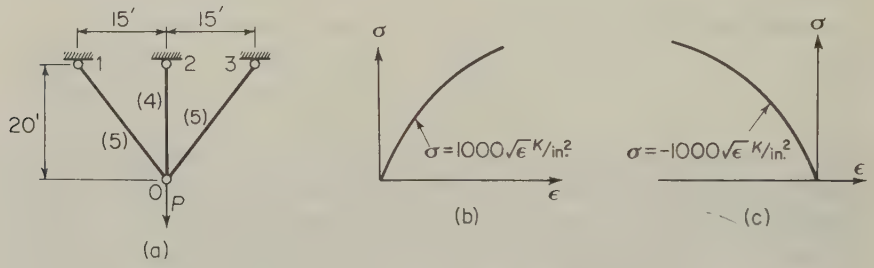

Figure 8-39

Since the structure is symmetrical, let all quantities pertaining to members 01 and 03 be denoted by the subscript 1 and those pertaining to member 02 be denoted by the subscript 2. Assuming that all bar forces are in tension, then from the equation of equilibrium. $\Sigma F_y = 0$, we have

$$(2F_1)(\tfrac{4}{5}) + F_2 = P$$

The structure is statically indeterminate to the first degree. We shall, therefore, consider one bar force, say F_2, as the redundant force. Then, the other bar force can be obtained in terms of F_2 from the equation of equilibrium as follows:

$$F_1 = \frac{1}{1.6}(P - F_2)$$

*See References 8–9 and 8–10 for further discussions.

The elongation of a member can be expressed in terms of the bar force from the stress-strain relation $\sigma = 1{,}000\sqrt{\epsilon}$. Then,

$$e = \epsilon L = 10^{-6}\sigma^2 L = 10^{-6}\left(\frac{F}{A}\right)^2 L = \frac{10^{-6}L}{A^2} F^2$$

Thus,

$$e_1 = \frac{(10^{-6})(25)(12)}{(5)^2} F_1^2 = 12 \times 10^{-6} F_1^2 = 4.68 \times 10^{-6}(P - F_2)^2$$

$$e_2 = \frac{(10^{-6})(20)(12)}{(4)^2} F_2^2 = 15 \times 10^{-6} F_2^2$$

Then,

$$\frac{\partial U_c}{\partial F_2} = 2e_1 \frac{\partial F_1}{\partial F_2} + e_2 \frac{\partial F_2}{\partial F_2} = (10^{-6})\left[(2)(4.68)(P - F_2)^2 \frac{1}{1.6} + 15F_2^2(1)\right]$$

or

$$\frac{\partial U_c}{\partial F_2} = (10^{-6})[-5.86(P - F_2)^2 + 15F_2^2] = 0$$

Multiplying through by a factor of $10^6/5.86$ leads to the quadratic equation

$$1.56F_2^2 + 2PF_2 - P^2 = 0$$

the roots of which are $F_2 = 0.385P$ and $-1.667P$. The corresponding values of F_1 are obtained as follows:

$$F_1 = \frac{1}{1.6}(P - F_2) = 0.385P \text{ and } + 1.667P$$

Note that each set of results represents a state of stress that is in equilibrium and automatically satisfies the requirement of compatibility. However, physically, there cannot be two sets of forces both of which satisfy the requirement of compatibility as well as conditions of equilibrium. In other words, the solution must be unique. The explanation for the multiplicity of answers lies in the fact that in computing the deformation e in a member, we take the square of the stress-strain relation $\sigma = 1{,}000\sqrt{\epsilon}$ given in Fig. 8-39(b). Thus, only one set of answers corresponds consistently to this stress-strain relation, while some or all answers in the other set may follow the stress-strain relation $\sigma = -1{,}000\sqrt{\epsilon}$, as shown in Fig. 8-39(c). We must therefore select the set of answers corresponding to the given stress-strain curve. Noting that $F_2 = -1.667P$ leads to a positive e_1, which represents the stress-strain relation in Fig. 8-39(c) rather than that in Fig. 8-39(b), this answer is unacceptable. Hence, the only set of answers for this problem is $F_1 = 0.385P$ and $F_2 = 0.385P$.

Generally, nonlinear stress-strain relations lead to a multiplicity of answers. If the strain is a function of an odd power of stress, or the stress is a function of an odd power of strain, this situation may not occur. However, there is always one and only one set of answers that satisfies all requirements. We must therefore observe the uniqueness of the solution and select only the correct one from the multiplicity of roots obtained by the complementary energy theorem.

8-18 *Summary*

In this chapter we have discussed the energy principles used in structural analysis and stressed the dual nature of these principles relating to forces and displacements. Since the computation of deflections of statically determinate structures is often a preliminary step in obtaining the equations of compatibility in the solution of redundant systems by the force method, special emphasis has been placed on the application of the energy principles to the computation of deflections of such structures. However, we made an attempt to give a balanced presentation in applying these principles to the direct solution of redundant systems by both the force and the displacement method. Although most of the examples cited involve linear elasticity, the application of energy principles is not confined to linear elastic systems, as we demonstrated with several examples of nonlinear elastic systems. The difficulty in the solution of nonlinear systems lies solely in the mathematical complexities inherent in such problems.

We also pointed out that the equilibrium and energy approaches are interrelated. Starting from the principle of conservation of energy, we can derive the requirements of equilibrium and compatibility. Hence, the energy principles should not be treated piecemeal as isolated methods of computing deflections. Only by studying the interrelations of various approaches can we gain insight into the unity of purpose underlying all principles of structural mechanics.

References

8-1 E. G. Coker, "An Optical Determination of the Variation of Stress in a Thin Rectangular Plate," *Proc. Royal Society of London*, ser. A, vol. 86, 1912, p. 291.

8-2 J. H. Argyris, "Energy Theorems and Structural Analysis," *Aircraft Engineering*, vol. 26, 1954, pp. 343, 383; vol. 27, 1955, pp. 42, 80, 125, 145.

8-3 N. J. Hoff, *The Analysis of Structures*, John Wiley & Sons, Inc., New York, 1956.

8-4 F. DiMaggio, "Principle of Virtual Work in Structural Analysis," *Proc. ASCE*, vol. 86, no. ST11, 1960, p. 65. See also subsequent discussions of the paper.

8-5 H. Cross, "Virtual Work: A Restatement," *Trans. ASCE*, vol. 90, 1926, p. 610.

8-6 A. Castigliano, *Théorème de l'Équilibre des Systèms Élastiques et ses Applications*, 1879; Eng. trans. E. S. Andrews, *Elastic Stresses in Structures*, Scott, Greenwood & Son, London, 1919.

8-7 R. V. Southwell, *An Introduction to the Theory of Elasticity*, 2nd Ed., Oxford University Press, Fair Lawn, N.J., 1941.

8-8 R. V. Southwell, "On Castigliano's Theorem of Least Work and the Principle of St. Venant," *Philosophical Magazine* (London), 6th ser., vol. 45, 1923, p. 193.

8-9 T. M. Charlton, *Energy Principles in Applied Statics*, Blackie & Son, London, 1959.

8-10 H. M. Westergaard, "On the Method of Complementary Energy," *Trans. ASCE*, vol. 107, 1942, p. 765.

8-11 J. C. Maxwell, "On the Calculation of the Equilibrium and Stiffness of Frames," *Philosophical Magazine* (London), 4th ser., vol. 27, 1864, p. 294.

8-12 G. F. Swain, "On the Application of the Principle of Virtual Velocities to the Determination of the Deflections and Stresses of Frames," *Journal of the Franklin Institute*, vol. 183, 1883, p. 102.

Problems

8-1 By the method of real work, determine the slope at end B of the beam due to a couple M applied at end B, as shown in Fig. P8-1. The bending stiffness EI of the beam is constant.

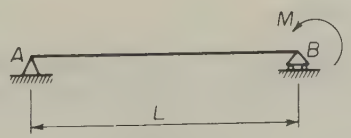

Figure P8–1

8-2 By the method of real work, determine the deflection at the center of the span of the simple beam shown in Fig. P8-2. The bending stiffness of the beam is constant.

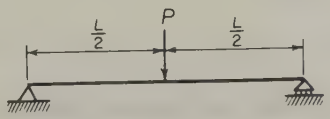

Figure P8–2

8-3 to **8-5** By the method of virtual work, compute the vertical deflection at point C of each of the beams shown in Figs. P7-3 to P7-5 at the end of Chapter 7.

8-6 By the method of virtual work, compute the horizontal and vertical displacements of joint D of the frame shown in Fig. P7-18 at the end of Chapter 7.

8-7 By the method of virtual work, compute the horizontal displacement at joint E of the frame shown in Fig. P7-20 at the end of Chapter 7.

8-8 and **8-9** By the method of virtual work, find the vertical displacement at joint B of each of the trusses shown in Figs. P7-24 and P7-25 at the end of Chapter 7.

8-10 By the method of virtual work, calculate the displacement of joint L_3 in a direction perpendicular to member U_2L_3 of the truss shown in Fig. P7-26 at the end of Chapter 7.

8-11 and **8-12** By the method of virtual work, determine the horizontal and vertical displacements at joint G of the trusses shown in Figs. P8-11 and P8-12. $E = 30 \times 10^3$ ksi.

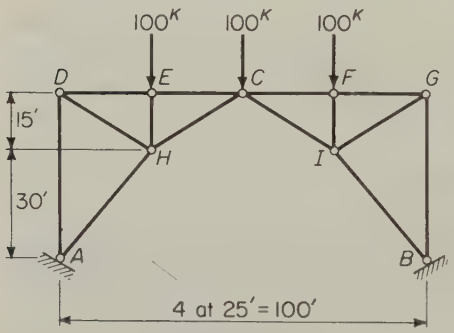

Figure P8–11

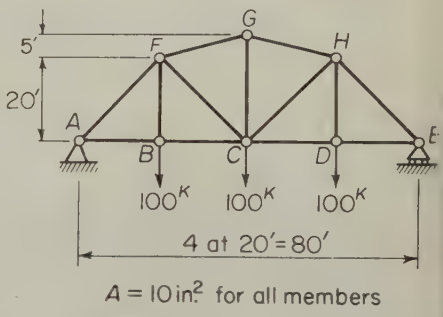

Figure P8–12

8-13 and **8-14** Using Castigliano's second theorem, compute the slope at point A of the beam shown in Figs. P8-13 and P8-14. The bending stiffness EI of the beams is constant.

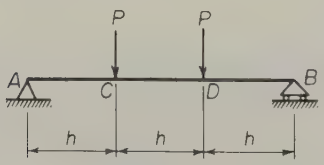

Figure P8–13

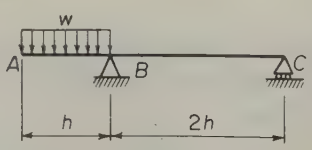

Figure P8–14

8-15 and **8-16** Using Castigliano's second theorem, compute the relative displacement of joints H and I of the trusses shown in Figs. P8-15 and P8-16. $E = 30 \times 10^3$ ksi.

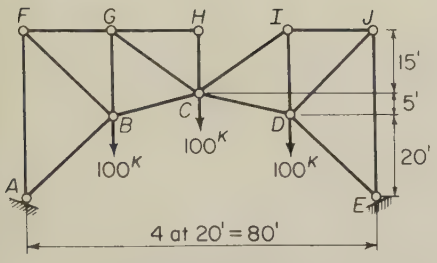

$E = 30 \times 10^3$ ksi
$A = 4$ in.^{2} for all members except bottom chord
$A = 20$ in.^{2} for bottom chord

Figure P8–15

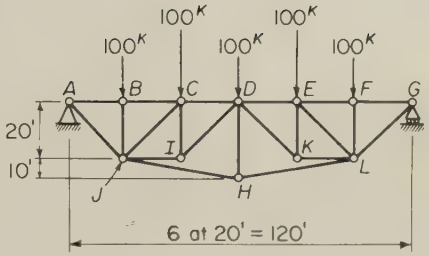

$E = 30 \times 10^3$ ksi
$A = 10$ in.^{2} for all members

Figure P8–16

8-17 and **8-18** If the material used for all members in a truss has a stress-strain relation $\sigma = 500\sqrt{\epsilon}$, determine the vertical displacement at point C of the trusses shown in Fig. P8-17 and P8-18.

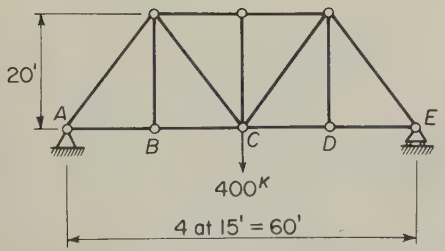

$A = 10$ in.^{2} for all members

Figure P8–17

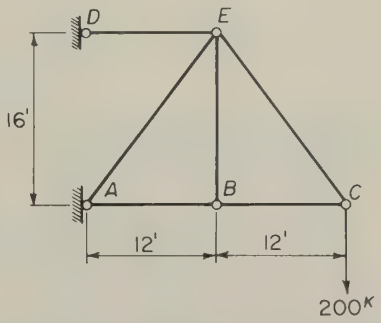

$A = 5$ in.^{2} for all members

Figure P8–18

8-19 and **8-20** By using the force method of analysis, determine the vertical reaction at support B of the structures shown in Figs. P8-19 and P8-20. $E = 30 \times 10^3$ ksi.

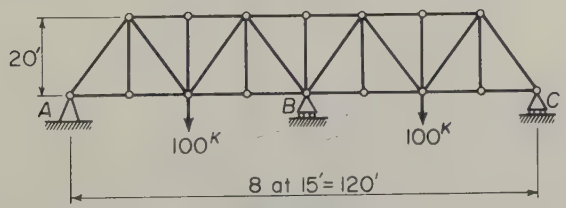

$E = 30 \times 10^3$ ksi
$A = 10$ in.^{2} for all members

Figure P8–19

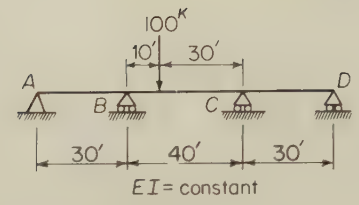

Figure P8–20

8-21 By using the force method of analysis, determine the horizontal reaction at support D of the frame shown in Fig. P8-21. $E = 30 \times 10^3$ ksi.

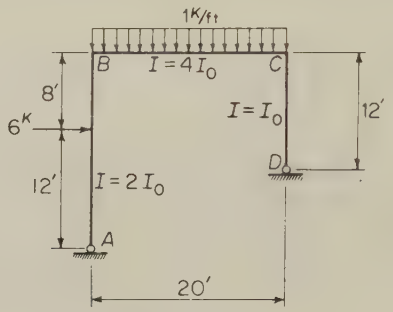

Figure P8–21

8-22 By using the force method of analysis, compute the moment at support B of the continuous beam shown in Fig. P8-22. $E = 30 \times 10^3$ ksi.

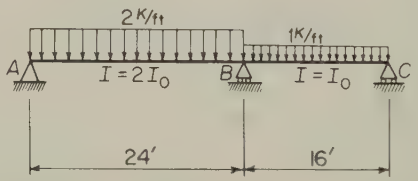

Figure P8–22

8-23 By using the displacement method of analysis, determine the horizontal and vertical displacements of joint 0 of the system shown in Fig. P8-23. The areas of the members in square inches are given along the members. $E = 30 \times 10^3$ ksi.

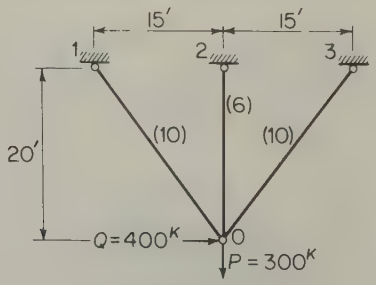

Figure P8–23

8-24 By using the displacement method of analysis, compute the vertical displacement of joint 0 of the system shown in Fig. P8-24. The area of the members in square inches are given along the members. $E = 30 \times 10^3$ ksi.

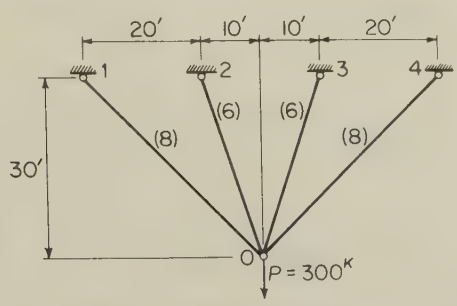

Figure P8–24

8-25 and **8-26** By applying Müller-Breslau's principle, construct influence lines for reactions at supports A and B of the beams shown in Figs. P8-25 and P8-26. Compute the ordinates of the influence lines at 10-ft intervals along the spans. The bending stiffness EI of the beams is constant.

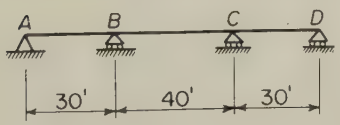

Figure P8–25

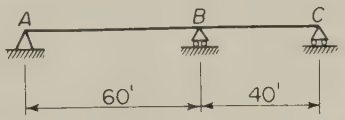

Figure P8–26

8-27 By applying Müller-Breslau's principle, construct an influence line for the horizontal component of reaction at point G due to a unit load moving from point F to point A of the truss shown in Fig. P8-27. Note that $E = 30 \times 10^3$ ksi and $A = 10$ in.^{2} for all members.

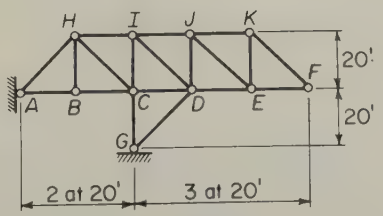

Figure P8–27

8-28 The parabolic arch shown in Fig. P8-28 has a moment of inertia at any section equal to $I = I_c \sec \beta$, in which I_c is the moment of inertia at the crown C and β is the angle between the tangent at the section and a horizontal line.

Construct an influence line for the moment at point D of the arch. Compute the ordinates of the influence line at the sixth points of the span.

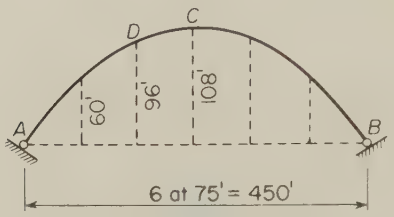

Figure P8–28

8-29 and **8-30** Work Problems 8-23 and 8-24 using Castigliano's first theorem.

8-31 to **8-34** Work Problems 8-19 to 8-22 using Castigliano's second theorem.

8-35 and **8-36** Work Problems 8-23 and 8-24 using the principle of minimum potential energy.

8-37 and **8-38** If the material used for all members in a system has a stress-strain relation $\sigma = 2{,}000\sqrt{\epsilon}$, determine the bar forces in each of the systems shown in Fig. P8-23 and P8-24.

ANSWERS TO PROBLEMS

Chapter 1

1-2. 14,100 lb
1-4. 138,400 lb
1-6. 3.24×10^6 lb-ft
1-8. $F_1 = 5.1$, $F_2 = 34.4$, $F_3 = 61.1$, $F_4 = 88.0$
$F_5 = 115.0$, $F_6 = 141.5$, $F_7 = 56.0$ kips
1-10. $n = 1.65$ for all beams
$K = 1.88, 2.49, 2.79$ for (a), (b), (c), respectively

Chapter 2

(*All answers are in kips*)

2-2. $H_a = 70$, $H_b = 70$, $V_b = 12.5$
2-4. $H_a = 81.4$, $H_b = 51.4$, $V_b = 60$
2-6. $V_a = 10$, $V_b = 28.7$, $V_c = 5.3$
2-8. $V_a = 19.3$, $H_a = 20$, $V_d = 35.7$
2-10. $V(L_2) = 100$, $H(L_2) = 70$, $V(L_3) = 40$, $V(L_7) = 40$, $H(L_7) = 40$
2-12. $V_a = 74.7$, $H_a = 80$, $V_c = 25.3$, $H_c = 0$
2-14. $V_a = 50$, $H_a = 0$, $V_b = 50$, $V_c = 60$, $V_d = 10$, $H_d = 0$
2-22. 25

Chapter 3

3-4. $N_f = 5.27^{k}$, $S_f = 14.1^{k}$, $M_f = 60^{k\text{-ft}}$, $N_g = 20.6^{k}$, $S_g = 20.6^{k}$, $M_g = 85^{k\text{-ft}}$
3-6. $M_b = -138^{k\text{-ft}}$
3-10. $M_c = +16^{k\text{-ft}}$, $M_e = -96^{k\text{-ft}}$
3-14. $M_c = -31^{k\text{-ft}}$
3-16. $M_d = -480^{k\text{-ft}}$
3-18. $M_b = +8.25^{k\text{-ft}}$

3-20. $S_{ab} = 296(\text{h}/24)^{\text{k}}$, $M_c = 523(h^2/24)^{\text{k-ft}}$
3-22. M (left support) $= -128(h^2/24)$
3-24. Shears (multiplied by a factor $h/24$): $S_{ab} = 5.0$, $S_{bc} = 21.0$, $S_{cd} = 20.9$, $S_{de} = 4.9$, $S_{ef} = -17.9$, $S_{fg} = -33.9$; Moments (multiplied by a factor $h^2/24$): $M_b = 5.0$, $M_c = 26.0$, $M_d = 46.9$, $M_e = 51.8$, $M_f = 33.9$
3-26. $M_b = -76^{\text{k-ft}}$, $M_e = -107^{\text{k-ft}}$
3-28. $N_d = 8.47^{\text{k}}$, $S_d = 8.47^{\text{k}}$, $M_d = 175^{\text{k-ft}}$
3-30. M (under 200^{k} load) $= +3240^{\text{k-ft}}$, M (under 160^{k} load) $= +1640^{\text{k-ft}}$
3-32. M (under 200^{k} load) $= +3230^{\text{k-ft}}$, M (under 160^{k} load) $= +2140^{\text{k-ft}}$
3-34. $r_c = 8'$, $r_d = 12'$, $r_e = 12'$, $T_{\max} = 256^{\text{k}}$
3-36. $T_{\max} = 122^{\text{k}}$
3-42. At C, $F_y = -35^{\text{k}}$, $M_x = -357.5^{\text{k-ft}}$, $M_z = 556^{\text{k-ft}}$
3-44. $V_0 = V_2 = 57.08^{\text{k}}$, $V_1 = 200^{\text{k}}$

Chapter 4

(*All answers are in kips*)

4-2. $AB = -125$, $AC = +70$, $BC = +35.2$, $BD = -84.3$, $CD = +14.3$, $CE = +65$
4-6. $a = 0$, $b = -240$, $c = +226$
4-9. $a = -27.4$, $b = -85$, $c = +80$
4-11. $a = -14.2$, $b = -12.5$, $c = +10$
4-12. $a = -30$, $b = +50$, $c = -63.4$
4-14. $a = +5$, $b = -3.78$, $c = -2.74$
4-17. $a = -56$, $b = -31.4$, $c = +38$
4-22. $AD = -100$, $DF = 0$, $FG = +30$, $GH = -70$, $HB = -70$, $BC = -20$, $CA = 0$, $DG = -70.7$, $DC = EG = EB = +70.7$, $EC = EH = +99$
4-24. $a = -85$, $b = 53.2$, $c = +25$
4-26. $a = +45$, $b = +112$, $c = -60$
4-28. $a = +158$, $b = -24.2$, $c = +84.2$
4-30. $a = -83.3$, $b = -17.3$, $c = -62.4$
4-31. $BC = -15.9$, $CD = -15.9$, $DE = -10.3$, $EF = +5.1$, $AF = +5.2$, $AB = -0.4$, $BE = -5.1$, $CF = +5.2$, $AD = +17.2$
4-36. $JG = +210$, $JH = -105$, $JI = -105$, $IH = 0$, $IG = 0$, $IF = -105$, $GF = -66.5$, $GD = +262$, $GH = -58$, $HD = +66.5$, $HE = -158$, $HF = 0$, $FD = +28.8$, $FE = 0$, $FC = -158$, $DC = -88$, $DE = -86.3$, $DA = +368$, $EA = +88$, $EB = -210$, $EC = 0$

Chapter 5

(*All answers are in kips*)

5-1. $R_a = 34.3$ ($H_a = 12$, $V_a = 32.3$), $R_b = 21.7$
5-3. $R_e = 14.8$, $R_f = 25.0$ ($H_f = 10$, $V_f = 11.2$)
5-19. $BC = -14.1$, $CD = -99$, $AD = +87.5$, $AB = -17.5$, $ED = -122.5$, $EB = +12.5$, $AE = -10$
5-21. $a = -60$, $b = 0$, $c = -150$

5-24. $AD = -88$, $DE = -78$, $EF = -75$, $FG = -66$, $GH = -56.5$, $HI = -53.5$, $AB = +69$, $BC = +56$, $DB = -8.3$, $EB = -8.3$, $FB = +12.3$, $FC = -21$, $FJ = +8$, $GJ = -8.5$, $HJ = -8.3$, $CJ = +16.5$, $IJ = +32$, $CK = +40$
5-27. 11.2 (to the left)
5-28. +17.2
5-29. 0

Chapter 6

6-3. (a) $Y_e = 2/5$ for S_e, $Y_e = 3/5\sqrt{2}$ for S_f; (b) $Y_e = 4$ for M_e, $Y_e = 6$ for M_f
6-5. (a) $Y_a = 1.25$, (b) $Y_a = 0.25$, (c) $Y_d = 1$, (d) $Y_d = -30$, (e) $Y_d = -15$
6-7. (a) $Y_c = 1.2$, (b) $Y_c = -8.0$, (c) $Y_c = -0.2$
6-9. (a) $Y_a = 0.25$ for R_a, $Y_e = +1.25$ for R_b; (b) $Y_e = -0.25$ for S_g, $Y_e = 1$ for S_h; (c) $Y_e = -5$ for M_g and M_h
6-12. (a) $Y_g = \frac{1}{6}$, (b) $Y_g = \frac{1}{6}$, (c) $Y_g = 3$
6-16. $Y_f = \frac{2}{3}$
6-18. $U_2L_3 = 67^k$, $L_3L_4 = 166^k$
6-20. $Y_a = 1$ for V_c, $Y_a = -8/7$ for H_c, $Y_a = +8/7$ for H_d
6-22. $Y(L_4) = -1.1$, $Y(L_3) = +5/4$, $Y(L_3) = -0.707$, $Y(L_4) = +0.566$, $Y(L_2) = -0.424$, $Y(L_3) = +1.0$
6-27. (a) 25.9^k, (b) 14.1^k, (c) $217^{k\text{-ft}}$
6-30. (b) $3{,}910^{k\text{-ft}}$
6-33. $U_1L_1 = +255^k$, $U_2L_2 = 0$, $U_1U_2 = -590^k$, $L_1L_2 = +379^k$, $U_1L_2 = +455^k$

Chapter 7

7-5. 1.38 in.
7-6. $-1143/EI$
7-11. At $\frac{1}{4}$ pt., $v = -72(w_0h^4/48EI_0)$; at center, $v = -95(w_0h^4/48EI_0)$
7-13. At center, $v = -51.47(M_0h^2/144EI_0)$
7-15. At free end, $v = -490\ h^2/EI_0 = -1.27$ in.; at center, $v = 110h^2/EI_0 = +0.247$ in.
7-18. $u = -42{,}200/EI_0$, $v = 195{,}000/EI_0$
7-20. 4.25 in.
7-22. 7.39 in.
7-24. 1.90 in.

Chapter 8

8-2. $PL^3/48EI$
8-5. 1.38 in.
8-10. 4.82 in.
8.12. $u = 0.77$ in., $v = 0.24$ in.
8-16. 0.303 in.
8-18. 0.618 in.
8-20. 89^k
8-21. 3.9^k
8-24. $u = 0$, $v = 0.226$ in.

8-26. Influence ordinates for $R_{\prime\prime}$, at 10 ft intervals starting from support A: 0, 0.288, 0.556, 0.787, 0.954, 1.023, 1.000, 0.859, 0.625, 0.328, 0

8-27. Influence ordinates from A to F inclusive: 0, -0.038, $+0.075$, $+0.61$, $+0.93$, $+1.27$

8-38. $F_1 = 92.0^{k}$, $F_2 = 89.4^{k}$

INDEX

A

Aeolian vibration, 29
Aerodynamic instability, 29
Analysis, defined, 1, 2
Angle change in:
  beams, 383
  trusses, 420
Axial force:
  definition, 123
  sign convention, 123
Arch:
  definition, 11
  deflection, 406
  influence lines, 314, 486
  three hinged, 163, 267, 314
  two hinged, 486
Argyris, 450

B

Bar chain method, 421
Bar force, 200
Beams:
  compound, 307
  definition, 10
  deflection, 373
  differential relationships, 130, 373
  influence lines, 295, 488
  simple, 130, 262
  statically indeterminate, 477
Bending moment:
  definition, 53, 123
  diagram, 139
  sign convention, 123
Bending stiffness, 370
Betti theorem, 472
Boundary conditions, 81
Bow girder, 184
Bow's notation, 279
Buckling, 35

C

Cable:
  definition, 173
  deflection, 425
  horizontal tension, 175
Castigliano's theorems:
  of internal work, 460
  of "least work," 490
Charlton, 491
Compatibility of displacements, 80
Complementary energy:
  definition, 112
  method, 450
  theorems, 503
Complementary work, 440
Complex trusses, 228
Compound beams, 307
Compound systems, 68

Compound trusses, 219, 282, 326
Configuration, 53
Conservation of energy, 9, 105, 438
Conservative systems, 105, 436
Construction, defined, 1, 5
Continuity, conditions of, 7
Continuum, 7
Cooper's loading, 24, 332, 333
Criteria for maximum effects of concentrated loads on:
  beam, 335
  girder supporting floor beams, 349
  truss, 349
Criteria of statical indeterminacy for:
  pin-connected trusses, 78
  rigid frames, 77
  structures with releases, 79
Cross, Hardy, 38
Curvature:
  definition, 88, 372
  radius of, 370
Curved bar, 92

D

d'Alembert's principle, 8
Deflection of:
  arches, 406
  beams, 373
  non-linear elastic systems, 465
  rigid frames, 397
  trusses, 408
Deflection theory, 53
Deformable system, 7, 436
Deformation, 53
Degrees of:
  freedom, 57
  kinematic indeterminacy, 84
  statical indeterminacy, 75
Design, defined, 1, 3
Design specifications, 38
Differential coefficients of internal work, theorem of, 460
Displacement:
  computation, 368
  definition, 53
Displacement boundary conditions, 81
Displacement method, 84, 476
Dummy unit load method, 454

E

Earthquake motions, 29
Elastic curve, 369
Elastic design, 4
Elastic theory, 53
Energy approach, 105, 436
Engesser, 450
Equilibrium:
  conditions of, 54
  dynamic, 8
  stable, 55
  static, 7
  unstable, 55
Equilibrium approach, 368
Equivalent static loads, 21

F

Factor of:
  safety, 37
  serviceability, 37
Flexibility coefficient, 482
Flexural rigidity, 370
Force, 6
Force boundary conditions, 81
Force-deformation relations, 84
Force method, 84, 476
Force parallelogram, 250
Force polygon, 250
Force triangle, 250
Forces:
  body, 21
  conservative, 106
  effective, 8
  external, 6
  inertia force, 8
  internal, 7, 52
  longitudinal, 25
  surface, 21
  transverse, 25
Fracture:
  brittle, 36
  fatigue, 36
Free body, defined, 52
Funicular polygon, 253

G

Galloping vibration, 29
Generalized coordinates, 57
Geometrical instability, 68
Girders supporting floorbeams:
  influence lines, 310
  shear and moment diagrams, 149

H

Henneberg's method, 230

I

Impact, 24
Influence coefficient, 296, 482
Influence diagram, 295
Influence line:
  definition, 295
  qualitative, 305

J

Joukowski lever, 287

K

Karman vortex trail, 29

L

Large deflection theory, 53
Load factor, 37
Loading:
  lane, 24
  train, 24, 332
Loads:
  blast, 32
  dead, 21
  dynamic, 21
  equivalent static, 21
  live, 22
  movable, 23
  moving, 23
  repeated, 36
  snow, 25
  standard truck, 23
  static, 21
  wind, 25
"Least work," theorem of, 490

M

Maxwell diagram, 278
Maxwell-Betti theorem, 471
Maxwell's theorem of reciprocal displacements, 471
Mechanism, 55
Membrane stresses, 11
Membrane theory, 15
Minimum potential energy for:
  deformable systems, 496
  linear elastic systems, 498
  rigid systems, 108
Moment:
  bending, 52
  twisting, 53
Moment-area method, 383
Moment-curvature relation, 369
Moment tables for concentrated loads, 330
Motion:
  definition, 7
  equation of, 8
Müller-Breslau's principle, 484

N

Newmark's method, 393
Newton's laws of motion, 7
Nodal point, 59
Normal force, 52
Normal strain, 53
Normal stress, 52
Numerical procedure for computing:
  deflections, 393
  equivalent concentrated loads, 152
  shears and moments, 157

P

Path of deformation, 54
Plain strain problems, 15
Plain stress problems, 14
Planning, defined, 1
Plastic deformation, 35
Plastic design, 4
Potential energy of:
  deformable systems, 496
  external forces, 106
  internal forces, 107
  rigid systems, 106
Pressure lines, 271
Prestressing, 95
Pseudo-uniform stress form, 11

Q

Qualitative influence line, 305

R

Reactions:
  computation, 60, 68
  definition, 52
  graphical determination, 255

Real work:
  definition, 438
  method of, 446
Redundant structures, analysis of, 476
Redundant systems, 75
Release, 68
Released structure, 82
Rigid frames:
  definition, 20
  deflection, 397
  shear and moment, 143
Rotation, 53

S

Saint-Venant's principle, 9
Schwedler dome, 237
Self-straining, 95, 490, 503
Shear:
  definition, 123
  diagram, 139
  sign convention, 123
Shearing force, 52
Shearing strain, 53
Shearing stress, 52
Simple trusses:
  definition, 206
  deflection, 408
  graphical solution, 278
  influence lines, 319
Singularity functions:
  definition, 135
  integration, 135
  successive integrations, 379
Small deflection theory, 53
Southwell, 491
Space diagram, 253
Space frame, 183
Space truss, 236
Statically determinate structures, defined, 44
Statically indeterminate structures, defined, 45
Stationary complementary energy, 502
Stationary potential energy of:
  deformable system, 496
  rigid systems, 107
Steinman loading, 24
Stiffening:
  girder, 18
  truss, 18
Stiffness coefficient, 482
Strain, 53
Strain energy, defined, 113
Strain energy:
  in linear elastic systems, 441
  method, 450
Stress, 52
Stress couple, 52
Stress energy, 113
Stress resultant, 52
Stresses in truss:
  primary, 201
  secondary, 201
String polygon, 253
Structures in space, 183
Superposition, principle of, 99
Suspension bridge, 179

T

Tension coefficients, method of, 238
Thermal effects, 96
Three-hinged arch, 163, 267, 314
Torque, 53
Trusses:
  Baltimore, 205
  common patterns, 203
  definition, 200
  Fink, 204
  Howe, 204, 205
  Parker, 205
  Petit or Pennsylvania, 205
  plane, 203
  Pratt, 204
  space, 236
  Warren, 204, 205
  Wichart, 206

U

Uniform stress form, 9
Unstable systems:
  geometrically, 62
  statically, 55

V

Varying stress form, 9
Vector, defined, 249
Vibration:
  aeolian, 29
  galloping, 29
  self-excited, 29
Virtual displacement, defined, 110

Virtual displacement diagram, 287
Virtual displacements:
  method of, 233
  principle of, 110, 452
Virtual force, principle of, 453
Virtual velocities, 111
Virtual work:
  method of, 454
  principle of, 110, 453
Virtual work for linear elastic systems, 457

W

Westergaard, 450
Williot diagram, 411
Williot-Mohr diagram, 413
Work, defined, 436

(Continued from front flap)

action of forces and displacements in structural systems.

- It brings up to date the energy principles that have long been neglected in elementary textbooks on structures, but are invaluable in structural analysis.
- Ample examples are completely worked out to illustrate the methods of approach for a great variety of problems.
- The unity of purpose of many different theorems and methods has been stressed throughout the entire book.

About the Author

TUNG AU received his Ph.D. degree from the University of Illinois in 1951, and for several years was a structural engineer for consulting offices in Detroit, Michigan. He has been an Associate Professor of Civil Engineering at Carnegie Institute of Technology since 1957. A registered professional engineer, Dr. Au is the author of several papers in structures and mechanics.

PRENTICE-HALL, Inc.
Englewood Cliffs, N. J.

574 • Printed in U.S. of America

Other books of interest in the
PRENTICE-HALL CIVIL ENGINEERING AND
ENGINEERING MECHANICS SERIES

THEORY OF PRESTRESSED CONCRETE

by MICHAEL CHI and FRANK A. BIBERSTEIN

Presents and analyzes the basic principles of prestressing, and uses these principles to develop a rational and direct method of designing a large variety of concrete structures. *Theory of Prestressed Concrete* emphasizes the theory rather than application of prestressing. A concise treatment of theory with minimal preoccupation with hardware and pragmatism is offered. Supplied also are unique design charts to enhance understanding of theory and to enable a rapid, accurate design.

Published April, 1963 *approx. 256 pages*

FOUNDATION DESIGN

by WAYNE C. TENG

The book furnishes the essential data for foundation design, incorporating both the latest advances in soil mechanics and the established principles of foundation engineering.

Part I contains the basic concepts and tools applicable to all foundations and retaining structures. It also furnishes a brief review of the basic principles of soil mechanics. Parts II and III deal with various types of foundations and retaining structures, including spread footings, combined footings, drilled caisson, sheetpiling walls, and cofferdams.

Published November, 1962 *466 pages*

PRENTICE-HALL, Inc.
Englewood Cliffs, New Jersey

13-260455-8